NEUROINFLAMMATION AND COGNITION

EDITED BY: Ashok Kumar, Brandi K Ormerod, Yogesh Dwivedi and Jakob W Streit

PUBLISHED IN: Frontiers in Aging Neuroscience

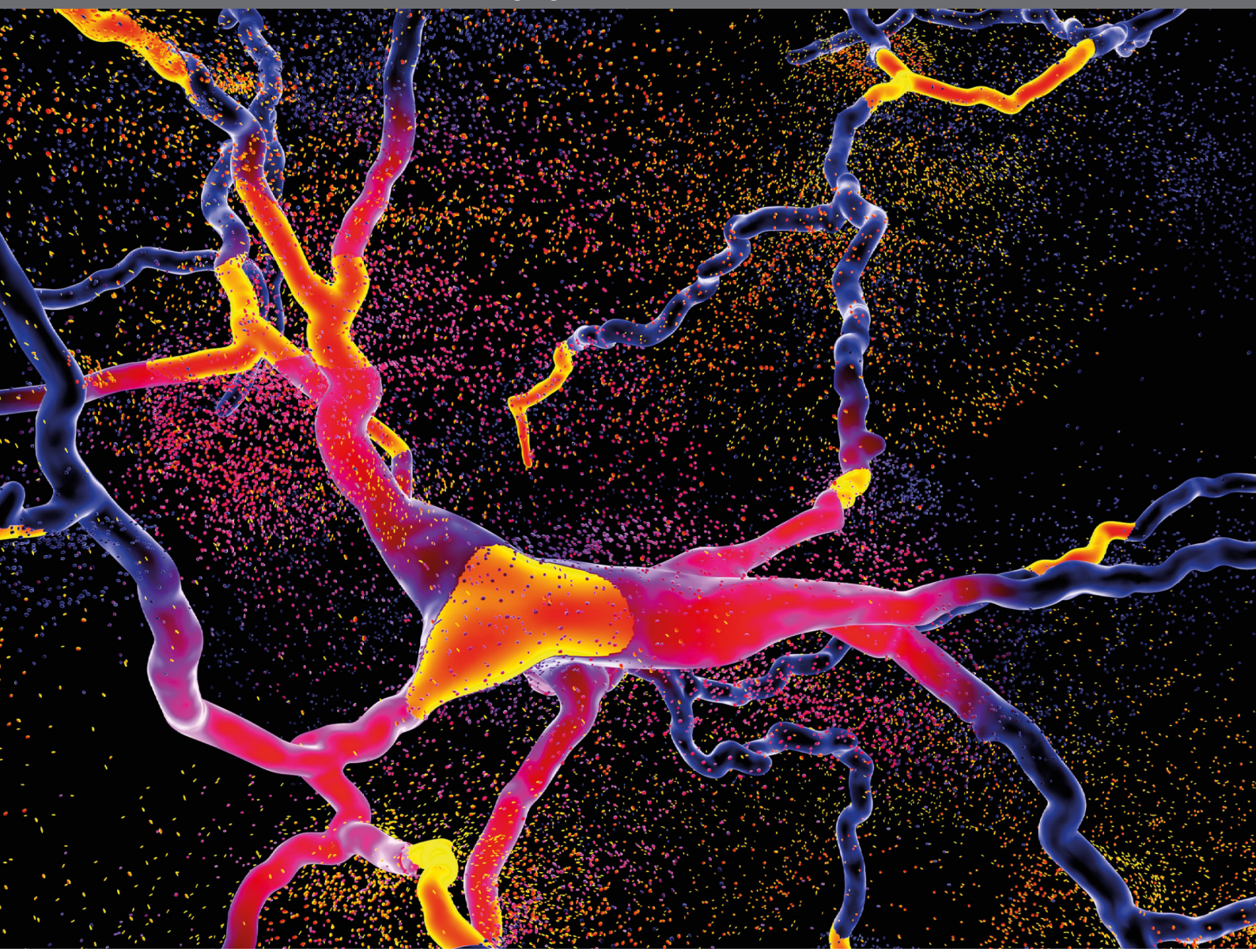

frontiers Research Topics

ISSN 1664-8714
ISBN 978-2-88945-760-1
DOI 10.3389/978-2-88945-760-1

About Frontiers

Frontiers is more than just an open-access publisher of scholarly articles: it is a pioneering approach to the world of academia, radically improving the way scholarly research is managed. The grand vision of Frontiers is a world where all people have an equal opportunity to seek, share and generate knowledge. Frontiers provides immediate and permanent online open access to all its publications, but this alone is not enough to realize our grand goals.

Frontiers Journal Series

The Frontiers Journal Series is a multi-tier and interdisciplinary set of open-access, online journals, promising a paradigm shift from the current review, selection and dissemination processes in academic publishing. All Frontiers journals are driven by researchers for researchers; therefore, they constitute a service to the scholarly community. At the same time, the Frontiers Journal Series operates on a revolutionary invention, the tiered publishing system, initially addressing specific communities of scholars, and gradually climbing up to broader public understanding, thus serving the interests of the lay society, too.

Dedication to Quality

Each Frontiers article is a landmark of the highest quality, thanks to genuinely collaborative interactions between authors and review editors, who include some of the world's best academicians. Research must be certified by peers before entering a stream of knowledge that may eventually reach the public - and shape society; therefore, Frontiers only applies the most rigorous and unbiased reviews.
Frontiers revolutionizes research publishing by freely delivering the most outstanding research, evaluated with no bias from both the academic and social point of view. By applying the most advanced information technologies, Frontiers is catapulting scholarly publishing into a new generation.

What are Frontiers Research Topics?

Frontiers Research Topics are very popular trademarks of the Frontiers Journals Series: they are collections of at least ten articles, all centered on a particular subject. With their unique mix of varied contributions from Original Research to Review Articles, Frontiers Research Topics unify the most influential researchers, the latest key findings and historical advances in a hot research area! Find out more on how to host your own Frontiers Research Topic or contribute to one as an author by contacting the Frontiers Editorial Office: researchtopics@frontiersin.org

NEUROINFLAMMATION AND COGNITION

Topic Editors:
Ashok Kumar, University of Florida, United States
Brandi K Ormerod, University of Florida, United States
Yogesh Dwivedi, University of Alabama, United States
Jakob W Streit, University of Florida, United States

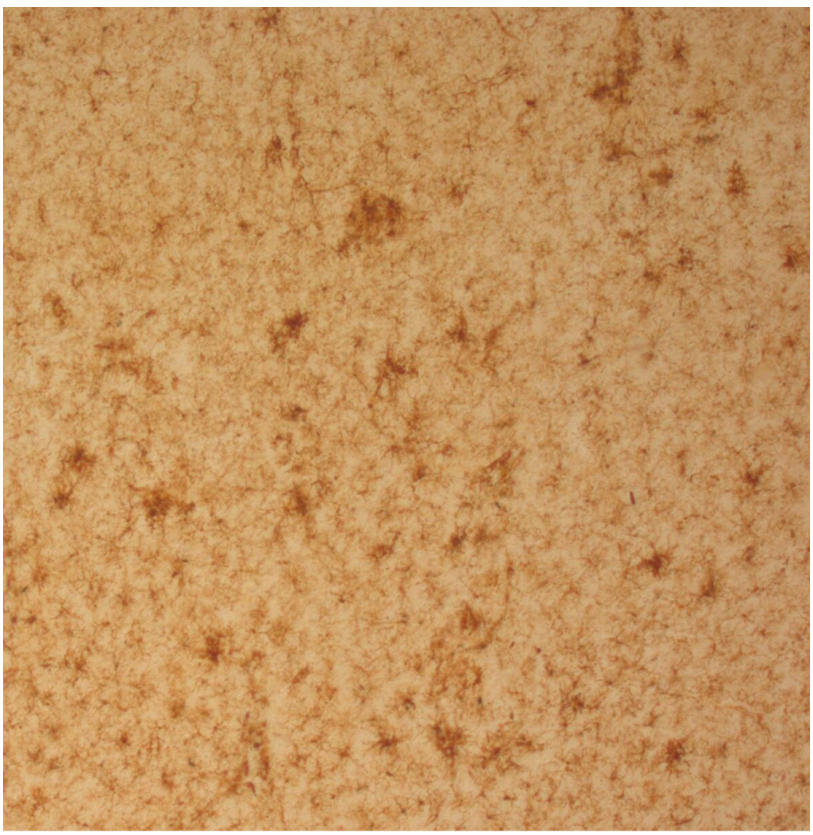

The micrograph illustrates neuroinflammation in Alzheimer's Disease, which presents as focal clusters of activated microglia. Microglia between clusters are non-activated and ramified. Human brain section stained with Iba1 antibody. The picture was taken by Jakob W. Streit, Department of Neuroscience, University of Florida.

Cover image: Kateryna Kon/Shutterstock.com

Aging is one of the major risk factors for the onset and progression of various neurodegenerative diseases. Neuroinflammation is a common feature of virtually every central nervous system disease, and is acknowledged as a likely mediator of cognitive impairments. Systemic inflammation levels are augmented with advanced age and neurodegeneration. The influence of age on neuroinflammatory responses including glial activation, increased production of proinflammatory cytokines, and aberrant neuronal signaling could magnify the deterioration of the central nervous

system microenvironment in disease, and may contribute to enhanced cognitive impairment. This eBook is a collection of highly informative original research articles, providing comprehensive aspect of neuroinflammation and possible therapeutic interventions in rescuing cognitive impairments.

Citation: Kumar, A., Ormerod, B. K., Dwivedi, Y., Streit, J. W., eds. (2019). Neuroinflammation and Cognition. Lausanne: Frontiers Media.
doi: 10.3389/978-2-88945-760-1

Table of Contents

frontiers in Aging Neuroscience

EDITORIAL
published: 11 December 2018
doi: 10.3389/fnagi.2018.00413

Editorial: Neuroinflammation and Cognition

*Ashok Kumar**

Department of Neuroscience, McKnight Brain Institute, University of Florida, Gainesville, FL, United States

Keywords: aging, inflammation, oxidative stress, cytokines, cognitive decline

Editorial on the Research Topic

Neuroinflammation and Cognition

Aging is a complex process, and one of the major risk factors for onset and progression of various neurodegenerative diseases. Increased human longevity has magnified the negative impact that aging can have on cognitive performance. The number of individuals 65 years or older will increase exponentially over the next several decades, and age-related cognitive impairment is expected to have a detrimental impact on individuals, their families, and society. An early sign of age-related cognitive decline in humans and rodent models is impaired executive function and spatial memory performance. Synaptic plasticity in the mammalian central nervous system has been the subject of intense investigation, and is regarded as a principal candidate for cellular mechanisms involved in learning and memory. Senescent physiology including altered synaptic plasticity and cell excitability contributes to the decline in cognitive function associated with aging and age associated neurodegenerative diseases. Neuroinflammation is a common feature of virtually every central nervous system disease, and is being increasingly recognized as a potential mediator of cognitive impairments. Systemic inflammation levels are increased with advanced age and neurodegeneration. The impact of age on neuroinflammatory responses including glial activation, increased production of proinflammatory cytokines, and aberrant neuronal signaling could magnify the deterioration of the central nervous system microenvironment in disease, and may contribute to accelerated cognitive impairment. However, a clear mechanistic understanding of these interactions is lacking. Given the high complexity of aging process and various mechanisms contributing to age-associated cognitive impairment, it is an arduous task to pinpoint on any single factor. This research topic in the *Frontiers in Aging Neuroscience* has produced a highly informative collection of original research articles (13), reviews (two), and a general commentary that cover comprehensive aspect of neuroinflammation and possible therapeutic interventions in rescuing cognitive impairments.

First, in their original research article, Ianov et al. provided detailed research findings related to gene expression profile in hippocampal sub regions and their association with aging and cognition.The authors employed two next-generation RNA sequencing platforms, Illumina, and Ion Proton, to examine gene expression differences related to brain aging and cognitive impairment in CA1, CA3, and dentate gyrus of the hippocampus. Their results demonstrate differences in gene expression in hippocampal sub regions and indicate regional differences in susceptibility to advanced age and cognitive performance.

OPEN ACCESS

Edited and reviewed by:
Panteleimon Giannakopoulos, Université de Genève, Switzerland

***Correspondence:**
Ashok Kumar
kash@ufl.edu

Received: *29 October 2018*
Accepted: *29 November 2018*
Published: *11 December 2018*

Citation:
Kumar A (2018) Editorial: Neuroinflammation and Cognition. Front. Aging Neurosci. 10:413. doi: 10.3389/fnagi.2018.00413

Rani et al. reported their exciting results in regards to miRNA in circulating microvesicles as being biomarkers for age-related cognitive deficit. The authors demonstrated that miRNA, from extracellular microvesicle enriched plasma samples, correlates with cognitive status in healthy elderly individuals. Bradburn et al. published their results in regards to elevated biomarkers of systemic inflammation and cognitive decline. The authors performed meta-analysis of prospective studies investigating the relationship between established markers of peripheral inflammation, the interleukin-6, with risk of cognitive impairment. Their results provide an evidence that individuals with high baseline interleukin-6 are more likely to develop cognitive decline. Rai et al. investigated the protective role of aqueous extract of Mucuna pruriens (Mp) against 1-methyl-4-phenyl-1,2,3,6-tetrahydropyridine (MPTP)-induced neuroinflammation and behavioral abnormalities, and delineated possible signaling pathways. The authors found that oral administration of MPTP in mice significantly and negatively influenced the behavioral performance and induced an increase in various inflammatory markers including glial fibrillary acidic protein, intercellular cell adhesion molecule, and tumor necrosis factor alpha in substantia nigra pars compacta. Treatment with Mp significantly reduced these inflammatory markers. The authors conclude that administration of Mp extract reversed MPTP-induced neuroinflammation and behavioral abnormalities by activating nuclear factor kB/pAKT signaling pathways. Nusrat et al. illustrated with their novel research on the role of acute and chronic cyclosporine A treatment on activation of endogenous neural precursor cells, neuroprotection, and tissue damage. The authors demonstrated that long-term treatment with cyclosporine A activated neural precursor cells, stimulated migration of neural precursor cells to the site of injury, and ameliorated cognitive recovery. Lee et al. in their original research investigated beneficial effects of Antler combined with Liuwei Dihuang pills (ALWPs) on cognition and lipopolysaccharide (LPS)-induced neuroinflammation. The authors found that oral administration of ALWPs rescued LPS-induced short and long-term memory impairment and attenuated microglial activation, possibly by modulating toll-like receptor/focal adhesion kinase/nuclear factor-kB signaling pathways. Hei et al. investigated the expression profile of growth factor neuregulin 1 (NRG1) and tyrosine kinase receptor ErbB4 in the CA1 region of the hippocampus following chronic cerebral hypoperfusion, and their possible relationship with neuronal degeneration and glial activation. The authors demonstrated that the expression of NRG1 and ErbB4/phospho ErbB4 peaked during acute phase and then decreased in the chronic phases of cerebral hypoperfusion. The expression of NRG1/ErbB4 in the CA1 region of the hippocampus was positively correlated with the degree of neuronal apoptosis, but not with glial activation. The study by Yang et al. investigated the influence of naringin dihydrochalcone on cognitive performance and the neuropathology of an Alzheimer's mouse model. Their results illustrate that oral administration of naringin dihydrochalcone ameliorated cognitive function, reduced amyloid plaque burden/Aβ levels, attenuated neuroinflammation, and augmented neurogenesis. The paper by Lin et al. provides evidence for a mediating role of systemic inflammation on the association between age and cognitive function. The study assessed serum concentrations of three inflammatory biomarkers, interleukin 6 (IL-6), tumor necrosis factor alpha, and C-reactive protein, as well as measured processing speed and short-term memory via performance-based tests in 47 young and 46 older generally healthy adults. A mediation analysis showed that the level of IL-6 partially accounted for differences in processing speed between young and older participants. IL-6 also mediated age-related impairment in processing speed within the older but not in the young participant group. The study observed no associations between any of the inflammatory biomarkers and short-term memory. Klein et al. in their innovative research investigated whether microglia in the middle-aged central nervous system responded differently to demyelination process. The authors reveal that in middle-aged animals, microglia, the resident immune cells of the central nervous system, are already altered, and react differently to demyelination. Cichoń et al. in their work evaluated the influence of extremely low-frequency electromagnetic field therapy on neuroplasticity in the rehabilitation of patients following moderate stroke. The authors report that electromagnetic field therapy significantly improved functional recovery in post-stroke patients by ameliorating neuroplasticity processes including upregulation of neurotrophic factors and plasma cytokines. In their original research article, Tiwari et al. explored for the first time the neuroprotective influence of withaferin A against amyloid beta pathology. The authors observed that amyloid beta significantly damaged the neuronal function and morphology, and withaferin A reduced the amyloid beta-induced neurotoxicity.

Rai et al. published their commentary on an article entitled "mild endoplasmic reticulum stress ameliorates LPS-induced neuroinflammation and cognitive impairment via regulation of microglial polarization" by Wang et al. (2017), suggesting that mild to moderate level of endoplasmic stress could provide an alternative therapeutic to delay neuroinflammatory-induced neurodegenerative diseases (Rai et al.).

In their review article, Musella et al. provided an overview of clinical and experimental studies emphasizing the various impacts of advanced age on motor disability and cognitive impairment in multiple sclerosis. The authors raised challenging questions on the putative age-related mechanisms including neuroinflammatory processes in contributing to the onset and progression of neurodegenerative processes related to multiple sclerosis. Sompol and Norris in their well-designed review article described age-associated alterations in Ca^{2+} regulation and the relation of these alterations to neurodegenerative diseases. The authors described that changes in Ca^{2+} regulation are usually attributed to neurons and are commonly discussed in the context of neuronal signaling pathways. However, astrocytes also exhibit striking aging and disease-related changes in Ca^{2+} regulation, especially in regions of marked pathology. The authors further report that the altered expression and activity of the Ca^{2+}-dependent protein phosphatase, calcineurin, in activated astrocytes is a function of age, injury, and disease. Calcineurin is found in a proteolized and highly activated state in astrocytes associated with amyloid deposits and damaged or

occluded cerebral blood vessels. Blockade of the calcineurin-dependent transcription factor, the nuclear factor of activated T cells-selectively activated astrocytes, improved synaptic function, reduced excitotoxic damage, and stabilized cognition in a variety of rodent models of injury and disease. Finally, the authors conclude that Ca^{2+} dysregulation in activated astrocytes results in neurologic dysfunction due to hyper activation of calcineurin.

Aging is characterized by a progressive increase in neuroinflammation, which contributes to cognitive impairment, associated with aging and age-related neurodegenerative diseases including Alzheimer's. However, mechanisms linking neuroinflammation and cognitive impairment are not yet clearly elucidated. Overall, this research topic attracted plenty of interesting original research articles as well as few reviews, and a general commentary, which brought comprehensive knowledge of age-related neuroinflammation and cognitive decline. This collection of remarkable articles delivered detail information on age-associated enhanced neuroinflammation and its influence on cognition. Finally, I hope that this research topic has provided understandings of therapeutic approaches for the treatment of aging-associated neuroinflammation-induced cognitive impairment.

AUTHOR CONTRIBUTIONS

The author confirms being the sole contributor of this work and has approved it for publication.

ACKNOWLEDGMENTS

I would like to thank Drs. Brandi K. Ormerod, Yogesh Dwivedi, and Jakob W. Streit who acted as co-editors on this research topic. Financial support by National Institutes of Aging Grant R01AG049711, R01AG052258, R01AG037984, and R37AG036800, and the Evelyn F. McKnight Brain Research Foundation is highly appreciated.

REFERENCES

Wang, Y. W., Zhou, Q., Zhang, X., Qian, Q. Q., Xu, J. W., Ni, P. F., et al. (2017). Mild endoplasmic reticulum stress ameliorates lipopolysaccharide-induced neuroinflammation and cognitive impairment via regulation of microglial polarization. *J. Neuroinflamm.* 14:233. doi: 10.1186/s12974-017-1002-7

Conflict of Interest Statement: The author declares that the research was conducted in the absence of any commercial or financial relationships that could be construed as a potential conflict of interest.

frontiers in Aging Neuroscience

REVIEW
published: 08 August 2018
doi: 10.3389/fnagi.2018.00238

Interplay Between Age and Neuroinflammation in Multiple Sclerosis: Effects on Motor and Cognitive Functions

Alessandra Musella[1,2], Antonietta Gentile[3,4], Francesca Romana Rizzo[3], Francesca De Vito[1,3], Diego Fresegna[1,3], Silvia Bullitta[1,3], Valentina Vanni[1,3], Livia Guadalupi[1], Mario Stampanoni Bassi[4], Fabio Buttari[4], Diego Centonze[3,4] and Georgia Mandolesi[1,2]*

[1]Laboratory of Synaptic Immunopathology, IRCCS San Raffaele Pisana, Rome, Italy, [2]San Raffaele University of Rome, Rome, Italy, [3]Laboratory of Synaptic Immunopathology, Department of Systems Medicine, University of Rome Tor Vergata, Rome, Italy, [4]Unit of Neurology, Istituto Neurologico Mediterraneo (IRCCS Neuromed), Pozzilli, Italy

Aging is one of the main risk factors for the development of many neurodegenerative diseases. Emerging evidence has acknowledged neuroinflammation as potential trigger of the functional changes occurring during normal and pathological aging. Two main determinants have been recognized to cogently contribute to neuroinflammation in the aging brain, i.e., the systemic chronic low-grade inflammation and the decline in the regulation of adaptive and innate immune systems (immunosenescence, ISC). The persistence of the inflammatory status in the brain in turn may cause synaptopathy and synaptic plasticity impairments that underlie both motor and cognitive dysfunctions. Interestingly, such inflammation-dependent synaptic dysfunctions have been recently involved in the pathophysiology of multiple sclerosis (MS). MS is an autoimmune neurodegenerative disease, typically affecting young adults that cause an early and progressive deterioration of both cognitive and motor functions. Of note, recent controlled studies have clearly shown that age at onset modifies prognosis and exerts a significant effect on presenting phenotype, suggesting that aging is a significant factor associated to the clinical course of MS. Moreover, some lines of evidence point to the different impact of age on motor disability and cognitive deficits, being the former most affected than the latter. The precise contribution of aging-related factors to MS neurological disability and the underlying molecular and cellular mechanisms are still unclear. In the present review article, we first emphasize the importance of the neuroinflammatory dependent mechanisms, such as synaptopathy and synaptic plasticity impairments, suggesting their potential exacerbation or acceleration with advancing age in the MS disease. Lastly, we provide an overview of clinical and

OPEN ACCESS

Edited by:
Brandi Ormerod, University of Florida, United States

Reviewed by:
Adelaide Fernandes, Faculdade de Farmácia, Universidade de Lisboa, Portugal
Daniel Ortuño-Sahagún, Universidad de Guadalajara, Mexico
Anna Maria Pittaluga, Università di Genova, Italy

***Correspondence:**
Diego Centonze
centonze@uniroma2.it

Received: *30 March 2018*
Accepted: *20 July 2018*
Published: *08 August 2018*

Citation:
Musella A, Gentile A, Rizzo FR, De Vito F, Fresegna D, Bullitta S, Vanni V, Guadalupi L, Stampanoni Bassi M, Buttari F, Centonze D and Mandolesi G (2018) Interplay Between Age and Neuroinflammation in Multiple Sclerosis: Effects on Motor and Cognitive Functions. Front. Aging Neurosci. 10:238. doi: 10.3389/fnagi.2018.00238

Abbreviations: AMPA, α-amino-3-hydroxy-5-methyl-4-isoxazole propionic acid; BDNF, brain derived neurotrophic factor; CI, cognitive impairment; CNS, central nervous system; CR, cognitive reserve; EAE, experimental autoimmune encephalomyelitis; GABA, γ-aminobutyric acid; IGF-1, insuline-like growth factor; IL-17, interleukin-17; IL-1β, Interleukin-1β; IL-6, Interleukin-6; ISC, immunosenescence; IFNγ, interferon-γ; LTD, long-term depression; LTP, long-term potentiation; MS, multiple sclerosis; NMDA, N-methyl-D-aspartate; PPMS, primary progressive MS; RNS, reactive nitrogen species; ROS, reactive oxygen species; RRMS, relapsing–remitting course; SNP, single nucleotide polymorphism; SPMS, secondary progressive MS; TMS, transcranial magnetic stimulation; TNF, tumor necrosis factor.

experimental studies highlighting the different impact of age on motor disability and cognitive decline in MS, raising challenging questions on the putative age-related mechanisms involved.

Keywords: aging, cognition, experimental autoimmune encephalomyelitis, multiple sclerosis, neurodegeneration, neuroinflammation, synaptic plasticity, synaptopathy

INTRODUCTION

Multiple sclerosis (MS) is an inflammatory neurodegenerative disease of the central nervous system (CNS), mainly affecting young adults. Its exact etiology remains unknown, but it is widely accepted that genetically susceptible individuals develop MS after exposure to undefined environmental triggers. MS is primarily characterized by a breakdown in immune tolerance to myelin and neuronal antigens and by a dysfunction of the blood brain barrier (Gourraud et al., 2012; Beecham et al., 2013; Olsson et al., 2017). Typically, infiltrating myelin-reactive lymphocytes (mainly T-cells but also B-cells) attack myelin sheaths and axon antigens on oligodendrocytes and neurons in the CNS. This event causes an inflammatory cascade, formation of large demyelinating plaques in the white matter and gliosis, neuroaxonal degeneration and synaptopathy, leading to an impairment of the neuronal signaling and, later on, to neurodegeneration (Compston and Coles, 2008; Dendrou et al., 2015; Mandolesi et al., 2015). Clinical manifestations include motor impairments, sensory and visual disturbances, fatigue, pain, mood disturbances and cognitive deficits, in relation to the spatiotemporal dissemination of pathological lesion sites in the CNS (Dendrou et al., 2015). Most of MS patients start with a relapsing remitting phase (RRMS), which later develops into a secondary progressive phase (SPMS). In primary progressive MS (PPMS) patients, the relapsing stage is absent and the disease starts already with a progressive loss of neurological functions (Compston and Coles, 2008; Disanto et al., 2010; Lassmann et al., 2012). Innate reparative processes can occur through remyelinating and neuronal repairing processes, which are highly variable among patients (Stangel, 2008; Bramow et al., 2010).

An important feature of adult MS is chronological age, consisting in a defined age interval between the mid-twenties and late-thirties for disease onset and a time limit, after the fifth decade, when the disorder is rarely diagnosed (Polliack et al., 2001; Sanai et al., 2016). Mounting evidence suggests that prognosis of MS appears to be, at least to some extent, dependent of age and not markedly influenced by the initial, exacerbating-remitting or progressive disease course (Confavreux and Vukusic, 2006; Scalfari et al., 2011; Cossburn et al., 2012; Sanai et al., 2016; Roy et al., 2017; Ruano et al., 2017). Many age-related changes affecting the brain could collectively affect neuronal viability and vulnerability in MS: increased iron accumulation, oxidative stress followed by mitochondrial injury, decrease of trophic support from the peri-plaque environment, decline of remyelination, chronic, systemic low grade inflammation as well as a broad increase in the production of inflammatory molecules such as pro-inflammatory cytokines ("inflammaging"; Pizza et al., 2011; Dorszewska, 2013; Dendrou et al., 2015; Di Benedetto et al., 2017; Bolton and Smith, 2018). Although further efforts are necessary to better clarify this aspect, the present review highlights common inflammatory processes occurring in both aging and MS brain that might be critical for understanding why age is an important risk factor for MS disability (motor and cognitive) and progression.

IMMUNE SYSTEM DYSREGULATION IN MS: THE IMPACT OF AGING

Key age-associated changes in the CNS are triggered by microglia, their impaired regulation (low-grade inflammation and inflammaging) and the inflammatory and oxidative stressful environment they build up. Immune challenges, such as infections, surgery, or traumatic brain injuries, result in greater susceptibility to memory impairments and altered synaptic plasticity during aging (Ojo et al., 2015; Cornejo and von Bernhardi, 2016; Matt and Johnson, 2016; Bettio et al., 2017; Di Benedetto et al., 2017). On the other hand, advanced age is associated with a phenomenon called immunosenescence (ISC) which refers to a weakening in integrity and efficiency of the adaptive and innate immune systems (Walford, 1969; Denkinger et al., 2015; Di Benedetto et al., 2017).

In past years, researchers have spent much effort to understand the impact of aging and ISC on adaptive immunity in MS and in its rodent model, experimental autoimmune encephalomyelitis (EAE). From these studies, which were primarily focused on the analysis of biomarkers of ISC at peripheral level (Bolton and Smith, 2018), emerged that a premature ISC might operate during the course of MS and of EAE (Bolton and Smith, 2018). The effects of a prematurely aged immune system and ISC on MS and EAE are still unknown, but emerging data justifies and encourages further investigation. ISC typically affects both adaptive and innate immune systems. The most relevant changes in the adaptive immunity are decreased peripheral naïve T cells and concomitant accumulation of late-stage differentiated memory T cells, with reduced antigen receptor repertoire diversity. This phenomenon results from age-related impairments in the hematopoietic stem cell compartment (which generates few T-cell precursors), and from thymic involution. An increase of circulating cytokines facilitates a systemic and chronic, low-grade, inflammatory state which is typical of aging (termed "inflammaging"). This systemic inflammation may promote neuroinflammation by modulating glial cells, leading to an increased risk for developing neurodegeneration and cognitive impairment (CIs) in healthy individuals (Pizza et al., 2011; von Bernhardi et al., 2015; Di Benedetto et al., 2017). In MS patients, the additional inflammation carried by peripheral immune cell infiltration and by CNS-resident immune cell activation may significantly

accelerate the inexorable aging processes in the CNS, and as the resulting stress response is excessive for homeostasis to be properly preserved (Dendrou et al., 2015), prominent neurodegenerative processes progressively follow (**Figure 1**).

Accumulating evidence suggests that an exacerbation of common neuropathological aspects of MS and of aging brain, such as synaptic dysfunction and loss (synaptopathy) and synaptic plasticity impairment (Di Filippo et al., 2008; Weiss et al., 2014; Mandolesi et al., 2015; Stampanoni Bassi et al., 2017), might contribute to explain why aging may impact on MS disability.

INFLAMMATORY SYNAPTOPATHY AND SYNAPTIC PLASTICITY IN MS/EAE AND IN AGING BRAIN

Synaptopathy

Synaptophaty refers to a progressive dysfunction and loss of the synaptic compartment of the CNS that is emerging as a pathophysiological feature of MS disease and of its mouse model EAE (Mandolesi et al., 2015; Henstridge et al., 2016). Along with demyelination and axonal damage, synaptopathy contributes to the neurodegenerative decline of the CNS starting since the early phase of the disease. In MS and EAE, neuroinflammation is responsible for an imbalance between the glutamatergic and GABAergic systems in the brain and spinal cord. During acute inflammatory attacks in MS and EAE, pro-inflammatory cytokines (such as tumor necrosis factor (TNF); interleukin-1β (IL-1β)), released from activated microglia and astroglia as well as from infiltrating lymphocytes, trigger a progressive increase of the glutamatergic transmission and an impairment of the GABAergic synaptic response, leading to uncontrolled excitability and possibly to neurodegeneration (Centonze et al., 2009; Rossi et al., 2011, 2012, 2014; Mandolesi et al., 2012, 2013, 2017a; Nisticò et al., 2013; Mori et al., 2014a). Synaptopathy has long-lasting effects (such as excitotoxic damage) that can give rise to motor and CIs. It is remarkable that traits of neuroinflammatory synaptopathy are evident also in normal aging brains (Viviani and Boraso, 2011; Barrientos et al., 2015; Bettio et al., 2017), strongly suggesting an exacerbation with age of pathological events occurring in MS (**Figure 1**). It has been indeed suggested that during aging, peripheral ISC and inflammaging may favor the activation of microglia cells, leading to loss of their neuroprotective functions, to neuronal dysfunctions and tissue damage (Henry et al., 2009; Norden and Godbout, 2013; Matt and Johnson, 2016). The over-production of pro-inflammatory mediators, such as IL-1β, interleukin-6 (IL-6) and TNF, disrupts the delicate balance needed for synaptic homeostasis by modulating ion channels and glutamate receptors (Viviani and Boraso, 2011). In particular, data mainly obtained in animal models suggest that IL-1β and TNF exacerbate or favor excitotoxicity by modulating the N-methyl-D-aspartate (NMDA) and α-amino-3-hydroxy-5-methyl-4-isoxazole propionic acid (AMPA) receptors in the aging brain, mimicking the alterations occurring in MS and EAE brains (Jasek and Griffith, 1998; Viviani et al., 2003, 2006; Stellwagen et al., 2005; Centonze et al., 2009; Viviani and Boraso, 2011; Grasselli et al., 2013). Inflammatory dependent glutamate excitotoxicity and reduced production of neurotrophic factors (brain derived neurotrophic factor, BDNF; insuline-like growth factor, IGF-1) may impact neuronal functions (**Figure 1**) in aging brain (von Bernhardi et al., 2010; Dorszewska, 2013; Di Benedetto et al., 2017).

Synaptic Plasticity

Compelling evidence suggests that during aging, neuroinflammation may contribute to impaired long-term potentiation (LTP), which has been classically regarded, together with long-term depression (LTD), as the substrate for learning and memory processes (Viviani and Boraso, 2011; Barrientos et al., 2015; Di Benedetto et al., 2017).

The aged brain seems to be remarkably sensitive to an immune challenge in the periphery due to an unusual hyperactivation of microglia cells that, in cooperation with impairments in key regulatory systems, causes a long lasting neuroinflammatory state and age-related neurobehavioral complications (Norden et al., 2015; Di Benedetto et al., 2017). Age-related cognitive decline following an immune challenge likely depends on an exaggerated inflammatory response. In particular it has been shown in rodents that the pro-inflammatory cytokines IL-1β can impair synaptic plasticity through activation of MAP-kinases JNK and p38 and/or inhibition of BDNF and Arc, essential mediators of hippocampal-dependent memory processes (Barrientos et al., 2015; Lynch, 2015). Furthermore, pro-inflammatory cytokines contribute to negatively influence hippocampal neurogenesis with detrimental consequences for synaptic plasticity phenomena. Therefore, by impairing microglial priming or blocking the excessive brain cytokine response (pharmacologically or through diet and voluntary exercise) it may be possible to effectively attenuate the harmful effects of an immune insult on memory processes, supporting the view that pro-inflammatory cytokines play a pivotal and direct role in inducing long-term memory and cognitive deficits in older individuals (Di Benedetto et al., 2017).

In both MS and EAE, recent studies have shown that inflammatory cytokines are involved in synaptic plasticity alterations. Hippocampal LTP deficits have been detected in EAE mice during the acute phase of the disease, in association with an increased microglial activation, elevated levels of IL-1β, and a selective reduction of NMDA receptors (Di Filippo et al., 2015; Mancini et al., 2017). In MS patients, studies based on transcranial magnetic stimulation (TMS), a non-invasive technique commonly used to detect motor cortex plasticity in humans (Lefaucheur, 2005; Rossini and Rossi, 2007; Ziemann et al., 2008), have shown that synaptic plasticity phenomena are impaired in the progressive forms of the disease, usually diagnosed in people in their 40s (Mori et al., 2013; Stampanoni Bassi et al., 2017). In these patients, that are proned to adaptive immune cell exhaustion form prolonged antigenic exposure, a chronic CNS-intrinsic inflammation and neurodegeneration are prominent, suggesting a concomitant occurrence of cerebral aging and the accumulation of structural brain deterioration

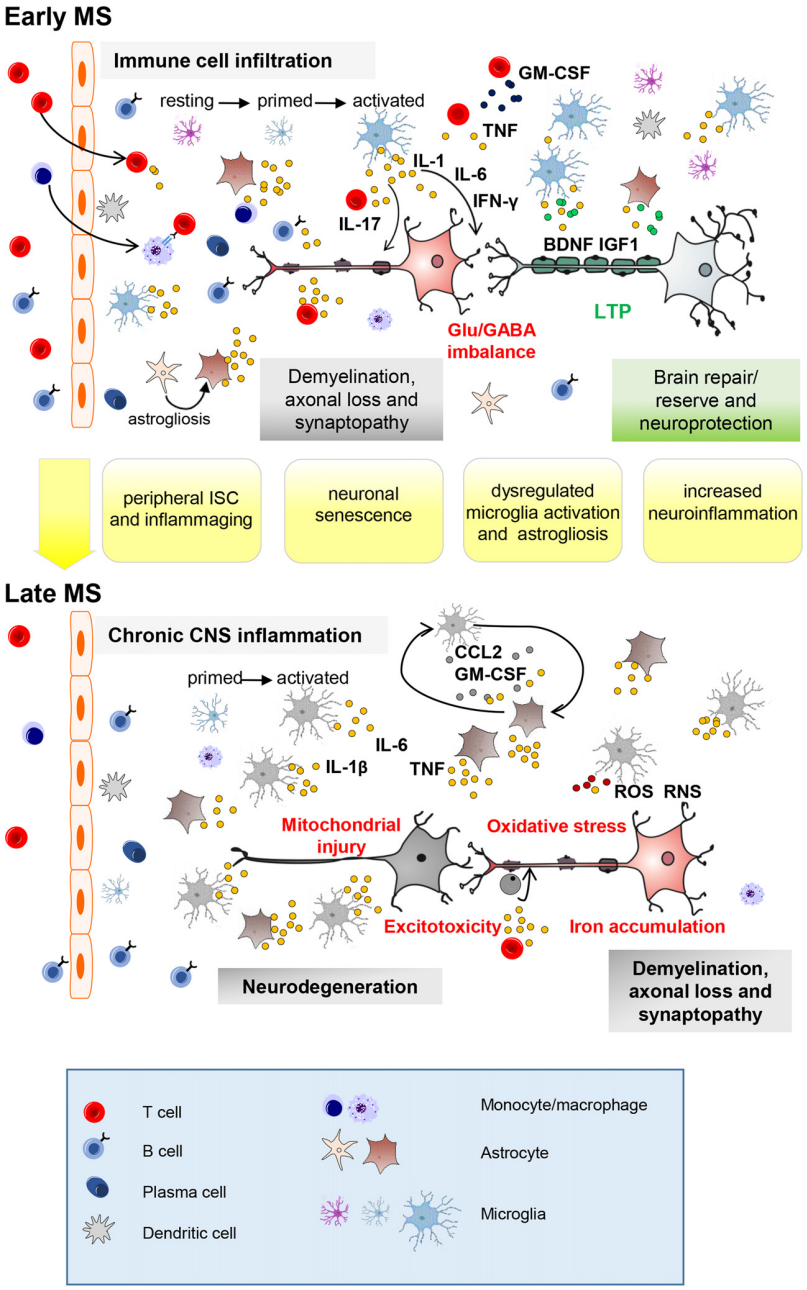

FIGURE 1 | Key neuroinflammatory processes occurring in the central nervous system (CNS) of multiple sclerosis (MS) patients influenced by aging. Immune cell infiltration from the periphery, mainly through the blood–brain barrier, is a prominent feature of early-stage MS (top panel). Peripheral innate and adaptive immune cells, along with activated CNS-resident microglia and astrocytes, promote demyelination, axonal injury and synaptopathy mainly through action of soluble inflammatory (IL-1β, Interleukin-1β; TNF, tumor necrosis factor; IFN-γ, interferon-γ; IL-17, interleukin-17) and neurotoxic mediators. Neuronal damage can be completely or partly resolved due to remyelination, resolution of inflammation and neuroprotective/reparative mechanisms (growth factors). Furthermore, additional mechanisms, from local synaptic plasticity to brain rewiring, intervene to functionally compensate synaptic loss (long-term potentiation, LTP). With advancing years, premature aging processes such as peripheral immunosenescence (ISC) and inflammaging may lead to age-related changes in the blood. Neuronal senescence and unusual microglia (primed) activation as well as astrogliosis (IL-1β; IL-6; TNF; granulocyte–macrophage colony-stimulating factor, GM-CSF; CC-chemokine ligand 2, CCL2) might contribute at exacerbating MS neuroinflammatory processes (synaptopathy, impaired synaptic plasticity, reduced production of brain derived neurotrophic factor (BDNF) and insuline-like growth factor (IGF-1)). Later on (bottom panel), immune cell infiltration wanes, perhaps due to adaptive immune cell exhaustion from chronic antigen exposure. However, chronic CNS-intrinsic inflammation, and other processes influenced by age (such as oxidative stress, mitochondrial injury, iron accumulation and excitotoxicity) might contribute at exacerbating early pathological processes leading to neurodegeneration. Further microglial recruitment and activation might be induced by interaction with astrocytes releasing CCL2 and GM-CSF as occur during aging. Astrocytes can prevent remyelination at sites of neuroaxonal injury by inhibiting progenitor cells from developing into mature oligodendrocyte cells (ODCs). RNS, reactive nitrogen species; ROS, reactive oxygen species.

(**Figure 1**). However, a second relevant aspect should be taken in consideration in MS patients. As in other pathological conditions, it is increasingly emerging that synaptic plasticity phenomena, besides having a physiological role in learning and memory processes, drive also important neuroreparative mechanisms (Malenka and Bear, 2004; Pelletier et al., 2009). During MS disease, in the event of an immunological attack, brain damage is eluded by mechanisms of neuroprotection and neurorepair (Weiss et al., 2014; Di Filippo et al., 2015). When these mechanisms eventually fail, an irreversible damage occurs with consequent neuronal denervation. It has been proposed that additional mechanisms, collectively known as brain plasticity, intervene to functionally compensate the deficit of synaptic inputs. The more appropriate synaptic mechanisms underlying brain plasticity and that depend also on the inflammatory milieu are LTP and LTD. In particular, LTP seems to be able to compensate neuronal damage bringing back excitability in synaptic injured neurons. Interestingly, it has been proposed that LTP enhancement might be secondary to alterations of the glutamatergic and GABAergic balance induced by the inflammatory milieu, suggesting that CNS inflammation in MS patients is able to subvert plasticity (Mori et al., 2011, 2012, 2014a; Weiss et al., 2014; Stampanoni Bassi et al., 2017). Furthermore, taking advantage of non-invasive TMS studies, specific brain plasticity alterations have been associated with different disease phenotypes (RR-MS; PP-MS), or phases (remitting, relapsing), indicating that plastic phenomena can modulate disability progression and the clinical manifestation of the disease (Weiss et al., 2014; Stampanoni Bassi et al., 2017).

AGE IS A RISK FACTOR FOR MS: MOTOR DISABILITY, COGNITIVE DECLINE AND PSYCHIATRIC SYMPTOMS

Motor Disability

Evidence exists that increasing age is a significant factor influencing the clinical course of MS. Indeed, age at onset modifies prognosis and exerts a significant effect on the presenting phenotype of this disease (Confavreux and Vukusic, 2006; Tremlett et al., 2006; Scalfari et al., 2011; Tedeholm et al., 2015). Clinical studies reported that a younger onset age was strongly associated with a slower rate of disability accumulation. As shown in an observational study on 1844 patients, aging negatively affects the prognosis in MS, independently of the type of the initial course of the disease, be it exacerbating-remitting or progressive (Confavreux and Vukusic, 2006). Clinical data from the London Ontario database highlight that onset age of patients with the relapsing form of MS strongly influences the time to conversion to secondary progression; compared to age 20, onset at age 40 and at age 50 doubled and tripled risks of developing SP respectively, compared to age 20 (Scalfari et al., 2011). A clinical study on 500 MS patients, grouped by cutoff in onset age, demonstrated that the severity of disabilities was increased during and after an age band of 30 years–35 years (Ramachandran et al., 2014). In agreement, it has been reported that a younger age (20 years–35 years) is correlated with a longer time to reach disability milestone compared with older patients (36 years–65 years; Trojano et al., 2002), confirming that age at onset predicts the disease course. All together these results are in agreement with previous evidence that neurological relapses have only a limited influence on the risk of entering secondary progressive phase and on the latency of entering progression (Confavreux et al., 2000; Scalfari et al., 2010, 2013).

Furthermore, age at onset strongly predicts the probability of a patient to evolve in a primary progressive form of the disease. Kis et al. (2008) reported that the majority (83%) of MS patients with late-onset MS had a primary progressive disease course, whereas the young-onset MS group (94%) developed a relapsing-remitting form. Accordingly, motor deficits were significantly more frequent in the late-onset MS than in patients with young-onset MS (90% vs. 67%; Kis et al., 2008). Similar results were obtained in a previous study on 957 patients with MS, since age at onset predicted the likelihood of developing a primary progressive form and, for RRMS patients, strongly determined the time to conversion to secondary progression (Stankoff et al., 2007).

The impact of aging on brain pathology was also supported by the observation that median age at the time of assigned disability is substantially similar between patients with different clinical course or symptomatology. Among primary progressive and RR-SP patients, median ages at reaching a given disability score were strikingly similar (Scalfari et al., 2011), suggesting that age at onset has a strong impact on the neurodegenerative component of MS.

Cognitive Impairment

Together with motor disability, CI is frequently observed in MS patients (with an occurrence estimates between 40% and 65% of MS patients) and tends to progress over time. CI is present since the clinical onset of MS, more frequently in progressive patients compared to RRMS patients (Huijbregts et al., 2004; Ruet et al., 2013; Planche et al., 2016; Matias-Guiu et al., 2017), although heterogeneous results have been reported (Rao, 1991; Potagas et al., 2008).

In a 10-year longitudinal study, Amato et al. (2001) comparing cognitive capacities of 50 MS patients, found that cognitive dysfunction progressed as MS advances and that neurological and cognitive involvement tended to converge during the follow-up. The percentage of cognitive preserved patients decreased from 74% to 51% during 4 years of follow-up, and to 44% after 10-year assessment. In parallel, at the end of the study about 56% MS patients showed mild and moderate CI (Amato et al., 2001).

The relationship between CI, physical disability and age was further investigated in a larger study that compared prevalence and profile of cognitive deficit across 1040 patients with different clinical phenotypes (Ruano et al., 2017), including 167 clinically isolated syndrome, 759 RR, 74 SPMS and 40 PPMS patients. The multivariable analysis showed that higher disability (evaluated by EDSS) and older patient age, rather than clinical subtype and disease duration were the main determinant of CI. Furthermore, the study supported the evidence that the frequency of CI is

increased in the progressive forms of the disease. Indeed, SP and PP patients showed approximately two-fold higher prevalence of CI when compared with RR and CIS patients.

The significant correlation with CI and age was reported also in two different Cross-Sectional studies. In the first study, 245 MS patients and 188 healthy control were evaluated using two measures of processing speed (the preliminary word reading and color naming trials of the Stroop) and the analysis were performed grouping participants into five age cohorts (Bodling et al., 2009).

In the second one, regression analyses were performed between age and several cognitive parameters (six outcomes T25FW, 9HPT, PASAT, SDMT, CVLT-II Learning and BVMT-R Learning) in 698 MS patients and 226 healthy subjects (Roy et al., 2017). Surprisingly in both clinical studies, although older MS patients were at higher risk of motor and cognitive disability, as expected, the interaction between MS and healthy control on cognitive test during lifespan was not significantly different, suggesting that age effects on CI are similar across healthy control and MS patients. Despite further longitudinal studies should be performed to determine and clarify the impact of aging on MS cognitive decline, these preliminary studies leave open interesting questions as discussed in the next paragraphs.

Psychiatric Symptoms

Recent studies have clearly demonstrated that also psychiatric affections are strongly associated with MS pathology. Depression and anxiety are known to be more prevalent among people with MS compared with the general population and individuals with other neurologic conditions (Boeschoten et al., 2017). Recently, several clinical (Imitola et al., 2005; Rossi et al., 2017) and preclinical studies (Haji et al., 2012; Gentile et al., 2016; Mandolesi et al., 2017b) have provided evidence that mood disturbances occur early in MS disease and its mouse model EAE and correlate with peripheral and central inflammation, independently of motor disability. Concerning the correlation between these psychological conditions and aging in MS, conflicting data are emerging. Several cross-sectional studies suggest that younger adults with MS are associated with greater risk for depressive symptoms respect to older patients (Patten et al., 2000, 2003; Chwastiak et al., 2002; Williams et al., 2005; Phillips and Stuifbergen, 2008). Accordingly, Kneebone et al. (2003) observed that older patients (70.6 $\pm$ 4.51 years) with MS were less affected by depressive symptoms with respect to younger patients (46.4 $\pm$ 8.35 years). Moreover, a significant correlation was found between the younger age at onset and the presence of depression in MS patients (Beiske et al., 2008). Interestingly, Williams et al. (2005) showed that a shorter duration of MS was associated with greater risk for depression. In contrast to these studies, da Silva et al. (2011) found that age was positively associated with depression in MS patients and Mattioli et al. (2011) reported that depressed MS patients were older than those not depressed (43.45 $\pm$ 12.15 years vs. 39.96 $\pm$ 10.88 years, $p = 0.02$). Finally, several cross-sectional studies on MS patients failed to replicate a relationship between depression and age (Galeazzi et al., 2005; Tsivgoulis et al., 2007; Bamer et al., 2008; Buchanan et al., 2009).

In conclusion, it is still not clear if aging may have an impact on MS psychiatric symptoms and further cross-sectional and longitudinal studies are needed to better investigate this challenging aspect, considering that a complex interplay of variables influences this form of comorbidity in MS (Boeschoten et al., 2017).

Collectively, these data support the hypothesis that in MS the shift from a predominantly inflammatory phase, dominated by clinical relapses, to a predominantly neurodegenerative phase, dominated by irreversible progression of neurological disability (motor and cognitive), may be mainly driven by biological factors related to aging (Lassmann et al., 2012; Friese et al., 2014; Mahad et al., 2015; Ruano et al., 2017; Zeydan and Kantarci, 2018).

AGING REDUCES THE ABILITY TO RECOVER AFTER A RELAPSE BY AFFECTING BRAIN PLASTICITY

Several results concur with the hypothesis that the capacity of the brain to manage MS pathology depends on the ability to recover after a relapse. Of note, the ability to recover was strongly correlated to reserve of brain plasticity, which are diminished in older patients. A poor recovery of early relapses is indeed associated with an earlier progression of the pathology (Kalincik et al., 2014; Novotna et al., 2015). On the other hand, relapses with a higher impact and poorer recovery in MS patients were positively correlated with age (Kalincik et al., 2014) as well as a reduced ability to recover from initial relapse significantly declined with age (Cossburn et al., 2012). Aging has been indeed related to a decreased capability of functional reorganization and plasticity in MS, likely due to an interaction between cerebral aging and the accumulation of structural brain damage (Schoonheim et al., 2010).

It is now well recognized that MS-associated pathological processes progressively modify brain networks essential for functional domains such as sensorimotor function (Rocca et al., 2005; Tomassini et al., 2012), vision (Jenkins et al., 2010) and cognition (Rocca et al., 2015), by activating adaptive or maladaptive mechanisms. A form of adaptive plasticity can be considered the functional reorganization observed in the brain of MS patients in association to the easily performance of simple tasks; by means of this compensatory mechanism, more complex brain systems are recruited relatively to normal subjects (Pelletier et al., 2009). On the other hand, forms of maladaptive plasticity might also occur, causing functional changes directly linked to disability (Reddy et al., 2002). Functional MRI has contributed notably to improve our understanding of the mechanisms associated with preserved function in MS (Mainero et al., 2006; Filippi and Rocca, 2009; Rocca et al., 2010b, 2005; Enzinger et al., 2016). Thanks to these studies, it has been proposed that (Filippi and Rocca, 2009; Rocca et al., 2015) an increased involvement of the cortical networks might help at containing the functional impact of MS-related damage (Rocca et al., 2002a) and that changes in the organization of cortical areas involved in motor or cognitive tasks at different stages of the disease (Reddy et al., 2000a,b, 2002; Filippi et al., 2002a,b; Pantano et al., 2002;

Rocca et al., 2002a,b, 2003a,b; Enzinger et al., 2016), might in part explain the discrepancy between brain injury and clinical disability. The progressive weakeaning of patterns of activation might account for progressive disability or CI in symptomatic MS patients, when compared to controls (Rocca et al., 2002b, 2010a; Ciccarelli et al., 2006) or asymptomatic MS patients (Penner et al., 2003; Mainero et al., 2006; Rocca et al., 2010a).

A deeper understanding of causal and functional relationships were achieved by neurophysiological techniques, predominantly by TMS (Zeller and Classen, 2014). Notably, accumulating evidence obtained through this technique have highlighted the ability of the brain to express LTP-like changes as a determinant factor to counteract disability progression in MS (Weiss et al., 2014; Stampanoni Bassi et al., 2017). Recently, it has been shown that a predictor of disease recovery from relapses is LTP induced by paired associative stimulation (Mori et al., 2014b). Furthermore, it has been observed that LTP induction in the primary motor cortex of patients in the early relapsing-remitting phases of the disease is possible and even enhanced. Conversely, LTP is absent in patients with a progressive form of MS (Mori et al., 2013; Weiss et al., 2014). Thus, it is conceivable that the capability of brain networks to adjust themselves in a plastic manner, allows a patient to accomplish with the focal and diffuse brain damage associated with the disease in the first years after MS onset. On the contrary, the disease likely enters in its more disabling progressive phase when the plastic reserve is exhausted. Accordingly, a study conducted on a cohort of RRMS patients with CI and on a group of cognitively preserved RRMS patients (Mori et al., 2011) revealed that LTP response was present only in the cognitively preserved group. Synaptic plasticity induction by PAS was also explored in RRMS and SPMS patients with stable clinical conditions in the last 3 months (Zeller et al., 2010), resulting in a comparable LTP amplitude between patients and gender, age-matched healthy controls. These observations suggest that alterations of synaptic plasticity emerge at the time of a relapse, as explored by other groups using paired associative stimulation (Mori et al., 2014b) or intermittent-theta burst stimulation (Mori et al., 2011).

Of note, LTP responses are variable among individuals and tend to decline with aging (Müller-Dahlhaus et al., 2008; Freitas et al., 2011). Accordingly, MS patients in their forties suffer from progressive forms during which LTP seems to be impaired. Current hypothesis to explain this inter-individual variability points to a combination of disease, age and likely genetic background (Pascual-Leone et al., 2011; Rossi et al., 2013) but further studies are necessary to clarify how population-level variability in LTP induction is related to MS disease phenotype and expression.

DOES AGING DIFFERENTIALLY AFFECT MOTOR AND COGNITIVE FUNCTION IN MS PATIENTS?

We have summarized several data concurring with the hypothesis that the interaction between cerebral aging and overload of structural brain injury decreases plasticity and capability of functional reorganization in MS (**Figure 1**). However, unexpectedly, recent studies suggest that aging processes differentially affect motor and cognitive performances in patients with MS (Bodling et al., 2009; Roy et al., 2017). It seems that older MS patients are more susceptible to motor disability, and less to cognitive dysfunction. Although longitudinal studies, which should include both healthy controls and different MS subgroups, are demanded to better clarify this aspect, some speculations on this topic might be raised. Among different hypotheses, it has been suggested that in older MS patients, shorter axonal fibers are more prone to resilience and compensation than single long fibers that intervene in motor function. It might be also possible that a prominent and progressive damage of the spinal cord would also have a greater consequence on motor function over time. Furthermore, it is possible that a considerable effect on cognitive rather than motor abilities is played by the influence of cognitive reserve (CR) and personality traits (Sumowski et al., 2013; Roy et al., 2016). CR is indeed emerging as a second mechanism that might contribute at limiting cognitive deficits in MS patients (Rocca et al., 2018). Of note, the theory of CR emerged from aging and dementia studies to justify the inter-individual differences in the ability of managing with brain damage and the consequent cognitive deficits by means of pre-existing compensatory mechanisms (Stern, 2002). According to the CR theory, recent studies showed that intellectual enrichment (such as educational level, vocabulary knowledge, employment status), protects MS patients against the negative effect of disease-related damage on cognitive performance (Sumowski et al., 2009; Benedict et al., 2010; Ghaffar et al., 2012; Amato et al., 2013; Pinter et al., 2014; Rocca et al., 2018). In particular, it has been suggested that CR may have a protective role in preserving cognitive functions, mitigating the effect of structural damage on cognitive performance. However, in recent 2-years MS longitudinal study emerged that the CR protective role may diminish with disease progression.

Notably, it should be also taken in consideration that brain compensatory and adaptive mechanisms might depend on a genetic background. In this regard, recent evidence suggests that genetic determinants influence inter-individual differences in both MS severity and synaptic excitability (Rossi et al., 2013). In particular, four single nucleotide polymorphism (SNPs: rs4880213, rs6293, rs1805247, rs7301328) of the NMDAR genes were evaluated to search for associations with both synaptic excitability and disease outcome in RRMS and PPMS patients, considering that LTP is dependent on the synaptic activation of the glutamate NMDA receptor. This study showed that the specific T allele of the rs4880213 SNP of the NR1 subunit was correlated to an increase of neuronal excitability measured by means of paired TMS protocol. Furthermore, the same SNP was associated with better compensation of brain damage in RR-MS but with higher severity of PP-MS. Accordingly, these results supported the idea that potentiation of glutamatergic NMDAR-dependent synaptic transmission has a role in both adaptive plasticity and excitoxicity in MS patients. More interestingly, enhanced NMDAR function was found to preserve cognitive abilities in that cohort of patients, thus confirming the role played by NMDARs and NMDAR-dependent synaptic plasticity during

learning and memory processes (Collingridge and Bliss, 1995; Nicoll and Malenka, 1999; Bennett, 2000; Cooke and Bliss, 2005, 2006). Notably, both RR-MS and PP-MS carrying the T allele of rs4880213 SNP showed a better performance at the Paced Auditory Serial Addition Test and the Symbol Digit Modalities Test, indicating residual NMDAR-dependent plasticity also in PP-MS. The above mentioned clinical tests explore cognitive domains frequently altered in MS, and impaired NMDAR-dependent synaptic plasticity in MS patients has been associated with poor performances at both tests (Mori et al., 2011). This evidence supports the idea that genetic determinants (SNPs) in combination with age and disease, might explain inter-individual variability of LTP responses (Pascual-Leone et al., 2011).

Although both genetic variability and CR could in part contribute to explain a potential less impact of age on cognitive decline, collectively these data clearly indicate that compensatory mechanisms of the brain can be potentially activated and responsive to therapeutic interventions even in PPMS patients (Feinstein et al., 2015). In this regard, despite some controversial results, it seems that increased physical activity is promising for cognitive benefits in MS (Dalgas and Stenager, 2012; Motl and Pilutti, 2012; Beier et al., 2014; Briken et al., 2014; Sandroff et al., 2014, 2016a; Motl et al., 2017). Indeed, in a randomized controlled trial of 42 patients with progressive MS (31 SPMS and 11 PPMS) with moderate physical disability (EDSS score 4–6), patients committed to several forms of exercise, rather than a wait list group, showed a significant amelioration in aerobic fitness and several secondary outcome measures, including cognitive performance (Briken et al., 2014). This study highlighted for the first time that physical activity specifically target cognition in patients with progressive MS but further studies are needed to identify the best type of exercise for cognitive recovery (Sandroff et al., 2016b; Motl et al., 2017; Ontaneda et al., 2017). Of note, in the aging context, it is emerging that exercise, as well as pharmacological treatments, may effectively block the detrimental effects of an immune challenge by preventing microglial priming or blocking the overstated brain cytokine response. This evidence not only suggests that these interventions may be useful therapeutic treatments, but also supports the view that a dysregulation of the fine interplay between the immune and nervous systems can have profound impacts on long-term plasticity and cognitive function in older individuals, as occurs in MS (Di Benedetto et al., 2017).

CONCLUSION

MS patients are indubitably exposed to the biological consequences of age, but the precise contribution of aging-related factors to MS neurological disability and the underlying molecular and cellular mechanisms are still unclear. Recent experimental and clinical investigations in the field of both aging and MS have shed a light onto common neuroinflammatory pathological mechanisms that are likely prematurely activated or exacerbated in MS patients, influencing the expression of the MS

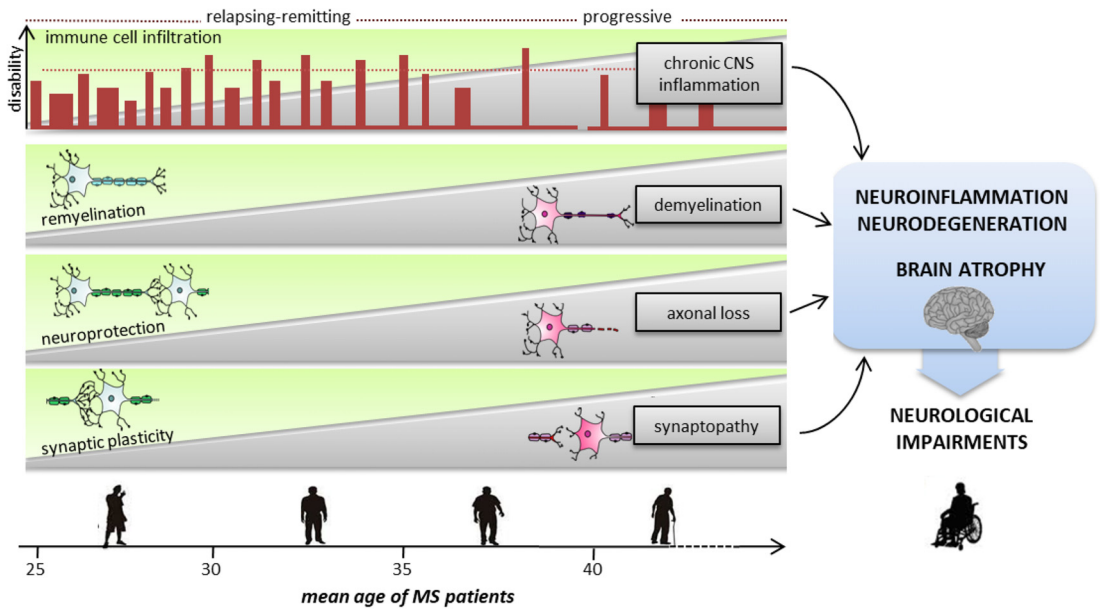

FIGURE 2 | Sequence of pathological and reparative events occurring during MS disease course, leading to severe neurological impairments. With advancing aging, neurodegenerative and neuroinflammatory processes are exacerbated causing severe cognitive and motor deficits. Inflammation is present at all stages of the disease, starting from an early phase dominated by peripheral immune cells invasion into the CNS to a progressive and chronic CNS inflammation. Since the early phase of the relapsing/remitting forms demyelination, synaptopathy and axonal damage occur causing progressive neurodegeneration. To avoid brain damage and to functionally compensate for eventual deficits of synaptic inputs, mechanisms of neuroprotection, remyelination and synaptic plasticity intervene. The transition from relapsing-remitting course MS (RRMS) to secondary progressive MS (SPMS) is likely to be the point at which the compensatory brain plasticity reserve bypassing of neuronal injury is exhausted. Usually after the fifth decade, regardless of the preceding disease course and severity, the inevitability and the rate of neurological decline are highly consistent.

disease course. Here, we emphasize how a dysregulated synergy between the immune and nervous systems in the course of MS disease causes inflammation-dependent synaptic dysfunction, plasticity and degeneration with important implications on motor and cognitive functions. Since the early phase of MS, inflammatory dependent synaptopathy and synaptic plasticity perturbations seem to occur even independently of demyelination. As MS disease progresses, besides a decrease in remyelinating processes, brain repair and plasticity become exhausted while excitotoxic and neurodegenerative processes are exacerbated in association to a chronic CNS inflammation, supporting a late contribution of aging processes (**Figure 2**). Accordingly, cognitive dysfunction is now recognized to be an early symptoms of MS disease and for this reason it is included in diagnostic, follow-up and therapeutic evaluations (Nasios et al., 2018).

Finally, we highlighted unexpected results obtained from clinical studies conducted on MS patients and healthy controls, revealing a milder effect of aging on MS cognitive function relative to motor disability. Although further investigations are necessary to clarify this aspect, it would be interesting to investigate also which compensatory mechanisms in MS brain are specifically involved. Considering the emerging view of a bidirectional communication between the nervous system and immune system, in which neuroinflammatory processes can be adaptive and beneficial (Schwartz and Deczkowska, 2016), it may be suggested that in the aging MS brains, a vicious interaction between the compromised immune and neuronal systems culminates in a protective and adaptive mechanisms of the neuro-immune system.

In conclusion, a more precise comprehension of the temporal (with age) and spatial distribution and activity of immune players in MS brain in association with specific stages of disease, genetic determinants and brain plasticity reserve is essential to determine the deep nature of the pathology, and thus the ideal strategy required to treat it.

AUTHOR CONTRIBUTIONS

AM, DC and GM conceived and designed the manuscript. All the other authors made significant contributions, reviewed and approved the manuscript.

FUNDING

This work was supported by the Italian Ministry of Health (Ricerca corrente—IRCCS San Raffaele Pisana; Ricerca corrente—IRCCS Neuromed and 5 × 1,000 IRCCS Neuromed).

ACKNOWLEDGMENTS

We would like to acknowledge funding from Umberto Veronesi Foundation for fellowship to AG.

REFERENCES

Amato, M. P., Ponziani, G., Siracusa, G., and Sorbi, S. (2001). Cognitive dysfunction in early-onset multiple sclerosis: a reappraisal after 10 years. *Arch. Neurol.* 58, 1602–1606. doi: 10.1001/archneur.58.10.1602

Amato, M. P., Razzolini, L., Goretti, B., Stromillo, M. L., Rossi, F., Giorgio, A., et al. (2013). Cognitive reserve and cortical atrophy in multiple sclerosis: a longitudinal study. *Neurology* 80, 1728–1733. doi: 10.1212/WNL.0b013e3182918c6f

Bamer, A. M., Cetin, K., Johnson, K. L., Gibbons, L. E., and Ehde, D. M. (2008). Validation study of prevalence and correlates of depressive symptomatology in multiple sclerosis. *Gen. Hosp. Psychiatry* 30, 311–317. doi: 10.1016/j.genhosppsych.2008.04.006

Barrientos, R. M., Kitt, M. M., Watkins, L. R., and Maier, S. F. (2015). Neuroinflammation in the normal aging hippocampus. *Neuroscience* 309, 84–99. doi: 10.1016/j.neuroscience.2015.03.007

Beecham, A. H., Patsopoulos, N. A., Xifara, D. K., Davis, M. F., Kemppinen, A., Cotsapas, C., et al. (2013). Analysis of immune-related loci identifies 48 new susceptibility variants for multiple sclerosis. *Nat. Genet.* 45, 1353–1360. doi: 10.1038/ng.2770

Beier, M., Bombardier, C. H., Hartoonian, N., Motl, R. W., and Kraft, G. H. (2014). Improved physical fitness correlates with improved cognition in multiple sclerosis. *Arch. Phys. Med. Rehabil.* 95, 1328–1334. doi: 10.1016/j.apmr.2014.02.017

Beiske, A. G., Svensson, E., Sandanger, I., Czujko, B., Pedersen, E. D., Aarseth, J. H., et al. (2008). Depression and anxiety amongst multiple sclerosis patients. *Eur. J. Neurol.* 15, 239–245. doi: 10.1111/j.1468-1331.2007.02041.x

Benedict, R. H. B., Morrow, S. A., Weinstock Guttman, B., Cookfair, D., and Schretlen, D. J. (2010). Cognitive reserve moderates decline in information processing speed in multiple sclerosis patients. *J. Int. Neuropsychol. Soc.* 16, 829–835. doi: 10.1017/s1355617710000688

Bennett, M. R. (2000). The concept of long term potentiation of transmission at synapses. *Prog. Neurobiol.* 60, 109–137. doi: 10.1016/s0301-0082(99)00006-4

Bettio, L. E. B., Rajendran, L., and Gil-Mohapel, J. (2017). The effects of aging in the hippocampus and cognitive decline. *Neurosci. Biobehav. Rev.* 79, 66–86. doi: 10.1016/j.neubiorev.2017.04.030

Bodling, A. M., Denney, D. R., and Lynch, S. G. (2009). Cognitive aging in patients with multiple sclerosis: a cross-sectional analysis of speeded processing. *Arch. Clin. Neuropsychol.* 24, 761–767. doi: 10.1093/arclin/acp076

Boeschoten, R. E., Braamse, A. M. J., Beekman, A. T. F., Cuijpers, P., van Oppen, P., Dekker, J., et al. (2017). Prevalence of depression and anxiety in Multiple Sclerosis: a systematic reviewand meta-analysis. *J. Neurol. Sci.* 372, 331–341. doi: 10.1016/j.jns.2016.11.067

Bolton, C., and Smith, P. A. (2018). The influence and impact of ageing and immunosenescence (ISC) on adaptive immunity during multiple sclerosis (MS) and the animal counterpart experimental autoimmune encephalomyelitis (EAE). *Ageing Res. Rev.* 41, 64–81. doi: 10.1016/j.arr.2017.10.005

Bramow, S., Frischer, J. M., Lassmann, H., Koch-Henriksen, N., Lucchinetti, C. F., Sørensen, P. S., et al. (2010). Demyelination versus remyelination in progressive multiple sclerosis. *Brain* 133, 2983–2998. doi: 10.1093/brain/awq250

Briken, S., Gold, S. M., Patra, S., Vettorazzi, E., Harbs, D., Tallner, A., et al. (2014). Effects of exercise on fitness and cognition in progressive MS: a randomized, controlled pilot trial. *Mult. Scler. J.* 20, 382–390. doi: 10.1177/1352458513507358

Buchanan, R. J., Chakravorty, B. J., Tyry, T., Hatcher, W., and Vollmer, T. (2009). Age-related comparisons of people with multiple sclerosis: demographic, disease, and treatment characteristics. *NeuroRehabilitation* 25, 271–278. doi: 10.3233/NRE-2009-0525

Centonze, D., Muzio, L., Rossi, S., Cavasinni, F., De Chiara, V., Bergami, A., et al. (2009). Inflammation triggers synaptic alteration and degeneration in experimental autoimmune encephalomyelitis. *J. Neurosci.* 29, 3442–3452. doi: 10.1523/JNEUROSCI.5804-08.2009

Chwastiak, L., Ehde, D. M., Gibbons, L. E., Sullivan, M., Bowen, J. D., and Kraft, G. H. (2002). Depressive symptoms and severity of illness in multiple sclerosis: epidemiologic study of a large community sample. *Am. J. Psychiatry* 159, 1862–1868. doi: 10.1176/appi.ajp.159.11.1862

Ciccarelli, O., Toosy, A. T., Marsden, J. E., Wheeler-Kingshott, C. M., Miller, D. H., Matthews, P. M., et al. (2006). Functional response to active and passive ankle movements with clinical correlations in patients with primary progressive multiple sclerosis. *J. Neurol.* 253, 882–891. doi: 10.1007/s00415-006-0125-z

Collingridge, G. L., and Bliss, T. V. P. (1995). Memories of NMDA receptors and LTP. *Trends Neurosci.* 18, 54–56. doi: 10.1016/0166-2236(95)80016-u

Compston, A., and Coles, A. (2008). Multiple sclerosis. *Lancet* 372, 1502–1517. doi: 10.1016/S0140-6736(08)61620-7

Confavreux, C., and Vukusic, S. (2006). Age at disability milestones in multiple sclerosis. *Brain* 129, 595–605. doi: 10.1093/brain/awh714

Confavreux, C., Vukusic, S., Moreau, T., and Adeleine, P. (2000). Relapses and progression of disability in multiple sclerosis. *N. Engl. J. Med.* 343, 1430–1438. doi: 10.1056/nejm200011163432001

Cooke, S. F., and Bliss, T. V. P. (2005). Long-term potentiation and cognitive drug discovery. *Curr. Opin. Investig. Drugs* 6, 25–34.

Cooke, S. F., and Bliss, T. V. P. (2006). Plasticity in the human central nervous system. *Brain* 129, 1659–1673. doi: 10.1093/brain/awl082

Cornejo, F., and von Bernhardi, R. (2016). Age-dependent changes in the activation and regulation of microglia. *Adv. Exp. Med. Biol.* 949, 205–226. doi: 10.1007/978-3-319-40764-7_10

Cossburn, M., Ingram, G., Hirst, C., Ben-Shlomo, Y., Pickersgill, T. P., and Robertson, N. P. (2012). Age at onset as a determinant of presenting phenotype and initial relapse recovery in multiple sclerosis. *Mult. Scler. J.* 18, 45–54. doi: 10.1177/1352458511417479

da Silva, A. M., Vilhena, E., Lopes, A., Santos, E., Gonçalves, M. A., Pinto, C., et al. (2011). Depression and anxiety in a Portuguese MS population: associations with physical disability and severity of disease. *J. Neurol. Sci.* 306, 66–70. doi: 10.1016/j.jns.2011.03.042

Dalgas, U., and Stenager, E. (2012). Exercise and disease progression in multiple sclerosis: can exercise slow down the progression of multiple sclerosis? *Ther. Adv. Neurol. Disord.* 5, 81–95. doi: 10.1177/1756285611430719

Dendrou, C. A., Fugger, L., and Friese, M. A. (2015). Immunopathology of multiple sclerosis. *Nat. Rev. Immunol.* 15, 545–558. doi: 10.1038/nri3871

Denkinger, M. D., Leins, H., Schirmbeck, R., Florian, M. C., and Geiger, H. (2015). HSC aging and senescent immune remodeling. *Trends Immunol.* 36, 815–824. doi: 10.1016/j.it.2015.10.008

Di Benedetto, S., Müller, L., Wenger, E., Düzel, S., and Pawelec, G. (2017). Contribution of neuroinflammation and immunity to brain aging and the mitigating effects of physical and cognitive interventions. *Neurosci. Biobehav. Rev.* 75, 114–128. doi: 10.1016/j.neubiorev.2017.01.044

Di Filippo, M., de Iure, A., Durante, V., Gaetani, L., Mancini, A., Sarchielli, P., et al. (2015). Synaptic plasticity and experimental autoimmune encephalomyelitis: implications for multiple sclerosis. *Brain Res.* 1621, 205–213. doi: 10.1016/j.brainres.2014.12.004

Di Filippo, M., Sarchielli, P., Picconi, B., and Calabresi, P. (2008). Neuroinflammation and synaptic plasticity: theoretical basis for a novel, immune-centred, therapeutic approach to neurological disorders. *Trends Pharmacol. Sci.* 29, 402–412. doi: 10.1016/j.tips.2008.06.005

Disanto, G., Berlanga, A. J., Handel, A. E., Para, A. E., Burrell, A. M., Fries, A., et al. (2010). Heterogeneity in multiple sclerosis: scratching the surface of a complex disease. *Autoimmune Dis.* 2011:932351. doi: 10.4061/2011/932351

Dorszewska, J. (2013). Cell biology of normal brain aging: synaptic plasticity-cell death. *Aging Clin. Exp. Res.* 25, 25–34. doi: 10.1007/s40520-013-0004-2

Enzinger, C., Pinter, D., Rocca, M. A., De Luca, J., Sastre-Garriga, J., Audoin, B., et al. (2016). Longitudinal fMRI studies: exploring brain plasticity and repair in MS. *Mult. Scler.* 22, 269–278. doi: 10.1177/1352458515619781

Feinstein, A., Freeman, J., and Lo, A. C. (2015). Treatment of progressive multiple sclerosis: what works, what does not, and what is needed. *Lancet Neurol.* 14, 194–207. doi: 10.1016/s1474-4422(14)70231-5

Filippi, M., and Rocca, M. A. (2009). Functional mr imaging in multiple sclerosis. *Neuroimaging Clin. N. Am.* 19, 59–70. doi: 10.1016/j.nic.2008.08.004

Filippi, M., Rocca, M. A., Colombo, B., Falini, A., Codella, M., Scotti, G., et al. (2002a). Functional magnetic resonance imaging correlates of fatigue in multiple sclerosis. *Neuroimage* 15, 559–567. doi: 10.1006/nimg.2001.1011

Filippi, M., Rocca, M. A., Falini, A., Caputo, D., Ghezzi, A., Colombo, B., et al. (2002b). Correlations between structural CNS damage and functional MRI changes in primary progressive MS. *Neuroimage* 15, 537–546. doi: 10.1006/nimg.2001.1023

Freitas, C., Perez, J., Knobel, M., Tormos, J. M., Oberman, L., Eldaief, M., et al. (2011). Changes in cortical plasticity across the lifespan. *Front. Aging Neurosci.* 3:5. doi: 10.3389/fnagi.2011.00005

Friese, M. A., Schattling, B., and Fugger, L. (2014). Mechanisms of neurodegeneration and axonal dysfunction in multiple sclerosis. *Nat. Rev. Neurol.* 10, 225–238. doi: 10.1038/nrneurol.2014.37

Galeazzi, G. M., Ferrari, S., Giaroli, G., Mackinnon, A., Merelli, E., Motti, L., et al. (2005). Psychiatric disorders and depression in multiple sclerosis outpatients: impact of disability and interferon β therapy. *Neurol. Sci.* 26, 255–262. doi: 10.1007/s10072-005-0468-8

Gentile, A., Fresegna, D., Musella, A., Sepman, H., Bullitta, S., De Vito, F., et al. (2016). Interaction between interleukin-1β and type-1 cannabinoid receptor is involved in anxiety-like behavior in experimental autoimmune encephalomyelitis. *J. Neuroinflammation* 13:231. doi: 10.1186/s12974-016-0682-8

Ghaffar, O., Fiati, M., and Feinstein, A. (2012). Occupational attainment as a marker of cognitive reserve in multiple sclerosis. *PLoS One* 7:e47206. doi: 10.1371/journal.pone.0047206

Gourraud, P. A., Harbo, H. F., Hauser, S. L., and Baranzini, S. E. (2012). The genetics of multiple sclerosis: an up-to-date review. *Immunol. Rev.* 248, 87–103. doi: 10.1111/j.1600-065X.2012.01134.x

Grasselli, G., Rossi, S., Musella, A., Gentile, A., Loizzo, S., Muzio, L., et al. (2013). Abnormal NMDA receptor function exacerbates experimental autoimmune encephalomyelitis. *Br. J. Pharmacol.* 168, 502–517. doi: 10.1111/j.1476-5381.2012.02178.x

Haji, N., Mandolesi, G., Gentile, A., Sacchetti, L., Fresegna, D., Rossi, S., et al. (2012). TNF-α-mediatedanxiety in a mouse model of multiple sclerosis. *Exp. Neurol.* 237, 296–303. doi: 10.1016/j.expneurol.2012.07.010

Henry, C. J., Huang, Y., Wynne, A. M., and Godbout, J. P. (2009). Peripheral lipopolysaccharide (LPS) challenge promotes microglial hyperactivity in aged mice that is associated with exaggerated induction of both pro-inflammatory IL-1β and anti-inflammatory IL-10 cytokines. *Brain Behav. Immun.* 23, 309–317. doi: 10.1016/j.bbi.2008.09.002

Henstridge, C. M., Pickett, E., and Spires-Jones, T. L. (2016). Synaptic pathology: a shared mechanism in neurological disease. *Ageing Res. Rev.* 28, 72–84. doi: 10.1016/j.arr.2016.04.005

Huijbregts, S. C. J., Kalkers, N. F., de Sonneville, L. M. J., de Groot, V., Reuling, I. E. W., and Polman, C. H. (2004). Differences in cognitive impairment of relapsing remitting, secondary, and primary progressive MS. *Neurology* 63, 335–339. doi: 10.1212/01.WNL.0000129828.03714.90

Imitola, J., Chitnis, T., and Khoury, S. J. (2005). Cytokines in multiple sclerosis: from bench to bedside. *Pharmacol. Ther.* 106, 163–177. doi: 10.1016/j.pharmthera.2004.11.007

Jasek, M. C., and Griffith, W. H. (1998). Pharmacological characterization of ionotropic excitatory amino acid receptors in young and aged rat basal forebrain. *Neuroscience* 82, 1179–1194. doi: 10.1016/s0306-4522(97)00337-0

Jenkins, T. M., Toosy, A. T., Ciccarelli, O., Miszkiel, K. A., Wheeler-Kingshott, C. A., Henderson, A. P., et al. (2010). Neuroplasticity predicts outcome of optic neuritis independent of tissue damage. *Ann. Neurol.* 67, 99–113. doi: 10.1002/ana.21823

Kalincik, T., Buzzard, K., Jokubaitis, V., Trojano, M., Duquette, P., Izquierdo, G., et al. (2014). Risk of relapse phenotype recurrence in multiple sclerosis. *Mult. Scler.* 20, 1511–1522. doi: 10.1177/1352458514528762

Kis, B., Rumberg, B., and Berlit, P. (2008). Clinical characteristics of patients with late-onset multiple sclerosis. *J. Neurol.* 255, 697–702. doi: 10.1007/s00415-008-0778-x

Kneebone, I. I., Dunmore, E. C., and Evans, E. (2003). Symptoms of depression in older adults with multiple sclerosis (MS): comparison with a matched sample of younger adults. *Aging Ment. Health* 7, 182–185. doi: 10.1080/1360786031000101148

Lassmann, H., van Horssen, J., and Mahad, D. (2012). Progressive multiple sclerosis: pathology and pathogenesis. *Nat. Rev. Neurol.* 8, 647–656. doi: 10.1038/nrneurol.2012.168

Lefaucheur, J.-P. (2005). Transcranial magnetic stimulation: applications in neurology. *Rev. Neurol.* 161, 1121–1130. doi: 10.1016/S0035-3787(05)85182-3

Lynch, M. A. (2015). Neuroinflammatory changes negatively impact on LTP: a focus on IL-1β. *Brain Res.* 1621, 197–204. doi: 10.1016/j.brainres.2014.08.040

Mahad, D. H., Trapp, P. B. D., and Lassmann, P. H. (2015). Pathological mechanisms in progressive multiple sclerosis. *Lancet Neurol.* 14, 183–193. doi: 10.1016/S1474-4422(14)70256-X

Mainero, C., Pantano, P., Caramia, F., and Pozzilli, C. (2006). Brain reorganization during attention and memory tasks in multiple sclerosis: insights from functional MRI studies. *J. Neurol. Sci.* 245, 93–98. doi: 10.1016/j.jns.2005.08.024

Malenka, R. C., and Bear, M. F. (2004). LTP and LTD: an embarrassment of riches. *Neuron* 44, 5–21. doi: 10.1016/j.neuron.2004.09.012

Mancini, A., Gaetani, L., Di Gregorio, M., Tozzi, A., Ghiglieri, V., Calabresi, P., et al. (2017). Hippocampal neuroplasticity and inflammation: relevance for multiple sclerosis. *Mult. Scler. Demyelinating Disord.* 2:2. doi: 10.1186/s40893-017-0019-1

Mandolesi, G., De Vito, F., Musella, A., Gentile, A., Bullitta, S., Fresegna, D., et al. (2017a). miR-142–3p is a key regulator of IL-1β-dependent synaptopathy in neuroinflammation. *J. Neurosci.* 37, 546–561. doi: 10.1523/JNEUROSCI.0851-16.2016

Mandolesi, G., Bullitta, S., Fresegna, D., Gentile, A., De Vito, F., Dolcetti, E., et al. (2017b). Interferon-γ causes mood abnormalities by altering cannabinoid CB1 receptor function in the mouse striatum. *Neurobiol. Dis.* 108, 45–53. doi: 10.1016/j.nbd.2017.07.019

Mandolesi, G., Grasselli, G., Musella, A., Gentile, A., Musumeci, G., Sepman, H., et al. (2012). GABAergic signaling and connectivity on Purkinje cells are impaired in experimental autoimmune encephalomyelitis. *Neurobiol. Dis.* 46, 414–424. doi: 10.1016/j.nbd.2012.02.005

Mandolesi, G., Musella, A., Gentile, A., Grasselli, G., Haji, N., Sepman, H., et al. (2013). Interleukin-1β alters glutamate transmission at purkinje cell synapses in a mouse model of multiple sclerosis. *J. Neurosci.* 33, 12105–12121. doi: 10.1523/JNEUROSCI.5369-12.2013

Mandolesi, G., Gentile, A., Musella, A., Fresegna, D., De Vito, F., Bullitta, S., et al. (2015). Synaptopathy connects inflammation and neurodegeneration in multiple sclerosis. *Nat. Rev. Neurol.* 11, 711–724. doi: 10.1038/nrneurol.2015.222

Matias-Guiu, J. A., Cortés-Martínez, A., Valles-Salgado, M., Oreja-Guevara, C., Pytel, V., Montero, P., et al. (2017). Functional components of cognitive impairment in multiple sclerosis: a cross-sectional investigation. *Front. Neurol.* 8:643. doi: 10.3389/fneur.2017.00643

Matt, S. M., and Johnson, R. W. (2016). Neuro-immune dysfunction during brain aging: new insights in microglial cell regulation. *Curr. Opin. Pharmacol.* 26, 96–101. doi: 10.1016/j.coph.2015.10.009

Mattioli, F., Bellomi, F., Stampatori, C., Parrinello, G., and Capra, R. (2011). Depression, disability and cognitive impairment in multiple sclerosis: a cross sectional Italian study. *Neurol. Sci.* 32, 825–832. doi: 10.1007/s10072-011-0624-2

Mori, F., Kusayanagi, H., Buttari, F., Centini, B., Monteleone, F., Nicoletti, C. G., et al. (2012). Early treatment with high-dose interferon β-1a reverses cognitive and cortical plasticity deficits in multiple sclerosis. *Funct. Neurol.* 27, 163–168.

Mori, F., Nisticò, R., Mandolesi, G., Piccinin, S., Mango, D., Kusayanagi, H., et al. (2014a). Interleukin-1β promotes long-term potentiation in patients with multiple sclerosis. *Neuromolecular Med.* 16, 38–51. doi: 10.1007/s12017-013-8249-7

Mori, F., Kusayanagi, H., Nicoletti, C. G., Weiss, S., Marciani, M. G., and Centonze, D. (2014b). Cortical plasticity predicts recovery from relapse in multiple sclerosis. *Mult. Scler.* 20, 451–457. doi: 10.1177/1352458513512541

Mori, F., Rossi, S., Piccinin, S., Motta, C., Mango, D., Kusayanagi, H., et al. (2013). Synaptic plasticity and PDGF signaling defects underlie clinical progression in multiple sclerosis. *J. Neurosci.* 33, 19112–19119. doi: 10.1523/JNEUROSCI.2536-13.2013

Mori, F., Rossi, S., Sancesario, G., Codecà, C., Mataluni, G., Monteleone, F., et al. (2011). Cognitive and cortical plasticity deficits correlate with altered amyloid-β CSF levels in multiple sclerosis. *Neuropsychopharmacology* 36, 559–568. doi: 10.1038/npp.2010.187

Motl, R. W., and Pilutti, L. A. (2012). The benefits of exercise training in multiple sclerosis. *Nat. Rev. Neurol.* 8, 487–497. doi: 10.1038/nrneurol.2012.136

Motl, R. W., Sandroff, B. M., Kwakkel, G., Dalgas, U., Feinstein, A., Heesen, C., et al. (2017). Exercise in patients with multiple sclerosis. *Lancet Neurol.* 16, 848–856. doi: 10.1016/S1474-4422(17)30281-8

Müller-Dahlhaus, J. F. M., Orekhov, Y., Liu, Y., and Ziemann, U. (2008). Interindividual variability and age-dependency of motor cortical plasticity induced by paired associative stimulation. *Exp. Brain Res.* 187, 467–475. doi: 10.1007/s00221-008-1319-7

Nasios, G., Messinis, L., Dardiotis, E., and Papathanasopoulos, P. (2018). Review article repetitive transcranial magnetic stimulation, cognition, and multiple sclerosis: an overview. *Behav. Neurol.* 2018:8584653. doi: 10.1155/2018/8584653

Nicoll, R. A., and Malenka, R. C. (1999). Expression mechanisms underlying NMDA receptor-dependent long-term potentiation. *Ann. N Y Acad. Sci.* 868, 515–525. doi: 10.1111/j.1749-6632.1999.tb11320.x

Nisticò, R., Mango, D., Mandolesi, G., Piccinin, S., Berretta, N., Pignatelli, M., et al. (2013). Inflammation subverts hippocampal synaptic plasticity in experimental multiple sclerosis. *PLoS One* 8:e54666. doi: 10.1371/journal.pone.0054666

Norden, D. M., and Godbout, J. P. (2013). Review: microglia of the aged brain: primed to be activated and resistant to regulation. *Neuropathol. Appl. Neurobiol.* 39, 19–34. doi: 10.1111/j.1365-2990.2012.01306.x

Norden, D. M., Muccigrosso, M. M., and Godbout, J. P. (2015). Microglial priming andenhanced reactivity to secondary insult in aging and traumatic CNS injury, and neurodegenerative disease. *Neuropharmacology* 96, 29–41. doi: 10.1016/j.neuropharm.2014.10.028

Novotna, M., Paz Soldán, M. M., Abou Zeid, N., Kale, N., Tutuncu, M., Crusan, D. J., et al. (2015). Poor early relapse recovery affects onset of progressive disease course in multiple sclerosis. *Neurology* 85, 722–729. doi: 10.1212/WNL.0000000000001856

Ojo, J. O., Rezaie, P., Gabbott, P. L., and Stewart, M. G. (2015). Impact of age-related neuroglial cell responses on hippocampal deterioration. *Front. Aging Neurosci.* 7:57. doi: 10.3389/fnagi.2015.00057

Olsson, T., Barcellos, L. F., and Alfredsson, L. (2017). Interactions between genetic, lifestyle and environmental risk factors for multiple sclerosis. *Nat. Rev. Neurol.* 13, 25–36. doi: 10.1038/nrneurol.2016.187

Ontaneda, D., Thompson, A. J., Fox, R. J., and Cohen, J. A. (2017). Progressive multiple sclerosis: prospects for disease therapy, repair, and restoration of function. *Lancet* 389, 1357–1366. doi: 10.1016/S0140-6736(16)31320-4

Pantano, P., Mainero, C., Domenico Iannetti, G., Caramia, F., Di Legge, S., Piattella, M. C., et al. (2002). Contribution of corticospinal tract damage to cortical motor reorganization after a single clinical attack of multiple sclerosis. *Neuroimage* 17, 1837–1843. doi: 10.1006/nimg.2002.1313

Pascual-Leone, A., Freitas, C., Oberman, L., Horvath, J. C., Halko, M., Eldaief, M., et al. (2011). Characterizing brain cortical plasticity and network dynamics across the age-span in health and disease with TMS-EEG and TMS-fMRI. *Brain Topogr.* 24, 302–315. doi: 10.1007/s10548-011-0196-8

Patten, S. B., Beck, C. A., Williams, J. V., Barbui, C., and Metz, L. M. (2003). Major depression in multiple sclerosis: a population-based perspective. *Neurology* 61, 1524–1527. doi: 10.1212/01.wnl.0000095964.34294.b4

Patten, S. B., Metz, L. M., and Reimer, M. A. (2000). Biopsychosocial correlates of lifetime major depression in a multiple sclerosis population. *Mult. Scler.* 6, 115–120. doi: 10.1177/135245850000600210

Pelletier, J., Audoin, B., Reuter, F., and Ranjeva, J. P. (2009). Plasticity in MS: from functional imaging to rehabilitation. *Int. MS J.* 16, 26–31.

Penner, I. K., Rausch, M., Kappos, L., Opwis, K., and Radü, E. W. (2003). Analysis of impairment related functional architecture in MS patients during performance of different attention tasks. *J. Neurol.* 250, 461–472. doi: 10.1007/s00415-003-1025-0

Phillips, L. J., and Stuifbergen, A. K. (2008). The influence of positive experiences on depression and quality of life in persons with multiple sclerosis. *J. Holist. Nurs* 26, 41–48. doi: 10.1177/0898010107301870

Pinter, D., Sumowski, J., DeLuca, J., Fazekas, F., Pichler, A., Khalil, M., et al. (2014). Higher education moderates the effect of T2 lesion load and third ventricle width on cognition in multiple sclerosis. *PLoS One* 9:e87567. doi: 10.1371/journal.pone.0087567

Pizza, V., Agresta, A., D'Acunto, C. W., Festa, M., and Capasso, A. (2011). Neuroinflamm-aging and neurodegenerative diseases: an overview.

CNS Neurol. Disord. Drug Targets 10, 621–634. doi: 10.2174/187152711796235014

Planche, V., Gibelin, M., Cregut, D., Pereira, B., and Clavelou, P. (2016). Cognitive impairment in a population-based study of patients with multiple sclerosis: differences between late relapsing-remitting, secondary progressive and primary progressive multiple sclerosis. *Eur. J. Neurol.* 23, 282–289. doi: 10.1111/ene.12715

Polliack, M. L., Barak, Y., and Achiron, A. (2001). Late-onset multiple sclerosis. *J. Am. Geriatr. Soc.* 49, 168–171. doi: 10.1046/j.1532-5415.2001.49038.x

Potagas, C., Giogkaraki, E., Koutsis, G., Mandellos, D., Tsirempolou, E., Sfagos, C., et al. (2008). Cognitive impairment in different MS subtypes and clinically isolated syndromes. *J. Neurol. Sci.* 267, 100–106. doi: 10.1016/j.jns.2007.10.002

Ramachandran, S., Strange, R. C., Jones, P. W., Kalra, S., Nayak, D., and Hawkins, C. P. (2014). Associations between onset age and disability in multiple sclerosis patients studied using MSSS and a progression model. *Mult. Scler. Relat. Disord.* 3, 593–599. doi: 10.1016/j.msard.2014.06.002

Rao, S. M. (1991). *A Manual for the Brief, Repeatable Battery of Neuropsychological Tests in Multiple Sclerosis.* New York, NY: National Multiple Sclerosis Society.

Reddy, H., Narayanan, S., Arnoutelis, R., Jenkinson, M., Antel, J., Matthews, P. M., et al. (2000a). Evidence for adaptive functional changes in the cerebral cortex with axonal injury from multiple sclerosis. *Brain* 123, 2314–2320. doi: 10.1093/brain/123.11.2314

Reddy, H., Narayanan, S., Matthews, P. M., Hoge, R. D., Pike, G. B., Duquette, P., et al. (2000b). Relating axonal injury to functional recovery in MS. *Neurology* 54, 236–239. doi: 10.1212/WNL.54.1.236

Reddy, H., Narayanan, S., Woolrich, M., Mitsumori, T., Lapierre, Y., Arnold, D. L., et al. (2002). Functional brain reorganization for hand movement in patients with multiple sclerosis: defining distinct effects of injury and disability. *Brain* 125, 2646–2657. doi: 10.1093/brain/awf283

Rocca, M. A., Amato, M. P., De Stefano, N., Enzinger, C., Geurts, J. J., Penner, I. K., et al. (2015). Clinical and imaging assessment of cognitive dysfunction in multiple sclerosis. *Lancet Neurol.* 14, 302–417. doi: 10.1016/S1474-4422(14)70250-9

Rocca, M. A., Ceccarelli, A., Rodegher, M., Misci, P., Riccitelli, G., Falini, A., et al. (2010a). Preserved brain adaptive properties in patients with benign multiple sclerosis. *Neurology* 74, 142–149. doi: 10.1212/WNL.0b013e3181c91a00

Rocca, M. A., Valsasina, P., Absinta, M., Riccitelli, G., Rodegher, M. E., Misci, P., et al. (2010b). Default-mode network dysfunction and cognitive impairment in progressive MS. *Neurology* 74, 1252–1259. doi: 10.1212/WNL.0b013e3181d9ed91

Rocca, M. A., Colombo, B., Falini, A., Ghezzi, A., Martinelli, V., Scotti, G., et al. (2005). Cortical adaptation in patients with MS: a cross-sectional functional MRI study of disease phenotypes. *Lancet Neurol.* 4, 618–626. doi: 10.1016/s1474-4422(05)70171-x

Rocca, M. A., Falini, A., Colombo, B., Scotti, G., Comi, G., and Filippi, M. (2002a). Adaptive functional changes in the cerebral cortex of patients with nondisabling multiple sclerosis correlate with the extent of brain structural damage. *Ann. Neurol.* 51, 330–339. doi: 10.1002/ana.10120

Rocca, M. A., Matthews, P. M., Caputo, D., Ghezzi, A., Falini, A., Scotti, G., et al. (2002b). Evidence for widespread movement-associated functional MRI changes in patients with PPMS. *Neurology* 58, 866–872. doi: 10.1212/WNL.58.6.866

Rocca, M. A., Gavazzi, C., Mezzapesa, D. M., Falini, A., Colombo, B., Mascalchi, M., et al. (2003a). A functional magnetic resonance imaging study of patients with secondary progressive multiple sclerosis. *Neuroimage* 19, 1770–1777. doi: 10.1016/s1053-8119(03)00242-8

Rocca, M. A., Mezzapesa, D. M., Falini, A., Ghezzi, A., Martinelli, V., Scotti, G., et al. (2003b). Evidence for axonal pathology and adaptive cortical reorganization in patients at presentation with clinically isolated syndromes suggestive of multiple sclerosis. *Neuroimage* 18, 847–855. doi: 10.1016/s1053-8119(03)00043-0

Rocca, M. A., Riccitelli, G. C., Meani, A., Pagani, E., Del Sette, P., Martinelli, V., et al. (2018). Cognitive reserve, cognition, and regional brain damage in MS: a 2 -year longitudinal study. *Mult. Scler.* doi: 10.1177/1352458517750767 [Epub ahead of print].

Rossi, S., Furlan, R., De Chiara, V., Motta, C., Studer, V., Mori, F., et al. (2012). Interleukin-1β causes synaptic hyperexcitability in multiple sclerosis. *Ann. Neurol.* 71, 76–83. doi: 10.1002/ana.22512

Rossi, S., Motta, C., Studer, V., Barbieri, F., Buttari, F., Bergami, A., et al. (2014). Tumor necrosis factor is elevated in progressive multiple sclerosis and causes excitotoxic neurodegeneration. *Mult. Scler.* 20, 304–312. doi: 10.1177/1352458513498128

Rossi, S., Muzio, L., De Chiara, V., Grasselli, G., Musella, A., Musumeci, G., et al. (2011). Impaired striatal GABA transmission in experimental autoimmune encephalomyelitis. *Brain Behav. Immun.* 25, 947–956. doi: 10.1016/j.bbi.2010.10.004

Rossi, S., Studer, V., Motta, C., Polidoro, S., Perugini, J., Macchiarulo, G., et al. (2017). Neuroinflammation drives anxiety and depression in relapsing-remitting multiple sclerosis. *Neurology* 89, 1338–1347. doi: 10.1212/WNL.0000000000004411

Rossi, S., Studer, V., Moscatelli, A., Motta, C., Coghe, G., Fenu, G., et al. (2013). Opposite roles of NMDA receptors in relapsing and primary progressive multiple sclerosis. *PLoS One* 8:e67357. doi: 10.1371/journal.pone.0067357

Rossini, P. M., and Rossi, S. (2007). Transcranial magnetic stimulation: diagnostic, therapeutic, and research potential. *Neurology* 68, 484–488. doi: 10.1212/01.wnl.0000250268.13789.b2

Roy, S., Frndak, S., Drake, A. S., Irwin, L., Zivadinov, R., Weinstock-Guttman, B., et al. (2017). Differential effects of aging on motor and cognitive functioning in multiple sclerosis. *Mult. Scler.* 23, 1385–1393. doi: 10.1177/1352458516679036

Roy, S., Schwartz, C. E., Duberstein, P., Dwyer, M. G., Zivadinov, R., Bergsland, N., et al. (2016). Synergistic effects of reserve and adaptive personality in multiple sclerosis. *J. Int. Neuropsychol. Soc.* 22, 920–927. doi: 10.1017/S1355617716000333

Ruano, L., Portaccio, E., Goretti, B., Niccolai, C., Severo, M., Patti, F., et al. (2017). Age and disability drive cognitive impairment in multiple sclerosis across disease subtypes. *Mult. Scler.* 23, 1258–1267. doi: 10.1177/1352458516674367

Ruet, A., Deloire, M., Charré-Morin, J., Hamel, D., and Brochet, B. (2013). Cognitive impairment differs between primary progressive and relapsing-remitting MS. *Neurology* 80, 1501–1508. doi: 10.1212/WNL.0b013e31828cf82f

Sanai, S. A., Saini, V., Benedict, R. H., Zivadinov, R., Teter, B. E., Ramanathan, M., et al. (2016). Aging and multiple sclerosis. *Mult. Scler.* 22, 717–725. doi: 10.1177/1352458516634871

Sandroff, B. M., Balto, J. M., Klaren, R. E., Sommer, S. K., DeLuca, J., and Motl, R. W. (2016a). Systematically developed pilot randomized controlled trial of exercise and cognition in persons with multiple sclerosis. *Neurocase* 22, 443–450. doi: 10.1080/13554794.2016.1237658

Sandroff, B. M., Motl, R. W., Scudder, M. R., and DeLuca, J. (2016b). Systematic, evidence-based review of exercise, physical activity and physical fitness effects on cognition in persons with multiple sclerosis. *Neuropsychol. Rev.* 26, 271–294. doi: 10.1007/s11065-016-9324-2

Sandroff, B. M., Klaren, R. E., Pilutti, L. A., Dlugonski, D., Benedict, R. H. B., and Motl, R. W. (2014). Randomized controlled trial of physical activity, cognition and walking in multiple sclerosis. *J. Neurol.* 261, 363–372. doi: 10.1007/s00415-013-7204-8

Scalfari, A., Neuhaus, A., Daumer, M., DeLuca, G. C., Muraro, P. A., and Ebers, G. C. (2013). Early relapses, onset of progression and late outcome in multiple sclerosis. *JAMA Neurol.* 70, 214–222. doi: 10.1001/jamaneurol.2013.599

Scalfari, A., Neuhaus, A., Daumer, M., Ebers, G. C., and Muraro, P. A. (2011). Age and disability accumulation in multiple sclerosis. *Neurology* 77, 1246–1252. doi: 10.1212/WNL.0b013e318230a17d

Scalfari, A., Neuhaus, A., Degenhardt, A., Rice, G. P., Muraro, P. A., Daumer, M., et al. (2010). The natural history of multiple sclerosis, a geographically based study 10: relapses and long-term disability. *Brain* 133, 1914–1929. doi: 10.1093/brain/awq118

Schoonheim, M. M., Geurts, J. J. G., and Barkhof, F. (2010). The limits of functional reorganization in multiple sclerosis. *Neurology* 74, 1246–1247. doi: 10.1212/WNL.0b013e3181db9957

Schwartz, M., and Deczkowska, A. (2016). Neurological disease as a failure of brain-immune crosstalk: the multiple faces of neuroinflammation. *Trends Immunol.* 37, 668–679. doi: 10.1016/j.it.2016.08.001

Stampanoni Bassi, M., Mori, F., Buttari, F., Marfia, G. A., Sancesario, A., Centonze, D., et al. (2017). Neurophysiology of synaptic functioning in multiple sclerosis. *Clin. Neurophysiol.* 128, 1148–1157. doi: 10.1016/j.clinph.2017.04.006

Stangel, M. (2008). Neuroprotection and neuroregeneration in multiple sclerosis. *J. Neurol.* 255, 77–81. doi: 10.1007/s00415-008-6014-x

Stankoff, B., Mrejen, S., Tourbah, A., Fontaine, B., Lyon-Caen, O., Lubetzki, C., et al. (2007). Age at onset determines the occurrence of the progressive phase of multiple sclerosis. *Neurology* 68, 779–781. doi: 10.1212/01.wnl.0000256732.36565.4a

Stellwagen, D., Beattie, E. C., Seo, J. Y., and Malenka, R. C. (2005). Differential regulation of AMPA receptor and GABA receptor trafficking by tumor necrosis factor-α. *J. Neurosci.* 25, 3219–3228. doi: 10.1523/JNEUROSCI.4486-04.2005

Stern, Y. (2002). What is cognitive reserve? Theory and research application of the reserve concept. *J. Int. Neuropsychol. Soc.* 8, 448–460. doi: 10.1017/s1355617702813248

Sumowski, J. F., Chiaravalloti, N., and DeLuca, J. (2009). Cognitive reserve protects against cognitive dysfunction in multiple sclerosis. *J. Clin. Exp. Neuropsychol.* 31, 913–926. doi: 10.1080/13803390902740643

Sumowski, J. F., Rocca, M. A., Leavitt, V. M., Riccitelli, G., Comi, G., DeLuca, J., et al. (2013). Brain reserve and cognitive reserve in multiple sclerosis: what you've got and how you use it. *Neurology* 80, 2186–2193. doi: 10.1212/WNL.0b013e318296e98b

Tedeholm, H., Skoog, B., Lisovskaja, V., Runmarker, B., Nerman, O., and Andersen, O. (2015). The outcome spectrum of multiple sclerosis: disability, mortality and a cluster of predictors from onset. *J. Neurol.* 262, 1148–1163. doi: 10.1007/s00415-015-7674-y

Tomassini, V., Matthews, P. M., Thompson, A. J., Fuglø, D., Geurts, J. J., Johansen-Berg, H., et al. (2012). Neuroplasticity and functional recovery in multiple sclerosis. *Nat. Rev. Neurol.* 8, 635–646. doi: 10.1038/nrneurol.2012.179

Tremlett, H., Paty, D., and Devonshire, V. (2006). Disability progression in multiple sclerosis is slower than previously reported. *Neurology* 66, 172–177. doi: 10.1212/01.wnl.0000194259.90286.fe

Trojano, M., Liguori, M., Bosco Zimatore, G., Bugarini, R., Avolio, C., Paolicelli, D., et al. (2002). Age-related disability in multiple sclerosis. *Ann. Neurol.* 51, 475–480. doi: 10.1002/ana.10147

Tsivgoulis, G., Triantafyllou, H., Papageorgiou, C., Evangelopoulos, M. E., Kararizou, E., Sfagos, C., et al. (2007). Associations of the expanded disability status scale with anxiety and depression in multiple sclerosis outpatients. *Acta Neurol. Scand.* 115, 67–72. doi: 10.1111/j.1600-0404.2006.00736.x

Viviani, B., and Boraso, M. S. (2011). Cytokines and neuronal channels: a molecular basis for age-related decline of neuronal function? *Exp. Gerontol.* 46, 199–206. doi: 10.1016/j.exger.2010.09.008

Viviani, B., Bartesaghi, S., Gardoni, F., Vezzani, A., Behrens, M. M., Bartfai, T., et al. (2003). Interleukin-1β enhances NMDA receptor-mediated intracellular calcium increase through activation of the Src family of kinases. *J. Neurosci.* 23, 8692–8700. doi: 10.1523/jneurosci.23-25-08692.2003

Viviani, B., Gardoni, F., Bartesaghi, S., Corsini, E., Facchi, A., Galli, C. L., et al. (2006). Interleukin-1β released by gp120 drives neural death through tyrosine phosphorylation and trafficking of NMDA receptors. *J. Biol. Chem.* 281, 30212–30222. doi: 10.1074/jbc.m602156200

von Bernhardi, R., Eugenín-von Bernhardi, L., and Eugenín, J. (2015). Microglial cell dysregulation in brain aging and neurodegeneration. *Front. Aging Neurosci.* 7:124. doi: 10.3389/fnagi.2015.00124

von Bernhardi, R., Tichauer, J. E., and Eugenín, J. (2010). Aging-dependent changes of microglial cells and their relevance for neurodegenerative disorders. *J. Neurochem.* 112, 1099–1114. doi: 10.1111/j.1471-4159.2009.06537.x

Walford, R. L. (1969). The immunological theory of aging. *Immunol. Rev.* 2, 171–171. doi: 10.1111/j.1600-065X.1969.tb00210.x

Weiss, S., Mori, F., Rossi, S., and Centonze, D. (2014). Disability in multiple sclerosis: when synaptic long-term potentiation fails. *Neurosci. Biobehav. Rev.* 43, 88–99. doi: 10.1016/j.neubiorev.2014.03.023

Williams, R. M., Turner, A. P., Hatzakis, M., Bowen, J. D., Rodriquez, A. A., and Haselkorn, J. K. (2005). Prevalence and correlates of depression among veterans with multiple sclerosis. *Neurology* 64, 75–80. doi: 10.1212/01.WNL.0000148480.31424.2A

Zeller, D., and Classen, J. (2014). Plasticity of the motor system in multiple sclerosis. *Neuroscience* 283, 222–230. doi: 10.1016/j.neuroscience.2014.05.043

Zeller, D., aufm Kampe, K., Biller, A., Stefan, K., Gentner, R., Schütz, A., et al. (2010). Rapid-onset central motor plasticity in multiple sclerosis. *Neurology* 74, 728–735. doi: 10.1212/WNL.0b013e3181d31dcf

Zeydan, B., and Kantarci, O. H. (2018). Progressive Forms of multiple sclerosis: distinct entity or age-dependent phenomena. *Neurol. Clin.* 36, 163–171. doi: 10.1016/j.ncl.2017.08.006

Ziemann, U., Paulus, W., Nitsche, M. A., Pascual-Leone, A., Byblow, W. D., Berardelli, A., et al. (2008). Consensus: motor cortex plasticity protocols. *Brain Stimul.* 1, 164–182. doi: 10.1016/j.brs.2008.06.006

Conflict of Interest Statement: The authors declare that the research was conducted in the absence of any commercial or financial relationships that could be construed as a potential conflict of interest.

frontiers in Aging Neuroscience

SYSTEMATIC REVIEW
published: 08 January 2018
doi: 10.3389/fnagi.2017.00438

Association of Peripheral Interleukin-6 with Global Cognitive Decline in Non-demented Adults: A Meta-Analysis of Prospective Studies

Steven Bradburn[1]*, *Jane Sarginson*[1,2] and *Christopher A. Murgatroyd*[1]

[1] School of Healthcare Science, Manchester Metropolitan University, Manchester, United Kingdom, [2] NIHR Greater Manchester Primary Care Patient Safety Translational Research Centre, University of Manchester, Manchester, United Kingdom

Background: Elevated biomarkers of systemic inflammation have been reported in individuals with cognitive decline, however, most of the literature concerns cross-sectional analyses that have produced mixed results. This study investigates the etiology of this association by performing meta-analyses on prospective studies investigating the relationship between baseline interleukin-6 (IL-6), an established marker of peripheral inflammation, with cognitive decline risk in non-demented adults at follow-up.

Methods: We reviewed studies reporting peripheral IL-6 with future cognitive decline, up to February 2017 by searching the PubMed, Science Direct, Scopus and Google Scholar databases. Studies which contained odds ratios (ORs) for the association between circulating baseline IL-6 and longitudinal cognitive performance in non-demented community dwelling older adults were pooled in random-effects models.

Results: The literature search retrieved 5,642 potential articles, of which 7 articles containing 8 independent aging cohorts were eligible for review. Collectively, these studies included 15,828 participants at baseline. Those with high circulating IL-6 were 1.42 times more likely to experience global cognitive decline at follow-up, over a 2–7-year period, compared to those with low IL-6 (OR 1.42, 95% CI 1.18–1.70; $p < 0.001$). Subgroup and sensitivity analyses suggests that this association is independent of the study sample size, duration of follow-up and cognitive assessments used.

Conclusions: These results add further evidence for the association between high peripheral inflammation, as measured by blood IL-6, and global cognitive decline. Measuring circulating IL-6 may be a useful indication for future cognitive health.

Keywords: inflammation, cognitive aging, inflammaging, interleukin-6, meta-analysis, cognitive decline, longitudinal studies, prospective studies

OPEN ACCESS

Edited by:
Brandi Ormerod,
University of Florida, United States

Reviewed by:
Elizabeta Blagoja Mukaetova-Ladinska,
Newcastle University, United Kingdom
Margaret Morris,
University of New South Wales, Australia

***Correspondence:**
Steven Bradburn
steven.bradburn@mmu.ac.uk

Received: *29 August 2017*
Accepted: *19 December 2017*
Published: *08 January 2018*

Citation:
Bradburn S, Sarginson J and Murgatroyd CA (2018) Association of Peripheral Interleukin-6 with Global Cognitive Decline in Non-demented Adults: A Meta-Analysis of Prospective Studies. Front. Aging Neurosci. 9:438. doi: 10.3389/fnagi.2017.00438

INTRODUCTION

Globally, the number of older adults (≥60 years old) is projected to increase by 56%, from 901 million to 1.4 billion, over the next 14 years and surpass 2 billion by the year 2050 (United Nations, 2015). Analysis involving European studies of aging suggest that the prevalence of cognitive decline in older adults is as high as 28% (Scafato et al., 2010). Some, but not all, of those who experience

cognitive decline may go on to develop mild cognitive impairment (MCI). Those with MCI are then at an increased risk of developing dementia (Korolev et al., 2016). The underlying pathogenesis behind this heterogenous transition from cognitive aging to dementia is still under debate but, evidence suggests that systemic inflammation may be a contributing factor (Cunningham and Hennessy, 2015).

Systemic inflammation gradually increases with age, commonly referred to as inflamm-aging. Of the cytokines implemented in the inflamm-aging process, interleukin-6 (IL-6) is regarded as one of the main inflammatory components resulting in the age-associated pathologies (Franceschi and Campisi, 2014). Physiologically, IL-6 is a hormone-like cytokine with pleiotropic capabilities including roles in immunological homeostasis (Hunter and Jones, 2015), such as upregulating acute phase response proteins (e.g., C-reactive protein), and signaling within the central nervous system (CNS) (Spooren et al., 2011; Erta et al., 2012).

Dysregulation of IL-6 has been implicated in the modulation of various cognitive functions (Donzis and Tronson, 2014) and previous meta-analyses have reported associations between upregulated peripheral IL-6 with Alzheimer's disease (AD) (Swardfager et al., 2010; Lai et al., 2017) and postoperative cognitive dysfunction (Peng et al., 2013). These studies report associations between peripheral inflammation during and after the onset of neuropathologies. Exploring these associations longitudinally in the non-demented, however, may provide a better insight into the pathological roles peripheral inflammation plays in the CNS.

The current state of the literature concerning IL-6 and cognitive decline in prospective cohorts of old adults has so far produced mixed findings (Weaver et al., 2002; Yaffe et al., 2003; Dik et al., 2005; Jordanova et al., 2007; Rafnsson et al., 2007; Schram et al., 2007; Singh-Manoux et al., 2014), with some stating a significant association between baseline IL-6 with cognitive decline while others failed to replicate such results. Further, systematic analyses remain inconclusive (Li and Yu, 2017).

The aim of this study was to collate the current data from the literature and perform a meta-analysis for longitudinal studies reporting the association between baseline peripheral IL-6 and future cognitive decline in adults without dementia. This approach is warranted in order to increase the statistical power and thus provide clarity to such an association.

METHODS

Search Strategy

All analyses were performed according to the PRISMA guidelines (Liberati et al., 2009). We searched the published literature in the Scopus, PubMed, Science Direct and Google Scholar databases up to February 2017.

Search terms were as follows: ("Interleukin-6" OR "IL-6") AND (cognition OR "cognitive decline" OR "cognitive function" OR "cognitive impairment" OR "cognitive loss" OR memory) AND (aging OR aging) AND (health OR healthy) AND (longitudinal OR prospective). We also manually searched any relevant references cited within retrieved articles. A standardized review protocol has not been published.

Eligibility Criteria

Studies were included if they met the following criteria: (i) a prospective cohort design; (ii) cognition performance was used at baseline and at follow-up; (iii) non-demented older subjects at baseline; (iv) IL-6 measured in unstimulated blood (e.g., *ex vivo* blood was not stimulated by lipopolysaccharide); (v) reported odds ratios (ORs) for the association of baseline IL-6 and future global cognitive decline; (vi) the study population consisted of community-dwelling adults; (vii) the article was available in English. Exclusion criteria included: (i) participants with dementia or cognitive impairment were included at baseline; (ii) the association between baseline IL-6 and cognitive decline was not reported; (iii) the study design was cross-sectional or interventional.

Where multiple publications utilized the same cohort source, the study containing the majority of required data was preferred. Where studies reported alternative statistics, as opposed to ORs, authors were contacted via e-mail and the desired logistical analysis was requested. Two authors agreed to this approach (Rafnsson et al., 2007; Schram et al., 2007) and provided ORs. Unsuccessful requests were otherwise discarded from the review.

Data Extraction

All data were reviewed and extracted by two independent investigators (SB and CM). Results were compared and disagreements were settled through discussion.

The following characteristics and data were extracted from each paper: number of subjects at baseline, proportion of females at baseline, age at baseline, length of study follow-up, assessment of global cognition, OR and 95% confidence intervals (CIs) for adjusted model, and confounders adjusted for in the regression analysis. Where studies stratified subjects into more than two groups (e.g., tertiles, quartiles), high and low IL-6 are defined as those in the highest and lowest grouping, respectively. For studies categorizing IL-6 into two groups, via a median split, high and low IL-6 subjects are defined as those above and below the median. For those reporting tertile groupings, those in the second tertile were classed as intermediate IL-6. Where multiple cognitive assessments were used to assess different cognitive domains, we chose the assessment and outcome reflecting global cognitive decline. Where multiple model testing was applied, we extracted the model with the most adjustments for potential confounders.

Quality Assessment

Each paper included within the meta-analyses was subject to quality assessment by two authors via the Newcastle-Ottawa Quality Assessment Scale for cohort studies (Wells et al., 2000). This scale is based on three categories (population selection, comparability and outcome) with a combined maximum score of 9 points. Ratings were compared between authors and disagreements were settled through discussion.

Statistical Analysis

The Review Manager (RevMan; version 5.3.5; Copenhagen, Denmark) software was used to pool the individual studies of interest. Results were deemed statistically significant when $p < 0.05$. Analysis is presented as ORs based on the likelihood of cognitive decline in the highest baseline IL-6 group compared to the lowest group using a random-effects method.

To investigate heterogeneity between studies, we used the I^2 index which describes the percentage of variation across the studies in the pooled analysis that is due to inconsistency rather than by chance.

Post-hoc sensitivity analyses were carried out to investigate the impact of between study methodological difference on the meta-analyses including, follow up time, cohort size, Newcastle-Ottawa Quality Assessment Scale score and IL-6 measurement method and grouping, as appropriate.

Publication bias was assessed through visual inspection of each Begg's funnel plot and the Egger's test. Analysis was performed using the Stata (StataCorp LP; version 14.2; College Station, TX, USA) software.

RESULTS

Study Selection

Our search strategy returned 5,642 potential articles for inclusion on baseline IL-6 and prospective cognitive functioning, of which 70 were deemed relevant through title and abstract screening (**Figure 1**). After the removal of duplicate findings, 34 articles remained for full-text analysis. Of these, 27 articles were excluded as they did not meet our inclusion criteria, leaving 7 articles eligible for review. Schram et al. (2007) reported two independent cohorts (Rotterdam and Leiden 85-plus), therefore these were treated as separate studies. Thus, in total 8 studies were included in the review and the study characteristics are described in **Table 1**. Quality assessment determined that all studies had a high quality score (range: 7–9) (**Table 2**) with an agreement rate of 86% between author ratings.

Study Characteristics

In total the studies contained 15,828 participants at baseline. Three studies (Yaffe et al., 2003; Rafnsson et al., 2007; Singh-Manoux et al., 2014) reported proportions of global cognitive decline upon follow-up (8,700 at baseline; 792 declined at follow-up; 9%). All the studies contained a mix of male and female participants. Follow-up periods ranged from 2 to 7 years.

Two studies measured IL-6 from the serum (Dik et al., 2005; Singh-Manoux et al., 2014) and six, including both independent cohorts presented in the Schram et al. study, measured IL-6 from plasma (Weaver et al., 2002; Yaffe et al., 2003; Jordanova et al., 2007; Rafnsson et al., 2007; Schram et al., 2007). All the studies quantified IL-6 from the blood by using an enzyme-linked immunosorbent assay (ELISA) technique.

Assessments of global cognitive functioning consisted of either the Mini-Mental State Examination (MMSE), Modified MMSE (3MS) or a battery of assessments (**Table 3**). Further, the definition of global cognitive decline differed between studies, however, three of the studies which used the MMSE as the assessment (Schram et al., 2007; Singh-Manoux et al., 2014) had identical definitions (**Table 3**). All studies included adjustments for age, gender and education at a minimum in their models (**Table 3**).

Association between High Baseline IL-6 and Global Cognitive Decline: Meta-Analysis

Those with high baseline IL-6 were 1.42 times more likely to encounter global cognitive decline at follow-up, compared to those with low IL-6 (OR 1.42, 95% CI 1.18–1.70, $p < 0.001$;

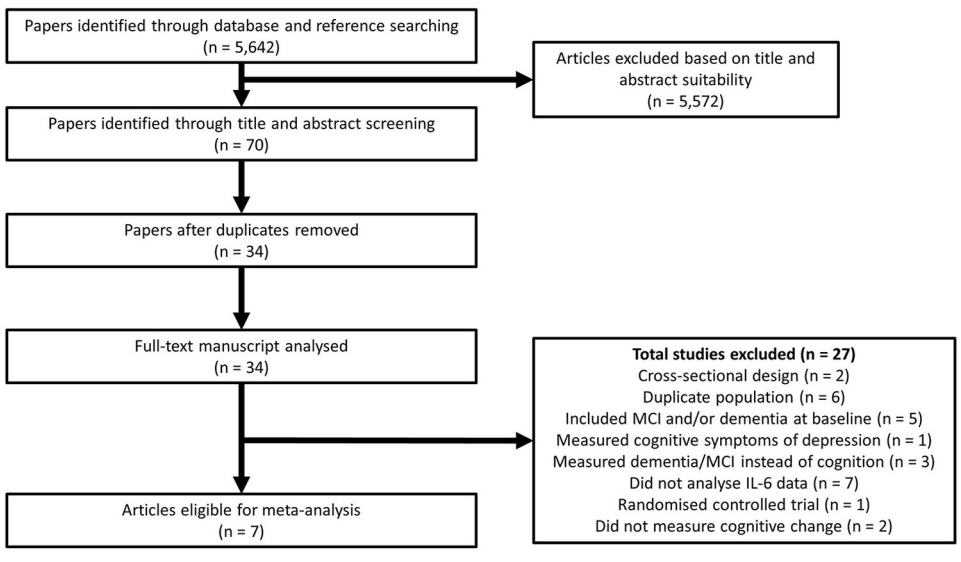

FIGURE 1 | Flowchart summarizing the literature search for the meta-analysis.

TABLE 1 | Study characteristics included in the meta-analysis.

Paper	Cohort (location)	Subjects at baseline (*n*)	Female (%)	Mean age at baseline (years)	Mean follow up (years)
Dik et al., 2005	Longitudinal Aging Study Amsterdam (The Netherlands)	1,284	51	75.4 ± 6.6	3
Jordanova et al., 2007	N/A (Britain)	290	57	65.5 ± 5.5	3
Rafnsson et al., 2007	Edinburgh Artery Study (Britain)	452	50	73.1 ± 5.0	4
(Schram et al., 2007) (Leiden 85-Plus cohort)	Leiden 85-Plus cohort (The Netherlands)	491	65	85	3.4
(Schram et al., 2007) (Rotterdam cohort)	Rotterdam cohort (The Netherlands)	3,874	58	72.1 ± 6.9	4.6
Singh-Manoux et al., 2014	The Whitehall II Study (Britain)	5,217	28	55.7 ± 6.0	5
Weaver et al., 2002	The MacArthur Study of Successful Aging (America)	1,189	55	74.3 ± 2.7	7
Yaffe et al., 2003	The Health ABC Study (America)	3,031	52	73.6 ± 2.9	2

Figure 2A). No study heterogeneity was evident ($I^2 = 14\%$, $p = 0.32$; **Figure 2A**).

Association between High Baseline IL-6 and Global Cognitive Decline: Subgroup Analysis

Subgroup analysis determined the association was independent of the sample size used (<1,000/≥1,000 participants at baseline), duration of follow-up (<4/≥4 years) and the method used to assess global cognitive performance (MMSE/others) (**Table 4**). The association, however, was no longer evident when including only studies of lower quality (<8 points). The significance remained after removing studies which categorized IL-6 as above/below median (Weaver et al., 2002; Dik et al., 2005), as opposed to upper and lower grouping (OR 1.41, 95% CI 1.16–1.71; $p < 0.001$; 6 studies) and those which used serum to measure IL-6 (Dik et al., 2005; Singh-Manoux et al., 2014) opposed to plasma (OR 1.39, 95% CI 1.14–1.69; $p = 0.001$; 6 studies).

Association between High Baseline IL-6 and Global Cognitive Decline: Risk of Bias Analysis

No publication bias was evident based on visual inspection of Begg's funnel plot (**Figure 3A**) or through an Egger's test ($p = 0.379$).

Association between Intermediate Baseline IL-6 and Global Cognitive Decline: Meta-Analysis

Five of the aforementioned studies (Weaver et al., 2002; Rafnsson et al., 2007; Schram et al., 2007; Singh-Manoux et al., 2014) also provided data for the association of cognitive decline in those with intermediate (second tertile group) baseline concentrations of IL-6. There was no significant association between those with intermediate baseline IL-6 and the likelihood of cognitive decline at follow-up, compared to those with low IL-6 (OR 1.13, 95% CI 0.90–1.42; $p = 0.28$; **Figure 2B**). No significant study heterogeneity ($I^2 = 0\%$, pP = 0.59; **Figure 2B**) was evident.

TABLE 2 | Quality assessment of the included studies via the Newcastle-Ottawa Quality Assessment Scale.

Study	Selection[a]	Comparability[b]	Outcome[c]	Total
Weaver et al., 2002	****	**	**	8
Yaffe et al., 2003	****	**	***	9
Dik et al., 2005	***	**	**	7
Jordanova et al., 2007	**	**	***	7
Rafnsson et al., 2007	***	**	***	8
(Schram et al., 2007) (Rotterdam cohort)	****	**	**	8
(Schram et al., 2007) (Leiden 85-plus cohort)	***	**	***	8
Singh-Manoux et al., 2014	**	**	***	7

*Scores per section are presented as asterisks. * = one point. Only those answers with an asterisk are given a score. [a]Selection; (1) **Representativeness of the exposed cohort (high/intermediate IL-6 group)**: (a) Truly representative of the average community-dwelling older adults*. (b) Somewhat representative of the average community-dwelling older adults*. (c) Selected group of users e.g., nurses, volunteers. (d) No description of the derivation of the cohort. (2) **Selection of the non-exposed cohort (low IL-6 group)**: (a) Drawn from the same community as the exposed cohort*. (b) Drawn from a different source. (c) No description of the derivation of the non-exposed cohort. (3) **Ascertainment of IL-6 category**: (a) Quantified from blood (unstimulated) using an appropriate technique (e.g., ELISA)*. (b) No description. (4) **Demonstration that dementia was not present at start of study**: (a) Yes – assessed via interview or using an established cognitive test*. (b) No - presumed. [b]Comparability; (1) **Comparability of cohorts on the basis of the design or analysis**: a) Study controls for age AND gender in analysis*. (b) Study controls for education level or prior cognitive ability in analysis*. [c]Outcome; (1) **Assessment of outcome**: (a) Cognitive test (e.g., MMSE) which was the same as baseline*. (b) Self report. (d) No description. (2) **Was follow-up long enough for outcomes to occur**: (a) Yes (average ≥ 2 years)*. (b) No (average < 2 years). (3) **Adequacy of follow up of cohorts**: a) Complete follow up - all subjects accounted for*. (b) Subjects lost to follow up unlikely to introduce bias - small number lost (≤ 25%), or description provided of those lost suggesting no different from those followed*. (c) Follow up rate ≤50% and no description of those lost. (d) No statement.*

Association between Intermediate Baseline IL-6 and Global Cognitive Decline: Risk of Bias Analysis

No publication bias was observed when visually inspecting the Begg's funnel plot (**Figure 3B**) and through an Egger's test ($p = 0.216$).

TABLE 3 | Summary of global cognitive assessments and definitions used in each study included in the meta-analysis.

Paper	Cognitive test	Global cognitive decline definition	IL-6 categories (pg/mL)	Blood specimen	Model adjustments
Dik et al., 2005	MMSE	Change based on cognitive test and regression to the mean.	Low: <5.0 High: 5.0–58.3	Serum	Age, gender, education.
Jordanova et al., 2007	Battery	Factor analysis based on cognitive score change.	Low: ≤3.1 High: >3.1	Plasma	Age, gender, education, stroke, hypertension, diabetes, smoking, alcohol status, BMI, NSAID use, disability.
Rafnsson et al., 2007	Battery	≥ 1 standard deviations from a general cognitive factor value.	Low: 0.55–1.66 Intermediate: 1.67–3.00 High: 3.01–100	Plasma	Age, gender, depressed mood, peak prior cognitive ability, lifetime smoking, alcohol intake, presence of major cardiovascular diseases, presence of diabetes mellitus.
(Schram et al., 2007) (Leiden 85-Plus cohort)	MMSE	≥3 points in MMSE scores.	Low: 0–4 Intermediate: 5–25 High: 26–75,001	Plasma	Age, gender, education.
(Schram et al., 2007) (Rotterdam cohort)	MMSE	≥3 points in MMSE scores.	Low: 0.53–1.82 Intermediate: 1.82–3.09 High: 3.10–80	Plasma	Age, gender, education.
Singh-Manoux et al., 2014	MMSE	≥3 points in MMSE scores.	Low: <1.18 Intermediate: 1.18–1.74 High: ≥1.75	Serum	Age, gender, ethnicity, education, smoking, obesity, Framingham cardiovascular disease risk score, coronary heart disease, stroke, cancer, diabetes antidepressant use.
Weaver et al., 2002	Battery	≥7 points in cognitive score.	Low: <2.13 Intermediate: 2.13–3.8 High: ≥3.8	Plasma	Age, race, gender, yearly income, education level, alcohol intake, activity level, BMI, self-reported history of cancer or diabetes, HBA1c levels, baseline cognitive scores.
Yaffe et al., 2003	3MS	>5 points in 3MS scores, or if taking cholesterase inhibitor, or hospitalized for dementia.	Low: 0.2–1.4 High: 2.4–16.0	Plasma	Age, education, race, gender, smoking, alcohol use, BMI, self-reported health, co-morbidities, baseline 3MS, use of NSAID.

DISCUSSION

Individually, many studies included within these analyses did not report significant findings. However, from a collective analysis containing 15,828 older adults who were community-dwelling at baseline, those with high baseline IL-6 were 1.42 times more likely to develop global cognitive decline during a follow-up period of 2–7 years, compared to those with low IL-6.

This is the first meta-analysis to investigate baseline IL-6 and longitudinal global cognitive decline in non-demented adults. Our results suggest that there is an association with high, but not intermediate, baseline concentrations of IL-6 and an increased likelihood of global cognitive decline upon follow-up. Interestingly, three of the included studies (Schram et al., 2007; Singh-Manoux et al., 2014) defined cognitive decline as a change of ≥3 points in MMSE scores between baseline and follow-up. The MMSE is a popular cognitive assessment frequently utilized in large, population based cohorts. It has previously been suggested that a change in MMSE scores of between 2 and 4 points indicated a reliable change at the 90% confidence level in non-demented older adults (Stein et al., 2012). Based on this and to reduce heterogeneity between studies, it may be useful if future studies adopt this definition when the MMSE is applied to define cognitive decline.

Mechanisms underlying bidirectional neuro-immune interactions are becoming increasingly understood (Engelhardt et al., 2017; Pavlov and Tracey, 2017) with numerous routes into the CNS being documented. For example, IL-6 has been shown

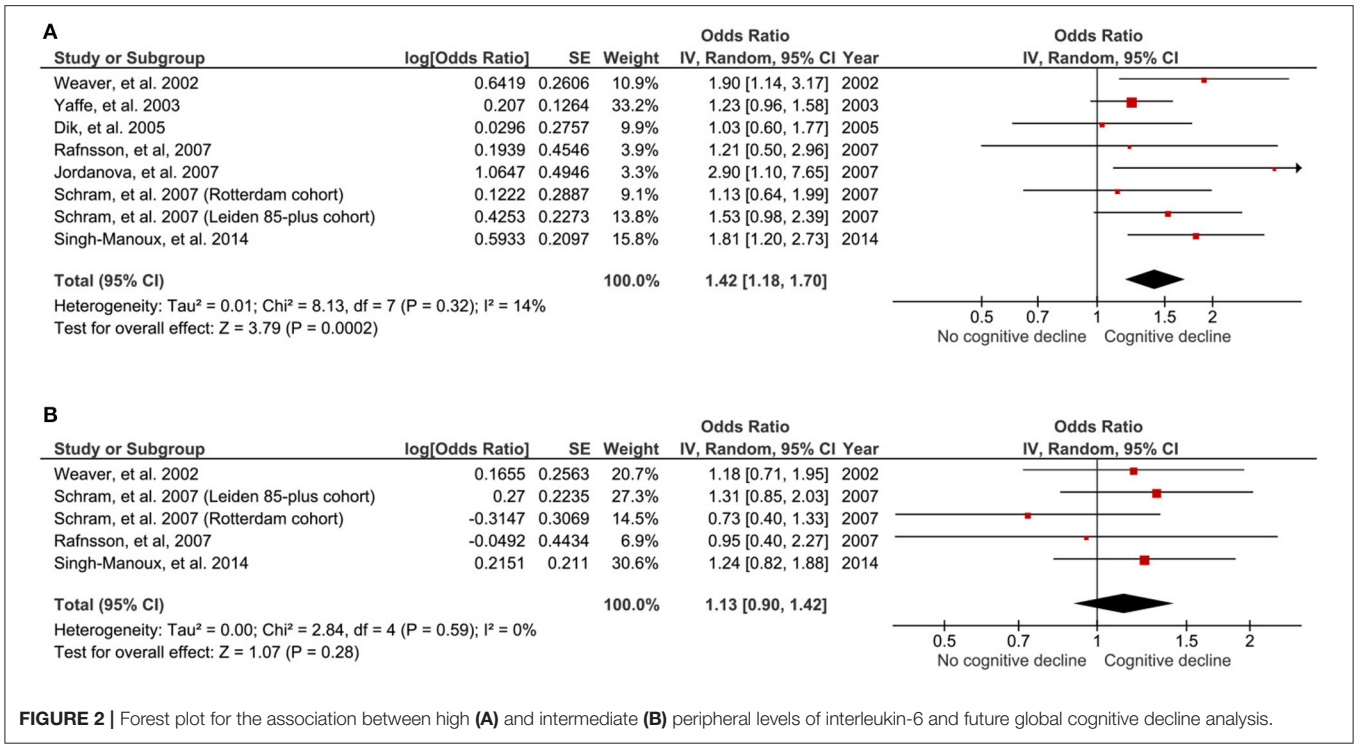

FIGURE 2 | Forest plot for the association between high **(A)** and intermediate **(B)** peripheral levels of interleukin-6 and future global cognitive decline analysis.

TABLE 4 | Subgroup analyses for the association between high peripheral IL-6 and global cognitive decline analysis.

		Main effect					Heterogeneity			
	Studies, *n*	Odds ratio	95% CI		*Z*	*p*	χ^2	df	p	I^2
DURATION OF FOLLOW-UP										
<4 years	4	1.33	1.03	1.73	2.15	0.03	4.05	3	0.26	26%
≥4 years	4	1.59	1.22	2.08	3.44	<0.01	2.60	3	0.46	0%
SAMPLE SIZE AT BASELINE										
<1,000	3	1.61	1.12	2.33	2.54	0.01	1.85	2	0.40	0%
≥1,000	5	1.37	1.10	1.72	2.79	<0.01	5.56	4	0.23	28%
METHOD USED TO ASSESS COGNITION										
MMSE	4	1.41	1.09	1.82	2.62	<0.01	3.43	3	0.33	13%
Others	4	1.51	1.07	2.13	2.37	0.02	4.67	3	0.20	36%
QUALITY SCORE										
<8	3	1.61	0.97	2.67	1.85	0.06	4.34	2	0.11	54%
≥8	5	1.34	1.11	1.61	3.10	<0.01	2.99	4	0.56	0%

CI, Confidence interval; MMSE, Mini Mental State Examination.

to directly cross the BBB in a murine model, albeit at a low level, via a saturable transport system (Banks et al., 1994). It is also proposed that peripheral cytokines may have greater access to the CNS through the circumventricular organs (CVOs), brain regions which have a high permeability to the circulating milieu. For example, in rats peripheral injections of IL-6 resulted in the activation of cells within the CVOs (Harré et al., 2003), suggesting a potential pathway from periphery to CNS. Other routes into the CNS include indirect signal propagation at the BBB (Eskilsson et al., 2014). There is also a significant relationship between IL-6 concentrations in the plasma and cerebrospinal fluid (CSF) in those with AD (Sun et al., 2003) and a lagged correlation has been observed in healthy subjects (Agorastos et al., 2014). It is also possible that the aged CNS is more susceptible to peripheral inflammatory cytokines. For example, Montagne and colleagues have shown that the BBB in humans becomes damaged and permeability is increased within regions responsible for learning and memory, such as the hippocampus, during aging (Montagne et al., 2015). Additionally, recurrent insults toward the BBB, due to recurrent infections or even increased exposure to exogenous IL-6 (de Vries et al., 1996), have also been shown to increase BBB permeability (Varatharaj and Galea, 2017). Therefore, it

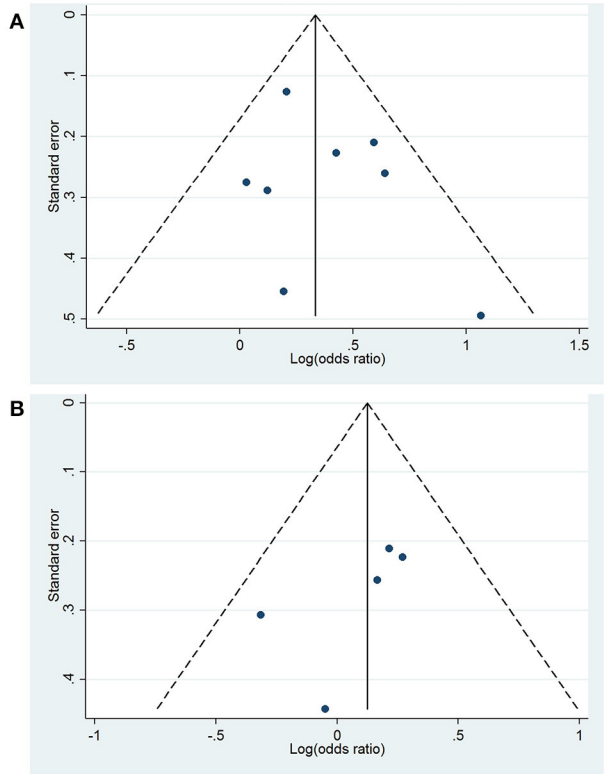

FIGURE 3 | Begg's funnel plots for the association between high **(A)** and intermediate **(B)** peripheral levels of interleukin-6 and future global cognitive decline analysis. Funnel plot displays the log(odds ratio) against the standard error, with the pooled effect (solid line) and pseudo 95% confidence limits (dashed lines).

is possible that BBB dysfunctions, both age-associated and the presence of underlying infections, may be present within these populations. Taken together, there is potential for peripheral IL-6 to gain access into the CNS and this is further exacerbated during aging.

The periphery to CNS routes raises the possibility of peripheral IL-6 as a contributing factor toward neuroinflammation. Conversely, raised IL-6 levels in the circulation may merely be a reflection of the neuroinflammatory processes occurring during neurodegeneration and cognitive decline. For example, in rats it has been shown that IL-6 is secreted from the brain following intracerebroventricular injections of labeled IL-6 (Chen et al., 1997) and following a cerebroventricular inflammatory insult (Romero et al., 1996). Further, in humans, the brain has been shown to secrete IL-6 into the circulation following prolonged exercise (Nybo et al., 2002). Considering the plethora of sources of IL-6 production within the CNS, including astrocytes, microglia and neurones and that IL-6 is upregulated during neurodegeneration (Erta et al., 2012), it could be possible that some CNS-derived IL-6 may spill over into the periphery. To elaborate on the cause or effect conundrum, future studies should explore the effect of chronic low-grade increases in peripheral IL-6 levels and the effect this has on the CNS *in vivo*.

Physiologically, IL-6 is essential for developmental functions within the CNS including promoting neural differentiation, modulating adult neurogenesis and controlling neurotrophic expression (Erta et al., 2012). However, prolonged and exacerbated IL-6 exposure to the brain has been associated with numerous neuropathological outcomes. For example, incubating rat hippocampal precursor cells *in vitro* with recombinant IL-6 reduced neurogenesis by approximately 50% and increased the number of apoptotic cells (Monje et al., 2003). Furthermore, the overproduction of IL-6 by astroglia in transgenic mice decreased neurogenesis rates within the dentate gyrus by 63% as well as reducing the proliferation, survival and differentiation of neural progenitor cells (Vallières et al., 2002). Corroborating this, and complementing our findings, research utilizing magnetic resonance imaging has found strong associations between high blood IL-6 concentrations with hippocampal gray matter volumes (Marsland et al., 2008; Satizabal et al., 2012), total brain volumes (Jefferson et al., 2007; Satizabal et al., 2012) and an increased rate of cortical thinning over time (McCarrey et al., 2014). These results suggest that long-term exposure of the brain to increased IL-6 can directly impede neurogenesis and neuronal health, which may manifest into cognitive decline.

The current findings that non-demented older adults with high baseline IL-6 are at an increased risk of future cognitive decline could make it possible of identifying at risk individuals. To bring this into a clinical setting, a considerable amount of methodological standardization is required. Firstly, IL-6 peripheral measures are heavily influenced by a circadian rhythm resulting in considerable inter- and intra-subject variability (Agorastos et al., 2014). Further, as noted in our literature analysis, other parameters such as, the type of commercially available ELISA used, the type of collection tubes used for blood collection, and the fasted state of participants, all varied between studies. These methodological issues have been shown to influence cytokine measurements in clinical research (Zhou et al., 2010) and is the reason why we chose to look at categorically defined IL-6 levels as opposed to continuous measures. Exactly what the specific concentrations of IL-6 classed as "high" and "low" will become clearer once these methodological discrepancies have been addressed.

LIMITATIONS

Despite high quality of the studies used in these analyses, we do accept that there are a few limitations. Firstly, the methodological designs varied considerably between the studies included. We anticipated such discrepancies by applying random-effects analysis throughout. Secondly, we cannot rule out publication bias since the power of statistical tests used here to assess publication bias are significantly reduced when there are fewer than 10 studies in the analysis. Also, we cannot rule out confounding effects by underlying factors that are linked to both elevated peripheral IL-6 levels and cognitive decline, such as cardiovascular disease (CVD) (Compté et al., 2013). We did, however, extract the most adjusted models, many included some adjustments for CVD risk (**Table 3**),

which would have minimized such an effect. Additionally, none of the included studies accounted for dietary factors which are known to influence cognition and IL-6 regulation. Recent insights utilizing the Whitehall II cohort indicate an association between dietary patterns, IL-6 concentrations and cognition in older adults (Ozawa et al., 2017). Also measures of obesity, such as BMI, are also known to correlate with peripheral IL-6 concentrations (Charles et al., 2011). Therefore, it would be interesting if future studies expand on this dietary and obesity association. Finally, almost all included studies reported a collated analysis involving a mix of males and females, therefore potential gender effects could not be explored.

CONCLUSION

In conclusion, these results add further evidence for the association between high peripheral inflammation, as measured by blood IL-6, with future cognitive decline. Specifically, those with high IL-6 were 1.42 times more likely to experience global cognitive decline, compared to those with low IL-6. Future studies should focus on exploring the use of circulating IL-6 as a biomarker for future cognitive health and standardizing the processing and measuring of this analyte.

AUTHOR CONTRIBUTIONS

SB: study design, literature search, statistical analysis, quality assessment, writing of the manuscript. JS: quality assessment, writing of the manuscript. CM: literature search, quality assessment, writing of the manuscript.

ACKNOWLEDGMENTS

We would like to thank Dr's Rafnsson and Schram for accepting and performing the requested repeat statistical analysis.

REFERENCES

Agorastos, A., Hauger, R. L., Barkauskas, D. A., Moeller-Bertram, T., Clopton, P. L., Haji, U., et al. (2014). Circadian rhythmicity, variability and correlation of interleukin-6 levels in plasma and cerebrospinal fluid of healthy men. *Psychoneuroendocrinology* 44, 71–82. doi: 10.1016/j.psyneuen.2014.02.020

Banks, W. A., Kastin, A. J., and Gutierrez, E. G. (1994). Penetration of interleukin-6 across the murine blood-brain barrier. *Neurosci. Lett.* 179, 53–56. doi: 10.1016/0304-3940(94)90933-4

Charles, B. A., Doumatey, A., Huang, H., Zhou, J., Chen, G., Shriner, D., et al. (2011). The Roles of IL-6, IL-10, and IL-1RA in obesity and insulin resistance in African-Americans. *J. Clin. Endocrinol. Metab.* 96, E2018–E2022. doi: 10.1210/jc.2011-1497

Chen, G., Castro, W. L., Chow, H. H., and Reichlin, S. (1997). Clearance of 125I-labeled interleukin-6 from brain into blood following intracerebroventricular injection in rats. *Endocrinology* 138, 4830–4836. doi: 10.1210/endo.138.11.5533

Compté, N., Boudjeltia, K. Z., Vanhaeverbeek, M., De, B., Pepersack, T., Tassignon, J., et al. (2013). Increased basal and alum-induced interleukin-6 levels in geriatric patients are associated with cardiovascular morbidity. *PLoS ONE* 8:e81911. doi: 10.1371/journal.pone.0081911

Cunningham, C., and Hennessy, E. (2015). Co-morbidity and systemic inflammation as drivers of cognitive decline: new experimental models adopting a broader paradigm in dementia research. *Alzheimers. Res. Ther.* 7:33. doi: 10.1186/s13195-015-0117-2

de Vries, H. E., Blom-Roosemalen, M. C. M., Oosten, M., van, de Boer, A. G., van Berkel, T. J. C., Breimer, D. D., et al. (1996). The influence of cytokines on the integrity of the blood-brain barrier *in vitro*. *J. Neuroimmunol.* 64, 37–43. doi: 10.1016/0165-5728(95)00148-4

Dik, M. G., Jonker, C., Hack, C. E., Smit, J. H., Comijs, H. C., and Eikelenboom, P. (2005). Serum inflammatory proteins and cognitive decline in older persons. *Neurology* 64, 1371–1377. doi: 10.1212/01.WNL.0000158281.08946.68

Donzis, E. J., and Tronson, N. C. (2014). Modulation of learning and memory by cytokines: signaling mechanisms and long term consequences. *Neurobiol. Learn. Mem.* 115, 68–77. doi: 10.1016/j.nlm.2014.08.008

Engelhardt, B., Vajkoczy, P., and Weller, R. O. (2017). The movers and shapers in immune privilege of the CNS. *Nat. Immunol.* 18, 123–131. doi: 10.1038/ni.3666

Erta, M., Quintana, A., and Hidalgo, J. (2012). Interleukin-6, a Major Cytokine in the Central Nervous System. *Int. J. Biol. Sci.* 8, 1254–1266. doi: 10.7150/ijbs.4679

Eskilsson, A., Mirrasekhian, E., Dufour, S., Schwaninger, M., Engblom, D., and Blomqvist, A. (2014). Immune-induced fever is mediated by IL-6 receptors on brain endothelial cells coupled to STAT3-dependent induction of brain endothelial prostaglandin synthesis. *J. Neurosci.* 34, 15957–15961. doi: 10.1523/JNEUROSCI.3520-14.2014

Franceschi, C., and Campisi, J. (2014). Chronic inflammation (inflammaging) and its potential contribution to age-associated diseases. *J. Gerontol. A Biol. Sci. Med. Sci.* 69(Suppl. 1), S4–S9. doi: 10.1093/gerona/glu057

Harré, E.-M., Roth, J., Gerstberger, R., and Hübschle, T. (2003). Interleukin-6 mediates lipopolysaccharide-induced nuclear STAT3 translocation in astrocytes of rat sensory circumventricular organs. *Brain Res.* 980, 151–155. doi: 10.1016/S0006-8993(03)02923-8

Hunter, C. A., and Jones, S. A. (2015). IL-6 as a keystone cytokine in health and disease. *Nat. Immunol.* 16, 448–457. doi: 10.1038/ni.3153

Jefferson, A. L., Massaro, J. M., Wolf, P. A., Seshadri, S., Au, R., Vasan, R. S., et al. (2007). Inflammatory biomarkers are associated with total brain volume. *Neurology* 68, 1032–1038. doi: 10.1212/01.wnl.0000257815.20548.df

Jordanova, V., Stewart, R., Davies, E., Sherwood, R., and Prince, M. (2007). Markers of inflammation and cognitive decline in an African-Caribbean population. *Int. J. Geriatr. Psychiatry* 22, 966–973. doi: 10.1002/gps.1772

Korolev, I. O., Symonds, L. L., and Bozoki, A. C. (2016). Predicting progression from mild cognitive impairment to Alzheimer's Dementia using clinical, MRI, and plasma biomarkers via probabilistic pattern classification. *PLoS ONE* 11:e0138866. doi: 10.1371/journal.pone.0138866

Lai, K. S. P., Liu, C. S., Rau, A., Lanctôt, K. L., Köhler, C. A., Pakosh, M., et al. (2017). Peripheral inflammatory markers in Alzheimer's disease: a systematic review and meta-analysis of 175 studies. *J. Neurol. Neurosurg. Psychiatry* 88, 876–882. doi: 10.1136/jnnp-2017-316201

Li, D., and Yu, F. (2017). Peripheral inflammatory biomarkers and cognitive decline in older adults with and without Alzheimer's Disease: a systematic review. *J. Gerontol. Nurs.* 43, 53–60. doi: 10.3928/00989134-20170519-01

Liberati, A., Altman, D. G., Tetzlaff, J., Mulrow, C., Gøtzsche, P. C., Ioannidis, J. P. A., et al. (2009). The PRISMA statement for reporting systematic reviews and meta-analyses of studies that evaluate healthcare interventions: explanation and elaboration. *BMJ* 339:b2700. doi: 10.1136/bmj.b2700

Marsland, A. L., Gianaros, P. J., Abramowitch, S. M., Manuck, S. B., and Hariri, A. R. (2008). Interleukin-6 covaries inversely with Hippocampal grey matter volume in middle-aged adults. *Biol. Psychiatry* 64, 484–490. doi: 10.1016/j.biopsych.2008.04.016

McCarrey, A. C., Pacheco, J., Carlson, O. D., Egan, J. M., Thambisetty, M., An, Y., et al. (2014). Interleukin-6 is linked to longitudinal rates of cortical thinning in aging. *Transl. Neurosci.* 5, 1–7. doi: 10.2478/s13380-014-0203-0

Monje, M. L., Toda, H., and Palmer, T. D. (2003). Inflammatory blockade restores adult hippocampal neurogenesis. *Science* 302, 1760–1765. doi: 10.1126/science.1088417

Montagne, A., Barnes, S. R., Sweeney, M. D., Halliday, M. R., Sagare, A. P., Zhao, Z., et al. (2015). Blood-brain barrier breakdown in the aging human hippocampus. *Neuron* 85, 296–302. doi: 10.1016/j.neuron.2014.12.032

Nybo, L., Nielsen, B., Klarlund Pedersen, B., Møller, K., and Secher, N. H. (2002). Interleukin-6 release from the human brain during prolonged exercise. *J. Physiol.* 542, 991–995. doi: 10.1113/jphysiol.2002.022285

Ozawa, M., Shipley, M., Kivimaki, M., Singh-Manoux, A., and Brunner, E. J. (2017). Dietary pattern, inflammation and cognitive decline: the Whitehall II prospective cohort study. *Clin. Nutr. Edinb. Scotl.* 36, 506–512. doi: 10.1016/j.clnu.2016.01.013

Pavlov, V. A., and Tracey, K. J. (2017). Neural regulation of immunity: molecular mechanisms and clinical translation. *Nat. Neurosci.* 20, 156–166. doi: 10.1038/nn.4477

Peng, L., Xu, L., and Ouyang, W. (2013). Role of Peripheral Inflammatory Markers in Postoperative Cognitive Dysfunction (POCD): a meta-analysis. *PLoS ONE* 8:e79624. doi: 10.1371/journal.pone.0079624

Rafnsson, S. B., Deary, I. J., Smith, F. B., Whiteman, M. C., Rumley, A., Lowe, G. D. O., et al. (2007). Cognitive decline and markers of inflammation and hemostasis: the Edinburgh Artery Study. *J. Am. Geriatr. Soc.* 55, 700–707. doi: 10.1111/j.1532-5415.2007.01158.x

Romero, L. I., Kakucska, I., Lechan, R. M., and Reichlin, S. (1996). Interleukin-6 (IL-6) is secreted from the brain after intracerebroventricular injection of IL-1 beta in rats. *Am. J. Physiol.* 270, R518–R524.

Satizabal, C. L., Zhu, Y. C., Mazoyer, B., Dufouil, C., and Tzourio, C. (2012). Circulating IL-6 and CRP are associated with MRI findings in the elderly: the 3C-Dijon Study. *Neurology* 78, 720–727. doi: 10.1212/WNL.0b013e318248e50f

Scafato, E., Gandin, C., Galluzzo, L., Ghirini, S., Cacciatore, F., Capurso, A., et al. (2010). Prevalence of Aging-Associated Cognitive Decline in an Italian elderly population: results from cross-sectional phase of Italian PRoject on Epidemiology of Alzheimer's disease (IPREA). *Aging Clin. Exp. Res.* 22, 440–449. doi: 10.3275/6970

Schram, M. T., Euser, S. M., de Craen, A. J. M., Witteman, J. C., Frölich, M., Hofman, A., et al. (2007). Systemic markers of inflammation and cognitive decline in old age. *J. Am. Geriatr. Soc.* 55, 708–716. doi: 10.1111/j.1532-5415.2007.01159.x

Singh-Manoux, A., Dugravot, A., Brunner, E., Kumari, M., Shipley, M., Elbaz, A., et al. (2014). Interleukin-6 and C-reactive protein as predictors of cognitive decline in late midlife. *Neurology* 83, 486–493. doi: 10.1212/WNL.0000000000000665

Spooren, A., Kolmus, K., Laureys, G., Clinckers, R., De Keyser, J., Haegeman, G., et al. (2011). Interleukin-6, a mental cytokine. *Brain Res. Rev.* 67, 157–183. doi: 10.1016/j.brainresrev.2011.01.002

Stein, J., Luppa, M., Maier, W., Wagner, M., Wolfsgruber, S., Scherer, M., et al. (2012). Assessing cognitive changes in the elderly: reliable change indices for the Mini-Mental State Examination. *Acta Psychiatr. Scand.* 126, 208–218. doi: 10.1111/j.1600-0447.2012.01850.x

Sun, Y. X., Minthon, L., Wallmark, A., Warkentin, S., Blennow, K., and Janciauskiene, S. (2003). Inflammatory markers in matched plasma and cerebrospinal fluid from patients with Alzheimer's disease. *Dement. Geriatr. Cogn. Disord.* 16, 136–144. doi: 10.1159/000071001

Swardfager, W., Lanctôt, K., Rothenburg, L., Wong, A., Cappell, J., and Herrmann, N. (2010). A Meta-Analysis of Cytokines in Alzheimer's Disease. *Biol. Psychiatry* 68, 930–941. doi: 10.1016/j.biopsych.2010.06.012

United Nations, (2015). *Population Division World Population Prospects 2015.* Available Online at: http://esa.un.org/unpd/wpp/Download/Probabilistic/Population/ (Accessed January 22, 2016).

Vallières, L., Campbell, I. L., Gage, F. H., and Sawchenko, P. E. (2002). Reduced hippocampal neurogenesis in adult transgenic mice with chronic astrocytic production of interleukin-6. *J. Neurosci.* 22, 486–492.

Varatharaj, A., and Galea, I. (2017). The blood-brain barrier in systemic inflammation. *Brain Behav. Immun.* 60, 1–12. doi: 10.1016/j.bbi.2016.03.010

Weaver, J. D., Huang, M. H., Albert, M., Harris, T., Rowe, J. W., and Seeman, T. E. (2002). Interleukin-6 and risk of cognitive decline: MacArthur studies of successful aging. *Neurology* 59, 371–378. doi: 10.1212/WNL.59.3.371

Wells, G., Shea, B., O'Connell, D., Peterson, J., Welch, V., Losos, M., et al. (2000). *The Newcastle - Scale for Assessing the Quality of Nonrandomised Studies in Meta-Analyses.pdf.* Available Online at: http://www.medicine.mcgill.ca/rtamblyn/Readings/The%20Newcastle%20-%20Scale%20for%20assessing%20the%20quality%20of%20nonrandomised%20studies%20in%20meta-analyses.pdf (Accessed October 21, 2016).

Yaffe, K., Lindquist, K., Penninx, B. W., Simonsick, E. M., Pahor, M., Kritchevsky, S., et al. (2003). Inflammatory markers and cognition in well-functioning African-American and white elders. *Neurology* 61, 76–80. doi: 10.1212/01.WNL.0000073620.42047.D7

Zhou, X., Fragala, M. S., McElhaney, J. E., and Kuchel, G. A. (2010). Conceptual and methodological issues relevant to cytokine and inflammatory marker measurements in clinical research. *Curr. Opin. Clin. Nutr. Metab. Care* 13, 541–547. doi: 10.1097/MCO.0b013e32833cf3bc

Conflict of Interest Statement: The authors declare that the research was conducted in the absence of any commercial or financial relationships that could be construed as a potential conflict of interest.

frontiers in Aging Neuroscience

ORIGINAL RESEARCH
published: 06 August 2018
doi: 10.3389/fnagi.2018.00236

Systemic Inflammation Mediates Age-Related Cognitive Deficits

*Tian Lin[1†], Gene A. Liu[1†], Eliany Perez[1], Robert D. Rainer[1], Marcelo Febo[2], Yenisel Cruz-Almeida[3,4] and Natalie C. Ebner[1,3,4]**

[1]Department of Psychology, University of Florida, Gainesville, FL, United States, [2]Department of Psychiatry, University of Florida, Gainesville, FL, United States, [3]Pain Research and Intervention Center of Excellence, University of Florida, Gainesville, FL, United States, [4]Center for Cognitive Aging and Memory, Department of Clinical and Health Psychology, University of Florida, Gainesville, FL, United States

The association between systemic inflammation and cognitive deficits is well-documented. Further, previous studies have shown that systemic inflammation levels increase with age. The present study took a novel approach by examining the extent to which systemic inflammation levels mediated age-related cognitive decline. Forty-seven young and 46 older generally healthy adults completed two cognitive tasks measuring processing speed and short-term memory, respectively. Serum concentrations of three inflammatory biomarkers (including interleukin 6 (IL-6), tumor necrosis factor alpha (TNF-α), C-reactive protein (CRP)) were measured in each participant. Both cognitive measures showed age-related deficits. In addition, levels of IL-6 and TNF-α were elevated with age. IL-6 partially mediated the difference in processing speed between the young and the older participant age group; there was no mediation effect for TNF-α and CRP. Considering chronological age, IL-6 partially accounted for age-related impairment in processing speed within older but not young participants. No effects were found for short-term memory. Evidence from this research supports the role of inflammatory processes in age-related cognitive decline. Processes involved in this mediation and differences in inflammatory influence on specific cognitive functions are discussed.

Keywords: systemic inflammation, IL-6, cognitive aging, processing speed, moderated mediation

OPEN ACCESS

Edited by:
Ashok Kumar,
University of Florida, United States

Reviewed by:
Lisa M. Renzi-Hammond,
University of Georgia, United States
Sarah J. Barber,
San Francisco State University, United States

****Correspondence:***
Natalie C. Ebner
natalie.ebner@ufl.edu

[†]These authors have contributed equally to this work.

Received: *30 March 2018*
Accepted: *18 July 2018*
Published: *06 August 2018*

Citation:
Lin T, Liu GA, Perez E, Rainer RD, Febo M, Cruz-Almeida Y and Ebner NC (2018) Systemic Inflammation Mediates Age-Related Cognitive Deficits. Front. Aging Neurosci. 10:236. doi: 10.3389/fnagi.2018.00236

INTRODUCTION

Systemic Inflammation and Cognitive Impairment

Mounting evidence associates cognitive impairment with systemic immune activation. For example, elevated serum levels of pro-inflammatory cytokines, including interleukin 6 (IL-6), tumor necrosis factor alpha (TNF-α) and C-reactive protein (CRP), lead to impairments in overall cognition (Weaver et al., 2002; Schram et al., 2007) as well as impairments in specific functions, such as reduced processing speed (Bettcher et al., 2014), executive function (Heringa et al., 2014) and memory (Teunissen et al., 2003). These associations between systemic inflammation and cognitive impairment have been found in young (Brydon et al., 2008), middle-aged (Marsland et al., 2008, 2015), and older (Athilingam et al., 2013; Tegeler et al., 2016) adults. Furthermore, within older adults, this inflammation–cognition link has been documented among generally healthy individuals (Brydon et al., 2008; Heringa et al., 2014; Nadkarni et al., 2016; Tegeler et al., 2016) and in clinical samples with conditions like dementia (Trollor et al., 2010), heart failure (Athilingam et al., 2013) and late-life depression (Charlton et al., 2018). However, to our knowledge, previous studies have not directly examined the mediatory role of systemic inflammation on cognitive aging.

Systemic inflammation leads to elevated circulating pro-inflammatory cytokines, including IL-6, TNF-α and CRP, which can interact with the central nervous system through three main routes: (i) pro-inflammatory cytokine transport proteins enable limited active transport across the blood brain barrier (BBB), allowing for central action (Dantzer et al., 2008; Fung et al., 2012). (ii) Systemically produced cytokines can stimulate afferent nerves (e.g., the vagal nerve), which then transmit the currently heightened inflammatory status to lower brain stem regions. In particular, the vagal nerve projects to the nucleus of the solitary tract and higher neural regions (e.g., hypothalamus, amygdala and bed nucleus of the stria terminals; McCusker and Kelley, 2013). (iii) Circulating cytokines reach the circumventricular organs, which reside outside the BBB. There, cells expressing toll-like receptors respond to the increased inflammatory state, eliciting further production and release of pro-inflammatory cytokines, which can then enter the brain through volume diffusion (Vitkovic et al., 2000; Dantzer et al., 2008; McCusker and Kelley, 2013; Sankowski et al., 2015).

These three pathways, when stimulated peripherally, will activate microglia and astrocytes in the brain to produce pro-inflammatory cytokines, propagating the signal into the neural environment (Dantzer et al., 2008; Sankowski et al., 2015). This leads to comparable inflammation levels in the brain and the periphery (McCusker and Kelley, 2013). Elevated neuroinflammation can result in structural and functional impairment in the brain (Varatharaj and Galea, 2017), such as hippocampal atrophy (Sankowski et al., 2015; Varatharaj and Galea, 2017) and increased substantia nigra activity (Brydon et al., 2008), both of which have been associated with cognitive deficits (Brydon et al., 2008; Sankowski et al., 2015; Varatharaj and Galea, 2017).

Systemic Inflammation and Cognitive Aging

Pro-inflammatory cytokines can alter mitochondrial dynamics, decreasing metabolic efficiency and producing reactive oxygen species (ROS; Sankowski et al., 2015; van Horssen et al., 2017). ROS, in turn, can further elicit inflammatory immune response (Giunta, 2008; van Horssen et al., 2017), resulting in a positive feedforward loop. With accumulating oxidative stress and free radical damage, microglia and astrocytes become more likely to express a "primed" phenotype and morphology (Norden et al., 2015), characterized by an elevated baseline inflammatory state, a more vigorous pro-inflammatory response after reaching a lowered threshold, and resistance to any efforts to return to homeostasis (Norden and Godbout, 2013; Norden et al., 2015). The likelihood of progressing towards this primed phenotype increases with age as individuals are exposed to a greater amount of immune challenges. This increased risk for chronic low-grade inflammation in advanced age has been termed "inflammaging" (Giunta, 2008; Perry and Teeling, 2013; Dev et al., 2017; Charlton et al., 2018). A heightened inflammatory state, as seen with inflammaging, could partially explain the cognitive declines commonly observed in normal aging (Ownby, 2010).

Supporting this argument, recent research has reliably correlated increased inflammatory biomarker levels and diminished cognitive function in older adults (Bettcher et al., 2014; Heringa et al., 2014; Papenberg et al., 2016; Tegeler et al., 2016; Dev et al., 2017). These studies indicate that elevated systemic inflammation could be a risk factor for cognitive decline in old age, but do not directly imply that systemic inflammation mediates the age effect on cognitive functions. While some studies reported lower baseline cognitive scores in older adults with higher levels of systemic inflammation, these studies did not find evidence associating levels of systemic inflammation and rate of cognitive decline (Alley et al., 2008; Gimeno et al., 2008; Todd, 2017; but see Schram et al., 2007; Singh-Manoux et al., 2014). The present study, therefore, directly tested the mediation effect of systemic inflammation on age-related cognitive impairment in a sample with a wide age range across adulthood. One previous study examined the link between systemic inflammation and cognition in a sample with a relatively wide range (mean age = 65 years, SD = 11; Teunissen et al., 2003), but did not specifically test the mediation of systemic inflammation on cognitive aging.

The Present Study

Adopting a novel methodological approach that considered between-group and within-group age effects, we expanded previous research in testing the role of systemic inflammation as a mediator of the age−cognition link in generally healthy adults. In particular, we addressed the following specific research questions: (i) Does systemic inflammation account for differences in cognitive performance between the young and the older age group? We predicted that greater systemic inflammation in the older compared to the young age group will mediate age-related cognitive impairment (i.e., reduced processing speed and short-term memory; *Hypothesis 1; mediation of the between-group age effect*). (ii) Does systemic inflammation account for age-related differences in cognitive performance within young and older age groups? We predicted that greater systemic inflammation associated with greater chronological age will mediate cognitive impairment in both the young and the older age group (*Hypothesis 2; mediation of the within-group age effect*). (iii) Does the extent to which systemic inflammation accounts for age-related differences in cognitive performance vary between young and older age groups? We predicted that the mediation of the within-group age effect will be more pronounced in the older compared to the young age group (*Hypothesis 3; moderated mediation of the within-group age effect)*.

MATERIALS AND METHODS

Participants

We recruited participants through: (i) handout and flyer distribution on campus and the community; (ii) HealthStreet, a university community outreach service; and (iii) mail-outs via two university participant registries particularly geared towards older individuals. Exclusion criteria were based on eligibility requirements for a larger project and included pregnancy (determined via pregnancy tests given to all women under 63 years), breastfeeding, psychological disorder, severe mental

illness, excessive smoking or drinking and magnetic resonance imaging (MRI) incompatibility (as reported elsewhere; Ebner et al., 2015, 2016). The final sample for this report included 47 young (M = 22.3 years, SD = 2.73, 18–31 years, 47% female) and 46 older (M = 71.2 years, SD = 5.08, 63–80 years, 52% female) generally healthy adults.[1] A basic metabolic panel, participants' responses to a series of questions related to overall health, including diagnoses and medication intake, and a review of bodily systems by a licensed physician confirmed health status. All participants were Caucasian and fluent in English. As summarized in **Table 1**, older participants had more years of education than young participants. There was no difference between young and older participants in their self-reported physical and mental health.

Procedure

This data analysis was part of a larger project that comprised a phone screening and two campus visits. This report only includes data from the phone screening and the first campus visit (for additional publications from the larger project, see Ebner et al., 2015, 2016, 2018).

[1]The original sample included 105 participants. Four young and eight older participants had missing inflammation biomarker data, resulting in a final sample size of 93 participants for the present analysis.

TABLE 1 | Means (SD)/median (Q1, Q3) and age-group differences in demographic, sleep, stress, health, cognitive and inflammation measures.

Construct	Young participants (n = 47)	Older participants (n = 46)
Years of education	**15.46 (2.16)**	**16.62 (3.06)**
Typical sleep duration (in hours)	7.46 (1.45)	7.25 (1.09)
Current stress level	**3.35 (1.35)**	**2.44 (1.85)**
Health		
Number of bodily symptoms	**1 (0, 2)**	**4 (2, 7)**
Physical health	8.50 (1.13)	8.49 (1.00)
Mental health	8.46 (1.20)	8.84 (1.21)
Cognitive measures		
Processing speed	**64.38 (10.15)**	**45.72 (7.71)**
Short-term memory	**9.23 (1.94)**	**7.63 (2.44)**
Inflammation markers		
IL-6	**0.97 (0.71, 1.49)**	**2.07 (1.12, 2.62)**
TNF-α	**0.65 (0.45, 0.78)**	**0.91 (0.66, 1.25)**
CRP	613.7 (316.56, 1812.73)	957.82 (438.13, 2276.4)

*Note. Q1 = First Quartile; Q3 = Third Quartile. Typical Sleep Duration "*How many hours do you normally sleep per night?*" was measured by a single self-report item in hours. Current Stress Level "*Please rate your current stress*" was measured by a single self-report item on a scale from 1 =* Not at all stressed *to 10 =* Extremely stressed*. Number of Bodily Symptoms indicated the total number of symptoms that participants reported based on a brief review of all major bodily systems, in which participants indicated the presence (Yes or No) of each of 66 symptoms. Physical Health "*Please rate your general physical health*" and Mental Health "*Please rate your general mental health/mood*" were measured by single self-report items on a scale ranging from 1 =* Poor *to 10 =* Excellent*. We presented the median as well as the first and third quartiles for Number of Bodily Symptoms and for the inflammation biomarkers, given the positively skewed distribution of these variables. We applied bias-corrected bootstrapping with 10,000 resampling for the examination of age-group differences in the three inflammation biomarkers. Bold indicates significant age-group differences at $p < 0.05$.*

During the initial phone screening, older adults first underwent the Telephone Interview for Cognitive Status (TICS; M = 35.45, SD = 2.38, Min = 30, Max = 41, cut off ≤30; Brandt et al., 1988). All participants then completed the lab's internal Health Screening and Demographics Form soliciting a range of information, including marital status, current medications, exercise habits and non-medicinal substance use such as caffeine, nicotine, alcohol and recreational drugs.

The phone screening was followed by a campus visit where, after receiving informed written consent, behavioral measures for short-term memory and processing speed (in this order; see details below) were administered. Next, a licensed physician conducted a review of all major bodily systems (i.e., eyes, ears, nose, throat; pulmonary; genito-urinary; gastrointestinal; neurological; cardiovascular; musculoskeletal) before a professional phlebotomist performed a blood draw to conduct the basic metabolic panel and to determine serum inflammation biomarker levels for IL-6, TNF-α and CRP. Personality and social relationship data were also collected, as reported elsewhere (Ebner et al., 2018). Participants were instructed to stay hydrated and avoid food, exercise and sexual activity for 2 h before the visit. They were also instructed to avoid smoking, caffeine, alcohol and recreational drugs for 24 h before the visit. Controlling for individual diurnal cycles, all screening visits began in the morning, usually around 8:00 a.m.

Cognitive Measures

Processing Speed

The Digit Symbol-Substitution Task (DSST) from the Wechsler Adult Intelligence Scale (WAIS; Wechsler, 1981) was used to measure processing speed. In this task, participants are given a table pairing the digits 1 through 9 with nine distinct symbols (e.g., the number three is paired with a cross). Next, participants are presented with a sequence of 93 digits, ranging from 1 through 9. The goal is to identify individual digits, consider their corresponding symbol, and write that symbol in the space provided immediately below each respective digit, as quickly and accurately as possible. Participants are given 90 s to work through as much of the sequence as time permits. The number of correct responses was used to indicate processing speed, with higher scores indicating faster processing speed.

Short-Term Memory

The Rey Auditory Verbal Learning Test (RAVLT; Rey, 1964) was used to measure short-term memory. In this task, participants read a list of 15 words (letters per word: M = 5.0; word frequency: M = 55.8, SD = 86.3), one every 2 s, for concrete objects (e.g., "desk", "ranger"). Immediately after, participants are asked to write down each word they can recall. The number of words correctly recalled was used to indicate short-term memory, with more recalled words indicating better short-term memory.

Inflammation Biomarker Collection and Assay

Using serum tubes, a professional phlebotomist drew 10 mL of blood. After five inversions, samples rested at room temperature

for 30–60 min to clot before 1600× *g* centrifugation at 4°C for 15 min and were immediately stored at −80°C. Before assays, samples thawed on ice. Using Human Quantikine Enzyme-linked Immunosorbent Assay (ELISA), serum IL-6, TNF-α and CRP levels were measured in duplicate according to instructions from the manufacturer (R and D System, Minneapolis, MA, USA; CRP: DCRP00; IL-6: HS600B; TNFα: HSTA00D). Intra-assay coefficient of variation (CV) was less than 6% for IL-6, 15% for TNF-α and 3% for CRP, and inter-assay CV was less than 14% for IL-6, 17% for TNF-α and 8% for CRP. IL-6 and TNF-α levels were significantly higher in older than young participants (**Table 1**). IL-6 levels were significantly related with CRP levels in both young and older participants and with TNF-α levels in older but not young participants. In contrast, TNF-α and CRP levels were not related in either of the age groups (**Table 2**).

Statistical Analysis

We conducted two separate analytic models to determine the extent to which systemic inflammation accounted for age effects on processing speed and short-term memory, respectively. In each model, the cognitive performance measure served as the dependent variable. Age-group contrast (categorical variable; young participants = −1; older participants = 1) and chronological age (continuous variable) served as the two independent variables in each model to capture both the between-group and the within-group age effects. To remove multicollinearity between the age-group contrast and the chronological age variables, we centered the chronological age variable separately in each age group. The three systemic inflammation biomarker levels served as mediators in the models. In addition, we considered the interaction between the age-group contrast and chronological age on the three systemic inflammation biomarkers and the cognitive performance measure and we considered the interaction between the age-group contrast and the three systemic inflammation biomarkers on the cognitive performance measure. This model specification allowed us to determine the extent to which the mediation of systemic inflammation of the within-group age effect on the cognitive measures varied between young and older participants (i.e., *moderated mediation of the within-group age effect*).

TABLE 2 | Bivariate correlations among the three inflammations markers in young and older participants.

	IL-6	TNF-α	CRP
IL-6		−0.03	**0.28**
TNF-α	**0.41**		0.18
CRP	**0.52**	0.34	

Note. Correlation coefficients above the diagonal refer to young participants; correlation coefficients below the diagonal refer to older participants. We applied bias-corrected bootstrapping with 10,000 resampling to determine the significance of each correlation. Bold indicates significant age-group differences at p < 0.05. According to Fisher z-test, the correlation between interleukin 6 (IL-6) and tumor necrosis factor alpha (TNF-α) was significantly higher in older than young participants (z = −2.17, p = 0.03). In contrast, correlations between IL-6 and C-reactive protein (CRP; z = −1.35, p = 0.18) and between TNF-α and CRP (z = −0.80, p = 0.42) did not differ between the age groups.

We used PROCESS macro on SPSS (Hayes, 2013) for model testing. The program reports the results for the mediation of the within-group age effects. However, it does not report the indirect effects of the between-group age effects. We followed guidelines by VanderWeele and Vanstellandt (VanderWeele and Vansteelandt, 2009; Valeri and VanderWeele, 2013) to calculate these indirect effects for each inflammation biomarker. We set significance thresholds of $p < 0.05$ (two-tailed test) for all main effects and interactions. We applied bias-corrected bootstrap with 10,000 resampling for calculation of the 95% confidence interval (CI) to determine the significance of each indirect effect.

RESULTS

Mediation Effect of Systemic Inflammation on the Link Between Age and Processing Speed

IL-6

The effect of age-group contrast on IL-6 was significant ($B = 0.31$, $t_{(89)} = 2.22$, $p = 0.03$) in the moderated mediation model (**Figure 1A**), with higher IL-6 levels in the older compared to the young group. In contrast, neither the main effect of chronological age ($B = 0.04$, $t_{(89)} = 0.88$, $p = 0.38$) nor its interaction with the age-group contrast ($B = 0.04$, $t_{(89)} = 0.92$, $p = 0.36$) was significant. That is, even though IL-6 levels were higher for individuals in the older compared to the young group, higher chronological age in each age group was not associated with higher IL-6 levels. The main effect of IL-6 levels on processing speed was significant ($B = -2.11$, $t_{(83)} = -2.52$, $p = 0.01$), while the interaction between IL-6 levels and age-group contrast was not significant ($B = -0.07$, $t_{(83)} = -0.08$, $p = 0.93$). That is, individuals with higher IL-6 levels had lower processing speed with comparable effects across the two age groups. Further, IL-6 levels mediated the between-group age effect on processing speed (Effect = −0.68, 95% CI = [−1.76, −0.06]) and the within-group age effect on processing speed in the older (Effect = −0.17, 95% CI = [−0.47, −0.02]) compared to the young (Effect = −0.003, 95% CI = [−0.27, 0.35]) group.

TNF-α

Similar to IL-6, the effect of age-group contrast on TNF-α was significant ($B = 0.22$, $t_{(89)} = 3.68$, $p < 0.001$) in the moderated mediation model (**Figure 1B**), with higher TNF-α levels in the older compared to the young group. In contrast, neither the main effect of chronological age ($B = -0.01$, $t_{(89)} = -0.41$, $p = 0.68$) nor its interaction with the age-group contrast ($B = 0.02$, $t_{(89)} = 0.95$, $p = 0.34$) on TNF-α levels was significant. That is, consistent with findings for IL-6, even though levels of TNF-α were higher for individuals in the older compared to the young group, higher chronological age in either age groups was not associated with higher TNF-α levels. Neither the main effect of TNF-α ($B = -1.79$, $t_{(83)} = -0.71$, $p = 0.48$) nor its interaction with age-group contrast ($B = 0.77$, $t_{(83)} = 0.31$, $p = 0.76$) on processing speed was significant, suggesting no association between TNF-α levels and processing speed in either

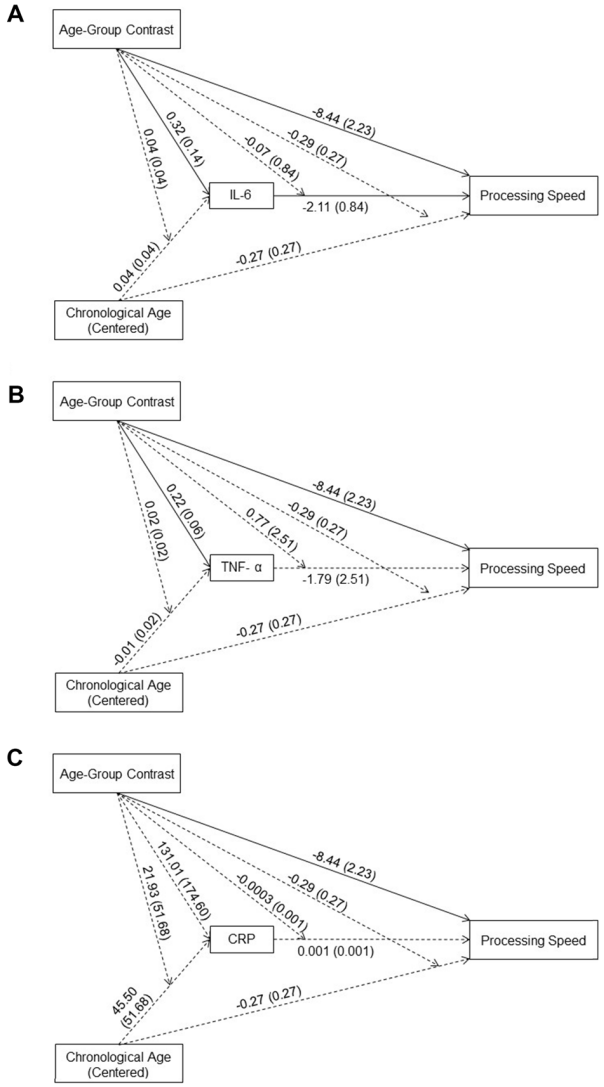

FIGURE 1 | Effects (*B* (*SE*)) of chronological age (centered), age-group contrast and interleukin 6 (IL-6) **(A)**, tumor necrosis factor alpha (TNF-α) **(B)**, and C-reactive protein (CRP) **(C)**, and their interactions on processing speed. To improve readability, separate figures show the results from the three systemic inflammation biomarkers while all variables were considered in a single model. Solid lines indicate significance at $p < 0.05$.

age group. Furthermore, TNF-α levels did not mediate the between-group age effect on processing speed (Effect = −0.22, 95% CI = [−1.21, 0.31]) nor the within-group age effect in either the young (Effect = 0.06, 95% CI = [−0.16, 0.81]) or the older (Effect = −0.01, 95% CI = [−0.14, 0.03]) group.

CRP

The effect of age-group contrast on CRP was not significant ($B = 131.01$, $t_{(89)} = 0.75$, $p = 0.46$) in the moderated mediation model (**Figure 1C**), suggesting comparable CRP levels in the young and older groups. Also, neither the main effect of chronological age ($B = 45.49$, $t_{(89)} = 0.88$, $p = 0.38$) nor its interaction with the age-group contrast ($B = 21.93$, $t_{(89)} = 0.42$, $p = 0.67$) on CRP was significant, suggesting no age-related changes in CRP in either age group. In addition, neither the main effect of CRP ($B = 0.001$, $t_{(83)} = 1.04$, $p = 0.30$) nor its interaction with the age-group contrast ($B = -0.0003$, $t_{(83)} = -0.50$, $p = 0.62$) was significant, suggesting no association between CRP levels and processing speed in either age group. Also, CRP did not mediate the between-group age effect on processing speed (Effect = 0.04, 95% CI = [−0.11, 0.50]) or the within-group age effect on processing speed in either the young (Effect = 0.02, 95% CI = [−0.15, 0.36]) or older (Effect = 0.02, 95% CI = [−0.07, 0.23]) group.

Direct Age Effects After Controlling for the Effects of IL-6, TNF-α and CRP

In the moderated mediation model, the effect of age-group contrast on processing speed was significant ($B = -8.44$, $t_{(83)} = -3.79$, $p < 0.001$). That is, after accounting for the effect of the three biomarkers on processing speed, the older group still showed lower processing speed than the young group. In addition, neither the main effect of chronological age ($B = -0.27$, $t_{(83)} = -0.99$, $p = 0.33$) nor its interaction with the age-group contrast ($B = -0.29$, $t_{(83)} = -1.06$, $p = 0.29$) on processing speed was significant.

Mediation Effect of Systemic Inflammation on the Link Between Age and Short-Term Memory

IL-6, TNF-α and CRP

As shown in **Figures 2A–C**, neither the main effects of the three inflammation biomarkers nor their interaction with age-group contrast on short-term memory was significant. Thus, our data did not support an effect of systemic inflammation on short-term memory in either age group. In addition, none of the inflammation biomarkers mediated the between-group age effects nor the within-group age effects on short-term memory in the young or older age groups. These results indicated that inflammation biomarker levels did not account for age-related difference in short-term memory in our sample.

Direct Age Effects After Controlling for the Effects of IL-6, TNF-α and CRP

In the moderated mediation model, the effect of age-group contrast on short-term memory was not significant ($B = -0.78$, $t_{(83)} = -1.37$, $p = 0.17$). In contrast, the main effect of chronological age on short-term memory was significant ($B = -0.16$, $t_{(83)} = -2.33$, $p = 0.02$), while its interaction with age-group contrast was not significant ($B = 0.06$, $t_{(83)} = 0.83$, $p = 0.41$). That is, after accounting for the effect of the three inflammation markers on short-term memory, the age-related decline in short-term memory was comparable for the age groups[2].

[2]Given an age-group difference in years of education in the current sample (**Table 1**), we conducted parallel analyses in which we considered years of education as covariate. The pattern of findings did not change by adding this covariate.

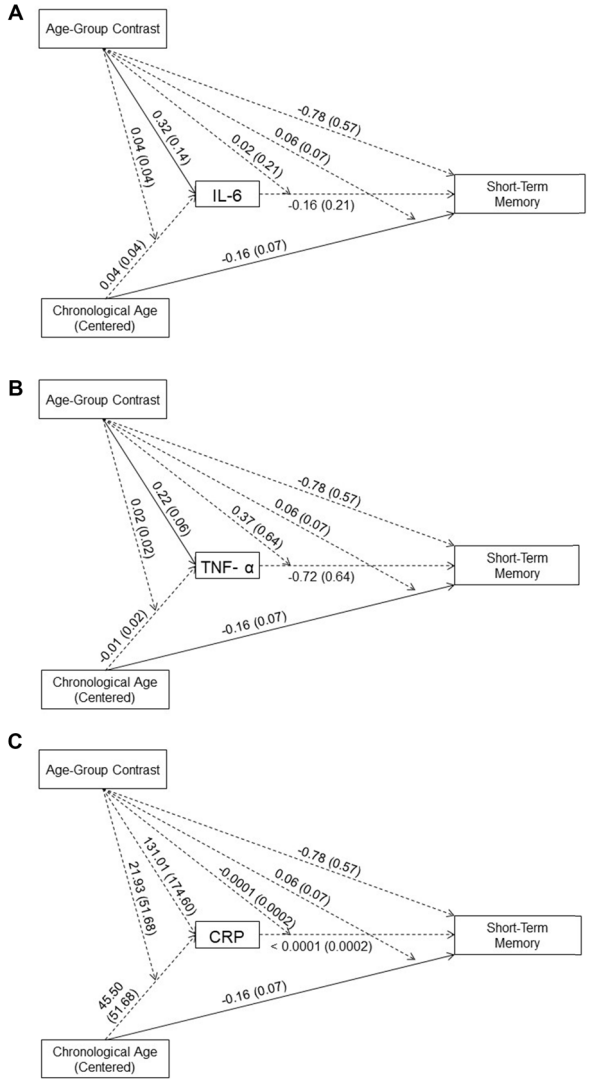

FIGURE 2 | Effects (*B* (*SE*)) of chronological age (centered), age-group contrast, and IL-6 **(A)**, TNF-α **(B)**, and CRP **(C)**, and their interactions on short-term memory. To improve readability, separate figures show the results from the three systemic inflammation biomarkers while all variables were considered in a single model. Solid lines indicate significance at $p < 0.05$.

DISCUSSION

Going beyond previous work, the present study took a novel methodological approach by examining the mediation of systemic inflammation (i.e., serum levels of IL-6, TNF-α and CRP) on age-related cognitive impairments (i.e., deficits in processing speed and short-term memory). We found that systemic inflammation partially explained differences in cognitive performance associated with increased age. In particular, IL-6 levels accounted for the age-group difference in processing speed, supporting Hypothesis 1 (*mediation of the between-group age effect*). Further, IL-6 levels accounted for the age-related differences in processing speed within the older but not the young age group, supporting Hypothesis 3 (*moderated mediation of the within-group age effect*). However, our data did not support Hypothesis 2 (*mediation of the within-group age effect*). Neither of the remaining two examined inflammatory biomarkers (i.e., TNF-α, CRP) nor short-term memory yielded any significant effects. Of note, the sample size in the present study was relatively small, limiting the statistical power to detect small effects and calling for future replication of our findings in a larger sample. Next, we discuss the novel findings generated in this work and their implications in more detail.

Age-Moderated Mediation of the Effect of Systemic Inflammation on Cognitive Aging

Previous work has documented a relationship between systemic inflammation and cognitive performance throughout adulthood, spanning young (Brydon et al., 2008), middle-aged (Marsland et al., 2008, 2015) and older (Athilingam et al., 2013; Tegeler et al., 2016) adults. The present study, however, represents the first direct test of a mediation effect of systemic inflammation on age-related cognitive impairment. In particular, our results suggest that the difference in systemic inflammation (measured by serum IL-6 levels) between young and older adults partially accounted for the difference in processing speed between these age groups. Additionally, IL-6 levels mediated age-related differences in processing speed within the older but not the young age group. Combining these two findings, the mediation of systemic inflammation on age-related variances in cognitive performance may become more pronounced with increased age (i.e., moderated mediation).

Two possible mechanisms may underlie the observed moderated mediation. First, age may increase the impact of systemic inflammation on cognition. In line with this suggestion, Baltes's (1997) life-span developmental theory (see also Kwasnicka et al., 2016) proposes that biological factors become increasingly influential on behavior as older adults experience reduced functioning and less effective compensatory processes to counter functional decline. However, in the present study we did not find a significant age-moderation of the effect of IL-6 levels on processing speed (**Figure 1A**). That is, the association between IL-6 levels and processing speed was comparable between young and older adults. Similarly, a previous study showed that an experimentally-induced elevation in inflammatory cytokine response (i.e., typhoid vaccination) consistently hindered reaction times among young participants (Brydon et al., 2008). This suggests that systemic inflammation produces similar impairments regardless of individual age. Therefore, individuals with higher systemic inflammatory levels, regardless of age, are more likely to show cognitive impairments. Thus, our data combined with previous studies, does not support the age-related enhancement in the association between systemic inflammation and cognitive impairment as an explanation for the observed moderated mediation.

Second, systemic inflammation levels increase with age, possibly because older adults face more immune challenges and become increasingly likely to display mild chronic inflammation (inflammaging; Giunta, 2008; Perry and Teeling, 2013; Dev et al., 2017; Charlton et al., 2018). With chronic conditions, primed microglia can yield deleterious effects on their local neuro-

environment, eliciting even greater inflammation, which may further prime microglia. This, in combination with continued accumulation of immune challenges, implies that inflammation levels, and their subsequent influence on cognition, may accelerate with time (Norden et al., 2015). Previous longitudinal studies, however, found no associations between systemic inflammation levels and the rate of cognitive decline (Alley et al., 2008; Gimeno et al., 2008; Todd, 2017). Importantly, these earlier studies focused on cohorts of older adults only. Further, while participants were tracked for about 10 year periods, this time span may have been too short to capture causal effects (Todd, 2017). Following from this argument, findings from the present study, which investigated a wider age range, showed that IL-6 levels partially accounted for the variance in processing speed between young and older adults. However, the cross-sectional nature of the present study does not allow causal conclusions of a mediation of inflammation on cognitive aging. Future longitudinal studies with longer data collection periods (e.g., across adulthood) are warranted.

Domain-Specificity of the Mediation Effect of Systemic Inflammation on Cognitive Aging

While participants showed age-related cognitive impairments in both cognitive tasks, systemic inflammation only accounted for the age-related differences in processing speed but not short-term memory. In line with these findings, previous work had documented domain-specificity in the inflammation−cognition link. Heringa et al. (2014), for example, showed that older adults' low-grade inflammation level, determined by the composite scores of various inflammatory biomarkers, including IL-6, IL-8, TNF-α and CRP, was negatively associated with processing speed, attention and executive functioning, but not other cognitive domains, including memory. Similarly, Tegeler et al. (2016) showed that higher levels of IL-6, IL-10 and CRP were associated with poorer executive function and processing speed, but not memory. In line with this correlational evidence, a recent intervention study found that participants who received antioxidant supplementation (e.g., resveratrol) for 90 days, compared to those in a control group who received placebo, showed improvement on processing speed (Anton et al., 2018; for a recent meta-analysis, also see Marx et al., 2018).

Importantly, microglial cells, which potentially represent the central mechanism for the neurological effects of inflammation, are widespread in the brain (Sankowski et al., 2015; van Horssen et al., 2017). This means that cognitive processes that integrate various areas across the brain may be more immediately vulnerable to inflammaging. Furthermore, a previous study reported a positive correlation between processing speed and whole-brain white matter volume, but not white matter volume from any sub-region in healthy young adults (Magistro et al., 2015). In addition, diffusion tensor imaging showed that processing speed in older adults was correlated with white matter integrity in diffuse areas of the frontal and parietal lobes (Kerchner et al., 2012). These results imply that processing speed is a cognitive process requiring coordination between various brain regions. Therefore, evidence from the present and previous studies associating systemic inflammation and processing speed, but not short-term memory (a more functionally localized process), supports the argument that systemic inflammation may cause global and diffuse brain damage with variable effects on individual cognitive domains.

We used the DSST to measure processing speed. Although the DSST has been commonly used as a measure of processing speed, previous research suggests that in addition to processing speed, other cognitive components such as executive function, visual scanning and memory contribute to performance in the DSST (Joy et al., 2003). Thus, participants' performance in the DSST may not only reflect their processing speed but represent a broader cognitive functioning composite. Future studies could apply multiple cognitive tasks and adopt a latent factor approach to clarify the associations between systemic inflammation and various cognitive functions.

In contrast, Charlton et al. (2018) reported an association between elevated inflammatory cytokines (i.e., IL-6) and memory impairment in older adults with late-life depression, but not in a healthy control group. Importantly, cytokine measures in individuals with late-life depression were compared with measures in relatively healthy older adults. The study showed a significant correlation between inflammation biomarker levels and the severity of depressive symptoms. Thus, it is possible that psychological conditions, like depression, introduce additional inflammation in peripheral and central immune systems, enhancing the impact of inflammation on various neurological structures and functions. As a result, more localized cognitive domains (e.g., memory) could become more vulnerable in these clinical conditions. Consistent with this notion is evidence of an age-related decline in hippocampal sub-region volume in adults with hypertension, but not individuals with normal blood pressure (Bender et al., 2013). Further supporting this argument, previous studies suggest elevated systemic inflammation as a risk factor for cognitive impairment (e.g., dementia, Fung et al., 2012; Hoogland et al., 2015; Marsland et al., 2015) among older adults. Thus, it is possible that the present study's exclusion criteria (e.g., no major illnesses, disorders, obesity), resulting in a sample of individuals with a relatively high health status, especially compared to older adults in the larger population, may have contributed to the lack of correlation between systemic inflammation and short-term memory.

The present study was embedded in the context of a larger project, which only included Caucasian individuals to avoid potential confounds in some of the central project outcomes. There is evidence, however, that racial minorities experience higher levels of inflammation (Paalani et al., 2011; Stepanikova et al., 2017), which may further contribute to age-related cognitive deficits within those populations (Windham et al., 2014; Goldstein et al., 2015). Thus, the lack of racial/ethnic diversity in the present sample limits the generalizability of our findings. Directly comparing racial/ethnic groups or analysis on a population-representative sample in future research will determine applicability of the present findings.

CONCLUSION

The present study directly tested the mediatory role of systemic inflammation on age-related differences in two cognitive domains (i.e., processing speed, short-term memory). Our findings establish systemic inflammation as a potential mechanism underlying cognitive impairments in aging. These results highlight the importance of reducing inflammation to promote cognitive health. Preventive measures, like regular erobic exercise and medications to reduce inflammation, adopted across the entire lifespan, may prove particularly important to protect against cognitive decline, especially among older adults.

ETHICS STATEMENT

This study was carried out in accordance with the recommendations of the Institutional Review Board at University of Florida. The protocol was approved by the Institutional Review Board at University of Florida. All subjects gave written informed consent in accordance with the Declaration of Helsinki.

AUTHOR CONTRIBUTIONS

TL conceptualized the study, collected and analyzed the data, and wrote the first draft of the manuscript. GL conceptualized the study, analyzed the data, and wrote the first draft of the manuscript. EP and RR assisted in article editing. MF and YC-A revised the final manuscript draft. NE conceptualized the study, supervised data collection and data analysis, and revised the manuscript.

FUNDING

This work was supported by the Department of Psychology at University of Florida, the McKnight Brain Research Foundation, and the University of Florida Center for Cognitive Aging and Memory, a University of Florida Clinical and Translational Science pilot award *(NIH/NCATS; UL*1 T*R000064)*, and a Scientific Research Network on Decision Neuroscience and Aging pilot award (*NIH/NIA, R24* A*G039350*) to NE. While working on this manuscript, NE was in part supported by the NIH-funded Claude D. Pepper Older Americans Independence Center (P30AG028740).

ACKNOWLEDGMENTS

The authors are grateful to the research teams and study staff from the Social-Cognitive and Affective Development lab and the Institute on Aging at the University of Florida for assistance in study implementation, data collection and data management. In addition, the authors wish to thank Brian Bouverat, Marvin Dirain and Jini Curry of the Metabolism and Translational Science Core at the Institute on Aging for technical assistance with the inflammation biomarker assays.

REFERENCES

Alley, D. E., Crimmins, E. M., Karlamangla, A., Hu, P., and Seeman, T. E. (2008). Inflammation and rate of cognitive change in high-functioning older adults. *J. Gerontol. A Biol. Sci. Med. Sci.* 63, 50–55. doi: 10.1093/gerona/63.1.50

Anton, S. D., Ebner, N. C., Dzierzewski, J. M., Zlatar, Z. Z., Gurka, M. J., Dotson, V. M., et al. (2018). Effects of 90 days of resveratrol supplementation on cognitive function in elders: a pilot study. *J. Altern. Complement. Med.* 24, 725–732. doi: 10.1089/acm.2017.0398

Athilingam, P., Moynihan, J., Chen, L., D'Aoust, R., Groer, M., and Kip, K. (2013). Elevated levels of interleukin 6 and C-reactive protein associated with cognitive impairment in heart failure. *Congest. Heart Fail.* 19, 92–98. doi: 10.1111/chf.12007

Baltes, P. B. (1997). On the incomplete architecture of human ontogeny. *Am. Psychol.* 52, 366–380. doi: 10.1037/0003-066x.52.4.366

Bender, A. R., Daugherty, A. M., and Raz, N. (2013). Vascular risk moderates associations between hippocampal subfield volumes and memory. *J. Cogn. Neurosci.* 25, 1851–1862. doi: 10.1162/jocn_a_00435

Bettcher, B. M., Watson, C. L., Walsh, C. M., Lobach, I. V., Neuhaus, J., Miller, J. W., et al. (2014). Interleukin-6, age and corpus callosum integrity. *PLoS One* 9:e106521. doi: 10.1371/journal.pone.0106521

Brandt, J., Spencer, M., and Folstein, M. (1988). The telephone interview for cognitive status. *Neuropsychiatry Neuropsychol. Behav. Neurol.* 1, 111–117.

Brydon, L., Harrison, N. A., Walker, C., Steptoe, A., and Critchley, H. D. (2008). Peripheral inflammation is associated with altered substantia nigra activity and psychomotor slowing in humans. *Biol. Psychiatry* 63, 1022–1029. doi: 10.1016/j.biopsych.2007.12.007

Charlton, R. A., Lamar, M., Zhang, A., Ren, X., Ajilore, O., Pandey, G. N., et al. (2018). Associations between pro-inflammatory cytokines, learning and memory in late-life depression and healthy aging. *Int. J. Geriatr. Psychiatry* 33, 104–112. doi: 10.1002/gps.4686

Dantzer, R., O'Connor, J. C., Freund, G. G., Johnson, R. W., and Kelley, K. W. (2008). From inflammation to sickness and depression: when the immune system subjugates the brain. *Nat. Rev. Neurosci.* 9, 46–56. doi: 10.1038/nrn2297

Dev, S. I., Moore, R. C., Soontornniyomkij, B., Achim, C. L., Jeste, D. V., and Eyler, L. T. (2017). Peripheral inflammation related to lower fMRI activation during a working memory task and resting functional connectivity among older adults: a preliminary study. *Int. J. Geriatr. Psychiatry* 32, 341–349. doi: 10.1002/gps.4482

Ebner, N. C., Chen, H., Porges, E., Lin, T., Fischer, H., Feifel, D., et al. (2016). Oxytocin's effect on resting-state functional connectivity varies by age and sex. *Psychoneuroendocrinology* 69, 50–59. doi: 10.1016/j.psyneuen.2016.03.013

Ebner, N. C., Horta, M., Lin, T., Feifel, D., Fischer, H., and Cohen, R. A. (2015). Oxytocin modulates meta-mood as a function of age and sex. *Front. Aging Neurosci.* 7:175. doi: 10.3389/fnagi.2015.00175

Ebner, N. C., Lin, T., Muradoglu, M., Weir, D. H., Plasencia, G. M., Lillard, T. S., et al. (2018). Associations between oxytocin receptor gene (OXTR) methylation, plasma oxytocin and attachment across adulthood. *Int. J. Psychophysiol.* doi: 10.1016/j.ijpsycho.2018.01.008 [Epub ahead of print].

Fung, A., Vizcaychipi, M., Lloyd, D., Wan, Y., and Ma, D. (2012). Central nervous system inflammation in disease related conditions: mechanistic prospects. *Brain Res.* 1446, 144–155. doi: 10.1016/j.brainres.2012.01.061

Gimeno, D., Marmot, M. G., and Singh-Manoux, A. (2008). Inflammatory markers and cognitive function in middle-aged adults: the whitehall II study. *Psychoneuroendocrinology* 33, 1322–1334. doi: 10.1016/j.psyneuen.2008.07.006

Giunta, S. (2008). Exploring the complex relations between inflammation and aging (inflamm-aging): anti-inflamm-aging remodelling of inflamm- aging, from robustness to frailty. *Inflamm. Res.* 57, 558–563. doi: 10.1007/s00011-008-7243-2

Goldstein, F. C., Zhao, L., Steenland, K., and Levey, A. I. (2015). Inflammation and cognitive functioning in African Americans and caucasians. *Int. J. Geriatr. Psychiatry* 30, 934–941. doi: 10.1002/gps.4238

Hayes, A. F. (2013). *Introduction to Mediation, Moderation and Conditional Process Analysis: A Regression-Based Approach.* New York, NY: The Guilford Press.

Heringa, S. M., van den Berg, E., Reijmer, Y. D., Nijpels, G., Stehouwer, C. D. A., Schalkwijk, C. G., et al. (2014). Markers of low-grade inflammation and endothelial dysfunction are related to reduced information processing speed and executive functioning in an older population–the Hoorn study. *Psychoneuroendocrinology* 40, 108–118. doi: 10.1016/j.psyneuen.2013.11.011

Hoogland, I. C. M., Houbolt, C., van Westerloo, D. J., van Gool, W. A., and van de Beek, D. (2015). Systemic inflammation and microglial activation: systematic review of animal experiments. *J. Neuroinflammation* 12:114. doi: 10.1186/s12974-015-0332-6

Joy, S., Fein, D., and Kaplan, E. (2003). Decoding digit symbol: speed, memory and visual scanning. *Assessment* 10, 56–65. doi: 10.1177/0095399702250335

Kerchner, G. A., Racine, C. A., Hale, S., Wilheim, R., Laluz, V., Miller, B. L., et al. (2012). Cognitive processing speed in older adults: relationship with white matter integrity. *PLoS One* 7:e50425. doi: 10.1371/journal.pone.0050425

Kwasnicka, D., Dombrowski, S. U., White, M., and Sniehotta, F. (2016). Theoretical explanations for maintenance of behaviour change: a systematic review of behaviour theories. *Health Psychol. Rev.* 10, 277–296. doi: 10.1080/17437199.2016.1151372

Magistro, D., Takeuchi, H., Nejad, K. K., Taki, Y., Sekiguchi, A., Nouchi, R., et al. (2015). The relationship between processing speed and regional white matter volume in healthy young people. *PLoS One* 10:e0136386. doi: 10.1371/journal.pone.0136386

Marsland, A. L., Gianaros, P. J., Abramowitch, S. M., Manuck, S. B., and Hariri, A. R. (2008). Interleukin-6 covaries inversely with hippocampal grey matter volume in middle-aged adults. *Biol. Psychiatry* 64, 484–490. doi: 10.1016/j.biopsych.2008.04.016

Marsland, A. L., Gianaros, P. J., Kuan, D. C. H., Sheu, L. K., Krajina, K., and Manuck, S. B. (2015). Brain morphology links systemic inflammation to cognitive function in midlife adults. *Brain Behav. Immun.* 48, 195–204. doi: 10.1016/j.bbi.2015.03.015

Marx, W., Kelly, J. T., Marshall, S., Cutajar, J., Annois, B., Pipingas, A., et al. (2018). Effect of resveratrol supplementation on cognitive performance and mood in adults: a systematic literature review and meta-analysis of randomized controlled trials. *Nutr. Rev.* 76, 432–443. doi: 10.1093/nutrit/nuy010

McCusker, R. H., and Kelley, K. W. (2013). Immune-neural connections: how the immune system's response to infectious agents influences behavior. *J. Exp. Biol.* 216, 84–98. doi: 10.1242/jeb.073411

Nadkarni, N. K., Boudreau, R. M., Studenski, S. A., Lopez, O. L., Liu, G., Kritchevsky, S., et al. (2016). Slow gait, white matter characteristics and prior 10-year interleukin-6 levels in older adults. *Neurology* 87, 1993–1999. doi: 10.1212/WNL.0000000000003304

Norden, D. M., and Godbout, J. P. (2013). Review: microglia of the aged brain: primed to be activated and resistant to regulation. *Neuropathol. Appl. Neurobiol.* 39, 19–34. doi: 10.1111/j.1365-2990.2012.01306.x

Norden, D. M., Muccigrosso, M. M., and Godbout, J. P. (2015). Microglial priming and enhanced reactivity to secondary insult in aging and traumatic CNS injury and neurodegenerative disease. *Neuropharmacology* 96, 29–41. doi: 10.1016/j.neuropharm.2014.10.028

Ownby, R. L. (2010). Neuroinflammation and cognitive aging. *Curr. Psychiatry Rep.* 12, 39–45. doi: 10.1007/s11920-009-0082-1

Paalani, M., Lee, J. W., Haddad, E., and Tonstad, S. (2011). Determinants of inflammatory markers in a bi-ethnic population. *Ethn. Dis.* 21, 142–149.

Papenberg, G., Ferencz, B., Mangialasche, F., Mecocci, P., Cecchetti, R., Kalpouzos, G., et al. (2016). Physical activity and inflammation: effects on gray-matter volume and cognitive decline in aging. *Hum. Brain Mapp.* 37, 3462–3473. doi: 10.1002/hbm.23252

Perry, V. H., and Teeling, J. (2013). Microglia and macrophages of the central nervous system: the contribution of microglia priming and systemic inflammation to chronic neurodegeneration. *Semin. Immunopathol.* 35, 601–612. doi: 10.1007/s00281-013-0382-8

Rey, A. (1964). *L'Examen Clinique en Psychologie.* Paris: Presses Universitaires de France.

Sankowski, R., Mader, S., and Valdés-Ferrer, S. I. (2015). Systemic inflammation and the brain: novel roles of genetic, molecular, and environmental cues as drivers of neurodegeneration. *Front. Cell. Neurosci.* 9:28. doi: 10.3389/fncel.2015.00028

Schram, M. T., Euser, S. M., De Craen, A. J. M., Witteman, J. C., Frölich, M., Hofman, A., et al. (2007). Systemic markers of inflammation and cognitive decline in old age. *J. Am. Geriatr. Soc.* 55, 708–716. doi: 10.1111/j.1532-5415.2007.01159.x

Singh-Manoux, A., Dugravot, A., Brunner, E., Kumari, M., Shipley, M., Elbaz, A., et al. (2014). Interleukin-6 and C-reactive protein as predictors of cognitive decline in late midlife. *Neurology* 83, 486–493. doi: 10.1212/WNL.0000000000000665

Stepanikova, I., Bateman, L. B., and Oates, G. R. (2017). Systemic inflammation in midlife: race, socioeconomic status and perceived discrimination. *Am. J. Prev. Med.* 52, S63–S76. doi: 10.1016/j.amepre.2016.09.026

Tegeler, C., O'Sullivan, J. L., Bucholtz, N., Goldeck, D., Pawelec, G., Steinhagen-Thiessen, E., et al. (2016). The inflammatory markers CRP, IL-6 and IL-10 are associated with cognitive function—data from the Berlin aging study II. *Neurobiol. Aging* 38, 112–117. doi: 10.1016/j.neurobiolaging.2015.10.039

Teunissen, C. E., van Boxtel, M. P. J., Bosma, H., Bosmans, E., Delanghe, J., De Bruijn, C., et al. (2003). Inflammation markers in relation to cognition in a healthy aging population. *J. Neuroimmunol.* 134, 142–150. doi: 10.1016/s0165-5728(02)00398-3

Todd, M. A. (2017). Inflammation and cognition in older adults: evidence from Taiwan. *Biodemography Soc. Biol.* 63, 309–323. doi: 10.1080/19485565.2017.1403305

Trollor, J. N., Smith, E., Baune, B. T., Kochan, N. A., Campbell, L., Samaras, K., et al. (2010). Systemic inflammation is associated with MCI and its subtypes: the sydney memory and aging study. *Dement. Geriatr. Cogn. Disord.* 30, 569–578. doi: 10.1159/000322092

Valeri, L., and VanderWeele, T. J. (2013). Mediation analysis allowing for exposure-mediator interactions and causal interpretation: theoretical assumptions and implementation with SAS and SPSS macros. *Psychol. Methods* 18, 137–150. doi: 10.1037/a0031034

VanderWeele, T. J., and Vansteelandt, S. (2009). Conceptual issues concerning mediation, interventions and composition. *Stat. Interface* 2, 457–468. doi: 10.4310/sii.2009.v2.n4.a7

van Horssen, J., van Schaik, P., and Witte, M. (2017). Inflammation and mitochondrial dysfunction: a vicious circle in neurodegenerative disorders? *Neurosci. Lett.* doi: 10.1016/j.neulet.2017.06.050 [Epub ahead of print].

Varatharaj, A., and Galea, I. (2017). The blood-brain barrier in systemic inflammation. *Brain Behav. Immun.* 60, 1–12. doi: 10.1016/j.bbi.2016.03.010

Vitkovic, L., Konsman, J. P., Bockaert, J., Dantzer, R., Homburger, V., and Jacque, C. (2000). Cytokine signals propagate through the brain. *Mol. Psychiatry* 5, 604–615. doi: 10.1038/sj.mp.4000813

Weaver, J. D., Huang, M.-H., Albert, M., Harris, T., Rowe, J. W., and Seeman, T. E. (2002). Interleukin-6 and risk of cognitive decline: MacArthur studies of successful aging. *Neurology* 59, 371–378. doi: 10.1212/wnl.59.3.371

Wechsler, D. (1981). *WAIS-R: Manual: Wechsler Adult Intelligence Scale—Revised.* New York, NY: Psychological Corporation.

Windham, B. G., Simpson, B. N., Lirette, S., Bridges, J., Bielak, L., Peyser, P. A., et al. (2014). Associations between inflammation and cognitive function in African Americans and European Americans. *J. Am. Geriatr. Soc.* 62, 2303–2310. doi: 10.1111/jgs.13165

Conflict of Interest Statement: The authors declare that the research was conducted in the absence of any commercial or financial relationships that could be construed as a potential conflict of interest.

The handling Editor declared a shared affiliation, though no other collaboration, with the authors.

frontiers in Aging Neuroscience

ORIGINAL RESEARCH
published: 20 September 2018
doi: 10.3389/fnagi.2018.00278

Age Influences Microglial Activation After Cuprizone-Induced Demyelination

Barbara Klein[1,2*†], *Heike Mrowetz*[1,2†], *Conor Michael Barker*[1,2], *Simona Lange*[1,2], *Francisco J. Rivera*[1,2,3,4] *and Ludwig Aigner*[1,2]

[1]*Institute of Molecular Regenerative Medicine, Paracelsus Medical University, Salzburg, Austria,* [2]*Spinal Cord Injury and Tissue Regeneration Center Salzburg (SCI-TReCS), Paracelsus Medical University, Salzburg, Austria,* [3]*Laboratory of Stem Cells and Neuroregeneration, Institute of Anatomy, Histology and Pathology, Faculty of Medicine, Universidad Austral de Chile, Valdivia, Chile,* [4]*Center for Interdisciplinary Studies on the Nervous System (CISNe), Universidad Austral de Chile, Valdivia, Chile*

Multiple sclerosis (MS) is a chronic inflammatory CNS disease, which causes demyelinated lesions and damages white and gray matter regions. Aging is a significant factor in the progression of MS, and microglia, the immune cells of the CNS tissue, play an important role in all disease stages. During aging, microglia are functionally altered. These age-related changes probably already begin early and might influence the progression of CNS pathologies. The aim of the present study was to investigate whether microglia in the middle-aged CNS already react differently to demyelination. For this purpose, several microglia markers (ionized calcium binding adaptor molecule 1 (Iba-1), P2RY12, F4/80, CD68, major histocompatibility complex II (MHCII), macrophage receptor with collagenous structure (Marco), Translocator protein 18 kD (TSPO), CD206, and CD163) were analyzed in the acute cuprizone demyelination model in young (2-month-old) and middle-aged (10-month-old) mice. In addition, microglial proliferation was quantified using double-labeling with proliferating cell nuclear antigen (PCNA) and bromodeoxyuridine (BrdU), which was injected with the onset of remyelination. To compare age-related microglial changes during de- and remyelination in both gray and white matter, the hilus of the dorsal hippocampal dentate gyrus (DG) and the splenium of the corpus callosum (CC) were analyzed in parallel. Age-related changes in microglia of healthy controls were more pronounced in the analyzed gray matter region (higher levels of F4/80 and Marco as well as lower expression of CD68 in middle-aged mice). During de- and remyelination, a stronger increase of the microglial markers Iba-1, CD68 and TSPO was observed in the splenium of the younger groups. There was a significant reduction of P2RY12 during demyelination, however, this was age- and region-dependent. The induction of the anti-inflammatory markers CD206 and CD163 was stronger in the middle-aged group, but also differed between the two analyzed regions. De- and remyelination led to a significant increase in $PCNA^+$ microglia only in young groups within the white matter region. The number of $BrdU^+$ microglia was not changed during de- or remyelination.

OPEN ACCESS

Edited by:
Ashok Kumar,
University of Florida, United States

Reviewed by:
Ting-Ting Huang,
Stanford University, United States
Chiara Cordiglieri,
Istituto Nazionale Genetica Molecolare (INGM), Italy

***Correspondence:**
Barbara Klein
barbara.klein@outlook.com

†These authors have contributed equally to this work

Received: *31 March 2018*
Accepted: *28 August 2018*
Published: *20 September 2018*

Citation:
Klein B, Mrowetz H, Barker CM, Lange S, Rivera FJ and Aigner L (2018) Age Influences Microglial Activation After Cuprizone-Induced Demyelination. Front. Aging Neurosci. 10:278. doi: 10.3389/fnagi.2018.00278

These results clearly show that microglia are already altered during middle-age and also react differently to CNS demyelination, however, this is highly region-dependent.

Keywords: microglia, aging, demyelination, cuprizone, hippocampus, corpus callosum, TSPO, P2RY12

INTRODUCTION

With increasing age, microglia, the resident immune cells of the CNS parenchyma, undergo functional changes (reviewed in Mosher and Wyss-Coray, 2014). Aging microglia seem to become more reactive to pro-inflammatory stimuli, and at the same time, also more resistant to deactivation, which together lead to an exaggerated and longer lasting inflammatory response. This process has been described as "microglial priming" (reviewed in Norden and Godbout, 2013; Norden et al., 2015), and may influence the progression of CNS pathologies (reviewed in Perry and Holmes, 2014). Additionally, there is evidence that microglia functions (such as phagocytosis and proteostasis), which are important for CNS homeostasis and in reaction to CNS pathologies, become impaired during aging (reviewed in Mosher and Wyss-Coray, 2014). These age-related microglial changes most likely already start during adulthood (e.g., Bardou et al., 2013; Lee et al., 2013; Hefendehl et al., 2014), until, at extreme ages, microglia become senescent and dystrophic (reviewed in Streit et al., 2014). The exact time sequence and functional impact of microglial age-related changes, however, need to be studied more extensively.

Multiple sclerosis (MS) is a chronic inflammatory disease of the CNS, which causes demyelination not only in white matter regions, but also damages gray matter and leads to axonal loss and neurodegeneration (reviews of MS pathology: Mallucci et al., 2015; Baecher-Allan et al., 2018). In young adults, MS is the main cause of non-traumatic neurological disabilities (Browne et al., 2014). Despite different MS disease patterns, aging is a very important factor in the progression of MS pathology and increasing disability (Confavreux and Vukusic, 2006; Manouchehrinia et al., 2017).

Microglia accumulate in active MS lesions and play an important role in all stages of MS pathology (reviewed in Jack et al., 2005; Rawji and Yong, 2013; O'Loughlin et al., 2018). There are indications that microglia can facilitate myelin repair by phagocytosing myelin and cell debris, secreting pro-regenerative signals (e.g., growth factors and cytokines), and by influencing oligodendrocyte lineage cells (reviewed in Napoli and Neumann, 2010; McMurran et al., 2016; Miron, 2017). However, with increasing disease duration and age, myelin regeneration becomes less successful, and it is possible that age-related changes in microglia are one factor contributing to this failure in myelin repair. Even though this hypothesis is not new, most preclinical studies on microglia in models for MS or demyelination used animals of a young age, which could conceivably influence the results.

The aim of the present study was to investigate whether microglia in the middle-aged (10-months-old) CNS react differently to demyelination than young microglia (2-months-old). For this purpose, we performed a comprehensive analysis of microglia using cell- and activity-specific markers in combination with markers for proliferation in the acute cuprizone demyelination model. This model is a well-studied and reproducible toxic model, which induces demyelination followed by spontaneous remyelination (Kipp et al., 2009; Praet et al., 2014; Tagge et al., 2016). Similar to the pathology in human MS patients, in the cuprizone model demyelination and axonal damage not only occur in white matter regions, like the corpus callosum (CC), but also in gray matter (Goldberg et al., 2015), for example, in the hippocampus (Hoffmann et al., 2008; Koutsoudaki et al., 2009; Norkute et al., 2009; Sun et al., 2016). To compare age-related microglial changes in both gray and white matter after demyelination, the hilus of the hippocampal dentate gyrus (DG) and the splenium of the CC were analyzed in parallel. The hippocampus was chosen as a target of our investigation, since MS patients often suffer from episodic memory impairment, which might be caused by pathological changes (such as altered connectivity, microstructural damage, atrophy and demyelination) in this region (Geurts et al., 2007; Sicotte et al., 2008; Dutta et al., 2011; Hulst et al., 2015; Planche et al., 2017). Recently, it has been shown that the CA4/DG subfield is the first region of the hippocampus that is atrophied at the earliest stages of MS (Planche et al., 2018). While studies about aging microglia often focus on changes affecting the old CNS, we specifically chose to analyze middle-aged—not old—animals, since in MS patients also around middle age, regeneration starts to fail and irreversible disabilities occur (Confavreux and Vukusic, 2006; Manouchehrinia et al., 2017). The results of this analysis should provide insight into the extent of age-related changes in middle-aged microglia, which could be a useful background for other studies, for example, to test new treatment strategies to enhance remyelination.

Studies about microglia largely depend on antibodies that recognize microglia activity state-specific antigens. This is an ongoing topic of research, and the list of useful markers and antibodies is constantly growing. Two markers that are strongly expressed in microglia surveying the healthy CNS, and thus, are ideal for general morphological analyses, are: (i) ionized calcium binding adaptor molecule 1 (Iba-1), which is (like most conventionally used microglia markers) expressed by microglia and infiltrating macrophages, and plays a role in calcium homeostasis (Imai et al., 1996; Ito et al., 1998); and (ii) the G-protein-coupled purinergic receptor P2RY12, which distinguishes microglia from CNS-infiltrating monocytes and other peripheral macrophages (Sasaki et al., 2003; Butovsky et al., 2014; Bennett et al., 2016). Despite their use as general markers for microglia, the expression of Iba-1 and P2RY12 is differentially affected by inflammatory stimuli, which lead to

an up-regulation of Iba-1 (e.g., Mori et al., 2000; Ito et al., 2001), whereas P2RY12 is increased during anti-inflammatory conditions (e.g., Moore et al., 2015; Beaino et al., 2017). Also F4/80, an adhesion G protein-coupled receptor that is expressed in mature mouse macrophages and microglia and may be involved in the induction of peripheral immune tolerance, is often analyzed (reviewed in Gordon et al., 2011). In contrast to Iba-1 and P2RY12, F4/80 is expressed at relatively low levels in microglia. One of the most widely used markers for microglial activation, CD68 (also ED1 or macrosialin), is a lysosomal/endosomal-associated protein, that plays a role in microglial phagocytosis (Fulci et al., 2007), however, its exact function is still unknown (reviewed in Sierra et al., 2013). Another popular microglia activation marker is major histocompatibility complex II (MHCII). In contrast to professional antigen-presenting cells, the expression of MHCII is low in microglia in the healthy CNS, however, it can be upregulated upon activation (reviewed in Sierra et al., 2013). The macrophage receptor with collagenous structure (Marco) is a class A scavenger receptor that has been associated with a pro-inflammatory microglial activation (reviewed in Colton, 2009; Sierra et al., 2013), and plays a role in defense against bacterial meningitis (Braun et al., 2011) and in binding amyloid-β (Brandenburg et al., 2010). Translocator protein 18 kD (TSPO), another pro-inflammatory marker, is involved in the transport of cholesterol across mitochondrial membranes, and is increased in neuroinflammatory diseases in microglia and astrocytes. TSPO is of particular interest, since it is used as a target for PET imaging, for example with the tracer PK11195 (reviewed in Jacobs and Tavitian, 2012). This PET signal is increased in healthy aged humans (Schuitemaker et al., 2012), and was also shown to correlate in MS patients with age, disease progression and clinical outcome (reviewed in Airas et al., 2018). Two markers that typically used to identify anti-inflammatory microglia are the mannose receptor CD206, which is not only expressed in microglia, but also in astrocytes (Burudi et al., 1999; Régnier-Vigouroux, 2003) and plays a role in the phagocytosis of pathogens (reviewed in Sierra et al., 2013), and the hemoglobin-haptoglobin scavenger receptor CD163, which is expressed in microglia and perivascular macrophages (reviewed in Colton, 2009; Thomsen et al., 2013). Proliferating microglia are often identified using co-labeling with proliferating cell nuclear antigen (PCNA). In addition, the generation and subsequent survival and fate of microglia can be detected after labeling proliferating cells *in vivo* using for example bromodeoxyuridine (BrdU).

MATERIALS AND METHODS

Animals and Cuprizone Treatment

Male C57BL/6J mice, at the ages of 2 and 10 months, were obtained from Janvier and afterwards kept in the animal facility of the Paracelsus Medical University in Salzburg, Austria under standard animal housing conditions with food and water *ad libitum*. Mice were divided into four different treatment groups per age, with six animals in each group, resulting in a total number of 48 animals. Control animals received a diet of standard food pellets (ssniff Spezialdiäten) for 8 weeks. For demyelination, animals in the respective groups received standard food pellets pre-mixed with 0.2% cuprizone (ssniff Spezialdiäten) for 6 weeks. To allow for remyelination, afterwards a normal diet consisting of standard food pellets was resumed for 1 or 2 weeks. For the analysis of proliferation of microglia and their subsequent survival during the remyelination period, animals received i.p. injections of BrdU (50 mg/kg body weight, in PBS) on six consecutive days starting on the first day after cuprizone administration. All experimental procedures were approved by the Federal State Government Salzburg, Austria (permit 20901-TVG/61/14-2016) and carried out in compliance with international ethical guidelines.

The percentage of weight change over the course of the experiment was calculated for each animal by subtracting the mean weight on the 2 days before the start of cuprizone treatment from the mean weight on the last 2 days before tissue collection.

Tissue Preparation

Perfusion fixation and tissue preparation were done as previously described (Couillard-Despres et al., 2005). In short, mice were terminally anesthetized by injection (i.p.) of ketamine (273 mg/kg body weight), xylazine (71 mg/kg body weight) and acepromazine (4 mg/kg body weight) in a physiological NaCl solution and then transcardially perfused with a 0.9% NaCl (w/v) solution followed by phosphate-buffered 4% paraformaldehyde (pH 7.4). Afterwards, brains were extracted, postfixed overnight in 4% paraformaldehyde, cryoprotected in 30% sucrose (w/v in PBS), and sectioned on dry ice with a sliding microtome (Leica SM 2000R). For quantitative analysis, a representative tenth of one brain hemisphere was collected (i.e., every tenth section, with an interval of 400 μm between sections). The 40 μm-thick sections were stored at −20°C in a cryoprotection solution (equal parts glycerin, 0.2 M phosphate buffer, ethylene glycol and H_2O).

Immunohistochemistry

Immunohistological stainings were done according to a protocol that was previously described in detail (Kandasamy et al., 2014), with the addition of an antigen retrieval step after the first washing of the tissue sections. In this step, the sections were incubated in 10 mM citrate buffer (pH 6.0) in a steamer at 100°C for 20 min, followed by washing in PBS for 3 × 5 min. For two antibodies, CD163 and CD206, the antigen retrieval was shortened, i.e., the hot citrate buffer was put on the sections only for 10 min at RT. For each staining, a tenth of a hemisphere was used for immunohistochemistry.

The following antibodies and dilutions were used: primary antibodies: rat anti-myelin basic protein (anti-MBP; 1:150, MCA409S, AbD Serotec), goat anti-Iba-1 (1:500, Ab107159, Abcam), rabbit anti-P2RY12 (1:500, 55043A, AnaSpec), rabbit anti-CD68 (1:500, AB125212, Abcam), rat anti-MHCII (1:100, 14-5321-82, eBioscience), rat anti-Marco (1:200, MCA1849, AbD Serotec), rabbit anti-TSPO (PBR; 1:250, Novus Biologicals, NBP1-95674), mouse anti-CD206 (1:200, Ab8918, Abcam),

rabbit anti-CD163 (1:200, Bs-2527R, Bioss), mouse anti-PCNA (1:500, A1111, Santa Cruz), rat anti-BrdU (1:500, OBT003G, Serotec), and rat anti-F4/80 (1:150, MCA497G, BioRad). Secondary antibodies (all diluted 1:1,000): rabbit anti-rat biotinylated (BA-4001, VectorLab), donkey anti-goat Alexa 488 (A11055, Mol Probes), donkey anti-rat Alexa 488 (A21208, Molecular Probes), donkey anti-mouse Alexa 488 (A21202, Life Tech), donkey anti-rabbit Alexa 568 (A10042, Life Tech), donkey anti-goat Alexa 647 (705605147, Jackson IR), donkey anti-rabbit Alexa 647 (A1573, Life Tech), and donkey anti-rat Alexa 647 (712-606-150, Jackson IR). Cell nuclei were stained with 4′,6-diamidino-2-phenylindole dihydrochloride (DAPI) at a concentration of 0.5 μg/μl (Sigma-Aldrich).

Microscopy and Image Processing

For quantitative analysis of the MBP staining, images were taken with a Zeiss Axioplan (5× objective) and the AxioCam MRC5 Zeiss Imaging Software (version 4.30.01). For the analysis of fluorescent stainings, z-stacks (spanning the whole 40 μm thickness of the section) were generated with a confocal scanning laser microscope (Zeiss LSM 700) equipped with LSM software (ZEN 2012) using the 20× objective and 0.5× zoom. For the figures, representative images were chosen from those taken for analysis. From the confocal images, orthogonal maximum intensity projections were created using the Zen 2012 blue edition software. If necessary, brightness and contrast were adjusted for the whole image.

Quantitative Analysis of Immunohistochemistry

All image analysis was done blinded (i.e., without knowing group or mouse number) using the software ImageJ 1.48 (GNU General Public License). The percentage area covered by an immunohistological staining was determined using the "Analyze particles" function of ImageJ. For each animal, four tissue sections were used to analyze staining in the two target regions. The light microscopic images of MBP staining were quantified in an area of 160 × 90 μm in the hilus of the dorsal hippocampal DG and an area of 220 × 220 μm in the splenium of the CC. For the fluorescent images of the other markers, first a maximum intensity projection of the z-stacks was created in ImageJ, and then an area of 200 × 100 μm was analyzed in the hilus of the dorsal hippocampal DG and an area of 320 × 320 μm in the splenium of the CC.

For analysis of cell numbers (of Iba-1$^+$ PCNA$^+$ and Iba-1$^+$ BrdU$^+$ cells), the total numbers of stained cells within the hilus of dorsal hippocampal DG (without the subgranular zone) and the splenium of the CC were counted in a tenth of a hemisphere using the "Cell Counter" plug-in (cell_counter.jar, version 2, GNU General Public License) for ImageJ and then multiplied per 10.

Statistical Analysis

Data are shown as means + standard deviation (SD). All statistical analysis was done with Prism 7 (Graphpad Software Inc., San Diego, CA, USA). For the analysis of the statistical significance of the effects of age and treatment on immunohistological parameters, statistical significance was determined with a two-way ANOVA (factors: age and treatment) followed by a Tukey's *post hoc* test in which each group was compared to all others. The effect of the different treatments on the change of body weight during the experiment were analyzed separately for each age group using a one-way ANOVA with a Tukey's *post hoc* test or a Kruskal-Wallis one-way analysis followed by a Dunn's multiple comparisons test depending on whether the data was normally distributed or not (as assessed by a Shapiro-Wilk test). The resulting p-values of the comparisons between different treatments of the same age group are represented as: $^*p < 0.05$, $^{**}p < 0.01$, $^{***}p < 0.001$ and $^{****}p < 0.0001$, whereas the p-values of age-related differences within the same treatment are shown as: $^{\#}p < 0.05$, $^{\#\#}p < 0.01$, $^{\#\#\#}p < 0.001$ and $^{\#\#\#\#}p < 0.0001$. Other significant differences (i.e., between different treatments across the two age groups) are not shown.

RESULTS

De- and Remyelination in Young and Middle-Aged Mice

To analyze age-related changes after demyelination, four different groups (control, demyelination, remyelination 1 week, and remyelination 2 weeks) were compared at two different ages. In the young group the 6–8 week treatment started at 2 months, and in the middle-aged group at 10 months of age (for experimental design see **Figure 1A**). For the analysis of the extent of de- and remyelination, a staining for MBP was used (**Figure 1B**). In the hilus of the dorsal DG of the hippocampus, both age groups were significantly demyelinated, which was followed by remyelination starting 1 week after cuprizone withdrawal. During demyelination, MBP levels were slightly, but significantly, lower in the younger group (**Figure 1C**). In the splenium of the CC, regardless of the age group, a reduction of MBP was found in the demyelination group. This observed change in myelination, however, was not significant (**Figure 1D**). In comparison to the control groups of the same age, no significant differences in the percentage change of body weight over the duration of the experiment were observed in the de- or remyelination groups (**Supplementary Figure S1**). This indicates that food intake was not negatively affected by the addition of cuprizone to the food pellets.

Divergent Spatial and Temporal Expression of "General" Microglia Markers

In the hilus of the hippocampal DG (**Figure 2A**) in both age groups, Iba-1 immunoreactivity was significantly increased during demyelination, which lasted until the first week of remyelination (**Figure 2B**). P2RY12, however, was significantly down-regulated in both age groups during demyelination (**Figure 2C**). In the older animals, the down-regulation of P2RY12 was significantly more pronounced than in the younger age group, and persisted for a longer duration (until the first week of remyelination; **Figure 2C**).

In the splenium of the CC (**Figure 3A**) in the young group, the upregulation of Iba-1 lasted longer than in the

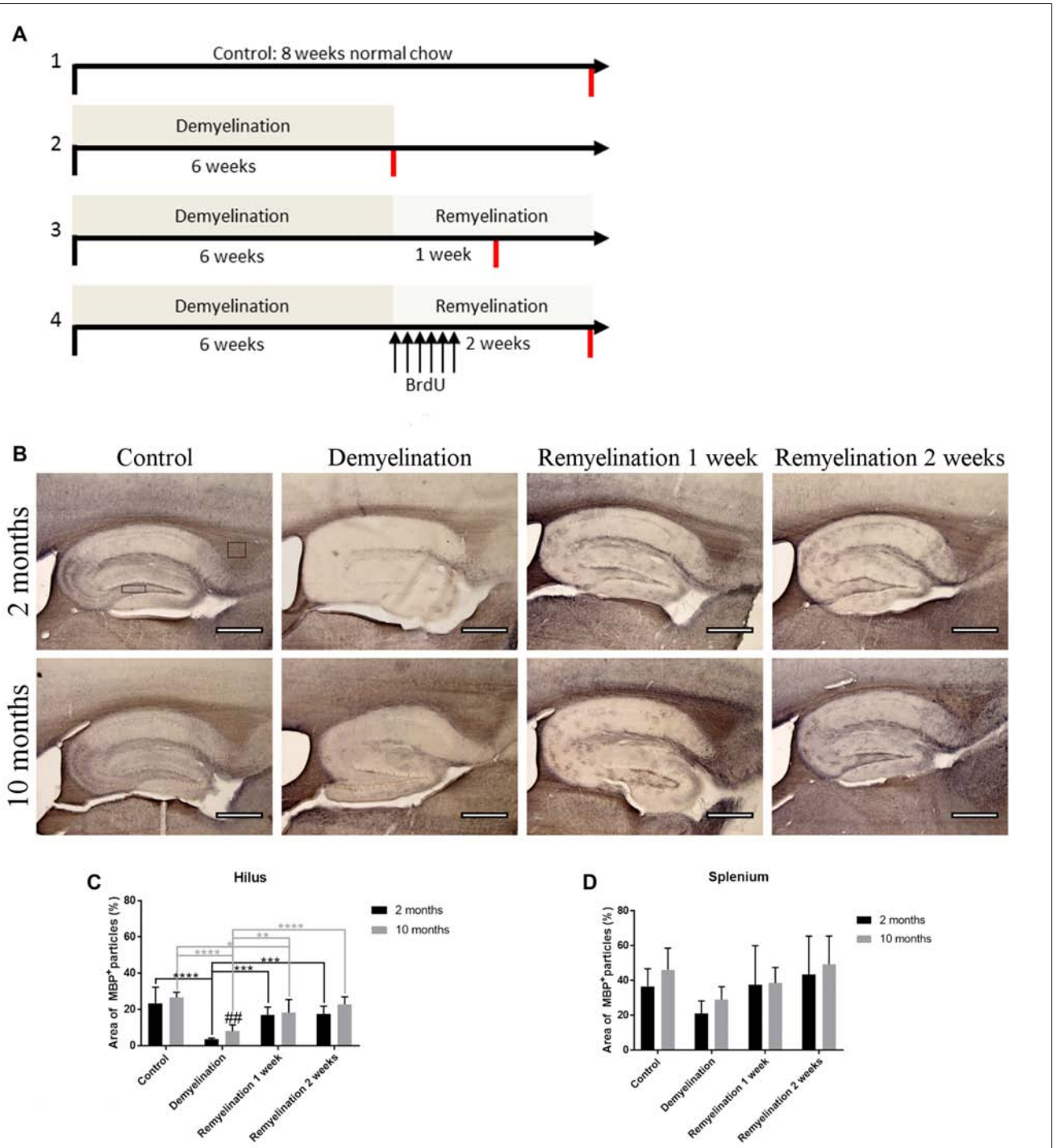

FIGURE 1 | Experimental design and analysis of de- and remyelination. **(A)** Overview of the different treatment groups and the timeline of the experiment. All four treatment groups (controls, demyelination, 1 week remyelination and 2 weeks remyelination) were compared at two different ages: young (starting in 2-month-old animals) and middle-aged (starting in 10-month-old animals). To analyze proliferation and subsequent survival of microglia during remyelination, controls and the remyelination groups received six BrdU injections starting as soon as the demyelination-inducing cuprizone treatment was stopped. The red lines indicate the time of tissue collection. **(B)** Myelination was analyzed using staining for myelin basic protein (MBP). The analyzed regions of interest are indicated by rectangles. **(C)** In the hilus of the dorsal hippocampal dentate gyrus (DG), both age groups were significantly demyelinated, followed by remyelination beginning 1 week after the end of the cuprizone treatment. After six weeks of cuprizone treatment, demyelination was slightly, but significantly, more severe in the young group. **(D)** In the splenium of the corpus callosum (CC), the observed myelin changes during de- and remyelination were less pronounced. Values are shown as means + standard deviation (SD $n = 6$ per group). Statistical significance was evaluated using a two-way ANOVA followed by a Tukey's *post hoc* test. The p-values are indicated in the graphs: treatment effects within the same age group: $^{*}p < 0.05$, $^{**}p < 0.01$, $^{***}p < 0.001$ and $^{****}p < 0.0001$, age-related differences: $^{\#\#}p < 0.01$. Bars: **(B)** 500 μm.

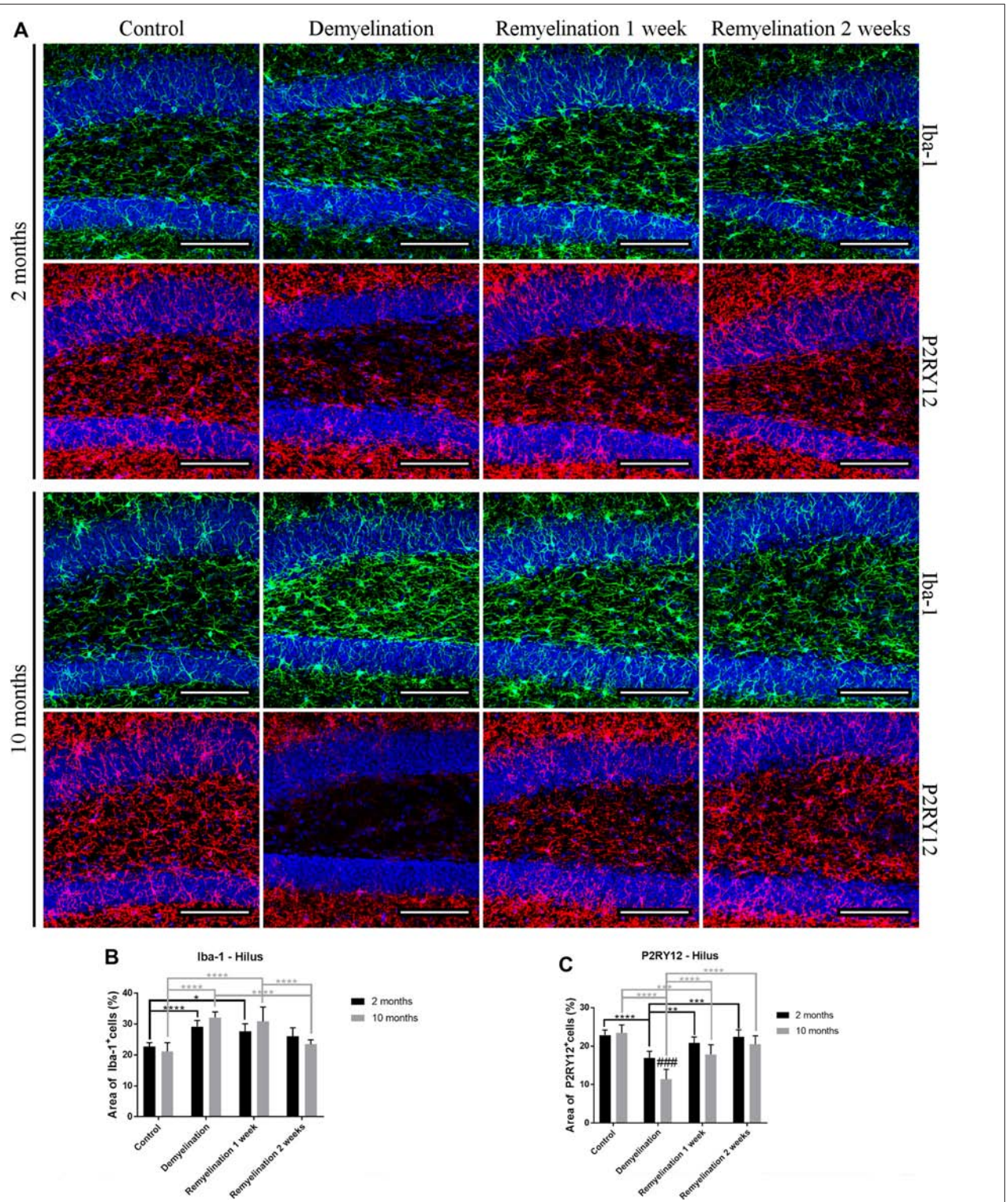

FIGURE 2 | Different patterns of ionized calcium binding adaptor molecule 1 (Iba-1), and P2RY12 during de- and remyelination in the hilus of the DG. **(A)** Iba-1 (green) and P2RY12 (red) labeling. Cell nuclei are stained with 4′,6-diamidino-2-phenylindole dihydrochloride (DAPI; blue). **(B)** In both age groups, Iba-1 staining was significantly increased during demyelination until the first week of remyelination. **(C)** P2RY12 labeling was significantly decreased in both age groups during demyelination, and this was more pronounced and longer lasting in the middle-aged animals. Values are shown as means + SD ($n = 6$ per group). Statistical significance was evaluated using a two-way ANOVA and a Tukey's *post hoc* test. The p-values are indicated in the graphs: treatment effects within the same age group: $^{*}p < 0.05$, $^{**}p < 0.01$, $^{***}p < 0.001$ and $^{****}p < 0.0001$, age-related differences: $^{\#\#\#}p < 0.001$. Bars: **(A)** 100 μm.

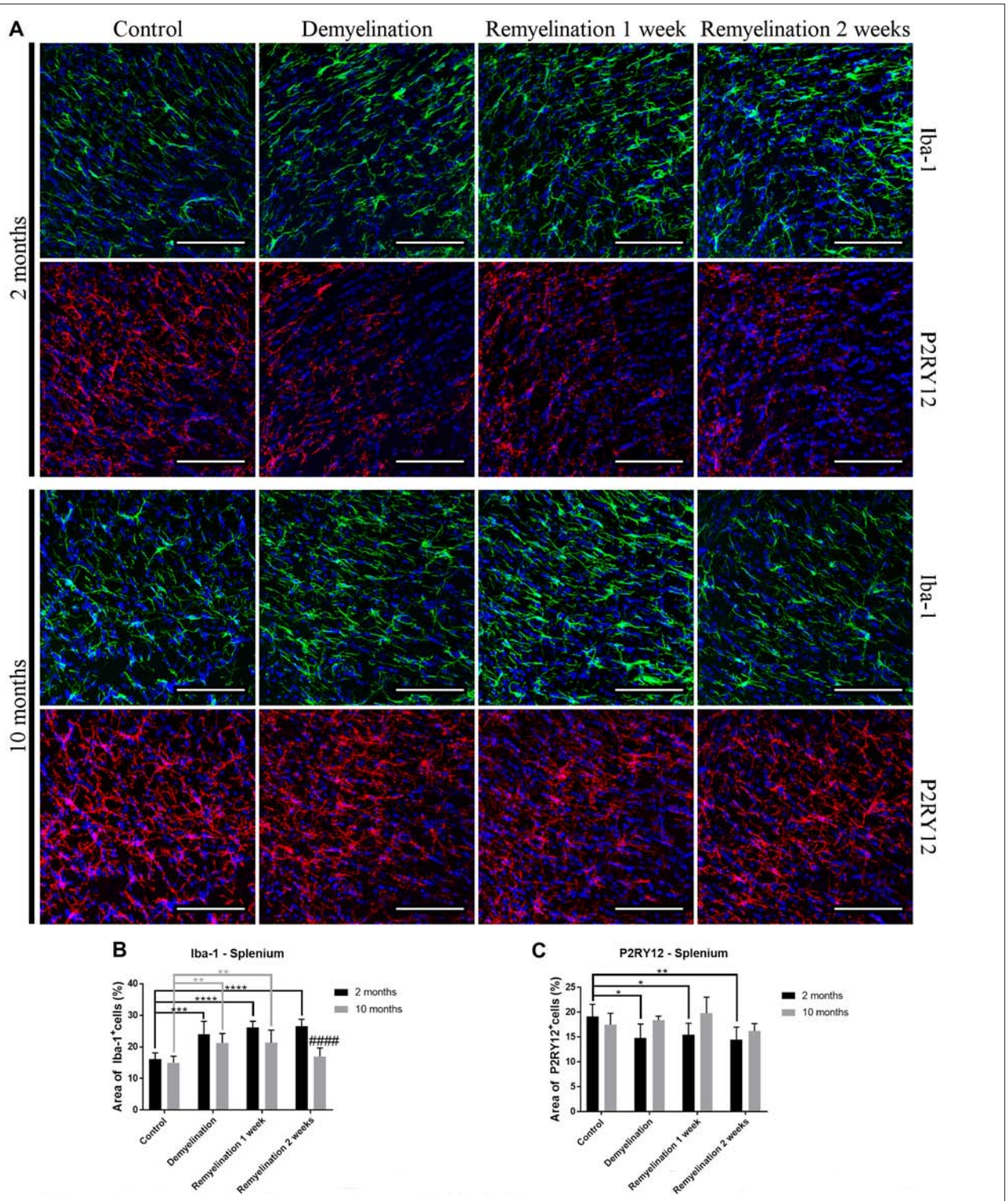

FIGURE 3 | Age- and region-dependent differences in Iba-1 and P2RY12 during de- and remyelination in the splenium of the CC. **(A)** Iba-1 (green) and P2RY12 (red) labeling. Cell nuclei are stained with DAPI (blue). **(B)** In young mice, Iba-1 was up-regulated during all phases of de- and remyelination, while in the middle-aged group Iba-1 returned to control levels after 2 weeks of remyelination, resulting in an age-related difference at this time point. **(C)** A significant reduction of P2RY12 in the splenium was observed only in the younger group during de- and remyelination. In the middle-aged group P2RY12 levels were not changed during de- or remyelination. Values are shown as means + SD ($n = 6$ per group). Statistical significance was evaluated using a two-way ANOVA and a Tukey's *post hoc* test. The p-values are indicated in the graphs: treatment effects within the same age group: $^{*}p < 0.05$, $^{**}p < 0.01$, $^{***}p < 0.001$ and $^{****}p < 0.0001$, age-related differences: $^{\#\#\#\#}p < 0.0001$. Bars: **(A)** 100 μm.

hilus of the DG (until the second week of remyelination; **Figure 3B**). At this time point, the level of Iba-1 expression in the splenium of the older group had already returned to control levels resulting in a significant age-related difference in Iba-1 expression (**Figure 3B**). Interestingly, a significant downregulation of P2RY12 in the splenium was observed only in the younger group during de- and remyelination (**Figure 3C**). In the older group, P2RY12 expression did not change significantly in the splenium in response to de- or remyelination (**Figure 3C**).

In the hilus of the hippocampal DG (**Figure 4A**, upper rows), we found a significantly higher F4/80 expression in all older groups compared to the young ones (**Figure 4B**). In addition, F4/80 was reduced in all young groups following de- and remyelination (significant after demyelination and 2 weeks of remyelination; **Figure 4B**). In contrast, in the splenium of the CC (**Figure 4A**, lower rows), no significant changes in F4/80 expression were observed (**Figure 4C**).

CD68 and MHCII React Differently to De- and Remyelination

When analyzing CD68 expression in the hilus of the hippocampal DG (**Figure 5A**), the first unexpected finding was that the expression of this marker was higher in the younger controls compared to the middle-aged ones (**Figure 5B**). In the younger de- and remyelination groups, the percentage of CD68 staining decreased significantly in comparison to controls, whereas the opposite was observed for the older groups (**Figure 5B**). These opposed regulation patterns resulted in a significantly higher CD68 expression in the middle-aged group after 2 weeks of remyelination in comparison to the younger one (**Figure 5B**). The percentage of MHCII staining was subtly, but significantly, reduced in the hippocampal hilus of the younger group after 2 weeks of remyelination (**Figure 6C**). In contrast, in the middle-aged group, a small, not significant, increase in MHCII was observed during de- and remyelination, which resulted in a significant age-related difference after 2 weeks of remyelination with higher levels of MHCII in the middle-aged group (**Figure 5C**).

In the splenium of the CC (**Figure 6A**), there were no differences between the controls of the two age groups, neither in the expression of CD68 (**Figure 6B**), nor MHCII (**Figure 6C**). Interestingly, de- and remyelination significantly increased CD68 only in the younger group resulting in significant age-related differences after demyelination and 2 weeks of remyelination (**Figure 5C**). MHCII expression was not significantly altered during de- or remyelination in both age groups in the splenium, and the expression of this marker was generally much lower than in the DG hilus (**Figure 6C**).

TSPO, but Not Marco, Is Influenced by De- and Remyelination

In the hilus of the hippocampal DG (**Figure 7A**), a significantly higher expression of Marco was found in the older control group compared to the younger one (**Figure 7B**). De- and remyelination, however, did not significantly affect the (very low) expression of this classical pro-inflammatory marker. In the same region, there were no age-related differences in TSPO expression, but in both age groups a significant TSPO increase was found during demyelination and the first week of remyelination (**Figure 7C**).

In the splenium of the CC (**Figure 8A**), no significant effects of age or treatment on Marco expression were found (**Figure 8B**). In contrast, TSPO was significantly increased in both age groups during de- and remyelination, however, the TSPO levels were significantly higher in the younger groups during de- and remyelination (**Figure 8C**).

Age and Region Affect Induction of CD206 and CD163 During Remyelination

In the hippocampal hilus (**Figure 9A**), de- and remyelination had no significant effect on the expression of CD206 in either age group (**Figure 9B**). In the middle-aged group, there was a significant upregulation of CD163 during the whole de- and remyelination phase, while in the younger group a similar pattern was observed, but the increase in CD163 was only significant 2 weeks after remyelination (**Figure 9C**). In the splenium (**Figure 10A**), CD206 was only significantly elevated in the middle-aged group after 2 weeks of remyelination (**Figure 10B**). For CD163, no significant changes were observed in this region (**Figure 10C**).

Increased Proliferation of Microglia in the Splenium of the CC in the Young Group

No significant increase in proliferating microglia ($PCNA^+$) was found during de- or remyelination in the hippocampal hilus (**Figure 11A**), which could be due to the very high variance within the demyelination groups in both age groups (**Figure 11C**). In accordance with these results, the number of Iba-1^+ $BrdU^+$ cells (**Figure 11B**) was also not increased during de- or remyelination in either age group (**Figure 11D**).

In the splenium of the CC (**Figure 12A**), the number of proliferating $PCNA^+$ microglia was significantly higher in the middle-aged controls than in the young ones. However, only the younger group was affected by the cuprizone treatment: in this age group, there was a significant increase in proliferating microglia after demyelination and the second week of remyelination. This dynamic resulted in age-related differences at all time points (**Figure 12C**). The number of $BrdU^+$ microglia in the splenium (**Figure 12B**) was higher in all middle-aged groups in comparison to the younger ones, however, this was only significant after 1 week of remyelination (**Figure 12D**). This increase of Iba-1^+ $BrdU^+$ cells fits together with the higher proliferation in the middle-aged groups that was observed in the PCNA staining in the controls and 1 week after remyelination during which BrdU was administered to the remyelination groups (**Figure 12C**). However, de- or remyelination did not affect the number of $BrdU^+$ Iba-1^+ microglia in either age group (**Figure 12D**). This is in accordance with the PCNA data, since in both age groups the number of proliferating $PCNA^+$ microglia was not

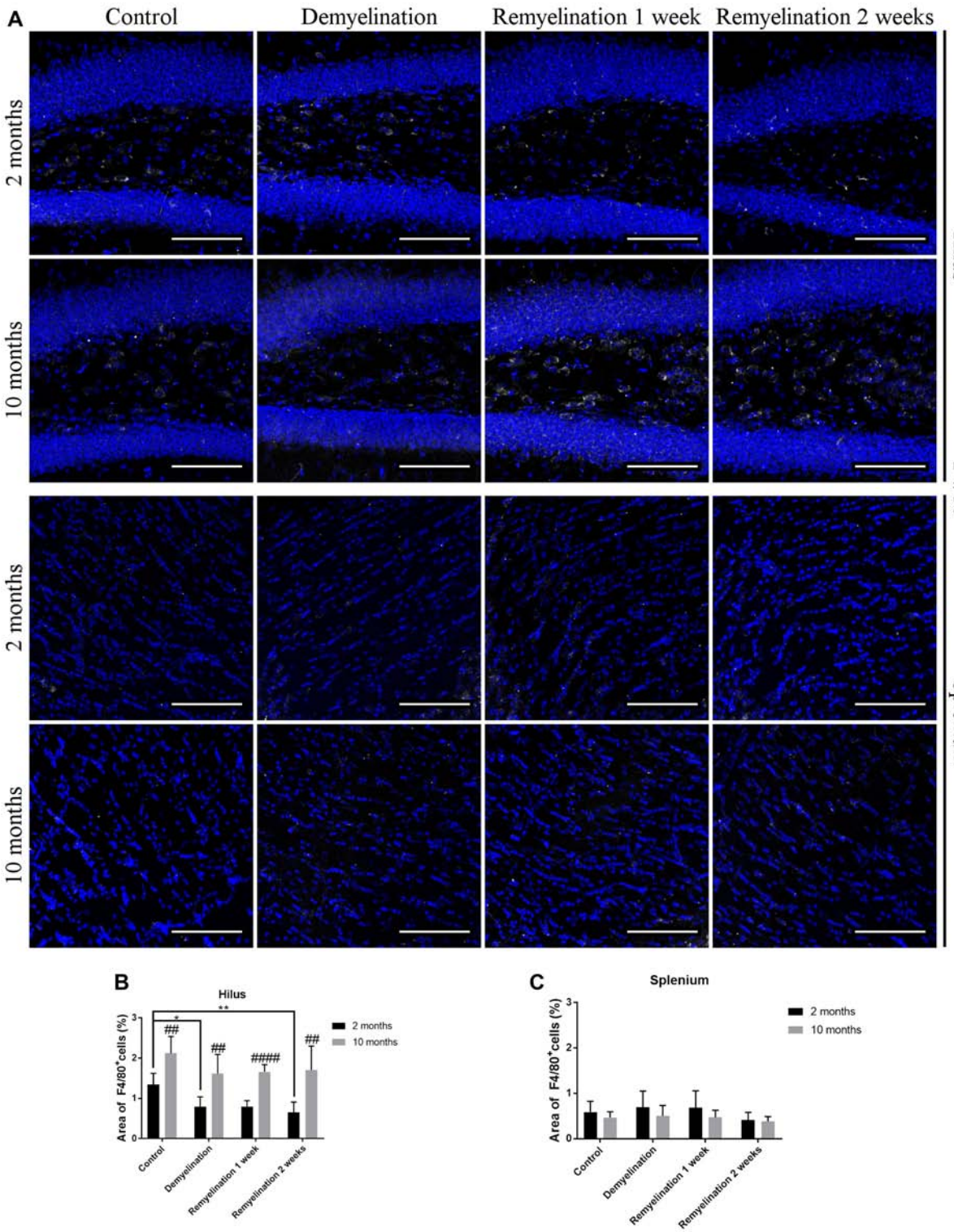

FIGURE 4 | F4/80 levels are affected by age and cuprizone treatment in the hilus of the DG, but not in the splenium of the CC. **(A)** F4/80 (white) staining in the hilus of the DG (two upper rows) and the splenium of the CC (two lower rows). Cell nuclei are stained with DAPI (blue). F4/80 is relatively low in all groups. **(B)** In the hilus of the hippocampal DG, F4/80 levels were higher in middle-aged groups compared to young ones. In young mice, F4/80 was significantly reduced after demyelination and 2 weeks of remyelination. **(C)** In contrast, in the splenium of the CC no significant changes in F4/80 expression were found. Values are shown as means + SD (n = 6 per group). Statistical significance was evaluated using a two-way ANOVA followed by a Tukey's *post hoc* test. The p-values are indicated in the graphs: treatment effects within the same age group: $^{*}p < 0.05$ and $^{**}p < 0.01$, age-related differences: $^{\#\#}p < 0.01$ and $^{\#\#\#\#}p < 0.0001$. Bars: **(A)** 100 μm.

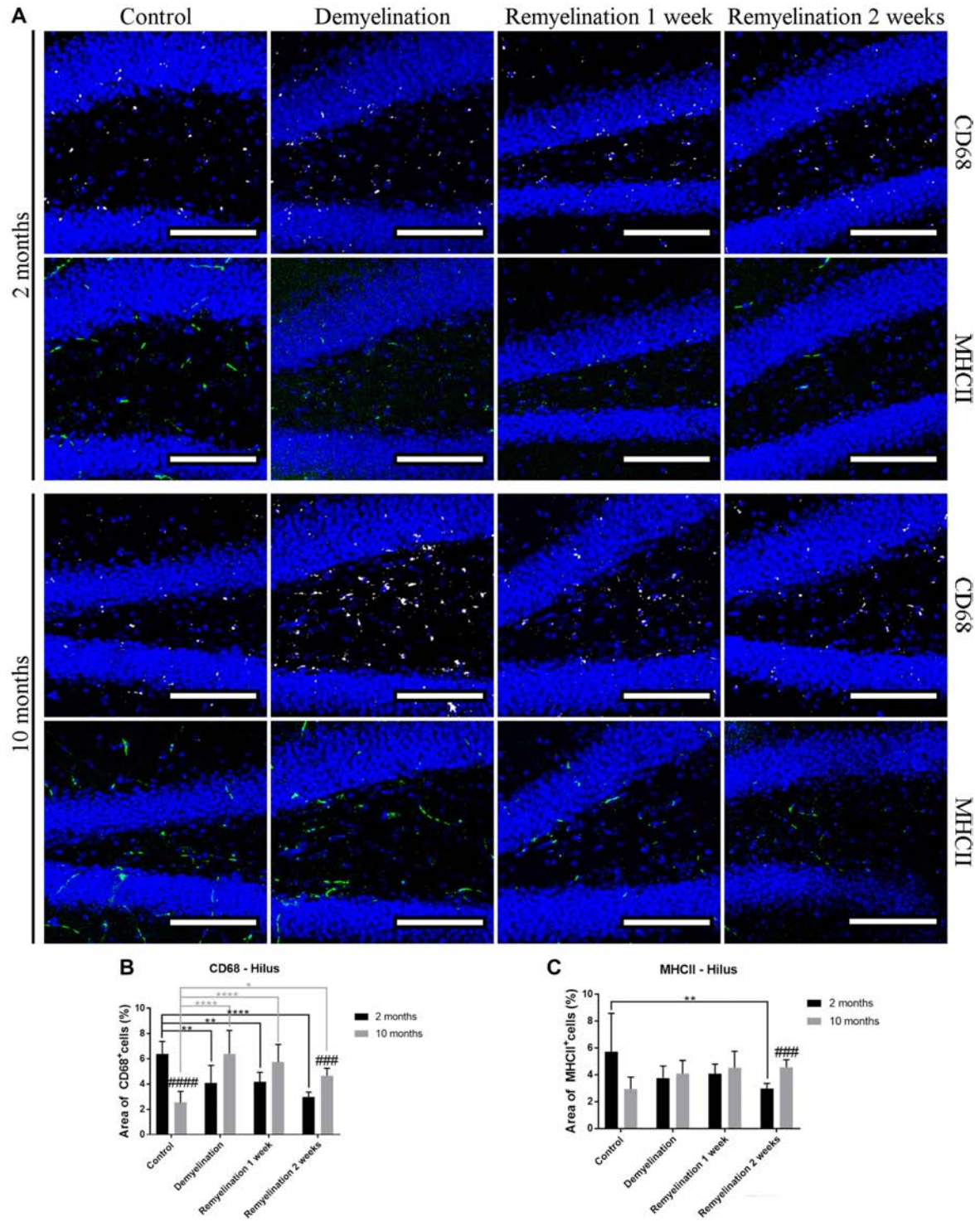

FIGURE 5 | Age-related heterogeneity in CD68 and major histocompatibility complex II (MHCII) in the hilus of the hippocampal DG. **(A)** CD68 (white) and MHCII (green) labeling. Cell nuclei are stained with DAPI (blue). **(B)** There was an age-related difference of CD68 staining in the control groups (higher in the younger controls). In the young groups, the percentage of CD68 staining decreased significantly during de- and remyelination, whereas the opposite was observed for the middle-aged groups. These different patterns led to a significantly higher CD68 level in the middle-aged group in comparison to the younger one after 2 weeks of remyelination. **(C)** MHCII expression was significantly reduced in the younger group after 2 weeks of remyelination. At the same time point, there was a significant age-related difference, with higher levels of MHCII in the middle-aged group. Values are shown as means + SD ($n = 6$ per group). Statistical significance was evaluated using a two-way ANOVA and a Tukey's *post hoc* test. The p-values are indicated in the graphs: treatment effects within the same age group: $^{*}p < 0.05$, $^{**}p < 0.01$ and $^{****}p < 0.0001$, age-related differences: $^{\#\#\#}p < 0.001$ and $^{\#\#\#\#}p < 0.0001$. Bars: **(A)** 100 μm.

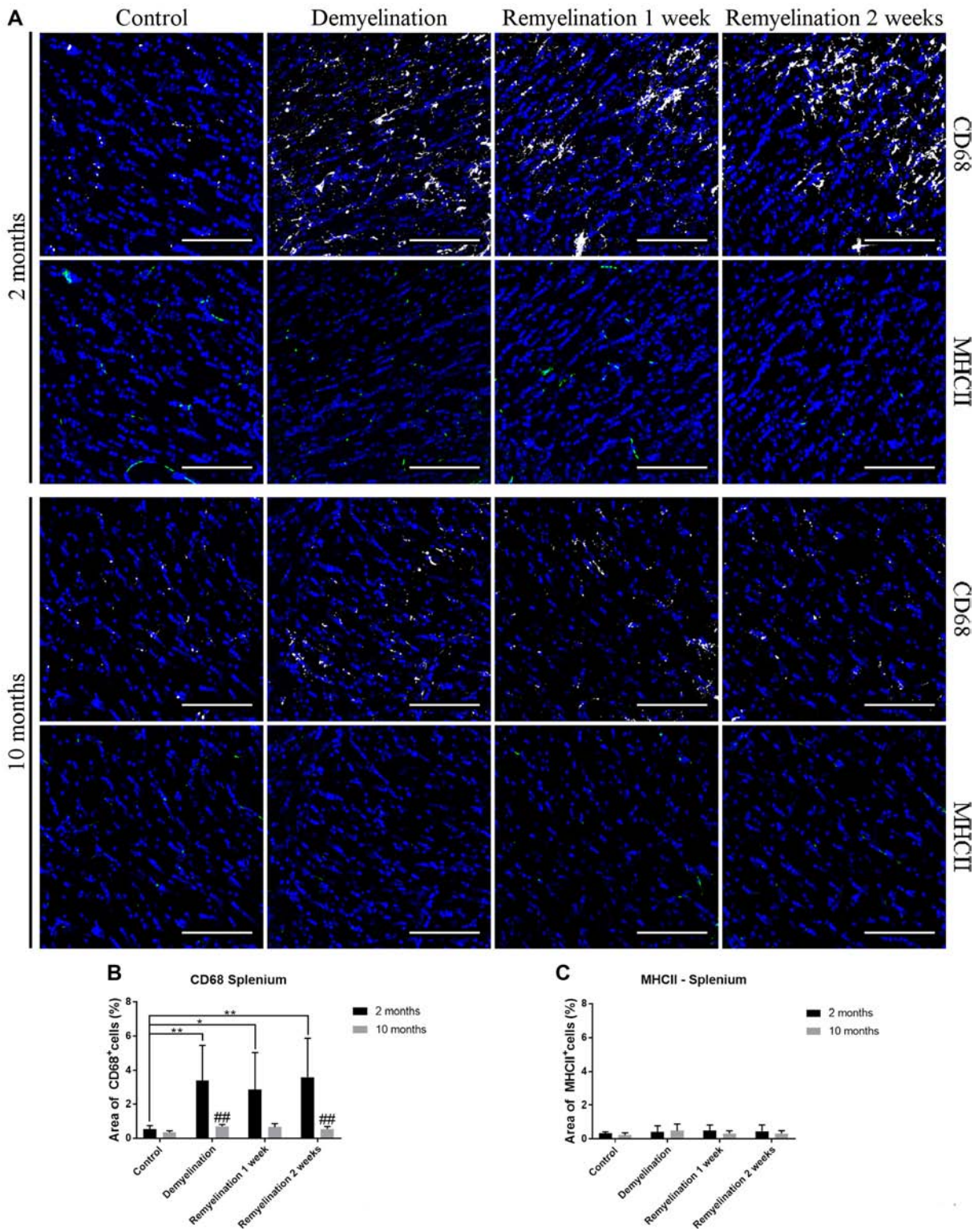

FIGURE 6 | Age-related differences in CD68, but not in MHCII, in splenium of the CC. **(A)** CD68 (white) and MHCII (green) labeling. Cell nuclei are stained with DAPI (blue). **(B)** CD68 was significantly increased during de- and remyelination only in the younger group leading to significant age-related differences (with higher values in the younger group) after demyelination and 2 weeks of remyelination. **(C)** MHCII staining was not significantly changed by de- or remyelination in both age groups. Values are shown as means + SD (n = 6 per group). Statistical significance was evaluated using a two-way ANOVA followed by a Tukey's *post hoc* test. The p-values are indicated in the graphs: treatment effects within the same age group: $^{*}p < 0.05$ and $^{**}p < 0.01$, age-related differences: $^{\#\#}p < 0.01$. Bars: **(A)** 100 μm.

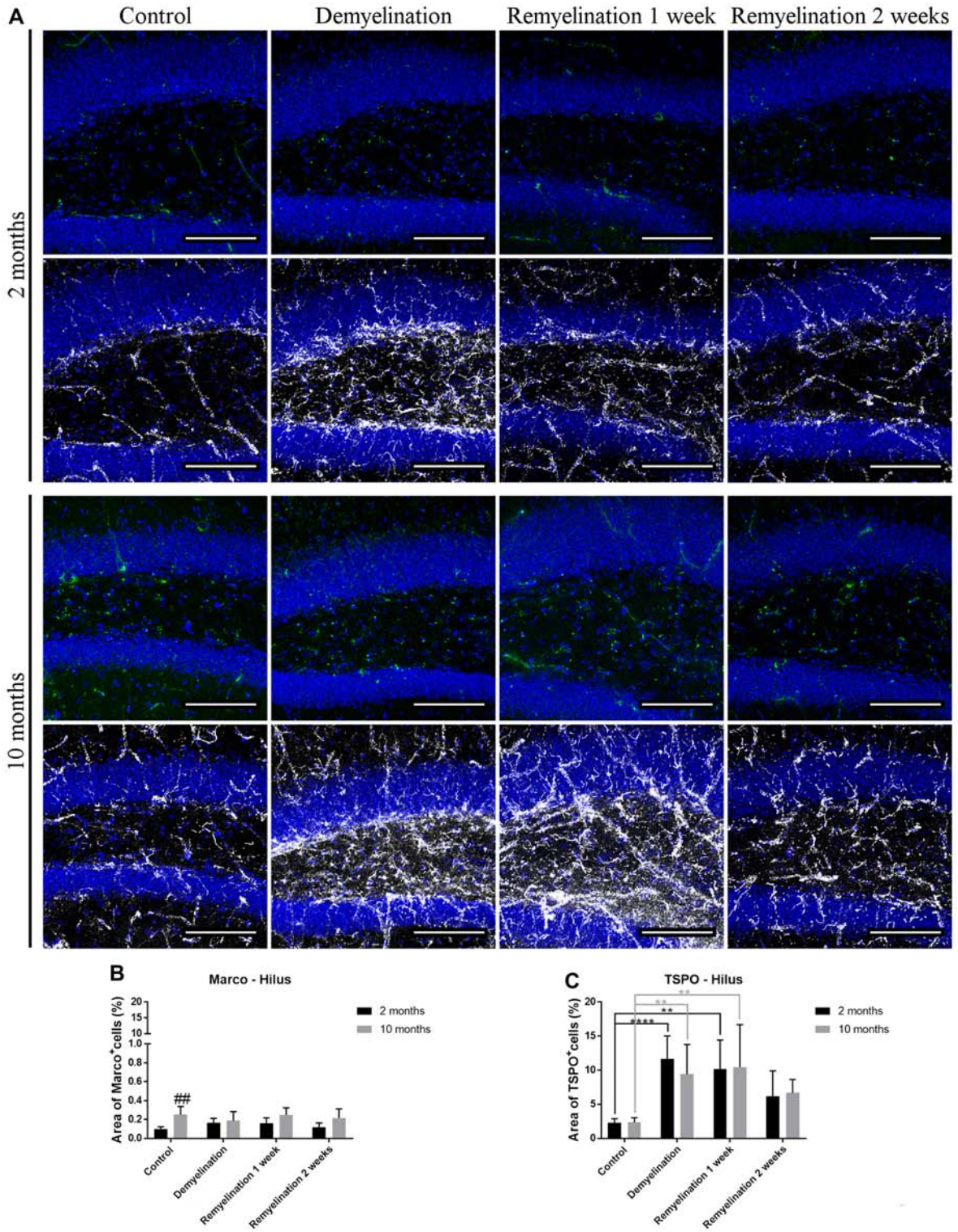

FIGURE 7 | Translocator protein 18 kD (TSPO), but not macrophage receptor with collagenous structure (Marco), reacts to de- and remyelination in the hilus of the hippocampal DG. **(A)** Marco (green) and TSPO (white) labeling. Cell nuclei are stained with DAPI (blue). **(B)** Marco staining was significantly higher in the middle-aged control group compared to the young one. De- and remyelination did not significantly change the levels of Marco. **(C)** TSPO was significantly increased during demyelination and the first week of remyelination in both age groups. Values are shown as means + SD ($n = 6$ per group). Statistical significance was evaluated using a two-way ANOVA followed by a Tukey's *post hoc* test **(C)**. The p-values are indicated in the graphs: treatment effects within the same age group: $^{**}p < 0.01$ and $^{****}p < 0.0001$, age-related differences: $^{\#\#}p < 0.01$. Bars: **(A)** 100 μm.

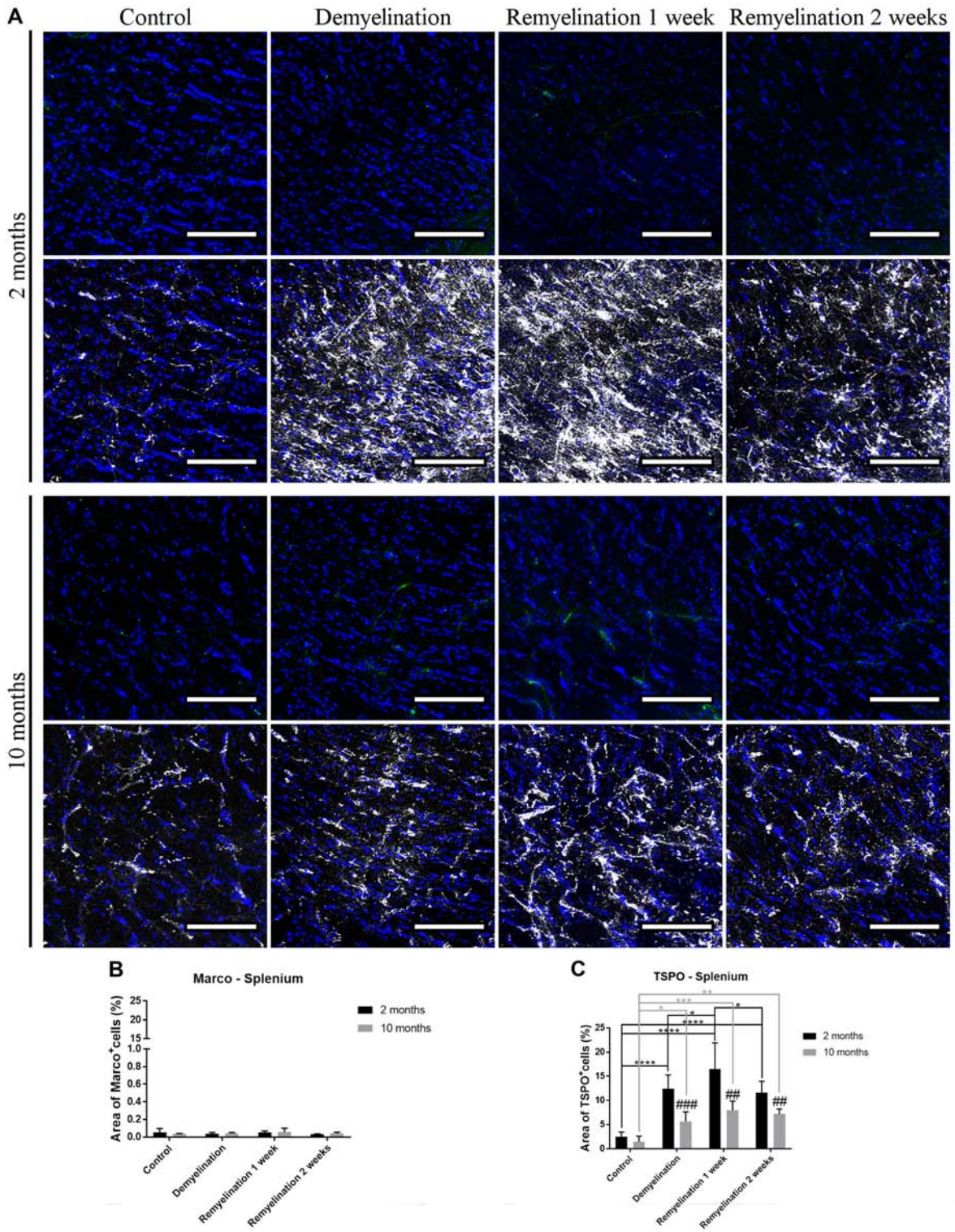

FIGURE 8 | Age-related differences in cuprizone-induced increase of TSPO in the splenium of the CC, while Marco remains unaffected. **(A)** Marco (green) and TSPO (white) labeling. Cell nuclei are stained with DAPI (blue). **(B)** No significant effects of age or treatment on Marco levels were observed. **(C)** In both age groups, TSPO was significantly increased during de- and remyelination. TSPO levels were significantly higher in the younger de- and remyelination groups. Values are shown as means + SD (n = 6 per group). Statistical significance was evaluated using a two-way ANOVA followed by a Tukey's *post hoc* test **(C)**. The p-values are indicated in the graphs: treatment effects within the same age group: $^{*}p < 0.05$, $^{**}p < 0.01$, $^{***}p < 0.001$ and $^{****}p < 0.0001$, age-related differences: $^{\#\#}p < 0.01$ and $^{\#\#\#}p < 0.001$. Bars: **(A)** 100 μm.

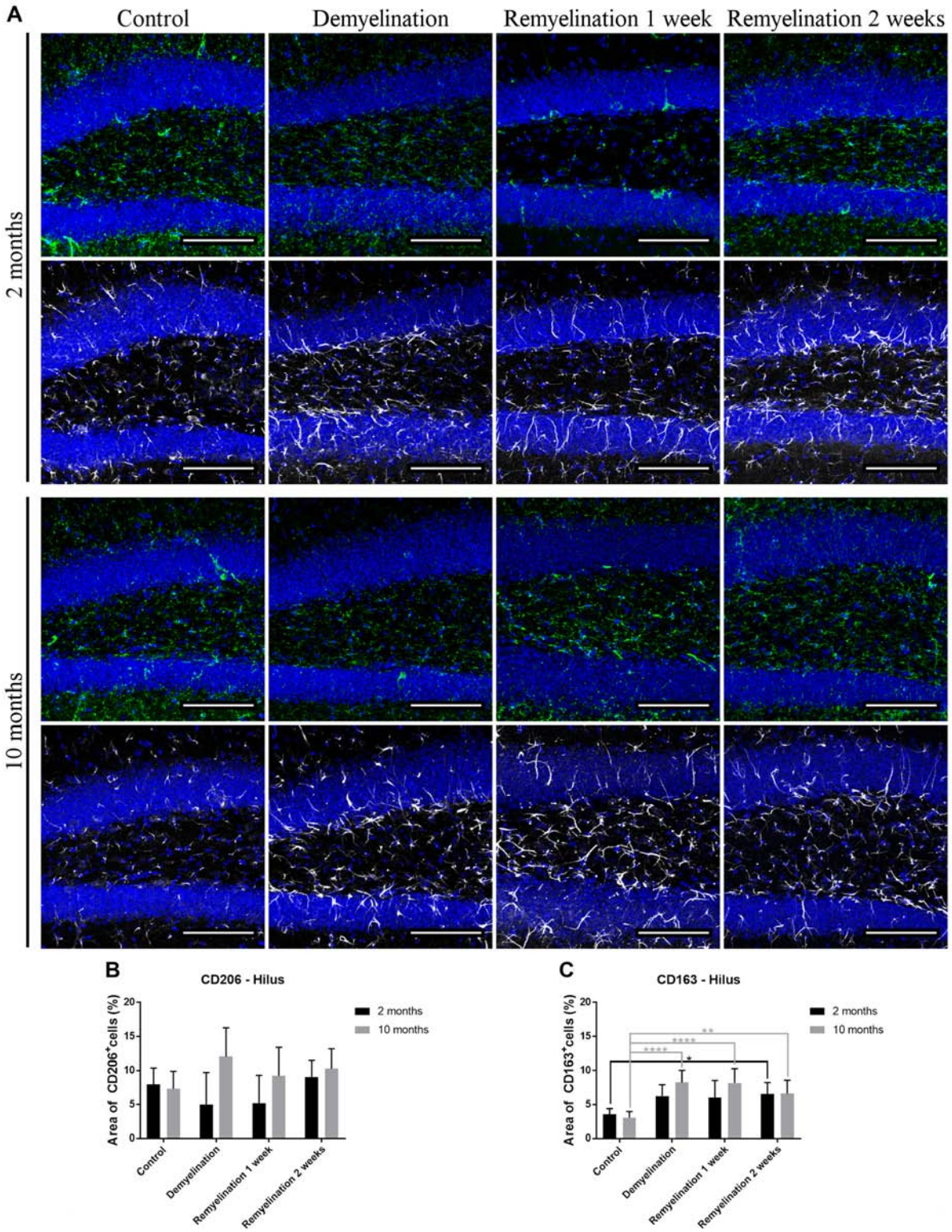

FIGURE 9 | Age-related differences in cuprizone-induced increase of CD163 in the hilus of the hippocampal DG, while CD206 is unchanged. **(A)** CD206 (green) and CD163 (white) labeling. Cell nuclei are stained with DAPI (blue). **(B)** In both age groups, de- and remyelination did not significantly affect CD206 staining. **(C)** In the middle-aged group, CD163 was significantly upregulated during de- and remyelination. In the younger group, the CD163 increase was only significant 2 weeks after remyelination. Values are shown as means + SD ($n = 6$ per group). Statistical significance was evaluated using a two-way ANOVA followed by a Tukey's *post hoc* test **(C)**. The p-values are indicated in the graphs: treatment effects within the same age group: $^{*}p < 0.05$, $^{**}p < 0.01$ and $^{****}p < 0.0001$. Bars: **(A)** 100 μm.

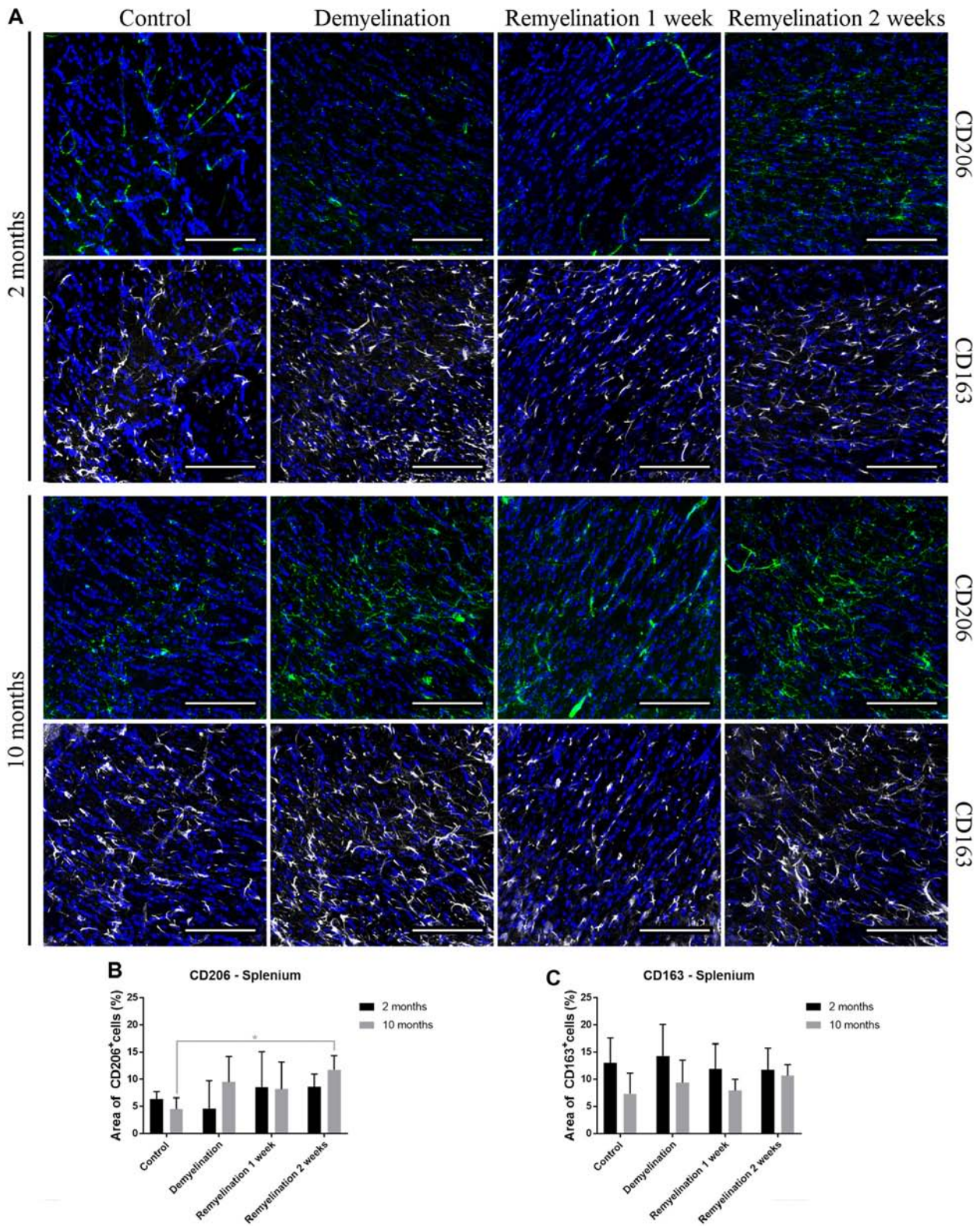

FIGURE 10 | Increase of CD206 during remyelination in middle-aged mice in the splenium of the CC, while CD163 is unaffected. **(A)** CD206 (green) and CD163 (white) labeling. Cell nuclei are stained with DAPI (blue). **(B)** CD206 was significantly elevated in the middle-aged group after 2 weeks of remyelination. **(C)** CD163 was not significantly affected by age or treatment. Values are shown as means + SD ($n = 6$ per group). Statistical significance was evaluated using a two-way ANOVA followed by a Tukey's *post hoc* test **(C)**. The p-values are indicated in the graphs: treatment effects within the same age group: $^*p < 0.05$. Bars: **(A)** 100 μm.

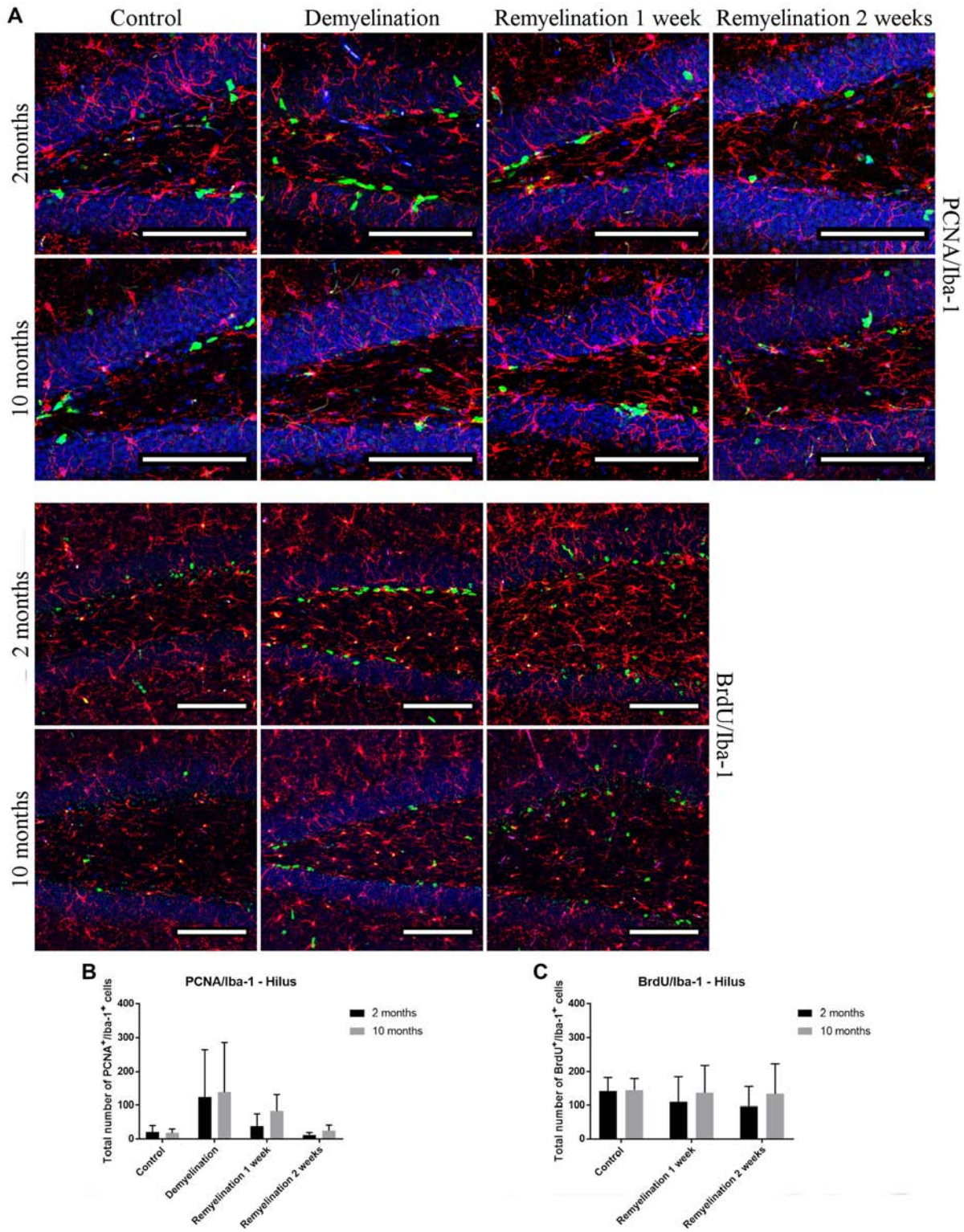

FIGURE 11 | No significant changes in numbers of proliferating microglia ($PCNA^+$ and $BrdU^+$) in the hilus of the hippocampal DG. **(A)** Proliferating cell nuclear antigen (PCNA; green) and Iba-1 (red) labeling. Cell nuclei are stained with DAPI (blue). **(B)** Bromodeoxyuridine (BrdU; green) and Iba-1 (red) labeling. Cell nuclei are stained with DAPI (blue). **(C)** No significant effects on the number of proliferating $PCNA^+$ microglia was observed. **(D)** The number of Iba-1^+ $BrdU^+$ cells was also not affected during de- or remyelination in either age group. Values are shown as means + SD (n = 6 per group). Statistical significance was evaluated using a two-way ANOVA and a Tukey's *post hoc* test. Bars: **(A)** 100 μm.

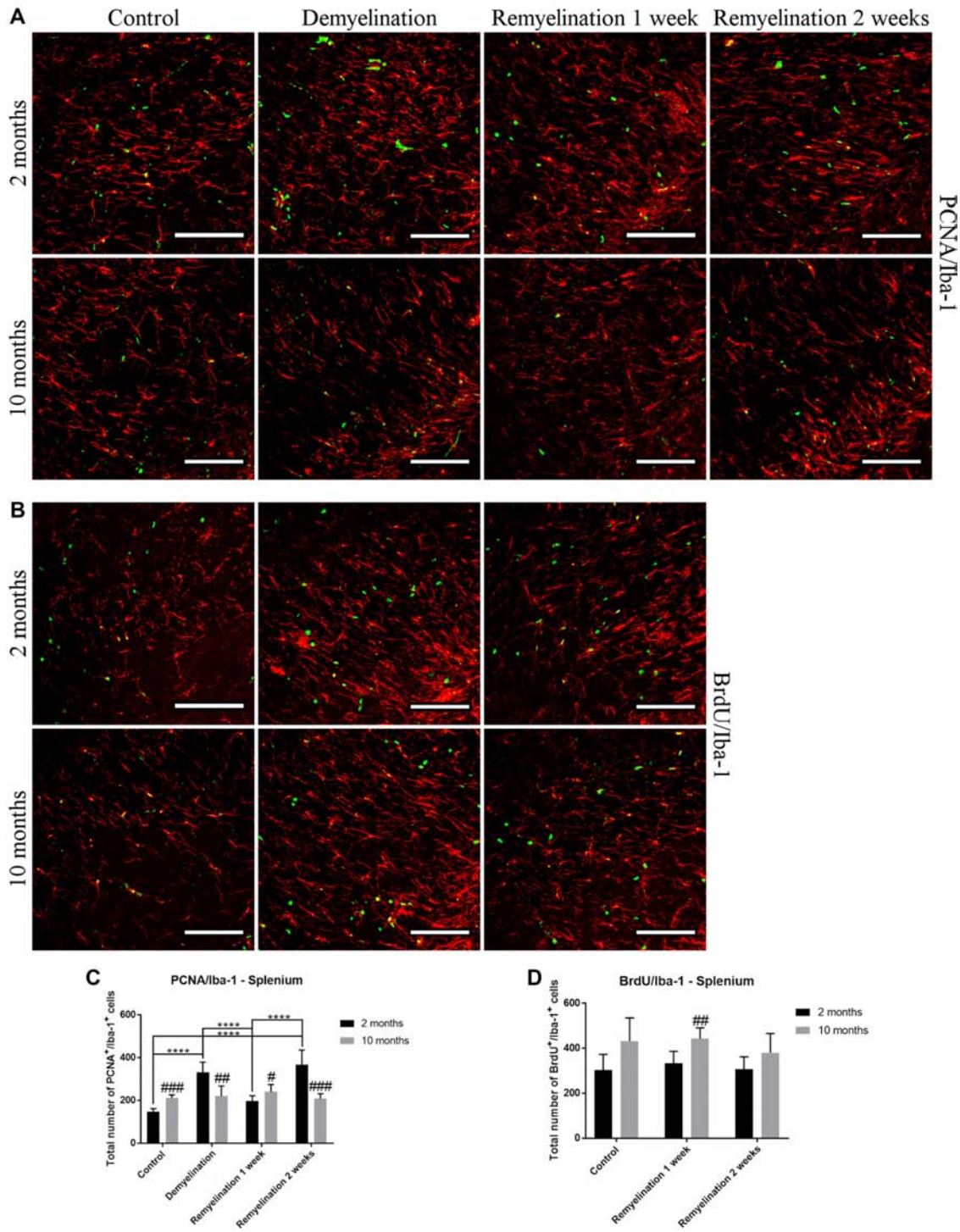

FIGURE 12 | Age-related differences in the number of proliferating microglia ($PCNA^+$ and $BrdU^+$) in the splenium of the CC. **(A)** PCNA (green) and Iba-1 (red) labeling. **(B)** BrdU (green) and Iba-1 (red) staining. **(C)** The number of proliferating $PCNA^+$ microglia was significantly increased in the middle-aged control group compared to the younger one. In young mice, there was a significant increase in $PCNA^+$ microglia after demyelination and 2 weeks of remyelination. Thus, age-related differences in $PCNA^+$ $Iba\text{-}1^+$ cell numbers were found in all treatment groups. **(D)** The number of $BrdU^+$ microglia was higher in the middle-aged group after 1 week of remyelination (a similar tendency was also observed in the other two groups). De- or remyelination did not affect the number of $BrdU^+$ $Iba\text{-}1^+$ microglia. Values are shown as means + SD ($n = 6$ per group). Statistical significance was evaluated using a two-way ANOVA and a Tukey's *post hoc* test. The p-values are indicated in the graphs: treatment effects within the same age group: $^{****}p < 0.0001$, age-related differences: $^{\#}p < 0.05$, $^{\#\#}p < 0.01$ and $^{\#\#\#}p < 0.001$. Bars: **(A)** 100 μm.

increased after 1 week of remyelination (during which BrdU was injected).

DISCUSSION

The results of the present study show that microglia in the middle-aged CNS are already subtly changed in comparison to young microglia and that they also react differently to demyelination in the cuprizone model. The observed age-related microglial changes differed between the two analyzed regions, hilus of the dorsal hippocampal DG a gray matter region functionally involved in learning and memory, and the splenium of the CC as a typical white matter region.

In both age groups, the analysis of MBP confirmed cuprizone-induced de- and remyelination, which was even more pronounced in the analyzed hippocampal region than the splenium of the CC. This is in agreement with work by others showing that in the cuprizone model demyelination occurs in the splenium of the CC (Steelman et al., 2012; Le Blon et al., 2016; Tagge et al., 2016) and the hippocampus (Hoffmann et al., 2008; Koutsoudaki et al., 2009; Norkute et al., 2009; Sun et al., 2016). Thus, the cuprizone model is well suited for studies on demyelination in the hippocampus, a region which is also affected in human MS patients (Geurts et al., 2007; Sicotte et al., 2008; Dutta et al., 2011; Hulst et al., 2015; Planche et al., 2017) with the hippocampal DG being particularly vulnerable at earliest stages of MS progression (Planche et al., 2018).

For analyzing differences between young and middle-aged mice during de- and remyelination, we first used Iba-1, a classical microglia marker, since it is highly expressed in microglia and is increased after pro-inflammatory stimulation (e.g., Mori et al., 2000; Ito et al., 2001). In the analyzed gray matter region, Iba-1 showed a similar pattern of increase during demyelination and the first week of remyelination for both age groups. However, in the splenium of the CC, the younger group showed a prolonged activation. This pattern fits to the observed changes in TSPO, a pro-inflammatory marker, which, in contrast to Iba-1, is not only expressed in microglia/macrophages, but also in astrocytes. For both Iba-1 and TSPO, a higher induction was observed in the younger group after cuprizone treatment in the analyzed white matter region, whereas there were no age-related differences in the gray matter region. TSPO is of particular interest, since PET tracer studies targeting TSPO have found convincing evidence that microglial activation indeed correlates with MS symptoms: in MS patients, this marker is not only increased in MS lesions and normal appearing gray and white matter, but also correlates with age, disease progression and disability (reviewed in Airas et al., 2018).

An unexpected finding was the significantly lower expression of CD68 in the hilus of the DG in the older controls, since it is well described that CD68 increases during aging in different brain regions (reviewed in Mosher and Wyss-Coray, 2014; Norden et al., 2015). However, one study, which performed a detailed analysis of microglia in different brain regions, found no significant increase in CD68 in old mice (20-months-old) in the DG under control conditions or after LPS injection (Hart et al., 2012). During de- and remyelination, CD68 expression tended to be higher in middle-aged mice than in the younger groups in the hilus of the DG, while the opposite was observed in the splenium of the CC, in which CD68 was up-regulated to much higher levels in the younger groups. Similar to the Iba-1 and TSPO results, this indicates a more extensive and longer lasting activation of microglia in the splenium of younger mice. However, at this point, we do not know how myelin repair is affected by the higher levels of activation markers in young microglia. It could be speculated, for example, that this age-related difference may be indicative for a more active phagocytosis in younger microglia, which has been found in a focal demyelination model (Rawji et al., 2018).

As expected, we found only low levels of MHCII in microglia under control conditions. However, the staining pattern of this marker seems to be associated at least in part with blood vessels, which could be explained by the staining of vessel-associated antigen presenting perivascular macrophages or dendritic cells. Moreover, brain pericytes are also able to express MHCII and inflammatory stimuli (such as IFN-γ) increase the MHCII expression in this perivascular cell type (Pieper et al., 2014). Surprisingly, a reduction of MHCII was found in the young group after 2 weeks of remyelination in the hippocampal DG. This, however, may be of limited functional relevance, since the observed MHCII levels are very low, and in particular are highly variable in the young control.

For two other markers that are induced by pro-inflammatory stimuli, F4/80 and Marco, the expected increase in expression was observed in middle-aged mice, but only in the analyzed gray matter region. Here, Marco was significantly higher in the older controls, and F4/80 was significantly up-regulated in all middle-aged groups, while surprisingly the F4/80 expression in the young groups was further reduced during de- and remyelination. Since most studies on microglial aging are done in old, not middle-aged mice, it is difficult to find comparable results in the literature. An age-related increase in F4/80 was found in the hippocampus of old mice (24-months-old) in one study (Boehme et al., 2014), whereas another group found that F4/80 increased in white matter regions, but not in the DG of old mice (20-months-old; Hart et al., 2012). While an injection of an M1-inducing cytokine cocktail increased Marco expression in young (6-month-old), middle-aged (12-month-old) and old mice (24-month-old mice), that study, however, reported no differences between vehicle-treated animals of different ages (Lee et al., 2013).

P2RY12 is expressed in microglia under physiological conditions, and it has been shown that it can also be used to distinguish microglia from infiltrating macrophages in mice, which is not possible with other commonly used microglia markers (Butovsky et al., 2014). Additionally, P2RY12 is being discussed as an M2-like anti-inflammatory marker, since it has been shown *in vitro* that P2RY12 expression is increased in microglia following anti-inflammatory stimuli (Moore et al., 2015; Beaino et al., 2017). In the present study, a significant reduction of P2RY12 was found in both age

groups in the hippocampal DG, which was even more severe in the middle-aged group. In the splenium, a similar pattern was only observed in the younger group. This reduction in P2RY12 coincided with an upregulation in Iba-1 and TSPO (which were both less pronounced in the splenium of the middle-aged group), suggesting that these markers are inversely regulated. These results are in accordance with other studies, which observed a reduced expression of P2RY12 in active inflammatory lesions in MS patients (Beaino et al., 2017; Mildner et al., 2017; Zrzavy et al., 2017). However, in a study investigating experimental autoimmune encephalomyelitis (EAE), an MS model in which pathology is driven mainly by $CD4^+$ T cells (reviewed in Sonar and Lal, 2017), an increased P2RY12 expression was found during the remission phase (Beaino et al., 2017), which indicates that the regulation of P2RY12 may be more complex. Zrzavy et al. (2017) analyzed P2RY12 and the anti-inflammatory microglia markers CD206 and CD163 in parallel in MS patients. This study showed a different pattern for these markers: P2RY12 was lost in active lesions but reappeared in the center of inactive lesions while the expression of CD163 and CD206 were highest in late active/inactive lesions (Zrzavy et al., 2017). In the present study, we also did not find a correlation between the changes in P2RY12 and the other analyzed M2-like markers, but rather it seems that P2RY12 is negatively correlated with pro-inflammatory markers.

Microglia have been shown to change their activation state during phagocytosis of myelin to more anti-inflammatory and pro-regenerative traits (Boven et al., 2006; van Rossum et al., 2008; Neumann et al., 2009). The anti-inflammatory marker CD206 (which is not only found in microglia, but also in astrocytes) was only significantly up-regulated in the analyzed white matter region after 2 weeks of remyelination in the middle-aged group. However, the CD206 expression was highly variable, particularly during demyelination and early remyelination. In contrast, CD163, a marker for microglia and perivascular macrophages, was significantly increased in both age groups, but this process started earlier in the middle-aged group and was only observed in the analyzed gray matter region. Thus, it seems that middle-aged mice are more likely to display M2-like characteristics than young ones. This difference may have consequences for remyelination, since in MS patients, the M2 marker CD206 is only increased in lesions with ongoing myelin repair (Butovsky et al., 2006; Miron et al., 2013). Others also have found an age-related increase in CD206 in microglia isolated from the cortex of old (24-month-old) mice (Zöller et al., 2018). In contrast, in a focal demyelination model using parabiotic pairs of aged mice (10–12 months-old), it has been shown that there is a lower number of M2-polarized microglia/macrophages (identified with the mannose receptor CD206) in demyelinated lesion, while at the same time remyelination efficiency is reduced. A parabiotic pairing of an aged mouse with a younger one (5–6 weeks-old) increased both the number of lesion-associated M2-polarized cells and remyelination in the older parabiotic partner (Miron et al., 2013). The contrasting results from Miron and colleagues and our study possibly could be due to differences in the investigated demyelination models—e.g., the longer de- and remyelination phases in the cuprizone model. Additionally, at the two analyzed time points, we did not find a difference in the extent of remyelination between the two age groups. However, it would be interesting to do functional studies with M2-polarized microglia/macrophages from aged mice after cuprizone-induced demyelination to find out whether they are indeed beneficial for myelin repair.

A significant increase of $PCNA^+$ proliferating microglia was only observed in the splenium of the CC of the younger group after demyelination and the second week of remyelination. A possible explanation for the few changes in proliferation could be that at 6 weeks of demyelination, which was analyzed in the present study, the peak of microglial proliferation that occurs at 4.5 weeks had already passed (Matsushima and Morell, 2001; Praet et al., 2014). The slightly higher number of Iba-1^+ $PCNA^+$ and Iba-1^+ $BrdU^+$ cells in the splenium of middle-aged healthy controls in comparison to young ones was unexpected, since it was shown that microglia have a relatively stable turnover rate during aging in different brain regions, such as the CC (Askew et al., 2017). However, in a stroke model an increased number of Iba-1^+ $BrdU^+$ microglia has been found in middle-aged mice (13–14 months; Moraga et al., 2015).

Traditionally, microglial activation has often been grouped into the classical pro-inflammatory or "M1" activation and the alternative, more anti-inflammatory, "M2" activation with functions in wound healing and regulation of immune responses (Colton, 2009; Olah et al., 2012; Boche et al., 2013). This classification has been derived originally from peripheral macrophages, however its usefulness has been increasingly challenged (Martinez and Gordon, 2014), in particular for the analysis of microglia (Ransohoff, 2016) as it is probably an oversimplification. Nevertheless, the markers which have been described as more M1- or M2-like are still popular targets for microglia analyses. Our results clearly show that immunohistochemical markers for microglia are useful, but great caution has to be taken when it comes to the interpretation of markers as being representative for specific microglia activity states such as M1, M2, pro- or anti-inflammatory. The markers which are currently used rather highlight the presence of a certain cell component, which, in turn, may more or less correlate with a certain microglia function. Along these lines, the present data clearly shows that the expression patterns of markers that are considered to be within the same "activation category," i.e., either pro- or anti-inflammatory, differ strongly.

The present study examines microglial alterations only after a relatively acute demyelination period. For follow-up studies, it would be interesting to examine age-related differences in microglial activation at different ages and after repeated and/or longer demyelination periods with the ultimate goal to better model the situation in MS patients suffering from cycles of relapse and remission or from chronic progressive pathology. Also, it would also be important to study both sexes in parallel—the present study only analyzed male mice.

Our results show that microglia changes already start during middle-age, but that they need to be carefully analyzed, in particular, because there are also region-dependent differences.

In healthy controls, age-related microglial changes were more pronounced in the analyzed gray matter region (resulting in more F4/80 and Marco as well as less CD68 in middle-aged mice). However, after cuprizone-induced demyelination, specifically in the analyzed white matter region, the activation of microglia in the young CNS seems to be stronger and longer lasting than in the middle-aged CNS (as indicated by increased Iba-1 and TSPO as well as reduced P2RY12). Interestingly, anti-inflammatory characteristics (increased CD206 and CD163) tend to be more pronounced in middle-aged mice. How these age-related microglial alterations might affect regeneration and myelin repair after prolonged or recurrent demyelination requires further investigation.

DATA AVAILABILITY

The datasets used and/or analyzed during the current study are available from the corresponding author on reasonable request.

AUTHOR CONTRIBUTIONS

BK designed the study, collected, analyzed and interpreted data and drafted the manuscript. HM collected, analyzed and interpreted data. SL and CB helped with data collection. FR participated in the discussion of the results. LA participated in the study design and coordination, and the discussion of the results. All authors contributed to revising the manuscript and approved the final version.

FUNDING

The research leading to these results has received funding from the European Union's Seventh Framework Programme (FP7/2007-2013) under grant agreement n° HEALTH-F2-2011-278850 (INMiND). FR was supported by research funds from Chilean FONDECYT Program CONICYT Grant #1161787 and Chilean PCI Program CONICYT Grant #REDES170233, as well as by a Stand-Alone Grant E-12/15/077-RIT from the research support funds of the Paracelsus Medical University (PMU-FFF).

ACKNOWLEDGMENTS

We are very thankful for the excellent technical assistance of Pia Zaunmair.

SUPPLEMENTARY MATERIAL

The Supplementary Material for this article can be found online at: https://www.frontiersin.org/articles/10.3389/fnagi.2018.00278/full#supplementary-material

FIGURE S1 | Weight changes during the experiment. Percentage weight changes between the first and the last 2 days of the experiment in **(A)** young and **(B)** middle-aged mice. In both age groups, no significant differences were observed in relative weight changes in comparison to the respective controls. Values are shown as means + SD (n = 6 per group). Statistical significance was evaluated using a one-way ANOVA and a Tukey's *post hoc* test **(A)** and a Kruskal-Wallis one-way analysis followed by a Dunn's multiple comparisons test **(B)**.

REFERENCES

Airas, L., Nylund, M., and Rissanen, E. (2018). Evaluation of microglial activation in multiple sclerosis patients using positron emission tomography. *Front. Neurol.* 9:181. doi: 10.3389/fneur.2018.00181

Askew, K., Li, K., Olmos-Alonso, A., Garcia-Moreno, F., Liang, Y., Richardson, P., et al. (2017). Coupled proliferation and apoptosis maintain the rapid turnover of microglia in the adult brain. *Cell Rep.* 18, 391–405. doi: 10.1016/j.celrep.2016.12.041

Baecher-Allan, C., Kaskow, B. J., and Weiner, H. L. (2018). Multiple sclerosis: mechanisms and immunotherapy. *Neuron* 97, 742–768. doi: 10.1016/j.neuron.2018.01.021

Bardou, I., Brothers, H. M., Kaercher, R. M., Hopp, S. C., and Wenk, G. L. (2013). Differential effects of duration and age on the consequences of neuroinflammation in the hippocampus. *Neurobiol. Aging* 34, 2293–2301. doi: 10.1016/j.neurobiolaging.2013.03.034

Beaino, W., Janssen, B., Kooij, G., van der Pol, S. M. A., van Het Hof, B., van Horssen, J., et al. (2017). Purinergic receptors P2Y12R and P2X7R: potential targets for PET imaging of microglia phenotypes in multiple sclerosis. *J. Neuroinflammation* 14:259. doi: 10.1186/s12974-017-1034-z

Bennett, M. L., Bennett, F. C., Liddelow, S. A., Ajami, B., Zamanian, J. L., Fernhoff, N. B., et al. (2016). New tools for studying microglia in the mouse and human CNS. *Proc. Natl. Acad. Sci. U S A* 113, E1738–E1746. doi: 10.1073/pnas.1525528113

Boche, D., Perry, V. H., and Nicoll, J. A. (2013). Review: activation patterns of microglia and their identification in the human brain. *Neuropathol. Appl. Neurobiol.* 39, 3–18. doi: 10.1111/nan.12011

Boehme, M., Guenther, M., Stahr, A., Liebmann, M., Jaenisch, N., Witte, O. W., et al. (2014). Impact of indomethacin on neuroinflammation and hippocampal neurogenesis in aged mice. *Neurosci. Lett.* 572, 7–12. doi: 10.1016/j.neulet.2014.04.043

Boven, L. A., Van Meurs, M., Van Zwam, M., Wierenga-Wolf, A., Hintzen, R. Q., Boot, R. G., et al. (2006). Myelin-laden macrophages are anti-inflammatory, consistent with foam cells in multiple sclerosis. *Brain* 129, 517–526. doi: 10.1093/brain/awh707

Brandenburg, L. O., Konrad, M., Wruck, C. J., Koch, T., Lucius, R., and Pufe, T. (2010). Functional and physical interactions between formyl-peptide-receptors and scavenger receptor MARCO and their involvement in amyloid beta 1–42-induced signal transduction in glial cells. *J. Neurochem.* 113, 749–760. doi: 10.1111/j.1471-4159.2010.06637.x

Braun, B. J., Slowik, A., Leib, S. L., Lucius, R., Varoga, D., Wruck, C. J., et al. (2011). The formyl peptide receptor like-1 and scavenger receptor MARCO are involved in glial cell activation in bacterial meningitis. *J. Neuroinflammation* 8:11. doi: 10.1186/1742-2094-8-11

Browne, P., Chandraratna, D., Angood, C., Tremlett, H., Baker, C., Taylor, B. V., et al. (2014). Atlas of multiple sclerosis 2013: a growing global problem with widespread inequity. *Neurology* 83, 1022–1024. doi: 10.1212/wnl.0000000000000768

Burudi, E. M. E., Riese, S., Stahl, P. D., and Regnier-Vigouroux, A. (1999). Identification and functional characterization of the mannose receptor in astrocytes. *Glia* 25, 44–55. doi: 10.1002/(sici)1098-1136(19990101)25:1<44::aid-glia5>3.0.co;2-c

Butovsky, O., Jedrychowski, M. P., Moore, C. S., Cialic, R., Lanser, A. J., Gabriely, G., et al. (2014). Identification of a unique TGF-β-dependent molecular and functional signature in microglia. *Nat. Neurosci.* 17, 131–143. doi: 10.1038/nn.3599

Butovsky, O., Landa, G., Kunis, G., Ziv, Y., Avidan, H., Greenberg, N., et al. (2006). Induction and blockage of oligodendrogenesis by differently activated microglia in an animal model of multiple sclerosis. *J. Clin. Invest.* 116, 905–915. doi: 10.1172/jci26836

Colton, C. A. (2009). Heterogeneity of microglial activation in the innate immune response in the brain. *J. Neuroimmune Pharmacol.* 4, 399–418. doi: 10.1007/s11481-009-9164-4

Confavreux, C., and Vukusic, S. (2006). Age at disability milestones in multiple sclerosis. *Brain* 129, 595–605. doi: 10.1093/brain/awh714

Couillard-Despres, S., Winner, B., Schaubeck, S., Aigner, R., Vroemen, M., Weidner, N., et al. (2005). Doublecortin expression levels in adult brain reflect neurogenesis. *Eur. J. Neurosci.* 21, 1–14. doi: 10.1111/j.1460-9568.2004.03813.x

Dutta, R., Chang, A., Doud, M. K., Kidd, G. J., Ribaudo, M. V., Young, E. A., et al. (2011). Demyelination causes synaptic alterations in hippocampi from multiple sclerosis patients. *Ann. Neurol.* 69, 445–454. doi: 10.1002/ana.22337

Fulci, G., Dmitrieva, N., Gianni, D., Fontana, E. J., Pan, X., Lu, Y., et al. (2007). Depletion of peripheral macrophages and brain microglia increases brain tumor titers of oncolytic viruses. *Cancer Res.* 67, 9398–9406. doi: 10.1158/0008-5472.can-07-1063

Geurts, J. J., Bo, L., Roosendaal, S. D., Hazes, T., Daniels, R., Barkhof, F., et al. (2007). Extensive hippocampal demyelination in multiple sclerosis. *J. Neuropathol. Exp. Neurol.* 66, 819–827. doi: 10.1097/nen.0b013e3181461f54

Goldberg, J., Clarner, T., Beyer, C., and Kipp, M. (2015). Anatomical distribution of cuprizone-induced lesions in C57BL6 mice. *J. Mol. Neurosci.* 57, 166–175. doi: 10.1007/s12031-015-0595-5

Gordon, S., Hamann, J., Lin, H. H., and Stacey, M. (2011). F4/80 and the related adhesion-GPCRs. *Eur. J. Immunol.* 41, 2472–2476. doi: 10.1002/eji.201141715

Hart, A. D., Wyttenbach, A., Perry, V. H., and Teeling, J. L. (2012). Age related changes in microglial phenotype vary between CNS regions: grey versus white matter differences. *Brain Behav. Immun.* 26, 754–765. doi: 10.1016/j.bbi.2011.11.006

Hefendehl, J. K., Neher, J. J., Sühs, R. B., Kohsaka, S., Skodras, A., and Jucker, M. (2014). Homeostatic and injury-induced microglia behavior in the aging brain. *Aging Cell* 13, 60–69. doi: 10.1111/acel.12149

Hoffmann, K., Lindner, M., Gröticke, I., Stangel, M., and Löscher, W. (2008). Epileptic seizures and hippocampal damage after cuprizone-induced demyelination in C57BL/6 mice. *Exp. Neurol.* 210, 308–321. doi: 10.1016/j.expneurol.2007.11.005

Hulst, H. E., Schoonheim, M. M., Van Geest, Q., Uitdehaag, B. M. J., Barkhof, F., and Geurts, J. J. G. (2015). Memory impairment in multiple sclerosis: relevance of hippocampal activation and hippocampal connectivity. *Mult. Scler.* 21, 1705–1712. doi: 10.1177/1352458514567727

Imai, Y., Ibata, I., Ito, D., Ohsawa, K., and Kohsaka, S. (1996). A novel gene iba1 in the major histocompatibility complex class III region encoding an EF hand protein expressed in a monocytic lineage. *Biochem. Biophys. Res. Commun.* 224, 855–862. doi: 10.1006/bbrc.1996.1112

Ito, D., Imai, Y., Ohsawa, K., Nakajima, K., Fukuuchi, Y., and Kohsaka, S. (1998). Microglia-specific localisation of a novel calcium binding protein, Iba1. *Mol. Brain Res.* 57, 1–9. doi: 10.1016/s0169-328x(98)00040-0

Ito, D., Tanaka, K., Suzuki, S., Dembo, T., and Fukuuchi, Y. (2001). Enhanced expression of Iba1, ionized calcium-binding adapter molecule 1, after transient focal cerebral ischemia in rat brain. *Stroke* 32, 1208–1215. doi: 10.1161/01.str.32.5.1208

Jack, C., Ruffini, F., Bar-Or, A., and Antel, J. P. (2005). Microglia and multiple sclerosis. *J. Neurosci. Res.* 81, 363–373. doi: 10.1002/jnr.20482

Jacobs, A. H., Tavitian, B., and INMiND consortium. (2012). Noninvasive molecular imaging of neuroinflammation. *J. Cereb. Blood Flow Metab.* 32, 1393–1415. doi: 10.1038/jcbfm.2012.53

Kandasamy, M., Lehner, B., Kraus, S., Sander, P. R., Marschallinger, J., Rivera, F. J., et al. (2014). TGF-beta signalling in the adult neurogenic niche promotes stem cell quiescence as well as generation of new neurons. *J. Cell. Mol. Med.* 18, 1444–1459. doi: 10.1111/jcmm.12298

Kipp, M., Clarner, T., Dang, J., Copray, S., and Beyer, C. (2009). The cuprizone animal model: new insights into an old story. *Acta Neuropathol.* 118, 723–736. doi: 10.1007/s00401-009-0591-3

Koutsoudaki, P. N., Skripuletz, T., Gudi, V., Moharregh-Khiabani, D., Hildebrandt, H., Trebst, C., et al. (2009). Demyelination of the hippocampus is prominent in the cuprizone model. *Neurosci. Lett.* 451, 83–88. doi: 10.1016/j.neulet.2008.11.058

Le Blon, D., Guglielmetti, C., Hoornaert, C., Quarta, A., Daans, J., Dooley, D., et al. (2016). Intracerebral transplantation of interleukin 13-producing mesenchymal stem cells limits microgliosis, oligodendrocyte loss and demyelination in the cuprizone mouse model. *J. Neuroinflammation* 13:288. doi: 10.1186/s12974-016-0756-7

Lee, D. C., Ruiz, C. R., Lebson, L., Selenica, M. L., Rizer, J., Hunt, J. B. Jr., et al. (2013). Aging enhances classical activation but mitigates alternative activation in the central nervous system. *Neurobiol. Aging* 34, 1610–1620. doi: 10.1016/j.neurobiolaging.2012.12.014

Mallucci, G., Peruzzotti-Jametti, L., Bernstock, J. D., and Pluchino, S. (2015). The role of immune cells, glia and neurons in white and gray matter pathology in multiple sclerosis. *Prog. Neurobiol.* 127–128, 1–22. doi: 10.1016/j.pneurobio.2015.02.003

Manouchehrinia, A., Westerlind, H., Kingwell, E., Zhu, F., Carruthers, R., Ramanujam, R., et al. (2017). Age related multiple sclerosis severity score: disability ranked by age. *Mult. Scler.* 23, 1938–1946. doi: 10.1177/1352458517690618

Martinez, F. O., and Gordon, S. (2014). The M1 and M2 paradigm of macrophage activation: time for reassessment. *F1000Prime Rep.* 6:13. doi: 10.12703/p6-13

Matsushima, G. K., and Morell, P. (2001). The neurotoxicant, cuprizone, as a model to study demyelination and remyelination in the central nervous system. *Brain Pathol.* 11, 107–116. doi: 10.1111/j.1750-3639.2001.tb00385.x

McMurran, C. E., Jones, C. A., Fitzgerald, D. C., and Franklin, R. J. (2016). CNS remyelination and the innate immune system. *Front. Cell Dev. Biol.* 4:38. doi: 10.3389/fcell.2016.00038

Mildner, A., Huang, H., Radke, J., Stenzel, W., and Priller, J. (2017). P2Y12 receptor is expressed on human microglia under physiological conditions throughout development and is sensitive to neuroinflammatory diseases. *Glia* 65, 375–387. doi: 10.1002/glia.23097

Miron, V. E. (2017). Microglia-driven regulation of oligodendrocyte lineage cells, myelination, and remyelination. *J. Leukoc. Biol.* 101, 1103–1108. doi: 10.1189/jlb.3ri1116-494r

Miron, V. E., Boyd, A., Zhao, J. W., Yuen, T. J., Ruckh, J. M., Shadrach, J. L., et al. (2013). M2 microglia and macrophages drive oligodendrocyte differentiation during CNS remyelination. *Nat. Neurosci.* 16, 1211–1218. doi: 10.1038/nn.3469

Moore, C. S., Ase, A. R., Kinsara, A., Rao, V. T., Michell-Robinson, M., Leong, S. Y., et al. (2015). P2Y12 expression and function in alternatively activated human microglia. *Neurol. Neuroimmunol. Neuroinflamm.* 2:e80. doi: 10.1212/NXI.0000000000000080

Moraga, A., Pradillo, J. M., García-Culebras, A., Palma-Tortosa, S., Ballesteros, I., Hernández-Jiménez, M., et al. (2015). Aging increases microglial proliferation, delays cell migration and decreases cortical neurogenesis after focal cerebral ischemia. *J. Neuroinflammation* 12:87. doi: 10.1186/s12974-015-0314-8

Mori, I., Imai, Y., Kohsaka, S., and Kimura, Y. (2000). Upregulated expression of Iba1 molecules in the central nervous system of mice in response to neurovirulent influenza A virus infection. *Microbiol. Immunol.* 44, 729–735. doi: 10.1111/j.1348-0421.2000.tb02556.x

Mosher, K. I., and Wyss-Coray, T. (2014). Microglial dysfunction in brain aging and Alzheimer's disease. *Biochem. Pharmacol.* 88, 594–604. doi: 10.1016/j.bcp.2014.01.008

Napoli, I., and Neumann, H. (2010). Protective effects of microglia in multiple sclerosis. *Exp. Neurol.* 225, 24–28. doi: 10.1016/j.expneurol.2009.04.024

Neumann, H., Kotter, M. R., and Franklin, R. J. (2009). Debris clearance by microglia: an essential link between degeneration and regeneration. *Brain* 132, 288–295. doi: 10.1093/brain/awn109

Norden, D. M., and Godbout, J. P. (2013). Review: microglia of the aged brain: primed to be activated and resistant to regulation. *Neuropathol. Appl. Neurobiol.* 39, 19–34. doi: 10.1111/j.1365-2990.2012.01306.x

Norden, D. M., Muccigrosso, M. M., and Godbout, J. P. (2015). Microglial priming and enhanced reactivity to secondary insult in aging and traumatic CNS injury and neurodegenerative disease. *Neuropharmacology* 96, 29–41. doi: 10.1016/j.neuropharm.2014.10.028

Norkute, A., Hieble, A., Braun, A., Johann, S., Clarner, T., Baumgartner, W., et al. (2009). Cuprizone treatment induces demyelination and astrocytosis in the mouse hippocampus. *J. Neurosci. Res.* 87, 1343–1355. doi: 10.1002/jnr.21946

Olah, M., Amor, S., Brouwer, N., Vinet, J., Eggen, B., Biber, K., et al. (2012). Identification of a microglia phenotype supportive of remyelination. *Glia* 60, 306–321. doi: 10.1002/glia.21266

O'Loughlin, E., Madore, C., Lassmann, H., and Butovsky, O. (2018). Microglial phenotypes and functions in multiple sclerosis. *Cold Spring Harb. Perspect. Med.* 8:a028993. doi: 10.1101/cshperspect.a028993

Perry, V. H., and Holmes, C. (2014). Microglial priming in neurodegenerative disease. *Nat. Rev. Neurol.* 10, 217–224. doi: 10.1038/nrneurol.2014.38

Pieper, C., Marek, J. J., Unterberg, M., Schwerdtle, T., and Galla, H. J. (2014). Brain capillary pericytes contribute to the immune defense in response to cytokines or LPS *in vitro*. *Brain Res.* 1550, 1–8. doi: 10.1016/j.brainres.2014.01.004

Planche, V., Koubiyr, I., Romero, J. E., Manjon, J. V., Coupé, P., Deloire, M., et al. (2018). Regional hippocampal vulnerability in early multiple sclerosis: dynamic pathological spreading from dentate gyrus to CA1. *Hum. Brain Mapp.* 39, 1814–1824. doi: 10.1002/hbm.23970

Planche, V., Ruet, A., Coupe, P., Lamargue-Hamel, D., Deloire, M., Pereira, B., et al. (2017). Hippocampal microstructural damage correlates with memory impairment in clinically isolated syndrome suggestive of multiple sclerosis. *Mult. Scler.* 23, 1214–1224. doi: 10.1177/1352458516675750

Praet, J., Guglielmetti, C., Berneman, Z., Van der Linden, A., and Ponsaerts, P. (2014). Cellular and molecular neuropathology of the cuprizone mouse model: clinical relevance for multiple sclerosis. *Neurosci. Biobehav. Rev.* 47, 485–505. doi: 10.1016/j.neubiorev.2014.10.004

Ransohoff, R. M. (2016). A polarizing question: do M1 and M2 microglia exist? *Nat. Neurosci.* 19, 987–991. doi: 10.1038/nn.4338

Rawji, K. S., Kappen, J., Tang, W., Teo, W., Plemel, J. R., Stys, P. K., et al. (2018). Deficient surveillance and phagocytic activity of myeloid cells within demyelinated lesions in aging mice visualized by *ex vivo* live multiphoton imaging. *J. Neurosci.* 38, 1973–1988. doi: 10.1523/jneurosci.2341-17.2018

Rawji, K. S., and Yong, V. W. (2013). The benefits and detriments of macrophages/microglia in models of multiple sclerosis. *Clin. Dev. Immunol.* 2013:948976. doi: 10.1155/2013/948976

Régnier-Vigouroux, A. (2003). The mannose receptor in the brain. *Int. Rev. Cytol.* 226, 321–342. doi: 10.1016/s0074-7696(03)01006-4

Sasaki, Y., Hoshi, M., Akazawa, C., Nakamura, Y., Tsuzuki, H., Inoue, K., et al. (2003). Selective expression of Gi/o-coupled ATP receptor P2Y12 in microglia in rat brain. *Glia* 44, 242–250. doi: 10.1002/glia.10293

Schuitemaker, A., van der Doef, T. F., Boellaard, R., van der Flier, W. M., Yaqub, M., Windhorst, A. D., et al. (2012). Microglial activation in healthy aging. *Neurobiol. Aging* 33, 1067–1072. doi: 10.1016/j.neurobiolaging.2010.09.016

Sicotte, N. L., Kern, K. C., Giesser, B. S., Arshanapalli, A., Schultz, A., Montag, M., et al. (2008). Regional hippocampal atrophy in multiple sclerosis. *Brain* 131, 1134–1141. doi: 10.1093/brain/awn030

Sierra, A., Abiega, O., Shahraz, A., and Neumann, H. (2013). Janus-faced microglia: beneficial and detrimental consequences of microglial phagocytosis. *Front. Cell. Neurosci.* 7:6. doi: 10.3389/fncel.2013.00006

Sonar, S. A., and Lal, G. (2017). Differentiation and transmigration of CD4 T cells in neuroinflammation and autoimmunity. *Front. Immunol.* 8:1695. doi: 10.3389/fimmu.2017.01695

Steelman, A. J., Thompson, J. P., and Li, J. (2012). Demyelination and remyelination in anatomically distinct regions of the corpus callosum following cuprizone intoxication. *Neurosci. Res.* 72, 32–42. doi: 10.1016/j.neures.2011.10.002

Streit, W. J., Xue, Q. S., Tischer, J., and Bechmann, I. (2014). Microglial pathology. *Acta Neuropathol. Commun.* 2:142. doi: 10.1186/s40478-014-0142-6

Sun, J., Zhou, H., Bai, F., Ren, Q., and Zhang, Z. (2016). Myelin injury induces axonal transport impairment but not AD-like pathology in the hippocampus of cuprizone-fed mice. *Oncotarget* 7, 30003–30017. doi: 10.18632/oncotarget.8981

Tagge, I., O'Connor, A., Chaudhary, P., Pollaro, J., Berlow, Y., Chalupsky, M., et al. (2016). Spatio-temporal patterns of demyelination and remyelination in the cuprizone mouse model. *PLoS One* 11:e0152480. doi: 10.1371/journal.pone.0152480

Thomsen, J. H., Etzerodt, A., Svendsen, P., and Moestrup, S. K. (2013). The haptoglobin-CD163-heme oxygenase-1 pathway for hemoglobin scavenging. *Oxid. Med. Cell. Longev.* 2013:523652. doi: 10.1155/2013/523652

van Rossum, D., Hilbert, S., Strassenburg, S., Hanisch, U. K., and Brück, W. (2008). Myelin-phagocytosing macrophages in isolated sciatic and optic nerves reveal a unique reactive phenotype. *Glia* 56, 271–283. doi: 10.1002/glia.20611

Zöller, T., Attaai, A., Potru, P. S., Ruß, T., and Spittau, B. (2018). Aged mouse cortical microglia display an activation profile suggesting immunotolerogenic functions. *Int. J. Mol. Sci.* 19:E706. doi: 10.3390/ijms19030706

Zrzavy, T., Machado-Santos, J., Christine, S., Baumgartner, C., Weiner, H. L., Butovsky, O., et al. (2017). Dominant role of microglial and macrophage innate immune responses in human ischemic infarcts. *Brain Pathol.* doi: 10.1111/bpa.12583 [Epub ahead of print].

Conflict of Interest Statement: The authors declare that the research was conducted in the absence of any commercial or financial relationships that could be construed as a potential conflict of interest.

frontiers in Aging Neuroscience

ORIGINAL RESEARCH
published: 26 September 2018
doi: 10.3389/fnagi.2018.00269

An Aqueous Extract of Herbal Medicine ALWPs Enhances Cognitive Performance and Inhibits LPS-Induced Neuroinflammation via FAK/NF-κB Signaling Pathways

Ju-Young Lee[1†], Bitna Joo[1,2†], Jin Han Nam[1], Hye Yeon Nam[1], Wonil Lee[1], Youngpyo Nam[1], Yongtaek Seo[3], Hye-Jin Kang[1], Hyun-Ji Cho[1], Young Pyo Jang[3], Jeongyeon Kim[1], Young-Man We[4,5], Ja Wook Koo[1,2]* and Hyang-Sook Hoe[1]**

[1] Department of Neural Development and Disease, Korea Brain Research Institute, Daegu, South Korea, [2] Department of Brain and Cognitive Sciences, Daegu Gyeongbuk Institute of Science & Technology, Daegu, South Korea, [3] Division of Pharmacology, College of Pharmacy, Kyung Hee University, Seoul, South Korea, [4] College of Korean Medicine, Wonkwang University, Iksan, South Korea, [5] Oriental Medical Clinic Center, Hyoo Medical Clinic, Seoul, South Korea

OPEN ACCESS

Edited by:
Brandi Ormerod,
University of Florida, United States

Reviewed by:
Marco Atzori,
Universidad Autónoma de San Luis Potosí, Mexico
Deep R. Sharma,
SUNY Downstate Medical Center, United States

***Correspondence:**
Young-Man We
hyooclinic@naver.com;
Young@kbri.re.kr
Ja Wook Koo
jawook.koo@kbri.re.kr
Hyang-Sook Hoe
sookhoe72@kbri.re.kr

† These authors have contributed equally to this work

Received: 12 March 2018
Accepted: 22 August 2018
Published: 26 September 2018

Citation:
Lee J-Y, Joo B, Nam JH, Nam HY, Lee W, Nam Y, Seo Y, Kang H-J, Cho H-J, Jang YP, Kim J, We Y-M, Koo JW and Hoe H-S (2018) An Aqueous Extract of Herbal Medicine ALWPs Enhances Cognitive Performance and Inhibits LPS-Induced Neuroinflammation via FAK/NF-κB Signaling Pathways. Front. Aging Neurosci. 10:269. doi: 10.3389/fnagi.2018.00269

Recent studies have shown that Liuwei Dihuang pills (LWPs) can positively affect learning, memory and neurogenesis. However, the underlying molecular mechanisms are not understood. In the present study, we developed ALWPs, a mixture of *Antler* and LWPs, and investigated whether ALWPs can affect neuroinflammatory responses. We found that ALWPs (500 μg/ml) inhibited lipopolysaccharide (LPS)-induced proinflammatory cytokine IL-1β mRNA levels in BV2 microglial cells but not primary astrocytes. ALWPs significantly reduced LPS-induced cell-surface levels of TLR4 to alter neuroinflammation. An examination of the molecular mechanisms by which ALWPs regulate the LPS-induced proinflammatory response revealed that ALWPs significantly downregulated LPS-induced levels of FAK phosphorylation, suggesting that ALWPs modulate FAK signaling to alter LPS-induced IL-1β levels. In addition, treatment with ALWPs followed by LPS resulted in decreased levels of the transcription factor NF-κB in the nucleus compared with LPS alone. Moreover, ALWPs significantly suppressed LPS-induced BV2 microglial cell migration. To examine whether ALWPs modulate learning and memory *in vivo*, wild-type C57BL/6J mice were orally administered ALWPs (200 mg/kg) or PBS daily for 3 days, intraperitoneally injected (i.p.) with LPS (250 μg/kg) or PBS, and assessed in Y maze and NOR tests. We observed that oral administration of ALWPs to LPS-injected wild-type C57BL/6J mice significantly rescued short- and long-term memory. More importantly, oral administration of ALWPs to LPS-injected wild-type C57BL/6J mice significantly reduced microglial activation in the hippocampus and cortex. Taken together, our results suggest that ALWPs can suppress neuroinflammation-associated cognitive deficits and that ALWPs have potential as a drug for neuroinflammation/neurodegeneration-related diseases, including Alzheimer's disease (AD).

Keywords: LPS, neuroinflammation, NF-κB, IL-1β, FAK

INTRODUCTION

Microglial cells represent 10–15% of the human brain. Microglia are resident innate immune cells in the central nervous system (CNS) and play a critical role in defending the host in response to exogenous toxins (Kreutzberg, 1996; Hanisch and Kettenmann, 2007; Kettenmann et al., 2011; Tremblay et al., 2011). Upon injury, microglia phagocytize dying cells and any cell debris (Neumann et al., 2009). In addition, microglia maintain brain homeostasis to ensure consistent cytokine levels. In aged brain and rodent models of neurodegenerative disease, microglial activation causes neuroinflammation, synaptic dysfunction and neuronal cell death (Hirsch et al., 2012; Cunningham, 2013; Asai et al., 2015), suggesting an association of neuroinflammation with neurodegenerative diseases. Activated microglial cells significantly increase proinflammatory cytokine levels and Aβ plaque deposition, resulting in impairment of learning and memory (Tan et al., 2013). In Alzheimer's disease (AD), soluble amyloid-β oligomers and fibrils interact with cell-surface receptors (e.g., integrin, CD14, and the Toll-like receptors TLR2 and TLR4) in microglial cells, and these interactions can also trigger a neuroinflammatory response (Solito and Sastre, 2012; Park et al., 2013; Zhang and Wang, 2014; Heneka et al., 2015). Significantly enhanced microglial activation has been observed in the cortex and hippocampus in mouse models of AD and AD patients, in addition to increased expression of proinflammatory cytokines in the brain, serum, and cerebrospinal fluid (CSF) (Oakley et al., 2006; Dursun et al., 2015; Shal et al., 2018). neuroinflammation has also been implicated in Parkinson's disease (PD), another neurodegenerative disease. For example, lipopolysaccharide (LPS)-injected wild-type C57BL/6J mice exhibit significantly induced microglial activation, which leads to functional changes such as dopaminergic neuron attenuation in an IL-1-dependent manner, resulting in PD-like behavioral impairment (Tanaka et al., 2013). Interestingly, microglial activation and proinflammatory cytokine levels [e.g., tumor necrosis factor-α (TNF-α), interleukin (IL)-1β, and IL-6] are significantly increased in the brain, CSF, and serum of PD patients postmortem, suggesting potential roles of these markers in predicting the progression of PD (Mogi et al., 1994; Williams-Gray et al., 2016). Although the molecular mechanisms by which neuroinflammation affects neurodegenerative diseases remain to be clarified, modulating microglia-mediated neuroinflammation in the brain may be a therapeutic strategy for treating or preventing neurodegenerative diseases.

Yukmijuhwang-tang (Liu-wei-di-huang-tang in China, Lokumijio-to in Japan) is a traditional Oriental herbal medicine that contains 6 different herb components: steamed *Rehmanniae radix*, *Discoreae radix*, *Corni fructus*, *Hoelen*, *Moutan Cortex Radicis,* and *Alismatis radix*. Yukmijuhwang-tang is widely used in Asia to treat diabetes mellitus, impaired neurogenesis, and malfunctions of the immune system (Park et al., 2005; Lee et al., 2012). Recent studies have shown that Liuwei Dihuang pills (LWPs), which are prescribed to prevent aging, regulate oxidant and free radical-scavenging activity (Ha et al., 2011; Lee et al., 2012). In addition, LWPs improve learning and memory in aged mice and promote neurogenesis in the dentate gyrus of the hippocampus in a stressed rat model (Wei, 2000; Hsieh et al., 2003; Park et al., 2005; Kang et al., 2006). However, whether LWPs can alter neuroinflammation is unknown.

Deer antler is a traditional herbal medicine that has been reported to restore the immune response, produce anti-inflammatory effects and improve learning and memory. For instance, pilose antler peptide regulates proinflammatory cytokines (e.g., TNF-α and IL-1β) in LPS-induced primary nucleus pulposus cells by inhibiting NF-κB pathways (Dong et al., 2018). Aqueous antler extract (AAE) restores memory impairment in scopolamine (SCOP)-induced memory deficit mice by regulating cholinergic marker enzyme activities (Lee et al., 2010). In addition, secreted molecules from antlers can affect neurite outgrowth and axonal growth (Gray et al., 1992; Li et al., 2007; Pita-Thomas et al., 2010). However, research on the possible roles of antler-derived molecules in inflammation in the brain has been limited.

Based on the literature, we developed ALWPs, which include antler and LWPs (Yukmijuhwang-tang). We anticipated synergistic effects of ALWPs on neuroinflammatory responses and cognitive function. Here, we determined that ALWPs suppressed the LPS-induced neuroinflammatory response in BV2 microglial cells but not primary astrocytes, suggesting that ALWPs can differentially affect neuroinflammatory responses depending on cell type. In addition, ALWPs altered TLR4/FAK/NF-κB signaling to regulate LPS-induced neuroinflammatory responses. Moreover, oral administration of ALWPs to LPS-injected wild-type C57BL/6J mice resulted in rescue of short- and long-term memory and significantly reduced microglial activation. Taken together, these data suggest that ALWPs have potential as an anti-inflammatory drug, including for AD.

MATERIALS AND METHODS

Ethics Statement

All experiments were approved by the Institutional Biosafety Committee (IBC) of the Korea Brain Research Institute (approval no. 2014-479).

Animals

All experiments were performed in accordance with the approved animal protocols and guidelines established by the Korea Brain Research Institute (IACUC-2016-0013). C57BL6/J mice were purchased from Orient-Bio Company (Gyeonggi-do, South Korea). Male wild-type C57BL6/J mice (8 weeks of age, 25–30 g) were housed in a pathogen-free facility with 12 h of light and dark per day at an ambient temperature of 22°C. Water and food were available *ad libitum*. Mice were housed in groups of 3–5 per cage, *randomly* assigning *animals* to control/treatment *groups* for all experiments. Cotton nestlets were provided to minimize stress effects. Data were analyzed in a semi-automated manner using ImageJ software, and the results were confirmed by an independent researcher who did not participate in the current experiments.

LPS Neuroinflammation Model

Lipopolysaccharide was injected intraperitoneally (i.p.) to evoke neuroinflammation in wild-type C57BL/6J mice as previously described (Lee et al., 2008). The animals were divided into three experimental groups for each experiment: group 1 was treated with phosphate-buffered saline (PBS); group 2 was treated with both LPS and PBS; and group 3 was treated with both LPS and ALWPs (200 mg/kg). To test the effects of ALWPs on cognitive function, 8- to 9-week-old wild-type mice were orally administered ALWPs (200 mg/kg, p.o.) or PBS daily for 3 days. On the third day, 1 h after administration of PBS or ALWPs, LPS was injected i.p. at a dose of 250 μg/kg. The injected dose of LPS was selected based on a previous study (Fruhauf et al., 2015). One hour after LPS injection, the Y-maze test and a training session for the novel object recognition test (NOR) were performed sequentially. The NOR test was conducted 24 h after the NOR training session. To examine the effects of ALWPs on cognitive performance, we used 29 mice for the Y-maze test and 24 mice for the NOR test. In the NOR test, mice that had less than 7 s of exploration time during training and test were excluded from analysis (Taglialatela et al., 2009; Wolf et al., 2016).

Y-Maze Test

The Y-maze test was performed to assess immediate working memory as described previously (Fruhauf et al., 2015). The mice were placed in a Y-shaped maze with 3 arms at angles of 120° from each other (36.5 cm × 7 cm × 15.5 cm) under low red light (4–5 lux). During a 3-min trial, the mice freely moved and explored the arms. The number of arms visited and their sequences were recorded, and alternation triplets were analyzed manually after video recording. The percentage of alternation (%) was calculated using the following formula: number of alternation triples/(total number of arm entries−2) × 100.

Novel Object Recognition (NOR)

The NOR task was performed to assess long-term memory as described previously (Fruhauf et al., 2015). On the training day, mice were placed in an experimental apparatus (30 cm × 30 cm × 25 cm) containing two identical objects under low red light (4–5 lux). The mice moved freely to explore the objects for 3 min. The next day, the mice were placed in the same apparatus with two objects for 5 min for the test sessions. One item was a familiar object, that is, the same object experienced previously, whereas the other was a novel object that the mouse had never experienced before. All trials were videotaped, and the interaction times were measured manually. The times during a mouse passed near or climbed above the object were not counted; only the time during which the mouse was heading to the object was measured. The relative interaction time was calculated as the preference (%) based on the following formula: $T_{Novel}/(T_{Familiar} + T_{Novel}) \times 100$, where T is the time of interaction with an object.

Antibodies and Chemicals

We used the following primary antibodies: mouse anti-β-actin (Cat No: sc-47778, Santa Cruz Biotechnology, Dallas, TX, United States), mouse anti-p-IκBα (B-9, Cat No: sc-8404, Santa Cruz Biotechnology), mouse anti-IκBα (Cat No: sc-1643, Santa Cruz Biotechnology), rabbit anti-NF-κB (P65, Cat No: sc-8008, Santa Cruz Biotechnology), mouse anti-PCNA (Cat No: sc-56, Santa Cruz Biotechnology), rat anti-mouse CD11b (M1/70, Cat No: ab8878, Abcam, Cambridge, MA, United States), rabbit anti-FAK (Cat No: 13009S, Cell Signaling Technology, Danvers, MA, United States), rabbit anti-p-FAK (Tyr397, Cat No: 8556S, Cell Signaling Technology), rabbit anti-p-NF-κB (Ser536, Cat No: 3033L, Cell Signaling Technology), rabbit anti-ERK (Cat No: 9102S, Cell Signaling Technology), rabbit anti-p-ERK (Thr202/Tyr204, Cat No:9101S, Cell Signaling Technology), rabbit anti-JNK (Cat No: MBS8509129, MyBioSource, San Diego, CA, United States), rabbit anti-p-JNK (Thr183/Tyr185, Cat No: MBS8508944, MyBioSource), rabbit anti-P38 (Cat No: 9212S, Cell Signaling Technology), rabbit anti-p-P38 (Cat No: 9211S, Cell Signaling Technology), rabbit anti-TLR4 (Cat No: PA5-11597, Thermo Scientific, Waltham, MA, United States), and rabbit anti-TLR4 (Cat No: NB100-56566, Novus Biologicals, Littleton, CO, United States). Horseradish peroxidase (HRP)-conjugated anti-mouse (Cat No: ADI-SAB-100-J, Enzo Life Science, NY, United States), and rabbit IgG (Cat No: ADI-SAB-300-J, Enzo Life Science, NY, United States) were used as the secondary antibodies. LPS from *Escherichia coli* O111:B4 (Cat No: L2880, Sigma, St. Louis, MO, United States) and the TLR4 inhibitor TAK-242 were purchased from Calbiochem (Cat No: 614316, San Diego, CA, United States), and the p-FAK inhibitor PF-573228 (Cat No: S2031) was purchased from Selleckchem (Houston, TX, United States).

Cell Lines and Culture Conditions

BV2 cells were derived from primary mouse microglial cells. BV2 microglial cells (a gift from Dr. Kyoungho Suk at Kyungpook National University) were maintained in high-glucose DMEM (HyClone, Logan, UT, United States) supplemented with 5% fetal bovine serum (FBS, HyClone) in a 5% CO_2 incubator. Treatments of BV2 microglial cells were always performed in serum-free DMEM. All BV2 microglial cells used in *in vitro* experiments were validated by immunostaining with anti-CD11b antibody, as a microglial cell marker. We also used BV2 microglia cells within 10 passages to ensure that healthy cells were used in the experiments. Data from all *in vitro* experiments were analyzed in a semi-automated manner using ImageJ software, and the results were confirmed by an independent researcher who did not participate in the current experiments.

Primary Astrocyte Cultures

Primary astrocytes were cultured from the cerebral cortices of 1-day-old Sprague Dawley rats. Briefly, the cortices were triturated into single cells in high-glucose DMEM containing 10% FBS and penicillin-streptomycin solution (5000 units/ml penicillin, 5 μg/ml streptomycin; Corning, NY, United States) and plated on 75-cm^2 T flasks (0.5 hemisphere/flask) for 2 weeks. To prepare astrocyte-enriched cultures, the microglia were detached by shaking for 2 h at 120 rpm, and the cells remaining in the flask were harvested with 0.1% trypsin. The astrocytes were

plated in 12-well culture plates (35-mm dish) pre-coated with poly-D-lysine (Sigma-Aldrich).

Cell-Surface Biotinylation

BV2 microglial cells were treated with ALWPs (500 μg/ml) or PBS for 30 min followed by LPS (1 μg/ml) or PBS for 5.5 h. Surface proteins were then labeled with Sulfo-NHS-SS-Biotin under gentle shaking at 4°C (Cat No: 89881, Thermo Scientific, United States). After 30 min, quenching solution was added to the cells. The surface-labeled cells were lysed in lysis buffer, disrupted by sonication on ice, incubated for 30 min, and clarified by centrifugation (10,000 × *g*, 10 min). After centrifugation, the lysate was added to immobilized NeutrAvidin™ gel and incubated for 1 h. After washing three times with wash buffer, the samples were incubated for 1 h in SDS–PAGE sample buffer with DTT. Surface proteins were then analyzed by immunoblotting with an antibody recognizing the N-terminus of TLR4.

Cytosol and Nuclear Fractionation

BV2 microglial cells were lysed in cytosol fractionation buffer (10 mM HEPES pH 8.0, 1.5 mM $MgCl_2$, 10 mM KCl, 0.5 mM DTT, 300 mM sucrose, 0.1% NP-40, and 0.5 mM PMSF) and centrifuged for 5 min at 10,000 rpm. The supernatant was collected as the cytosolic fraction. The remaining pellet was resuspended in nuclear fractionation buffer (10 mM HEPES pH 8.0, 20% glycerol, 100 mM KCl, 100 mM NaCl, 0.2 mM EDTA, 0.5 mM DTT, and 0.5 mM PMSF), incubated on ice for 15 min, and centrifuged for 1 min at 10,000 rpm. The supernatant was collected as the nuclear fraction (Nam et al., 2017).

Reverse Transcription PCR (RT-PCR)

To examine the effects of ALWPs on IL-1β, IL-6, COX-2, iNOS, and TNF-α mRNA levels, BV2 or primary astrocyte cells were pretreated with PBS or ALWPs (250 or 500 μg/ml) for 30 min and then treated with PBS or LPS (1 μg/ml) for 5.5 h. RNA was then extracted using TRIzol (Ambion, United States). RT-PCR was performed with the following primers for BV2 cells: IL-1β: Forward (F)′, AGC TGG AGA GTG TGG ATC CC and Reverse (R)′, CCT GTC TTG GCC GAG GAC TA; IL-6: F′, CCA CTT CAC AAG TCG GAG GC and R′, GGA GAG CAT TGG AAA TTG GGG T; IL-18: F′, TTT CTG GAC TCC TGC CTG CT and R′, ATC GCA GCC ATT GTT CCT GG; COX-2: F′, GCC AGC AAA GCC TAG AGC AA and R′, GCC TTC TGC AGT CCA GGT TC; iNOS: F′, CCG GCA AAC CCA AGG TCT AC and R′, GCA TTT CGC TGT CTC CCC AA; TNF-α: F′, CTA TGG CCC AGA CCC TCA CA and R′, TCT TGA CGG CAG AGA GGA GG; GAPDH: F′, CAG GAG CGA GAC CCC ACT AA and R′, ATC ACG CCA CAG CTT TCC AG. For primary astrocytes, the following primers were used for RT-PCR:COX-2: F′, TCC AAC TCA AGT TCG ACC CA and R′, TCC TCC GAA GGT GCT AGG TT; IL-1β: F′, AAA ATG CCT CGT GCT GTC TG and R′, CAG AAT GTG CCA CGG TTT TC; IL-6: F′, TTG CCT TCT TGG GAC TGA TG and R′, TGG AAG TTG GGG TAG GAA GG; iNOS: F′, ATC ATG GAC CAC CAC ACA GC and R′, GGT GTT GAA GGC GTA GCT GA; TNF-α: F′, AGC ACA GAA AGC ATG ATC CG and R′, CTC CCT CAG GGG TGT CCT TA; GAPDH: F′, GTT ACC AGG GCT GCC TTC TC and R′, GTG ATG GCA TGG ACT GTG GT. Image analyses were performed using ImageJ software to measure the average band intensities.

Preparation of ALWPs

ALWPs included LWPs (Yukmijuhwang-tang: *Rehmannia glutinosa*, *Cornus officinalis*, *Dioscoreae rhizoma, Paeonia suffruticosa*, *Poria cocos*, and *Alisma orientale*), *Lycium chinense*, *Polygala tenuifolia*, *Acorus gramineus*, and *Antler*. The ALWP formula was prepared via a three-step extraction process. First, *L. chinense* (1000 g), *R. glutinosa* (1200 g), *D. rhizoma* (500 g), *C. officinalis* (500 g), *P. suffruticosa* (360 g), *A. orientale* (360 g), *P. cocos* (360 g), and *Antler* (240 g) were boiled for 12 h at 120°C. Second, the heated mixture was sifted through a filter to remove debris. *P. tenuifolia* (180 g), *A. gramineus* (180 g), and *P. cocos* (90 g) were added to the reaction mixture from the first step and boiled for 1 h to prepare a cohesive agent. Finally, the cohesive agent was air-dried for 72 h and molded into a pill. The pills were stored at 4°C, and the extract was dissolved in PBS and diluted with medium before each experiment. To verify each herbal component of ALWPs and to determine the content of the principal markers, ultra-high-performance liquid chromatography (UHPLC) was performed. In addition, to examine the effects of the individual components of ALWPs on LPS-induced proinflammatory cytokine levels, we calculated the doses of the individual components of the mixture from the composition formula of ALWPs and conducted further experiments.

Liquid Chromatography

Reverse-phase UHPLC was performed on a Waters ACQUITYUHPLC H-Class system (Milford, MA, United States) consisting of a quaternary solvent manager pump, sample manager – TN and photodiode array (PDA) detector. Empower 3 Pro software (Milford, MA, United States) was used for UHPLC data analysis. Chromatographic separation was accomplished on a Perkin Elmer C18 reverse-phase column (Brownlee SPP 100 mm × 1.0 mm I.D., 1.7 μm) at 30°C and monitored at 283 nm for 5-HMF (5-hydroxymethyl-2-furaldehyde, Sigma Aldrich), 231 nm for paeoniflorin (MFDS, Osong, South Korea), 240 nm for morroniside (ChemFaces, Wuhan, China), and 237 nm for loganin (MFDS). A solvent system consisting of acetonitrile (solvent A) and 0.1% formic acid DW (solvent B) was used with a gradient from 2% (solvent A): 98% (solvent B) to 100% (solvent A): 0% (solvent B) over 18 min at a flow rate of 0.4 ml/min. Standard stock solutions were prepared by dissolving standards in 100% methanol to obtain a final concentration of 10 μg/ml. After ultracentrifugation at 9000 rpm and filtration through a syringe filter (0.2 μg, Whatman™, Maidstone, United Kingdom), 4 ml of sample was injected six times.

MTT Assays

Cell viability was assessed using the 3-(4,5-dimethylthiazol-2-yl)-2,5-diphenyltetrazolium bromide (MTT) assay. Cells were seeded in 96-well plates and treated with various concentrations of ALWPs (50–250 μg/ml) for 6 or 24 h in the absence of FBS. The cells were then treated with 0.5 μg/ml MTT and incubated for 3 h at 37°C in a 5% CO_2 incubator. After discarding the culture

medium, dimethyl sulfoxide (DMSO) was added to dissolve the formazan dye, and the absorbance was measured at 580 nm.

Immunocytochemistry

Cells were plated at a density of 20,000 cells/well on cover slips in 12-well plates (Eppendorf, Hamburg, Germany). Twenty four hour after exchanging the culture medium with serum-free high-glucose DMEM (HyClone), the cells were pretreated with ALWPs (250 μg/ml) or PBS for 30 min, followed by treatment with LPS (1 μg/ml) or PBS for 5.5 h. The cells were then fixed in cold methanol for 8 min, washed with PBS three times, and incubated with one of the following primary antibodies in GDB buffer [0.1% gelatin, 0.3% Triton X-100, 16 mM sodium phosphate (pH 7.4), and 450 mM NaCl] overnight at 4°C: anti-CD11b (M1/70, Cat No: ab8878, 1:200, Abcam), anti-IL-1β (Cat No: sc-7884, 1:200, Santa Cruz Biotechnology), or p-NF-κB (Ser536, Cat No: 3033L, 1:100, Cell Signaling Technology). The next day, the cells were washed with PBS three times and incubated with the following secondary antibodies for 1 h at room temperature: Alexa Fluor 488 and Alexa Fluor 555 (1:200, Molecular Probes, OR, United States). The cells were mounted in DAPI-containing solution (Vector Laboratories, CA, United States), and images were acquired on a single plane using a confocal microscope (Nikon, Japan) and analyzed using ImageJ software.

Immunofluorescence Analysis

To examine the effects of ALWPs on microglial activation, 3-month-old wild-type C57BL/6J mice were orally administered ALWPs (200 mg/kg, p.o.) or PBS daily for 3 days. On the third day, LPS (10 mg/kg) was injected i.p. Three hours later, the mice were perfused and fixed in 4% paraformaldehyde (PFA) solution, and brain tissues were flash-frozen and dissected using a cryostat (35 μm thick). Each brain section was processed for immunofluorescence staining. The sections were rinsed with PBS and incubated with rabbit anti-Iba-1 (1:500, Wako, Japan) to detect microglia. Primary antibodies were diluted with 0.5% bovine serum albumin (BSA) and incubated at 4°C overnight. The following day, the tissues were rinsed with 0.5% BSA and incubated with Alexa Fluor 555-conjugated anti-rabbit IgG (1:500, Molecular Probes) for 1 h at room temperature. The tissues were subsequently mounted on gelatin-coated cover glass and covered with DAPI-containing mounting solution (Vector Laboratories). The stained tissues were imaged using confocal microscopy (TI-RCP, Nikon). Nine mice were used for immunofluorescence analysis.

Western Blotting

Cells were lysed using IPH lysis buffer (50 mM Tris-Cl, 150 mM NaCl, 1 % NP-40, 0.5 M EDTA, 1 mM PMSF, 0.1 M DTT) containing protease and phosphatase inhibitor tablets (Roche, Basel, Switzerland). Equal amounts of protein (10 or 20 μg) were mixed with sample loading buffer (Bio-Rad, Hercules, CA, United States), boiled for 5 min, and separated by SDS–PAGE using a Mini protein Tetra cell system. The separated proteins were transferred to polyvinylidene difluoride membranes (PVDF, Millipore, Temecula, CA, United States) using an electrophoretic transfer system (Bio-Rad). After blocking with 5% non-fat dry milk or 5% BSA for 1 h at room temperature, the membranes were incubated with specific primary antibodies as follows: mouse β-actin (1:5000), mouse anti-p-IκBα (1:1000), rabbit anti-IκBα (1:1000), rabbit anti-NF-κB (P65, 1:1000), mouse anti-PCNA (1:1000), rabbit anti-FAK (1:1000), rabbit anti-p-FAK (Tyr397, 1:1000), rabbit anti-ERK (1:1000), rabbit anti-p-ERK (Thr202/Tyr204, 1:1000), rabbit anti-JNK (1:1000), rabbit anti-p-JNK (Thr183/Tyr185, 1:1000), rabbit anti-P38 (1:1000), rabbit anti-p-P38 (1:1000), rabbit anti-TLR4 (1:1000), and rabbit anti-TLR4 (1:1000) or secondary antibodies (HRP-conjugated anti-rabbit or mouse, 1:10,000). Finally, the membrane were developed with enhanced chemiluminescence detection reagents (ATTO, Japan) (Song et al., 2016). Images were analyzed using Fusion software or ImageJ software.

Cell Migration Assay (Wound-Healing Assay)

The wound-healing assay was performed as previously described (Nam et al., 2017). BV2 microglial cells were seeded in 12-well plates and incubated until the cells reached 80–90% confluence. The cells were then scratched with a cell scratcher (SPL, Gyeonggi-do, South Korea) to create a wound. Images were captured immediately or after 24 h.

Statistical Analyses

All data were analyzed using either unpaired two-tailed *t*-tests with Welch's correction for comparisons between two groups or one-way ANOVA for multiple comparisons in GraphPad Prism 6 software. *Post hoc* analyses were completed with Tukey's multiple comparison test with significance set at $^{*}p < 0.05$, $^{**}p < 0.01$, $^{***}p < 0.0001$. Data are presented as the mean ± SEM.

RESULTS

Effects of ALWPs on Cell Viability and Morphology in BV2 Microglial Cells

To assess the effects of ALWPs on cell viability, we treated BV2 microglial cells with PBS or ALWPs (50, 250, 500, 750, or 1000 μg/ml) for 6 h and then conducted MTT assays. ALWPs did not cause cell toxicity at concentrations up to 500 μg/ml, but cell viability was reduced when the ALWPs concentration was 750 μg/ml or higher (**Figure 1A**).

Next, we examined whether ALWPs affected cell viability under longer treatment times. BV2 microglial cells were treated with PBS or ALWPs (50, 250, 500, 750, or 1000 μg/ml) for 24 h, and MTT assays were conducted. ALWPs slightly decreased BV2 microglial cell viability at the highest doses, with reductions of 17.5 and 19.8% at 750 and 1000 μg/ml, respectively (**Figure 1B**). Based on these findings, we selected 250 and 500 μg/ml as optimal ALWP concentrations for the subsequent experiments.

To examine whether ALWPs affect cell morphology, we treated BV2 microglial cells with either PBS or ALWPs (500 μg/ml) for 30 min followed by LPS (1 μg/ml) or PBS for 5.5 h. The cells were then fixed and immunostained with an anti-CD11b antibody as a marker for microglia. Compared

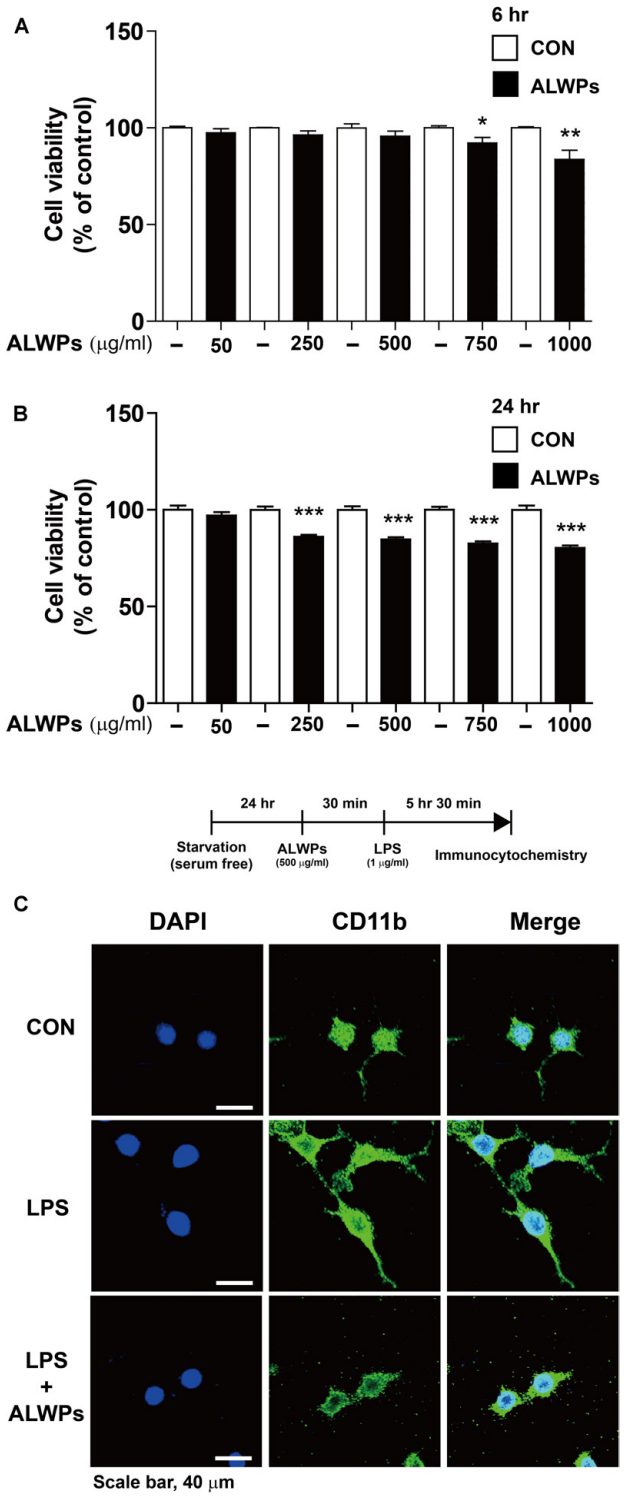

FIGURE 1 | The effects of ALWPs on cell viability and morphology in BV2 microglial cells. **(A,B)** BV2 microglial cells were treated with PBS or ALWPs (50, 250, 500, 750, and 1000 μg/ml) at various concentrations for 6 h [**(A)**, $n = 8$ for each dose] or 24 h [**(B)**, $n = 16$ for each dose], and cell viability was measured. **(C)** Morphological changes of LPS-induced and ALWP-treated BV2 microglial cells, scale bar 40 μm (40× confocal images). $^{*}p < 0.05$, $^{**}p < 0.01$, $^{***}p <$ 0.001.

with the control, LPS-treated cells displayed long, thin, fiber-like structures extending from the cell body (**Figure 1C**, middle panel), consistent with previous studies (Sheng et al., 2011; Dang et al., 2014). However, cells treated with ALWPs followed by LPS exhibited shorter branches and a rounder cell body shape compared with cells treated with LPS (**Figure 1C**, lower panel).

ALWPs Significantly Decrease LPS-Mediated IL-1β Levels in BV2 Microglial Cells

Several studies have shown that the components of ALWPs, specifically *R. glutinosa* and *Corni fructus*, can regulate inflammation in several organs (Park et al., 2005; Lee et al., 2012). However, whether the components of ALWPs can alter neuroinflammation has not been determined. Thus, we examined whether ALWPs can regulate LPS-mediated proinflammatory cytokine levels. BV2 microglial cells were pretreated with ALWPs (250 μg/ml) or PBS for 30 min, followed by treatment with LPS (1 μg/ml) or PBS for 5.5 h. Total RNA was isolated, and the mRNA levels of proinflammatory cytokines were measured by RT-PCR. Surprisingly, 250 μg/ml ALWPs did not alter any LPS-induced proinflammatory cytokine levels in BV2 microglial cells (**Figures 2A–G**).

We then examined whether higher concentrations of ALWPs can alter LPS-induced proinflammatory responses. BV2 microglial cells were pretreated with ALWPs (500 μg/ml) or PBS for 30 min, followed by treatment with either LPS (1 μg/ml) or PBS for 5.5 h. Total RNA was isolated, and the mRNA levels of proinflammatory cytokines were examined by RT-PCR. Interestingly, pretreatment with ALWPs followed by LPS significantly reduced the mRNA levels of IL-1β in LPS-stimulated BV2 microglial cells but not the mRNA levels of other proinflammatory cytokines (**Figures 2H–N**).

To further confirm the findings described above, BV2 microglial cells were pretreated with ALWPs (500 μg/ml) or PBS for 30 min, followed by treatment with either LPS (1 μg/ml) or PBS for 5.5 h. Immunostaining was performed with anti-CD11b and anti-IL-1β antibodies. Consistent with the findings described above, LPS alone significantly increased IL-1β levels compared with the control treatment, but pretreatment with ALWPs followed by LPS treatment significantly decreased IL-1β levels compared with LPS treatment (**Figures 2O,P**). These results suggest that ALWPs can selectively affect LPS-induced proinflammatory cytokine levels in BV2 microglial cells.

To determine whether the individual components of ALWPs can alter proinflammatory cytokine IL-1β levels compared with treatment with ALWPs and LPS or with LPS alone, BV2 microglial cells were pretreated with *P. cocos* or ALWPs (500 μg/ml) for 30 min, followed by treatment with either LPS (1 μg/ml) or PBS for 5.5 h. Total RNA was isolated, and the mRNA levels of IL-1β were examined by RT-PCR. The same methodology was used to treat BV2 microglial cells with *A. orientale*, *D. rhizoma*, *Antler, P. suffruticosa Andrews*, *C. officinalis*, *L. chinense*, or *R. glutinosa*. Consistent with the findings described above, ALWPs blocked LPS-induced

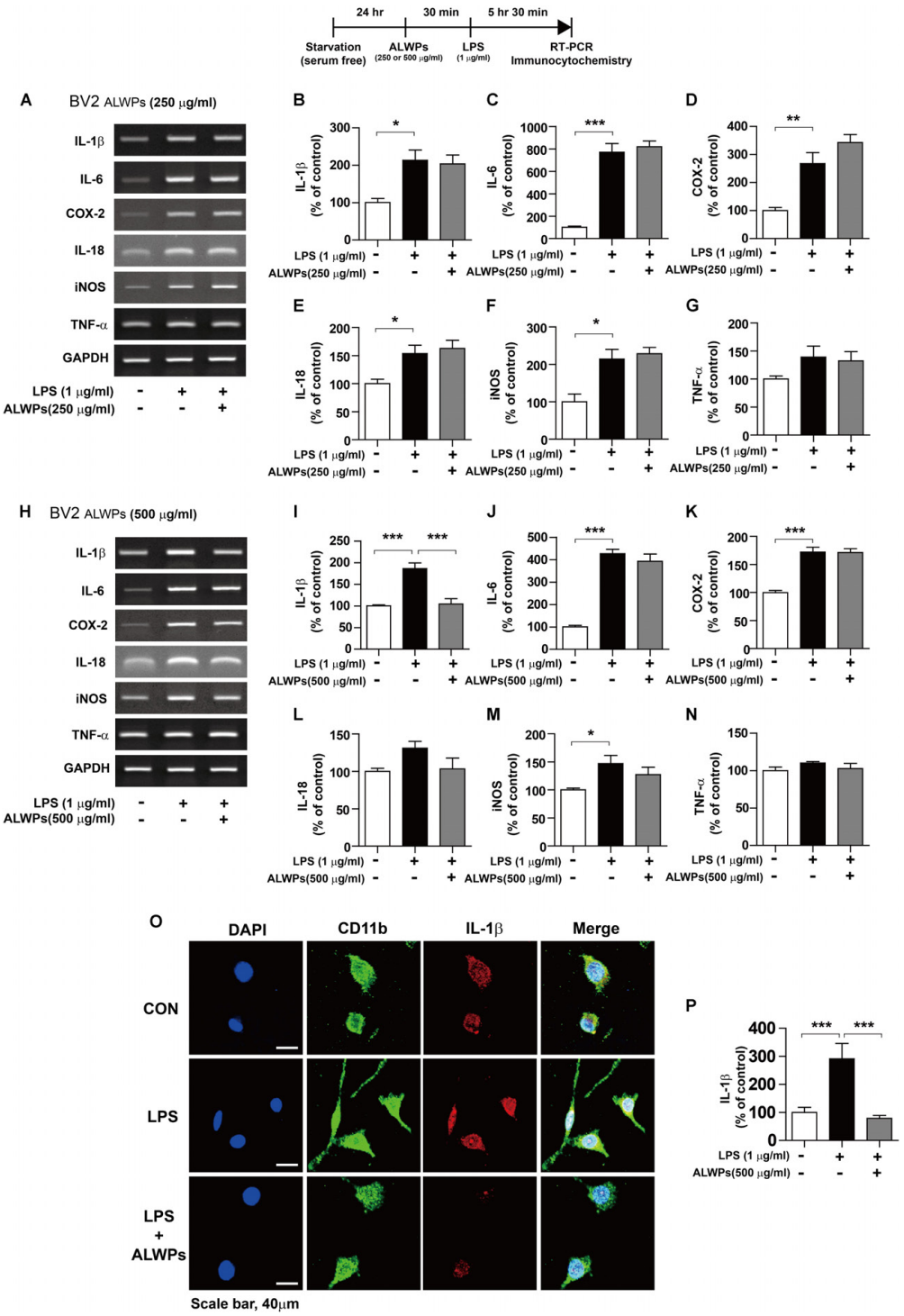

FIGURE 2 | ALWPs inhibit LPS-induced IL-1β levels in BV2 microglial cells. **(A–G)** BV2 microglial cells were pretreated with ALWPs (250 μg/ml) or PBS for 30 min, followed by treatment with LPS (1 μg/ml) or PBS for 5.5 h. Total RNA was isolated, and the mRNA levels of proinflammatory cytokines were measured by RT-PCR (con, $n = 4$; LPS, $n = 4$; ALWPs + LPS, $n = 4$). **(H–N)** BV2 microglial cells were pretreated with ALWPs (500 μg/ml) or PBS for 30 min, followed by treatment with LPS (1 μg/ml) or PBS for 5.5 h. Total RNA was isolated, and the mRNA levels of proinflammatory cytokines were measured by RT-PCR (IL-1β, IL-6, IL-18, iNOS, and TNF-α: con, $n = 4$; LPS, $n = 4$; ALWPs + LPS; $n = 4$, COX-2: con, $n = 8$; LPS, $n = 8$; ALWPs + LPS, $n = 8$). **(O)** BV2 microglial cells were pretreated with ALWPs (500 μg/ml) or PBS for 30 min, followed by treatment with LPS (1 μg/ml) or PBS for 5.5 h. Cells were fixed and immunostained with anti-CD11b and anti-IL-1β antibodies. **(P)** Quantification of the data from **(O)** (con, $n = 70$ cells; LPS, $n = 80$ cells; LPS + ALWPs, $n = 82$, 40× confocal images). $^{*}p < 0.05$, $^{**}p < 0.01$, $^{***}p < 0.001$.

proinflammatory cytokine IL-1β mRNA levels compared with LPS (**Figures 3A–P**, ANOVA with *post hoc* Tukey's test, two-tailed *t*-test of LPS vs. ALWPs + LPS). In addition, we observed that pretreatment with the individual components of ALWPs followed by LPS treatment did not significantly alter IL-1β mRNA levels compared with treatment with LPS alone (**Figures 3A–P**). These data suggest that the combination of these ten components in ALWPs may have additive/synergistic effects on the neuroinflammatory response.

ALWPs Do Not Alter LPS-Induced Proinflammatory Cytokine Levels in Primary Astrocytes

To examine whether ALWPs can regulate proinflammatory cytokine levels in primary astrocytes, primary astrocytes were first treated with either ALWPs (500 μg/ml) or PBS for 30 min and then treated with LPS (1 μg/ml) or PBS for 5.5, 11.5, or 23.5 h. After the specified treatment period, total RNA was isolated from the cells, and proinflammatory cytokine mRNA levels were measured by RT-PCR. We found that ALWP treatment did not alter LPS-mediated proinflammatory cytokine levels at any time point in primary astrocytes (**Supplementary Figure 1**).

We then examined whether ALWPs affect proinflammatory cytokine levels in a dose-dependent manner. Primary astrocytes were treated with either ALWPs (500, 750, and 1000 μg/ml) or PBS for 30 min and then treated with LPS (1 μg/ml) or PBS for 5.5 h. The cells were harvested to isolate total RNA, and proinflammatory cytokine levels were measured by RT-PCR. Again, we found that no dosage of ALWPs regulated LPS-mediated proinflammatory cytokine levels in primary astrocytes (**Supplementary Figure 2**). These data suggest that ALWPs may differentially regulate LPS-induced proinflammatory responses in specific cell types.

ALWPs Decrease LPS-Induced Cell-Surface TLR4 in BV2 Microglial Cells

Several studies have implied that LPS can activate microglial cells by interacting with Toll-like receptors (e.g., TLR4) (Chen et al., 2012; Hines et al., 2013; Yao et al., 2013b; Dai et al., 2015). Therefore, we examined whether TLR4 can alter LPS-induced IL-1β mRNA levels in the presence of ALWPs. BV2 microglial cells were treated with TAK-242 (a TLR4 inhibitor, 500 nM) for 30 min, ALWPs (500 μg/ml) or PBS for 30 min, and finally LPS (1 μg/ml) or PBS for 5 h. Total RNA was then isolated, and IL-1β mRNA levels were measured by RT-PCR. Consistent with the results shown in **Figure 3**, ALWP treatment followed by LPS decreased IL-1β mRNA levels compared with LPS alone (**Figures 4A,B**). In addition, treatment with TAK-242, ALWPs, and LPS did not reduce IL-1β mRNA levels compared with treatment with TAK-242 and LPS (**Figures 4A,B**). These data suggest that ALWPs alter TLR4 to affect LPS-induced proinflammatory cytokine levels.

Next, we examined whether ALWPs can modulate cell-surface levels of TLR4. BV2 microglial cells were first treated with ALWPs (500 μg/ml) or PBS for 30 min and then treated with LPS (1 μg/ml) or PBS for 5.5 h. Cell-surface biotinylation was performed with a TLR4 antibody recognizing the N-terminus of TLR4. LPS treatment significantly increased the cell-surface levels of TLR4 (**Figures 4C,D**). In addition, treatment with ALWPs followed by LPS significantly reduced the cell-surface levels of TLR4 compared with LPS alone (**Figures 4C,D**). These results suggest that ALWPs inhibit cell-surface levels of TLR4 and thereby decrease the interaction between LPS and TLR4 on the cell surface to regulate proinflammatory responses.

ALWPs Alter FAK Signaling to Modulate LPS-Induced IL-1β mRNA Levels

To investigate the molecular mechanisms by which ALWPs modulate LPS-stimulated proinflammatory responses, we initially tested whether ALWPs modulate MAP kinase signaling cascades, a downstream LPS-induced signaling pathway (Kaminska et al., 2009; Dang et al., 2014; Guo et al., 2016). BV2 microglial cells were treated with ALWPs (500 μg/ml) or PBS for 5 h and then treated with LPS (1 μg/ml) or PBS for 45 min, and western blotting was performed with anti-p-ERK and anti-ERK antibodies. ALWPs did not alter p-ERK or total ERK levels in LPS-stimulated BV2 microglial cells (**Supplementary Figures 3A,B**). We then examined whether ALWPs can regulate other MAP kinase signaling pathways, including P38 and JNK signaling. Again, ALWPs did not alter the phosphorylation status and total level of P38/JNK in LPS-induced BV2 microglial cells (**Supplementary Figures 3C–F**).

Next, we examined whether ALWPs can regulate the phosphorylation of focal adhesion kinase (FAK) as a potential target involved in inflammation (Zeisel et al., 2005; Wong et al., 2011; Choi et al., 2015; Lian et al., 2015). BV2 microglial cells were pretreated with ALWPs (500 μg/ml) or PBS for 5 h and then treated with LPS (1 μg/ml) or PBS for 45 min, and western blotting was performed with anti-p-FAK and anti-FAK antibodies. Cells treated with LPS alone showed an increase in the phosphorylation of FAK compared with the control treatment (**Figures 5A,B**), and ALWPs significantly decreased LPS-induced FAK phosphorylation compared with LPS treatment in BV2 microglial cells (**Figures 5A,B**).

To investigate whether ALWPs alter FAK signaling to affect LPS-induced IL-1β mRNA levels, BV2 microglial cells were treated with PF-573228 (a FAK inhibitor, 5 μM) or vehicle (1% DMSO) for 30 min, ALWPs (500 μg/ml) or PBS for 30 min, and finally LPS (1 μg/ml) or PBS for 5 h. Total RNA was isolated, and IL-1β mRNA levels were measured by RT-PCR. Treatment with PF-573228, ALWPs, and LPS did not reduce LPS-induced IL-1β mRNA levels compared with treatment with PF-573228 and LPS (**Figures 5C,D**). These results suggest that ALWPs regulate FAK signaling to modulate LPS-stimulated proinflammatory responses.

ALWPs Suppress LPS-Induced NF-κB Levels in the Nucleus

NF-κB plays an important role in neuroinflammation (Lawrence, 2009; Cao et al., 2010; Tilstra et al., 2011; Yao et al., 2013a). NF-κB in microglia is activated by viruses and bacterial toxins

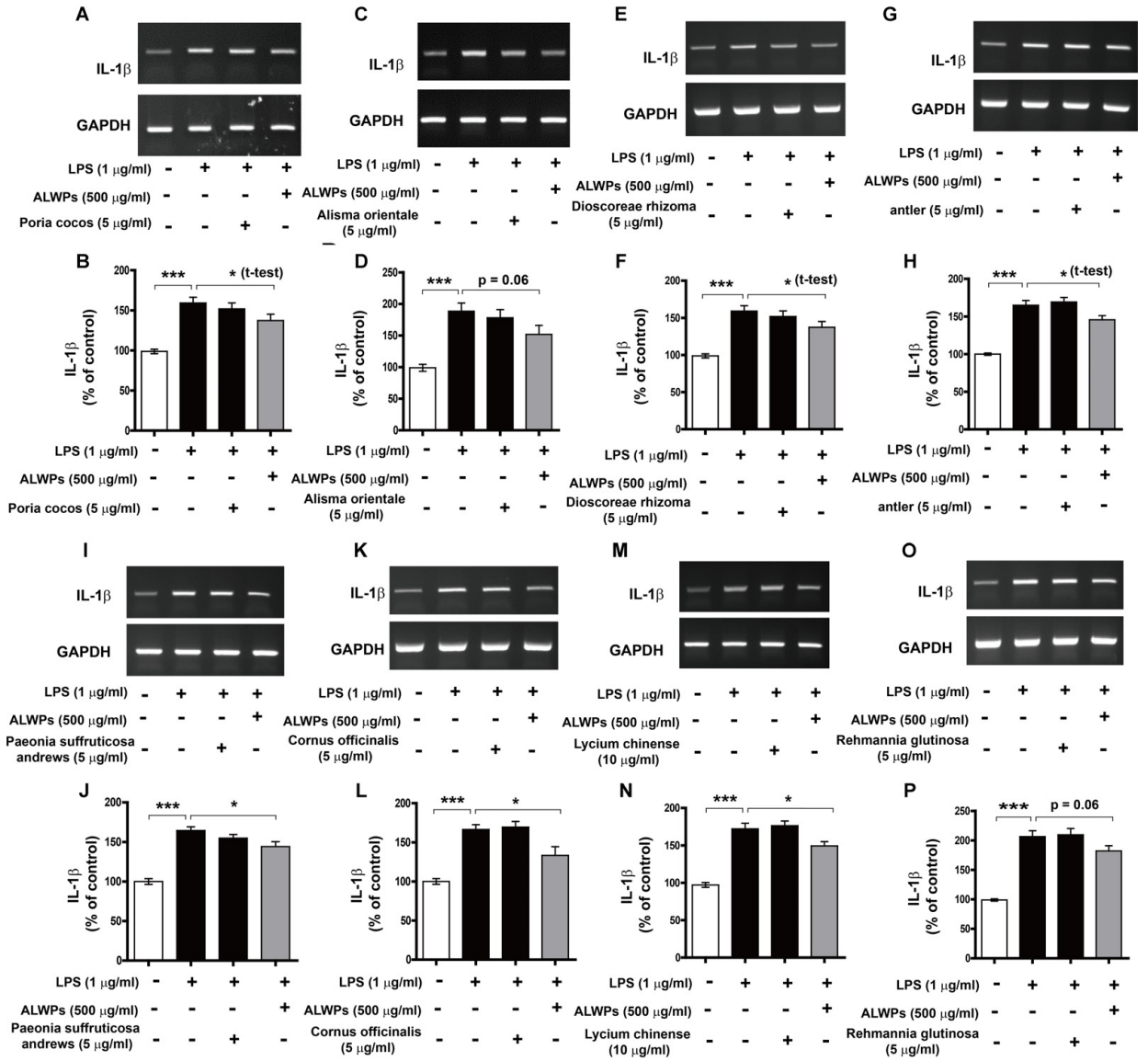

FIGURE 3 | The effects of each component of ALWPs on LPS-induced IL-1β mRNA levels. **(A,B)** BV2 microglial cells were pretreated with *Poria cocos* (5 μg/ml), ALWPs (500 μg/ml), or PBS for 30 min, followed by treatment with LPS (1 μg/ml) or PBS for 5.5 h. **(C,D)** BV2 microglial cells were pretreated with *Alisma orientale* (5 μg/ml), ALWPs (500 μg/ml), or PBS for 30 min, followed by treatment with LPS (1 μg/ml) or PBS for 5.5 h. **(E,F)** BV2 microglial cells were pretreated with *Dioscoreae rhizoma* (5 μg/ml), ALWPs (500 μg/ml), or PBS for 30 min, followed by treatment with LPS (1 μg/ml) or PBS for 5.5 h. **(G,H)** BV2 microglial cells were pretreated with *Antler* (5 μg/ml), ALWPs (500 μg/ml), or PBS for 30 min, followed by treatment with LPS (1 μg/ml) or PBS for 5.5 h. **(I,J)** BV2 microglial cells were pretreated with *Paeonia suffruticosa Andrews* (5 μg/ml), ALWPs (500 μg/ml), or PBS for 30 min, followed by treatment with LPS (1 μg/ml) or PBS for 5.5 h. **(K,L)** BV2 microglial cells were pretreated with *Cornus officinalis* (5 μg/ml), ALWPs (500 μg/ml), or PBS for 30 min, followed by treatment with LPS (1 μg/ml) or PBS for 5.5 h. **(M,N)** BV2 microglial cells were pretreated with *Lycium chinense* (10 μg/ml), ALWPs (500 μg/ml), or PBS for 30 min, followed by treatment with LPS (1 μg/ml) or PBS for 5.5 h. **(O,P)** BV2 microglial cells were pretreated with *Rehmannia glutinosa* (5 μg/ml), ALWPs (500 μg/ml), or PBS for 30 min, followed by treatment with LPS (1 μg/ml) or PBS for 5.5 h. After treatment, total RNA was isolated, and the mRNA levels of proinflammatory cytokines were measured by RT-PCR **(B,D,F,H,J,L,N,P)**. Quantification of the data from **(A)** (vehicle, $n = 31$; LPS, $n = 31$; *P. cocos* + LPS, $n = 31$; ALWPs + LPS, $n = 31$), **(C)** (vehicle, $n = 13$; LPS, $n = 13$; *A. orientale* + LPS, $n = 13$; ALWPs + LPS, $n = 13$), **(E)** (vehicle, $n = 9$; LPS, $n = 9$; *D. rhizoma* + LPS, $n = 9$; ALWPs + LPS, $n = 9$), **(G)** (vehicle, $n = 12$; LPS, $n = 12$; *Antler* + LPS, $n = 12$; ALWPs + LPS, $n = 12$), **(I)** (vehicle, $n = 12$; LPS, $n = 12$; *P. suffruticosa Andrews* + LPS, $n = 12$; ALWPs + LPS, $n = 12$), **(K)** (vehicle, $n = 9$; LPS, $n = 9$; *C. officinalis* + LPS, $n = 9$; ALWPs + LPS, $n = 9$), **(M)** (vehicle, $n = 17$; LPS, $n = 17$; *L. chinense* + LPS, $n = 17$; ALWPs + LPS, $n = 17$), and **(O)** (vehicle, $n = 41$; LPS, $n = 41$; *R. glutinosa* + LPS, $n = 41$; ALWPs + LPS, $n = 41$). $^*p < 0.05$, $^{***}p < 0.001$.

such as LPS. For instance, the activation of NF-κB in patients with chronic inflammation has been found to be a critical factor for AD, PD, and osteoporosis, which are autoimmune/inflammatory diseases (Vallabhapurapu and Karin, 2009). Therefore, we examined whether ALWPs can regulate NF-κB subcellular localization. BV2 microglial cells were pretreated with ALWPs

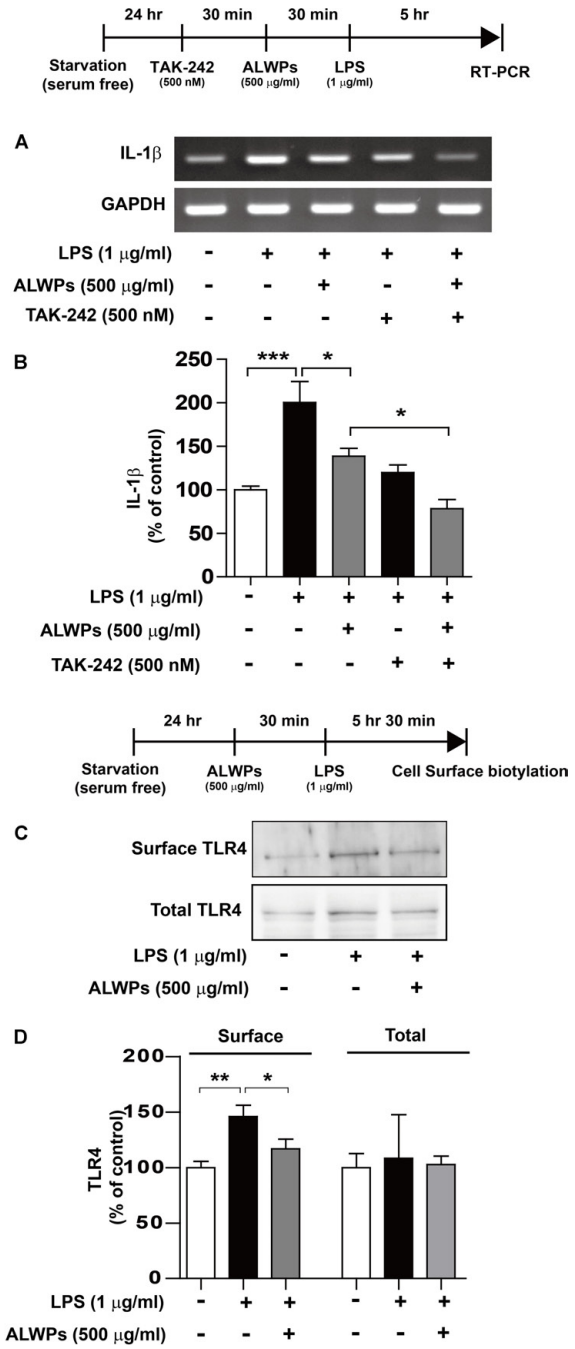

FIGURE 4 | ALWPs significantly reduced LPS-induced cell-surface levels of TLR4. **(A)** BV2 microglial cells were pretreated with TAK-242 (a TLR4 inhibitor, 500 nM) for 30 min, followed by treatment with ALWPs (500 μg/ml) or PBS for 30 min and finally LPS (1 μg/ml) or PBS for 5 h. Total RNA was isolated, and IL-1β mRNA levels were measured by RT-PCR. **(B)** Quantification of the data from **(A)** (con, $n = 20$; LPS, $n = 20$; ALWPs + LPS, $n = 20$; TAK-242 + LPS, $n = 20$; TAK-242 + ALWPs + LPS, $n = 20$). **(C)** BV2 microglial cells were pretreated with ALWPs (500 μg/ml) or PBS for 30 min, followed by treatment with LPS (1 μg/ml) or PBS for 5.5 h. Cell-surface biotinylation was then conducted with a TLR4 antibody recognizing the N-terminal region of TLR4. **(D)** Quantification of the data from **(C)** (Surface TLR4: con, $n = 10$; LPS, $n = 10$; ALWPs + LPS, $n = 10$; Total TLR4: con, $n = 4$; LPS, $n = 4$; ALWPs + LPS, $n = 4$). $^*p < 0.05$, $^{**}p < 0.01$, $^{***}p < 0.001$.

(500 μg/ml) or PBS for 5 h, treated with LPS (1 μg/ml) or PBS for 45 min, and then subjected to subcellular fractionation (nucleus vs. cytosol). We observed that pretreatment with ALWPs followed by LPS did not alter p-IκBα, IκBα, or NF-κB levels in the cytosol compared with LPS treatment (**Figures 6A–D**). In the nuclear fraction, LPS increased NF-κB levels compared with control treatment (**Figures 6E,F**). Pretreatment with ALWPs followed by LPS resulted in decreased LPS-induced nuclear NF-κB levels compared with treatment with LPS alone in BV2 microglial cells (**Figures 6E,F**).

To further confirm our findings, BV2 microglial cells were pretreated with ALWPs (500 μg/ml) or PBS for 5 h, followed by treatment with LPS (1 μg/ml) or PBS for 45 min. Immunocytochemistry was then performed with anti-CD11b and anti-p-NF-κB antibodies. LPS alone significantly increased nuclear p-NF-κB levels, whereas ALWPs significantly decreased LPS-induced nuclear p-NF-κB levels in BV2 microglial cells (**Figures 6G,H**). These data suggest that ALWPs modulate LPS-induced NF-κB nuclear translocation in BV2 microglial cells.

We then examined whether ALWPs modulate FAK signaling to alter LPS-induced nuclear p-NF-κB levels. BV2 microglial cells were pretreated with the FAK inhibitor PF-573228 (5 μM) for 30 min, followed by treatment with ALWPs (500 μg/ml) or PBS for 30 min and finally LPS (1 μg/ml) or PBS for 5 h. Immunocytochemistry was then conducted with anti-CD11b and anti-p-NF-κB antibodies. Treatment with PF-573228, ALWPs, and LPS further decreased LPS-stimulated nuclear p-NF-κB levels compared with treatment with PF-573228 and LPS or ALWPs and LPS (**Figures 6I,J**). These data suggest that ALWPs alter FAK signaling to affect nuclear p-NF-κB signaling to modulate the neuroinflammatory response.

ALWPs Reduce LPS-Induced Microglial Cell Migration

Several studies have shown that microglial cell migration is associated with the neuroinflammatory response (Choi et al., 2010; Karlstetter et al., 2011; Bose et al., 2016). To examine whether ALWPs can regulate microglial cell migration, we conducted wound-healing assays in which BV2 microglial cells were pretreated with PBS or ALWPs (500 μg/ml) for 1 h and treated with LPS (0.1 μg/ml) or PBS for 24 h. We found that LPS alone significantly increased BV2 microglial cell migration compared with control treatment (**Figures 7A,B**). In addition, pretreatment with ALWPs followed by LPS treatment significantly suppressed BV2 microglial cell migration compared with LPS treatment (**Figures 7A,B**). These data suggest that ALWPs can inhibit LPS-mediated BV2 microglial cell migration.

ALWPs Rescue Cognitive Performance and Inhibit Microglial Activation in LPS-Injected Wild-Type Mice

Several studies have shown that microglial activation is a cause of AD and other neurological disorders (Wee Yong, 2010; Hirsch et al., 2012; Asai et al., 2015; Heneka et al., 2015). In addition, enhanced neuroinflammation can lead to memory impairment

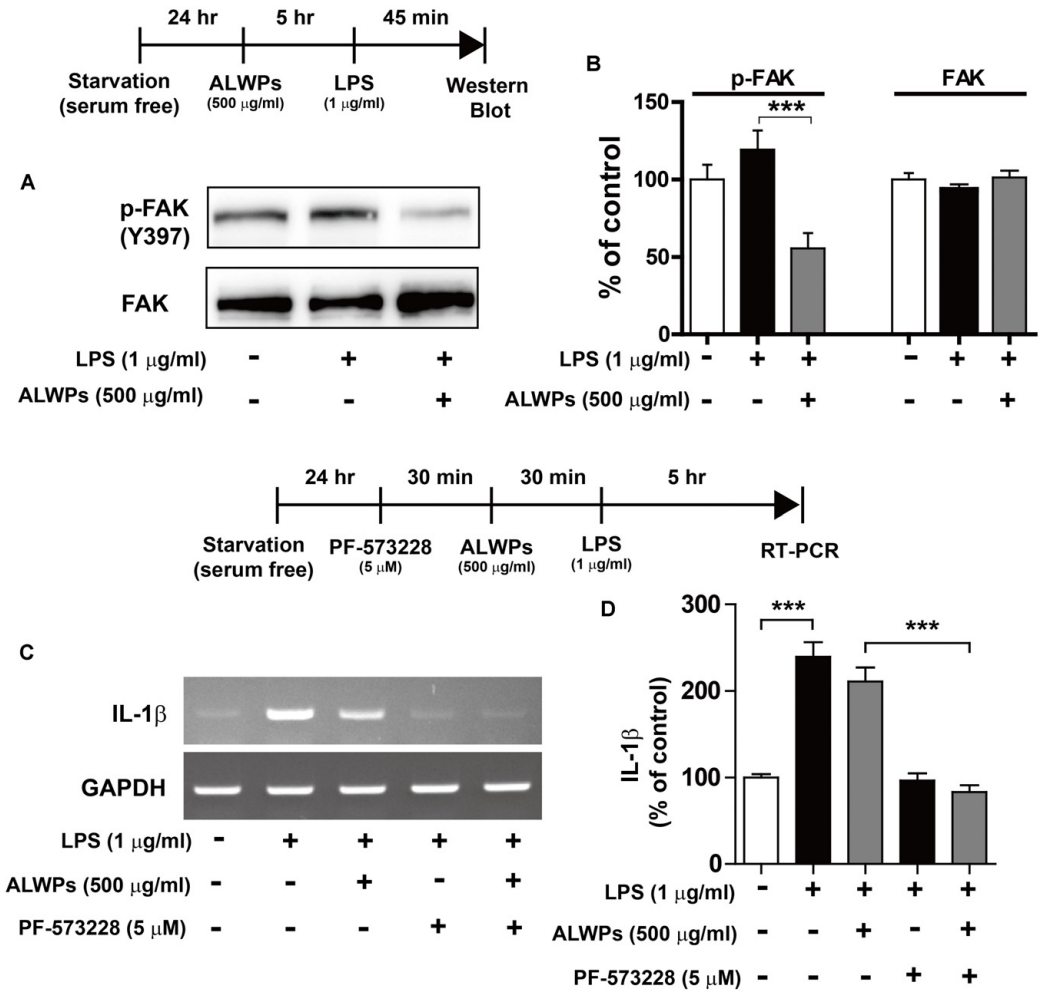

FIGURE 5 | ALWPs decreased LPS-induced FAK phosphorylation in BV2 microglial cells. **(A)** BV2 microglial cells were pretreated with ALWPs (500 μg/ml) or PBS for 5 h, followed by treatment with LPS (1 μg/ml) or PBS for 45 min, and western blotting was performed with anti-p-FAK and anti-FAK antibodies. **(B)** Quantification of the data from **(A)** (p-FAK and FAK: con, $n = 8$; LPS, $n = 8$; ALWPs + LPS, $n = 8$). **(C)** BV2 microglial cells were pretreated with PF-573228 (a FAK inhibitor, 5 μM) for 30 min, followed by treatment with ALWPs (500 μg/ml) or PBS for 30 min and finally LPS (1 μg/ml) or PBS for 5 h. Total RNA was isolated, and IL-1β mRNA levels were measured by RT-PCR. **(D)** Quantification of the data from **(C)** (con, $n = 30$; LPS, $n = 30$; ALWPs + LPS, $n = 30$; PF-573228 + LPS, $n = 30$; PF-573228 + ALWPs + LPS, $n = 30$). ***$p < 0.001$.

and eventually results in neurodegenerative diseases (Fang et al., 2010; Tweedie et al., 2012; Kempuraj et al., 2016). Thus, we investigated whether ALWPs can regulate cognitive function *in vivo*. Wild-type C57BL/6J mice were orally administered ALWPs (200 mg/kg) or PBS daily for 3 days. On the last day, after the treatment with PBS or ALWPs, LPS (250 μg/kg) was injected i.p., and Y-maze tests were performed. In addition, training sessions of the novel object recognition test (NOR) were performed 1 h after LPS injection, followed by the NOR test 24 h later. The LPS-injected wild-type mice exhibited significantly reduced short- and long-term memory compared with PBS-injected wild-type mice (**Figures 8A,B**). Pretreatment with ALWPs and injection with LPS rescued short- and long-term memory compared with LPS injection alone (**Figures 8A,B**), suggesting that ALWPs can affect learning and memory in LPS-injected wild-type mice.

Next, we examined whether ALWPs can regulate microglial activation *in vivo*. Wild-type C57BL/6J mice were orally administered ALWPs (200 mg/kg) or PBS daily for 3 days. On the last day, after the treatment with PBS or ALWPs, LPS (10 μg/kg) was injected i.p. Three hours later, immunohistochemistry was conducted with an anti-Iba-1 antibody, a marker for activated microglia. The LPS-injected wild-type mice exhibited significantly increased microglial activation in the hippocampus (**Figures 8C–E**) and cortex (**Figures 8F,G**) compared with PBS-injected wild-type mice. However, pretreatment with ALWPs significantly reduced microglial activation in the hippocampus (**Figures 8C–E**) and cortex (**Figures 8F,G**) in LPS-injected wild-type C57BL/6J mice. Taken together, these data suggest that ALWPs not only suppress microglial activation but also rescue impaired short-and long-term memory in LPS-injected wild-type C57BL/6J mice.

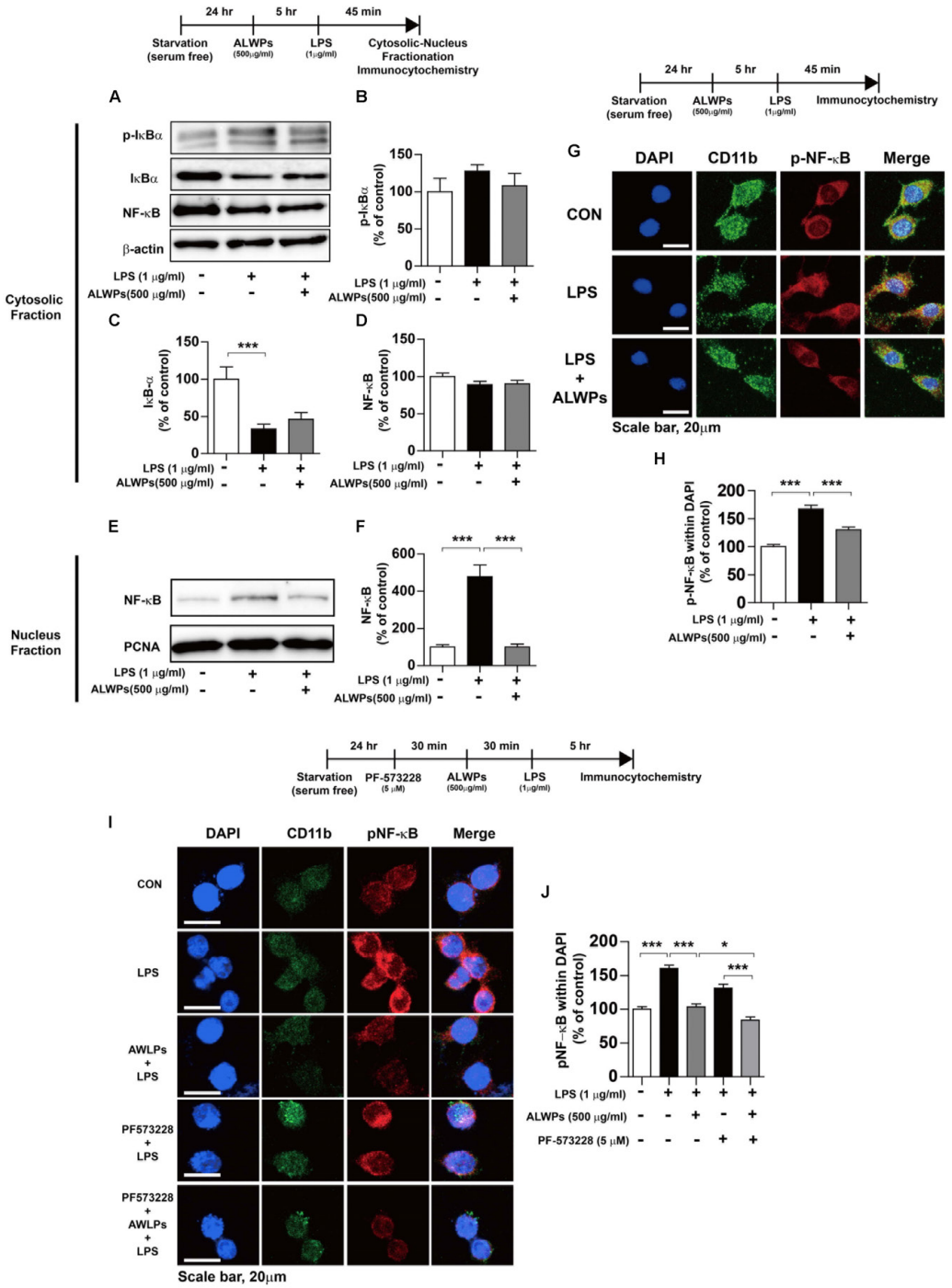

FIGURE 6 | ALWPs decreased LPS-induced nuclear NF-κB (Ser536) levels. **(A)** BV2 microglial cells were pretreated with ALWPs (500 μg/ml) or PBS for 5 h, followed by treatment with LPS (1 μg/ml) or PBS for 45 min and subcellular fractionation (nucleus vs. cytosol). Western blotting was conducted on the cytosolic fraction using antibodies against p-IκBα, IκBα, NF-κB, and β-actin (as a cytosolic marker). **(B–D)** Quantification of the data from **(A)** (p-IκBα: con, $n = 12$; LPS, $n = 12$; ALWPs + LPS, $n = 12$; IκBα: con, $n = 12$; LPS, $n = 12$; ALWPs + LPS, $n = 12$; NF-κB: con, $n = 12$; LPS, $n = 12$; ALWPs + LPS, $n = 12$). **(E)** Western blotting was performed on the nuclear fraction using antibodies against NF-κB and PCNA (as a nuclear marker). **(F)** Quantification of the data from **(E)** (con, $n = 12$; LPS, $n = 12$; ALWPs + LPS, $n = 12$). **(G)** BV2 microglial cells were pretreated with ALWPs (500 μg/ml) or PBS for 5 h and then treated with LPS (1 μg/ml) or PBS for 45 min. Cells were fixed and immunostained with anti-CD11b and anti-p-NF-κB (Ser536) antibodies (40× confocal images). **(H)** Quantification of the data from **(G)** (con, $n = 122$ cells; LPS, $n = 129$ cells; LPS + ALWPs, $n = 111$ cells). **(I)** BV2 microglial cells were pretreated with PF-573228 (a FAK inhibitor, 5 μM) or vehicle (1% DMSO) for 30 min, followed by treatment with ALWPs (500 μg/ml) or PBS for 30 min and finally LPS (1 μg/ml) or PBS for 5 h. Cells were fixed and immunostained with anti-CD11b and anti-p-NF-κB (Ser536) antibodies. **(J)** Quantification of the data from **(I)** (con, $n = 260$ cells; LPS, $n = 331$ cells; LPS + ALWPs, $n = 265$ cells; LPS + FAK inhibitor, $n = 188$ cells; LPS + FAK inhibitor + ALWPs, $n = 199$ cells). Scale bar 20 μm (40× confocal images). $^{*}p < 0.05$, $^{***}p < 0.001$.

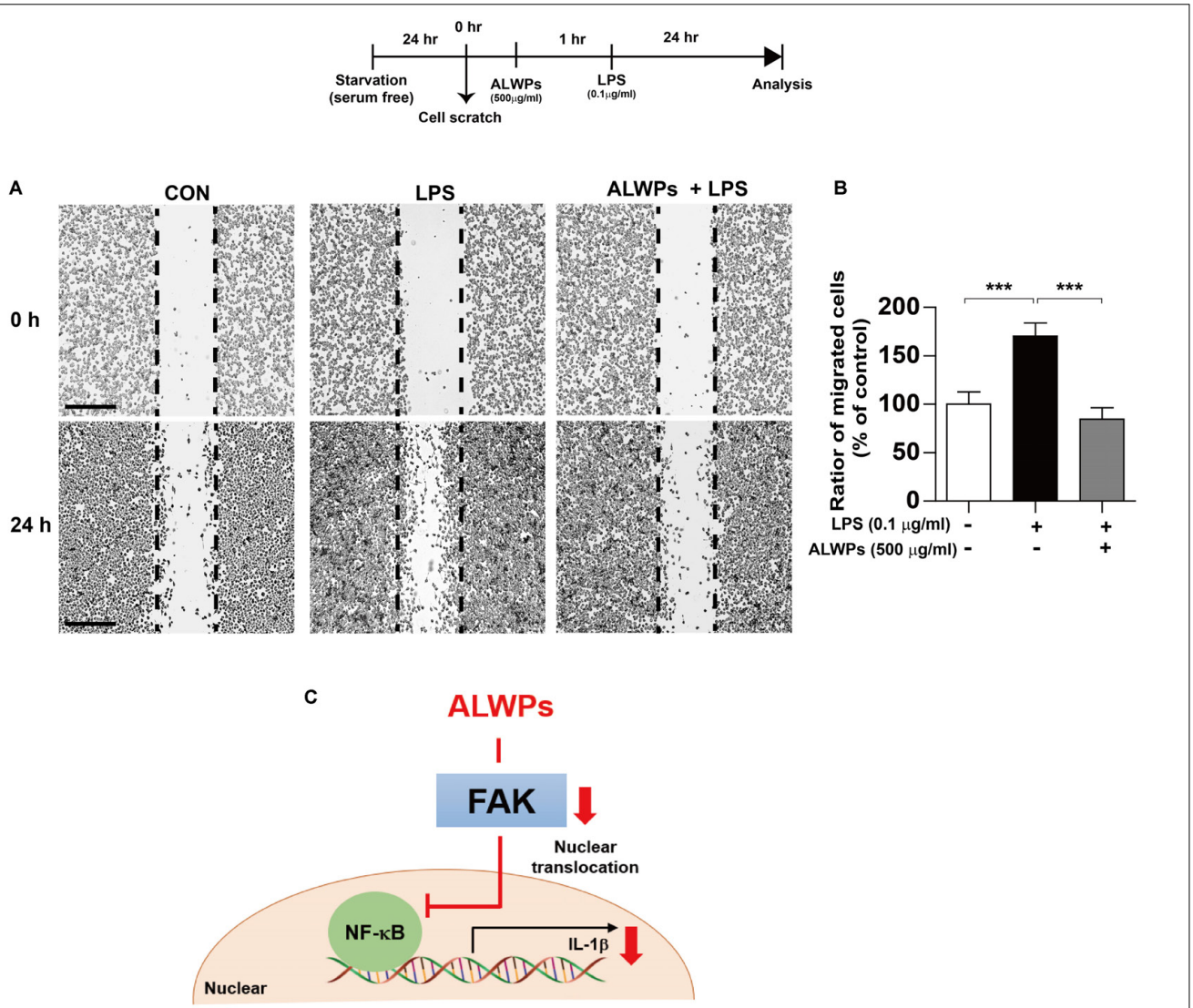

FIGURE 7 | ALWPs inhibited LPS-induced BV2 microglial cell migration. **(A)** BV2 microglial cell monolayers were scratched with a fine tip, pretreated with PBS or ALWPs (500 μg/ml) for 1 h, and then treated with LPS (0.1 μg/ml) or PBS for 23 h. Images of the wound gap were acquired at 0 h (i.e., immediately after scratching) and after 24 h. Scale bar 200 μm (4× confocal images). **(B)** Quantification of the data from **(A)** (con, $n = 16$; LPS, $n = 16$; ALWPs + LPS, $n = 16$). **(C)** A working model of the regulation of the LPS-induced neuroinflammatory response by ALWPs. $^{***}p < 0.001$.

Analysis of the Chemical Components of ALWPs by UHPLC

Four chemical standards corresponding to components of ALWPs were used to confirm the ALWP formula by UHPLC as described in the Materials and Methods: 5-hydroxymethyl-2-furaldehyde (5-HMF), morroniside, loganin and paeoniflorin. 5-HMF is one of the components of *R. glutinosa*, morroniside is present in *L. chinense*, loganin is present in *C. Officinalis* in, and paeoniflorin is present in *Moutan Cortex Radicis*. We observed that the retention times of 5-HMF, morroniside, loganin and paeoniflorin were approximately 4.059, 10.160, 11.494, and 12.019 min, respectively (**Supplementary Figure 4**). These results indicate that ALWPs contain the corresponding herbal ingredients.

To verify each herbal component of ALWPs by identifying the principal markers and to determine the content of the principal markers, UHPLC was performed. Calibration curves for 5-HMF, morroniside, and paeoniflorin were constructed with standard concentrations ranging from 10 to 100 μg/ml. The calibration curve of loganin was constructed with standard concentrations ranging from 10 to 1000 μg/ml. The regression equations and correlation coefficients (R^2) of 5-HMF, morroniside, loganin, and paeoniflorin were as follows: $y = 15200\times - 8020$, $R^2 = 0.999969$; $y = 1820\times + 760$, $R^2 = 0.999232$; $y = 397\times - 1550$, $R^2 = 0.999733$; and $y = 1910\times - 455$, $R^2 = 0.999335$, respectively (**Supplementary Figure 5**). Using these equations, the quantities of 5-HMF, morroniside, loganin, and paeoniflorin in ALWPs were calculated (**Table 1**).

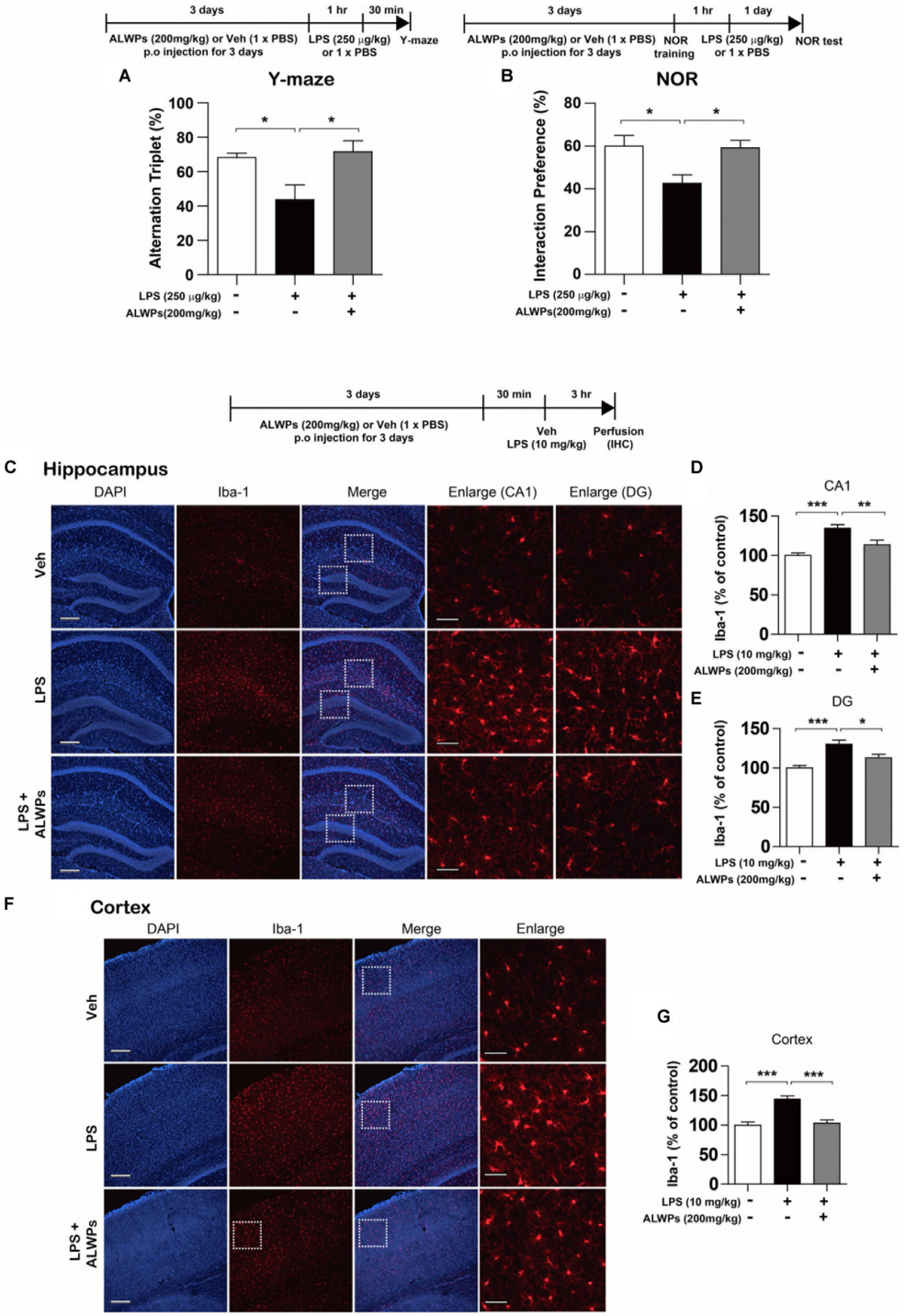

FIGURE 8 | ALWPs rescued impaired short- and long-term memory in LPS-injected wild-type C57BL6/J mice. **(A,B)** Wild-type C57BL6/J mice were orally administered ALWPs (200 mg/kg) or PBS daily for 3 days. On the third day, 1 h after treatment with PBS or ALWPs, LPS (250 μg/kg) was injected intraperitoneally (i.p.). Y-maze tests and training sessions of the novel object recognition test (NOR) were performed 1 h after LPS injection. NOR tests were conducted 24 h after the NOR training session (Y-maze: Veh, n = 9/mice; LPS + Veh, n = 9/mice; LPS + ALWPs, n = 11/mice; NOR test: Veh, n = 6/mice; LPS + Veh, n = 10/mice; LPS + ALWPs, n = 8/mice). **(C–G)** Wild-type C57BL6/J mice were orally administered ALWPs (200 mg/kg, p.o.) or PBS daily for 3 days. On the third day, LPS (10 mg/kg) was injected i.p Three hours later, immunohistochemistry was performed with an anti-Iba1 antibody in the hippocampus [**(C–E)**, CA1: Veh, n = 3/mice; LPS + Veh, n = 3/mice; LPS + ALWPs, n = 3/mice, DG: Veh, n = 3/mice; LPS + Veh, n = 3/mice; LPS + ALWPs, n = 3/mice] and cortex [**(F–G)**, Cortex: Veh, n = 3/mice; LPS + Veh, n = 3/mice; LPS + ALWPs, n = 3/mice]. Scale bar 200 μm (10× confocal images), Scale bar 50 μm (enlarged images), $^{*}p < 0.05$, $^{**}p < 0.01$, $^{***}p < 0.001$.

TABLE 1 | The contents of 5-HMF, morroniside, loganin, and paeoniflorin in ALWPs.

Origin	Marker compound	RT (min)	UV wavelength	Amount (μg/mL)
Rehmannia glutinosa	5-HMF	4.059	238	0.534 ± 0.002
Cornus officinalis	Morroniside	10.160	240	1.493 ± 0.015
C. officinalis	Loganin	11.494	237	9.390 ± 0.289
Moutan Cortex Radicis	Paeoniflorin	12.019	231	1.222 ± 0.006

DISCUSSION

Many studies have shown that neuroinflammation is tightly associated with neurodegenerative diseases, including AD. However, very little research has focused on elucidating the molecular mechanisms underlying neuroinflammation. In this study, we examined the novel effects of ALWPs on cognitive performance and neuroinflammatory responses. Specifically, we found that ALWPs suppressed LPS-induced IL-1β levels in BV2 microglial cells but not in primary astrocytes. ALWPs also modulated TLR4/FAK signaling to decrease LPS-induced IL-1β levels. In addition, ALWPs regulated the nuclear localization of the transcription factor NF-κB, thereby alleviating neuroinflammatory responses. Moreover, we observed that oral administration of ALWPs to LPS-injected wild-type C57BL/6J mice rescued short- and long-term memory and reduced microglial activation.

Proinflammatory cytokines and neuroinflammation have been linked to neurodegenerative disease (Downen et al., 1999; Norden et al., 2016). IL-1 exists in two isoforms, IL-1a and IL-1β, and both are highly involved in neurodegenerative diseases (Shaftel et al., 2008). A recent study showed that chronic activation of LPS or IFN-γ regulates proinflammatory cytokines, including IL-1β, leading to neuronal dysfunction and neuronal death (Papageorgiou et al., 2016). Another study found that activated microglial cells release IL-1β, leading to dopaminergic neuronal death in a PD animal model (Chung et al., 2017). Other studies have demonstrated that the natural compound resveratrol inhibits LPS-induced IL-1β expression in a murine microglial cell line (N9 cells) and in primary microglial cells but not in primary astrocytes (Lu et al., 2010). Interestingly, we observed that ALWPs affected LPS-stimulated IL-1β levels in BV2 microglial cells (**Figure 2**), whereas no effect on LPS-induced changes in proinflammatory cytokine levels was observed in primary astrocytes (**Supplementary Figures 1, 2**). Our findings indicate that ALWPs specifically modulate LPS-induced proinflammatory cytokine IL-1β levels and have different effects depending on cell type. We speculate that ALWPs reduce IL-1β levels to regulate neuroinflammation as well as cognitive function. However, we have not fully addressed why ALWPs only regulate IL-1β levels in microglial cells. The effects of ALWPs on LPS-induced IL-1β levels will be investigated at the molecular level in future studies.

Lipopolysaccharide binds to TLR4 on the cell surface of microglial cells, which then release proinflammatory cytokines (Gaikwad et al., 2016). Therefore, TLR4 inhibitors or antagonists are candidates as therapeutic agents targeting neuroinflammation-related diseases. In the present study, ALWPs altered TLR4 signaling to modulate LPS-induced IL-1β levels (**Figure 4**). It is possible that ALWPs interfere with the association between LPS and TLR4 or between LPS and unknown receptors that interact with LPS because we observed that ALWPs decreased LPS-induced IL-1β levels in the absence of a TLR4 inhibitor. In addition, we observed that ALWPs significantly decreased cell-surface levels of TLR4 (**Figure 4**). Thus, ALWPs inhibit the interaction between LPS and TLR4 on the cell surface, thereby affecting neuroinflammatory responses. However, it is not clear whether ALWPs affect the interaction between LPS and unknown receptors to alter neuroinflammation. A future study will explore whether ALWPs can modulate the interaction between LPS and TLR4 or unknown receptors to regulate the LPS-induced neuroinflammatory response.

Lipopolysaccharide activates TLR4 and downstream signaling cascades such as MAP kinase signaling (EKR1/2, JNK and P38). MAPK signaling is a key factor for regulating proinflammatory cytokines in microglial cells. The expression of IL-1β is regulated by the MAPK signaling pathway in neuroglial cells, including microglia, astrocytes, and a microglial cell line (BV2) (Kaminska et al., 2009; Dang et al., 2014; Guo et al., 2016). Unexpectedly, we found that ALWPs did not alter the LPS-induced MAPK signaling pathway (**Supplementary Figure 3**). Thus, we examined another potential target, the FAK signaling pathway, which is a downstream signaling pathway activated by LPS (Wong et al., 2011). LPS treatment increases autophosphorylation of FAK (Tyr397) in murine macrophages and human synoviocytes. In addition, a study has shown that LPS-induced IL-6 levels are associated with FAK phosphorylation (Tyr397) (Zeisel et al., 2005). Thus, we examined the effects of ALWPs on FAK phosphorylation and observed that ALWPs decreased p-FAK (Tyr 397) in LPS-stimulated BV2 microglial cells (**Figure 5**). In addition, treatment with a FAK inhibitor, ALWPs, and LPS did not reduce LPS-induced IL-1β levels compared with treatment with a FAK inhibitor and LPS (**Figure 5**). These data suggest that ALWPs suppress FAK phosphorylation (Tyr 397) to regulate LPS-induced IL-1β levels.

NF-κB is a key transcription factor regulating inflammatory cytokines (Shaftel et al., 2008; Lawrence, 2009). Several studies have shown that LPS increases the phosphorylation of NF-κB-p65 *in vivo* and *in vitro* (Stylianou et al., 1992; Schutze et al., 1995; Bonaiuto et al., 1997; Dai et al., 2015). In addition, NF-κB binds to the IL-1β promoter region (Hiscott et al., 1993), and treatment with IL-1 agonists increases the phosphorylation of NF-κB (Malinin et al., 1997). Here, we observed that ALWPs downregulated p-NF-κB and translocation in the nucleus in LPS-stimulated BV2 microglial cells (**Figure 6**). In addition, ALWPs but not the individual components significantly decreased LPS-stimulated proinflammatory cytokine IL-1β levels (**Figure 3**),

suggesting that ALWPs play an important role in regulating NF-κB and IL-1β levels and providing a new mechanism of the anti-inflammatory response.

Microglial cell migration is associated with neuroinflammation. Specifically, microglial migration and the related phagocytic activity can be activated by G-coupled receptors, which include chemokines (Guida et al., 2017). A recent study demonstrated that the chemokine CCL2 modulates microglial cell migration through the MEK/ERK and PI3K pathways (Bose et al., 2016). Karlstetter et al. found that curcumin, one of the major components of turmeric, has anti-inflammatory effects by inhibiting microglial cell migration (Choi et al., 2010; Karlstetter et al., 2011). Therefore, we examined the effects of ALWPs on microglial cell migration and found that ALWPs significantly inhibited LPS-induced BV2 microglial cell migration (**Figure 7**). Based on the literature and our findings, we speculate that ALWPs modulate BV2 microglial cell migration by altering LPS-mediated IL-1β levels. Thus, we will further investigate how ALWPs regulate BV2 microglial cell migration.

In this study, we examined the anti-inflammatory effects of ALWPs. ALWPs contain ten different herbs, and some of the components of ALWPs are known to be involved in inflammation. For instance, 5-HMF, one of the components of *R. glutinosa*, a component of ALWPs, inhibits reactive oxygen species (ROS) and NF-κB activity in TNF-α-induced vascular endothelial cells (Kim et al., 2013). *Corni fructus,* a component of ALWPs, has anti-inflammatory effects by suppressing COX-2 and iNOS levels through the downregulation of NF-κB binding activity in macrophages (Sung et al., 2009). Morroniside is a major component of *C. officinalis,* a component of ALWPs, and reduces proinflammatory cytokine IL-6 and IL-1β levels in a rat model of acute myocardial infarction (Yu et al., 2018). In addition, type 2 diabetic rats orally administered morroniside, a component of ALWPs, exhibit downregulated NF-κB activity in hepatic tissue (Park et al., 2009). Loganin is one of the components of *C. officinalis,* a component of ALWPs, and has been shown to suppress ApoCIII-induced proinflammatory cytokines and NF-κB phosphorylation in mouse adipocytes (Li et al., 2016). Thus, each component of ALWPs has antioxidant and anti-inflammatory effects in vascular endothelial cells, hepatic tissue, or adipose cells. However, whether the ten individual components of ALWPs have anti-inflammatory effects in LPS-induced BV2 microglial cells and in the brain is not clear. To test this, we examined the effects of each component of ALWPs on proinflammatory cytokine IL-1β levels and found that ALWPs but not the individual components decreased LPS-mediated IL-1β mRNA levels in BV2 microglial cells (**Figure 3**). Although each component of ALWPs is known to have a positive effect at the cellular level, we suggest that the combination of these ten ingredients in ALWPs has synergistic effects to reduce neuroinflammation.

Memory loss is one of the clinical symptoms of neurodegenerative diseases and is most commonly associated with AD. Memory deficits have been shown to be closely related to neuroinflammation. Specifically, activated microglia release proinflammatory cytokines that exacerbate memory loss in various diseases (Perry and Holmes, 2014; Lelios and Greter, 2018; Wendeln et al., 2018). In particular, several studies have demonstrated critical roles for IL-1β and TNF-α in the formation of learning and memory. For instance, increased levels of IL-1β are correlated with cognitive deficits in sepsis-associated encephalopathy and a repeated social defeat model (Imamura et al., 2011; McKim et al., 2016). Other studies reported that intrahippocampal injection or chronic overexpression of IL-1β in the hippocampus region leads to impairments of spatial memory (Gonzalez et al., 2009; Moore et al., 2009). Wang et al. reported that the proinflammatory cytokine IL-1β induces memory deficits by modulating the expression of $GABA_A$ receptors through the P38 signaling pathway (Wang et al., 2012). Similarly, overexpression of TNF-α in neurons or glial cells impairs synaptic plasticity and learning and memory (Fiore et al., 2000). In addition, chronic LPS administration impairs learning and memory via TNF-α (Belarbi et al., 2012). These studies indicate that inflammation can affect cognitive function. Accordingly, several studies have evaluated the potential of traditional herbal medicines to inhibit neuroinflammation and ameliorate memory loss in inflammation-related diseases. For example, chrysophanol (a component extracted from *Rhubarb*), a traditional herbal medicine, attenuates memory deficits and neuronal death by inhibiting inflammation in diabetic mice (Chu et al., 2018). Anthocyanins, another herbal medicine, ameliorate hippocampus-dependent memory impairment and prevent neuroinflammation via the JNK/Akt/GSK3β axis in LPS-injected wild-type mice (Khan et al., 2018). In addition, Gu et al. (2016) have shown that paeoniflorin, a component of ALWPs, improves learning and memory and inhibits proinflammatory cytokine levels in a mouse model of AD. Another group reported that loganin, a component of ALWPs, decreases Aβ-induced inflammatory responses and ameliorates memory deficits induced by scopolamine (Hwang et al., 2017). However, there are few studies on the therapeutic effects and related mechanisms of each of the components of ALWPs in inflammation-related cognitive deficits. Based on the literature, we hypothesized that ALWPs affect cognitive performance by inhibiting neuroinflammation. To test this hypothesis, we examined the effects of ALWPs on cognitive function in LPS-injected wild-type mice. Interestingly, we found that ALWPs had anti-inflammatory effects (**Figures 2**, **3**) and attenuated LPS-induced short- and long-term memory deficits in wild-type mice (**Figure 8**). Future studies will examine whether ALWPs regulate cognitive function through IL-1β as well as whether the individual components of ALWPs are sufficient to enhance learning and memory.

CONCLUSION

In summary, this study showed that traditional herbal medicine ALWPs are a regulator of anti-inflammatory TLR4/FAK signaling cascades in LPS-induced BV2 microglial cells. In addition, treatment with ALWPs followed by LPS alters the subcellular localization of the transcriptional factor NF-κB. Moreover, ALWPs promote short- and long-term memory and inhibit

microglial activation. Taken together, these data indicate that ALWPs might be a potential therapeutic anti-neuroinflammatory drug for neuroinflammation-related diseases, including AD.

AUTHOR CONTRIBUTIONS

Y-MW, JWK, and H-SH conceived and designed the study. J-YL, JN, WL, BJ, HN, H-JC, H-JK, YN, and YS acquired the data. J-YL, HN, JN, BJ, YN, and JK prepared the figures. YS, YJ, and Y-MW prepared the tables. J-YL, JN, JK, YN, YJ, Y-MW, JWK, YN, and H-SH wrote the manuscript.

FUNDING

Confocal microscopy (Nikon, TI-RCP) data were acquired at the Advanced Neural Imaging Center at the Korea Brain Research Institute (KBRI). This work was supported by the KBRI basic research program through the Korea Brain Research Institute funded by the Ministry of Science, ICT and Future Planning (Grant No. 18-BR-02-03, JWK; Grant No. 18-BR-02-04, H-SH), and the National Research Foundation of Korea (Grant No. 2016R1A2B4011393, H-SH).

ACKNOWLEDGMENTS

We thank So Yeon Koo, Dr. Young-Pyo Choi, and Bae-Jin Kim for editing, valuable comments, and assistance with the behavior studies in our manuscript.

SUPPLEMENTARY MATERIAL

The Supplementary Material for this article can be found online at: https://www.frontiersin.org/articles/10.3389/fnagi.2018.00269/full#supplementary-material

REFERENCES

Asai, H., Ikezu, S., Tsunoda, S., Medalla, M., Luebke, J., Haydar, T., et al. (2015). Depletion of microglia and inhibition of exosome synthesis halt tau propagation. *Nat. Neurosci.* 18, 1584–1593. doi: 10.1038/nn.4132

Belarbi, K., Jopson, T., Tweedie, D., Arellano, C., Luo, W., Greig, N. H., et al. (2012). TNF-alpha protein synthesis inhibitor restores neuronal function and reverses cognitive deficits induced by chronic neuroinflammation. *J. Neuroinflamm.* 9:23. doi: 10.1186/1742-2094-9-23

Bonaiuto, C., McDonald, P. P., Rossi, F., and Cassatella, M. A. (1997). Activation of nuclear factor-kappa B by beta-amyloid peptides and interferon-gamma in murine microglia. *J. Neuroimmunol.* 77, 51–56. doi: 10.1016/S0165-5728(97)00054-4

Bose, S., Kim, S., Oh, Y., Moniruzzaman, M., Lee, G., and Cho, J. (2016). Effect of CCL2 on BV2 microglial cell migration: involvement of probable signaling pathways. *Cytokine* 81, 39–49. doi: 10.1016/j.cyto.2016.02.001

Cao, Q., Li, P., Lu, J., Dheen, S. T., Kaur, C., and Ling, E. A. (2010). Nuclear factor-kappaB/p65 responds to changes in the Notch signaling pathway in murine BV-2 cells and in amoeboid microglia in postnatal rats treated with the gamma-secretase complex blocker DAPT. *J. Neurosci. Res.* 88, 2701–2714. doi: 10.1002/jnr.22429

Chen, Z., Jalabi, W., Shpargel, K. B., Farabaugh, K. T., Dutta, R., Yin, X., et al. (2012). Lipopolysaccharide-induced microglial activation and neuroprotection against experimental brain injury is independent of hematogenous TLR4. *J. Neurosci.* 32, 11706–11715. doi: 10.1523/JNEUROSCI.0730-12.2012

Choi, I., Kim, B., Byun, J. W., Baik, S. H., Huh, Y. H., Kim, J. H., et al. (2015). LRRK2 G2019S mutation attenuates microglial motility by inhibiting focal adhesion kinase. *Nat. Commun.* 6:8255. doi: 10.1038/ncomms9255

Choi, M. S., Cho, K. S., Shin, S. M., Ko, H. M., Kwon, K. J., Shin, C. Y., et al. (2010). ATP induced microglial cell migration through non-transcriptional activation of matrix metalloproteinase-9. *Arch. Pharm. Res.* 33, 257–265. doi: 10.1007/s12272-010-0211-8

Chu, X., Zhou, S., Sun, R., Wang, L., Xing, C., Liang, R., et al. (2018). Chrysophanol relieves cognition deficits and neuronal loss through inhibition of inflammation in diabetic mice. *Neurochem. Res.* 43, 972–983. doi: 10.1007/s11064-018-2503-1

Chung, Y. C., Baek, J. Y., Kim, S. R., Ko, H. W., Bok, E., Shin, W. H., et al. (2017). Capsaicin prevents degeneration of dopamine neurons by inhibiting glial activation and oxidative stress in the MPTP model of Parkinson's disease. *Exp. Mol. Med.* 49:e298. doi: 10.1038/emm.2016.159

Cunningham, C. (2013). Microglia and neurodegeneration: the role of systemic inflammation. *Glia* 61, 71–90. doi: 10.1002/glia.22350

Dai, X. J., Li, N., Yu, L., Chen, Z. Y., Hua, R., Qin, X., et al. (2015). Activation of BV2 microglia by lipopolysaccharide triggers an inflammatory reaction in PC12 cell apoptosis through a toll-like receptor 4-dependent pathway. *Cell Stress Chaperones* 20, 321–331. doi: 10.1007/s12192-014-0552-1

Dang, Y., Xu, Y., Wu, W., Li, W., Sun, Y., Yang, J., et al. (2014). Tetrandrine suppresses lipopolysaccharide-induced microglial activation by inhibiting NF-kappaB and ERK signaling pathways in BV2 cells. *PLoS One* 9:e102522. doi: 10.1371/journal.pone.0102522

Dong, Y., Liu, L., Shan, X., Tang, J., Xia, B., Cheng, X., et al. (2018). Pilose antler peptide attenuates LPS-induced inflammatory reaction. *Int. J. Biol. Macromol.* 108, 272–276. doi: 10.1016/j.ijbiomac.2017.11.176

Downen, M., Amaral, T. D., Hua, L. L., Zhao, M. L., and Lee, S. C. (1999). Neuronal death in cytokine-activated primary human brain cell culture: role of tumor necrosis factor-alpha. *Glia* 28, 114–127. doi: 10.1002/(SICI)1098-1136(199911)28:2<114::AID-GLIA3>3.0.CO;2-O

Dursun, E., Gezen-Ak, D., Hanagasi, H., Bilgic, B., Lohmann, E., Ertan, S., et al. (2015). The interleukin 1 alpha, interleukin 1 beta, interleukin 6 and alpha-2-macroglobulin serum levels in patients with early or late onset Alzheimer's disease, mild cognitive impairment or Parkinson's disease. *J. Neuroimmunol.* 283, 50–57. doi: 10.1016/j.jneuroim.2015.04.014

Fang, S. J., Wu, X. S., Han, Z. H., Zhang, X. X., Wang, C. M., Li, X. Y., et al. (2010). Neuregulin-1 preconditioning protects the heart against ischemia/reperfusion injury through a PI3K/Akt-dependent mechanism. *Chin. Med. J. (Engl.)* 123, 3597–3604.

Fiore, M., Angelucci, F., Alleva, E., Branchi, I., Probert, L., and Aloe, L. (2000). Learning performances, brain NGF distribution and NPY levels in transgenic mice expressing TNF-alpha. *Behav. Brain Res.* 112, 165–175. doi: 10.1016/S0166-4328(00)00180-7

Fruhauf, P. K., Ineu, R. P., Tomazi, L., Duarte, T., Mello, C. F., and Rubin, M. A. (2015). Spermine reverses lipopolysaccharide-induced memory deficit in mice. *J. Neuroinflamm.* 12:3. doi: 10.1186/s12974-014-0220-5

Gaikwad, S., Naveen, C., and Agrawal-Rajput, R. (2016). Toll-like receptor-4 antagonism mediates benefits during neuroinflammation. *Neural Regen Res.* 11, 552–553. doi: 10.4103/1673-5374.180732

Gonzalez, P. V., Schioth, H. B., Lasaga, M., and Scimonelli, T. N. (2009). Memory impairment induced by IL-1beta is reversed by alpha-MSH through central melanocortin-4 receptors. *Brain Behav. Immun.* 23, 817–822. doi: 10.1016/j.bbi.2009.03.001

Gray, C., Hukkanen, M., Konttinen, Y. T., Terenghi, G., Arnett, T. R., Jones, S. J., et al. (1992). Rapid neural growth: calcitonin gene-related peptide and substance P-containing nerves attain exceptional growth rates in regenerating deer antler. *Neuroscience* 50, 953–963. doi: 10.1016/0306-4522(92)90218-Q

Gu, X., Cai, Z., Cai, M., Liu, K., Liu, D., Zhang, Q., et al. (2016). Protective effect of paeoniflorin on inflammation and apoptosis in the cerebral cortex of a transgenic mouse model of Alzheimer's disease. *Mol. Med. Rep.* 13, 2247–2252. doi: 10.3892/mmr.2016.4805

Guida, F., Luongo, L., Boccella, S., Giordano, M. E., Romano, R., Bellini, G., et al. (2017). Palmitoylethanolamide induces microglia changes associated with increased migration and phagocytic activity: involvement of the CB2 receptor. *Sci. Rep.* 7:375. doi: 10.1038/s41598-017-00342-1

Guo, C., Yang, L., Wan, C. X., Xia, Y. Z., Zhang, C., Chen, M. H., et al. (2016). Anti-neuroinflammatory effect of sophoraflavanone G from *Sophora alopecuroides* in LPS-activated BV2 microglia by MAPK, JAK/STAT and Nrf2/HO-1 signaling pathways. *Phytomedicine* 23, 1629–1637. doi: 10.1016/j.phymed.2016.10.007

Ha, H., Lee, J. K., Lee, H. Y., Koh, W. S., Seo, C. S., Lee, M. Y., et al. (2011). Safety evaluation of yukmijihwang-tang: assessment of acute and subchronic toxicity in rats. *Evid. Based Complem. Alternat. Med.* 2011:672136. doi: 10.1155/2011/672136

Hanisch, U. K., and Kettenmann, H. (2007). Microglia: active sensor and versatile effector cells in the normal and pathologic brain. *Nat. Neurosci.* 10, 1387–1394. doi: 10.1038/nn1997

Heneka, M. T., Carson, M. J., El Khoury, J., Landreth, G. E., Brosseron, F., Feinstein, D. L., et al. (2015). Neuroinflammation in Alzheimer's disease. *Lancet Neurol.* 14, 388–405. doi: 10.1016/s1474-4422(15)70016-5

Hines, D. J., Choi, H. B., Hines, R. M., Phillips, A. G., and MacVicar, B. A. (2013). Prevention of LPS-induced microglia activation, cytokine production and sickness behavior with TLR4 receptor interfering peptides. *PLoS One* 8:e60388. doi: 10.1371/journal.pone.0060388

Hirsch, E. C., Vyas, S., and Hunot, S. (2012). Neuroinflammation in Parkinson's disease. *Parkinsonism Relat. Disord.* 18(Suppl. 1), S210–S212. doi: 10.1016/s1353-8020(11)70065-7

Hiscott, J., Marois, J., Garoufalis, J., D'Addario, M., Roulston, A., Kwan, I., et al. (1993). Characterization of a functional NF-kappaB site in the human interleukin 1 beta promoter: evidence for a positive autoregulatory loop. *Mol. Cell Biol.* 13, 6231–6240. doi: 10.1128/MCB.13.10.6231

Hsieh, M. T., Cheng, S. J., Lin, L. W., Wang, W. H., and Wu, C. R. (2003). The ameliorating effects of acute and chronic administration of LiuWei Dihuang Wang on learning performance in rodents. *Biol. Pharm. Bull.* 26, 156–161. doi: 10.1248/bpb.26.156

Hwang, E. S., Kim, H. B., Lee, S., Kim, M. J., Lee, S. O., Han, S. M., et al. (2017). Loganin enhances long-term potentiation and recovers scopolamine-induced learning and memory impairments. *Physiol. Behav.* 171, 243–248. doi: 10.1016/j.physbeh.2016.12.043

Imamura, Y., Wang, H., Matsumoto, N., Muroya, T., Shimazaki, J., Ogura, H., et al. (2011). Interleukin-1beta causes long-term potentiation deficiency in a mouse model of septic encephalopathy. *Neuroscience* 187, 63–69. doi: 10.1016/j.neuroscience.2011.04.063

Kaminska, B., Gozdz, A., Zawadzka, M., Ellert-Miklaszewska, A., and Lipko, M. (2009). MAPK signal transduction underlying brain inflammation and gliosis as therapeutic target. *Anat. Rec. (Hoboken)* 292, 1902–1913. doi: 10.1002/ar.21047

Kang, M., Kim, J. H., Cho, C., Lee, K. Y., Shin, M., Hong, M., et al. (2006). Effects of Yukmijihwang-tang derivatives (YMJd) on ibotenic acid-induced amnesia in the rat. *Biol. Pharm. Bull.* 29, 1431–1435. doi: 10.1248/bpb.29.1431

Karlstetter, M., Lippe, E., Walczak, Y., Moehle, C., Aslanidis, A., Mirza, M., et al. (2011). Curcumin is a potent modulator of microglial gene expression and migration. *J Neuroinflamm.* 8:125. doi: 10.1186/1742-2094-8-125

Kempuraj, D., Thangavel, R., Natteru, P. A., Selvakumar, G. P., Saeed, D., Zahoor, H., et al. (2016). Neuroinflammation induces neurodegeneration. *J. Neurol. Neurosurg. Spine* 1:1003.

Kettenmann, H., Hanisch, U. K., Noda, M., and Verkhratsky, A. (2011). Physiology of microglia. *Physiol. Rev.* 91, 461–553. doi: 10.1152/physrev.00011.2010

Khan, M. S., Ali, T., Kim, M. W., Jo, M. H., Chung, J. I., and Kim, M. O. (2018). Anthocyanins improve hippocampus-dependent memory function and prevent neurodegeneration via JNK/Akt/GSK3beta signaling in LPS-treated adult mice. *Mol. Neurobiol.* doi: 10.1007/s12035-018-1101-1 [Epub ahead of print].

Kim, M.-C., Lee, C.-H., and Yook, T.-H. (2013). Effects of anti-inflammatory and *Rehmanniae radix* pharmacopuncture on atopic dermatitis in NC/Nga mice. *J. Acupunct. Meridian Stud.* 6, 98–109. doi: 10.1016/j.jams.2012.10.007

Kreutzberg, G. W. (1996). Microglia: a sensor for pathological events in the CNS. *Trends Neurosci.* 19, 312–318. doi: 10.1016/0166-2236(96)10049-7

Lawrence, T. (2009). The nuclear factor NF-kappaB pathway in inflammation. *Cold Spring Harb. Perspect. Biol.* 1:a001651. doi: 10.1101/cshperspect.a001651

Lee, J. W., Lee, Y. K., Yuk, D. Y., Choi, D. Y., Ban, S. B., Oh, K. W., et al. (2008). Neuro-inflammation induced by lipopolysaccharide causes cognitive impairment through enhancement of beta-amyloid generation. *J. Neuroinflamm.* 5:37. doi: 10.1186/1742-2094-5-37

Lee, J. W., Pak, S. C., Jeon, S., and Kim, D. I. (2012). Modified yukmijihwangtang suppresses the production of proinflammatory cytokines in the intravesical hydrochloric acid-induced cystitis rat model via the NF-kappaB pathway. *Am. J. Chin. Med.* 40, 321–334. doi: 10.1142/S0192415X12500255

Lee, M.-R., Yun, B.-S., Zhang, D.-L., Liu, L., Wang, Z., Wang, C.-L., et al. (2010). Effect of aqueous antler extract on scopolamine-induced memory impairment in mice and antioxidant activities. *Food Sci. Biotechnol.* 19, 655–661. doi: 10.1007/s10068-010-0092-0

Lelios, I., and Greter, M. (2018). Trained microglia trigger memory loss. *Immunity* 48, 849–851. doi: 10.1016/j.immuni.2018.04.033

Li, C., Stanton, J. A., Robertson, T. M., Suttie, J. M., Sheard, P. W., Harris, A. J., et al. (2007). Nerve growth factor mRNA expression in the regenerating antler tip of red deer (*Cervus elaphus*). *PLoS One* 2:e148. doi: 10.1371/journal.pone.0000148

Li, Y., Li, Z., Shi, L., Zhao, C., Shen, B., Tian, Y., et al. (2016). Loganin inhibits the inflammatory response in mouse 3T3L1 adipocytes and mouse model. *Int. Immunopharmacol.* 36, 173–179. doi: 10.1016/j.intimp.2016.04.026

Lian, X., Wang, X. T., Wang, W. T., Yang, X., Suo, Z. W., and Hu, X. D. (2015). Peripheral inflammation activated focal adhesion kinase signaling in spinal dorsal horn of mice. *J. Neurosci. Res.* 93, 873–881. doi: 10.1002/jnr.23551

Lu, X., Ma, L., Ruan, L., Kong, Y., Mou, H., Zhang, Z., et al. (2010). Resveratrol differentially modulates inflammatory responses of microglia and astrocytes. *J. Neuroinflamm.* 7:46. doi: 10.1186/1742-2094-7-46

Malinin, N. L., Boldin, M. P., Kovalenko, A. V., and Wallach, D. (1997). MAP3K-related kinase involved in NF-kappaB induction by TNF, CD95 and IL-1. *Nature* 385, 540–544. doi: 10.1038/385540a0

McKim, D. B., Niraula, A., Tarr, A. J., Wohleb, E. S., Sheridan, J. F., and Godbout, J. P. (2016). Neuroinflammatory dynamics underlie memory impairments after repeated social defeat. *J. Neurosci.* 36, 2590–2604. doi: 10.1523/JNEUROSCI.2394-15.2016

Mogi, M., Harada, M., Riederer, P., Narabayashi, H., Fujita, K., and Nagatsu, T. (1994). Tumor necrosis factor-alpha (TNF-alpha) increases both in the brain and in the cerebrospinal fluid from parkinsonian patients. *Neurosci. Lett.* 165, 208–210. doi: 10.1016/0304-3940(94)90746-3

Moore, A. H., Wu, M., Shaftel, S. S., Graham, K. A., and O'Banion, M. K. (2009). Sustained expression of interleukin-1beta in mouse hippocampus impairs spatial memory. *Neuroscience* 164, 1484–1495. doi: 10.1016/j.neuroscience.2009.08.073

Nam, J. H., Cho, H. J., Kang, H., Lee, J. Y., Jung, M., and Chang, Y. C. (2017). A mercaptoacetamide-based class II histone deacetylase inhibitor suppresses cell migration and invasion in monomorphic malignant human glioma cells by inhibiting FAK/STAT3 signaling. *J. Cell. Biochem.* 118, 4672–4685. doi: 10.1002/jcb.26133

Neumann, H., Kotter, M. R., and Franklin, R. J. (2009). Debris clearance by microglia: an essential link between degeneration and regeneration. *Brain* 132(Pt 2), 288–295. doi: 10.1093/brain/awn109

Norden, D. M., Trojanowski, P. J., Villanueva, E., Navarro, E., and Godbout, J. P. (2016). Sequential activation of microglia and astrocyte cytokine expression precedes increased Iba-1 or GFAP immunoreactivity following systemic immune challenge. *Glia* 64, 300–316. doi: 10.1002/glia.22930

Oakley, H., Cole, S. L., Logan, S., Maus, E., Shao, P., Craft, J., et al. (2006). Intraneuronal beta-amyloid aggregates, neurodegeneration, and neuron loss in transgenic mice with five familial Alzheimer's disease mutations: potential factors in amyloid plaque formation. *J. Neurosci.* 26, 10129–10140. doi: 10.1523/jneurosci.1202-06.2006

Papageorgiou, I. E., Lewen, A., Galow, L. V., Cesetti, T., Scheffel, J., Regen, T., et al. (2016). TLR4-activated microglia require IFN-gamma to induce severe neuronal dysfunction and death in situ. *Proc. Natl. Acad. Sci. U.S.A.* 113, 212–217. doi: 10.1073/pnas.1513853113

Park, C. H., Yamabe, N., Noh, J. S., Kang, K. S., Tanaka, T., and Yokozawa, T. (2009). The beneficial effects of morroniside on the inflammatory response and lipid metabolism in the liver of db/db mice. *Biol. Pharm. Bull.* 32, 1734–1740. doi: 10.1248/bpb.32.1734

Park, E., Kang, M., Oh, J. W., Jung, M., Park, C., Cho, C., et al. (2005). Yukmijihwang-tang derivatives enhance cognitive processing in normal young adults: a double-blinded, placebo-controlled trial. *Am. J. Chin. Med.* 33, 107–115. doi: 10.1142/S0192415X05002709

Park, J. Y., Kang, K. A., Kim, K. C., Cha, J. W., Kim, E. H., and Hyun, J. W. (2013). Morin induces heme oxygenase-1 via ERK-Nrf2 signaling pathway. *J. Cancer Prev.* 18, 249–256. doi: 10.15430/JCP.2013.18.3.249

Perry, V. H., and Holmes, C. (2014). Microglial priming in neurodegenerative disease. *Nat. Rev. Neurol.* 10, 217–224. doi: 10.1038/nrneurol.2014.38

Pita-Thomas, W., Nieto-Sampedro, M., Maza, R. M., and Nieto-Diaz, M. (2010). Factors promoting neurite outgrowth during deer antler regeneration. *J. Neurosci. Res.* 88, 3034–3047. doi: 10.1002/jnr.22459

Schutze, S., Wiegmann, K., Machleidt, T., and Kronke, M. (1995). TNF-induced activation of NF-kappaB. *Immunobiology* 193, 193–203. doi: 10.1016/S0171-2985(11)80543-7

Shaftel, S. S., Griffin, W. S., and O'Banion, M. K. (2008). The role of interleukin-1 in neuroinflammation and Alzheimer disease: an evolving perspective. *J. Neuroinflamm.* 5:7. doi: 10.1186/1742-2094-5-7

Shal, B., Ding, W., Ali, H., Kim, Y. S., and Khan, S. (2018). Anti-neuroinflammatory potential of natural products in attenuation of Alzheimer's disease. *Front. Pharmacol.* 9:548. doi: 10.3389/fphar.2018.00548

Sheng, W., Zong, Y., Mohammad, A., Ajit, D., Cui, J., Han, D., et al. (2011). Pro-inflammatory cytokines and lipopolysaccharide induce changes in cell morphology, and upregulation of ERK1/2, iNOS and $sPLA_2$-IIA expression in astrocytes and microglia. *J. Neuroinflammation* 8:121. doi: 10.1186/1742-2094-8-121

Solito, E., and Sastre, M. (2012). Microglia function in Alzheimer's disease. *Front. Pharmacol.* 3:14. doi: 10.3389/fphar.2012.00014

Song, X., Shukla, S., Lee, G., Park, S., and Kim, M. (2016). Detection of *Cronobacter* genus in powdered infant formula by enzyme-linked immunosorbent assay using anti-*Cronobacter* antibody. *Front. Microbiol.* 7:1124. doi: 10.3389/fmicb.2016.01124

Stylianou, E., O'Neill, L. A., Rawlinson, L., Edbrooke, M. R., Woo, P., and Saklatvala, J. (1992). Interleukin 1 induces NF-kappaB through its type I but not its type II receptor in lymphocytes. *J. Biol. Chem.* 267, 15836–15841.

Sung, Y. H., Chang, H. K., Kim, S. E., Kim, Y. M., Seo, J. H., Shin, M. C., et al. (2009). Anti-inflammatory and analgesic effects of the aqueous extract of corni fructus in murine RAW 264.7 macrophage cells. *J. Med. Food* 12, 788–795. doi: 10.1089/jmf.2008.1011

Taglialatela, G., Hogan, D., Zhang, W. R., and Dineley, K. T. (2009). Intermediate- and long-term recognition memory deficits in Tg2576 mice are reversed with acute calcineurin inhibition. *Behav. Brain Res.* 200, 95–99. doi: 10.1016/j.bbr.2008.12.034

Tan, M. S., Yu, J. T., Jiang, T., Zhu, X. C., Wang, H. F., Zhang, W., et al. (2013). NLRP3 polymorphisms are associated with late-onset Alzheimer's disease in Han Chinese. *J. Neuroimmunol.* 265, 91–95. doi: 10.1016/j.jneuroim.2013.10.002

Tanaka, S., Ishii, A., Ohtaki, H., Shioda, S., Yoshida, T., and Numazawa, S. (2013). Activation of microglia induces symptoms of Parkinson's disease in wild-type, but not in IL-1 knockout mice. *J. Neuroinflamm.* 10:143. doi: 10.1186/1742-2094-10-143

Tilstra, J. S., Clauson, C. L., Niedernhofer, L. J., and Robbins, P. D. (2011). NF-kappaB in aging and disease. *Aging Dis.* 2, 449–465.

Tremblay, M. E., Stevens, B., Sierra, A., Wake, H., Bessis, A., and Nimmerjahn, A. (2011). The role of microglia in the healthy brain. *J. Neurosci.* 31, 16064–16069. doi: 10.1523/jneurosci.4158-11.2011

Tweedie, D., Ferguson, R. A., Fishman, K., Frankola, K. A., Van Praag, H., Holloway, H. W., et al. (2012). Tumor necrosis factor-alpha synthesis inhibitor 3,6'-dithiothalidomide attenuates markers of inflammation, Alzheimer pathology and behavioral deficits in animal models of neuroinflammation and Alzheimer's disease. *J. Neuroinflamm.* 9:106. doi: 10.1186/1742-2094-9-106

Vallabhapurapu, S., and Karin, M. (2009). Regulation and function of NF-κB transcription factors in the immune system. *Annu. Rev. Immunol.* 27, 693–733. doi: 10.1146/annurev.immunol.021908.132641

Wang, D. S., Zurek, A. A., Lecker, I., Yu, J., Abramian, A. M., Avramescu, S., et al. (2012). Memory deficits induced by inflammation are regulated by alpha5-subunit-containing GABAA receptors. *Cell Rep.* 2, 488–496. doi: 10.1016/j.celrep.2012.08.022

Wee Yong, V. (2010). Inflammation in neurological disorders: a help or a hindrance? *Neuroscientist* 16, 408–420. doi: 10.1177/1073858410371379

Wei, X. L. (2000). [Studies on learning and memory function-related genes in the hippocampus and the relationship between the cognitive enhancing effect of liuwei dihuang decoction (LW) and gene expression]. *Sheng Li Ke Xue Jin Zhan* 31, 227–230.

Wendeln, A. C., Degenhardt, K., Kaurani, L., Gertig, M., Ulas, T., Jain, G., et al. (2018). Innate immune memory in the brain shapes neurological disease hallmarks. *Nature* 556, 332–338. doi: 10.1038/s41586-018-0023-4

Williams-Gray, C. H., Wijeyekoon, R., Yarnall, A. J., Lawson, R. A., Breen, D. P., Evans, J. R., et al. (2016). Serum immune markers and disease progression in an incident Parkinson's disease cohort (ICICLE-PD). *Mov. Disord.* 31, 995–1003. doi: 10.1002/mds.26563

Wolf, A., Bauer, B., Abner, E. L., Ashkenazy-Frolinger, T., and Hartz, A. M. (2016). A comprehensive behavioral test battery to assess learning and memory in 129S6/Tg2576 mice. *PLoS One* 11:e0147733. doi: 10.1371/journal.pone.0147733

Wong, V. W., Rustad, K. C., Akaishi, S., Sorkin, M., Glotzbach, J. P., Januszyk, M., et al. (2011). Focal adhesion kinase links mechanical force to skin fibrosis via inflammatory signaling. *Nat. Med.* 18, 148–152. doi: 10.1038/nm.2574

Yao, L., Kan, E. M., Kaur, C., Dheen, S. T., Hao, A., Lu, J., et al. (2013a). Notch-1 signaling regulates microglia activation via NF-kappaB pathway after hypoxic exposure in vivo and in vitro. *PLoS One* 8:e78439. doi: 10.1371/journal.pone.0078439

Yao, L., Kan, E. M., Lu, J., Hao, A., Dheen, S. T., Kaur, C., et al. (2013b). Toll-like receptor 4 mediates microglial activation and production of inflammatory mediators in neonatal rat brain following hypoxia: role of TLR4 in hypoxic microglia. *J. Neuroinflamm.* 10:23. doi: 10.1186/1742-2094-10-23

Yu, B., Zhang, G., An, Y., and Wang, W. (2018). Morroniside on anti-inflammation activities in rats following acute myocardial infarction. *Korean J. Physiol. Pharmacol.* 22, 17–21. doi: 10.4196/kjpp.2018.22.1.17

Zeisel, M. B., Druet, V. A., Sibilia, J., Klein, J. P., Quesniaux, V., and Wachsmann, D. (2005). Cross talk between MyD88 and focal adhesion kinase pathways. *J. Immunol.* 174, 7393–7397. doi: 10.4049/jimmunol.174.11.7393

Zhang, L., and Wang, C.-C. (2014). Inflammatory response of macrophages in infection. *Hepatob. Pancreatic Dis. Int.* 13, 138–152. doi: 10.1016/S1499-3872(14)60024-2

Conflict of Interest Statement: The authors declare that the research was conducted in the absence of any commercial or financial relationships that could be construed as a potential conflict of interest.

frontiers in Aging Neuroscience

REVIEW
published: 09 July 2018
doi: 10.3389/fnagi.2018.00199

Ca^{2+}, Astrocyte Activation and Calcineurin/NFAT Signaling in Age-Related Neurodegenerative Diseases

Pradoldej Sompol[1] *and Christopher M. Norris*[1,2]*

[1]Sanders-Brown Center on Aging, University of Kentucky College of Medicine, Lexington, KY, United States, [2]Department of Pharmacology and Nutritional Sciences, University of Kentucky College of Medicine, Lexington, KY, United States

Mounting evidence supports a fundamental role for Ca^{2+} dysregulation in astrocyte activation. Though the activated astrocyte phenotype is complex, cell-type targeting approaches have revealed a number of detrimental roles of activated astrocytes involving neuroinflammation, release of synaptotoxic factors and loss of glutamate regulation. Work from our lab and others has suggested that the Ca^{2+}/calmodulin dependent protein phosphatase, calcineurin (CN), provides a critical link between Ca^{2+} dysregulation and the activated astrocyte phenotype. A proteolyzed, hyperactivated form of CN appears at high levels in activated astrocytes in both human tissue and rodent tissue around regions of amyloid and vascular pathology. Similar upregulation of the CN-dependent transcription factor nuclear factor of activated T cells (NFAT4) also appears in activated astrocytes in mouse models of Alzheimer's disease (ADs) and traumatic brain injury (TBI). Major consequences of hyperactivated CN/NFAT4 signaling in astrocytes are neuroinflammation, synapse dysfunction and glutamate dysregulation/excitotoxicity, which will be covered in this review article.

Keywords: Alzheimer's disease, Ca^{2+}, glia, dementia, astrocytes, neuroinflammation, synapse

OPEN ACCESS

Edited by:
Ashok Kumar,
University of Florida, United States

Reviewed by:
Giulio Taglialatela,
University of Texas Medical Branch, United States
Carole Escartin,
UMR9199 Laboratoire de Maladies Neurodégénératives Mécanismes, Thérapies, Imagerie, France

***Correspondence:**
Christopher M. Norris
cnorr2@uky.edu

Received: *03 April 2018*
Accepted: *12 June 2018*
Published: *09 July 2018*

Citation:
Sompol P and Norris CM (2018) Ca^{2+}, Astrocyte Activation and Calcineurin/NFAT Signaling in Age-Related Neurodegenerative Diseases. Front. Aging Neurosci. 10:199. doi: 10.3389/fnagi.2018.00199

INTRODUCTION

The central role of Ca^{2+} dysregulation in age-related memory deficits and neurodegenerative disease, proposed more than 30 years ago (Gibson and Peterson, 1987; Khachaturian, 1987; Landfield, 1987; Abdul et al., 2009), has been supported time and again by molecular, electrophysiological, biochemical and behavioral studies and is the subject of many excellent reviews (Alzheimer's Association Calcium Hypothesis Workgroup, 2017; Frazier et al., 2017; Gibson and Thakkar, 2017; Pchitskaya et al., 2018). Neurons are often the focus of studies on Ca^{2+} dysregulation, and for good reason. Ca^{2+} signaling is an absolutely essential mechanism for both intra- and interneuronal communication. Moreover, disruption of any of the many neuronal Ca^{2+} regulatory checkpoints can lead to the structural deterioration of neurons and neuronal death, which are defining features of most neurodegenerative diseases. Nonetheless, it is becoming increasingly clear that Ca^{2+} dysregulation underlies altered function and viability of other non-neuronal cells during aging and disease, especially astrocytes. Several recent articles have provided comprehensive reviews of Ca^{2+} signaling mechanisms and Ca^{2+} dyregulation in astrocytes as a function of disease (Vardjan et al., 2017; Verkhratsky et al., 2017; Zorec et al., 2018). The following review will instead focus on the protein phosphatase calcineurin (CN) as an

emerging mechanism for linking astrocytic Ca^{2+} dysregulation to neuroinflammation, glutamate dysregulation, amyloid pathology and synaptotoxicity. Particular emphasis will be placed on CN interactions with the nuclear factor of activated T cells (NFATs), though other CN-sensitive transcription factors such as nuclear factor κB (NFκB) and forkhead O3 (FOXO3) will also be considered.

Ca^{2+} DYSREGULATION IN ACTIVATED ASTROCYTES

Astrocytes are abundant and versatile cells that play critical roles in brain metabolism, vascular regulation, interneuronal signaling and defense. Fundamental to many of these duties are Ca^{2+} ions, which are handled by a sophisticated network of plasma membrane channels, Ca^{2+} pumps, Ca^{2+} binding proteins and intracellular stores (for recent comprehensive reviews see; Rusakov, 2015; Bazargani and Attwell, 2016; Shigetomi et al., 2016; Guerra-Gomes et al., 2017). Together, these mechanisms, and others, coordinate dynamic Ca^{2+} responses (e.g., Ca^{2+} waves and sparks) that can be propagated within the confines of individual astrocytes and also across large astrocyte syncytia via interconnecting gap junction channels (De Bock et al., 2014; Zheng et al., 2015; Fujii et al., 2017). The recent application of three-dimensional multiphoton imaging to astrocyte Ca^{2+} transients has highlighted the complexity and heterogeneity of Ca^{2+} signaling within different astrocyte compartments (e.g., soma, processes and endfeet) and perhaps points to an approaching renaissance in our understanding of the role of astrocytes in brain function and disease. Astrocytic Ca^{2+} dysregulation appears to be indelibly linked to morphologic transformations (i.e., astrocyte "activation" or "reactivity") characterized by hypertrophic somata and processes and upregulation of the intermediate filament protein, GFAP (Pekny and Nilsson, 2005; Sofroniew, 2009; Rodríguez-Arellano et al., 2016; Bindocci et al., 2017). Astrocyte activation is triggered by a diverse range of injurious stimuli and is frequently localized to regions of frank pathology (e.g., damaged blood vessels, necrotic tissues and protein aggregates). Along with activated microglia, activated astrocytes provide one of the best neuroanatomical hallmarks of neuroinflammation.

Immunohistochemical studies have revealed the upregulation of numerous Ca^{2+} signaling mediators in activated astrocytes including: Ca^{2+} related proteases (Shields et al., 1998, 2000; Feng et al., 2011), L-type voltage-sensitive Ca^{2+} channels (Xu et al., 2007, 2010; Willis et al., 2010; Daschil et al., 2013; Wang et al., 2015), transient receptor potential vanilloid channels (Shirakawa et al., 2010; Butenko et al., 2012), endoplasmic reticulum Ca^{2+}-release channels and Ca^{2+} pumps (Grolla et al., 2013), Ca^{2+}-dependent K^+ channels (Yi et al., 2016), and Ca^{2+} binding proteins (McAdory et al., 1998). Most extracellular factors that promote robust astrocyte activation *in vivo* (e.g., cytokines, reactive oxygen species, protein aggregates, excitotoxins, . . .etc) also trigger Ca^{2+} dysregulation (e.g., elevated Ca^{2+} levels, augmented Ca^{2+} transients) in primary culture and brain slices (Sama and Norris, 2013). Similar functional indices of Ca^{2+} dysregulation have been noted in animal models of AD (Takano et al., 2007; Kuchibhotla et al., 2009; Delekate et al., 2014), brain edema (Thrane et al., 2011), stroke (Ding et al., 2009; Rakers and Petzold, 2017) and epilepsy (Ding et al., 2007; Tian et al., 2010). The relationship between Ca^{2+} dysregulation and astrocyte activation is very likely to be bi-directional in nature. Indeed, Ca^{2+} modulates the activity of numerous transcription factor pathways (Mellstrom et al., 2008), several of which (e.g., NFκB, JAK/STAT, FOX proteins, peroxisome proliferator-activated receptors (PPARs) and activator protein-1 (AP-1), among others) have been implicated in shaping gene expression programs involved in astrocyte activation (Perez-Nievas and Serrano-Pozo, 2018). So, once astrocytic Ca^{2+} dysregulation is set in motion by injurious and/or neuroinflammatory factors, there are multiple routes through which Ca^{2+} could maintain astrocytes in an activated state. Perhaps the most direct link between Ca^{2+} and the gene regulatory machinery in astrocytes (and most other cell types) is provided by NFAT transcription factors, which are directly activated by the Ca^{2+}-dependent protein phosphatase, CN. Mounting evidence, discussed below, shows that CN/NFATs exhibit clear signs of hyperactivation, and/or increased expression, in subsets of activated astrocytes, while cell-specific targeting approaches suggest that CN/NFAT signaling drives or exacerbates multiple forms of neuropathology.

CN DYSREGULATION AND NEURODEGENERATIVE DISEASE

CN is a highly abundant protein found throughout the brain, appearing at high levels in neurons and low levels in glia in healthy adult animals (Goto et al., 1986a,b; Polli et al., 1991; Kuno et al., 1992). Hyperactive CN signaling is observed in human postmortem brain tissue at early stages of cognitive decline associated with AD, ramping up in later disease stages in parallel with worsening amyloid pathology, neurofibrillary pathology and/or cognitive decline (Liu et al., 2005; Abdul et al., 2009; Wu et al., 2010; Mohmmad Abdul et al., 2011; Qian et al., 2011; Watanabe et al., 2015; Pleiss et al., 2016b). Other human neurodegenerative conditions associated with increased CN signaling include Parkinson's disease (Caraveo et al., 2014), dementia with Lewy bodies (Martin et al., 2012; Caraveo et al., 2014) and vascular pathology (Pleiss et al., 2016b). Similar changes are often recapitulated to a significant degree in corresponding animal models of aging and neurodegeneration (Foster et al., 2001; Huang et al., 2005; Norris et al., 2005; Shioda et al., 2006; Reese et al., 2008; Mukherjee et al., 2010; Wu et al., 2010; D'Amelio et al., 2011; Martin et al., 2012; Rosenkranz et al., 2012; Furman et al., 2016; Sompol et al., 2017). Moreover, inhibition of CN signaling with the commercial immunosuppressant drugs, tacrolimus and cyclosporine, commonly imparts neuroprotection in experimental models of injury and disease (Kuchibhotla et al., 2008; Wu et al., 2010; Rozkalne et al., 2011; O'Donnell et al., 2016; Xiong et al., 2018), reduces neuroinflammation (Yoshiyama et al., 2007; Rojanathammanee et al., 2015;

Fields et al., 2016; Manocha et al., 2017a; Shah et al., 2017), improves synapse function (Chen et al., 2002; Dineley et al., 2010; Cavallucci et al., 2013; Kim et al., 2015), inhibits cognitive loss (Taglialatela et al., 2009; Dineley et al., 2010; Kumar and Singh, 2017; Liu et al., 2017), and may even extend lifespan (Yoshiyama et al., 2007). Consistent with the animal literature, an epidemiological investigation found that daily tacrolimus use reduced the risk of dementia in kidney transplant patients relative to age-matched healthy individuals in the general population (Taglialatela et al., 2015).

The CN holoenzyme consists of a catalytic subunit and a Ca^{2+}-binding regulatory subunit (Norris, 2014). The catalytic subunit contains a critical autoinhibitory domain (AID) and a calmodulin binding site. Ca^{2+}/calmodulin binding to CN is the primary stimulus for driving maximal CN phosphatase activity (**Figure 1**). When cellular Ca^{2+} levels are low, the AID masks the catalytic core and maintains CN in an inactive state. Cooperative binding of Ca^{2+} to the CN regulatory subunit and to calmodulin lead to the rapid displacement of the AID and robust activation of CN. When Ca^{2+} levels fall, Ca^{2+}/calmodulin rapidly dissociates from CN, reinstating inhibition by the AID. CN is highly sensitive to Ca^{2+}, with a Kd to Ca^{2+}-saturated calmodulin in the picomolar range (Quintana et al., 2005). Thus, even small perturbations in cellular Ca^{2+} can lead to hyperactivation of CN. Under these conditions, CN activity can still be normalized if Ca^{2+} levels recover. However, large surges in Ca^{2+} can trigger the calpain-mediated proteolytic removal or disruption of the CN AID. Without the AID, CN becomes partially (but permanently) uncoupled from local Ca^{2+} changes and exhibits constitutively high levels of activity (i.e., in the presence or absence of Ca^{2+}). Appearance of the CN proteolytic fragment (ΔCN) is one of the most clear-cut indicators of hyperactive CN signaling (**Figure 1**). Many commercial CN antibodies (directed to the CN carboxyl terminus) do not detect ΔCN in Western blot applications, which may explain why earlier studies failed to observe elevated CN in neurodegenerative conditions like AD (Gong et al., 1993; Ladner et al., 1996; Lian et al., 2001). In contrast, more recent work (using N terminus antibodies) has found that ΔCN is increased in human AD tissue (Liu et al., 2005; Wu et al., 2010; Mohmmad Abdul et al., 2011; Watanabe et al., 2015), in parallel with calpain activation (Liu et al., 2005; Mohmmad Abdul et al., 2011). The ΔCN fragment has been reported in numerous other experimental models of brain injury and disease including traumatic brain injury (TBI), ischemia and glaucoma (Norris, 2014).

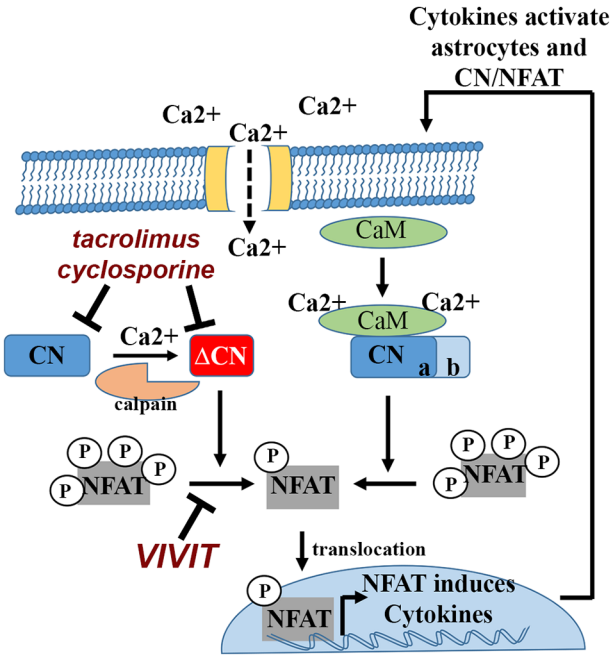

FIGURE 1 | Calcineurin (CN)/nuclear factor of activated T cells (NFATs) signaling in astrocytes and bidirectional interactions with cytokines. Cytokines and other inflammatory factors lead to Ca^{2+} elevations in astrocytes. Ca^{2+} binds to calmodulin (CaM), which in turn, binds to and activates CN. CN dephosphorylates NFAT transcription factors, leading to nuclear translocation and induction of cytokine genes. CN activity can be inhibited using the commercially available immunosuppressants, tacrolimus and cyclosporine. Physical interactions between CN and NFATs can be blocked using peptide based reagents like VIVIT. Many cytokines that are induced by the CN/NFAT pathway can stimulate astrocytes in an autocrine or paracrine manner, triggering elevations in intracellular Ca^{2+}, which can lead to further CN activation. Severe Ca^{2+} dysregulation can convert CN into a constitutively active proteolytic fragment (ΔCN) via calpain dependent proteolysis. Hyperactivation of CN/NFAT maintains chronic neuroinflammation (and astrocyte activation) through continued induction (i.e., a positive feedback loop) of pro-inflammatory cytokine genes.

CN EXPRESSION IS INCREASED IN ACTIVATED ASTROCYTES IN HUMANS AND ANIMAL MODELS

Cell-specific expression patterns of CN in both humans and animal models can exhibit striking changes characterized by intense upregulation in subsets of activated astrocytes (Hashimoto et al., 1998; Celsi et al., 2007; Abdul et al., 2009; Lim et al., 2013; Liu et al., 2015; Watanabe et al., 2015; Pleiss et al., 2016b; Sompol et al., 2017). Recent work using custom antibodies generated toward calpain-dependent proteolysis sites in the CN catalytic subunit, observed extensive labeling for a 45–48 kDa ΔCN proteolytic fragment in astrocytes and, to a seemingly lesser extent, neurons (Pleiss et al., 2016b). ΔCN was especially prominent in activated astrocytes bordering amyloid deposits and microinfarcts in human specimens (Pleiss et al., 2016b). Interestingly, ΔCN-positive and ΔCN-negative astrocytes were often found in the same regions (sometimes side-by-side) and appeared morphologically similar, highlighting the biochemical heterogeneity of activated astrocytes. In an aggressive mouse model of AD (i.e., 5xFAD mice), ΔCN was similarly observed in activated astrocytes in the hippocampus, increasing in direct proportion to elevated GFAP levels (Sompol et al., 2017). These observations are consistent with previous reports that found high levels of calpain activity in activated astrocytes (Shields et al., 1998, 2000; Feng et al., 2011) and suggest that Ca^{2+} dependent proteolysis of CN is a major outcome of astrocytic Ca^{2+} dysregulation.

NFATs

There are five primary NFAT family members: NFAT1 (or NFATp, NFATc2), NFAT2 (or NFATc, NFATc1), NFAT3 (or NFATc4), NFAT4 (or NFATc3) and NFAT5, all of which exhibit DNA-binding domains that are structurally similar to the Rel/NFκB family of transcription factors (Rao et al., 1997). Elevations in Ca^{2+} activate CN, which binds to and dephosphorylates NFATs 1–4 in the cytosol (**Figure 1**). NFAT5 is activated by osmotic stress and does not interact with CN. Dephosphorylation of NFATs exposes a nuclear localization signal, leading to transport into the nucleus and interaction with specific DNA binding elements. Similar to CN, NFAT activation is typically elevated under neurodegenerative conditions like AD (Abdul et al., 2009; Wu et al., 2010), Parkinson's disease (Caraveo et al., 2014), and acute brain injury (Serrano-Pérez et al., 2011; Furman et al., 2016). As with other previously mentioned transcription factors (e.g., NFkB, JAK-STAT, AP-1,. . .etc), NFATs exert broad control over several transcriptional programs via the up- and downregulation of numerous genes, many of which involve cytokines and other classic inflammatory mediators (Im and Rao, 2004; **Figure 1**). NFATs are very strongly inhibited by the CN-inhibiting drugs tacrolimus and cyclosporine, but can be specifically targeted by a variety of peptide-based reagents. The VIVIT peptide, based on the endogenous CN docking sequence (PxIxIT) located in the N terminus of the regulatory region of NFATs 1–4, prevents CN from binding to and dephosphorylating NFATs (Aramburu et al., 1999). Thus, unlike commercial CN inhibitors, VIVIT impairs CN-mediated activation of NFATs without inhibiting CN activity *per se*, providing a powerful reagent for teasing apart NFAT-dependent signaling from the broader NFAT-independent actions of CN (**Figure 1**).

In peripheral tissues, NFATs play key roles in phenotype switching. Activation/anergy of T lymphocytes (Hogan, 2017), myotube formation and fiber-type commitment (Horsley and Pavlath, 2002; McCullagh et al., 2004; Rana et al., 2008), cardiomyocyte hypertrophy (Molkentin, 2004), vascular smooth muscle cell migration and proliferation (Liu et al., 2004; Karpurapu et al., 2010; Kundumani-Sridharan et al., 2013), and bone and joint remodeling (Sitara and Aliprantis, 2010) all depend critically on the NFAT pathway. Though not as extensively investigated in the CNS, several studies suggest that NFATs play a key role in the activation of astrocytes and microglia, as well (Nagamoto-Combs and Combs, 2010; Furman and Norris, 2014). All four CN-dependent NFATs have been identified in primary astrocytes at the mRNA and protein levels (Canellada et al., 2008). NFAT1 was found at higher levels in astrocyte nuclei in postmortem brain sections taken from human subjects with mild cognitive impairment (Abdul et al., 2009). NFAT1 has also been identified in microglia of AD mouse models (Manocha et al., 2017b). However, relative to all other NFAT isoforms, NFAT4 appears to show the greatest association with astrocytes in intact animals, with comparatively much less expression in neurons (Filosa et al., 2007; Serrano-Pérez et al., 2011; Neria et al., 2013; Caraveo et al., 2014; Yan et al., 2014; Furman et al., 2016; Sompol et al., 2017). While one study observed a reduction in NFAT4 protein levels in rats exposed to TBI (Yan et al., 2014), several other studies found that NFAT4 is strongly induced in activated astrocytes as a result of acute injury or progressive amyloid or synuclein pathology (Serrano-Pérez et al., 2011; Neria et al., 2013; Caraveo et al., 2014; Furman et al., 2016; Sompol et al., 2017).

GLIAL CN/NFAT PATHWAY AND NEUROINFLAMMATORY SIGNALING

Similar to actions in lymphocytes, glial CN/NFAT activity appears to play a critical role in regulating immune/inflammatory responses. In primary astrocytes and microglia, the CN/NFAT pathway is robustly activated by many key inflammatory mediators, including cytokines, Aβ, glutamate and vascular injury-associated factors (Fernandez et al., 2007; Canellada et al., 2008; Pérez-Ortiz et al., 2008; Sama et al., 2008; Abdul et al., 2009; Furman et al., 2010; Nagamoto-Combs and Combs, 2010; Rojanathammanee et al., 2015). Little is known about the Ca^{2+} sources that are responsible for glial CN activation but L-type voltage sensitive Ca^{2+} channels have been specifically implicated in astrocytes (Canellada et al., 2008; Sama et al., 2008). Overexpression of the hyperactive ΔCN fragment in astrocytes leads to the upregulation of numerous immune/inflammatory related genes (Norris et al., 2005; Fernandez et al., 2007) and functional gene categories linked to the activated astrocyte phenotype (i.e., morphogenesis, cell adhesion and immune response; Norris et al., 2005). Interestingly, many of the genes identified in Norris et al. (2005) are part of the A1 "neurotoxic" astrocyte transcriptional signature described by the Barres lab (Zamanian et al., 2012; Liddelow et al., 2017). Of note, ΔCN triggered a two-to-three fold increase in the A1-associated complement component C3, found recently to drive microglia-mediated synapse loss in mouse models of AD (Hong et al., 2016; Shi et al., 2017). In addition to CN-activation studies, inhibitory approaches in primary cultures have revealed similar roles for CN/NFATs in neuroinflammation. Immune/inflammatory factors sensitive to CN/NFAT inhibition in glial cells include TNFα, GM-CSF, IL-6, CCL2 and Cox2, among others (Canellada et al., 2008; Sama et al., 2008; Nagamoto-Combs and Combs, 2010; Kim et al., 2011; Watanabe et al., 2015; Manocha et al., 2017b).

Bidirectional interactions between CN/NFAT and cytokine factors suggest that the CN/NFAT pathway is ideally suited to maintain positive feedback cycles underlying chronic neuroinflammation (Griffin et al., 1998; **Figure 1**). Consistent with this possibility, hyperactive CN/NFAT activity has been shown to propagate across local astrocyte networks through a paracrine signaling mechanism (Sama et al., 2008). A significant question remains about the mechanisms that keep these feedback cycles in check. One possibility is that CN/NFAT activity is limited by the expression of endogenous CN inhibitors. Regulator of CN 1 (RCAN1), for instance, is strongly induced by NFAT activity in multiple cell types

including astrocytes (Canellada et al., 2008; Sobrado et al., 2012). RCANs are widely considered as CN inhibitors, though, it deserves noting that several studies have revealed permissive effects of RCAN on CN, depending on the presence of key accessory proteins (Liu et al., 2009). Whether RCANs provide a negative feedback mechanism for guarding against progressive Ca^{2+} dysregulation and neuroinflammation in astrocytes, in the context of neurodegeneration, will require further investigation.

Finally, caution should be taken when interpreting immune/inflammatory actions of CN/NFATs in primary glia which are very sensitive to culturing conditions. When investigated in serum-containing media, primary astrocytes may exhibit a quasi-activated state characterized by elevated basal levels of CN/NFAT activity (Furman et al., 2010). Indeed, addition of standard (10% fetal calf) serum alone induces robust CN/NFAT activity in primary astrocytes previously maintained in serum-free media (Furman et al., 2010). Moreover, treatment with IL1-β, IF-γ, or TNFα, which strongly induce NFAT activity in the absence of sera, elicited significantly muted responses when delivered in the presence of sera. Similar caution is also warranted in studies on intact animals, where the effects of CN/NFAT inhibition may have very different effects on glial activity and neuroinflammation, depending on the nature of the insult. For instance, intracerebroventricular delivery of the VIVIT peptide, or astrocyte-specific expression of VIVIT using adeno-associated virus (AAV), reduced signs of astrocyte and microglial activation in mouse models of AD characterized by progressive amyloid pathology (Abdul et al., 2010; Furman et al., 2012; Rojanathammanee et al., 2015; Sompol et al., 2017), but not in a rat model of TBI characterized by acute trauma (Furman et al., 2016). The reason for these discrepancies is unclear, but could involve CN/NFAT interactions with multiple other transcription factors and signaling pathways (as discussed further below). In any case, the results highlight the importance of context in understanding astrocytic CN/NFAT signaling.

ASTROCYTIC CN/NFAT PATHWAY IN GLUTAMATE DYSREGULATION

Mounting evidence suggest that activated astrocytes may lose protective glutamate buffering properties in some forms of injury and disease. Astrocytes control extracellular glutamate levels, in part, through the use of several excitatory amino acid transporters (EAATs) located in the astrocyte plasmalemma. The EAAT2/GLT-1 protein is responsible for the bulk of glutamate uptake in several brain regions, including hippocampus (Robinson and Jackson, 2016). Loss of EAAT2 has been observed in several human neurodegenerative conditions including AD (Masliah et al., 1996; Abdul et al., 2009; Simpson et al., 2010), Alexander disease (Tian et al., 2010), epilepsy with hippocampal sclerosis (Mathern et al., 1999; Proper et al., 2002), and TBI (van Landeghem et al., 2006). Similar changes have been reported in corresponding animal models (Masliah et al., 2000; Mookherjee et al., 2011; Schallier et al., 2011; Hefendehl et al., 2016; Sompol et al., 2017). Functional knockdown of EAAT2/GLT-1 very typically causes synaptic hyperexcitability, altered synaptic plasticity, excitotoxicity and a variety of functional deficits depending on the brain region affected (Rothstein et al., 1996; Rao et al., 2001; Selkirk et al., 2005; Petr et al., 2015; Moidunny et al., 2016). In contrast, increased expression/function of EAAT2/GLT-1 provides strong neuroprotection from exogenously delivered excitotoxins as well as from acute and chronic CNS injury and disease (Harvey et al., 2011; Rozkalne et al., 2011; Zumkehr et al., 2015; Karklin Fontana et al., 2016).

The human EAAT2 promoter has putative binding sites for numerous transcription factors linked to neuroinflammation, including NFATs (Kim et al., 2003; Su et al., 2003; Mallolas et al., 2006), and is activated (and in some cases, inhibited) by a number of cytokine factors. Several studies suggest that the CN/NFAT pathway provides a putative link between Ca^{2+} dysregulation, neuroinflammation and glutamate dysregulation in activated astrocytes through modulation of EAAT/GLT-1 expression. Recent work found that overexpression of the ΔCN fragment significantly reduced EAAT-mediated glutamate uptake in primary astrocytes (Sompol et al., 2017). In contrast, inhibition of CN/NFAT activity with the VIVIT peptide protected EAAT2-GLT-1 protein levels and reduced extracellular glutamate and/or neuronal hyperexcitability in primary cultures following treatment with either IL1-β or oligomeric Aβ (Sama et al., 2008; Abdul et al., 2009). Under the same treatment conditions, significantly greater neuronal survival was observed when astrocytic CN/NFAT activity was inhibited with VIVIT. Similar effects were found following VIVIT treatment in an intact mouse model of AD (Sompol et al., 2017). Specifically, VIVIT increased protein levels of the astrocytic glutamate transporter, GLT-1, especially around Aβ deposits, and reduced the frequency and duration of spontaneous glutamate transients in intact 5xFAD mice. VIVIT also quelled hyperactive synaptic transients in *in situ* brain slices from 5xFAD mice and reduced the augmented NMDA receptor-mediated component of basal synaptic transmission. The reduction in glutamate hyperexcitability in 5xFAD mice was accompanied by the normalization of dendrite morphology and integrity, suggesting that astrocyte activation and astrocytic CN/NFAT signaling can drive excitotoxic damage in some disease states, like AD.

ASTROCYTIC CN/NFAT PATHWAY IN AMYLOID PATHOLOGY

Amyloid pathology has long been recognized as a potent stimulus for CN and/or NFAT activity in multiple neural cell types (Agostinho et al., 2008; Reese et al., 2008; Abdul et al., 2009; Li et al., 2010; Wu et al., 2010, 2012; Mohmmad Abdul et al., 2011; Fang et al., 2016). Mice with parenchymal amyloid pathology show clear Ca^{2+} dysregulation in astrocytes: i.e., higher basal Ca^{2+} levels and bigger and more frequent Ca^{2+} transients (Kuchibhotla et al., 2009), providing a permissive environment for CN/NFAT activity. In human postmortem tissue, elevations

in CN/NFAT activity increase in direct proportion with soluble Aβ levels, within the same subjects (Abdul et al., 2009). In primary neuron/astrocyte cultures, Aβ stimulates CN/NFAT activity and generates ΔCN proteolytic fragments (Mohmmad Abdul et al., 2011). Moreover, CN/ΔCN is found at especially high levels in activated astrocytes surrounding amyloid deposits in both mouse and human tissue (Norris et al., 2005; Celsi et al., 2007; Abdul et al., 2009; Jin et al., 2012; Lim et al., 2013; Watanabe et al., 2015; Pleiss et al., 2016b).

In addition to responding to Aβ, several studies have suggested that astrocytic CN/NFAT activity stimulates the generation of Aβ peptides (Hong et al., 2010; Furman et al., 2012; Jin et al., 2012; Sompol et al., 2017). Peripheral administration of the CN inhibitor, tacrolimus, to 8-month-old APP/PS1 transgenic mice over a period of 2 months led to a large (>75%) significant reduction in amyloid plaque burden in both the hippocampus and cortex (Hong et al., 2010). A smaller (20%–30%), but statistically significant decrease in amyloid plaque load and soluble Aβ peptide levels was also observed when CN/NFAT activity was specifically inhibited in hippocampal astrocytes of 2x and 5xAPP/PS1 mice using AAV-mediated delivery of VIVIT (Furman et al., 2012; Sompol et al., 2017). Though reductions in Aβ could have simply stemmed from the increased viability of neurons in tacrolimus/VIVIT treated mice, an additional report by Sompol et al. (2017) demonstrated that Ca^{2+} overload can lead to elevated Aβ production—specifically within astrocytes—through a CN/NFAT4-dependent mechanism. In this study, NFAT4 was shown to bind to the promoter of BACE1 (the rate limiting enzyme for Aβ generation) and induce BACE1 transcription. These results suggest that astrocytic CN/NFATs may help to drive parenchymal Aβ plaque pathology in AD. Given the intimate association between astrocytes and the cerebrovasculature, it would be interesting to determine if astrocytic CN/NFATs play a particularly important role in cerebral amyloid angiopathy.

ASTROCYTIC CN/NFAT PATHWAY IN SYNAPSE DYSFUNCTION

As discussed, commercial CN inhibitors are commonly associated with neuroprotective, anti-inflammatory and nootropic properties across a wide-range of experimental models of neural injury and disease. Within our lab, synaptoprotection has emerged as the single most consistent functional outcome of inhibiting CN/NFAT activity in astrocytes. To inhibit CN/NFATs, we have relied heavily on AAV vectors expressing the NFAT inhibitor, VIVIT, under the control of the human GFAP promoter (Gfa2). Delivery of AAVGfa2-VIVIT to the hippocampus of adult rodents results in widespread, astrocyte-selective transgene expression, coincident with the inhibition of NFAT4 nuclear translocation (Furman et al., 2012, 2016; Sompol et al., 2017). AAV-Gfa2-VIVIT improves basal hippocampal synaptic strength in double transgenic APP/PS1 transgenic mice (Furman et al., 2012), 5xFAD mice (Sompol et al., 2017), rats with TBI (Furman et al., 2016), and mice with hyperhomocysteinemia (HHcy)-associated vascular pathology (Pleiss et al., 2016a). In regards to synaptic plasticity, AAV-Gfa2-VIVIT improves long-term potentiation (LTP) in double transgenic APP/PS1 mice (Furman et al., 2012) and suppresses the induction of long-term depression in TBI rats (Furman et al., 2016). Investigations on LTP in HHcy mice have shown very similar outcomes. In contrast, hyperactivation of CN in astrocytes of otherwise healthy adult rats, using AAV-Gfa delivery of the ΔCN fragment, induces local deficits in CA3-CA1 synaptic strength (Pleiss et al., 2016b). Though not investigated in every study, we have also found that delivery of AAV-Gfa2-VIVIT to hippocampal astrocytes of AD mouse models improves hippocampal-dependent cognition (Furman et al., 2012; Sompol et al., 2017).

It is presently unclear how or why astrocytic CN/NFAT signaling negatively affects synapses. Many of the CN-dependent cytokines released from astrocytes are known to disrupt synaptic viability under certain conditions. In fact, several cytokine-inhibiting drugs appear to have remarkably similar effects to astrocyte-VIVIT treatment in AD mouse models (Kotilinek et al., 2008; Bachstetter et al., 2012; MacPherson et al., 2017). In addition, CN-dependent TGF-β release from astrocytes was recently found to suppress PSD-95 levels in nearby neurons (Tapella et al., 2018). In addition to cytokines, gene microarray studies in primary cells and protein measurements in TBI rats suggest that CN/NFATs drive the induction of factors involved in synapse turnover and/or remodeling, including complement cascade components (e.g., C3) and matricellular factors (e.g., SPARC and hevin; Norris et al., 2005; Furman et al., 2016). As mentioned, C3 was recently identified as a key component of the "neurotoxic" A1 activated astrocyte phenotype (Liddelow et al., 2017). During development, C3 release from astrocytes tags synapses for microglia-mediated phagocytosis, leading to synapse removal/remodeling (Stevens et al., 2007). C3 levels drop during maturation, but then reappear under pathological conditions, like AD (Eikelenboom and Veerhuis, 1996; Zabel and Kirsch, 2013). Recent work found that C3 upregulation in activated astrocytes in an APP/PS1 mouse model of AD guides microglia-mediated synapse loss, similar to that observed during development (Lian et al., 2015; Hong et al., 2016; Shi et al., 2017). In the Lian et al.'s (2015) study, C3 induction in astrocytes was attributable to the activation of NFκB (which can be activated by CN, see below), though a role for NFAT was not investigated. The matricellular proteins SPARC and hevin are also developmentally regulated factors that become induced in activated astrocytes in mature brain following injury and/or disease (Jones and Bouvier, 2014; Blakely et al., 2015; Furman et al., 2016). These factors regulate adhesion and de-adhesion of astrocytes with the extracellular matrix where they influence interactions with the vasculature, with other astrocytes, and also with neurons, especially at synapses, leading to synaptogenesis and re-modeling (Jones et al., 2011; Kucukdereli et al., 2011; Jones and Bouvier, 2014; Blakely et al., 2015). Hevin, a pro-synaptogenic factor,

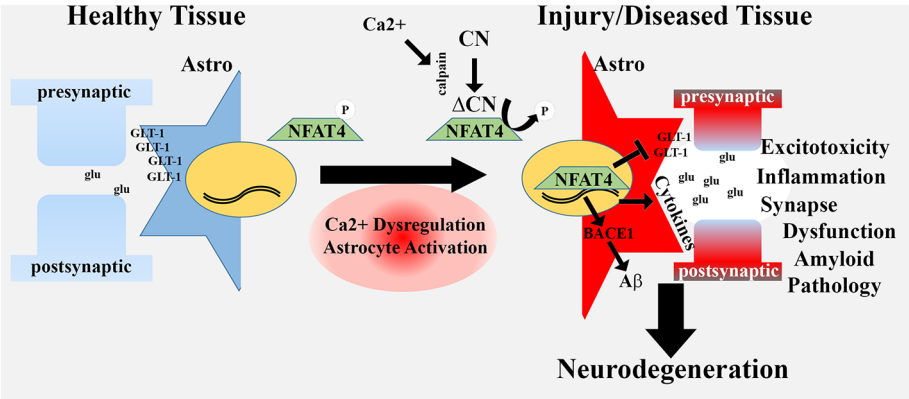

FIGURE 2 | Hyperactivated CN/NFAT signaling in astrocytes may give rise to a neurotoxic astrocyte phenotype. In healthy tissue, astrocytes fine-tune synaptic communication and protect neuronal viability through numerous mechanisms, including uptake of excitotoxic glutamate (glu) at synapses, via GLT-1 transporters. During aging, injury and disease, many astrocytes exhibit an activated phenotype that includes Ca^{2+} dysregulation, proteolysis of CN to a high activity fragment (ΔCN) and induction of the NFAT4 isoform. Hyperactivation of NFAT4 leads to the downregulation of GLT-1, production and release of numerous pro-inflammatory cytokines, and induction of BACE1. These changes underlie a neurotoxic astrocyte phenotype associated with glutamate dysregulation/excitotoxicity, neuroinflammation, synapse dysfunction and amyloid pathology. Neurotoxic astrocytes contribute to or hasten neurodegenerative processes leading to dementia.

is very strongly induced in TBI rats treated with AAV-Gfa2-VIVIT, suggesting that activated astrocytes and hyperactive CN/NFAT signaling inhibit the formation of new synapses by suppressing hevin levels, at least in the context of acute neural injury (Furman et al., 2016). Finally, it seems likely that glutamate dysregulation and Aβ pathology play a significant and non-specific role in synapse dysfunction. Indeed, synapses are very sensitive to excitotoxic insults and circulating oligomeric Aβ peptide levels. By contributing to glutamate dysregulation and amyloid toxicity, activated astrocytes and hyperactive CN/NFAT signaling may simply promote an inhospitable working environment for synapses. Of course, all of these mechanisms could be working in concert as part of a broader neurotoxic astrocyte phenotype, with Ca^{2+} dysregulation and hyperactive CN/NFAT4 activity as central driving features (**Figure 2**).

NON-NFAT TARGETS OF CN IN ASTROCYTES AND CURRENT CONTROVERSIES

NFATs may be the most studied, but they are certainly not the only substrates for CN. In fact, CN has been shown to interact with most transcription factors involved in immune/inflammatory signaling. NFκB, for instance, is strongly regulated by CN activity, though in a fairly indirect manner. CN does not appear to physically bind to or dephosphorylate NFκB, but instead interacts with upstream targets that drive NFκB activation (Pons and Torres-Aleman, 2000; Frischbutter et al., 2011; Palkowitsch et al., 2011). CN-dependent activation of NFκB in astrocytes has been shown to modulate the expression of immune/inflammatory genes (Fernandez et al., 2007) and genes involved in Ca^{2+} signaling and homeostasis (e.g., mGluR5 type glutamate receptors and inositol triphosphate (IP3)-dependent Ca^{2+} release channels; Lim et al., 2013). IP3-receptors play an important role in regulating intracellular Ca^{2+} transients and waves in astrocytes (Filosa et al., 2004; Wu et al., 2017) and have been suggested to mediate neurotoxic actions of activated astrocytes in Alexander disease (Saito et al., 2018). CN/NFκB-dependent upregulation of mGluR5 and IP3 receptors occurs in direct response to pathogenic Aβ peptides and provides an intriguing CN-based mechanism for driving astrocytic Ca^{2+} dysregulation in AD mouse models (Kuchibhotla et al., 2009).

In addition to NFATs and NFκB, recent work suggests that CN can exert transcriptional control in astrocytes through novel interactions with the forkhead transcription factor, FOX03 (Fernandez et al., 2012, 2016). Proinflammatory cytokines, like TNFα, or Aβ peptides, stimulated the physical association between CN and FOX03, leading to dephosphorylation of FOXO3 and association with NFκB. The CN/FOX03/NFκB complex is thought to drive gene programs underlying deleterious neuro-immune/inflammatory signaling. Using an approach similar to the VIVIT strategy for inhibiting CN-NFAT interactions, Fernandez et al. (2016) developed a mimetic peptide that selectively disrupts CN-FOXO3 interactions. When delivered to primary astrocytes the CN-FOX03 interfering peptide reduced Aβ production and reduced the expression of pro-inflammatory cytokines. Interestingly, treatment of astrocytes with the neurotrophic factor, insulin like growth factor 1 (IGF-1), inhibited CN/FOX03/NFκB interactions and instead promoted the association of CN with NFκB and the peroxisome proliferator-activated receptor-γ (PPAR-γ). Formation of the CN/PPAR-γ/NFκB complex in astrocytes was associated with reduced amyloid pathology and improved cognitive function in an AD mouse model (Fernandez et al., 2012). These results suggest that CN activation in astrocytes can drive either deleterious or protective processes depending

on which transcription factors are engaged. This work is consistent with other studies that find both beneficial and detrimental actions of activated astrocytes in disease models (Pekny and Pekna, 2014; Pekny et al., 2016). Moreover, there is good precedence for divergent actions of CN on gene expression programs in other non-neural cell types. For instance, CN activation in T lymphocytes can drive or inhibit expression of immune/inflammatory factors by interacting with different transcription factors in different T cell subtypes or in response to changing environmental conditions (Im and Rao, 2004; Wu et al., 2006).

Interestingly, overexpression of a ΔCN proteolytic fragment in astrocytes using a GFAP promoter was shown to have similar effects as IGF-1 stimulation, yielding beneficial effects in an AD mouse model, and in mice exposed to acute stab wound or LPS insult (Fernandez et al., 2007, 2012). The mechanisms of ΔCN's beneficial effects are unclear. It is unknown whether ΔCN interacts with the PPARγ/NFκB complex, or if ΔCN opposes the interaction of NFκB with FOXO3, or if NFATs are involved in any of these pathways. The beneficial effects of ΔCN from the Fernandez et al. (2007, 2012) studies are especially unusual as this fragment is largely uncoupled from its normal mode of regulation (Ca^{2+}/calmodulin) and is most commonly associated with cellular dysfunction and cell death in many different cell types, though there are some rare exceptions e.g., (Bousette et al., 2010). These results are also in apparent contrast to recent work showing that ΔCN expression in healthy rats drives (rather than prevents) local synapse dysfunction (Pleiss et al., 2016b). An alternative possibility for ΔCN-mediated neuroprotection in the Fernandez et al. (2007, 2012) studies may relate to an interaction between existing brain pathology and the over-expression system used (i.e., genetically modified ΔCN under the control of a GFAP promoter). Preexisting injury or amyloid pathology may be expected to strongly induce the GFAP promoter, leading to the intense upregulation of ΔCN in target cells, which could, possibly, lead to the death/deterioration of the most reactive and/or the most harmful astrocytes. Loss of harmful astrocytes may ultimately improve the viability of nearby neurons. Clearly, further research will be necessary to test this possibility.

Finally, CN is a versatile enzyme with numerous functions that are independent of transcriptional regulation. Nonetheless, very few non-transcription factor substrates of CN have been investigated in astrocytes. In most cases, CN's interactions with other targets has been implied based on sensitivity to commercial CN inhibitors. For instance, tacrolimus and cyclosporine partially blocked the dephosphorylation of GFAP and vimentin in primary astrocytes and in brain slices from neonatal rat pups (Vinadé et al., 1997; Carvalho et al., 2016), suggesting that CN may regulate astrocyte morphology through a posttranscriptional mechanism. These results are reminiscent of studies in neurons, where CN has been long-known to regulate rapid cytoskeletal reorganization in dendritic spines and growth cones (Halpain et al., 1998; Wen et al., 2004). Given the dynamic nature of astrocyte processes and endfeet, it seems likely that CN would play a similar role in cytoskeletal reorganization in astrocytes. In addition to intermediate filaments, the astrocyte hemichannel protein, connexin 43, has also been revealed as a potential CN substrate (Li and Nagy, 2000; Tence et al., 2012). The cytoplasmic tail of connexin 43 is dephosphorylated in a tacrolimus/cyclosporine sensitive manner during hypoxic/ischemic insults. Interestingly, this dephosphorylation was associated with reduced gap junction coupling, which could have important implications for potassium and glutamate buffering during neural injury and disease. And, as with many other cell types, mitochondria function in astrocytes appears to be very sensitive to tacrolimus/cyclosporine (Kahraman et al., 2011; O'Donnell et al., 2016), though, it should be noted that cyclosporine can inhibit formation of the mitochondrial transition pore in a CN-independent manner (Halestrap et al., 1997). In one recent study, both tacrolimus and cyclosporine prevented the loss of mitochondria from astrocyte processes during hypoxic/ischemic insult (O'Donnell et al., 2016). However, it remains unclear how CN specifically contributed to this loss.

SUMMARY

Mounting evidence suggests that the CN/NFAT pathway links astrocytic Ca^{2+} dysregulation to molecular and phenotypic changes involved with neuroinflammation, glutamate dysregulation, amyloid pathology and synapse dysfunction. We hypothesize that the increased expression and/or hyperactivation of CN/NFAT in activated astrocytes—found in human neurodegenerative disease and animal models of disease—plays a predominantly deleterious role in the brain, arising early in neurodegenerative diseases, like AD, and progressing as disease symptoms worsen (**Figure 2**). The numerous beneficial effects reported in disease models treated with CN and/or NFAT inhibitors is largely consistent with this hypothesis. These observations provide a very important extension and/or reconceptualization of the Ca^{2+} hypothesis of aging and disease to include glial Ca^{2+} dyshomeostasis and altered CN signaling as a critical component in the initiation and progression of neurodegeneration. Further work will be needed to tease apart the actions of CN on different transcriptional pathways and how these pathways interact to modulate neural function in healthy and diseased brain.

AUTHOR CONTRIBUTIONS

PS and CN researched and wrote this manuscript.

FUNDING

This work was supported by National Institutes of Health Grants AG027297, AG051945 and AG056998 and a gift from the Hazel Embry Research Trust.

REFERENCES

Abdul, H. M., Furman, J. L., Sama, M. A., Mathis, D. M., and Norris, C. M. (2010). NFATs and Alzheimer's disease. *Mol. Cell. Pharmacol.* 2, 7–14. doi: 10.4255/mcpharmacol.10.02

Abdul, H. M., Sama, M. A., Furman, J. L., Mathis, D. M., Beckett, T. L., Weidner, A. M., et al. (2009). Cognitive decline in Alzheimer's disease is associated with selective changes in calcineurin/NFAT signaling. *J. Neurosci.* 29, 12957–12969. doi: 10.1523/JNEUROSCI.1064-09.2009

Agostinho, P., Lopes, J. P., Velez, Z., and Oliveira, C. R. (2008). Overactivation of calcineurin induced by amyloid-β and prion proteins. *Neurochem. Int.* 52, 1226–1233. doi: 10.1016/j.neuint.2008.01.005

Alzheimer's Association Calcium Hypothesis Workgroup. (2017). Calcium Hypothesis of Alzheimer's disease and brain aging: a framework for integrating new evidence into a comprehensive theory of pathogenesis. *Alzheimers Dement.* 13, 178.e17–182.e17. doi: 10.1016/j.jalz.2016.12.006

Aramburu, J., Yaffe, M. B., López-Rodríguez, C., Cantley, L. C., Hogan, P. G., and Rao, A. (1999). Affinity-driven peptide selection of an NFAT inhibitor more selective than cyclosporin A. *Science* 285, 2129–2133. doi: 10.1126/science.285.5436.2129

Bachstetter, A. D., Norris, C. M., Sompol, P., Wilcock, D. M., Goulding, D., Neltner, J. H., et al. (2012). Early stage drug treatment that normalizes proinflammatory cytokine production attenuates synaptic dysfunction in a mouse model that exhibits age-dependent progression of Alzheimer's disease-related pathology. *J. Neurosci.* 32, 10201–10210. doi: 10.1523/JNEUROSCI.1496-12.2012

Bazargani, N., and Attwell, D. (2016). Astrocyte calcium signaling: the third wave. *Nat. Neurosci.* 19, 182–189. doi: 10.1038/nn.4201

Bindocci, E., Savtchouk, I., Liaudet, N., Becker, D., Carriero, G., and Volterra, A. (2017). Three-dimensional Ca^{2+} imaging advances understanding of astrocyte biology. *Science* 356:eaai8185. doi: 10.1126/science.aai8185

Blakely, P. K., Hussain, S., Carlin, L. E., and Irani, D. N. (2015). Astrocyte matricellular proteins that control excitatory synaptogenesis are regulated by inflammatory cytokines and correlate with paralysis severity during experimental autoimmune encephalomyelitis. *Front. Neurosci.* 9:344. doi: 10.3389/fnins.2015.00344

Bousette, N., Chugh, S., Fong, V., Isserlin, R., Kim, K. H., Volchuk, A., et al. (2010). Constitutively active calcineurin induces cardiac endoplasmic reticulum stress and protects against apoptosis that is mediated by α-crystallin-B. *Proc. Natl. Acad. Sci. U S A* 107, 18481–18486. doi: 10.1073/pnas.1013555107

Butenko, O., Dzamba, D., Benesova, J., Honsa, P., Benfenati, V., Rusnakova, V., et al. (2012). The increased activity of TRPV4 channel in the astrocytes of the adult rat hippocampus after cerebral hypoxia/ischemia. *PLoS One* 7:e39959. doi: 10.1371/journal.pone.0039959

Canellada, A., Ramirez, B. G., Minami, T., Redondo, J. M., and Cano, E. (2008). Calcium/calcineurin signaling in primary cortical astrocyte cultures: Rcan1–4 and cyclooxygenase-2 as NFAT target genes. *Glia* 56, 709–722. doi: 10.1002/glia.20647

Caraveo, G., Auluck, P. K., Whitesell, L., Chung, C. Y., Baru, V., Mosharov, E. V., et al. (2014). Calcineurin determines toxic versus beneficial responses to α-synuclein. *Proc. Natl. Acad. Sci. U S A* 111, E3544–E3552. doi: 10.1073/pnas.1413201111

Carvalho, R. V., da Silva Ferreira, F., Heimfarth, L., Pierozan, P., Fernandes, C., and Pessoa-Pureur, R. (2016). Acute hyperammonemia induces NMDA-mediated hypophosphorylation of intermediate filaments through PP1 and PP2B in cerebral cortex of young rats. *Neurotox. Res.* 30, 138–149. doi: 10.1007/s12640-016-9607-7

Cavallucci, V., Berretta, N., Nobili, A., Nisticò, R., Mercuri, N. B., and D'Amelio, M. (2013). Calcineurin inhibition rescues early synaptic plasticity deficits in a mouse model of Alzheimer's disease. *Neuromolecular Med.* 15, 541–548. doi: 10.1007/s12017-013-8241-2

Celsi, F., Svedberg, M., Unger, C., Cotman, C. W., Carrì, M. T., Ottersen, O. P., et al. (2007). β-amyloid causes downregulation of calcineurin in neurons through induction of oxidative stress. *Neurobiol. Dis.* 26, 342–352. doi: 10.1016/j.nbd.2006.12.022

Chen, Q. S., Wei, W. Z., Shimahara, T., and Xie, C. W. (2002). Alzheimer amyloid β-peptide inhibits the late phase of long-term potentiation through calcineurin-dependent mechanisms in the hippocampal dentate gyrus. *Neurobiol. Learn. Mem.* 77, 354–371. doi: 10.1006/nlme.2001.4034

D'Amelio, M., Cavallucci, V., Middei, S., Marchetti, C., Pacioni, S., Ferri, A., et al. (2011). Caspase-3 triggers early synaptic dysfunction in a mouse model of Alzheimer's disease. *Nat. Neurosci.* 14, 69–76. doi: 10.1038/nn.2709

Daschil, N., Obermair, G. J., Flucher, B. E., Stefanova, N., Hutter-Paier, B., Windisch, M., et al. (2013). CaV1.2 calcium channel expression in reactive astrocytes is associated with the formation of amyloid-β plaques in an Alzheimer's disease mouse model. *J. Alzheimers Dis.* 37, 439–451. doi: 10.3233/JAD-130560

De Bock, M., Decrock, E., Wang, N., Bol, M., Vinken, M., Bultynck, G., et al. (2014). The dual face of connexin-based astroglial Ca^{2+} communication: a key player in brain physiology and a prime target in pathology. *Biochim. Biophys. Acta* 1843, 2211–2232. doi: 10.1016/j.bbamcr.2014.04.016

Delekate, A., Füchtemeier, M., Schumacher, T., Ulbrich, C., Foddis, M., and Petzold, G. C. (2014). Metabotropic P2Y1 receptor signalling mediates astrocytic hyperactivity *in vivo* in an Alzheimer's disease mouse model. *Nat. Commun.* 5:5422. doi: 10.1038/ncomms6422

Dineley, K. T., Kayed, R., Neugebauer, V., Fu, Y., Zhang, W., Reese, L. C., et al. (2010). Amyloid-β oligomers impair fear conditioned memory in a calcineurin-dependent fashion in mice. *J. Neurosci. Res.* 88, 2923–2932. doi: 10.1002/jnr.22445

Ding, S., Fellin, T., Zhu, Y., Lee, S. Y., Auberson, Y. P., Meaney, D. F., et al. (2007). Enhanced astrocytic Ca^{2+} signals contribute to neuronal excitotoxicity after status epilepticus. *J. Neurosci.* 27, 10674–10684. doi: 10.1523/JNEUROSCI.2001-07.2007

Ding, S., Wang, T., Cui, W., and Haydon, P. G. (2009). Photothrombosis ischemia stimulates a sustained astrocytic Ca^{2+} signaling *in vivo*. *Glia* 57, 767–776. doi: 10.1002/glia.20804

Eikelenboom, P., and Veerhuis, R. (1996). The role of complement and activated microglia in the pathogenesis of Alzheimer's disease. *Neurobiol. Aging* 17, 673–680. doi: 10.1016/s0197-4580(96)00108-x

Fang, M., Zhang, P., Zhao, Y., Jin, A., and Liu, X. (2016). Aβ mediates Sigma receptor degradation via CaN/NFAT pathway. *Am. J. Transl. Res.* 8, 3471–3481.

Feng, Z. H., Hao, J., Ye, L., Dayao, C., Yan, N., Yan, Y., et al. (2011). Overexpression of mu-calpain in the anterior temporal neocortex of patients with intractable epilepsy correlates with clinicopathological characteristics. *Seizure* 20, 395–401. doi: 10.1016/j.seizure.2011.01.010

Fernandez, A. M., Fernandez, S., Carrero, P., Garcia-Garcia, M., and Torres-Aleman, I. (2007). Calcineurin in reactive astrocytes plays a key role in the interplay between proinflammatory and anti-inflammatory signals. *J. Neurosci.* 27, 8745–8756. doi: 10.1523/JNEUROSCI.1002-07.2007

Fernandez, A. M., Hervas, R., Dominguez-Fraile, M., Garrido, V. N., Gomez-Gutierrez, P., Vega, M., et al. (2016). Blockade of the interaction of calcineurin with FOXO in astrocytes protects against amyloid-β-induced neuronal death. *J. Alzheimers Dis.* 52, 1471–1478. doi: 10.3233/jad-160149

Fernandez, A. M., Jimenez, S., Mecha, M., Dávila, D., Guaza, C., Vitorica, J., et al. (2012). Regulation of the phosphatase calcineurin by insulin-like growth factor I unveils a key role of astrocytes in Alzheimer's pathology. *Mol. Psychiatry* 17, 705–718. doi: 10.1038/mp.2011.128

Fields, J. A., Overk, C., Adame, A., Florio, J., Mante, M., Pineda, A., et al. (2016). Neuroprotective effects of the immunomodulatory drug FK506 in a model of HIV1-gp120 neurotoxicity. *J. Neuroinflammation* 13:120. doi: 10.1186/s12974-016-0585-8

Filosa, J. A., Bonev, A. D., and Nelson, M. T. (2004). Calcium dynamics in cortical astrocytes and arterioles during neurovascular coupling. *Circ. Res.* 95, e73–e81. doi: 10.1161/01.res.0000148636.60732.2e

Filosa, J. A., Nelson, M. T., and Gonzalez Bosc, L. V. (2007). Activity-dependent NFATc3 nuclear accumulation in pericytes from cortical parenchymal microvessels. *Am. J. Physiol. Cell Physiol.* 293, C1797–C1805. doi: 10.1152/ajpcell.00554.2006

Foster, T. C., Sharrow, K. M., Masse, J. R., Norris, C. M., and Kumar, A. (2001). Calcineurin links Ca^{2+} dysregulation with brain aging. *J. Neurosci.* 21, 4066–4073. doi: 10.1523/JNEUROSCI.21-11-04066.2001

Frazier, H. N., Maimaiti, S., Anderson, K. L., Brewer, L. D., Gant, J. C., Porter, N. M., et al. (2017). Calcium's role as nuanced modulator of cellular physiology in the brain. *Biochem. Biophys. Res. Commun.* 483, 981–987. doi: 10.1016/j.bbrc.2016.08.105

Frischbutter, S., Gabriel, C., Bendfeldt, H., Radbruch, A., and Baumgrass, R. (2011). Dephosphorylation of Bcl-10 by calcineurin is essential for canonical NF-kappaB activation in Th cells. *Eur. J. Immunol.* 41, 2349–2357. doi: 10.1002/eji.201041052

Fujii, Y., Maekawa, S., and Morita, M. (2017). Astrocyte calcium waves propagate proximally by gap junction and distally by extracellular diffusion of ATP released from volume-regulated anion channels. *Sci. Rep.* 7:13115. doi: 10.1038/s41598-017-13243-0

Furman, J. L., and Norris, C. M. (2014). Calcineurin and glial signaling: neuroinflammation and beyond. *J. Neuroinflammation* 11:158. doi: 10.1186/s12974-014-0158-7

Furman, J. L., Artiushin, I. A., and Norris, C. M. (2010). Disparate effects of serum on basal and evoked NFAT activity in primary astrocyte cultures. *Neurosci. Lett.* 469, 365–369. doi: 10.1016/j.neulet.2009.12.029

Furman, J. L., Sama, D. M., Gant, J. C., Beckett, T. L., Murphy, M. P., Bachstetter, A. D., et al. (2012). Targeting astrocytes ameliorates neurologic changes in a mouse model of Alzheimer's disease. *J. Neurosci.* 32, 16129–16140. doi: 10.1523/JNEUROSCI.2323-12.2012

Furman, J. L., Sompol, P., Kraner, S. D., Pleiss, M. M., Putman, E. J., Dunkerson, J., et al. (2016). Blockade of astrocytic calcineurin/NFAT signaling helps to normalize hippocampal synaptic function and plasticity in a rat model of traumatic brain injury. *J. Neurosci.* 36, 1502–1515. doi: 10.1523/JNEUROSCI.1930-15.2016

Gibson, G. E., and Peterson, C. (1987). Calcium and the aging nervous system. *Neurobiol. Aging* 8, 329–343. doi: 10.1016/0197-4580(87)90077-7

Gibson, G. E., and Thakkar, A. (2017). Interactions of mitochondria/metabolism and calcium regulation in Alzheimer's disease: a calcinist point of view. *Neurochem. Res.* 42, 1636–1648. doi: 10.1007/s11064-017-2182-3

Gong, C. X., Singh, T. J., Grundke-Iqbal, I., and Iqbal, K. (1993). Phosphoprotein phosphatase activities in Alzheimer disease brain. *J. Neurochem.* 61, 921–927. doi: 10.1111/j.1471-4159.1993.tb03603.x

Goto, S., Matsukado, Y., Mihara, Y., Inoue, N., and Miyamoto, E. (1986a). Calcineurin in human brain and its relation to extrapyramidal system. Immunohistochemical study on postmortem human brains. *Acta Neuropathol.* 72, 150–156. doi: 10.1007/bf00685977

Goto, S., Matsukado, Y., Mihara, Y., Inoue, N., and Miyamoto, E. (1986b). The distribution of calcineurin in rat brain by light and electron microscopic immunohistochemistry and enzyme-immunoassay. *Brain Res.* 397, 161–172. doi: 10.1016/0006-8993(86)91381-8

Griffin, W. S., Sheng, J. G., Royston, M. C., Gentleman, S. M., Mckenzie, J. E., Graham, D. I., et al. (1998). Glial-neuronal interactions in Alzheimer's disease: the potential role of a 'cytokine cycle' in disease progression. *Brain Pathol.* 8, 65–72. doi: 10.1111/j.1750-3639.1998.tb00136.x

Grolla, A. A., Fakhfouri, G., Balzaretti, G., Marcello, E., Gardoni, F., Canonico, P. L., et al. (2013). Aβ leads to Ca^{2+} signaling alterations and transcriptional changes in glial cells. *Neurobiol. Aging* 34, 511–522. doi: 10.1016/j.neurobiolaging.2012.05.005

Guerra-Gomes, S., Sousa, N., Pinto, L., and Oliveira, J. F. (2017). Functional roles of astrocyte calcium elevations: from synapses to behavior. *Front. Cell. Neurosci.* 11:427. doi: 10.3389/fncel.2017.00427

Halestrap, A. P., Connern, C. P., Griffiths, E. J., and Kerr, P. M. (1997). Cyclosporin A binding to mitochondrial cyclophilin inhibits the permeability transition pore and protects hearts from ischaemia/reperfusion injury. *Mol. Cell. Biochem.* 174, 167–172. doi: 10.1007/978-1-4615-6111-8_25

Halpain, S., Hipolito, A., and Saffer, L. (1998). Regulation of F-actin stability in dendritic spines by glutamate receptors and calcineurin. *J. Neurosci.* 18, 9835–9844. doi: 10.1523/JNEUROSCI.18-23-09835.1998

Harvey, B. K., Airavaara, M., Hinzman, J., Wires, E. M., Chiocco, M. J., Howard, D. B., et al. (2011). Targeted over-expression of glutamate transporter 1 (GLT-1) reduces ischemic brain injury in a rat model of stroke. *PLoS One* 6:e22135. doi: 10.1371/journal.pone.0022135

Hashimoto, T., Kawamata, T., Saito, N., Sasaki, M., Nakai, M., Niu, S., et al. (1998). Isoform-specific redistribution of calcineurin Aα and Aβ in the hippocampal CA1 region of gerbils after transient ischemia. *J. Neurochem.* 70, 1289–1298. doi: 10.1046/j.1471-4159.1998.70031289.x

Hefendehl, J. K., LeDue, J., Ko, R. W., Mahler, J., Murphy, T. H., and Macvicar, B. A. (2016). Mapping synaptic glutamate transporter dysfunction *in vivo* to regions surrounding Aβ plaques by iGluSnFR two-photon imaging. *Nat. Commun.* 7:13441. doi: 10.1038/ncomms13441

Hogan, P. G. (2017). Calcium-NFAT transcriptional signalling in T cell activation and T cell exhaustion. *Cell Calcium* 63, 66–69. doi: 10.1016/j.ceca.2017.01.014

Hong, S., Beja-Glasser, V. F., Nfonoyim, B. M., Frouin, A., Li, S., Ramakrishnan, S., et al. (2016). Complement and microglia mediate early synapse loss in Alzheimer mouse models. *Science* 352, 712–716. doi: 10.1126/science.aad8373

Hong, H. S., Hwang, J. Y., Son, S. M., Kim, Y. H., Moon, M., and Inhee, M. J. (2010). FK506 reduces amyloid plaque burden and induces MMP-9 in AβPP/PS1 double transgenic mice. *J. Alzheimers Dis.* 22, 97–105. doi: 10.3233/jad-2010-100261

Horsley, V., and Pavlath, G. K. (2002). NFAT: ubiquitous regulator of cell differentiation and adaptation. *J. Cell Biol.* 156, 771–774. doi: 10.1083/jcb.200111073

Huang, W., Fileta, J. B., Dobberfuhl, A., Filippopolous, T., Guo, Y., Kwon, G., et al. (2005). Calcineurin cleavage is triggered by elevated intraocular pressure and calcineurin inhibition blocks retinal ganglion cell death in experimental glaucoma. *Proc. Natl. Acad. Sci. U S A* 102, 12242–12247. doi: 10.1073/pnas.0505138102

Im, S. H., and Rao, A. (2004). Activation and deactivation of gene expression by Ca^{2+}/calcineurin-NFAT-mediated signaling. *Mol. Cells* 18, 1–9.

Jin, S. M., Cho, H. J., Kim, Y. W., Hwang, J. Y., and Mook-Jung, I. (2012). Aβ-induced Ca^{2+} influx regulates astrocytic BACE1 expression via calcineurin/NFAT4 signals. *Biochem. Biophys. Res. Commun.* 425, 649–655. doi: 10.1016/j.bbrc.2012.07.123

Jones, E. V., Bernardinelli, Y., Tse, Y. C., Chierzi, S., Wong, T. P., and Murai, K. K. (2011). Astrocytes control glutamate receptor levels at developing synapses through SPARC-β-integrin interactions. *J. Neurosci.* 31, 4154–4165. doi: 10.1523/JNEUROSCI.4757-10.2011

Jones, E. V., and Bouvier, D. S. (2014). Astrocyte-secreted matricellular proteins in CNS remodelling during development and disease. *Neural Plast.* 2014:321209. doi: 10.1155/2014/321209

Kahraman, S., Bambrick, L. L., and Fiskum, G. (2011). Effects of FK506 and cyclosporin a on calcium ionophore-induced mitochondrial depolarization and cytosolic calcium in astrocytes and neurons. *J. Neurosci. Res.* 89, 1973–1978. doi: 10.1002/jnr.22709

Karklin Fontana, A. C., Fox, D. P., Zoubroulis, A., Valente Mortensen, O., and Raghupathi, R. (2016). Neuroprotective effects of the glutamate transporter activator (*R*)-(−)-5-methyl-1-nicotinoyl-2-pyrazoline (MS-153) following traumatic brain injury in the adult rat. *J. Neurotrauma* 33, 1073–1083. doi: 10.1089/neu.2015.4079

Karpurapu, M., Wang, D., Van Quyen, D., Kim, T. K., Kundumani-Sridharan, V., Pulusani, S., et al. (2010). Cyclin D1 is a bona fide target gene of NFATc1 and is sufficient in the mediation of injury-induced vascular wall remodeling. *J. Biol. Chem.* 285, 3510–3523. doi: 10.1074/jbc.M109.063727

Khachaturian, Z. S. (1987). Hypothesis on the regulation of cytosol calcium concentration and the aging brain. *Neurobiol. Aging* 8, 345–346. doi: 10.1016/0197-4580(87)90073-x

Kim, S. Y., Chao, W., Choi, S. Y., and Volsky, D. J. (2003). Cloning and characterization of the 3′-untranslated region of the human excitatory amino acid transporter 2 transcript. *J. Neurochem.* 86, 1458–1467. doi: 10.1046/j.1471-4159.2003.01958.x

Kim, B., Jeong, H. K., Kim, J. H., Lee, S. Y., Jou, I., and Joe, E. H. (2011). Uridine 5′-diphosphate induces chemokine expression in microglia and astrocytes through activation of the P2Y6 receptor. *J. Immunol.* 186, 3701–3709. doi: 10.4049/jimmunol.1000212

Kim, S., Violette, C. J., and Ziff, E. B. (2015). Reduction of increased calcineurin activity rescues impaired homeostatic synaptic plasticity in presenilin 1 M146V mutant. *Neurobiol. Aging* 36, 3239–3246. doi: 10.1016/j.neurobiolaging.2015.09.007

Kotilinek, L. A., Westerman, M. A., Wang, Q., Panizzon, K., Lim, G. P., Simonyi, A., et al. (2008). Cyclooxygenase-2 inhibition improves amyloid-β-mediated suppression of memory and synaptic plasticity. *Brain* 131, 651–664. doi: 10.1093/brain/awn008

Kuchibhotla, K. V., Goldman, S. T., Lattarulo, C. R., Wu, H. Y., Hyman, B. T., and Bacskai, B. J. (2008). Aβ plaques lead to aberrant regulation of calcium homeostasis *in vivo* resulting in structural and functional disruption

of neuronal networks. *Neuron* 59, 214–225. doi: 10.1016/j.neuron.2008.06.008

Kuchibhotla, K. V., Lattarulo, C. R., Hyman, B. T., and Bacskai, B. J. (2009). Synchronous hyperactivity and intercellular calcium waves in astrocytes in Alzheimer mice. *Science* 323, 1211–1215. doi: 10.1126/science.1169096

Kucukdereli, H., Allen, N. J., Lee, A. T., Feng, A., Ozlu, M. I., Conatser, L. M., et al. (2011). Control of excitatory CNS synaptogenesis by astrocyte-secreted proteins Hevin and SPARC. *Proc. Natl. Acad. Sci. U S A* 108, E440–E449. doi: 10.1073/pnas.1104977108

Kumar, A., and Singh, N. (2017). Calcineurin inhibitors improve memory loss and neuropathological changes in mouse model of dementia. *Pharmacol. Biochem. Behav.* 153, 147–159. doi: 10.1016/j.pbb.2016.12.018

Kundumani-Sridharan, V., Singh, N. K., Kumar, S., Gadepalli, R., and Rao, G. N. (2013). Nuclear factor of activated T cells c1 mediates p21-activated kinase 1 activation in the modulation of chemokine-induced human aortic smooth muscle cell F-actin stress fiber formation, migration, and proliferation and injury-induced vascular wall remodeling. *J. Biol. Chem.* 288, 22150–22162. doi: 10.1074/jbc.M113.454082

Kuno, T., Mukai, H., Ito, A., Chang, C. D., Kishima, K., Saito, N., et al. (1992). Distinct cellular expression of calcineurin Aα and Aβ in rat brain. *J. Neurochem.* 58, 1643–1651. doi: 10.1111/j.1471-4159.1992.tb10036.x

Ladner, C. J., Czech, J., Maurice, J., Lorens, S. A., and Lee, J. M. (1996). Reduction of calcineurin enzymatic activity in Alzheimer's disease: correlation with neuropathologic changes. *J. Neuropathol. Exp. Neurol.* 55, 924–931. doi: 10.1097/00005072-199608000-00008

Landfield, P. W. (1987). 'Increased calcium-current' hypothesis of brain aging. *Neurobiol. Aging* 8, 346–347. doi: 10.1016/0197-4580(87)90074-1

Li, Q., Fang, J., Yang, M., Wu, D., Zhang, L., and Zhang, Y. (2010). Galantamine inhibits calpain-calcineurin signaling activated by β-amyloid in human neuroblastoma SH-SY5Y cells. *Neurosci. Lett.* 480, 173–177. doi: 10.1016/j.neulet.2010.06.005

Li, W. E., and Nagy, J. I. (2000). Connexin43 phosphorylation state and intercellular communication in cultured astrocytes following hypoxia and protein phosphatase inhibition. *Eur. J. Neurosci.* 12, 2644–2650. doi: 10.1046/j.1460-9568.2000.00162.x

Lian, Q., Ladner, C. J., Magnuson, D., and Lee, J. M. (2001). Selective changes of calcineurin (protein phosphatase 2B) activity in Alzheimer's disease cerebral cortex. *Exp. Neurol.* 167, 158–165. doi: 10.1006/exnr.2000.7534

Lian, H., Yang, L., Cole, A., Sun, L., Chiang, A. C., Fowler, S. W., et al. (2015). NFκB-activated astroglial release of compement C3 compromises neuronal morphology and function associated with Alzheimer's disease. *Neuron* 85, 101–115. doi: 10.1016/j.neuron.2014.11.018

Liddelow, S. A., Guttenplan, K. A., Clarke, L. E., Bennett, F. C., Bohlen, C. J., Schirmer, L., et al. (2017). Neurotoxic reactive astrocytes are induced by activated microglia. *Nature* 541, 481–487. doi: 10.1038/nature21029

Lim, D., Iyer, A., Ronco, V., Grolla, A. A., Canonico, P. L., Aronica, E., et al. (2013). Amyloid β deregulates astroglial mGluR5-mediated calcium signaling via calcineurin and Nf-κB. *Glia* 61, 1134–1145. doi: 10.1002/glia.22502

Liu, Q., Busby, J. C., and Molkentin, J. D. (2009). Interaction between TAK1-TAB1-TAB2 and RCAN1-calcineurin defines a signalling nodal control point. *Nat. Cell Biol.* 11, 154–161. doi: 10.1038/ncb1823

Liu, Z., Dronadula, N., and Rao, G. N. (2004). A novel role for nuclear factor of activated T cells in receptor tyrosine kinase and G protein-coupled receptor agonist-induced vascular smooth muscle cell motility. *J. Biol. Chem.* 279, 41218–41226. doi: 10.1074/jbc.M406917200

Liu, F., Grundke-Iqbal, I., Iqbal, K., Oda, Y., Tomizawa, K., and Gong, C. X. (2005). Truncation and activation of calcineurin A by calpain I in Alzheimer disease brain. *J. Biol. Chem.* 280, 37755–37762. doi: 10.1074/jbc.M507475200

Liu, J., Li, X., Chen, L., Xue, P., Yang, Q., and Wang, A. (2015). Increased calcineurin expression after pilocarpine-induced status epilepticus is associated with brain focal edema and astrogliosis. *Int. J. Neurosci.* doi: 10.3109/00207454.2015.1045975 [Epub ahead of print].

Liu, J., Si, Z., Li, S., Huang, Z., He, Y., Zhang, T., et al. (2017). The calcineurin inhibitor fk506 prevents cognitive impairment by inhibiting reactive astrogliosis in pilocarpine-induced status epilepticus rats. *Front. Cell. Neurosci.* 11:428. doi: 10.3389/fncel.2017.00428

MacPherson, K. P., Sompol, P., Kannarkat, G. T., Chang, J., Sniffen, L., Wildner, M. E., et al. (2017). Peripheral administration of the soluble TNF inhibitor XPro1595 modifies brain immune cell profiles, decreases β-amyloid plaque load, and rescues impaired long-term potentiation in 5xFAD mice. *Neurobiol. Dis.* 102, 81–95. doi: 10.1016/j.nbd.2017.02.010

Mallolas, J., Hurtado, O., Castellanos, M., Blanco, M., Sobrino, T., Serena, J., et al. (2006). A polymorphism in the EAAT2 promoter is associated with higher glutamate concentrations and higher frequency of progressing stroke. *J. Exp. Med.* 203, 711–717. doi: 10.1084/jem.20051979

Manocha, G. D., Floden, A. M., Puig, K. L., Nagamoto-Combs, K., Scherzer, C. R., and Combs, C. K. (2017a). Defining the contribution of neuroinflammation to Parkinson's disease in humanized immune system mice. *Mol. Neurodegener.* 12:17. doi: 10.1186/s13024-017-0158-z

Manocha, G. D., Ghatak, A., Puig, K. L., Kraner, S. D., Norris, C. M., and Combs, C. K. (2017b). NFATc2 modulates microglial activation in the AβPP/PS1 Mouse model of Alzheimer's disease. *J. Alzheimers Dis.* 58, 775–787. doi: 10.3233/JAD-151203

Martin, Z. S., Neugebauer, V., Dineley, K. T., Kayed, R., Zhang, W., Reese, L. C., et al. (2012). α-Synuclein oligomers oppose long-term potentiation and impair memory through a calcineurin-dependent mechanism: relevance to human synucleopathic diseases. *J. Neurochem.* 120, 440–452. doi: 10.1111/j.1471-4159.2011.07576.x

Masliah, E., Alford, M., DeTeresa, R., Mallory, M., and Hansen, L. (1996). Deficient glutamate transport is associated with neurodegeneration in Alzheimer's disease. *Ann. Neurol.* 40, 759–766. doi: 10.1002/ana.410400512

Masliah, E., Alford, M., Mallory, M., Rockenstein, E., Moechars, D., and Van Leuven, F. (2000). Abnormal glutamate transport function in mutant amyloid precursor protein transgenic mice. *Exp. Neurol.* 163, 381–387. doi: 10.1006/exnr.2000.7386

Mathern, G. W., Mendoza, D., Lozada, A., Pretorius, J. K., Dehnes, Y., Danbolt, N. C., et al. (1999). Hippocampal GABA and glutamate transporter immunoreactivity in patients with temporal lobe epilepsy. *Neurology* 52, 453–472. doi: 10.1212/wnl.52.3.453

McAdory, B. S., Van Eldik, L. J., and Norden, J. J. (1998). S100B, a neurotropic protein that modulates neuronal protein phosphorylation, is upregulated during lesion-induced collateral sprouting and reactive synaptogenesis. *Brain Res.* 813, 211–217. doi: 10.1016/s0006-8993(98)01014-2

McCullagh, K. J., Calabria, E., Pallafacchina, G., Ciciliot, S., Serrano, A. L., Argentini, C., et al. (2004). NFAT is a nerve activity sensor in skeletal muscle and controls activity-dependent myosin switching. *Proc. Natl. Acad. Sci. U S A* 101, 10590–10595. doi: 10.1073/pnas.0308035101

Mellstrom, B., Savignac, M., Gomez-Villafuertes, R., and Naranjo, J. R. (2008). Ca^{2+}-operated transcriptional networks: molecular mechanisms and *in vivo* models. *Physiol. Rev.* 88, 421–449. doi: 10.1152/physrev.00041.2005

Mohmmad Abdul, H., Baig, I., Levine, H. III., Guttmann, R. P., and Norris, C. M. (2011). Proteolysis of calcineurin is increased in human hippocampus during mild cognitive impairment and is stimulated by oligomeric Aβ in primary cell culture. *Aging Cell* 10, 103–113. doi: 10.1111/j.1474-9726.2010.00645.x

Moidunny, S., Matos, M., Wesseling, E., Banerjee, S., Volsky, D. J., Cunha, R. A., et al. (2016). Oncostatin M promotes excitotoxicity by inhibiting glutamate uptake in astrocytes: implications in HIV-associated neurotoxicity. *J. Neuroinflammation* 13:144. doi: 10.1186/s12974-016-0613-8

Molkentin, J. D. (2004). Calcineurin-NFAT signaling regulates the cardiac hypertrophic response in coordination with the MAPKs. *Cardiovasc. Res.* 63, 467–475. doi: 10.1016/j.cardiores.2004.01.021

Mookherjee, P., Green, P. S., Watson, G. S., Marques, M. A., Tanaka, K., Meeker, K. D., et al. (2011). GLT-1 loss accelerates cognitive deficit onset in an Alzheimer's disease animal model. *J. Alzheimers Dis.* 26, 447–455. doi: 10.3233/JAD-2011-110503

Mukherjee, A., Morales-Scheihing, D., Gonzalez-Romero, D., Green, K., Taglialatela, G., and Soto, C. (2010). Calcineurin inhibition at the clinical phase of prion disease reduces neurodegeneration, improves behavioral alterations and increases animal survival. *PLoS Pathog.* 6:e1001138. doi: 10.1371/journal.ppat.1001138

Nagamoto-Combs, K., and Combs, C. K. (2010). Microglial phenotype is regulated by activity of the transcription factor, NFAT (nuclear factor of activated T cells). *J. Neurosci.* 30, 9641–9646. doi: 10.1523/JNEUROSCI.0828-10.2010

Neria, F., del Carmen Serrano-Perez, M., Velasco, P., Urso, K., Tranque, P., and Cano, E. (2013). NFATc3 promotes Ca^{2+}-dependent MMP3 expression in astroglial cells. *Glia* 61, 1052–1066. doi: 10.1002/glia.22494

Norris, C. M. (2014). "Calpain interactions with the protein phosphatase calcineurin in neurodegeneration," in *Advances in Biochemistry in Health and Disease*, (Vol. 8) eds N. Dhalla and S. Chakraborti (New York, NY: Springer), 17–45.

Norris, C. M., Kadish, I., Blalock, E. M., Chen, K. C., Thibault, V., Porter, N. M., et al. (2005). Calcineurin triggers reactive/inflammatory processes in astrocytes and is upregulated in aging and Alzheimer's models. *J. Neurosci.* 25, 4649–4658. doi: 10.1523/JNEUROSCI.0365-05.2005

O'Donnell, J. C., Jackson, J. G., and Robinson, M. B. (2016). Transient oxygen/glucose deprivation causes a delayed loss of mitochondria and increases spontaneous calcium signaling in astrocytic processes. *J. Neurosci.* 36, 7109–7127. doi: 10.1523/JNEUROSCI.4518-15.2016

Palkowitsch, L., Marienfeld, U., Brunner, C., Eitelhuber, A., Krappmann, D., and Marienfeld, R. B. (2011). The Ca^{2+}-dependent phosphatase calcineurin controls the formation of the Carma1-Bcl10-Malt1 complex during T cell receptor-induced NF-κB activation. *J. Biol. Chem.* 286, 7522–7534. doi: 10.1074/jbc.M110.155895

Pchitskaya, E., Popugaeva, E., and Bezprozvanny, I. (2018). Calcium signaling and molecular mechanisms underlying neurodegenerative diseases. *Cell Calcium* 70, 87–94. doi: 10.1016/j.ceca.2017.06.008

Pekny, M., and Nilsson, M. (2005). Astrocyte activation and reactive gliosis. *Glia* 50, 427–434. doi: 10.1002/glia.20207

Pekny, M., and Pekna, M. (2014). Astrocyte reactivity and reactive astrogliosis: costs and benefits. *Physiol. Rev.* 94, 1077–1098. doi: 10.1152/physrev.00041.2013

Pekny, M., Pekna, M., Messing, A., Steinhauser, C., Lee, J. M., Parpura, V., et al. (2016). Astrocytes: a central element in neurological diseases. *Acta Neuropathol.* 131, 323–345. doi: 10.1007/s00401-015-1513-1

Perez-Nievas, B. G., and Serrano-Pozo, A. (2018). Deciphering the astrocyte reaction in Alzheimer's disease. *Front. Aging Neurosci.* 10:114. doi: 10.3389/fnagi.2018.00114

Pérez-Ortiz, J. M., Serrano-Pérez, M. C., Pastor, M. D., Martin, E. D., Calvo, S., Rincon, M., et al. (2008). Mechanical lesion activates newly identified NFATc1 in primary astrocytes: implication of ATP and purinergic receptors. *Eur. J. Neurosci.* 27, 2453–2465. doi: 10.1111/j.1460-9568.2008.06197.x

Petr, G. T., Sun, Y., Frederick, N. M., Zhou, Y., Dhamne, S. C., Hameed, M. Q., et al. (2015). Conditional deletion of the glutamate transporter GLT-1 reveals that astrocytic GLT-1 protects against fatal epilepsy while neuronal GLT-1 contributes significantly to glutamate uptake into synaptosomes. *J. Neurosci.* 35, 5187–5201. doi: 10.1523/JNEUROSCI.4255-14.2015

Pleiss, M. M., Sompol, P., Artiushin, I. A., Kraner, S. D., Powell, D. K., Bakshi, V., et al. (2016a). Inhibition of astrocytic calcineurin/NFAT signaling in a mouse model of vascular cognitive impairment and dementia. *Soc. Neurosci. Abs.* 46:482.09.

Pleiss, M. M., Sompol, P., Kraner, S. D., Abdul, H. M., Furman, J. L., Guttmann, R. P., et al. (2016b). Calcineurin proteolysis in astrocytes: implications for impaired synaptic function. *Biochim. Biophys. Acta* 1862, 1521–1532. doi: 10.1016/j.bbadis.2016.05.007

Polli, J. W., Billingsley, M. L., and Kincaid, R. L. (1991). Expression of the calmodulin-dependent protein phosphatase, calcineurin, in rat brain: developmental patterns and the role of nigrostriatal innervation. *Dev. Brain Res.* 63, 105–119. doi: 10.1016/0165-3806(91)90071-p

Pons, S., and Torres-Aleman, I. (2000). Insulin-like growth factor-I stimulates dephosphorylation of IκB through the serine phosphatase calcineurin (protein phosphatase 2B). *J. Biol. Chem.* 275, 38620–38625. doi: 10.1074/jbc.M004531200

Proper, E. A., Hoogland, G., Kappen, S. M., Jansen, G. H., Rensen, M. G., Schrama, L. H., et al. (2002). Distribution of glutamate transporters in the hippocampus of patients with pharmaco-resistant temporal lobe epilepsy. *Brain* 125, 32–43. doi: 10.1093/brain/awf001

Qian, W., Yin, X., Hu, W., Shi, J., Gu, J., Grundke-Iqbal, I., et al. (2011). Activation of protein phosphatase 2B and hyperphosphorylation of Tau in Alzheimer's disease. *J. Alzheimers Dis.* 23, 617–627. doi: 10.3233/JAD-2010-100987

Quintana, A. R., Wang, D., Forbes, J. E., and Waxham, M. N. (2005). Kinetics of calmodulin binding to calcineurin. *Biochem. Biophys. Res. Commun.* 334, 674–680. doi: 10.1016/j.bbrc.2005.06.152

Rakers, C., and Petzold, G. C. (2017). Astrocytic calcium release mediates peri-infarct depolarizations in a rodent stroke model. *J. Clin. Invest.* 127, 511–516. doi: 10.1172/JCI89354

Rana, Z. A., Gundersen, K., and Buonanno, A. (2008). Activity-dependent repression of muscle genes by NFAT. *Proc. Natl. Acad. Sci. U S A* 105, 5921–5926. doi: 10.1073/pnas.0801330105

Rao, V. L., Dogan, A., Bowen, K. K., Todd, K. G., and Dempsey, R. J. (2001). Antisense knockdown of the glial glutamate transporter GLT-1 exacerbates hippocampal neuronal damage following traumatic injury to rat brain. *Eur. J. Neurosci.* 13, 119–128. doi: 10.1111/j.1460-9568.2001.01367.x

Rao, A., Luo, C., and Hogan, P. G. (1997). Transcription factors of the NFAT family: regulation and function. *Annu. Rev. Immunol.* 15, 707–747. doi: 10.1146/annurev.immunol.15.1.707

Reese, L. C., Zhang, W., Dineley, K. T., Kayed, R., and Taglialatela, G. (2008). Selective induction of calcineurin activity and signaling by oligomeric amyloid β. *Aging Cell* 7, 824–835. doi: 10.1111/j.1474-9726.2008.00434.x

Robinson, M. B., and Jackson, J. G. (2016). Astroglial glutamate transporters coordinate excitatory signaling and brain energetics. *Neurochem. Int.* 98, 56–71. doi: 10.1016/j.neuint.2016.03.014

Rodríguez-Arellano, J. J., Parpura, V., Zorec, R., and Verkhratsky, A. (2016). Astrocytes in physiological aging and Alzheimer's disease. *Neuroscience* 323, 170–182. doi: 10.1016/j.neuroscience.2015.01.007

Rojanathammanee, L., Floden, A. M., Manocha, G. D., and Combs, C. K. (2015). Attenuation of microglial activation in a mouse model of Alzheimer's disease via NFAT inhibition. *J. Neuroinflammation* 12:42. doi: 10.1186/s12974-015-0255-2

Rosenkranz, K., May, C., Meier, C., and Marcus, K. (2012). Proteomic analysis of alterations induced by perinatal hypoxic-ischemic brain injury. *J. Proteome Res.* 11, 5794–5803. doi: 10.1021/pr3005869

Rothstein, J. D., Dykes-Hoberg, M., Pardo, C. A., Bristol, L. A., Jin, L., Kuncl, R. W., et al. (1996). Knockout of glutamate transporters reveals a major role for astroglial transport in excitotoxicity and clearance of glutamate. *Neuron* 16, 675–686. doi: 10.1016/s0896-6273(00)80086-0

Rozkalne, A., Hyman, B. T., and Spires-Jones, T. L. (2011). Calcineurin inhibition with FK506 ameliorates dendritic spine density deficits in plaque-bearing Alzheimer model mice. *Neurobiol. Dis.* 41, 650–654. doi: 10.1016/j.nbd.2010.11.014

Rusakov, D. A. (2015). Disentangling calcium-driven astrocyte physiology. *Nat. Rev. Neurosci.* 16, 226–233. doi: 10.1038/nrn3878

Saito, K., Shigetomi, E., Yasuda, R., Sato, R., Nakano, M., Tashiro, K., et al. (2018). Aberrant astrocyte Ca^{2+} signals "AxCa signals" exacerbate pathological alterations in an Alexander disease model. *Glia* 66, 1053–1067. doi: 10.1002/glia.23300

Sama, M. A., Mathis, D. M., Furman, J. L., Abdul, H. M., Artiushin, I. A., Kraner, S. D., et al. (2008). Interleukin-1β-dependent signaling between astrocytes and neurons depends critically on astrocytic calcineurin/NFAT activity. *J. Biol. Chem.* 283, 21953–21964. doi: 10.1074/jbc.M800148200

Sama, D. M., and Norris, C. M. (2013). Calcium dysregulation and neuroinflammation: discrete and integrated mechanisms for age-related synaptic dysfunction. *Ageing Res. Rev.* 12, 982–995. doi: 10.1016/j.arr.2013.05.008

Schallier, A., Smolders, I., Van Dam, D., Loyens, E., De Deyn, P. P., Michotte, A., et al. (2011). Region- and age-specific changes in glutamate transport in the AβPP23 mouse model for Alzheimer's disease. *J. Alzheimers Dis.* 24, 287–300. doi: 10.3233/JAD-2011-101005

Selkirk, J. V., Nottebaum, L. M., Vana, A. M., Verge, G. M., Mackay, K. B., Stiefel, T. H., et al. (2005). Role of the GLT-1 subtype of glutamate transporter in glutamate homeostasis: the GLT-1-preferring inhibitor WAY-855 produces marginal neurotoxicity in the rat hippocampus. *Eur. J. Neurosci.* 21, 3217–3228. doi: 10.1111/j.1460-9568.2005.04162.x

Serrano-Pérez, M. C., Martín, E. D., Vaquero, C. F., Azcoitia, I., Calvo, S., Cano, E., et al. (2011). Response of transcription factor NFATc3 to excitotoxic and traumatic brain insults: identification of a subpopulation of reactive astrocytes. *Glia* 59, 94–107. doi: 10.1002/glia.21079

Shah, S. Z. A., Zhao, D., Taglialatela, G., Khan, S. H., Hussain, T., Dong, H., et al. (2017). Early minocycline and late FK506 treatment improves survival and alleviates neuroinflammation, neurodegeneration, and behavioral deficits in prion-infected hamsters. *Neurotherapeutics* 14, 463–483. doi: 10.1007/s13311-016-0500-0

Shi, Q., Chowdhury, S., Ma, R., Le, K. X., Hong, S., Caldarone, B. J., et al. (2017). Complement C3 deficiency protects against neurodegeneration in aged plaque-rich APP/PS1 mice. *Sci. Transl. Med.* 9:eaaf6295. doi: 10.1126/scitranslmed.aaf6295

Shields, D. C., Schaecher, K. E., Hogan, E. L., and Banik, N. L. (2000). Calpain activity and expression increased in activated glial and inflammatory cells in penumbra of spinal cord injury lesion. *J. Neurosci. Res.* 61, 146–150. doi: 10.1002/1097-4547(20000715)61:2<146::aid-jnr5>3.3.co;2-3

Shields, D. C., Tyor, W. R., Deibler, G. E., Hogan, E. L., and Banik, N. L. (1998). Increased calpain expression in activated glial and inflammatory cells in experimental allergic encephalomyelitis. *Proc. Natl. Acad. Sci. U S A* 95, 5768–5772. doi: 10.1073/pnas.95.10.5768

Shigetomi, E., Patel, S., and Khakh, B. S. (2016). Probing the complexities of astrocyte calcium signaling. *Trends Cell Biol.* 26, 300–312. doi: 10.1016/j.tcb.2016.01.003

Shioda, N., Moriguchi, S., Shirasaki, Y., and Fukunaga, K. (2006). Generation of constitutively active calcineurin by calpain contributes to delayed neuronal death following mouse brain ischemia. *J. Neurochem.* 98, 310–320. doi: 10.1111/j.1471-4159.2006.03874.x

Shirakawa, H., Sakimoto, S., Nakao, K., Sugishita, A., Konno, M., Iida, S., et al. (2010). Transient receptor potential canonical 3 (TRPC3) mediates thrombin-induced astrocyte activation and upregulates its own expression in cortical astrocytes. *J. Neurosci.* 30, 13116–13129. doi: 10.1523/JNEUROSCI.1890-10.2010

Simpson, J. E., Ince, P. G., Lace, G., Forster, G., Shaw, P. J., Matthews, F., et al. (2010). Astrocyte phenotype in relation to Alzheimer-type pathology in the ageing brain. *Neurobiol. Aging* 31, 578–590. doi: 10.1016/j.neurobiolaging.2008.05.015

Sitara, D., and Aliprantis, A. O. (2010). Transcriptional regulation of bone and joint remodeling by NFAT. *Immunol. Rev.* 233, 286–300. doi: 10.1111/j.0105-2896.2009.00849.x

Sobrado, M., Ramirez, B. G., Neria, F., Lizasoain, I., Arbones, M. L., Minami, T., et al. (2012). Regulator of calcineurin 1 (Rcan1) has a protective role in brain ischemia/reperfusion injury. *J. Neuroinflammation* 9:48. doi: 10.1186/1742-2094-9-48

Sofroniew, M. V. (2009). Molecular dissection of reactive astrogliosis and glial scar formation. *Trends Neurosci.* 32, 638–647. doi: 10.1016/j.tins.2009.08.002

Sompol, P., Furman, J. L., Pleiss, M. M., Kraner, S. D., Artiushin, I. A., Batten, S. R., et al. (2017). Calcineurin/NFAT signaling in activated astrocytes drives network hyperexcitability in aβ-bearing mice. *J. Neurosci.* 37, 6132–6148. doi: 10.1523/JNEUROSCI.0877-17.2017

Stevens, B., Allen, N. J., Vazquez, L. E., Howell, G. R., Christopherson, K. S., Nouri, N., et al. (2007). The classical complement cascade mediates CNS synapse elimination. *Cell* 131, 1164–1178. doi: 10.1016/j.cell.2007.10.036

Su, Z. Z., Leszczyniecka, M., Kang, D. C., Sarkar, D., Chao, W., Volsky, D. J., et al. (2003). Insights into glutamate transport regulation in human astrocytes: cloning of the promoter for excitatory amino acid transporter 2 (EAAT2). *Proc. Natl. Acad. Sci. U S A* 100, 1955–1960. doi: 10.1073/pnas.0136555100

Taglialatela, G., Hogan, D., Zhang, W. R., and Dineley, K. T. (2009). Intermediate- and long-term recognition memory deficits in Tg2576 mice are reversed with acute calcineurin inhibition. *Behav. Brain Res.* 200, 95–99. doi: 10.1016/j.bbr.2008.12.034

Taglialatela, G., Rastellini, C., and Cicalese, L. (2015). Reduced incidence of dementia in solid organ transplant patients treated with calcineurin inhibitors. *J. Alzheimers Dis.* 47, 329–333. doi: 10.3233/JAD-150065

Takano, T., Han, X., Deane, R., Zlokovic, B., and Nedergaard, M. (2007). Two-photon imaging of astrocytic Ca^{2+} signaling and the microvasculature in experimental mice models of Alzheimer's disease. *Ann. N Y Acad. Sci.* 1097, 40–50. doi: 10.1196/annals.1379.004

Tapella, L., Cerruti, M., Biocotino, I., Stevano, A., Rocchio, F., Canonico, P. L., et al. (2018). TGF-β2 and TGF-β3 from cultured β-amyloid-treated or 3xTg-AD-derived astrocytes may mediate astrocyte-neuron communication. *Eur. J. Neurosci.* 47, 211–221. doi: 10.1111/ejn.13819

Tence, M., Ezan, P., Amigou, E., and Giaume, C. (2012). Increased interaction of connexin43 with zonula occludens-1 during inhibition of gap junctions by G protein-coupled receptor agonists. *Cell Signal* 24, 86–98. doi: 10.1016/j.cellsig.2011.08.006

Thrane, A. S., Rappold, P. M., Fujita, T., Torres, A., Bekar, L. K., Takano, T., et al. (2011). Critical role of aquaporin-4 (AQP4) in astrocytic Ca^{2+} signaling events elicited by cerebral edema. *Proc. Natl. Acad. Sci. U S A* 108, 846–851. doi: 10.1073/pnas.1015217108

Tian, R., Wu, X., Hagemann, T. L., Sosunov, A. A., Messing, A., McKhann, G. M., et al. (2010). Alexander disease mutant glial fibrillary acidic protein compromises glutamate transport in astrocytes. *J. Neuropathol. Exp. Neurol.* 69, 335–345. doi: 10.1097/NEN.0b013e3181d3cb52

van Landeghem, F. K., Weiss, T., Oehmichen, M., and von Deimling, A. (2006). Decreased expression of glutamate transporters in astrocytes after human traumatic brain injury. *J. Neurotrauma* 23, 1518–1528. doi: 10.1089/neu.2006.23.1518

Vardjan, N., Verkhratsky, A., and Zorec, R. (2017). Astrocytic pathological calcium homeostasis and impaired vesicle trafficking in neurodegeneration. *Int. J. Mol. Sci.* 18:E358. doi: 10.3390/ijms18020358

Verkhratsky, A., Rodríguez-Arellano, J. J., Parpura, V., and Zorec, R. (2017). Astroglial calcium signalling in Alzheimer's disease. *Biochem. Biophys. Res. Commun.* 483, 1005–1012. doi: 10.1016/j.bbrc.2016.08.088

Vinadé, L., Gonçalves, C. A., Wofchuk, S., Gottfried, C., and Rodnight, R. (1997). Evidence for a role for calcium ions in the dephosphorylation of glial fibrillary acidic protein (GFAP) in immature hippocampal slices and in astrocyte cultures from the rat. *Dev. Brain Res.* 104, 11–17. doi: 10.1016/s0165-3806(97)00114-4

Wang, F., Du, T., Liang, C., Verkhratsky, A., and Peng, L. (2015). Ammonium increases Ca^{2+} signalling and upregulates expression of $Ca_v1.2$ gene in astrocytes in primary cultures and in the *in vivo* brain. *Acta Physiol.* 214, 261–274. doi: 10.1111/apha.12500

Watanabe, K., Uemura, K., Asada, M., Maesako, M., Akiyama, H., Shimohama, S., et al. (2015). The participation of insulin-like growth factor-binding protein 3 released by astrocytes in the pathology of Alzheimer's disease. *Mol. Brain* 8:82. doi: 10.1186/s13041-015-0174-2

Wen, Z., Guirland, C., Ming, G. L., and Zheng, J. Q. (2004). A CaMKII/calcineurin switch controls the direction of Ca^{2+}-dependent growth cone guidance. *Neuron* 43, 835–846. doi: 10.1016/j.neuron.2004.08.037

Willis, M., Kaufmann, W. A., Wietzorrek, G., Hutter-Paier, B., Moosmang, S., Humpel, C., et al. (2010). L-type calcium channel CaV 1.2 in transgenic mice overexpressing human AβPP751 with the London (V717I) and Swedish (K670M/N671L) mutations. *J. Alzheimers Dis.* 20, 1167–1180. doi: 10.3233/JAD-2010-091117

Wu, Y., Borde, M., Heissmeyer, V., Feuerer, M., Lapan, A. D., Stroud, J. C., et al. (2006). FOXP3 controls regulatory T cell function through cooperation with NFAT. *Cell* 126, 375–387. doi: 10.1016/j.cell.2006.05.042

Wu, D. C., Chen, R. Y., Cheng, T. C., Chiang, Y. C., Shen, M. L., Hsu, L. L., et al. (2017). Spreading depression promotes astrocytic calcium oscillations and enhances gliotransmission to hippocampal neurons. *Cereb. Cortex* doi: 10.1093/cercor/bhx192[Epub ahead of print].

Wu, H. Y., Hudry, E., Hashimoto, T., Kuchibhotla, K., Rozkalne, A., Fan, Z., et al. (2010). Amyloid β induces the morphological neurodegenerative triad of spine loss, dendritic simplification and neuritic dystrophies through calcineurin activation. *J. Neurosci.* 30, 2636–2649. doi: 10.1523/JNEUROSCI.4456-09.2010

Wu, H. Y., Hudry, E., Hashimoto, T., Uemura, K., Fan, Z. Y., Berezovska, O., et al. (2012). Distinct dendritic spine and nuclear phases of calcineurin activation after exposure to amyloid-β revealed by a novel fluorescence resonance energy transfer assay. *J. Neurosci.* 32, 5298–5309. doi: 10.1523/JNEUROSCI.0227-12.2012

Xiong, T. Q., Chen, L. M., Tan, B. H., Guo, C. Y., Li, Y. N., Zhang, Y. F., et al. (2018). The effects of calcineurin inhibitor FK506 on actin cytoskeleton, neuronal survival and glial reactions after pilocarpine-induced status epilepticus in mice. *Epilepsy Res.* 140, 138–147. doi: 10.1016/j.eplepsyres.2018.01.007

Xu, J. H., Long, L., Tang, Y. C., Hu, H. T., and Tang, F. R. (2007). $Ca_v1.2$, $Ca_v1.3$, and $Ca_v2.1$ in the mouse hippocampus during and after pilocarpine-induced status epilepticus. *Hippocampus* 17, 235–251. doi: 10.1002/hipo.20263

Xu, J. H., Long, L., Wang, J., Tang, Y. C., Hu, H. T., Soong, T. W., et al. (2010). Nuclear localization of $Ca_v2.2$ and its distribution in the mouse central nervous system, and changes in the hippocampus during and after pilocarpine-induced status epilepticus. *Neuropathol. Appl. Neurobiol.* 36, 71–85. doi: 10.1111/j.1365-2990.2009.01044.x

Yan, H. Q., Shin, S. S., Ma, X., Li, Y., and Dixon, C. E. (2014). Differential effect of traumatic brain injury on the nuclear factor of activated T Cells C3 and C4 isoforms in the rat hippocampus. *Brain Res.* 1548, 63–72. doi: 10.1016/j.brainres.2013.12.028

Yi, M., Yu, P., Lu, Q., Geller, H. M., Yu, Z., and Chen, H. (2016). KCa3.1 constitutes a pharmacological target for astrogliosis associated with Alzheimer's disease. *Mol. Cell. Neurosci.* 76, 21–32. doi: 10.1016/j.mcn.2016.08.008

Yoshiyama, Y., Higuchi, M., Zhang, B., Huang, S. M., Iwata, N., Saido, T. C., et al. (2007). Synapse loss and microglial activation precede tangles in a P301S tauopathy mouse model. *Neuron* 53, 337–351. doi: 10.1016/j.neuron.2007.01.010

Zabel, M. K., and Kirsch, W. M. (2013). From development to dysfunction: microglia and the complement cascade in CNS homeostasis. *Ageing Res. Rev.* 12, 749–756. doi: 10.1016/j.arr.2013.02.001

Zamanian, J. L., Xu, L., Foo, L. C., Nouri, N., Zhou, L., Giffard, R. G., et al. (2012). Genomic analysis of reactive astrogliosis. *J. Neurosci.* 32, 6391–6410. doi: 10.1523/JNEUROSCI.6221-11.2012

Zheng, K., Bard, L., Reynolds, J. P., King, C., Jensen, T. P., Gourine, A. V., et al. (2015). Time-resolved imaging reveals heterogeneous landscapes of nanomolar Ca^{2+} in neurons and astroglia. *Neuron* 88, 277–288. doi: 10.1016/j.neuron.2015.09.043

Zorec, R., Parpura, V., and Verkhratsky, A. (2018). Astroglial vesicular network: evolutionary trends, physiology and pathophysiology. *Acta Physiol.* 222:e12915. doi: 10.1111/apha.12915

Zumkehr, J., Rodriguez-Ortiz, C. J., Cheng, D., Kieu, Z., Wai, T., Hawkins, C., et al. (2015). Ceftriaxone ameliorates tau pathology and cognitive decline via restoration of glial glutamate transporter in a mouse model of Alzheimer's disease. *Neurobiol. Aging* 36, 2260–2271. doi: 10.1016/j.neurobiolaging.2015.04.005

Conflict of Interest Statement: The authors declare that the research was conducted in the absence of any commercial or financial relationships that could be construed as a potential conflict of interest.

frontiers in Aging Neuroscience

ORIGINAL RESEARCH
published: 24 April 2018
doi: 10.3389/fnagi.2018.00093

Cyclosporin A-Mediated Activation of Endogenous Neural Precursor Cells Promotes Cognitive Recovery in a Mouse Model of Stroke

*Labeeba Nusrat[1], Jessica M. Livingston-Thomas[1], Vaakiny Raguthevan[1], Kelsey Adams[2], Ilan Vonderwalde[3], Dale Corbett[4,5] and Cindi M. Morshead[1,2,3]**

[1]Department of Surgery, University of Toronto, Toronto, ON, Canada, [2]Institute of Medical Sciences, University of Toronto, Toronto, ON, Canada, [3]Institute of Biomaterials and Biomedical Engineering, University of Toronto, Toronto, ON, Canada, [4]Department of Cellular & Molecular Medicine, University of Ottawa, Ottawa, ON, Canada, [5]Canadian Partnership for Stroke Recovery, Ottawa, ON, Canada

Cognitive dysfunction following stroke significantly impacts quality of life and functional independance; yet, despite the prevalence and negative impact of cognitive deficits, post-stroke interventions almost exclusively target motor impairments. As a result, current treatment options are limited in their ability to promote post-stroke cognitive recovery. Cyclosporin A (CsA) has been previously shown to improve post-stroke functional recovery of sensorimotor deficits. Interestingly, CsA is a commonly used immunosuppressant and also acts directly on endogenous neural precursor cells (NPCs) in the neurogenic regions of the brain (the periventricular region and the dentate gyrus). The immunosuppressive and NPC activation effects are mediated by calcineurin-dependent and calcineurin-independent pathways, respectively. To develop a cognitive stroke model, focal bilateral lesions were induced in the medial prefrontal cortex (mPFC) of adult mice using endothelin-1. First, we characterized this stroke model in the acute and chronic phase, using problem-solving and memory-based cognitive tests. mPFC stroke resulted in early and persistent deficits in short-term memory, problem-solving and behavioral flexibility, without affecting anxiety. Second, we investigated the effects of acute and chronic CsA treatment on NPC activation, neuroprotection, and tissue damage. Acute CsA administration post-stroke increased the size of the NPC pool. There was no effect on neurodegeneration or lesion volume. Lastly, we looked at the effects of chronic CsA treatment on cognitive recovery. Long-term CsA administration promoted NPC migration toward the lesion site and rescued cognitive deficits to control levels. This study demonstrates that CsA treatment activates the NPC population, promotes migration of NPCs to the site of injury, and leads to improved cognitive recovery following long-term treatment.

Keywords: stroke, cognitive dysfunction, neural precursor cells, immunosuppression, neural precursor activation, cognitive recovery, endogenous repair

OPEN ACCESS

Edited by:
Brandi Ormerod, University of Florida, United States

Reviewed by:
Ashok K. Shetty, Texas A&M University College of Medicine, United States
Aurel Popa-Wagner, Department of Neurology, University Hospital Essen, Germany

****Correspondence:***
Cindi M. Morshead
cindi.morshead@utoronto.ca

Received: *01 February 2018*
Accepted: *19 March 2018*
Published: *24 April 2018*

Citation:
Nusrat L, Livingston-Thomas JM, Raguthevan V, Adams K, Vonderwalde I, Corbett D and Morshead CM (2018) Cyclosporin A-Mediated Activation of Endogenous Neural Precursor Cells Promotes Cognitive Recovery in a Mouse Model of Stroke. Front. Aging Neurosci. 10:93. doi: 10.3389/fnagi.2018.00093

INTRODUCTION

Stroke is a leading cause of death and chronic disability. Prevalence of post-stroke cognitive dysfunction can be up to 80% of stroke survivors (Sun et al., 2014), including impairments in learning and memory and deficits in executive functions (Zinn et al., 2007; Hofmann et al., 2012; Douiri et al., 2013). Such impairments can persist for years (Poulin et al., 2012) and are associated with higher rates of long-term post-stroke disability (Cumming et al., 2013; Mullick et al., 2015), impacting the quality of life of survivors. Areas of the prefrontal cortex, such as anterior cingulate and dorsolateral prefrontal cortices, are responsible for regulating executive functioning which is commonly affected after stroke (Kumral et al., 2002; Pohjasvaara et al., 2002; Poulin et al., 2012). Executive functions include an array of complex behaviors that govern self-regulatory actions and goal-management such as problem solving, cognitive flexibility, decision making and working memory (Zinn et al., 2007; Hofmann et al., 2012; Cordova et al., 2014) Despite the profound impact of cognitive deficits after stroke, therapeutic strategies to promote long-term cognitive recovery have attracted relatively little attention (Zinn et al., 2007; Cumming et al., 2013). Currently, cognitive rehabilitation which targets spared skills to develop compensatory strategies is the only treatment option for stroke survivors, and has limited efficacy (Adams et al., 2007; Poulin et al., 2012). Thus, it is timely to consider the development of strategies to enhance neural repair for the treatment of post-stroke cognitive deficits.

The adult mammalian brain contains neural stem cells that possess the ability to self-renew and generate progeny that differentiate into neural phenotypes, making them promising therapeutic targets to promote neural regeneration and plasticity. Stem cells and their progeny (together termed neural precursor cells, NPCs) exist in the subependyma (SE) lining the walls of the lateral ventricles, and the subgranular zone of dentate gyrus, where they contribute to ongoing neurogenesis in the olfactory bulb and hippocampus, respectively (Doetsch, 2003). A number of factors have been shown to activate endogenous NPCs. For example, brain injury activates endogenous NPCs, leading to an expansion of the size of the NPC pool, migration, and neurogenesis (Parent et al., 2002; Jin et al., 2003; Ahmed et al., 2014) Administration of growth factors and small molecules can similarly promote NPC expansion, migration and differentiation (Kolb et al., 2007; Hunt et al., 2010; Dadwal et al., 2015). We have previously demonstrated that the commonly used immunosuppressant, Cyclosporin A (CsA), has direct pro-survival effects on NPCs both *in vitro* and *in vivo*, thereby expanding the size of the NPC pool (Hunt et al., 2010; Chow and Morshead, 2016). Interestingly, while the immunosuppressant effects of CsA are mediated by a calcineurin-dependent pathway, with downstream effects resulting in T-cell regulation, the NPC pro-survival effects of CsA result from activation of a calcineurin-independent pathway (Sachewsky et al., 2014), which inhibits mitochondrial pore formation and effectively blocks apoptotic pathways. In models of sensorimotor stroke, CsA administration leads to NPC pool expansion, tissue regeneration, and motor recovery (Erlandsson et al., 2011; Sachewsky et al., 2014). Thus, CsA shows therapeutic promise, and herein we propose to study its efficacy for the treatment of cognitive impairments after stroke.

To investigate the potential of this endogenous repair strategy to promote cognitive recovery following stroke, we first established a reproducible cognitive stroke model in mice. Based on a similar model in rats (Livingston-Thomas et al., 2015), bilateral focal lesions were produced using endothelin-1 (ET-1) in the medial prefrontal cortex, which is analogous to the human cingulate and dorsolateral prefrontal cortices (Seamans et al., 2008; Cordova et al., 2014). Stroke-injured mice displayed significant short- and long-term cognitive deficits, and an expansion in the size of the NPC pool similar to that observed following ET-1-induced sensorimotor stroke (Sachewsky et al., 2014). Chronic CsA treatment promoted migration of NPCs to the site of the lesion, and rescued cognitive performance to control levels following stroke, demonstrating the therapeutic potential of this endogenous NPC activation strategy to enhance cognitive recovery following stroke.

MATERIALS AND METHODS

Animals

This study was carried out in accordance with the recommendations of guidelines of the University of Toronto Animal Care Committee and the Canadian Council of Animal Care. The protocol was approved by the University of Toronto Animal Care Committee. Sixty adult male C57BL/6 mice (6–8 weeks of age; 20–25 g; Charles River) were single housed on a 12-h light/dark cycle with food and water *ad libitum*. For each experiment, specific *n*-numbers are presented in the figure captions. Mice were acclimated to the facility for 1 week prior to the experiment. Mice were randomly assigned to the uninjured Control, Stroke-alone, or Stroke+CsA group.

Stroke and CsA Administration

To induce mPFC stroke, mice received stereotaxic microinjections of ET-1 (0.76 μl; 800 picomolar; Calbiochem) at two bilateral injection sites (for a total of four injections): (1) anteroposterior (AP) +2.2 mm from Bregma; mediolateral (ML) ±0.4 mm from midline; dorsoventral (DV) −2.4 mm from skull surface, and (2) AP +1.5 mm; ML ±0.4 mm; DV 2.6 mm. Immediately following injections, mini osmotic pumps (Alzet, Cupertino, CA, USA) filled with CsA (15 mg/kg/day; dissolved in 65% ethanol and 35% cremaphor) were implanted subcutaneously and replaced as required based on the length of the experiment. Sensorimotor stroke was induced as described previously (Sachewsky et al., 2014).

Neurosphere Assay

Animals were anesthetized with isoflurane, quickly decapitated, and the brain was removed. The adult SE was dissected and cultured as previously described. Briefly, tissue was collected and enzymatically dissociated, triturated into a single cell suspension and plated at clonal density (10 cells/μl) in serum free media (SFM) supplemented with EGF (20 ng/ml), FGF (10 ng/ml) and

heparin (7.35 ng/ml; all from Sigma; Coles-Takabe et al., 2008). The number of neurospheres was counted following 7 days in culture. Neurospheres originate from a single stem cell; hence, the number of neurospheres reflects the size of the NPC pool (Hunt et al., 2010). The assay was performed at 7 and 60 days following stroke. For cortical neurosphere assays, tissue was dissected from the lesioned bilateral mPFC region and plated as described (Erlandsson et al., 2011).

Behavioral Testing

All behavioral testing took place after stroke surgery, with the exception of the adhesive removal test which included baseline testing prior to injury. Prior to testing, all animals were acclimated to the testing room for at least 10 min.

Adhesive Removal Test

To screen for sensorimotor deficits, the adhesive removal test was performed as previously described (Bouet et al., 2009). A 0.3 × 0.4 cm piece of tape was placed on the center of each forepaw, and the latency to contact and then remove the tape was measured. A functional score was calculated as ([latency to remove] − [latency to contact]). The task consisted of 7 days of training to ensure performance under 1 min, and 2 days of testing on day 4 and day 5 after stroke. Post-stroke performance was averaged from the 2 days of testing for analysis.

Puzzle Box Task

The Puzzle Box (PB) task is used to assess cognitive functions including problem-solving, and short- and long-term memory (Ben Abdallah et al., 2011). Mice were placed into a brightly-lit start zone of a rectangular box, and were required to travel to a dark, enriched goal zone. The test was performed as three trials per day (maximum 300 s) with a 2 min inter-trial interval, for three consecutive days. The test was performed at three time points throughout the experiment: post stroke days 4–6, 22–24 and 45–47. Trials were filmed from above using Viewer software (Bioserve, Bonn, Germany).

On Trial 1, mice were allowed easy access to the goal zone through an open door and clear underpass. Trials 2 and 3 required access through the underpass only, and the doorway blocked. The following day, the same paradigm was repeated (Trial 4; long term memory), following which accessibility was made more difficult by blocking the underpass with bedding, requiring which mice to remove it in order to enter the goal zone (Trial 5; problem solving). That paradigm was then repeated in Trial 6 (short-term memory). On the last day, the paradigm is repeated once more (Trial 7; long-term memory), following which the underpass is blocked with a cardboard plug that must be removed (Trial 8; problem solving). Lastly, that paradigm is repeated (Trial 9; short-term memory).

Morris Water Maze

The morris water maze (MWM) evaluates spatial learning, long-term memory, and behavioral flexibility. The test takes place over three phases: acquisition (5 days), probe (1 day) and reversal (4 days). During the acquisition phase, animals must locate a static hidden platform located in a circular pool of water. Mice were given four trials/day, each from a pseudorandomly assigned quadrant, with a maximum trial time of 60 s. Once the platform was located, mice were returned to their home cage for a 15 min inter-trial interval. The latency to locate the platform was recorded as the average trial time over 5 days. Twenty-four hours following the last acquisition trial, a probe test was performed. The platform was removed, mice were placed into the pool at a randomly assigned start location, and allowed to search for the platform for 60 s. The proportion of time spent searching in the maze quadrant that previously contained the platform was recorded. Twenty-four hours later the reversal phase began, for which the platform was replaced in the quadrant opposite from the original location, and trials were run as described in the acquisition phase. Mice were tested from days 35–44 post-stroke.

Open Field Task

The open field task was used to assess anxiety-related behavior. Mice were placed into a 60 × 60 cm chamber conceptually divided into 16 equal squares. The central eight squares were defined as the central zone, and the remaining squares were considered the edge. Animals were allowed to explore the environment for 10 min. Locomotor activity in the central and edge zones were evaluated on day 7 and 48 post-stroke.

Tissue Preparation and Histology

All animals were deeply anesthetized with tribromoethanol (250 mg/kg; Sigma-Aldrich) and transcardially perfused with 0.01 M phosphate buffered saline (PBS), followed by 4% paraformaldehyde. Brains were collected and stored in 4% paraformaldehyde overnight, then transferred to 20% sucrose solution until saturated. Coronal brain sections (20 μm) were collected in series.

Lesion Volume and Neural Degeneration

Coronal sections were collected at days 1, 4 and 10 post-stroke. Sections were stained with cresyl violet (Sigma-Aldrich) for lesion volume analysis. Lesion, defined as morphological changes in tissue, lack of staining, or pallor, was measured in a pre-calculated reference area using ImageJ software (National Institute of Health, Bethesda, MA, USA). The sections were imaged at 240 μm intervals and the lesion volume was calculated using the formula (lesion area) × (distance between sections).

To assess neural degeneration, Fluoro Jade (FJ) C staining was performed. A stock solution of FJC was prepared (25 mg FJC in 250 mL dH_2O). Slides were immersed in 1% NaOH in 80% ethanol for 5 min, rinsed in 70% ethanol and distilled H_2O for 2 min, each. Next, slides were in incubated in 0.06% $KMnO_4$ for 10 min and then rinsed again in dH_2O for 2 min. The following day, slides were incubated in a working solution of FJC (2 ml of stock solution in 198 mL dH_2O and 198 mL acetic acid) for 30 min and washed in dH_2O prior to cover slipping. The total numbers of FJC+ cells were manually counted using ImageJ (NIH) from every 10th section (i.e., 200 μm apart) between +2.3 and +1.10 mm from Bregma, within a pre-determined region of interest. Within a brain, coronal sections were divided into two clusters based on morphological characteristics (anterior and posterior

to the genu of the corpus callosum). The total volume of the region of interest was 4.64 mm^3, a sum of cluster 1 (2.55 × 1.0 × 1.6 mm) and cluster 2 (1.5 × 1.0 × 1.16 mm) volumes. The region of interest was kept consistent between all brains.

Statistical Analysis

Statistical analyses were performed using Graphpad Prism v6.0 and Microsoft Excel 2011. Two-tailed *t*-tests were used for two group comparisons and two-way repeated measures ANOVAs were used for multiple group comparisons across more than one trial. For multiple group comparisons, *post hoc* tests Tukey or Dunnett were used when required based on group comparisons against each other, or group comparisons against one fixed control group, respectively. All data are reported as mean ± SEM. Statistical significance was considered when $p \leq 0.05$.

RESULTS

mPFC Stroke Leads to Targeted Lesions and Persistent Cognitive Impairments

We first sought to establish a stroke model in mice that would result in persistent cognitive impairments using a bilateral injury model similar to those previously described in rats (Cordova et al., 2014; Livingston-Thomas et al., 2015). Bilateral ET-1 injections resulted in damage confined to the prelimbic, infralimbic and anterior cingulate subdivisions of the mPFC. Lesions spanned from approximately 2.34 mm to 1.10 mm anterior to Bregma, producing an average volume of 4.98 ± 0.92 mm^3 at 4 days post-stroke (**Figure 1A**).

To assess cognitive outcome in the acute post-stroke phase, performance in the PB task was assessed at 4–6 days following injury. A cognitive deficit was defined as a significantly increased latency to enter the goal box compared to controls. In Stroke-alone mice, a significant deficit was detected on Trials 5, 6 and 9 (Stroke-alone: Trial 5: 249.94 ± 14 s; Trial 6: 164.39 ± 27 s; Trial 9: 208.39 ± 22 s; Controls: Trial 5: 185.67 ± 21 s; Trial 6: 90.13 ± 21 s; Trial 9: 145.67 ± 31 s; $p < 0.05$; **Figure 1B**). Therefore, bilateral mPFC stroke produced acute cognitive impairments in problem-solving and short-term memory after stroke.

Separate cohorts of mice were used to evaluate chronic cognitive impairment using the MWM test and Y-maze task. In the MWM test, there were no deficits detected in the acquisition or probe phases of the test ($p > 0.05$ for both); however, in the reversal phase, mPFC stroke animals exhibited a significant impairment, with a higher overall latency to find the platform compared to controls (Control: 17.5 ± 1.8 s; Stroke-alone: 22.6 ± 2.1 s; $F_{(1,20)} = 4.751$, $p = 0.045$; **Figure 1C**).

The Y-maze spontaneous alternation task was used to assess whether mPFC stroke resulted in deficits in frontal lobe-mediated spatial working memory on day 49 post-stroke. There were no significant differences in the spontaneous alternation percentage (SAP) between groups (data not shown). This demonstrates that mPFC stroke resulted in persistent chronic impairment in behavioral flexibility without affecting spatial working memory.

To rule out any confounding effect of sensorimotor impairments on cognitive tests, we used the adhesive removal test (Bouet et al., 2009). As predicted, mice with unilateral sensorimotor stroke lesions exhibited a significant contralateral (left) impairment (125.67 ± 43.44 s (left), 6.25 ± 0.39 s (right); $p < 0.01$; **Figure 1D**). Sensorimotor impairment was not observed in the mPFC lesioned mice ($p > 0.05$), consistent with histological examination of affected brain regions revealing no damage to the sensorimotor cortex.

CsA Administration Expands the Size of the NPC Pool but Is Not Neuroprotective

Next we investigated whether administration of CsA from the time of stroke would have an effect on recovery. First, the neurosphere assay was performed on the SE at day 7 post-stroke to evaluate the effect of stroke and CsA treatment on the size of the NPC pool (**Figure 2Ai**). We observed a significant expansion in the size of the NPC pool in Stroke+CsA mice (1.7 ± 0.04 fold; **Figure 2Aii**). A slight non-significant expansion was observed in Stroke-alone mice (Control: 39 ± 8 neurospheres; Stroke-alone: 54 ± 2 neurospheres; Stroke+CsA: 65 ± 16 neurospheres per 5000 cells; $p < 0.01$). Thus, CsA treatment following mPFC stroke significantly expands the NPC population within the first week.

To determine if CsA delivery was neuroprotective post-stroke, the numbers of FJC+ cells and the lesion volume were analyzed on days 1, 4 and 10 after mPFC stroke. There were no significant differences in the number of FJC+ cells in Stroke-alone vs. Stroke+CsA groups at any of these time points (day 1 Stroke-alone: 2,68,799 ± 24,878 cells, Stroke+CsA: 2,80,089 ± 47,471 cells; day 4 Stroke-alone: 1,34,071 ± 36,015 cells; Stroke+CsA: 1,89,036 ± 71,746 cells; day 10 Stroke-alone: 18,480 ± 2372 cells; Stroke+CsA: 6209 ± 655 cells; **Figures 2Bi,ii**). In both the Stroke-alone and Stroke+CsA groups, the number of FJC+ cells declined from day 1 to 10 post-stroke ($p < 0.05$). There were no significant differences in lesion volume between the Stroke-alone and Stroke+CsA groups at any time point (**Figure 2C**). Taken together, these findings demonstrate that CsA treatment did not have neuroprotective effects when administration was started immediately after stroke.

Chronic CsA Administration Rescues Cognitive Impairment Following mPFC Stroke in the Puzzle Box Task

Cognitive performance following CsA treatment was assessed at early (post-stroke days 4–6), middle (post-stroke days 22–24), and late (post-stroke days 45–47) time points using the PB (**Figure 3A**). Early post-stroke deficits were not improved in the CsA-treated mice. However, at both middle and late time points, Stroke+CsA animals were recovered to control level performance, while Stroke-alone animals continued to exhibit deficits (**Figure 3B**). Late time point data were combined, revealing that overall, the Stroke-alone mice exhibited significant

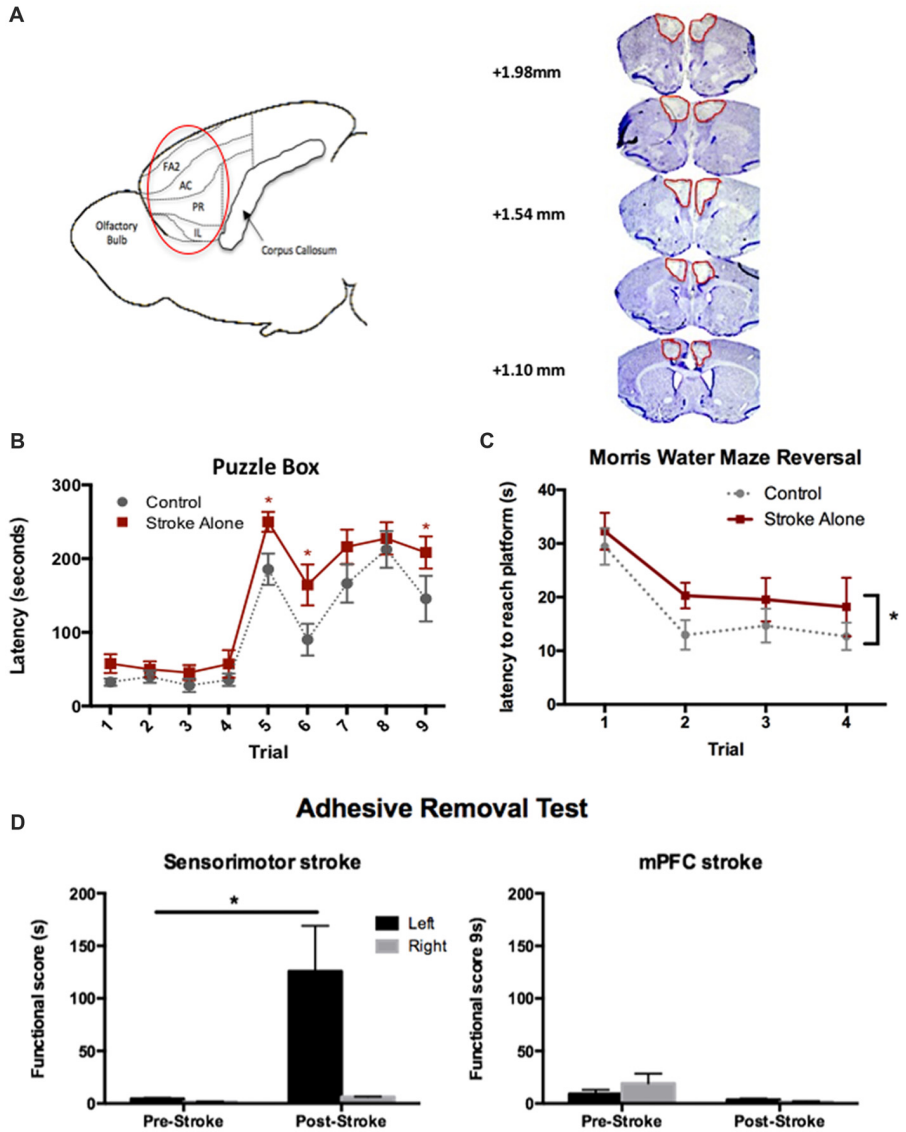

FIGURE 1 | Endothelin-1 (ET-1)-induced cognitive model of stroke in mice. **(A)** Sagittal representation of the lesioned areas of the brain (circled). FA2, frontal area 2; AC, anterior cingulate cortex; PR, prelimbic; IL, infralimbic; cresyl violet stained coronal sections depicting typical medial prefrontal cortex (mPFC) lesion on day 4 post-stroke. **(B)** Significant cognitive impairments following stroke were detected using the Puzzle Box (PB) task at day 4–6 compared to control (n = 18 stroke; 16 control). **(C)** Following stroke, a significant cognitive deficit was detected up to 45 days, using the Morris Water Maze (MWM) reversal test (n = 12 stroke; 10 control). **(D)** Post-stroke functional scores in the adhesive removal test. Unilateral sensory-motor (n = 3), but not bilateral mPFC (n = 7) stroke, resulted in contralesional (left) forepaw deficits compared to baseline performance. *$p < 0.05$.

impairments on Trials 5 (Stroke-alone: 217.25 ± 18 s; Control: 159.79 ± 23 s; $p < 0.05$), Trial 7 (Stroke-alone: 269.11 ± 11 s; Control: 211.82 ± 23 s; $p < 0.05$) and Trial 8 (Stroke-alone: 179.67 ± 21 s; Control: 119.79 ± 25 s; $p < 0.05$), whereas the Stroke+CsA group had recovered to Control performance (Trial 5: 180.44 ± 15 s; Trial 7: 243.19 ± 17 s; Trial 8: 146.38 ± 19 s). Hence, CsA administration reduced long-term cognitive deficits.

We further compared the PB performance in Stroke-alone and Stroke+CsA mice at each of the time points tested. At day 22–24, Stroke+CsA mice showed reduced latency to reach the goal box on Trials 5 and 8 (Trial 5: 178.50 ± 20 s; Trial 8: 139.42 ± 20 s) compared to performance on day 4–6 (Trial 5: 256.94 ± 12 s; Trial 8: 244.00 ± 17 s; $p < 0.01$, $p < 0.001$), suggesting an improvement in the problem-solving deficit that persisted until day 45–47 (Trial 5: 177.13 ± 20 s; Trial 8: 138.56 ± 23 s; **Figure 3C**). The Stroke-alone group did not show any significant changes in performance on Trials 5 and 8 at any of the long-term test points (**Figure 3D**). These findings further support the hypothesis that long-term CsA treatment reduces cognitive impairments following stroke.

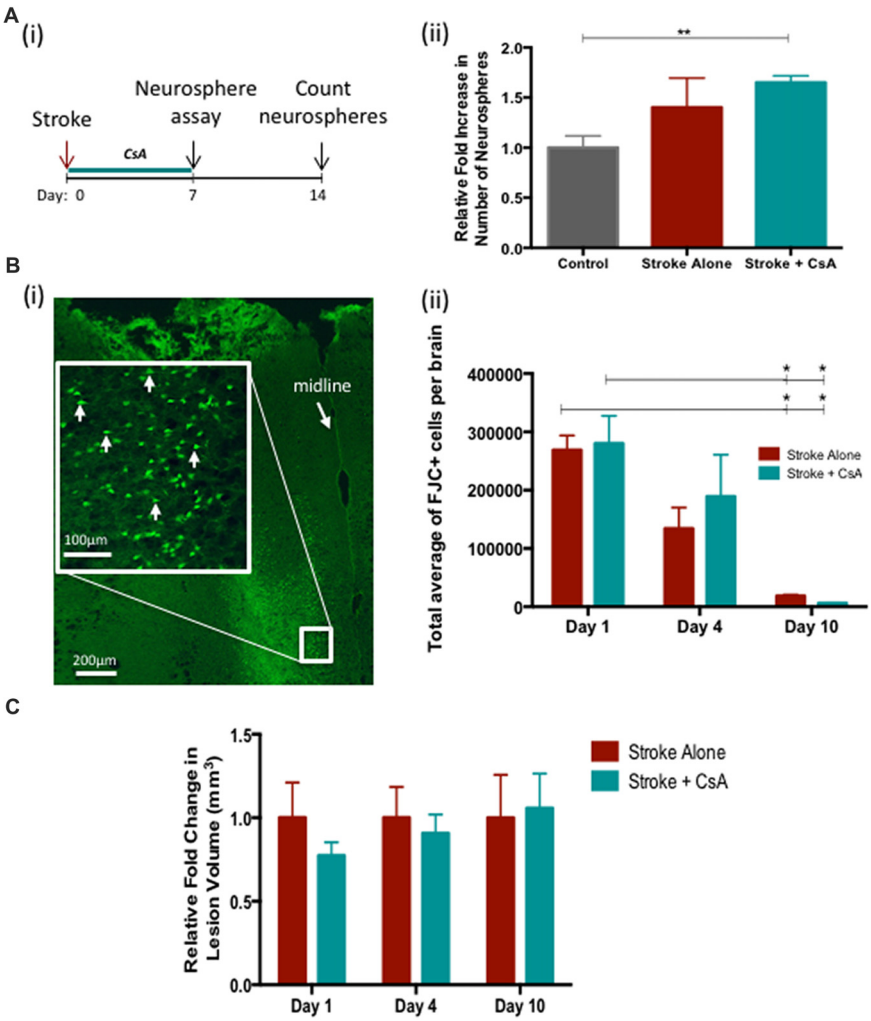

FIGURE 2 | Cyclosporin A (CsA) expands the neural precursor cell (NPC) pool and is not neuroprotective. **(Ai)** Timeline of the experiment. Neurosphere assay was performed on day 7 following Stroke and counted 7 days later. **(ii)** Stroke-Alone (n = 6) results in a slight 1.4 fold increase, while Stroke+CsA (n = 5) caused a significant 1.7 fold increase (n = 7 controls); $^{**}p < 0.01$. **(Bi)** Fluoro Jade C+ (FJC+) cells in the lesioned mPFC (white arrows). **(ii)** There was no significant difference in FJC+ cell counts between Stroke-Alone and Stroke+CsA groups on day 1 (n = 5/group), 4 (n = 5/group) or 10 (n = 3/group) post-stroke. **(C)** Lesion volumes are not significantly different between stroke-alone and stroke+CsA groups (n = 5/group) $^{*}p < 0.05$.

To confirm that the increased latency for stroke animals to complete trials in the PB task was not confounded by alterations in anxiety, the open field task was performed at early (day 7) and late (day 48) time points post-stroke (**Figure 3A**). No significant differences were observed in the amount of time spent in corner zones in any of the groups at either time point (**Figure 3E**). Similarly, the total distance traveled in the corner zones was not significantly different (data not shown). Hence, locomotion and anxiety were not affected by mPFC stroke.

NPCS Migrate to the Site of Injury Following mPFC Stroke

Previous findings have shown NPC migration to the site of the injury following sensorimotor stroke, in the presence and absence of CsA treatment (Sachewsky et al., 2014; Faiz et al., 2015). We investigated whether similar NPC migration was seen in this mPFC stroke model. On day 60 post-stroke, neurospheres were observed in the cortex of the stroke injured mice, but not controls (Stroke-alone and Stroke+CsA cortical neurospheres in 14% and 43% of brains, respectively, compared to 0% of brains in controls). Hence, mPFC stroke can promote NPC migration toward the site of injury, and this migration can be enhanced following CsA administration.

DISCUSSION

In this study, we investigated the efficacy of endogenous NPC activation using CsA to promote cognitive recovery

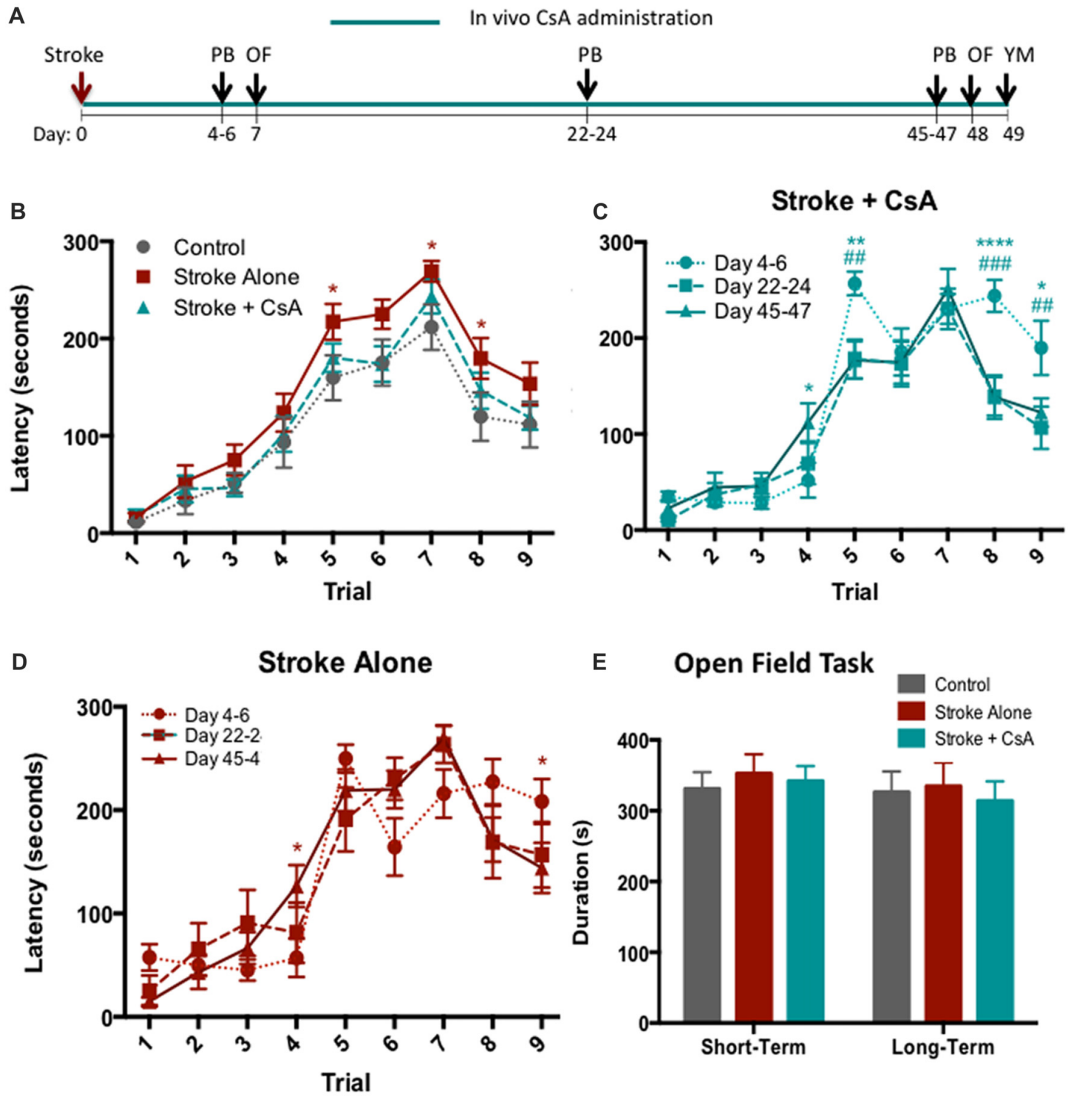

FIGURE 3 | Chronic CsA treatment reduces cognitive impairments. **(A)** Experimental timeline. PB, puzzle box; OF, Open Field; YM, Y-Maze. **(B)** Stroke-Alone (n = 18), but not Stroke+CsA (n = 16), showed persisting cognitive deficits compared to controls (n = 14) in the PB task; $^{*}p < 0.05$. **(C)** Stroke+CsA animals show significant improvement at day 22–24 (#) and 45–47 (*) compared to day 4–6. **(D)** Stroke-alone animals show spontaneous recovery in trial 9 at long-term time points. **(E)** No significant differences were observed in the amount of time spent in the corner zones of the maze between Stroke-alone (n = 11), Stroke+CsA (n = 11), and control (n = 8) groups. Day 22–24: $^{*}p < 0.05$, $^{**}p < 0.01$, $^{****}p < 0.0001$; Day 45–47: $^{\#}p < 0.05$, $^{\#\#}p < 0.01$, $^{\#\#\#}p < 0.001$.

following mPFC stroke. We successfully reproduced a cognitive stroke model in mice. Using the PB and MWM tasks, we demonstrated that mPFC injury resulted in cognitive deficits across various cognitive domains, detectable as early as 4 days and persisting up to 45 days post-stroke, similar to previous findings in rats (Cordova et al., 2014; Livingston-Thomas et al., 2015). Short-term CsA treatment expanded the SE-derived NPC pool early after stroke, and chronic post-stroke CsA administration promoted migration of NPCs and recovery of persistent long-term cognitive deficits. Hence, we have demonstrated that an endogenous NPC activation strategy using the immunosuppressant CsA has the potential to enhance recovery following mPFC stroke.

Sensorimotor stroke results in the transient expansion of the SE NPC pool 7 days post-injury, a phenomenon not observed in the present study. It is possible that the injury induced expansion of the NPC pool in this model at an earlier time post-stroke. Alternatively, the lack of effect observed in this model may be due to the location of the injury; the mPFC is more distant from the SE than the sensorimotor cortex. This finding could have implications for the translation of NPC migration approaches as the degree of NPC activation would vary depending on the site of the stroke lesion. Nonetheless, post-stroke administration of CsA led to a significant expansion of the NPC pool, similar to the effect seen following CsA administration in sensorimotor stroke (Sachewsky et al., 2014).

Our findings reveal that despite CsA's well-documented neuroprotective effects (Sullivan et al., 2011; Yousuf et al., 2011), delivery of CsA did not result in sparing of tissue or neuroprotection post-stroke. Our data suggest that activation of endogenous precursors is sufficient for promoting recovery post-stroke. This is consistent with our previous work showing that a CsA analog, NIM811, is able to promote sensorimotor functional recovery following cortical stroke despite its non-immunosuppressive effects (Sachewsky et al., 2014). Notably, our current findings do not eliminate a potential role for suppressing neuroinflammation in cognitive recovery. To test whether NPC activation is sufficient for recovery as suggested herein, and not due in part to immunosuppression, it would be interesting to explore the effects of NIM811 in this model.

The development of this reproducible model of mPFC stroke provides a foundation to examine the efficacy of novel therapeutics to enhance recovery. Here, we showed that following injury, administration of the immunosuppressant drug CsA can activate NPCs in the adult forebrain and reduce cognitive impairments. Investigating the efficacy of combinatorial strategies (i.e., rehabilitation) alongside small molecule activation strategies to accelerate post-stroke cognitive recovery, as previously shown in sensorimotor stroke (Jeffers et al., 2014), would be a logical next step toward advancing knowledge in this area.

AUTHOR CONTRIBUTIONS

LN was responsible for performing surgeries, experiments, data analyses and interpretation and writing of the manuscript. JML-T conducted the MWM task to assess chronic cognitive impairments and contributed in writing the manuscript. VR was responsible for lesion volume and neural degeneration analyses. KA assisted in performing the neurosphere assays. IV assisted in conducting adhesive tape removal test and subsequent data analyses. DC was involved in providing technical and academic guidance on the project and editing of the manuscript. CMM was the principal investigator of this project and was involved in writing of the manuscript.

FUNDING

This work has been supported by the Heart and Stroke Foundation of Canada and Canadian Institutes of Health Research (CMM and DC).

ACKNOWLEDGMENTS

We thank the Ramsey and Hampson labs (University of Toronto) for providing behavioral equipment for our studies.

REFERENCES

Adams, H. P. Jr., del Zoppo, G., Alberts, M. J., Bhatt, D. L., Brass, L., Furlan, A., et al. (2007). Guidelines for the early management of adults with ischemic stroke: a guideline from the American Heart Association/American Stroke Association Stroke Council, Clinical Cardiology Council, Cardiovascular Radiology and Intervention Council and the Atherosclerotic Peripheral Vascular Disease and Quality of Care Outcomes in Research Interdisciplinary Working Groups: the American Academy of Neurology affirms the value of this guideline as an educational tool for neurologists. *Circulation* 115, e478–e534. doi: 10.1161/CIRCULATIONAHA.107.181486

Ahmed, A., Shtaya, A., Zaben, M., and Gray, W. (2014). Activation of endogenous neural stem cells after traumatic brain injury. *Lancet* 383:S18. doi: 10.1016/s0140-6736(14)60281-6

Ben Abdallah, N. M.-B., Fuss, J., Trusel, M., Galsworthy, M. J., Bobsin, K., Colacicco, G., et al. (2011). The puzzle box as a simple and efficient behavioral test for exploring impairments of general cognition and executive functions in mouse models of schizophrenia. *Exp. Neurol.* 227, 42–52. doi: 10.1016/j.expneurol.2010.09.008

Bouet, V., Boulouard, M., Toutain, J., Divoux, D., Bernaudin, M., Schumann-Bard, P., et al. (2009). The adhesive removal test: a sensitive method to assess sensorimotor deficits in mice. *Nat. Protoc.* 4, 1560–1564. doi: 10.1038/nprot.2009.125

Chow, A., and Morshead, C. M. (2016). Cyclosporin A enhances neurogenesis in the dentate gyrus of the hippocampus. *Stem Cell Res.* 16, 79–87. doi: 10.1016/j.scr.2015.12.007

Coles-Takabe, B. L. K., Brain, I., Purpura, K. A., Karpowicz, P., Zandstra, P. W., Morshead, C. M., et al. (2008). Don't look: growing clonal versus nonclonal neural stem cell colonies. *Stem Cells* 26, 2938–2944. doi: 10.1634/stemcells.2008-0558

Cordova, C. A., Jackson, D., Langdon, K. D., Hewlett, K. A., and Corbett, D. (2014). Impaired executive function following ischemic stroke in the rat medial prefrontal cortex. *Behav. Brain Res.* 258, 106–111. doi: 10.1016/j.bbr.2013.10.022

Cumming, T. B., Marshall, R. S., and Lazar, R. M. (2013). Stroke, cognitive deficits, and rehabilitation: still an incomplete picture. *Int. J. Stroke* 8, 38–45. doi: 10.1111/j.1747-4949.2012.00972.x

Dadwal, P., Mahmud, N., Sinai, L., Azimi, A., Fatt, M., Wondisford, F. E., et al. (2015). Activating endogenous neural precursor cells using metformin leads to neural repair and functional recovery in a model of childhood brain injury. *Stem Cell Rep.* 5, 166–173. doi: 10.1016/j.stemcr.2015.06.011

Doetsch, F. (2003). A niche for adult neural stem cells. *Curr. Opin. Genet. Dev.* 13, 543–550. doi: 10.1016/j.gde.2003.08.012

Douiri, A., Rudd, A. G., and Wolfe, C. D. A. (2013). Prevalence of poststroke cognitive impairment: south london stroke register 1995-2010. *Stroke* 44, 138–145. doi: 10.1161/STROKEAHA.112.670844

Erlandsson, A., Lin, C.-H. A., Yu, F., and Morshead, C. M. (2011). Immunosuppression promotes endogenous neural stem and progenitor cell migration and tissue regeneration after ischemic injury. *Exp. Neurol.* 230, 48–57. doi: 10.1016/j.expneurol.2010.05.018

Faiz, M., Sachewsky, N., Gascón, S., Bang, K. W. A., Morshead, C. M., and Nagy, A. (2015). Adult neural stem cells from the subventricular zone give rise to reactive astrocytes in the cortex after stroke. *Cell Stem Cell* 17, 624–634. doi: 10.1016/j.stem.2015.08.002

Hofmann, W., Schmeichel, B. J., and Baddeley, A. D. (2012). Executive functions and self-regulation. *Trends Cogn. Sci.* 16, 174–180. doi: 10.1016/j.tics.2012.01.006

Hunt, J., Cheng, A., Hoyles, A., Jervis, E., and Morshead, C. M. (2010). Cyclosporin A has direct effects on adult neural precursor cells. *J. Neurosci.* 30, 2888–2896. doi: 10.1523/JNEUROSCI.5991-09.2010

Jeffers, M. S., Hoyles, A., Morshead, C., and Corbett, D. (2014). Epidermal growth factor and erythropoietin infusion accelerate functional recovery in combination with rehabilitation. *Stroke* 45, 1856–1858. doi: 10.1161/STROKEAHA.114.005464

Jin, K., Sun, Y., Xie, L., Peel, A., Mao, X. O., Batteur, S., et al. (2003). Directed migration of neuronal precursors into the ischemic cerebral cortex and striatum. *Mol. Cell. Neurosci.* 24, 171–189. doi: 10.1016/s1044-7431(03)00159-3

Kolb, B., Morshead, C., Gonzalez, C., Kim, M., Gregg, C., Shingo, T., et al. (2007). Growth factor-stimulated generation of new cortical tissue and functional recovery after stroke damage to the motor cortex of rats. *J. Cereb. Blood Flow Metab.* 27, 983–997. doi: 10.1038/sj.jcbfm.9600402

Kumral, E., Bayulkem, G., Evyapan, D., and Yunten, N. (2002). Spectrum of anterior cerebral artery territory infarction: clinical and MRI findings. *Eur. J. Neurol.* 9, 615–624. doi: 10.1046/j.1468-1331.2002.00452.x

Livingston-Thomas, J. M., Jeffers, M. S., Nguemeni, C., Shoichet, M. S., Morshead, C. M., and Corbett, D. (2015). Assessing cognitive function following medial prefrontal stroke in the rat. *Behav. Brain Res.* 294, 102–110. doi: 10.1016/j.bbr.2015.07.053

Mullick, A. A., Subramanian, S. K., and Levin, M. F. (2015). Emerging evidence of the association between cognitive deficits and arm motor recovery after stroke: a meta-analysis. *Restor. Neurol. Neurosci.* 33, 389–403. doi: 10.3233/RNN-150510

Parent, J. M., Vexler, Z. S., Gong, C., Derugin, N., and Ferriero, D. M. (2002). Rat forebrain neurogenesis and striatal neuron replacement after focal stroke. *Ann. Neurol.* 52, 802–813. doi: 10.1002/ana.10393

Pohjasvaara, T., Leskelä, M., Vataja, R., Kalska, H., Ylikoski, R., Hietanen, M., et al. (2002). Post-stroke depression, executive dysfunction and functional outcome. *Eur. J. Neurol.* 9, 269–275. doi: 10.1046/j.1468-1331.2002.00396.x

Poulin, V., Korner-Bitensky, N., Dawson, D. R., and Bherer, L. (2012). Efficacy of executive function interventions after stroke: a systematic review. *Top. Stroke Rehabil.* 19, 158–171. doi: 10.1310/tsr1902-158

Sachewsky, N., Hunt, J., Cooke, M. J., Azimi, A., Zarin, T., Miu, C., et al. (2014). Cyclosporin A enhances neural precursor cell survival in mice through a calcineurin-independent pathway. *Dis. Model. Mech.* 7, 953–961. doi: 10.1242/dmm.014480

Seamans, J. K., Lapish, C., and Durstewitz, D. (2008). Comparing the prefrontal cortex of rats and primates: insights from electrophysiology. *Neurotox Res.* 14, 249–262. doi: 10.1007/BF03033814

Sullivan, P. G., Sebastian, A. H., and Hall, E. D. (2011). Therapeutic window analysis of the neuroprotective effects of cyclosporine A after traumatic brain injury. *J. Neurotrauma* 28, 311–318. doi: 10.1089/neu.2010.1646

Sun, J.-H., Tan, L., and Yu, J.-T. (2014). Post-stroke cognitive impairment: epidemiology, mechanisms and management. *Ann. Transl. Med.* 2:80. doi: 10.3978/j.issn.2305-5839.2014.08.05

Yousuf, S., Atif, F., Kesherwani, V., and Agrawal, S. K. (2011). Neuroprotective effects of Tacrolimus (FK-506) and Cyclosporin (CsA) in oxidative injury. *Brain Behav.* 1, 87–94. doi: 10.1002/brb3.16

Zinn, S., Bosworth, H. B., Hoenig, H. M., and Swartzwelder, H. S. (2007). Executive function deficits in acute stroke. *Arch. Phys. Med. Rehabil.* 88, 173–180. doi: 10.1016/j.apmr.2006.11.015

Conflict of Interest Statement: The authors declare that the research was conducted in the absence of any commercial or financial relationships that could be construed as a potential conflict of interest.

frontiers in Aging Neuroscience

ORIGINAL RESEARCH
published: 08 December 2017
doi: 10.3389/fnagi.2017.00383

Hippocampal Transcriptomic Profiles: Subfield Vulnerability to Age and Cognitive Impairment

Lara Ianov[1,2], Matt De Both[3], Monica K. Chawla[4], Asha Rani[1], Andrew J. Kennedy[5], Ignazio Piras[3], Jeremy J. Day[5], Ashley Siniard[3], Ashok Kumar[1], J. David Sweatt[5,6], Carol A. Barnes[4,7], Matthew J. Huentelman[3,4] and Thomas C. Foster[1]**

[1] Departments of Neuroscience and Genetics and Genomics Program, Evelyn F. and William L. McKnight Brain Institute, University of Florida, Gainesville, FL, United States, [2] Civitan International Research Center, University of Alabama at Birmingham, Birmingham, AL, United States, [3] Neurogenomics Division, Translational Genomics Research Institute, Phoenix, AZ, United States, [4] Evelyn F. McKnight Brain Institute, University of Arizona, Tucson, AZ, United States, [5] Evelyn F. McKnight Brain Institute, University of Alabama, Birmingham, AL, United States, [6] Department of Pharmacology, Vanderbilt University, Nashville, TN, United States, [7] Departments of Psychology, Neurology and Neuroscience, University of Arizona, Tucson, AZ, United States

The current study employed next-generation RNA sequencing to examine gene expression differences related to brain aging, cognitive decline, and hippocampal subfields. Young and aged rats were trained on a spatial episodic memory task. Hippocampal regions CA1, CA3, and the dentate gyrus were isolated. Poly-A mRNA was examined using two different sequencing platforms, Illumina, and Ion Proton. The Illumina platform was used to generate seed lists of genes that were statistically differentially expressed across regions, ages, or in association with cognitive function. The gene lists were then retested using the data from the Ion Proton platform. The results indicate hippocampal subfield differences in gene expression and point to regional differences in vulnerability to aging. Aging was associated with increased expression of immune response-related genes, particularly in the dentate gyrus. For the memory task, impaired performance of aged animals was linked to the regulation of Ca^{2+} and synaptic function in region CA1. Finally, we provide a transcriptomic characterization of the three subfields regardless of age or cognitive status, highlighting and confirming a correspondence between cytoarchitectural boundaries and molecular profiling.

Keywords: aging, hippocampus, cognitive function, transcription, gene expression, Illumina HiSeq, Ion proton

OPEN ACCESS

Edited by:
Nibaldo C. Inestrosa, Pontificia Universidad Católica de Chile, Chile

Reviewed by:
Ana M. Daugherty, University of Illinois at Urbana–Champaign, United States
Stephen D. Ginsberg, Nathan Kline Institute for Psychiatric Research, United States

***Correspondence:**
Ashok Kumar
kash@ufl.edu
Thomas C. Foster
foster1@ufl.edu

Received: *03 August 2017*
Accepted: *07 November 2017*
Published: *08 December 2017*

Citation:
Ianov L, De Both M, Chawla MK, Rani A, Kennedy AJ, Piras I, Day JJ, Siniard A, Kumar A, Sweatt JD, Barnes CA, Huentelman MJ and Foster TC (2017) Hippocampal Transcriptomic Profiles: Subfield Vulnerability to Age and Cognitive Impairment. Front. Aging Neurosci. 9:383. doi: 10.3389/fnagi.2017.00383

INTRODUCTION

Regional variation in brain aging may explain differential susceptibility to impairment in specific cognitive domains over the course of aging. Deficits in hippocampal-dependent episodic memory emerges in middle-age, and the degree or propensity for impairment increases with advancing age in humans and animal models (Uttl and Graf, 1993; Ronnlund et al., 2005; Cansino, 2009; Foster, 2012). There has been a notable increase in recent efforts to accurately identify boundaries that define distinct hippocampal subfields in humans (Yushkevich et al., 2015; Wisse et al., 2016; Berron et al., 2017) and to link behavioral impairments in older individuals to subfield-specific hippocampal volume or activity changes (Mueller and Weiner, 2009; Yassa et al., 2011; Daugherty et al., 2016). Computational approaches, as well as research from brain damaged humans

and animal models, suggest that the different subfields of the hippocampus (CA1, CA3, and dentate gyrus-DG) contribute to various aspects of episodic memory (Rolls and Kesner, 2006; Goodrich-Hunsaker et al., 2008; Maass et al., 2014; Wang and Diana, 2016). This includes pattern separation and completion mechanisms, rapid acquisition, and retention across different time scales. In addition, each region may employ different mechanisms to modulate the strength of their synaptic communication to alter connectivity during the formation of episodic memories. Furthermore, the three regions exhibit differential vulnerability to the aging process (Jackson et al., 2009; Wang et al., 2009; Zeier et al., 2011; Chapman et al., 2012). To address the complexity of the molecular mechanisms linked to age-related changes in hippocampal-dependent cognition, it is necessary to consider the variability in region-specific responses to aging and memory mechanisms.

The current study investigated changes in gene expression within each of the three hippocampal regions in relation to both aging and to cognitive decline in aging. Previous work suggests that brain aging is associated with altered genes and proteins linked to biological processes for cell maintenance and repair, reactions to oxidative stress, neuroinflammation, and neuron-specific signaling, including cell excitability and synaptic plasticity (Blalock et al., 2003; Lu et al., 2004; Fraser et al., 2005; Wang et al., 2009; Burger, 2010; Zeier et al., 2011; Cribbs et al., 2012; Haberman et al., 2013; Masser et al., 2014). It is unclear; however, which biomarkers may represent causative factors for cognitive decline, compensation to maintain cognitive function, or epiphenomenon associated with the aging process (Gray and Barnes, 2015). For example, studies that examine gene expression soon after behavioral testing indicate a decrease in expression of neural activity-related genes; however, it is unclear if altered expression represents the cause of the age-related deficit, or whether the genes are not expressed because learning did not occur (Rowe et al., 2007; Penner et al., 2011; Chawla et al., 2013). Similarly, brain aging can be characterized by an increase in molecular markers of oxidative stress and neuroinflammation (Foster, 2006; Droge and Schipper, 2007; Craft et al., 2012) and it is unclear whether such changes represent precursors to cognitive decline, age-related factors independent of cognition, neuroprotective elements in cognitively unimpaired individuals, or compensation due to changes in afferent connections.

Next-generation sequencing technology is a powerful tool for examining complex processes by monitoring the parallel expression of tens of thousands of genes. Along with the advantage of examining large numbers of transcripts, comes the necessity for validation of the differentially expressed genes. Normally this would occur using a different technique, such as qRT-PCR. We have taken advantage of two different next-generation platforms to confirm differential expression. Our study was designed to increase experimental robustness by utilizing two different laboratories to perform the behavioral characterization of the animals and by using two different next-generation sequencing chemistries on the same RNA samples to minimize false positives and negatives in a staged discovery/validation approach. In this case, transcriptome analysis of the same tissue was performed using Illumina fluorescent labeling and Ion Proton semiconductor measures of proton release during sequencing-by-synthesis. Each technology has pros and cons (Jessri and Farah, 2014); however, previous reports indicate a good concordance in the accuracy of expression profiling between the different platforms (Kusko et al., 2014; Li et al., 2015; Reuter et al., 2015). This study was designed to lead to a high probability of independent validation in other laboratories.

METHODS

Animals

Procedures involving animal subjects have been reviewed and approved by the Institutional Animal Care and Use Committee at the University of Arizona (AZ) and University of Florida (FL) and were in accordance with guidelines established by the U.S. Public Health Service Policy on Humane Care and Use of Laboratory. Male Fischer 344 rats of two ages, young (5–6 months, total $n = 10$; $n = 5$ AZ, $n = 5$ FL) and aged (17–22 months, total $n = 24$; $n = 11$ AZ, $n = 13$ FL) were obtained from National Institute on Aging's colonies (Taconic, FL; Charles River, AZ). Animals were maintained on a 12:12 h light/dark schedule, and provided *ad libitum* access to food and water. Animal characterization was performed at two sites—University of Arizona and University of Florida—and the resulting data were combined and analyzed as a single cohort.

Morris Water Maze

Procedures for the water maze have previously been published (Foster et al., 1991; Bean et al., 2015). Animals were trained in a tank, 1.7 m (FL), 1.8 m (AZ) in diameter, positioned in room that provided cues for the animals. Water ($27 \pm 2^{\circ}$C) was maintained at a level approximately 8 cm below the surface of the tank. For cue and spatial tasks, training consisted of five blocks with three trials per block and training on each task was massed into a single day. Inter-trial intervals were 20 s and inter-block intervals were ∼15 min. Rats remained on the platform between trials and in home cages under the heat lamp after each block. Behavioral data were acquired with either Noldus EthoVision computer tracking software (Noldus Information Technology, (Leesburg, VA) in FL or AnyMaze (Wood Dale, IL) in AZ and included path-length and time in the goal and opposite quadrants.

Rats were first trained on the cue discrimination version of the water escape task. The escape platform was extended approximately 1 cm above the water level and its location was signaled by a visual cue. For each trial, the platform position and start location were randomized. If an animal did not escape the water maze within 60 s, the rat was gently guided to the platform. Three days following cue training, animals were trained on the spatial discrimination task. For spatial discrimination, the escape platform was hidden approximately 1.5 cm beneath the water level and remained in the same location relative to the distal cues in the room for the duration of the initial spatial training. Fifteen minutes following the end of training on block 5, a free-swim probe trial was administered as a measure of learning. For the probe trial, the platform was removed and the animal placed in the tank for 60 s. A spatial discrimination index was computed

according to the formula (G − O)/(G + O) where G and O represent the percent of time spent in the goal quadrant and quadrant opposite the goal, respectively.

Statistical Analysis of Behavior

The mean distance to find the platform during the first training block was used as a baseline for the water maze cue and spatial tasks and the mean percent change from the baseline was calculated for each subsequent block. Repeated measures analyses of variance (ANOVAs) were used to examine age and training effects over blocks of trials. One-way ANOVAs were used to examine age effects for the water maze probe trial discrimination index. Fisher's protected least significant difference comparisons, with the *p*-value set at 0.05, were used as *post hoc* tests to localize differences. Pearson's correlations were calculated between the distance measures for the last block of cue and spatial discrimination trials in order to determine if differences in sensory-motor function or procedural learning contributed to spatial learning. Correlations were limited to within each age group.

Tissue Collection

Two weeks following water maze testing, rats were briefly anesthetized using isoflurane (Piramal Healthcare) and then quickly decapitated. The brains were rapidly removed, briefly rinsed in sterile saline, and the hippocampus was dissected out using a microspatula, razor blade, and surgical scissors. Methods for dissection of hippocampal subfields was adapted from previous work, which enabled isolation of CA1, CA3, and the dentate gyrus (DG) along the rostral and ventral hippocampus (Lein et al., 2004; Zeier et al., 2011). The hippocampus was placed ventral side up on a microdissection tray on ice, the hippocampal fissure was identified, and the dentate gyrus (DG) was dissected free of the CA and subicular fields by gently teasing it away along the hippocampal fissure. Further dissection along the margin of the free blade produced a block consisting of subiculum/cortex, CA1 and most of CA3. The subiculum was separated from CA regions, which was then further cut into CA1 and CA3 subfields. The tissues (CA1, CA3, and DG) were quickly frozen in liquid nitrogen then stored at −80°C. The tissue for one hippocampus from each animal was used for RNA isolation. Due to the dissection along the length of the hippocampus, other subfields including region CA2 and the subiculum were not isolated.

RNA Isolation

The tissue was sent to University of Alabama at Birmingham for RNA isolation. Total RNA was extracted (Qiagen, miRNeasy #217004), DNase-treated (Qiagen), and quality was assessed (Bioanalyzer, Agilent), which indicated a RNA integrity of 8.83 ± 0.04 (mean ± standard error) for the cohort.

Ion Proton Sequencing and Analysis

Sequencing and analysis by using Ion Proton was performed at the University of Florida. Poly-A selection for the Ion Proton sequencer was performed with 250 ng of total RNA using the Dynabeads mRNA DIRECT Micro kit (Thermo Fisher, catalog number 61021) followed by library preparations with the Ion Total RNA-seq Kit v2 (Thermo Fisher, catalog number 4475936) with the addition of the Ion Xpress barcodes for multiplex sequencing (Thermo Fisher, catalog number 4475485). In brief, poly-A selection was performed by the base pairing of the poly-A tail of mRNA to the oligo $(dT)_{25}$ sequence of the magnetic Dynabeads. Further, the mRNA was enzymatically fragmented by RNAse III, purified, ligated to the Ion adaptor mix, and reverse transcribed. The cDNA was uniquely barcoded per biological replicate and amplified with 16 cycles of PCR. The concentration of the libraries was quantified by the Qubit dsDNA HS Assay (Thermo Fisher, catalog number Q32851), and size distribution was evaluated with the High Sensitivity D1000 ScreenTape in the 2200 Tapestation system (Agilent Technologies).

Template preparation was performed in the Ion Chef system and sequencing was completed in the Ion Proton (Thermo Fisher). Low quality reads were removed from the FASTQ files resulting in reads containing an average length of 134 bp. The Ion Proton data were aligned to the *rattus norvegicus* (rn5) genome using the two step alignment method with TopHat2 and Bowtie2 in the Partek Flow servers (Partek, Inc.). Aligned reads were summarized as gene-level counts (featureCounts 1.4.4). The FASTQ files from the Ion Proton have been submitted to NCBI's Gene Expression Omnibus (GEO) under the accession number: GSE97608.

Illumina HiSeq Sequencing and Analysis

Sequencing and analysis by using Illumina HiSeq was performed at the Translational Genomics Research Institute, Arizona. Sequencing libraries were prepared with 250 ng of total RNA using Illumina's Truseq RNA Sample Preparation Kit v2 (Illumina, Inc.) following the manufacturer's protocol. In brief, poly-A containing mRNA molecules were purified using poly-T oligo attached magnetic beads. The mRNA was then thermally fragmented and converted to double-stranded cDNA. The cDNA fragments were end-repaired, a single "A" nucleotide was incorporated, sequencing adapters were ligated, and fragments were enriched with 15 cycles of PCR. Final PCR-enriched fragments were validated on a 2200 TapeStation (Agilent Technologies) and quantitated via qPCR using Kapa's Library Quantification Kit (Kapa Biosystems) on the QuantStudio 6 Flex Instrument (ThermoFisher). The final library was sequenced by 50 bp paired-end sequencing on a HiSeq 2500 (Illumina). Illumina BCL files were converted and demultiplexed (bcl2fastq 2.17). FASTQ files were trimmed of adapter sequences (CutAdapt 1.8.3) and aligned to rn5 (STAR 2.5). Aligned reads were summarized as gene-level counts (featureCounts 1.4.4). Sequencing and quality control reports were generated (FastQC 0.11.4 and Qualimap 2.1.3). The FASTQ files from the Illumina platform have been separately submitted to GEO under the accession number: GSE101798.

Analysis

For poly-A mRNA gene expression sequenced by Illumina and Ion Proton, pairwise differential expression analysis was conducted with the R package *DESeq2* (1.10.1) to identify transcriptional changes due to age, cognitive performance,

or subfield. For the transcriptional changes due to age and cognitive performance, a significant cut-off was set at $p < 0.01$. The resulting data sets for each region represent seed lists of differentially expressed genes. Validation of expression was performed using poly-A mRNA sequenced on the Ion Proton. For Ion Proton mRNA, a significance cut-off was set at $p < 0.05$ for one tailed-tests, with the tail specified by the direction of fold change (FC) determined by the Illumina seed list. Thus, the adjusted p-value for the combined tests was $p < 0.0005$. The following formula was used to calculate the false discovery rate (FDR) = (number of genes identified by Illumina * 0.0005/the number genes from this list identified by Ion Proton). Heat maps were generated in R with "gplots" (3.0.1) and "ComplexHeatmap" (1.14.0) using counts which were standardized to z-scores from genes validated with the Ion Proton, and the box plots were generated with "ggplot2" (2.2.1).

To be labeled subfield-specific in CA1, CA3, or DG, gene counts had to be significantly different (Benjamini-Hochberg adj-$p < 0.05$) from both of the other two subfields with a concordant direction of fold change and validated by Ion Proton sequencing at the same significance threshold. Finally, pathway analysis was conducted with the ToppGene web portal against KEGG, PantherDB, and Reactome databases. An additional analysis was conducted using DAVID (version 6.8), considering Gene Ontology for biological processes and cellular components in the "Direct" and "FAT" categories with the Benjamini FDR set at $p < 0.05$ as a cut-off for cluster selection.

RESULTS

Behavior

Cue Discrimination

A repeated measures ANOVA indicated an effect of training [$F_{(4, 128)} = 5.81, p < 0.0005$] and age [$F_{(1, 32)} = 11.57, p < 0.005$], and an interaction [$F_{(4, 128)} = 2.46$, $p < 0.05$] (**Figure 1A**). Despite the age difference, all animals were able to locate the platform by the end of training and an ANOVA in each age group confirmed decreased path length with training ($p < 0.05$). *Post hoc* analysis indicated that young rats exhibited a rapid rate of learning observed as a decrease in escape path length for blocks 2–5 relative to block 1. For aged animals, learning was slower, such that escape path length decreased on blocks 4–5 relative to blocks 2–3.

Spatial Discrimination

A repeated measures ANOVA on performance in the spatial task indicated an effect of training [$F_{(4, 128)} = 11.28, p < 0.0001$] and age [$F_{(1, 32)} = 16.81, p < 0.001$], in the absence of an interaction (**Figure 1B**). An ANOVA in each age group confirmed decreased path length with training ($p < 0.005$), indicating that both groups exhibited improved performance with training. *Post hoc* analysis indicated that young rats exhibited a rapid rate of learning observed as a decrease in escape path length for blocks 2–5 relative to block 1. For aged animals, learning was observed as a decrease in escape path length for blocks 4–5 relative to blocks 1–2.

Regression analysis performed within each age group indicated no relationship between performance on the cue task (block 5 distance) and the spatial task (block 5 distance) (young: $r = 0.43$, $p = 0.22$; aged: $r = 0.078$, $p = 0.72$). The results indicate that age differences in sensory-motor function or acquisition of the procedural aspects of the task did not mediate impairments in acquisition of a spatial search strategy.

Probe Trial Discrimination Index (DI) Scores

An ANOVA on the discrimination index scores using age and testing site as factors indicated an age difference [$F_{(1, 30)} = 8.41$, $p < 0.01$] in the absence of a training site difference or interaction (**Figure 1C**). As expected, from the age range of 17–22 months in this strain of rat, there was considerable variability for aged animals, with some animals performing as well as young.

The observed lowest DI score for young animals was 0.24. This value was used as cut-off to classify aged animals as aged-impaired (AI) (DI < 0.24) or aged-unimpaired (AU; DI > 0.24). A repeated measures ANOVA was computed comparing AI and AU groups for the cue task. No group difference was observed for distance to escape to the platform on the cue task ($p = 0.82$). Thus, the difference for the DI scores is not likely due to sensory-motor function or learning the procedural aspects of the task.

Gene Expression across Regions: Comparison of Illumina and Ion Proton Technologies

Sequence Quality Metrics

We sequenced a total of 17.1 and 18.9 million reads per sample, the total mapping rate was 94.1 and 96.8%, with exonic mapping 63.8 and 58.0%, intronic 15.2 and 13.1% and the percentage of intergenic reads was 21.0 and 28.9% on the Illumina and Ion Proton platforms, respectively.

The correlation of number of counts for the common genes is shown in **Figure S1**. We conducted pairwise differential expression analysis between the three subfields regardless of age or cognitive status. For each pairwise comparison, we retained the differentially expressed genes (DEGs) that were statistically significant with both platforms (adj-$p < 0.05$) and concordant for FC direction. A summary of the number of genes detected in all the pairwise comparisons in both platforms is reported in **Table 1**. A total of 24 DEGs were discordant for FC between the two platforms in the 3 comparisons (specifically: 5 for CA1 vs. CA3, 14 for CA1 vs. DG and 5 for CA3 vs. DG). Finally, the significant genes showing concordant FC in both platforms were: 2,379 (CA1 vs. CA3), 4,352 (CA1 vs. DG), and 4,642 (CA3 vs. DG). The complete results of the differential analysis for the genes detected with both platforms are reported in Tables S1–S3, and the overlap is represented in the proportional Venn diagram in **Figure 2A**.

We computed the correlation coefficient for the Log2 FC between the two platforms in each pairwise comparison for all detected genes. The Pearson coefficients demonstrated a strong positive correlation for all of the comparisons ($p < 2.2e\text{-}16$), ranging from $R = 0.776$ (CA1 vs. CA3) to R = 0.836 (CA3 vs. DG). In **Figure 2B,** we illustrate the corresponding

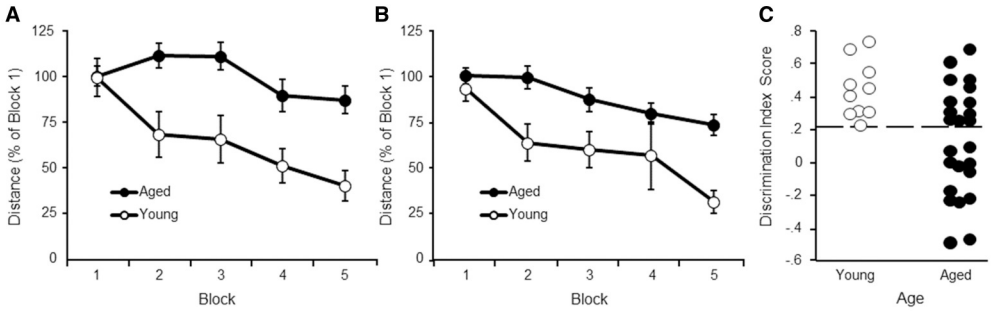

FIGURE 1 | Performance on the water maze task. Symbols indicate the mean (±SEM) escape path length to the escape platform during 5 training blocks on the **(A)** cue and **(B)** spatial discrimination tasks for young (open symbols) and aged (filled symbols) animals. **(C)** Acquisition of a spatial search strategy. Individual discrimination index scores for young (open symbols) and aged (filled symbols) animals. The dashed line indicates the cut-off for behavioral classification of aged-impaired (AI) and aged-unimpaired (AU) animals.

TABLE 1 | Number of genes that were statistically significant (adj-$p < 0.05$) and detected in both platforms.

Test	Illumina		Ion Proton		Cross-Platform Comparison		
	Total Genes Detected	adj-$p < 0.05$	Total Genes Detected	adj-$p < 0.05$	Mutual Found	adj-$p < 0.05$	adj-$p < 0.05$ and FC Concordant
CA1 vs. *CA3*	18,987	5,722	19,506	3,062	18,263	2,384	2,379
CA1 vs. *DG*	19,427	8,675	19,506	5,515	18,436	4,366	4,352
CA3 vs. *DG*	19,870	8,903	19,972	5,589	18,929	4,647	4,642

Total Genes Detected are the number of genes detected that were not filtered out by DESeq2 and for which an adj-p-value was computed.

scatterplots from these comparisons with the blue points indicating genes that were significantly differentially expressed across both platforms (adj-$p < 0.05$).

Gene Expression across Regions: Subfield Specific Transcriptome Profiling

We looked for subfield specific transcriptomic signatures for genes that met the criteria of significantly differentially expressed on both platforms and concordant for fold change across platforms. We detected a total of 908 (CA1), 1,063 (CA3), and 2,431 (DG) specific genes. The results for all three regions are reported in Tables S4–S6. The heatmap including the specific genes for each region is reported in **Figure S2**.

In the CA1 region, 898 of the DEGs were protein coding, whereas the remaining 10 were pseudogenes or processed transcripts. A total of 359 genes (39.5%) were overexpressed and 549 (60.5%) underexpressed with respect to the CA3 and DG regions. The boxplots for all of the specific genes are illustrated in **Figure S3**, and in **Figure S4** we show the Allen Brain Atlas data from mouse for *Wfs1*, *Nov*, *Ndst4*, and *Gpr161*. The first 5 genes ranked by absolute average fold change were: *Vgll3*, *Mx1*, *Gnrhr* (underexpressed), and *Wnt3*, *Ackr2* (overexpressed). Pathway analysis conducted with ToppGene using genes with average FC $> |0.50|$ ($n = 379$) reveals one significant pathway after Bonferroni correction (KEGG: neuroactive ligand-receptor interaction; adj-p = 7.40E-04) that included 20 genes (Table S7). The enrichment analysis conducted with DAVID did not identify any significant results after Benjamini correction.

In the CA3 region a total of 1,051 of the differentially expressed genes were protein coding, whereas the remaining 12 were processed transcripts or pseudogenes. A total of 551 genes (51.8%) were overexpressed, whereas 512 were underexpressed (48.2%) with respect to the CA1 and DG (Table S5). The boxplots for all of the specific genes are illustrated in **Figure S5**, and in **Figure S6** we show the Allen Brain Atlas data from mouse for *Col6a6* and *Nnat*. The first 5 genes ranked by absolute average fold change were *Lnp1*, *RGD1562638*, *Plk5* (underexpressed), and *Mmp3*, *Mx1* (overexpressed). Pathway and enrichment analysis conducted using genes with average FC $> |0.50|$ ($n = 535$) revealed 11 significant pathways after Bonferroni correction. Top results were: KEGG calcium signaling (adj-$p = 4.27E-04$; 17 genes) and REACTOME potassium channel (adj-$p = 1.73E-03$) (Table S7). The analysis conducted with DAVID allowed us to detect 3 significant GO biological processes after Benjamini correction: cilium movement, outer dynein arm, and potassium ion transmembrane transport (Table S7). The last process was also detected using ToppGene.

In the DG region 2,403 of the differentially expressed genes were protein coding, whereas the remaining 28 were pseudogenes, miRNA, processed transcripts or lincRNA. 975 genes (40.1%) were overexpressed and 1,456 underexpressed (59.9%) with respect to CA1 and CA3 regions (Table S6). The first 5 genes ranked by absolute FC were: *Bhlhe23*, *Met*, *Abca12*, *RGD1562638*, and *Ptpru*. The boxplots for all the specific genes are illustrated in **Figure S7**; in **Figure S8** we show the Allen Brain Atlas data from mouse for genes *Pdin*, *Plk5*, *C1ql2*, and *Dsp*. The enrichment analysis conducted with ToppGene using

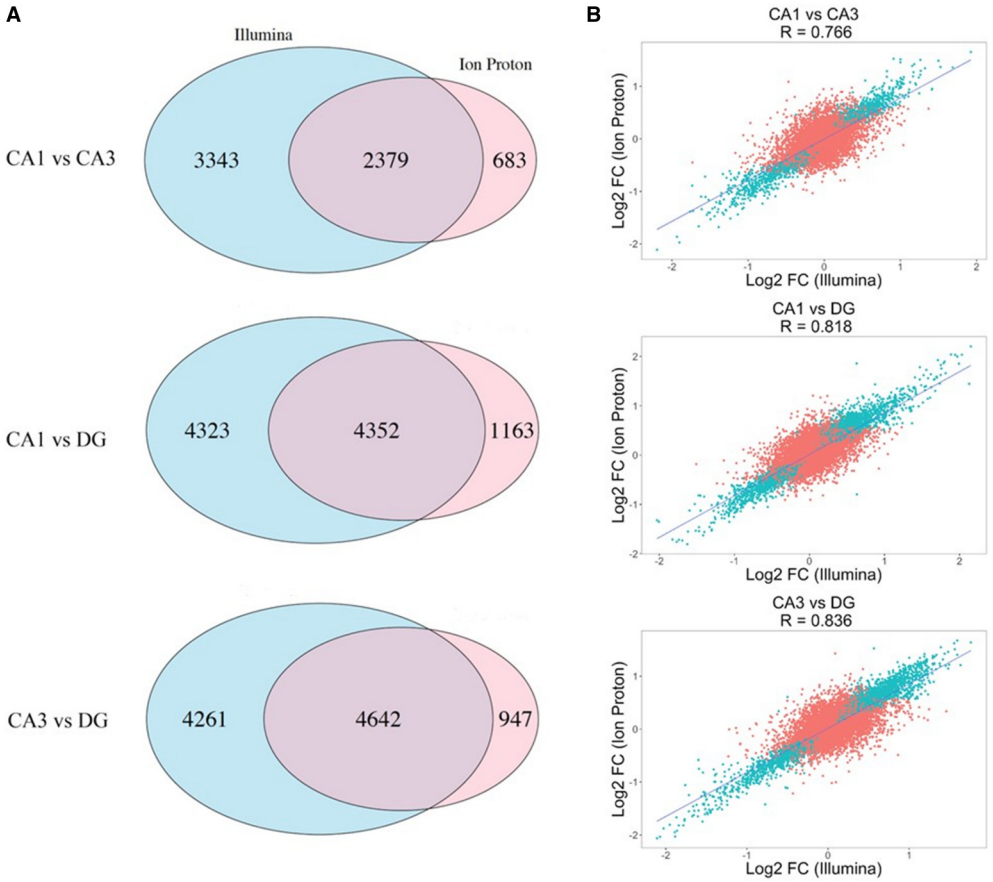

FIGURE 2 | Differential expression across the Illumina and Ion Proton platforms. **(A)** Proportional Venn diagrams showing the concordance for genes that were significant after *p*-value adjustment for the Illumina and Ion Proton in each pairwise comparison indicated (CA1 vs. CA3; CA1 vs. DG; CA3 vs. DG). For example, total number of significant genes for CA1 vs. CA3 were 5722 and 3062 for Illumina and Ion Proton, respectively, with an overlap of 2379. **(B)** Scatterplot of the fold changes for all detected genes across both platforms. Blue points are the genes differentially expressed in Illumina and Ion Proton (adj-$p < 0.05$).

genes with absolute average FC $> |0.50|$ ($n = 927$) revealed 7 significant pathways after Bonferroni correction. The most significant pathways were: KEGG axon guidance (adj-$p = 4.70$E-05; 23 genes) and REACTOME adherens junctions interactions (adj-$p = 6.20$E-04; 10 genes). The remaining significant pathways are reported in Table S7. In this same subfield we also detected the KEGG pathway neuroactive ligand-receptor interaction (adj-$p = 4.92$E-03; 32 genes), the only one shared with CA1 and CA3. In contrast, REACTOME gastrin-CREB signaling pathway via PKC and MAPK and REACTOME neuronal system were detected in CA3 region. The analysis conducted with DAVID revealed enrichment for 8 biological processes: neural crest cell migration (FDR adj-$p = 1.77$E-03; 12 genes), semaphorin-plexin signaling (FDR adj-$p = 2.11$E-03) and myosin complex (FDR adj-$p = 7.65$E-03). All the remaining processes (FDR adj-$p < 0.05$) are reported in Table S7.

Gene Expression Related to Aging

The data sets for differential expression using the cross platform validation method described above were used to investigate age-related changes in gene expression. The CA1 Illumina poly-A mRNA analysis produced 228 DEGs that passed the statistical filter. From this seed list the number of genes that was detected for Ion Proton poly-A mRNA was 104 (FDR $= 1.1^{-3}$). All 104 of these genes were in the NIH DAVID database. Among these, 90 genes were up regulated and 14 genes were down regulated in aged rats. Enrichment analysis indicated clusters related to immune function including the lysosome (GO:0005764, 14 genes, FDR adj-$p = 1.3^{-.3}$), regulation of leukocyte mediated immunity (GO:0002443, 14 genes, FDR adj-$p = 1.6^{-5}$), immune response (GO:0006955, 28 genes, FDR adj-$p = 1.8^{-7}$), and neutrophil activation (GO:0042119, 4 genes, FDR adj-$p = 9.8^{-3}$). In addition, clusters related to cell adhesion (GO:0007155, 25 genes FDR adj-$p = 2.9^{-4}$) and regulation of ERK1 and ERK2 cascade (GO:0070372, 8 genes, FDR adj-$p = 2.2^{-2}$) were also present. Furthermore, a KEGG pathway for the lysosome (rno04142, 8 genes, FDR adj-$p = 5.2^{-3}$) was identified. Enrichment analysis using the ToppGene web tool confirmed the enrichment of pathways related to immune function (i.e.: Lysosome, B cell receptor signaling pathway and adaptive immune system). All genes under the indicated immune related functional clusters were up regulated genes (**Figure S9**).

For region CA3, analysis of Illumina poly-A mRNA indicated 189 DEGs in the seed list and the number validated with the Ion Proton poly-A mRNA was 81 (FDR adj-$p = 1.2^{-3}$). All 81 genes were in the NIH DAVID database, with 61 genes up regulated and 20 down regulated genes in aged rats. As with area CA1, clustering analysis was related to immune function including leukocyte activation (GO:0045321, 17 genes, FDR adj-$p = 4.9^{-5}$) immune response (GO:0006955, 20 genes, FDR adj-$p = 8.8^{-5}$), cytokine production (GO:0001816, 12 genes, FDR adj-$p = 2.4^{-3}$), antigen processing and presentation of peptide antigen via MHC class II (GO:0002495, 7 genes, FDR adj-$p = 4.4^{-7}$), and interleukin-10 production (GO:0032613, 5 genes, FDR adj-$p = 3.0^{-3}$). Additionally, a cluster for biological adhesion (GO:0022610, 21 genes, FDR adj-$p = 4.4^{-4}$) and a KEGG pathway for cell adhesion molecules (rno04514, 7 genes, FDR adj-$p = 2.3^{-3}$) were found. Enrichment analysis conducted with ToppGene confirmed the presence of pathways correlated with the immune system (i.e., immunoregulatory interactions between a lymphoid and a non-lymphoid cell, adaptive immune system, and phagosome). All genes under the indicated immune related functional clusters were up regulated (**Figure S10**).

The DG region exhibited similar aging patterns in relation to the CA1 and CA3, with 280 DEGs in the Illumina poly-A mRNA data set. From this list, 162 genes were validated by the Ion Proton (FDR $= 8.6^{-4}$), and all 161 genes were in the DAVID database. From the validated gene list, 134 genes were up regulated and 27 genes decreased with aging. Enriched clusters included immune response (GO:0006955, 41 genes, FDR adj-$p = 2.9^{-11}$), defense response (GO:0006952, 40 genes, FDR adj-$p = 5.8^{-9}$), inflammatory response (GO:0006954, 26 genes, FDR adj-$p = 1.1^{-8}$), response to wounding (GO:0009611, 15 genes, FDR adj-$p = 9.3^{-3}$), response to steroid hormone (GO:0048545, 14 genes, FDR adj-$p = 1.3^{-2}$) and cell-cell adhesion (GO:0098609, 30 genes, FDR adj-$p = 2.7^{-6}$). KEGG pathways were identified for lysosome (rno04142, 10 genes, FDR adj-$p = 3.2^{-4}$), antigen processing and presentation (rno04612, 11 genes, FDR adj-$p = 5.2^{-6}$), and cell adhesion molecules (rno04514, 10 genes, FDR adj-$p = 2.8^{-3}$). All genes under the indicated immune related functional clusters were up regulated genes (**Figure S11**). Again, the analysis conducted with ToppGene confirmed the immunologic processes detected with DAVID. In addition, we detected 3 pathways involving the complement system: initial triggering of complement, complement and coagulation cascades, complement cascade, and activation of C3 and C5. Beside the immunological pathways, we detected the cadherin signaling and Wnt signaling.

In examining genes that were differentially expressed with age across regions it is clear that each region contains a number of age-related genes that are unique relative to the other hippocampal regions. For the most part, more genes were up regulated in older rats within each region and several up regulated genes overlapped across regions. Among the genes that overlapped regions, several were related to immune function (**Table 2**). Only one gene, *Col4a5,* exhibited a decrease across all three regions. Interestingly, the DG region showed the highest number of gene changes related to the age of the animal (162), including the greatest number of distinct genes (91 genes) (**Figure 3**). Among the 69 genes that were uniquely up regulated in the DG, 68 matched DAVID for functional annotation clustering analysis with the top clusters involved in immune function. Together, the results indicate that the DG region may be more sensitive to aging effects.

TABLE 2 | Genes, which significantly increased expression across all three regions in aged animals from both the Illumina and Ion Proton data.

Gene symbol	Gene Name	Immune related
C3	Complement component 3	x
Card11	Caspase recruitment domain family, member 11	x
Cd4	Cd4 molecule	x
Cd74	Cd74 molecule, major histocompatibility complex, class II invariant chain	x
Cdh1	Cadherin 1	
Cdh23	Cadherin 23 (otocadherin)	
Csf1r	Colony stimulating factor 1 receptor	x
Ctss	Cathepsin S	x
Ctsz	Cathepsin Z	
Cx3cr1	Chemokine (C-X3-C motif) receptor 1	x
Fcgr2b	Fc fragment of IgG, low affinity IIb, receptor (CD32)	x
Gfap	Glial fibrillary acidic protein	x
Gpr183	G protein-coupled receptor 183	x
Gpr84	G protein-coupled receptor 84	x
Itgb2	Integrin beta 2	x
Ncf1	Neutrophil cytosolic factor 1	x
Nckap1l	NCK associated protein 1 like	x
Npc2	Niemann-Pick disease, type C2	
Pcdhb4	protocadherin beta 4	
Pld4	Phospholipase D family, member 4	
Slc14a1	Solute carrier family 14 (urea transporter), member 1	
Trem2	Triggering receptor expressed on myeloid cells 2	x
Bpifb4	BPI Fold Containing Family B, Member 4	
Wdfy4	WDFY Family Member 4	

Genes that are related to immune function are indicated.

Gene Expression Related to Behavior

For examination of genes linked to cognitive status, only aged animals were included in order to avoid age as a confound. Aged animals were subdivided into AI and AU according to the water maze DI score. **Figure 4** illustrates the number of genes that were differentially expressed in CA1, CA3, and the DG according to cognitive status, and were annotated in DAVID. The Illumina analysis of CA1 poly-A mRNA produced 235 sequences that passed the statistical filter. From the seed list, the number of genes that was detected for Ion Proton mRNA was 107 (FDR $= 1.1^{-3}$) (Table S8). For the 107 genes, 106 were in the NIH DAVID database, with 48 up regulated and 58 down regulated genes in aged impaired animals. The CA3 Illumina mRNA analysis contained 32 sequences in the seed list and the number validated with the Ion Proton poly-A mRNA was 8 (FDR $= 2.0^{-3}$) (Table S8). All 8 genes were annotated in DAVID (increased: *Prl*, *Pcdh19*,

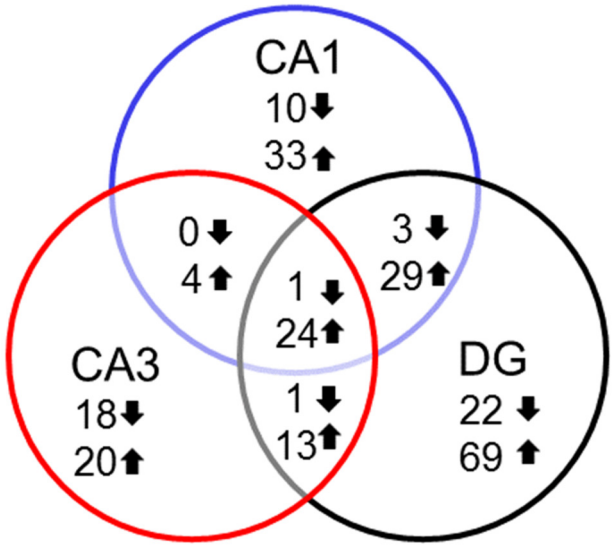

FIGURE 3 | Number of genes altered during aging across hippocampal regions. Summary of the total number of genes across the hippocampal subfields whose expression increased (up arrow) or decreased (down arrow) using Illumina DEGs with $p < 0.01$ validated with Ion Proton mRNA with $p < 0.05$.

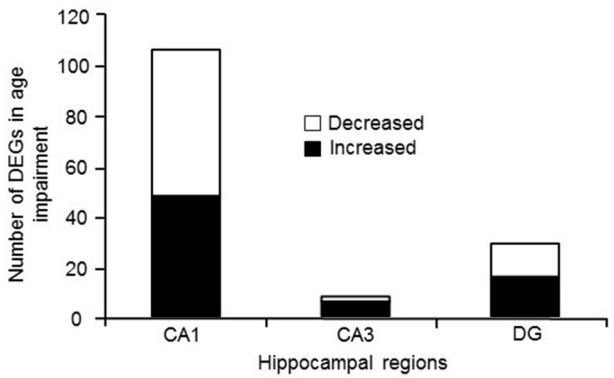

FIGURE 4 | Number of genes differentially expressed in regions CA1, CA3, and DG according to cognitive function. In each case, the number of genes down regulated (open portion) and up regulated (filled portion) in aged-cognitively impaired animals are represented.

Pcdh17, *Gabrb1*, *Gda*, *Als2*; decreased: *Msrb2*, *Wnt6*). The DG Illumina poly-A mRNA analysis contained 97 sequences in the seed list and the number validated with the Ion Proton mRNA was 30 (FDR = 1.6^{-3}) (Table S8), which included 29 genes that were annotated in DAVID (16 up regulated and 13 down regulated). Only one gene, *Prl*, was increased across all regions.

Up and down regulated genes were combined within each region and submitted for cluster analysis. The results indicated that only CA1 exhibited significant enrichment. Clustering was observed for cellular components with CA1 genes linked to synapse (GO:0045202, 20 genes, FDR adj-p = 2.6^{-5}), cell junction (GO:0030054, 18 genes, FDR adj-p = 1.2^{-2}), neuron part (GO:0097458, 22 genes, FDR adj-p = 5.6^{-3}), postsynapse (GO:0098794, 10 genes, FDR adj-p = 1.3^{-2}), ion channel complex (GO:0034702, 9 genes, FDR adj-p = 5.9^{-3}) and plasma membrane region (GO:0098590, 16 genes, FDR adj-p = 6.1^{-3}) (**Table 3**). In addition, enrichment for biological processes included regulation of signaling (GO:0023051, 34 genes, FDR adj-p = 4.7^{-3}), the KEGG pathways for calcium signaling (rno04020, 7 genes, FDR adj-$p = 1.7^{-2}$) and long-term potentiation (rno04720, 4 genes, FDR adj-$p = 3.5^{-2}$). ToppGene identified five significant pathways after Bonferroni correction: glutamatergic synapse, neuronal system, heterotrimeric G-protein signaling pathway-Gq alpha and Go alpha mediated pathway, calcium signaling, and phosphatidylinositol signaling system. The results confirmed the presence of neuronal genes, but pointed to more specific processes, including the glutamatergic synapse.

A closer examination of the direction of gene changes suggested that there was decreased expression of genes that regulated Ca^{2+} entry by modulating the function of NMDA receptors (*Neto1, Prickle2*), or voltage-gated Ca^{2+} channels (*Cacnb2*) (**Figure 5**). Decreased expression was also observed for genes linked to receptor mediated release of Ca^{2+} from intracellular Ca^{2+} stores (*Adra1d, Homer3, Itpr1*). A decline in protein expression for these genes might be expected to decrease intracellular Ca^{2+}. Similarly, increased expression was observed for the membrane Ca^{2+} ATPase pump (*Atp2b4*), which would remove intracellular Ca^{2+}. Moreover, decreased expression was observed for genes linked to downstream Ca^{2+} signaling (*Hpca, Dclk2, Prkca*). Together, the results suggest that in impaired animals, transcription is altered in an attempt to limit intracellular Ca^{2+} signaling (**Figure 5**).

Closer examination of the direction of change for genes linked to synaptic activity suggests differential expression in genes for regulating synaptic receptors and K^+ channels (**Figure 6**). For example, there was a decrease in the GABA receptor subunit (*Gabra5*) and *Nptxr*, which are involved in clustering of AMPA receptors at the synapse. Increased expression was observed for two K^+ channels, *Hcn4* and *Kcnk1*, and *Kcnab2*, a cytoplasmic potassium channel subunit that modulates K^+ channel activity was down regulated. Finally, there was down regulation of genes for proteins that are downstream of G-protein coupled receptor activation (*Mpp3*, *Ksr1*, *Akap13*) and an increase expression of the glutamate metabotropic receptor (*Grm2*).

Finally, we examined the specificity of gene changes. In this case, aged animals were separated by performance on the cue task, using a mean split for block 5. Relative to gene expression associated with spatial discrimination performance, fewer genes were associated with performance on the cue task. Analysis of the CA1 region poly-A mRNA using Illumina produced 135 sequences that differed according to cue discrimination performance. From this seed list the number of genes that was detected for Ion Proton poly-A mRNA was 24 (FDR = 2.8^{-3}). For region CA3, 38 differentially expressed genes were detected by Illumina and 3 genes were confirmed by the Ion Proton (FDR = 6.3^{-3}). For the dentate gyrus, Illumina detected 71 sequences and 4 were confirmed by the Ion Proton (FDR = 8.8^{-3}). No gene clusters were observed for any region.

TABLE 3 | Genes of age impaired and age unimpaired animals, which were significantly differentially expressed in region CA1 in both the Illumina and Ion Proton data.

Gene symbol	Gene Name	Ca^{2+} binding	Synaptic function
Adra1d	Adrenergic, alpha-1D-, receptor	x	x
Akap13	A kinase (PRKA) anchor protein 13		x
Arpc5	Actin related protein 2/3 complex, subunit 5		x
Dclk2	Doublecortin-like kinase 2		x
Dgkz	Diacylglycerol kinase zeta		x
Gabra5	Gamma-aminobutyric acid (GABA) A receptor, alpha 5		x
Homer3	Homer homolog 3 (Drosophila)		x
Itpr1	Inositol 1,4,5-triphosphate receptor, type 1		x
Kcnab2	Potassium voltage-gated channel, shaker-related subfamily, beta member 2		x
Ksr1	Kinase suppressor of ras 1		x
Mpp3	Membrane protein, palmitoylated 3 (MAGUK p55 subfamily member 3)		x
Neto1	Neuropilin (NRP) and tolloid (TLL)-like 1	x	x
Nptxr	Chromobox homolog 6; neuronal pentraxin receptor	x	x
Pragmin	Pragma of Rnd2		x
Prickle2	Prickle homolog 2 (Drosophila)	x	x
Rem2	RAS (RAD and GEM) like GTP binding 2	x	x
Slc17a8	Solute carrier family 17, member 8		x
Vav2	vav 2 guanine nucleotide exchange factor		x
Cacnb2	Calcium channel, voltage-dependent, beta 2 subunit	x	x
Dgka	Diacylglycerol kinase, alpha	x	
Hpca	hippocalcin	x	
Itpr1	Inositol 1,4,5-triphosphate receptor, type 1	x	
Prkca	Protein kinase C, alpha	x	
Scube2	Signal peptide, CUB domain, EGF-like 2	x	
Sulf2	Sulfatase 2	x	

Genes that are related to Ca^{2+} binding and synaptic function are indicated.

DISCUSSION

Gene Expression across Subfields: Subfield Specific Transcriptome Profiling

We report the results of the transcriptional differences among hippocampus brain subfields (CA1, CA3, and DG) regardless of the animal's age or cognitive status. Our approach was based on retaining for each subfield, genes significant and concordant in FC in both pairwise comparisons. We were able to detect a high number of specific genes for each subfield, specifically: 908 (CA1), 1,063 (CA3), and 2,431 (DG) genes. These lists include genes highly or lowly expressed in each subfield with respect to the others. In CA1, the top gene with high values of expression compared to the other subfields was *Wnt3* (Wnt Family Member 3), which is considered to play a central role in synaptogenesis and adult neurogenesis (Varela-Nallar and Inestrosa, 2013). In area CA1, Wnt signaling has been linked to synaptic plasticity and associated hippocampal-dependent memory processes (Xu et al., 2015; Ivanova et al., 2016). At the pathway level, those genes with higher expression in CA1 exhibited enrichment for Neuroactive ligand-receptor interaction, including *Nts* (neurotensin), *Htr1b* (5-hydroxytryptamine receptor 1B) and *Gpr161* (G Protein-Coupled Receptor 161).

For subfield CA3, we observed increased expression of genes linked to processes involving potassium channel activity in both ToppGene (Potassium channels, Voltage gated potassium channels) and DAVID enrichment analysis (GO:0071805 Potassium ion transmembrane transport). Potassium channels are central to intrinsic excitability in region CA3 of the hippocampus, which is highly vulnerable to cell death due to seizure activity (Ben-Ari, 1985; Cooper, 2012). Indeed, many of the top overexpressed genes (*Mmp3*, *Pagl1Zac1*, *Galr1*, *Glra1*, and *Nk3r*) are regulated by neural activity and linked to epiletogenesis of the hippocampus (Elmslie and Gardiner, 1995; Valente et al., 2004; Mazarati et al., 2006; McColl et al., 2006; Dubey et al., 2017).

Enrichment analysis of genes that are highly expressed in the DG relative to other subfields indicated that the most significant processes were "Axon guidance" (KEGG) and "Neural crest cell migration" (GO:0001755). In general, the genes and the biological processes detected as enriched in the DG may be due to the known neurogenesis activity in this subfield. In the DG, the top genes overexpressed with respect the other regions included *Bhlhe23* (basic helix-loop-helix family member E23) and *Msx3* (msh like homeobox 3), which are involved in neurogenesis and specification of neuronal subtype (Bramblett et al., 2004; Liu et al., 2004; Hesse et al., 2011). *EphA8* (EPH receptor A8), a member of the ephrin receptor subfamily and *C1ql2* (complement C1q like 2) are implicated in neurite growth and establishing synaptic connections (Buchser et al., 2010; Iijima et al., 2010). *Plk5* (polo like kinase 5) modulates the formation of neuritic processes upon stimulation of the brain-derived neurotrophic factor (BDNF)/nerve growth factor (NGF)-Ras pathway in neurons (de Carcer et al., 2011). Interestingly, we also found *Bdnf* specifically overexpressed in this subfield (average FC = 0.948).

Subfield Vulnerability to Aging

It is likely that regional differences in transcription during aging are associated with differences in connectivity and molecular make-up of each subfield. For example, relative to CA3 pyramidal neurons, CA1 pyramidal neurons are more sensitive to metabolic perturbations (Jackson et al., 2009). Blalock and associates have suggested that metabolic changes precede neuroinflammation and have linked increased vulnerability of gene changes in CA1, relative to CA3, to biomarkers of metabolic syndrome in nonhuman primates (Blalock et al., 2010). In considering

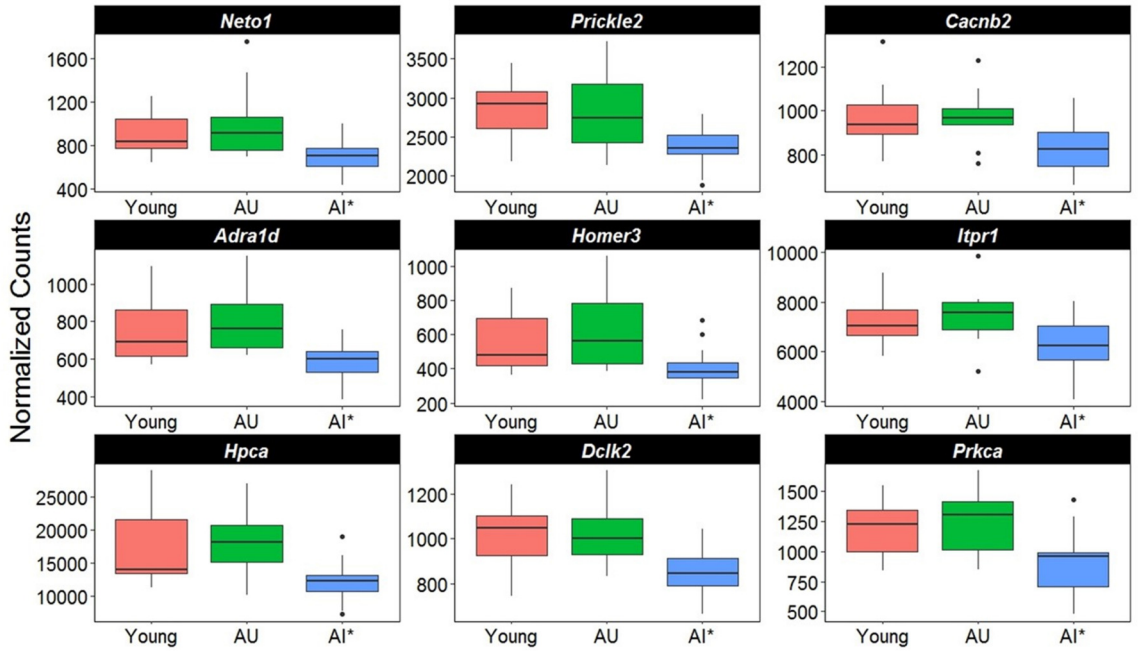

FIGURE 5 | Altered transcription of genes linked to calcium regulation. The y-axis represents Illumina normalized counts and the asterisk in the x-axis represent differential expression of AI rats relative to AU in the Illumina platform ($p < 0.01$) validated with the Ion Proton ($p < 0.05$).

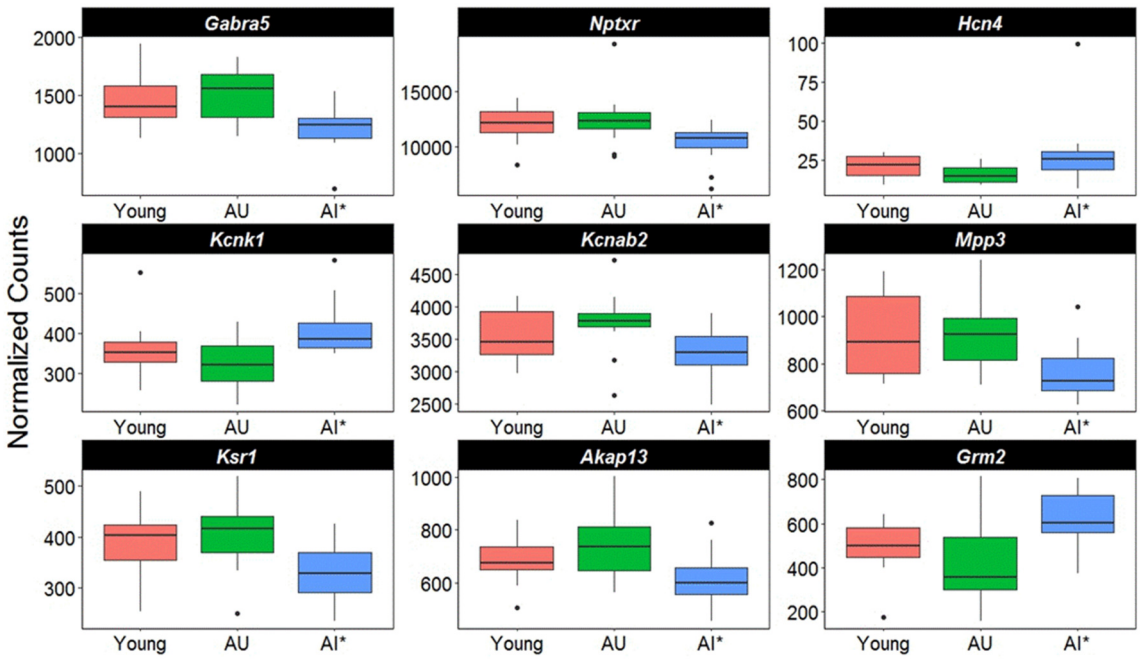

FIGURE 6 | Altered transcription of genes linked to cell excitability. The y-axis represents Illumina normalized counts and the asterisk in the x-axis represent differential expression of AI rats relative to AU in the Illumina platform ($p < 0.01$) validated with the Ion Proton ($p < 0.05$).

the increase in age-related shift in transcription in the DG, it is important to note that neurogenesis in the DG exhibits a robust decline between adult and middle-age (Kuhn et al., 1996; Lemaire et al., 2000; Driscoll et al., 2006). Similarly, the rat DG exhibits a loss of perforant path input (Geinisman, 1979; Barnes and McNaughton, 1980), and loss of neuronal connections underlie the altered expression of genes related to cell-cell adhesion or axon guidance and increased markers of

inflammation (Ianov et al., 2016). Interestingly, older memory-impaired humans also show reduced white matter volume in the vicinity of the major axon input pathway to the hippocampus, the perforant pathway (Rogalski et al., 2012). Thus, while we observed that the DG exhibits robust changes in transcription during aging, it remains to be discovered how these changes specifically relate to DG function and to anatomical or physiological changes associated with aging. The subfield-specific changes observed in activity of the human dentate gyrus/CA3 region, however, does suggest that these alterations occur across species, and may contribute to memory deficits during aging in humans and other animals (Yassa et al., 2011).

Consistent with a number of previous studies, we observed that brain aging was associated with an increase in markers of neuroinflammation including expression of immune response genes (Rowe et al., 2007; Kadish et al., 2009; Blalock et al., 2010; Zeier et al., 2011; Cribbs et al., 2012; Ianov et al., 2016). Typical genes include *Gfap*, complement genes (*C3*, *C4b*), and genes associated with antigen processing through the lysosome (*Cd74, Ctsd*, *Ctsz*, *Laptm5, Dnase2*) or phagosome (*Fcgr2b*, *Ncf1*). In the current study, the DG region showed the highest number of gene changes related to the age of the animal. This is in contrast to previous microarray studies, which suggest that for BNxF344 rats examined between middle-age (12–18) and advanced age (26–28 months), region CA1 is more vulnerable than DG (Zeier et al., 2011; Masser et al., 2014). In this case the differences likely relate to the animal model, age of onset for gene changes, and differences in the age range examined (Ianov et al., 2016). In F344 rats, for ages similar to those employed in the current study (5–6 and 17–22 months), the CA1 region of older animals exhibited relatively smaller transcriptional changes compared to the prefrontal cortex and white matter (Ianov et al., 2016). Similarly, a decline in interneuron markers occurs in all hippocampal regions from adult to middle-age in F344 rats and the decline is observed in CA1 but not the DG when analysis is limited to middle-age and aged BNxF344 rats (Shi et al., 2004; Stanley and Shetty, 2004). Thus, one possibility is that changes in the DG emerge earlier than in CA1, minimizing age-related changes between middle-age and older animals. Alternatively, we have observed that the majority of gene changes in region CA1 of F344 rats occurs between adult and middle-age (Blalock et al., 2010), suggesting possible species differences.

The increase in immune response genes suggests activation of astrocytes and microglia. However, it is important to note that the age-related increase in expression of inflammation genes does not necessarily predict memory impairment or the stage of neurodegeneration (Blalock et al., 2003; Cribbs et al., 2012). In the case of neurodegeneration, neuroinflammation may initially have beneficial and neuroprotective effects (Chakrabarty et al., 2010; Streit et al., 2014; Sochocka et al., 2017). Glial activation during aging is associated with a decline in synaptic density (Rozovsky et al., 2005) and the ability to maintain or form new synapses may underlie resiliency in the face of aging or neurodegenerative disease (Arnold et al., 2013; Ianov et al., 2016, 2017).

Genes Associated with Impaired Episodic Memory

The identification and specificity of genes related to cognition is a function of the brain region sampled and the type of cognitive process examined (Ianov et al., 2016). In the current study, within each region, more genes were correlated with episodic memory scores relative to sensory-motor performance on the cue discrimination task, suggesting specificity of gene changes. While the hippocampus is required for spatial memory, different hippocampal-dependent processes depend on specific regional and molecular mechanisms. For example, the DG is involved in spatial pattern separation and region CA1 with memory for topological relationships in space (Kesner et al., 2004; Goodrich-Hunsaker et al., 2008; Kesner and Rolls, 2015). Thus, if the task had focused on spatial pattern separation we would expect a greater correspondence between behavior and transcription in the DG. Regardless, aging of the DG likely contributes to impaired spatial episodic memory. While no functional gene clusters were observed, several of the DG genes that were down regulated in impaired animals (*Bcl6*, *Crim1*, *Dapk1*, *Mtss1*, *Oas1a*) have been linked to cell growth/apoptosis and neurogenesis or neuronal development.

The results on CA1 transcriptional changes associated with cognitive decline are in confirmation of previous studies employing microarray technology, which indicate that impaired cognition is associated with altered expression of synaptic genes, genes involved in Ca^{2+} regulation, and glutamatergic synapses (Toescu et al., 2004; Burger, 2010; Uddin and Singh, 2013; Volk et al., 2015). However, rarely are the same genes observed to change in the same direction across studies. The difference may be due to different cognitive processes examined including reference memory and episodic memory, differences in ages, and the time after behavioral training in which transcription is examined. Previous work has established that Ca^{2+} dysregulation and impaired Ca^{2+}-dependent synaptic plasticity in region CA1 is associated with poor performance on episodic spatial memory (Landfield, 1988; Foster and Norris, 1997; Foster, 1999, 2007; Burke and Barnes, 2010; Oh and Disterhoft, 2010) and these processes are influenced by behavioral training. We examined transcription 2 weeks after testing. Thus, the differences observed here are not likely due to differential response to training and may represent an underlying and chronic shift in transcription for this region. In our experiments, the changes in expression of genes involved in the glutamatergic synapses in aging are concordant with the evidence that P301L tau expression increased hippocampal glutamate release and decreased glutamate uptake, and these alterations in glutamate signaling correlated with cognitive deficits in the hippocampal-dependent Barnes maze task (Hunsberger et al., 2015).

Finally, it is important to point out the advantages or disadvantages of the experimental design. The current study was conducted across multiple testing sites and employed two different methods for transcriptional analysis. The advantage of multiple testing sites includes the ability to pool data across sites. However, there is the challenge of equating data due to differences in hardware or protocols. Episodic memory is sensitive to age-related cognitive decline across species; however,

there is considerable variability in cognition with advancing age. Furthermore, aged animals can exhibit sensory-motor impairment and acquire the procedural aspects of the task much more slowly than young animals, which could influence the validity of cognitive measures. Thus, in the current study possible sensory-motor and procedural learning contributions to behavior on the spatial task were controlled by first testing the animals on the cue discrimination task. Characterization of spatial episodic memory was based on a DI score, which would tend to standardize scores for animals tested on mazes of different sizes. The testing procedure and use of a DI score likely contributed to the good correspondence of behavioral results across the different testing sites, such that all young animals performed above chance (DI score = 0) and approximately half the aged animals at each site exhibited impaired performance. Finally, behavior on the spatial task was not related to behavior on the cue discrimination task.

Due to the large numbers of transcripts examined, the possibility of false positives or false negatives should be controlled. In order to reduce the instance of false discovery we were able to increase the power of the analysis by pooling a relatively large number of animals that were tested across the two sites (young = 10; aged unimpaired = 12; aged impaired = 12). In addition, it is advised that transcriptional profiling studies should use another method to confirm suspected changes. Each method has its benefits and limitations and there are major differences in the nature of the approaches. In the current study, we have taken advantage of two different next-generation platforms, Illumina fluorescent labeling and Ion Proton semiconductor measures of proton release, to confirm differential expression of thousands of genes (Kusko et al., 2014; Li et al., 2015; Reuter et al., 2015). Consistent with previous reports, we observed a good concordance in the gene counts between the different platforms (R = 0.909), increasing the confidence in the observed transcriptional changes. We now expand this idea by showing considerable concordance between the two platforms in detecting differences in expression. Thus, coefficients for the Log2 FC between the two platforms across regions was highly significant (**Figure 2B**), with the correlation coefficients ranging from 0.776 (CA1 vs. CA3) to 0.836 (CA3 vs DG). Indeed, for genes that changed in relation to age or cognitive function, the probability of false discovery across the platforms was generally $<2.0^{-3}$.

CONCLUSION

The two next-generation sequencing platforms were able to validate variability in gene expression associated with several variables. Due to the high number of specific genes detected in each subfield, our findings confirm previous studies conducted on the same hippocampal subfields in other animal models with the microarray technology, demonstrating a correspondence between cytoarchitectural boundaries, transcriptome distribution, and underlying differences in physiology and vulnerability to insults (Datson et al., 2004; Lein et al., 2004; Newrzella et al., 2007). The results confirm that brain aging is associated with increased expression of genes linked to the immune response; however, we noted regional differences with more robust changes observed in the DG. Finally, the literature suggests several physiological and transcriptional processes that may underlie cognitive decline; however, there is considerable diversity in the literature concerning which specific genes are altered. Our results confirm that cognitive decline is associated with differential expression of CA1 genes linked to Ca^{2+} homeostasis and synaptic plasticity. Furthermore, due to the time between testing and examination of transcription, we would suggest that these changes represent an underlying and chronic shift in transcription.

AUTHOR CONTRIBUTIONS

LI performed experiments, analyzed data, wrote the manuscript, and constructed figures; AR, MC, AS, and AJK, performed experiments; AK and IP performed experiments, contributed in writing the manuscript and figures. MD analyzed data and constructed figures. MH and TF designed the experiments, analyzed the data, constructed figures, wrote the manuscript. JD, CB, and JS designed the experiments, contributed to the manuscript.

ACKNOWLEDGMENTS

Financial support by National Institutes of Health Grants AG036800, AG037984, AG049711, and AG052258 (TF), MH57014 (JS), DA034681 (JD), AG028740, and by the McKnight Brain Research Foundation. This work was partially supported by the University of Florida Claude D. Pepper Older Americans Independence Center (P30-AG028740).

SUPPLEMENTARY MATERIAL

The Supplementary Material for this article can be found online at: https://www.frontiersin.org/articles/10.3389/fnagi.2017.00383/full#supplementary-material

Supplementary Figure 1 | Correlation ($R^2 = 0.938$) of gene counts across sequencing platforms, Illumina and Ion Proton.

Supplementary Figure 2 | Heatmap of hippocampal subfield changes in gene expression. Plotted for each hippocampal subfield, are genes found with both sequencing platforms to be differentially expressed compared to the other two subfields at a significance of adj-$p < 0.05$. Each row represents the z-scores from the DEGs, and the columns are the biological replicates for each region.

Supplementary Figure 3 | Boxplots for the CA1 specific genes reported in Table S4. The normalized counts are from the Illumina experiment, and the genes are ranked according the average Fold Change computed from the pairwise comparisons CA1 vs. CA3 and CA1 vs. DG.

Supplementary Figure 4 | Expression of genes *Wsf1, Nov, Ndst4,* and *Gpr161,* (specific to CA1 in our study) as reported in the Allen Brain Atlas (Mouse).

Supplementary Figure 5 | Boxplots for the CA3 specific genes reported in Table S5. The normalized counts are from the Illumina experiment, and the genes are ranked according the average Fold Change computed from the pairwise comparisons CA3 vs. CA1 and CA3 vs. DG.

Supplementary Figure 6 | Expression of genes *Col6a6* and *Nnat* (specific to CA3 in our study) as reported in the Allen Brain Atlas (Mouse).

Supplementary Figure 7 | Boxplots for the DG specific genes reported in Table S6. The normalized counts are from the Illumina experiment, and the genes are ranked according the average Fold Change computed from the pairwise comparisons DG vs. CA1 and DG vs. CA3.

Supplementary Figure 8 | Expression of genes *Pdin, Plk5, C1ql2,* and *Dsp* (specific to DG in our study) as reported in the Allen Brain Atlas (Mouse).

Supplementary Figure 9 | Heatmap of age-related changes in gene expression in the CA1 region. Each row represents a DEG (Illumina $p < 0.01$; Ion Proton $p < 0.05$) associated with aging. Gene-level counts were standardized to z-scores and the color represents the standard deviation increasing (yellow) or decreasing (blue) relative to the mean (black). The age-related gene enrichment clusters (FDR adj-$p < 0.05$) in the CA1 region included immune related GOs, neutrophil activation, cell adhesion and regulation of ERK1 and ERK2 cascade.

Supplementary Figure 10 | Heatmap of age-related changes in gene expression in the CA3 region. Each row represents a DEG (Illumina $p < 0.01$; Ion Proton $p < 0.05$) associated with aging. Gene-level counts were standardized to z-scores and the color represents the standard deviation increasing (yellow) or decreasing (blue) relative to the mean (black). The age-related gene enrichment clusters (FDR adj-$p < 0.05$) in the CA3 region included immune related GOs such as leukocyte activation, cytokine production, and antigen processing and presentation.

Supplementary Figure 11 | Heatmap of age-related changes in gene expression in the DG region. Each row represents a DEG (Illumina $p < 0.01$; Ion Proton $p < 0.05$) associated with aging. Gene-level counts were standardized to z-scores and the color represents the standard deviation increasing (yellow) or decreasing (blue) relative to the mean (black). The age-related gene enrichment clusters (FDR adj-$p < 0.05$) in the DG region included immune related GOs such as defense response, and inflammatory response. Cell-cell adhesion GO was also detected.

REFERENCES

Arnold, S. E., Louneva, N., Cao, K., Wang, L. S., Han, L. Y., Wolk, D. A., et al. (2013). Cellular, synaptic, and biochemical features of resilient cognition in Alzheimer's disease. *Neurobiol. Aging* 34, 157–168. doi: 10.1016/j.neurobiolaging.2012.03.004

Barnes, C. A., and McNaughton, B. L. (1980). Physiological compensation for loss of afferent synapses in rat hippocampal granule cells during senescence. *J. Physiol.* 309, 473–485. doi: 10.1113/jphysiol.1980.sp013521

Bean, L. A., Kumar, A., Rani, A., Guidi, M., Rosario, A. M., Cruz, P. E., et al. (2015). Re-opening the critical window for estrogen therapy. *J. Neurosci.* 35, 16077–16093. doi: 10.1523/JNEUROSCI.1890-15.2015

Ben-Ari, Y. (1985). Limbic seizure and brain damage produced by kainic acid: mechanisms and relevance to human temporal lobe epilepsy. *Neuroscience* 14, 375–403. doi: 10.1016/0306-4522(85)90299-4

Berron, D., Vieweg, P., Hochkeppler, A., Pluta, J. B., Ding, S. L., Maass, A., et al. (2017). A protocol for manual segmentation of medial temporal lobe subregions in 7 Tesla MRI. *Neuroimage Clin.* 15, 466–482. doi: 10.1016/j.nicl.2017.05.022

Blalock, E. M., Chen, K. C., Sharrow, K., Herman, J. P., Porter, N. M., Foster, T. C., et al. (2003). Gene microarrays in hippocampal aging: statistical profiling identifies novel processes correlated with cognitive impairment. *J. Neurosci.* 23, 3807–3819.

Blalock, E. M., Grondin, R., Chen, K. C., Thibault, O., Thibault, V., Pandya, J. D., et al. (2010). Aging-related gene expression in hippocampus proper compared with dentate gyrus is selectively associated with metabolic syndrome variables in rhesus monkeys. *J. Neurosci.* 30, 6058–6071. doi: 10.1523/JNEUROSCI.3956-09.2010

Bramblett, D. E., Pennesi, M. E., Wu, S. M., and Tsai, M. J. (2004). The transcription factor Bhlhb4 is required for rod bipolar cell maturation. *Neuron* 43, 779–793. doi: 10.1016/j.neuron.2004.08.032

Buchser, W. J., Slepak, T. I., Gutierrez-Arenas, O., Bixby, J. L., and Lemmon, V. P. (2010). Kinase/phosphatase overexpression reveals pathways regulating hippocampal neuron morphology. *Mol. Syst. Biol.* 6:391. doi: 10.1038/msb.2010.52

Burger, C. (2010). Region-specific genetic alterations in the aging hippocampus: implications for cognitive aging. *Front. Aging Neurosci.* 2:140. doi: 10.3389/fnagi.2010.00140

Burke, S. N., and Barnes, C. A. (2010). Senescent synapses and hippocampal circuit dynamics. *Trends Neurosci.* 33, 153–161. doi: 10.1016/j.tins.2009.12.003

Cansino, S. (2009). Episodic memory decay along the adult lifespan: a review of behavioral and neurophysiological evidence. *Int. J. Psychophysiol.* 71, 64–69. doi: 10.1016/j.ijpsycho.2008.07.005

Chakrabarty, P., Jansen-West, K., Beccard, A., Ceballos-Diaz, C., Levites, Y., Verbeeck, C., et al. (2010). Massive gliosis induced by interleukin-6 suppresses Abeta deposition *in vivo*: evidence against inflammation as a driving force for amyloid deposition. *FASEB J.* 24, 548–559. doi: 10.1096/fj.09-141754

Chapman, T. R., Barrientos, R. M., Ahrendsen, J. T., Hoover, J. M., Maier, S. F., and Patterson, S. L. (2012). Aging and infection reduce expression of specific brain-derived neurotrophic factor mRNAs in hippocampus. *Neurobiol. Aging* 33:832 e1–14. doi: 10.1016/j.neurobiolaging.2011.07.015

Chawla, M. K., Penner, M. R., Olson, K. M., Sutherland, V. L., Mittelman-Smith, M. A., and Barnes, C. A. (2013). Spatial behavior and seizure-induced changes in c-fos mRNA expression in young and old rats. *Neurobiol. Aging* 34, 1184–1198. doi: 10.1016/j.neurobiolaging.2012.10.017

Cooper, E. C. (2012). "Potassium Channels (including KCNQ) and Epilepsy," in *Jasper's Basic Mechanisms of the Epilepsies*, eds J. L. Noebels, M. Avoli, M. Rogawski, R. Olsen, and A. Delgado-Escueta (Bethesda, MD: National Center for Biotechnology Information (US)).

Craft, S., Foster, T. C., Landfield, P. W., Maier, S. F., Resnick, S. M., and Yaffe, K. (2012). Session III: mechanisms of age-related cognitive change and targets for intervention: inflammatory, oxidative, and metabolic processes. *J. Gerontol. A Biol. Sci. Med. Sci.* 67, 754–759. doi: 10.1093/gerona/gls112

Cribbs, D. H., Berchtold, N. C., Perreau, V., Coleman, P. D., Rogers, J., Tenner, A. J., et al. (2012). Extensive innate immune gene activation accompanies brain aging, increasing vulnerability to cognitive decline and neurodegeneration: a microarray study. *J. Neuroinflammation* 9:179. doi: 10.1186/1742-2094-9-179

Datson, N. A., Meijer, L., Steenbergen, P. J., Morsink, M. C., van der Laan, S., Meijer, O. C., et al. (2004). Expression profiling in laser-microdissected hippocampal subregions in rat brain reveals large subregion-specific differences in expression. *Eur. J. Neurosci.* 20, 2541–2554. doi: 10.1111/j.1460-9568.2004.03738.x

Daugherty, A. M., Bender, A. R., Yuan, P., and Raz, N. (2016). Changes in search path complexity and length during learning of a virtual water maze: age differences and differential associations with hippocampal subfield volumes. *Cereb. Cortex* 26, 2391–2401. doi: 10.1093/cercor/bhv061

de Cárcer, G., Escobar, B., Higuero, A. M., García, L., Ansón, A., Pérez, G., et al. (2011). Plk5, a polo box domain-only protein with specific roles in neuron differentiation and glioblastoma suppression. *Mol. Cell. Biol.* 31, 1225–1239. doi: 10.1128/MCB.00607-10

Driscoll, I., Howard, S. R., Stone, J. C., Monfils, M. H., Tomanek, B., Brooks, W. M., et al. (2006). The aging hippocampus: a multi-level analysis in the rat. *Neuroscience* 139, 1173–1185. doi: 10.1016/j.neuroscience.2006.01.040

Dröge, W., and Schipper, H. M. (2007). Oxidative stress and aberrant signaling in aging and cognitive decline. *Aging Cell.* 6, 361–370. doi: 10.1111/j.1474-9726.2007.00294.x

Dubey, D., McRae, P. A., Rankin-Gee, E. K., Baranov, E., Wandrey, L., Rogers, S., et al. (2017). Increased metalloproteinase activity in the hippocampus following status epilepticus. *Epilepsy Res.* 132, 50–58. doi: 10.1016/j.eplepsyres.2017.02.021

Elmslie, F., and Gardiner, M. (1995). Genetics of the epilepsies. *Curr. Opin. Neurol.* 8, 126–129. doi: 10.1097/00019052-199504000-00007

Foster, T. C. (1999). Involvement of hippocampal synaptic plasticity in age-related memory decline. *Brain Res. Brain Res. Rev.* 30, 236–249. doi: 10.1016/S0165-0173(99)00017-X

Foster, T. C. (2006). Biological markers of age-related memory deficits: treatment of senescent physiology. *CNS Drugs* 20, 153–166. doi: 10.2165/00023210-200620020-00006

Foster, T. C. (2007). Calcium homeostasis and modulation of synaptic plasticity in the aged brain. *Aging Cell* 6, 319–325. doi: 10.1111/j.1474-9726.2007.00283.x

Foster, T. C. (2012). Dissecting the age-related decline on spatial learning and memory tasks in rodent models: N-methyl-D-aspartate receptors and voltage-dependent Ca^{2+} channels in senescent synaptic plasticity. *Prog. Neurobiol.* 96, 283–303. doi: 10.1016/j.pneurobio.2012.01.007

Foster, T. C., Barnes, C. A., Rao, G., and McNaughton, B. L. (1991). Increase in perforant path quantal size in aged F-344 rats. *Neurobiol. Aging* 12, 441–448. doi: 10.1016/0197-4580(91)90071-Q

Foster, T. C., and Norris, C. M. (1997). Age-associated changes in Ca(2+)-dependent processes: relation to hippocampal synaptic plasticity. *Hippocampus* 7, 602–612. doi: 10.1002/(SICI)1098-1063(1997)7:6<602::AID-HIPO3>3.0.CO2-G

Fraser, H. B., Khaitovich, P., Plotkin, J. B., Pääbo, S., and Eisen, M. B. (2005). Aging and gene expression in the primate brain. *PLoS Biol.* 3:e274. doi: 10.1371/journal.pbio.0030274

Geinisman, Y. (1979). Loss of axosomatic synapses in the dentate gyrus of aged rats. *Brain Res.* 168, 485–492. doi: 10.1016/0006-8993(79)90304-4

Goodrich-Hunsaker, N. J., Hunsaker, M. R., and Kesner, R. P. (2008). The interactions and dissociations of the dorsal hippocampus subregions: how the dentate gyrus, CA3, and CA1 process spatial information. *Behav. Neurosci.* 122, 16–26. doi: 10.1037/0735-7044.122.1.16

Gray, D. T., and Barnes, C. A. (2015). Distinguishing adaptive plasticity from vulnerability in the aging hippocampus. *Neuroscience* 309, 17–28. doi: 10.1016/j.neuroscience.2015.08.001

Haberman, R. P., Colantuoni, C., Koh, M. T., and Gallagher, M. (2013). Behaviorally activated mRNA expression profiles produce signatures of learning and enhanced inhibition in aged rats with preserved memory. *PLoS ONE* 8:e83674. doi: 10.1371/journal.pone.0083674

Hesse, K., Vaupel, K., Kurt, S., Buettner, R., Kirfel, J., and Moser, M. (2011). AP-2delta is a crucial transcriptional regulator of the posterior midbrain. *PLoS ONE* 6:e23483. doi: 10.1371/journal.pone.0023483

Hunsberger, H. C., Rudy, C. C., Batten, S. R., Gerhardt, G. A., and Reed, M. N. (2015). P301L tau expression affects glutamate release and clearance in the hippocampal trisynaptic pathway. *J. Neurochem.* 132, 169–182. doi: 10.1111/jnc.12967

Ianov, L., Rani, A., Beas, B. S., Kumar, A., and Foster, T. C. (2016). Transcription profile of aging and cognition-related genes in the medial prefrontal cortex. *Front. Aging Neurosci.* 8:113. doi: 10.3389/fnagi.2016.00113

Ianov, L., Riva, A., Kumar, A., and Foster, T. C. (2017). DNA methylation of synaptic genes in the prefrontal cortex is associated with aging and age-related cognitive impairment. *Front. Aging Neurosci.* 9:249. doi: 10.3389/fnagi.2017.00249

Iijima, T., Miura, E., Watanabe, M., and Yuzaki, M. (2010). Distinct expression of C1q-like family mRNAs in mouse brain and biochemical characterization of their encoded proteins. *Eur. J. Neurosci.* 31, 1606–1615. doi: 10.1111/j.1460-9568.2010.07202.x

Ivanova, O. Y., Dobryakova, Y. V., Salozhin, S. V., Aniol, V. A., Onufriev, M. V., Gulyaeva, N. V., et al. (2016). Lentiviral modulation of Wnt/beta-catenin signaling affects *in vivo* LTP. *Cell Mol. Neurobiol.* 37, 1227–1241. doi: 10.1007/s10571-016-0455-z

Jackson, T. C., Rani, A., Kumar, A., and Foster, T. C. (2009). Regional hippocampal differences in AKT survival signaling across the lifespan: implications for CA1 vulnerability with aging. *Cell Death Differ.* 16, 439–448. doi: 10.1038/cdd.2008.171

Jessri, M., and Farah, C. S. (2014). Next generation sequencing and its application in deciphering head and neck cancer. *Oral Oncol.* 50, 247–253. doi: 10.1016/j.oraloncology.2013.12.017

Kadish, I., Thibault, O., Blalock, E. M., Chen, K. C., Gant, J. C., Porter, N. M., et al. (2009). Hippocampal and cognitive aging across the lifespan: a bioenergetic shift precedes and increased cholesterol trafficking parallels memory impairment. *J. Neurosci.* 29, 1805–1816. doi: 10.1523/JNEUROSCI.4599-08.2009

Kesner, R. P., Lee, I., and Gilbert, P. (2004). A behavioral assessment of hippocampal function based on a subregional analysis. *Rev. Neurosci.* 15, 333–351. doi: 10.1515/REVNEURO.2004.15.5.333

Kesner, R. P., and Rolls, E. T. (2015). A computational theory of hippocampal function, and tests of the theory: new developments. *Neurosci. Biobehav. Rev.* 48, 92–147. doi: 10.1016/j.neubiorev.2014.11.009

Kuhn, H. G., Dickinson-Anson, H., and Gage, F. H. (1996). Neurogenesis in the dentate gyrus of the adult rat: age-related decrease of neuronal progenitor proliferation. *J. Neurosci.* 16, 2027–2033.

Kusko, R., LeClerc, A., Swahn, S., Lenburg, M., and Spira, A. (2014). Comparison of illumina and ion torrent RNA-sequencing and microarray-based approaches for profiling the transcriptome. *J. Biomol. Tech.* 25, S14.

Landfield, P. W. (1988). Hippocampal neurobiological mechanisms of age-related memory dysfunction. *Neurobiol. Aging* 9, 571–579. doi: 10.1016/S0197-4580(88)80116-7

Lein, E. S., Zhao, X., and Gage, F. H. (2004). Defining a molecular atlas of the hippocampus using DNA microarrays and high-throughput *in situ* hybridization. *J. Neurosci.* 24, 3879–3889. doi: 10.1523/JNEUROSCI.4710-03.2004

Lemaire, V., Koehl, M., Le Moal, M., and Abrous, D. N. (2000). Prenatal stress produces learning deficits associated with an inhibition of neurogenesis in the hippocampus. *Proc. Natl. Acad. Sci. U.S.A.* 97, 11032–11037. doi: 10.1073/pnas.97.20.11032

Li, W., Turner, A., Aggarwal, P., Matter, A., Storvick, E., Arnett, D. K., et al. (2015). Comprehensive evaluation of AmpliSeq transcriptome, a novel targeted whole transcriptome RNA sequencing methodology for global gene expression analysis. *BMC Genomics* 16:1069. doi: 10.1186/s12864-015-2270-1

Liu, Y., Helms, A. W., and Johnson, J. E. (2004). Distinct activities of Msx1 and Msx3 in dorsal neural tube development. *Development* 131, 1017–1028. doi: 10.1242/dev.00994

Lu, T., Pan, Y., Kao, S. Y., Li, C., Kohane, I., Chan, J., et al. (2004). Gene regulation and DNA damage in the ageing human brain. *Nature* 429, 883–891. doi: 10.1038/nature02661

Maass, A., Schütze, H., Speck, O., Yonelinas, A., Tempelmann, C., Heinze, H. J., et al. (2014). Laminar activity in the hippocampus and entorhinal cortex related to novelty and episodic encoding. *Nat. Commun.* 5, 5547. doi: 10.1038/ncomms6547

Masser, D. R., Bixler, G. V., Brucklacher, R. M., Yan, H., Giles, C. B., Wren, J. D., et al. (2014). Hippocampal subregions exhibit both distinct and shared transcriptomic responses to aging and nonneurodegenerative cognitive decline. *J. Gerontol. A Biol. Sci. Med. Sci.* 69, 1311–1324. doi: 10.1093/gerona/glu091

Mazarati, A., Lundström, L., Sollenberg, U., Shin, D., Langel, U., and Sankar, R. (2006). Regulation of kindling epileptogenesis by hippocampal galanin type 1 and type 2 receptors: the effects of subtype-selective agonists and the role of G-protein-mediated signaling. *J. Pharmacol. Exp. Ther.* 318, 700–708. doi: 10.1124/jpet.106.104703

McColl, C. D., Jacoby, A. S., Shine, J., Iismaa, T. P., and Bekkers, J. M. (2006). Galanin receptor-1 knockout mice exhibit spontaneous epilepsy, abnormal EEGs and altered inhibition in the hippocampus. *Neuropharmacology* 50, 209–218. doi: 10.1016/j.neuropharm.2005.09.001

Mueller, S. G., and Weiner, M. W. (2009). Selective effect of age, Apo e4, and Alzheimer's disease on hippocampal subfields. *Hippocampus* 19, 558–564. doi: 10.1002/hipo.20614

Newrzella, D., Pahlavan, P. S., Krüger, C., Boehm, C., Sorgenfrei, O., Schröck, H., et al. (2007). The functional genome of CA1 and CA3 neurons under native conditions and in response to ischemia. *BMC Genomics* 8:370. doi: 10.1186/1471-2164-8-370

Oh, M. M., and Disterhoft, J. F. (2010). Cellular mechanisms for altered learning in aging. *Future Neurol.* 5, 147–155. doi: 10.2217/fnl.09.74

Penner, M. R., Roth, T. L., Chawla, M. K., Hoang, L. T., Roth, E. D., Lubin, F. D., et al. (2011). Age-related changes in Arc transcription and DNA methylation within the hippocampus. *Neurobiol. Aging* 32, 2198–2210. doi: 10.1016/j.neurobiolaging.2010.01.009

Reuter, J. A., Spacek, D. V., and Snyder, M. P. (2015). High-throughput sequencing technologies. *Mol. Cell* 58, 586–597. doi: 10.1016/j.molcel.2015.05.004

Rogalski, E., Stebbins, G. T., Barnes, C. A., Murphy, C. M., Stoub, T. R., George, S., et al. (2012). Age-related changes in parahippocampal white matter integrity: a diffusion tensor imaging study. *Neuropsychologia* 50, 1759–1765. doi: 10.1016/j.neuropsychologia.2012.03.033

Rolls, E. T., and Kesner, R. P. (2006). A computational theory of hippocampal function, and empirical tests of the theory. *Prog. Neurobiol.* 79, 1–48. doi: 10.1016/j.pneurobio.2006.04.005

Rönnlund, M., Nyberg, L., Bäckman, L., and Nilsson, L. G. (2005). Stability, growth, and decline in adult life span development of declarative memory: cross-sectional and longitudinal data from a population-based study. *Psychol. Aging* 20, 3–18. doi: 10.1037/0882-7974.20.1.3

Rowe, W. B., Blalock, E. M., Chen, K. C., Kadish, I., Wang, D., Barrett, J. E., et al. (2007). Hippocampal expression analyses reveal selective association of immediate-early, neuroenergetic, and myelinogenic pathways with cognitive impairment in aged rats. *J. Neurosci.* 27, 3098–3110. doi: 10.1523/JNEUROSCI.4163-06.2007

Rozovsky, I., Wei, M., Morgan, T. E., and Finch, C. E. (2005). Reversible age impairments in neurite outgrowth by manipulations of astrocytic GFAP. *Neurobiol. Aging* 26, 705–715. doi: 10.1016/j.neurobiolaging.2004.06.009

Shi, L., Argenta, A. E., Winseck, A. K., and Brunso-Bechtold, J. K. (2004). Stereological quantification of GAD-67-immunoreactive neurons and boutons in the hippocampus of middle-aged and old Fischer 344 x Brown Norway rats. *J. Comp. Neurol.* 478, 282–291. doi: 10.1002/cne.20303

Sochocka, M., Diniz, B. S., and Leszek, J. (2017). Inflammatory response in the CNS: friend or foe? *Mol. Neurobiol.* 54, 8071–8089. doi: 10.1007/s12035-016-0297-1

Stanley, D. P., and Shetty, A. K. (2004). Aging in the rat hippocampus is associated with widespread reductions in the number of glutamate decarboxylase-67 positive interneurons but not interneuron degeneration. *J. Neurochem.* 89, 204–216. doi: 10.1111/j.1471-4159.2004.02318.x

Streit, W. J., Xue, Q. S., Braak, H., and del Tredici, K. (2014). Presence of severe neuroinflammation does not intensify neurofibrillary degeneration in human brain. *Glia* 62, 96–105. doi: 10.1002/glia.22589

Toescu, E. C., Verkhratsky, A., and Landfield, P. W. (2004). Ca^{2+} regulation and gene expression in normal brain aging. *Trends Neurosci.* 27, 614–620. doi: 10.1016/j.tins.2004.07.010

Uddin, R. K., and Singh, S. M. (2013). Hippocampal gene expression meta-analysis identifies aging and age-associated spatial learning impairment (ASLI) genes and pathways. *PLoS ONE* 8:e69768. doi: 10.1371/journal.pone.0069768

Uttl, B., and Graf, P. (1993). Episodic spatial memory in adulthood. *Psychol. Aging* 8, 257–273. doi: 10.1037/0882-7974.8.2.257

Valente, T., Domínguez, M. I., Bellmann, A., Journot, L., Ferrer, I., and Auladell, C. (2004). Zac1 is up-regulated in neural cells of the limbic system of mouse brain following seizures that provoke strong cell activation. *Neuroscience* 128, 323–336. doi: 10.1016/j.neuroscience.2004.06.056

Varela-Nallar, L., and Inestrosa, N. C. (2013). Wnt signaling in the regulation of adult hippocampal neurogenesis. *Front. Cell. Neurosci.* 7:100. doi: 10.3389/fncel.2013.00100

Volk, L., Chiu, S. L., Sharma, K., and Huganir, R. L. (2015). Glutamate synapses in human cognitive disorders. *Annu. Rev. Neurosci.* 38, 127–149. doi: 10.1146/annurev-neuro-071714-033821

Wang, F., and Diana, R. A. (2016). Temporal context processing within hippocampal subfields. *Neuroimage* 134, 261–269. doi: 10.1016/j.neuroimage.2016.03.048

Wang, X., Zaidi, A., Pal, R., Garrett, A. S., Braceras, R., Chen, X. W., et al. (2009). Genomic and biochemical approaches in the discovery of mechanisms for selective neuronal vulnerability to oxidative stress. *BMC Neurosci.* 10:12. doi: 10.1186/1471-2202-10-12

Wisse, L. E., Adler, D. H., Ittyerah, R., Pluta, J. B., Robinson, J. L., Schuck, T., et al. (2016). Comparison of *in vivo* and *ex vivo* MRI of the human hippocampal formation in the same subjects. *Cereb. Cortex* 27, 5185–5196. doi: 10.1093/cercor/bhw299

Xu, N., Zhou, W. J., Wang, Y., Huang, S. H., Li, X., and Chen, Z. Y. (2015). Hippocampal Wnt3a is necessary and sufficient for contextual fear memory acquisition and consolidation. *Cereb. Cortex* 25, 4062–4075. doi: 10.1093/cercor/bhu121

Yassa, M. A., Mattfeld, A. T., Stark, S. M., and Stark, C. E. (2011). Age-related memory deficits linked to circuit-specific disruptions in the hippocampus. *Proc. Natl. Acad. Sci. U.S.A.* 108, 8873–8878. doi: 10.1073/pnas.1101567108

Yushkevich, P. A., Amaral, R. S., Augustinack, J. C., Bender, A. R., Bernstein, J. D., Boccardi, M., et al. (2015). Quantitative comparison of 21 protocols for labeling hippocampal subfields and parahippocampal subregions in *in vivo* MRI: towards a harmonized segmentation protocol. *Neuroimage* 111, 526–541. doi: 10.1016/j.neuroimage.2015.01.004

Zeier, Z., Madorsky, I., Xu, Y., Ogle, W. O., Notterpek, L., and Foster, T. C. (2011). Gene expression in the hippocampus: regionally specific effects of aging and caloric restriction. *Mech. Ageing Dev.* 132, 8–19. doi: 10.1016/j.mad.2010.10.006

Conflict of Interest Statement: The authors declare that the research was conducted in the absence of any commercial or financial relationships that could be construed as a potential conflict of interest.

frontiers in Aging Neuroscience

ORIGINAL RESEARCH
published: 26 September 2018
doi: 10.3389/fnagi.2018.00294

Increase in Blood Levels of Growth Factors Involved in the Neuroplasticity Process by Using an Extremely Low Frequency Electromagnetic Field in Post-stroke Patients

Natalia Cichoń[1], Michał Bijak[1], Piotr Czarny[2], Elżbieta Miller[3,4], Ewelina Synowiec[5], Tomasz Sliwinski[5] and Joanna Saluk-Bijak[1]*

[1] Department of General Biochemistry, Faculty of Biology and Environmental Protection, University of Lodz, Łódź, Poland, [2] Department of Medical Biochemistry, Medical University of Lodz, Łódź, Poland, [3] Department of Physical Medicine, Medical University of Lodz, Łódź, Poland, [4] Neurorehabilitation Ward, III General Hospital in Lodz, Łódź, Poland, [5] Laboratory of Medical Genetics, Department of Molecular Genetics, Faculty of Biology and Environmental Protection, University of Lodz, Łódź, Poland

OPEN ACCESS

Edited by:
Ashok Kumar,
University of Florida, United States

Reviewed by:
Eduardo Candelario-Jalil,
University of Florida, United States
Hyacinth Idu Hyacinth,
Emory University, United States

***Correspondence:**
Natalia Cichoń
natalia.cichon@biol.uni.lodz.pl

Received: *13 April 2018*
Accepted: *06 September 2018*
Published: *26 September 2018*

Citation:
Cichoń N, Bijak M, Czarny P, Miller E, Synowiec E, Sliwinski T and Saluk-Bijak J (2018) Increase in Blood Levels of Growth Factors Involved in the Neuroplasticity Process by Using an Extremely Low Frequency Electromagnetic Field in Post-stroke Patients. Front. Aging Neurosci. 10:294. doi: 10.3389/fnagi.2018.00294

Background: Neuroplasticity ensures the improvement of functional status in patients after stroke. The aim of this study was to evaluate the effect of extremely low-frequency electromagnetic field therapy (ELF-EMF) on brain plasticity in the rehabilitation of patients after stroke.

Methods: Forty-eight patients were divided into two groups underwent the same rehabilitation program, but in the study group, the patients additionally were exposed to a standard series of 10 ELF-EMF treatments. To determine the level of neuroplasticity, we measured the plasma level of the brain-derived neurotrophic factor (BDNF), the vascular-endothelial growth factor, as well as BDNF mRNA expression. Additionally, we determined the molecule levels for hepatocyte growth factor, stem cell factor, stromal cell-derived factor 1α, nerve growth factor β, and leukemia inhibitory factor, using 5plex cytokine panel in plasma. After 4 weeks, during which patients had undergone neurorehabilitation and neurological examinations, we assessed functional recovery using the Barthel Index, Mini-Mental State Examination (MMSE), Geriatric Depression Scale, National Institutes of Health Stroke Scale (NIHSS), and the modified Rankin Scale (mRS).

Results: We observed that ELF-EMF significantly increased growth factors and cytokine levels involved in neuroplasticity, as well as promoted an enhancement of functional recovery in post-stroke patients. Additionally, we presented evidence that these effects could be related to the increase of gene expression on the mRNA level. Moreover, a change of BDNF plasma level was positively correlated with the Barthel Index, MMSE, and negatively correlated with GDS.

Conclusion: Extremely low-frequency electromagnetic field therapy improves the effectiveness of rehabilitation of post-stroke patients by improving neuroplasticity processes.

Keywords: extremely low-frequency electromagnetic field, neuroplasticity, brain-derived neurotrophic factor, stroke, rehabilitation

INTRODUCTION

Regenerative processes within the brain tissue are limited and regulated by tissue environmental properties, which are affected by changes in the physiology of the organism (Hagg, 2009). Neurotrophic factors affect neurogenesis through the condition of the growth of new neurons and the survival of existing ones (Hylin et al., 2017). Traditionally, neurotrophic factors are divided into three protein families: the classic neurotrophin, ligands of Glial Cell Derived Neurotrophic Factor (GDNF), and neuropoietic cytokines. Neurotrophins are synthesized and secreted by nerve cells in the brain and spinal cord, and the cells of dependent tissue (Hagg, 2009; Lindholm and Saarma, 2010).

Compensatory plasticity of the damaged brain is a completely different process from the plasticity occurring in a normally functioning, healthy brain. This process is initiated under critical conditions: in interactions with oedema, inflammation, apoptosis, metabolic disturbances, and fiber degeneration. It starts immediately after an ischaemic event (Liguz-Lecznar and Kossut, 2013). Moreover, neuroplasticity consists of strengthening the existing nerve pathways and then establishing new connections. Existing, but weaker connections between brain centers undergo activation (Martin et al., 2017). As a result, the defective function can be restored partially or completely, because other cortical or subcortical structures will take over the function of the damaged area. In the brain in animal models, synaptogenesis was found in the area adjacent to tissue damaged by the stroke, and also in regions of the undammed hemisphere (Law et al., 2017).

Neuroplasticity is closely related to neurogenesis, wherein fully functioning neuronal cells are generated, resulting from the differentiation of neuronal stem cells (NSCs) present in the adult, fully formed brain. NSCs are characterized by the ability of indefinite mitotic division, potential divisions, and to differentiate into the appropriate morphological phenotype (Klein et al., 2016). The process of neurogenesis occurs in certain brain structures throughout life, nevertheless the rate of proliferation and the ability of the newly formed neurons to survive to reduce with age. Nerve cells are generated in brain regions responsible for learning, memory, and reception of olfactory sensation, primarily in the sub-ventricular zone (SVZ) and the subgranular zone (SGZ), and also in the migration of emergent neuroblasts toward injury (Zelentsova-Levytskyi et al., 2017). Neurogenesis is regulated by many factors, including neurotrophins, growth factors, hormones, neurotransmitters, and microenvironmental factors (Aimone et al., 2014).

Physical therapy, including the use of extremely low-frequency electromagnetic field (ELF-EMF) therapy, is beneficial in restoring the patients after stroke. ELF-EMF demonstrates anti-inflammatory, regenerative, analgesic, and osteogenic action. Moreover, ELF-EMF promotes cell proliferation, protein synthesis, ion transport, and changes in cellular signal transmission (Li, 2017). Our previous studies have shown that ELF-EMF therapy reduces oxidative stress during rehabilitation of post-acute stroke patients (Cichoń et al., 2017a, 2018). Additionally, our recent research, for the first time focused on the effect of ELF-EMF on the potential factors of brain plasticity, indicate that ELF-EMF therapy increases the generation and metabolism of NO – neurotransmitter regulating neurogenesis, and synaptic plasticity (Cichoń et al., 2017b). As part of the broadening the examined issue, the present analyses are a continuation of the parameter evaluation of the same group of post-stroke patients but currently relate to changes in blood levels of growth factors involved in the neuroplasticity process, induced by ELF-EMF therapy. We selected two significant growth factors for analysis, i.e., brain-derived neurotrophic factor (BDNF) and vascular endothelial growth factor (VEGF). BDNF is the most common neurotrophin in the nervous system, and playing an important role as an effective indicator for rehabilitation interventions in relation to brain neuroplasticity improvement (Qiao et al., 2017). VEGF is one of the most important pro-angiogenic factors and is critical for blood vessel growth in the nervous system of vertebrates. VEGF-induced blood vessel growth may be essential for nervous tissue regeneration during the recovery process. Moreover, several recent studies demonstrate that VEGF has significant non-vascular functions in the nervous system, and it can be considered as an important agent for promoting neurogenesis, glial growth, and nerve repair (Rosenstein et al., 2010). It is well documented that the cytokine-mediated inflammatory mechanisms within the central nervous system (CNS) contribute to cognitive impairment due to disorders of neurons and glial cells in acute stroke patients. Therefore, we have also chosen a panel of 5 cytokines (HGF, SCF, SDF-1α, β-NGF, and LIF) simultaneous measured using Bio-Plex System, which may be the important factors involved in the neurochemical features of brain tissue damage and repair.

MATERIALS AND METHODS

Blood Sample Collection

Blood samples were taken twice: before and after a standard ten sessions of therapy (with an interval of 14 days). They were collected into $CPDA_1$ containing tubes (Sarstedt, Nümbrecht, Germany). For analysis of mRNA expression, a portion of the sample was frozen at −80°C immediately upon collection. The rest of the samples were centrifuged (15 min at 1,500 *g*) at 25°C, to isolate the plasma. All blood samples were collected at the same

time of day (between 7 am and 9 am), under conditions of dietary fasting, and stored using the same protocol.

Subject Presentation

Post-stroke patients with moderate stroke severity (n = 48) were recruited to the study, and were then randomly divided into a study group [ELF-EMF (n = 25; NIHSS scores of 4.9 ± 3.1; aged 48.0 ± 8.0)], and a control group [non-ELF-EMF (n = 23; NIHSS scores of 5.4 ± 2.9; aged 44.8 ± 7.7)]. Clinical and demographic characteristics are shown in **Table 1**. The same patients were enrolment to our previous study (Cichoń et al., 2017b). Subjects with neurological illness other than stroke, haemorrhagic stroke, chronic or significant acute inflammatory factors, dementia, and/or decreased consciousness in their medical pre-stroke history, were all excluded. The patients had undergone neurorehabilitation as well as internal and neurological examinations, for 4 weeks in Neurorehabilitation Ward III of the General Hospital in Łódź, Poland.

In both subject groups the same therapeutic program (aerobic exercise 30 min, neurophysiological routines 60 min, and 15 min psychological therapy) was used. Furthermore, ELF-EMF therapy was conducted using a Magnetronic MF10 generator (EiE Elektronika i Elektromedycyna, Otwock, Poland). Both groups were treated for the same amount of time (15 min), but sham exposures were administrated to the non-ELF-EMF subjects. Subjects were excluded from the ELF-EMF group who had electronic and/or metal implants (pacemakers, etc.). ELF-EMF therapy with specific parameters (magnetic induction of 5 mT, 40 Hz, rectangular and bipolar waveforms) was conducted in the ELF-EMF group. The pelvic girdle of the patients was exposed to the electromagnetic field.

TABLE 1 | Demographic characteristics.

	Non-ELF-EMF group	ELF-EMF group	*p*
Demographics			
Age [mean ± *SD*]	44.8 ± 7.7	48.0 ± 8.0	0.84
Sex (man) [%]	48 vs. 52	60 vs. 40	0.27
Living alone [%]	32.1	34.2	0.59
Vascular risk			
Hypertension [%]	97.3	98.5	0.07
Diabetes [%]	31.4	39.2	0.21
Dyslipidemia [%]	78.8	72.2	0.7
BMI ≥ 30 [%]	21	34	0.78
Concomitant medications			
Antidepressants [%]	29	34	0.5
ASA [%]	70	65	0.42
NSAID [%]	25	27	0.8
Stroke characteristics			
Weeks since stroke [mean ± *SD*]	3.9 ± 0.6	3.2 ± 0.4	
NIHSS scores [mean ± *SD*]	5.4 ± 2.9	4.9 ± 3.1	
ADL [mean ± *SD*]	8.89 ± 2.87	9.95 ± 2.35	0.22
Lesion location			
Anterior [*n*]	3	5	
Posterior [*n*]	7	6	
Intermediate [*n*]	13	14	
Lesion side			
Left [*n*]	15	13	
Right [*n*]	8	12	

Determination of BDNF Level in Plasma

Plasma samples were diluted ten times (using a diluents buffer) before measurement of BDNF concentration, using a Human BDNF ELISA Kit (Abcam, Cambridge, MA, United States), in accordance with the manufacturer's protocol. The intensity of the color was measured at 450 nm (Schiavone et al., 2017).

Determination of *BDNF* Expression in Whole Blood Samples

Isolation of RNA and Reverse Transcription

Frozen whole blood samples (−80°C) were lysed using TRI Reagent® (Sigma-Aldrich, St. Louis, MO, United States), after which phase separation was performed. Then, an InviTrap Spin Universal RNA Mini Kit (Stratec Biomedical Systems, Birkenfeld, Germany) was used to purify the RNA-containing aqueous phase. The quantity and purity of RNA were estimated using a Synergy HTX Multi-Mode Microplate Reader, equipped with a Take3 Micro-Volume Plate (BioTek Instruments, Inc., Winooski, VT, United States). RNA samples were diluted to 20 ng/μL and transcribed into cDNA with a High-Capacity cDNA Reverse Transcription Kit (Applied Biosystems^{TM}, Waltham, MA, United States). All steps were performed according to the manufacturers' recommendations.

Real-Time PCR

Expression levels of the studied genes were obtained using the following TaqMan probes: Hs02718934_s1 for human *BDNF* gene, and Hs02786624_g1 as an endogenous control, which was a human *GAPDH* gene (Life Technologies, Carlsbad, CA, United States). Real-time PCRs were performed in a CFX96 real-time PCR system (Bio-Rad Laboratories, Hercules, CA, United States) using a TaqMan Universal Master Mix II, without UNG (Life Technologies, Carlsbad, CA, United States). All procedures were performed according to the manufacturers' protocols. Relative expressions of the studied genes were calculated using the equation $2^{-\Delta Ct}$, where $\Delta Ct = Ct_{targetgene} - Ct_{GAPDH}$.

Determination of VEGF in Plasma

Measurement of VEGF concentration was conducted using a VEGF Human ELISA Kit (Novex® Life Technologies, Carlsbad, CA, United States), according to the manufacturer's protocol. The intensity of the color was measured at 450 nm (Ling et al., 2015).

Analysis of Plasma Cytokine Levels

The level of HGF, SCF, SDF-1α, β-NGF, and LIF plasma growth factors were indicated using a Human Cytokine 5-plex assay kit (Bio-Rad, Hercules, CA, United States), on a Bio-Plex® 200 system (Bio-Rad, Hercules, CA, United States). Growth factors were measured in accordance with the manufacturer's protocol (Zanotta et al., 2016).

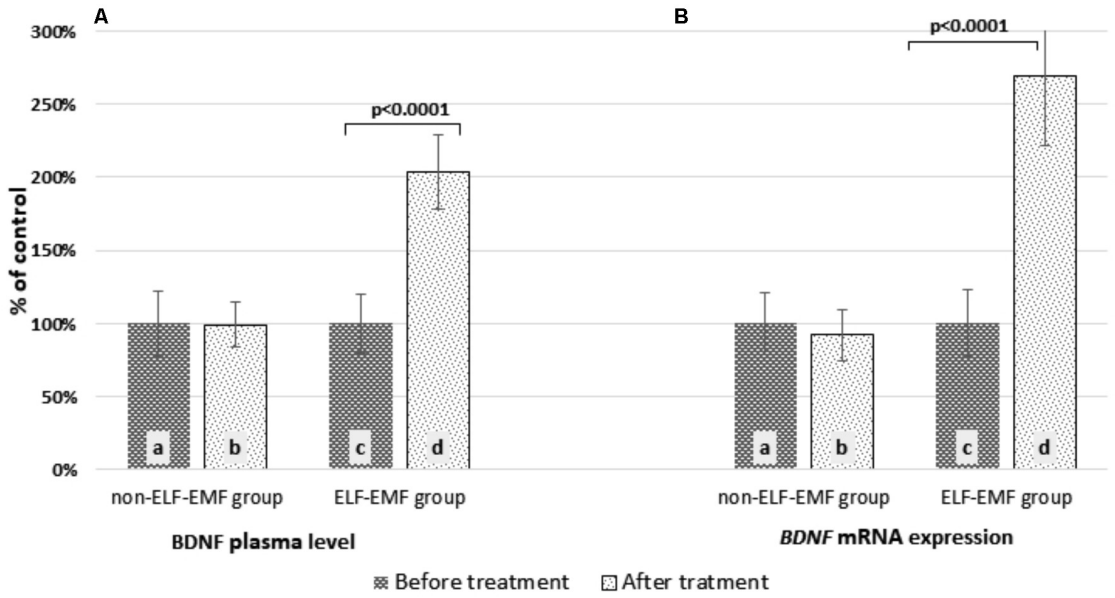

FIGURE 1 | Comparison of the BDNF level obtained from the ELF-EMF group vs. the non-ELF-EMF group. **(A)** BDNF plasma concentration. Statistical significance between ELF-EMF and non-ELF-EMF groups: b vs. d: $p < 0.0001$. **(B)** *BDNF* mRNA expression. Statistical significance between ELF-EMF and non-ELF-EMF groups: b vs. d: $p < 0.0001$.

Clinical Parameters Determination

The stroke-related neurologic deficit was measured using The National Institutes of Health Stroke Scale (NIHSS). Functional status was evaluated using the Barthel Index of Activities of Daily Living (ADL) and modified Rankin Scale (mRS), and cognitive status using the Mini-Mental State Examination (MMSE). Depression, the most common affective complication after stroke, was estimated using the Geriatric Depression Scale (GDS) (Cichoń et al., 2017a). The NIHSS, ADL, MMSE, GDS, and mRS were conducted either on the same day as the blood sampling or the afternoon before, in both groups.

Data Analysis

All experiments were performed in duplicate and calculated as mean values. For all subjects, the values of parameters before their treatments were used as the output value (100%). Data from the experiments performed on these same subjects after appropriate treatments were expressed as a percentage of the output value. Values obtained in this way were expressed as mean ± SD.

The all statistical analyses were performed using Stats Direct statistical software v.2.7.2. To avoid committing a type 1 error statistical analysis was performed using multiple comparison methods. First, the Shapiro–Wilk test was used to assess normal distribution of variables. Next, the results were analyzed for equality of variance using Levene's test. The significance of the differences between the values was analyzed using ANOVA, followed by Tukey's range test for multiple comparisons (for data with normal distribution and equality of variance) or non-parametric the Kruskal–Wallis test (when variables had other than normal distribution or had no equality of variance) (Bijak et al., 2012, 2013).

Additionally, we performed a correlation analysis between the changes in both experimental and clinical parameters. For these analyses, a Spearman's rank correlation was used, with the Spearman's rank correlation coefficient and the probability of correlation designated. For all analyses, a level of $p < 0.05$ was accepted as statistically significant.

RESULTS

In our comparative analysis, we demonstrated the effect of ELF-EMF therapy on various neurotrophic factors. Particularly relevant findings relate to the level of BDNF as the most prevalent growth factor in the CNS, which is essential for the development of CNS and neuronal plasticity. The plasma level of BDNF in the ELF-EMF group after ten sessions of rehabilitation was significantly higher compared to the non-ELF-EMF group ($p < 0.0001$). The increase of the BDNF level in the ELF-EMF group was about 200% ($p < 0.0001$), while in the non-ELF-EMF group it was comparable ($p > 0.05$) (**Figure 1A**). We also evaluated the effect of ELF-EMF on gene expression in the whole blood samples of *BDNF*. We demonstrated that after ELF-EMF therapy, expression of *BDNF* increased about 195% ($p < 0.0001$), while in the non-ELF-EMF group it did not change (**Figure 1B**). Because of the crucial role of BDNF participates in the formation of appropriate synaptic connections in the brain, it seems that ELF-EMF may serve as a therapeutic treatment to improve the neuroplasticity after stroke. Moreover, as proved to be significant differences in the level of VEGF caused by ELF-EMF application. VEGF is crucial for cross-talk between the cardiovascular and nervous systems, which is particularly important in the case

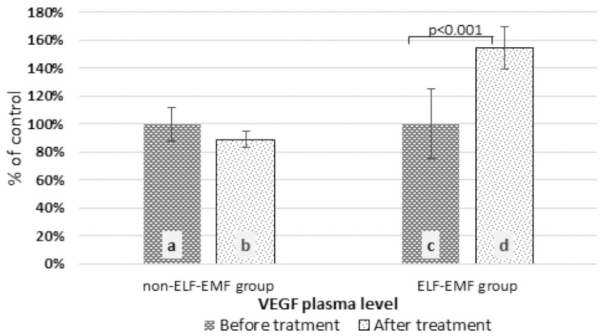

FIGURE 2 | Comparison of the plasma VEGF level obtained from the ELF-EMF group vs. the non-ELF-EMF group. Statistical significance between ELF-EMF and non-ELF-EMF groups: b vs. d: $p < 0.001$.

TABLE 2 | Plasma levels (in pg/ml) of BDNF and VEGF measured before and after treatment in ELF-EMF and non-ELF-EMF groups.

		Non-ELF-EMF group	ELF-EMF group
BDNF [pg/ml]	Before treatment	25.57	23.68
	After treatment	23.31	36.36
	p	>0.05	<0.001
VEGF [pg/ml]	Before treatment	37.67	30.75
	After treatment	34.79	46.29
	p	>0.05	<0.001

TABLE 3 | Cytokine plasma profile.

		Non-ELF-EMF group	ELF-EMF group
HGF [pg/ml]	Before treatment	369.55	274.43
	After treatment	390.83	366.62
	p	>0.05	<0.001
SCF [pg/ml]	Before treatment	96.21	85.66
	After treatment	98.68	105.29
	p	>0.05	<0.05
SDF-1α [pg/ml]	Before treatment	105.55	122.45
	After treatment	108.65	120.40
	p	>0.05	>0.05
βNGF [pg/ml]	Before treatment	<2.57	<2.57
	After treatment	<2.57	<2.57
LIF [pg/ml]	Before treatment	<1.92	<1.92
	After treatment	<1.92	<1.92

of brain stroke that damages both blood vessels and nervous tissue. After treatment, the VEGF plasma concentration in the ELF-EMF group increased about 50% ($p < 0.001$), but in the non-ELF-EMF group it remained unchanged ($p > 0.05$) (**Figure 2**). The raw data of both BDNF and VEGF plasma level has been shown in **Table 2**). We also assessed five cytokine concentrations in plasma using the Luminex platform. Two of these (βNGF and LIF) presented as out of range, both before and after treatment (<2.57 pg/ml and 1.92 pg/ml, respectively) (**Table 3**). After treatments, hepatocyte growth factor (HGF) and stem cell factor (SCF) levels in plasma were elevated in the ELF-EMF group ($p < 0.01$ and $p < 0.05$, respectively), but the SDF-1α level was comparable in both groups ($p > 0.05$) (**Table 3** and **Figure 3**). HGF is another (like VEGF) angiogenic factor that also produces neurotrophic effects in CNS. HGF plays pivotal roles in the nervous system during nerve regeneration process, by acting on neuronal or non-neuronal cells. HGF concentration after ELF-EMF therapy increased about 35% ($p < 0.01$), and in the non-ELF-EMF group remained unchanged ($p > 0.05$) (**Figure 3A**). SCF is a cytokine belonging to the control factors of the differentiation of stem cells to neurons and glia. Given the capacity of SCF to induction of regenerate of cells lost through brain injury, this cytokine seems particularly essential for the course of neuroplasticity processes. SCF level in the ELF-EMF group was higher by about 25% after treatment ($p < 0.05$), and in the non-ELF-EMF group was unchanged ($p > 0.05$) (**Figure 3B**). After therapy, the change of SDF-1α concentration was low and not statistically significant in either group (**Table 3** and **Figure 3C**).

Additionally, we estimated the clinical status of patients using NIHSS, ADL, mRS, MMSE, and the GDS in both groups. Stroke-related neurologic deficit estimated using NIHSS in ELF-EMF group decreased about 65% more than in non-ELF-EMF group ($p < 0.001$) (**Figure 4**). Functional status assessed by ADL in both groups increased ($p < 0.001$ and $p < 0.001$), but ΔADL in both groups was comparable ($p > 0.05$), whereas assessed by mRS decreased in both group, and decline in ELF-EMF group was more about 50% than in non-ELF-EMF group ($p < 0.01$) (**Figure 4**). A better improvement after ELF-EMF therapy was observed in cognitive impairment estimated by MMSE, with about a 35% higher growth (**Figure 4**). Depressive syndrome measured in GDS decreased significantly, while ΔGDS gained about 45% better results in the ELF-EMF group than the non-ELF-EMF group (**Figure 4**).

Subsequently, we performed a correlation analysis between the plasma level of the most important neurotrophic factor, BDNF, and clinical parameters. Correlation parameters indicated a significant positive correlation between changes (Δ) of BDNF plasma level and ΔADL, as well as between ΔBNDF and ΔMMSE, and a negative correlation between ΔBNDF and ΔGDS (**Figure 5**). The detailed process of these relationships, which confirms the correlation and the numeric data shown, is presented in **Table 3**.

DISCUSSION

Post-stroke rehabilitation is intended to restore the patient to a healthy condition and return them to a functional state, as prior to their illness, or allow them to adapt and achieve an optimal level of independence. Active post-stroke therapy should be begun as soon as possible, immediately upon stabilization of the general medical state. The rehabilitation process should be continued until obtaining a good result on an actual improvement index, which should also include cognitive disorders and behavioral changes (Jia et al., 2017).

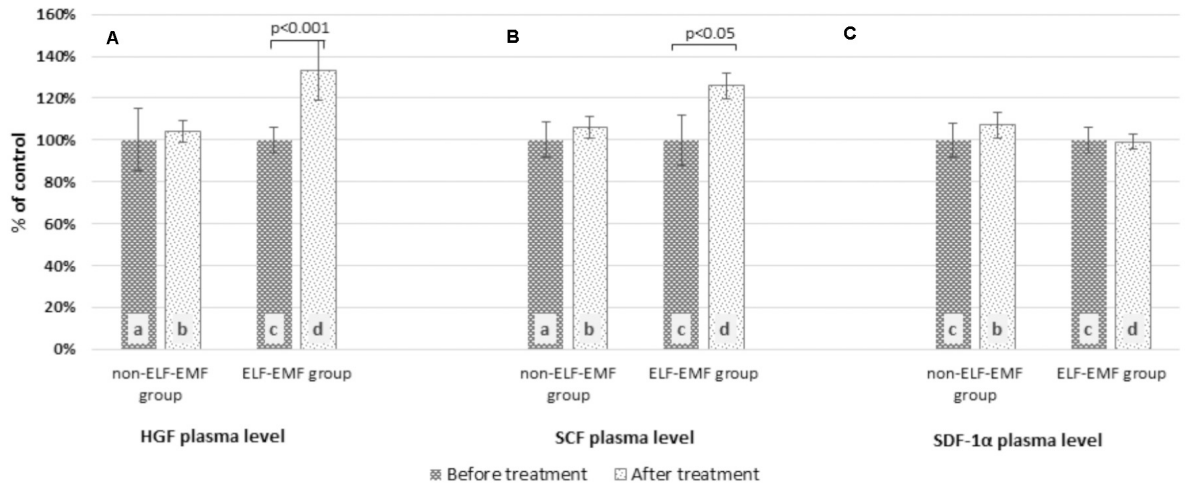

FIGURE 3 | Comparison of the plasma cytokine profile obtained from the ELF-EMF group vs the non-ELF-EMF group. **(A)** HGF plasma level. Statistical significance between ELF-EMF and non-ELF-EMF groups: b vs. d: $p < 0.01$. **(B)** SCF plasma level. Statistical significance between ELF-EMF and non-ELF-EMF groups: b vs. d: $p < 0.05$. **(C)** SDF-1α plasma level.

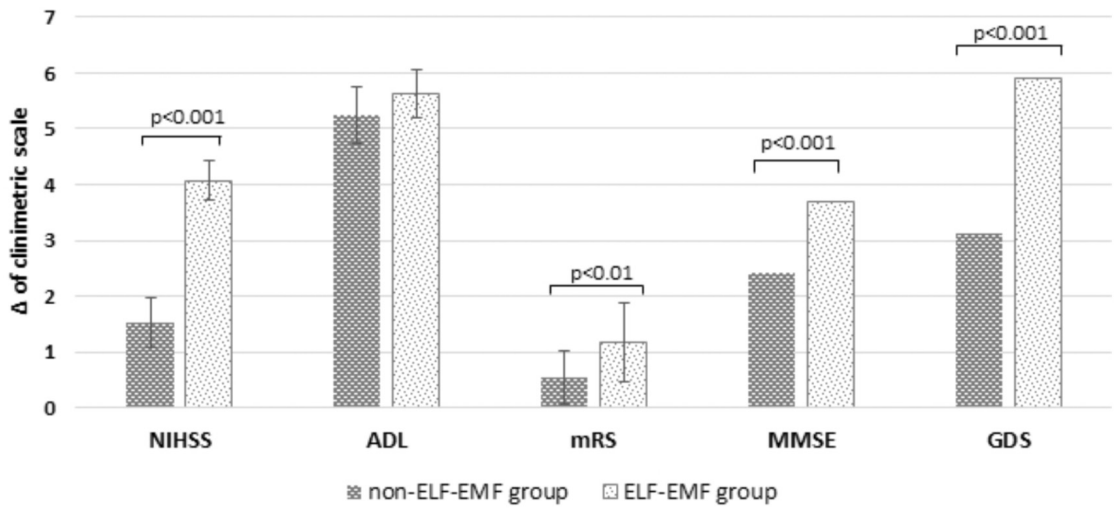

FIGURE 4 | Clinical parameters NIHSS, ADL, mRS, MMSE, and GDS as measured in the study vs. the control group. Data is shown here as a delta of scores obtained before and after the standard series of treatments (Δ NIHSS = the decline of NIHSS; ΔADL = the gain of ADL; Δ mRS = the decline of mRS; Δ MMSE = the gain of MMSE; Δ GDS = the decline of GDS).

Ischaemic stroke and other acute CNS injury indicates an increase of neuronal progenitor's proliferation in the SVZ zone identifying the lesion area and neuroblast migration to the ischaemic area within the striatum and cortex (Hu et al., 2013; Liu et al., 2015b; Choi et al., 2017).

In current research on brain plasticity processes, particular attention has been focused on BDNF an activator of various signaling pathways involved in regulation of neurogenesis and survival of neurons. The BDNF function may also be related to the formation and maintenance of dendritic spines and dendrites, as well as regulation of synaptic function during long-term potentiation, learning, and memory process (Greenberg et al., 2009). The source of BDNF is an active microglial, as well as the endothelium and neurons (Gomes et al., 2012). BDNF is involved in the regulation of neurogenesis in the SVZ zone and the migration of progenitor cells from the SVZ to the damaged striatum (Bathina and Das, 2015). BDNF infusions into lateral ventricles cause duplication of a number of neurons in the olfactory bulb region and production of synaptic connections (Bath and Lee, 2010).

In this study, we showed for the first time that ELF-EMF increased BDNF concentration (**Figure 1A**), as well as *BDNF* mRNA expression *in vivo* in humans (**Figure 1B**). Our results coincide with those of studies conducted by Di Loreto et al. (2009). They investigated changes in the expression profile of cytokine and the growth factor profile in rat cortical neurons

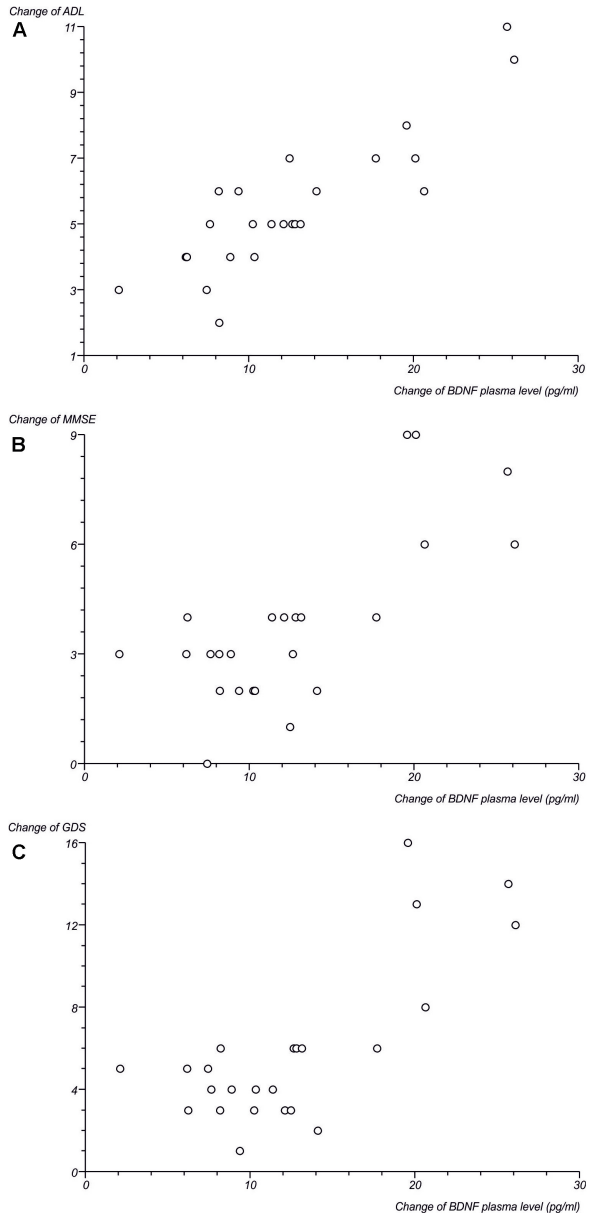

FIGURE 5 | Scatterplots presenting correlation between changes of BDNF plasma level (in pg/ml) in ELF-EMF group and **(A)** changes of ADL; **(B)** changes of MMSE; **(C)** changes of GDS.

with exposure to ELF-EMF (50 Hz, 0.1 and 1 mT) during maturation of cells. They observed that ELF-EMF exposure induced an increased mRNA and protein expression of BNDF and its receptor. As such, they found that ELF-EMF caused up-regulation in neurons (Di Loreto et al., 2009).

The regenerative ability of ELF-EMF has been confirmed by Hei et al. (2016) They observed that pulsating electromagnetic fields (50 Hz, 1 mT) caused increased *BDNF* gene expression in immortalized rat Schwann cells. They suggested that the electromagnetic field improved regeneration of peripheral nerves by enhancing proliferation of cells, and *BDNF* and *S100* gene expression (Hei et al., 2016). Similar evidence was provided by Urnukhsaikhan et al. (2017). The increase of BDNF, protein level after EMF treatment, confirmed the neuroprotective action of EMF in mice during recovery process after stroke (Urnukhsaikhan et al., 2017).

The probable mechanism of increase of *BDNF* mRNA expression after EMF treatment was explained by Li et al. (2014). They investigated L-type voltage-gated calcium channels-and Erk-dependent signaling pathways and sampled *BNDF* mRNA expression in cultured dorsal root ganglion neurons (Li et al., 2014). Sun et al. (2016) investigated membrane capacitance and calcium influx in the calyx of Held. They certified the significance of the effect of ELF-EMF on plasticity and synaptic transmission by facilitation of synaptic plasticity in a calcium-dependent manner, and vesicle endocytosis. Exposition of ELF-EMF causes increases in the impact of calcium influx on the enhancement of calcium channel expression at the presynaptic nerve terminal (Sun et al., 2016).

The primary function of VEGF is a pro-angiogenic action, but there is much evidence of its neurotrophic and neuroprotective effect, both on the central and peripheral nervous system (Saban et al., 2011; Yao et al., 2016; Shahhoseini and Bigdeli, 2017). VEGF generated by ependymal cells activates and enhances neuronal precursor proliferation and growth in the SCZ and SGZ zones (Chodobski et al., 2003). Moreover, VEGF enhances astrocytes proliferation and migration (Lenzer-Fanara et al., 2017), as well as stimulates growth and survival of Schwann cells after hypoxia (Cattin et al., 2015). Its neurogenesis effect is assessed by stimulation of the endothelium to release neurotrophic factors (Feng et al., 2012).

In the current study, we observed that the VEGF plasma level increased in the group exposed to ELF-EMF (**Figure 2**). However, our results are compatible with studies conducted by Delle Monache et al. (2008), who suggested ELF-EMF's impact on *in vitro* modulation of endothelial functions through VEGF-dependent signal transduction pathways. Liu et al. (2015a) estimated the effect of a pulsating electromagnetic field on neurotrophic genes' expression and proliferation in Schwann cells in rats. They observed that EMF increased both protein levels and the gene expression of VEGF, BDNF, and GDNF. They thereby confirm that EMF therapy improves nerve regeneration (Liu et al., 2015a).

We also measured the cytokine plasma levels involved in neuroplasticity processes: HGF, SCF, SDF-1α, β-NGF, and LIF. We observed that after the application of ELF-EMF, hepatocyte growth factor increased (**Table 3** and **Figure 3A**). HGF is expressed in many different tissues, including the brain (Sharma, 2010). HGF by cMet receptor impacts morphogenesis, cell motility, and proliferation of neuronal and non-neuronal tissues. It also activates the migration and proliferation of the progenitors of oligodendrocyte, Schwann cells, as well as intensifying the differentiation and survival of hippocampal, cortical, and midbrain dopaminergic neurons (Wang et al., 2011). Shang et al. (2011) found that in Wistar rats, after transient middle cerebral artery occlusion (tMCAO), exogenous administration of HGF caused a decrease in infarct size, intensification of synaptogenesis and angiogenesis, and a reduction of scar thickness of the pia

mater and glial scar formation (Shang et al., 2011). Similarly, Doeppner et al. (2011) investigated the impact of intrastriatal HGF treatment on the long-term effects of and neurologic recovery and brain injury. They suggested that long-term neuroprotection caused by HGF was associated with enhanced neurovascular remodeling, and maintained recruitment of proliferating cells (Doeppner et al., 2011).

Stem cell factor (SCF) also has an impact on neuroprotection and neurogenesis. It is involved in the development of the cortex, and migration and proliferation of neural progenitor cells. SCF in microglia enhances BNDF and NGF expression and reduces pro-inflammatory cytokine expression. Furthermore, SCF participates in neuron-glia, and neuron-neuron interaction (Benedetti et al., 2016). Liu et al. (2016) estimated the effect of administration of SCF and granulocyte-colony stimulating factor (G-CSF) on the effectiveness of recovery in aged mice after stroke. A similar study was conducted by Cui et al., who investigated the effect of the SCF and G-CSF combination on brain repair, 6 months after cortical injury in transgenic mice. They also suggested that SCF + G-SCF treatment enhanced motor function through vascular and synaptic regeneration (Cui et al., 2016). In this study, we showed that the plasma concentration of SCF increased about 25% in the ELF-EMF group (**Table 3** and **Figure 3B**), and this is consistent with Fan et al. whose evaluated the effect of ELF-EMF (50 Hz, 1 mT) on cytokine production and proliferation of mesenchymal stem cells (MSC) in rats. They found that *SCF* mRNA expression after ELF-EMF increased in comparison to their control group. They suggested that ELF-EMF enhanced the proliferation of MSC, as well as up-regulated haematopoietic growth factor expression (Fan et al., 2015).

Stromal derived factor-1α (SDF-1α) is a chemokine secreted from the endothelium which can induce neuroblast migration from SVZ to the ischemic area in rats (Zhao et al., 2015). Luo et al. (2014) demonstrated the impact of physical exercise on functional recovery by improving migration, differentiation, and proliferation of NSCs in SDF-1α rats after MCAO. In our study, we observed no change in SDF-1α, in both the ELF-EMF and non-ELF-EMF groups (**Table 3** and **Figure 3C**).

Despite nerve growth factor (NGF) being a neurotrophic factor predominantly involved in neuroplasticity (Isaev et al., 2017), in our study, the βNGF level in both groups before and after treatment was out of range (**Table 3**). Similarly, leukemia inhibitory factor (LIF), which is an anti-inflammatory cytokine involved in brain plasticity (Vidal et al., 2013), was out of range (**Table 3**). In research by Sarchielli et al. (2013) the level of these molecules was also below the detection limit.

In our study we suggested that ELF-EMF improved neuroplasticity, which idea is compatible with data from the existing literature (Oda and Koike, 2004; Cuccurazzu et al., 2010; Balassa et al., 2013; Cheng et al., 2015). Cuccurazzu et al. (2010) investigated the effect of ELF-EMF (50Hz, 1mT) on hippocampal neurogenesis in adult mice. They observed that ELF-EMF exposition increased the expression of Mash1, NeuroD2, and Hes1 (pro-neuronal transcription genes), and genes encoding Ca(v)1.2 channel α(1C) subunits, thus promoted neurogenesis in the dentate gyrus (Cuccurazzu et al., 2010). On the other hand, Balassa et al. estimated the impact of long-term ELF-EMF (50 Hz, 3mT) synaptic functions in the developing brain. They found that exposure to ELF-EMF enhanced synaptic plasticity and basic neuronal functions in the brain, both in newborn and fetal rats (Balassa et al., 2013). Oda and Koike examined the effect of ELF-EMF (50 Hz, 0.3 mT) on neuronal apoptosis. They observed that application of ELF-EMF inhibited apoptosis and enhanced the survival of immature cerebellar granule neurons (Oda and Koike, 2004). Moreover, Cheng et al. investigated the impact of ELF-EMF (50 Hz, 0.4 mT) on hippocampal neural progenitor cells from both ischaemic and embryonic brains. They observed that application of ELF-EMF intensified the ability of neural progenitor cells to proliferate in both kinds of the brain (Cheng et al., 2015).

In our study, we also found a relationship between ELF-EMF and the enhancement of the clinical parameters of tested subjects, as well as a correlation between BDNF level and clinical parameters (**Figure 5**). The results we obtained show that the ADL value was comparable in both groups of patients (**Figure 4**) and that there was a significant positive correlation between an increase of BDNF level and ΔADL in the ELF-EMF group (**Figure 5** and **Table 4**). Our findings are compatible with results obtained by Zhang et al. (2017). They evaluated functional recovery and serum BDNF level in post-stroke patients and the relationship between the two. They observed a positive correlation between BNDF level and Barhel Index, and between BNDF level and mRS, which indicated functional status (Zhang et al., 2017). The increase in the MMSE parameter before and after ELF-EMF treatment was about 15% (**Figure 4**), and we proved a significantly positive correlation between ΔBDNF level and ΔMMSE in our study group (**Figure 5** and **Table 4**). A positive correlation between BDNF level and the MMSE scale was previously shown by Belviranli et al. (2016) who investigated the dependence of cognitive parameters (assessed by MMSE) and BDNF plasma level in endurance athletes. Similarity, Levada et al. (2016) observed that after BDNF administration in patients with mild neurocognitive disorders, their MMSE level increased. The decline in parameters on the GDS scale was about 50% greater in the ELF-EMF group, in comparison to the non-ELF-EMF group. We also demonstrated a significant positive correlation between changes of BDNF level and ΔGDS (**Figure 5** and **Table 4**). Importantly, a low BDNF level is associated with post-stroke depression and acute stroke (Yang et al., 2011), and over-expression of BDNF in

TABLE 4 | Correlation coefficient values obtained for the change in BDNF plasma level (ΔBDNF) and parameters of functional status (ADL, MMSE, and GDS) after ELF-EMF treatment.

Δ BDNF plasma level		
ADL	**MMSE**	**GDS**
Rho = 0.7720	Rho = 0.5979	Rho = −0.55924
$p < 0.0001$	$p < 0.01$	$p < 0.01$
H1: positive correlation	H1: positive correlation	H1: negative correlation

The correlation was made using Spearman's rank correlation method. This table includes Spearman's rank correlation coefficient (Rho), the probability of correlation (p), and hypotheses verification (H1).

the hippocampus moderates depression behaviors in post-stroke depressive rats (Chen et al., 2015).

CONCLUSION

ELF-EMF improves functional recovery in stroke patients by improving neuroplasticity processes. Intensifying brain plasticity using ELF-EMF therapy is associated with an increased level of neurotrophic factors, which could be caused by the impact of ELF-EMF on gene expression. We also suggested that the inclusion of ELF-EMF treatment in post-stroke therapy could enhance the effectiveness of the therapy.

ETHICS STATEMENT

This study was approved by the Bioethics Committee of the Faculty of Biology and Environmental Protection of University of Lodz, Poland with Resolution No. 13/KBBN-UŁ/II/2016. All participants gave their written informed consent before participation. The study was executed according to the principles of the Helsinki Declaration.

AUTHOR CONTRIBUTIONS

NC was involved in the preparation of the research project, preparation, collection and interpretation of data, as well as preparation of the manuscript. MB was involved in the interpretation of data, statistical analysis, and preparation of the manuscript. PC was involved in the preparation of samples (isolation of RNA) and determination of VEGF. EM was responsible for patient recruitment and was involved in the analysis and interpretation of clinical data. ES was involved in the evaluation of the quality of RNA and preparation of cDNA. TS analyzed and interpreted of obtained data and was responsible for language correction. JS-B was involved in the preparation of the research project, critically revision, analysis and interpretation of the data, and preparation of the manuscript. All authors read and approved the final manuscript.

FUNDING

This study was supported by the Department of General Biochemistry, Faculty of Biology and Environmental Protection, University of Lodz (No. 506/1136) and Grants for Young Scientists and PhD Students (B1611000001145.02).

REFERENCES

Aimone, J. B., Li, Y., Lee, S. W., Clemenson, G. D., Deng, W., and Gage, F. H. (2014). Regulation and function of adult neurogenesis: from genes to cognition. *Physiol. Rev.* 94, 991–1026. doi: 10.1152/physrev.00004.2014

Balassa, T., Varró, P., Elek, S., Drozdovszky, O., Szemerszky, R., Világi, I., et al. (2013). Changes in synaptic efficacy in rat brain slices following extremely low-frequency magnetic field exposure at embryonic and early postnatal age. *Int. J. Dev. Neurosci.* 31, 724–730. doi: 10.1016/j.ijdevneu.2013.08.004

Bath, K. G., and Lee, F. S. (2010). Neurotrophic factor control of adult SVZ neurogenesis. *Dev. Neurobiol.* 70, 339–349. doi: 10.1002/dneu.20781

Bathina, S., and Das, U. N. (2015). Brain-derived neurotrophic factor and its clinical implications. *Arch. Med. Sci.* 11, 1164–1178. doi: 10.5114/aoms.2015.56342

Belviranli, M., Okudan, N., Kabak, B., Erdoğan, M., and Karanfilci, M. (2016). The relationship between brain-derived neurotrophic factor, irisin and cognitive skills of endurance athletes. *Phys. Sportsmed.* 44, 290–296. doi: 10.1080/00913847.2016.1196125

Benedetti, F., Poletti, S., Hoogenboezem, T. A., Locatelli, C., Ambrée, O., de Wit, H., et al. (2016). Stem cell factor (SCF) is a putative biomarker of antidepressant response. *J. Neuroimmune Pharmacol.* 11, 248–258. doi: 10.1007/s11481-016-9672-y

Bijak, M., Kolodziejczyk-Czepas, J., Ponczek, M. B., Saluk, J., and Nowak, P. (2012). Protective effects of grape seed extract against oxidative and nitrative damage of plasma proteins. *Int. J. Biol. Macromol.* 51, 183–187. doi: 10.1016/j.ijbiomac.2012.05.009

Bijak, M., Saluk, J., Antosik, A., Ponczek, M. B., Zbikowska, H. M., Borowiecka, M., et al. (2013). Aronia melanocarpa as a protector against nitration of fibrinogen. *Int. J. Biol. Macromol.* 55, 264–268. doi: 10.1016/j.ijbiomac.2013.01.019

Cattin, A. L., Burden, J. J., Van Emmenis, L., Mackenzie, F. E., Hoving, J. J., Garcia Calavia, N., et al. (2015). Macrophage-induced blood vessels guide schwann cell-mediated regeneration of peripheral nerves. *Cell* 162, 1127–1139. doi: 10.1016/j.cell.2015.07.021

Chen, H. H., Zhang, N., Li, W. Y., Fang, M. R., Zhang, H., Fang, Y. S., et al. (2015). Overexpression of brain-derived neurotrophic factor in the hippocampus protects against post-stroke depression. *Neural Regen. Res.* 10, 1427–1432. doi: 10.4103/1673-5374.165510

Cheng, Y., Dai, Y., Zhu, X., Xu, H., Cai, P., Xia, R., et al. (2015). Extremely low-frequency electromagnetic fields enhance the proliferation and differentiation of neural progenitor cells cultured from ischemic brains. *Neuroreport* 26, 896–902. doi: 10.1097/WNR.0000000000000450

Chodobski, A., Chung, I., Koźniewska, E., Ivanenko, T., Chang, W., Harrington, J. F., et al. (2003). Early neutrophilic expression of vascular endothelial growth factor after traumatic brain injury. *Neuroscience* 122, 853–867. doi: 10.1016/j.neuroscience.2003.08.055

Choi, J. Y., Kim, J. Y., Park, J., Lee, W. T., and Lee, J. E. (2017). M2 phenotype microglia-derived cytokine stimulates proliferation and neuronal differentiation of endogenous stem cells in ischemic brain. *Exp. Neurobiol.* 26, 33–41. doi: 10.5607/en.2017.26.1.33

Cichoń, N., Bijak, M., Miller, E., and Saluk, J. (2017a). Extremely low frequency electromagnetic field (ELF-EMF) reduces oxidative stress and improves functional and psychological status in ischemic stroke patients. *Bioelectromagnetics* 38, 386–396. doi: 10.1002/bem.22055

Cichoń, N., Czarny, P., Bijak, M., Miller, E., Śliwinñski, T., Szemraj, J., et al. (2017b). Benign effect of extremely low-frequency electromagnetic field on brain plasticity assessed by nitric oxide metabolism during poststroke rehabilitation. *Oxid. Med. Cell. Longev.* 2017:2181942. doi: 10.1155/2017/2181942

Cichoń, N., Rzeźnicka, P., Bijak, M., Miller, E., Miller, S., and Saluk, J. (2018). Extremely low frequency electromagnetic field reduces oxidative stress during the rehabilitation of post-acute stroke patients. *Adv. Clin. Exp. Med.* doi: 10.17219/acem/73699 [Epub ahead of print].'

Cuccurazzu, B., Leone, L., Podda, M. V., Piacentini, R., Riccardi, E., Ripoli, C., et al. (2010). Exposure to extremely low-frequency (50 Hz) electromagnetic fields enhances adult hippocampal neurogenesis in C57BL/6 mice. *Exp. Neurol* 226, 173–182. doi: 10.1016/j.expneurol.2010.08.022

Cui, L., Wang, D., McGillis, S., Kyle, M., and Zhao, L. R. (2016). Repairing the brain by SCF+G-CSF Treatment at 6 months postexperimental stroke: mechanistic determination of the causal link between neurovascular regeneration and motor functional recovery. *ASN Neuro* 8:1759091416655010. doi: 10.1177/1759091416655010

Delle Monache, S., Alessandro, R., Iorio, R., Gualtieri, G., and Colonna, R. (2008). Extremely low frequency electromagnetic fields (ELF-EMFs) induce in vitro angiogenesis process in human endothelial cells. *Bioelectromagnetics* 29, 640–648. doi: 10.1002/bem.20430

Di Loreto, S., Falone, S., Caracciolo, V., Sebastiani, P., D'Alessandro, A., Mirabilio, A., et al. (2009). Fifty hertz extremely low-frequency magnetic field exposure elicits redox and trophic response in rat-cortical neurons. *J. Cell. Physiol.* 219, 334–343. doi: 10.1002/jcp.21674

Doeppner, T. R., Kaltwasser, B., ElAli, A., Zechariah, A., Hermann, D. M., and Bähr, M. (2011). Acute hepatocyte growth factor treatment induces long-term neuroprotection and stroke recovery via mechanisms involving neural precursor cell proliferation and differentiation. *J. Cereb. Blood Flow Metab.* 31, 1251–1262. doi: 10.1038/jcbfm.2010.211

Fan, W., Qian, F., Ma, Q., Zhang, P., Chen, T., Chen, C., et al. (2015). 50 Hz electromagnetic field exposure promotes proliferation and cytokine production of bone marrow mesenchymal stem cells. *Int. J. Clin. Exp Med.* 8, 7394–7404.

Feng, S., Zhuang, M., and Wu, R. (2012). Secretion of nerve growth factor, brain-derived neurotrophic factor, and glial cell-line derived neurotrophic factor in co-culture of four cell types in cerebrospinal fluid-containing medium. *Neural Regen. Res.* 7, 2907–2914. doi: 10.3969/j.issn.1673-5374.2012.36.008

Gomes, J. R., Costa, J. T., Melo, C. V., Felizzi, F., Monteiro, P., Pinto, M. J., et al. (2012). Excitotoxicity downregulates TrkB.FL signaling and upregulates the neuroprotective truncated TrkB receptors in cultured hippocampal and striatal neurons. *J. Neurosci.* 32, 4610–4622. doi: 10.1523/JNEUROSCI.0374-12.2012

Greenberg, M. E., Xu, B., Lu, B., and Hempstead, B. L. (2009). New insights in the biology of BDNF synthesis and release: implications in CNS function. *J. Neurosci.* 29, 12764–12767. doi: 10.1523/JNEUROSCI.3566-09.2009

Hagg, T. (2009). From neurotransmitters to neurotrophic factors to neurogenesis. *Neuroscientist* 15, 20–27. doi: 10.1177/1073858408324789

Hei, W. H., Byun, S. H., Kim, J. S., Kim, S., Seo, Y. K., Park, J. C., et al. (2016). Effects of electromagnetic field (PEMF) exposure at different frequency and duration on the peripheral nerve regeneration: in vitro and in vivo study. *Int. J. Neurosci.* 126, 739–748. doi: 10.3109/00207454.2015.1054032

Hu, X., Zhang, F., Leak, R. K., Zhang, W., Iwai, M., Stetler, R. A., et al. (2013). Transgenic overproduction of omega-3 polyunsaturated fatty acids provides neuroprotection and enhances endogenous neurogenesis after stroke. *Curr. Mol. Med.* 13, 1465–1473. doi: 10.2174/15665240113139990075

Hylin, M. J., Kerr, A. L., and Holden, R. (2017). Understanding the mechanisms of recovery and/or compensation following injury. *Neural Plast.* 2017:7125057. doi: 10.1155/2017/7125057

Isaev, N. K., Stelmashook, E. V., and Genrikhs, E. E. (2017). Role of nerve growth factor in plasticity of forebrain cholinergic neurons. *Biochemistry* 82, 291–300. doi: 10.1134/S0006297917030075

Jia, H., Pei, Q., Sullivan, C. T., Cowper Ripley, D. C., Wu, S. S., Vogel, W. B., et al. (2017). Regional variation in post-stroke multidisciplinary rehabilitation care among veteran residents in community nursing homes. *J. Multidiscip. Healthc.* 10, 75–85. doi: 10.2147/JMDH.S123905

Klein, R., Mahlberg, N., Ohren, M., Ladwig, A., Neumaier, B., Graf, R., et al. (2016). The neural cell adhesion molecule-derived (NCAM)-peptide FG loop (FGL) mobilizes endogenous neural stem cells and promotes endogenous regenerative capacity after stroke. *J. Neuroimmune Pharmacol.* 11, 708–720. doi: 10.1007/s11481-016-9694-5

Law, H. C., Szeto, S. S., Quan, Q., Zhao, Y., Zhang, Z., Krakovska, O., et al. (2017). Characterization of the molecular mechanisms underlying the chronic phase of stroke in a cynomolgus monkey model of induced cerebral ischemia. *J. Proteome. Res.* 16, 1150–1166. doi: 10.1021/acs.jproteome.6b00651

Lenzer-Fanara, J. R., Li, T., Salerni, E. A., Payen, F., and Croll, S. D. (2017). VEGF treatment during status epilepticus attenuates long-term seizure-associated alterations in astrocyte morphology. *Epilepsy Behav.* 70(Pt A), 33–44. doi: 10.1016/j.yebeh.2017.02.019

Levada, O. A., Cherednichenko, N. V., Trailin, A. V., and Troyan, A. S. (2016). Plasma brain-derived neurotrophic factor as a biomarker for the main types of mild neurocognitive disorders and treatment efficacy: a preliminary study. *Dis. Mark.* 2016:4095723. doi: 10.1155/2016/4095723

Li, S. (2017). Spasticity, motor recovery, and neural plasticity after stroke. *Front. Neurol.* 8:120. doi: 10.3389/fneur.2017.00120

Li, Y., Yan, X., Liu, J., Li, L., Hu, X., Sun, H., et al. (2014). Pulsed electromagnetic field enhances brain-derived neurotrophic factor expression through L-type voltage-gated calcium channel- and Erk-dependent signaling pathways in neonatal rat dorsal root ganglion neurons. *Neurochem. Int.* 75, 96–104. doi: 10.1016/j.neuint.2014.06.004

Liguz-Lecznar, M., and Kossut, M. (2013). Influence of inflammation on poststroke plasticity. *Neural Plast.* 2013, 258582. doi: 10.1155/2013/258582

Lindholm, P., and Saarma, M. (2010). Novel CDNF/MANF family of neurotrophic factors. *Dev. Neurobiol.* 70, 360–371. doi: 10.1002/dneu.20760

Ling, G. Q., Liu, Y. J., Ke, Y. Q., Chen, L., Jiang, X. D., Jiang, C. L., et al. (2015). All-trans retinoic acid impairs the vasculogenic mimicry formation ability of U87 stem-like cells through promoting differentiation. *Mol. Med. Rep.* 12, 165–172. doi: 10.3892/mmr.2015.3449

Liu, L., Liu, Z., Huang, L., Sun, Z., Ma, T., Zhu, S., et al. (2015a). Pulsed magnetic field promotes proliferation and neurotrophic genes expression in Schwann cells in vitro. *Int. J. Clin. Exp. Pathol.* 8, 2343–2353.

Liu, X. Y., Zhou, X. Y., Hou, J. C., Zhu, H., Wang, Z., Liu, J. X., et al. (2015b). Ginsenoside Rd promotes neurogenesis in rat brain after transient focal cerebral ischemia via activation of PI3K/Akt pathway. *Acta Pharmacol. Sin.* 36, 421–428. doi: 10.1038/aps.2014.156

Liu, Y., Popescu, M., Longo, S., Gao, M., Wang, D., McGillis, S., et al. (2016). Fibrinogen reduction and motor function improvement by hematopoietic growth factor treatment in chronic stroke in aged mice: a treatment frequency study. *Cell Transplant.* 25, 729–734. doi: 10.3727/096368916X690791

Luo, J., Hu, X., Zhang, L., Li, L., Zheng, H., Li, M., et al. (2014). Physical exercise regulates neural stem cells proliferation and migration via SDF-1α/CXCR4 pathway in rats after ischemic stroke. *Neurosci. Lett.* 578, 203–208. doi: 10.1016/j.neulet.2014.06.059

Martin, B., Wang, R., Cong, W. N., Daimon, C. M., Wu, W. W., Ni, B., et al. (2017). Altered learning, memory, and social behavior in type 1 taste receptor subunit 3 knock-out mice are associated with neuronal dysfunction. *J. Biol. Chem.* 292, 11508–11530. doi: 10.1074/jbc.M116.773820

Oda, T., and Koike, T. (2004). Magnetic field exposure saves rat cerebellar granule neurons from apoptosis in vitro. *Neurosci. Lett.* 365, 83–86. doi: 10.1016/j.neulet.2004.04.068

Qiao, H. J., Li, Z. Z., Wang, L. M., Sun, W., Yu, J. C., and Wang, B. (2017). Association of lower serum brain-derived neurotrophic factor levels with larger infarct volumes in acute ischemic stroke. *J. Neuroimmunol.* 307, 69–73. doi: 10.1016/j.jneuroim.2017.04.002

Rosenstein, J. M., Krum, J. M., and Ruhrberg, C. (2010). VEGF in the nervous system. *Organogenesis* 6, 107–114. doi: 10.4161/org.6.2.11687

Saban, M. R., Davis, C. A., Avelino, A., Cruz, F., Maier, J., Bjorling, D. E., et al. (2011). VEGF signaling mediates bladder neuroplasticity and inflammation in response to BCG. *BMC Physiol.* 11:16. doi: 10.1186/1472-6793-11-16

Sarchielli, P., Nardi, K., Chiasserini, D., Eusebi, P., Tantucci, M., Di Piero, V., et al. (2013). Immunological profile of silent brain infarction and lacunar stroke. *PLoS One* 8:e68428. doi: 10.1371/journal.pone.0068428

Schiavone, S., Tucci, P., Mhillaj, E., Bove, M., Trabace, L., and Morgese, M. G. (2017). Antidepressant drugs for beta amyloid-induced depression: a new standpoint? *Prog. Neuropsychopharmacol. Biol. Psychiatry* 78, 114–122. doi: 10.1016/j.pnpbp.2017.05.004

Shahhoseini, M., and Bigdeli, M. R. (2017). Time course of neuroprotection induced by. *Iran J. Basic Med. Sci.* 20, 67–74.

Shang, J., Deguchi, K., Ohta, Y., Liu, N., Zhang, X., Tian, F., et al. (2011). Strong neurogenesis, angiogenesis, synaptogenesis, and antifibrosis of hepatocyte growth factor in rats brain after transient middle cerebral artery occlusion. *J. Neurosci. Res.* 89, 86–95. doi: 10.1002/jnr.22524

Sharma, S. (2010). Hepatocyte growth factor in synaptic plasticity and Alzheimer's disease. *Sci. World J.* 10, 457–461. doi: 10.1100/tsw.2010.49

Sun, Z. C., Ge, J. L., Guo, B., Guo, J., Hao, M., Wu, Y. C., et al. (2016). Extremely low frequency electromagnetic fields facilitate vesicle endocytosis by increasing presynaptic calcium channel expression at a central synapse. *Sci. Rep.* 6:21774. doi: 10.1038/srep21774

Urnukhsaikhan, E., Mishig-Ochir, T., Kim, S. C., Park, J. K., and Seo, Y. K. (2017). Neuroprotective effect of low frequency-pulsed electromagnetic fields in ischemic stroke. *Appl. Biochem. Biotechnol.* 181, 1360–1371. doi: 10.1007/s12010-016-2289-z

Vidal, P. M., Lemmens, E., Dooley, D., and Hendrix, S. (2013). The role of "anti-inflammatory" cytokines in axon regeneration. *Cytokine Growth Factor Rev.* 24, 1–12. doi: 10.1016/j.cytogfr.2012.08.008

Wang, T. W., Zhang, H., Gyetko, M. R., and Parent, J. M. (2011). Hepatocyte growth factor acts as a mitogen and chemoattractant for postnatal

subventricular zone-olfactory bulb neurogenesis. *Mol. Cell. Neurosci.* 48, 38–50. doi: 10.1016/j.mcn.2011.06.003

Yang, L., Zhang, Z., Sun, D., Xu, Z., Yuan, Y., Zhang, X., et al. (2011). Low serum BDNF may indicate the development of PSD in patients with acute ischemic stroke. *Int. J. Geriatr. Psychiatry* 26, 495–502. doi: 10.1002/gps.2552

Yao, Y., Zheng, X. R., Zhang, S. S., Wang, X., Yu, X. H., Tan, J. L., et al. (2016). Transplantation of vascular endothelial growth factor-modified neural stem/progenitor cells promotes the recovery of neurological function following hypoxic-ischemic brain damage. *Neural Regen. Res.* 11, 1456–1463. doi: 10.4103/1673-5374.191220

Zanotta, N., Tornesello, M. L., Annunziata, C., Stellato, G., Buonaguro, F. M., and Comar, M. (2016). Candidate soluble immune mediators in young women with high-risk human papillomavirus infection: high expression of chemokines promoting angiogenesis and cell proliferation. *PLoS One* 11:e0151851. doi: 10.1371/journal.pone.0151851

Zelentsova-Levytskyi, K., Talmi, Z., Abboud-Jarrous, G., Capucha, T., Sapir, T., Burstyn-Cohen, T., et al. (2017). Negatively regulates neural stem cell self-renewal through Bmi-1 signaling. *Front. Mol. Neurosci.* 10:124. doi: 10.3389/fnmol.2017.00124

Zhang, J., Mu, X., Breker, D. A., Li, Y., Gao, Z., and Huang, Y. (2017). Atorvastatin treatment is associated with increased BDNF level and improved functional recovery after atherothrombotic stroke. *Int. J. Neurosci.* 127, 92–97. doi: 10.3109/00207454.2016.1146882

Zhao, S., Qu, H., Zhao, Y., Xiao, T., Zhao, M., Li, Y., et al. (2015). CXCR4 antagonist AMD3100 reverses the neurogenesis and behavioral recovery promoted by forced limb-use in stroke rats. *Restor. Neurol Neurosci.* 33, 809–821. doi: 10.3233/RNN-150515

Conflict of Interest Statement: The authors declare that the research was conducted in the absence of any commercial or financial relationships that could be construed as a potential conflict of interest.

The reviewer EC-J and handling Editor declared their shared affiliation at the time of the review.

frontiers in Aging Neuroscience

ORIGINAL RESEARCH
published: 04 October 2017
doi: 10.3389/fnagi.2017.00323

miRNA in Circulating Microvesicles as Biomarkers for Age-Related Cognitive Decline

Asha Rani[1], Andrew O'Shea[2,3], Lara Ianov[1,4], Ronald A. Cohen[2,3], Adam J. Woods[1,2,3] and Thomas C. Foster[1,4]**

[1] Department of Neuroscience, McKnight Brain Institute, University of Florida, Gainesville, FL, United States, [2] Department of Clinical and Health Psychology, University of Florida, Gainesville, FL, United States, [3] Center for Cognitive Aging and Memory, McKnight Brain Institute, University of Florida, Gainesville, FL, United States, [4] Genetics and Genomics Program, Genetics Institute, University of Florida, Gainesville, FL, United States

Community dwelling older individuals from the North Florida region were examined for health status and a comprehensive neuropsychological battery, including the Montreal Cognitive Assessment (MoCA), was performed on each participant. A subpopulation (58 females and 39 males) met the criteria for age (60–89) and no evidence of mild cognitive impairment, with a MoCA score ≥23. Despite the stringent criteria for participation, MoCA scores were negatively correlated within the limited age range. Extracellular microvesicles were isolated from the plasma and samples were found to be positive for the exosome marker CD63, with an enrichment of particles within the size range for exosomes. miRNA was extracted and examined using next generation sequencing with a stringent criterion (average of ≥10 counts per million reads) resulting in 117 miRNA for subsequent analysis. Characterization of expression confirmed pervious work concerning the relative abundance and overall pattern of expression of miRNA in plasma. Correlation analysis indicated that most of the miRNAs (74 miRNAs) were positively correlated with age (p <0.01). Multiple regression was employed to identify the relationship of miRNA expression and MoCA score, accounting for age. MoCA scores were negatively correlated with 13 miRNAs. The pattern of expression for cognition-related miRNA did not match that previously described for Alzheimer's disease. Enrichment analysis was employed to identify miRNA–gene interactions to reveal possible links to brain function.

Keywords: exosome, microRNA, biomarker, normal aging, Alzheimer's disease

OPEN ACCESS

Edited by:
Yogesh Dwivedi, The University of Alabama at Birmingham, United States

Reviewed by:
Gianluca Serafini, University of Genoa, Italy
Hermona Soreq, Hebrew University of Jerusalem, Israel

****Correspondence:***
Thomas C. Foster
foster1@ufl.edu
Asha Rani
hope2003@ufl.edu

Received: *22 August 2017*
Accepted: *20 September 2017*
Published: *04 October 2017*

Citation:
Rani A, O'Shea A, Ianov L, Cohen RA, Woods AJ and Foster TC (2017) miRNA in Circulating Microvesicles as Biomarkers for Age-Related Cognitive Decline. Front. Aging Neurosci. 9:323. doi: 10.3389/fnagi.2017.00323

INTRODUCTION

Normal aging in humans and animal models is associated with changes in specific cognitive processes. Impaired memory, executive function, and processing speed have been well-characterized with advancing age (Alexander et al., 2012; Woods et al., 2013; Febo and Foster, 2016; O'Shea et al., 2016; Nissim et al., 2017; Porges et al., 2017). However, age-related cognitive decline is not uniform, environmental and biological factors including genes, exercise, diet, inflammation, and stress, which are thought to influence the age of onset and the trajectory of cognitive decline (Foster, 2006; Barrientos et al., 2010; Craft et al., 2012; Kumar et al., 2012; Speisman et al., 2013;

Cai et al., 2014; Fan et al., 2017). Further complicating the field is the ability to distinguish age-related cognitive decline from diseases that influence cognition (Foster, 2006; Foster et al., 2016).

Neuroimaging, genetics, and circulating biomarkers are being developed to differentiate normal aging from diseases that affect cognition. While genetic markers may suggest susceptibility to disease, these gene markers are not diagnostic. Similarly, more accurate techniques for identifying pathology, such as positron emission computed tomography, are expensive and may miss early diagnosis, which is critical for treatment. Due to the relative ease of collecting blood, blood based biomarkers could provide a simple and relatively inexpensive means for tracking the progression of cognitive decline and effectiveness of treatments, as well as providing information on mechanism for cognitive impairment. Previous work has examined the relationship between cognition and blood biomarkers, based on theories concerning a role for lipids and cholesterol, oxidative stress, hormones, and inflammation in promoting disease and senescent physiology (Foster, 2006). Recent research suggests that non-coding RNAs found in the circulation can act as biomarkers for diseases of aging including cancer, cardiovascular and neurodegenerative disease (Sheinerman and Umansky, 2013; Schwarzenbach et al., 2014; Mushtaq et al., 2016; Schulte et al., 2016).

MicroRNAs (miRNAs) are small, phylogenetically conserved, 18–25 base pair sections of RNA that influences biological processes through the post-transcriptional regulation of RNA. miRNA acts as a template for target mRNA, binding to the 3′ untranslated region (UTR) of mRNA to silence genes by inhibiting translation and initiating mRNA degradation of the target mRNA. Some miRNAs are ubiquitously expressed in order to regulate fundamental metabolic pathways and variability in expression is influenced by ongoing physiology, including aging. In other cases, miRNAs are preferentially expressed in specific tissues or during different times of development and maturation (Landgraf et al., 2007; Shao et al., 2010; Fehlmann et al., 2016). Finally, examination of the brain suggests that intracellular miRNA signaling influences neural circuits, including those associated with psychiatric diseases (Impey et al., 2010; Serafini et al., 2014; Jovasevic et al., 2015; Rajman et al., 2017).

Within the circulation, miRNAs can be found attached to proteins or in extracellular vesicles, small (50 nm to 1 μm) vesicles of endocytic origin that are released from cells into the extracellular environment. Some (e.g., exosomes) are able to cross membranes (e.g., blood–brain barrier) and can be detected in bodily fluids including serum, urine, and saliva. In this way, microvesicles can provide intercellular and inter-organ communication by delivery of miRNAs to influence transcription and altering genetic processes. Indeed, studies suggest that circulating levels of miRNAs in plasma (Kumar et al., 2013) or in exosomes (Cheng et al., 2015; Lugli et al., 2015) may be able to identify Alzheimer's disease. The current study employs the datasets from previous studies examining the relationship of brain structural and cognitive function in older adults (O'Shea et al., 2016; Nissim et al., 2017). We now include additional analysis of the expression of miRNAs, isolated from plasma enriched for microvesicles, and relate the expression to cognition in advanced age.

MATERIALS AND METHODS

Participants

The study was approved by the Ethics Review Committee on Human Research of the University of Florida (Gainesville, FL, United States) and written informed consent was obtained from all participants. The participants were selected from previous studies (O'Shea et al., 2016; Nissim et al., 2017) in which healthy community dwelling older individuals were recruited from Gainesville and the North Florida region. A thorough medical history questionnaire for each participant provided detailed information on health status, medication status, and a comprehensive neuropsychological battery was performed on each participant (O'Shea et al., 2016; Nissim et al., 2017). No participants in this sample were clinically indicated to have mild cognitive impairment (MCI) or other age-related brain disorders. The Montreal Cognitive Assessment (MoCA) was given to assess general cognitive ability as well as rule out possible MCI (Nasreddine et al., 2005). From this group, we selected those between the ages of 60–89, with a MoCA $\geq$23. The 97 participants met the criteria for inclusion in this study, with 58 females and 39 males.

Sample Collection and Microvesicle Characterization

The plasma samples were collected into EDTA Tubes- Plasma (Cat# 367863). The tubes were inverted five times, stored on ice and processed within 30 min of blood draw. The samples were centrifuged at 1600 × *g* for 15 min at 4°C and the isolated plasma samples were stored at −80°C until RNA isolation. The plasma was filtered (0.22 μm filter; Millipore, Billicera, MA, United States) to remove cellular material, including thrombocyte fragments. Microvesicles were isolated using the exoEasy Maxi and exoRNeasy kit (Qiagen).

For a subset of samples, the size distribution and concentration of the microvesicles were determined by University of Florida Interdisciplinary Center for Biotechnology Research using the NanoSight 300 Instrument (Malvern Instruments), according to the manufacture instruction. In addition, morphological assessment of microvesicles was determined by University of Florida Interdisciplinary Center for Biotechnology Research using the transmission electron Microscopy (TEM). A glow discharged carbon coated Formvar copper 400 mesh grid, was floated onto 10 microliter aliquots of re-suspended microvesicle pellet and incubated for 5 min. Excess solution was drawn off with filter paper and the grids were floated on 1% aqueous uranyl acetate for 30 s. Stain was removed with filter paper, air dried and examined using FEI Tecnai G2 Spirit Twin TEM (FEI Corp., Hillsboro, OR, United States) and digital images were acquired with Gatan UltraScan 2k × 2k camera and Digital Micrograph software (Gatan Inc., Pleasanton, CA, United States).

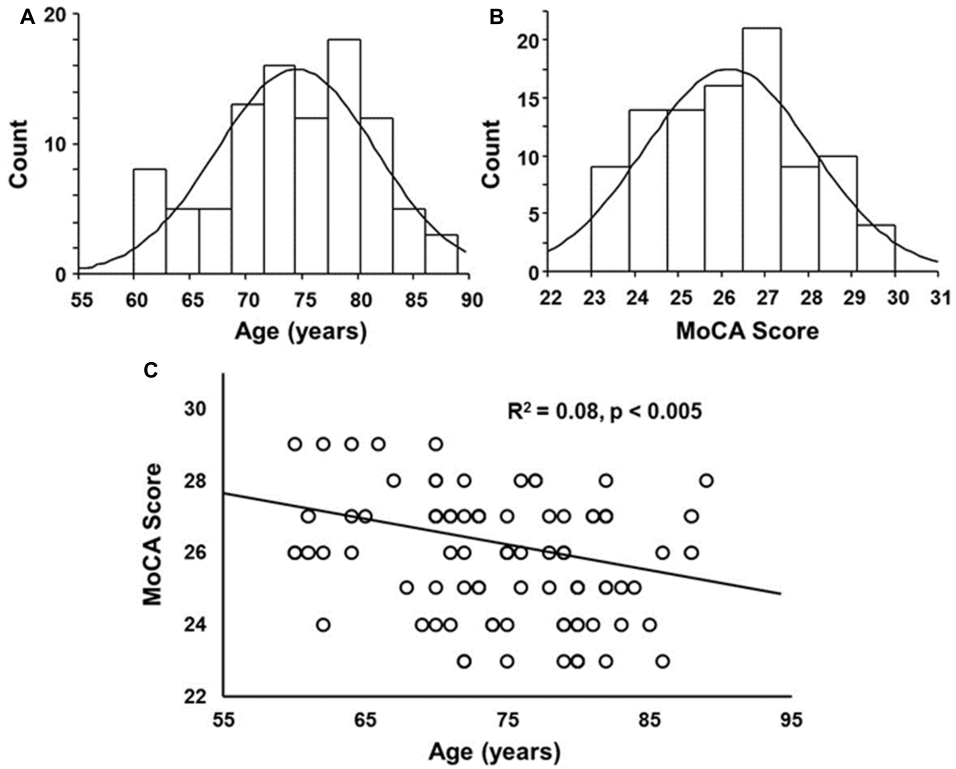

FIGURE 1 | Histograms of the distribution of **(A)** ages and **(B)** Montreal Cognitive Assessment (MoCA) scores overlaid with a normal distribution curve based on the mean and SD. **(C)** A correlation was observed between age and MoCA score, such that the MoCA score decreased with increasing age.

RNA Isolation

RNA was isolated using exoRNeasy Serum/Plasma Maxi kit (Cat# 77064, Qiagen) according to the manufacturer's instructions with the final elution volume of 12 μl. The quantity and quality of the RNA were determined by University of Florida Interdisciplinary Center for Biotechnology Research using the Agilent RNA 6000 Pico Kit to determine the concentration of total RNA, and a Small RNA Kit Chip was used to measure the concentration of exosomal micro RNA (miRNA) on the Agilent Bioanalyzer instrument (Agilent Technologies). Total RNA samples contained a range of 49–90% miRNA.

Small RNA Library Preparation

Sequencing libraries were constructed using ∼2 ng of total exosomal RNA with the library preparation kit Ion Total RNA-Seq kit v2 (Thermo Fisher, Cat# 4475936). Each library was barcoded with Ion Xpress RNA Seq-Barcode 01-16 Kit (Thermo Fisher, Cat# 4475485) to enable multiplex sequencing. The concentration of the libraries was quantified by the Qubit dsDNA HS Assay (Thermo Fisher, Cat# Q32851). In addition, the size distribution and molar concentration was determined with the High Sensitivity D1000 Screen Tape Kit (5067–5584) on 2200 TapeStation system (Agilent Technologies, Cat# G2964A) according to the manufacture's protocol.

Sequencing, Data Acquisition, and Bioinformatics

Templates were prepared with 25 μl of the pooled libraries at a final concentration of 50 pM using Ion Chef instrument (Thermo Fisher) and then sequenced in the Ion Proton System (Thermo Fisher). FASTQ files were extracted from Ion Torrent server and uploaded to the Partek Flow (Partek Inc., St. Louis, MO, United States) servers for bioinformatics analysis. On average, each sample contained 13.8 million reads of 32 base pair (bp) length. Reads were trimmed based on size such that reads below 15 bp and reads above 35 bp were discarded. Following trimming, reads were aligned using Bowtie (version 1.0.0) against the human genome reference (hg38) followed by a post-alignment quality check to assess the performance of the alignment. Gene annotation was completed with the miRBase mature miRNAs model (release version 21) and normalization was performed on total counts. In order to consider genes that are not present in miRBase, gene annotation was also done using hg38-Ensembl Transcripts (release version 85) followed by total count normalization. (Gene Expression Omnibus accession number: The data for this study has been uploaded to the Gene Expression Omnibus under the accession number GSE97644.

To study functionally related genes and their relationship, a biological interpretation was performed by gene ontology (GO) enrichment analysis using DIANA tool web-based software using mirPath (v.3) for miRNA pathway analysis and TarBase

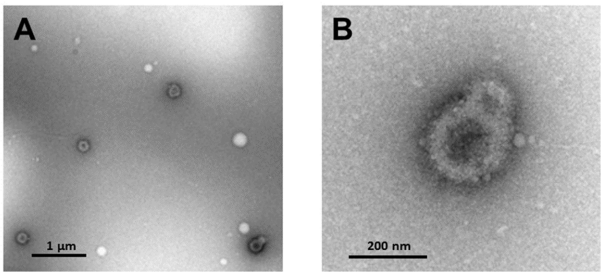

FIGURE 2 | Transmission electron microscopy of **(A)** extracellular microvesicles isolated from plasma and negatively stained with 1% uranyl acetate. **(B)** Enhanced magnification of microvesicles shown in lower right corner of **(A)**.

(v7.0) (Vlachos et al., 2015) was employed to identify miRNA–gene interactions. The statistical cutoff for GO analysis was based on corrected *p*-values with the Benjamini–Hochberg's False Discovery Rate (FDR) $p < 0.05$.

Statistical Analysis

For statistical analysis, miRNA counts were first log-transformed. Differences associated with sex were determined using analyses of variance (ANOVAs). Pearson's regression analysis was used to examine correlations associated with age and miRNA expression. Due to the correspondence of age and cognitive function, multiple regression was employed to determine correlation of miRNA with MoCA score after adjusting for age.

RESULTS

Cognitive testing and plasma were collected from a total of 134 participants, age range 44–102 years. From this population, five were removed due to a history suggesting possible brain disorders due to stroke, concussion, or epilepsy, 22 were removed due to a MoCA score less than 23 (MoCA score range 18–22), and 10 were outside the specified age range of 60–89 years, with one person age 92 and 9 individuals 44–59 years. The remaining 97 participants that met the criteria for inclusion in this study included 58 females and 39 males. The distribution of ages and MoCA scores was approximately normal (**Figure 1**). No age difference was observed between females (75.4 ± 1.0 years mean ± SEM) and males (mean 73.0 ± 1.0 years). While we cannot rule out that some participants may have been pre-symptomatic for MCI or Alzheimer's disease, the MoCA scores were negatively correlated with age ($R^2 = 0.08$, $p < 0.005$) (**Figure 1C**), suggesting that this population exhibited an age-related cognitive decline.

Extracellular Microvesicle Characterization

Characterization of extracellular microvesicle markers was performed for five samples. Elisa assays indicated that all samples were positive for the exosome marker CD63 (OD_{450} 4.08^{-1} ± 0.24, mean ± SD) (Peterson et al., 2015). NanoSight analysis indicated an average vesicle size of 188.82 ± 22.9 nm (mean ± SD), average mode 152.18 ± 34.7 (mean ± SD), and the percent of particles that were <200 nm averaged 65%. Electron microscopy confirmed the recovery of small vesicles with an expected size range from 50 to 200 nm (**Figure 2**).

miRNA

For expression of miRNA, a cut-off was set such that expression had to average at least 10 across the 97 participants. This filtering resulted in data for 117 miRNAs for analysis. Similar to previous reports (Hunter et al., 2008; Mooney et al., 2015), we observed that mir-223-3p exhibited the highest level expression and relatively high level expression (>300 average counts) was observed for mir-191-5p, mir-126-3p, mir-126-5p, mir-484, and mir-26a-5p (**Table 1**).

An examination of differential expression between the males and females indicated no difference in miRNA expression. Previous work suggests expression of circulating miRNAs increases with increasing age (Freedman et al., 2016). Therefore, Pearson's regression analysis with a cut-off of $r = \pm 0.263$ ($p < 0.01$) was employed to examine correlations of miRNA expression with age. The results revealed 74 miRNAs that were positively correlated with age (**Table 2**), confirming that most plasma miRNA that changes with age, exhibit increased expression with advancing age (Freedman et al., 2016). Interestingly, several miRNA that are consistently reported to decrease in blood, plasma, and serum of Alzheimer's patients (hsa-let-7g-5p, hsa-let-7e-5p, and hsa-miR-103a-3p) (Kumar et al., 2013; Leidinger et al., 2013; Tan et al., 2014; Satoh et al., 2015; Nagaraj et al., 2017), were positively correlated with age.

Due to the correspondence of age with miRNA expression and cognitive function, multiple regression was performed to

TABLE 1 | Highly expressed miRNA.

miRNA	Average expression
hsa-miR-223-3p	8760.771
hsa-miR-451a	2372.06
hsa-miR-191-5p	1548.376
hsa-miR-126-3p	1174.333
hsa-miR-126-5p	1021.754
hsa-miR-103a-3p	824.9511
hsa-miR-23a-3p	804.3156
hsa-miR-26a-5p	796.5815
hsa-miR-19b-3p	717.237
hsa-miR-150-5p	697.2409
hsa-miR-484	654.5321
hsa-let-7a-5p	557.691
hsa-miR-185-5p	436.1216
hsa-miR-320a	361.9573
hsa-miR-22-3p	349.7947
hsa-let-7b-5p	325.3197
hsa-let-7g-5p	302.027

For all tables, expression represents averaged counts.

TABLE 2 | miRNA correlated with age.

miRNA	*r*-Value	Average expression	miRNA	*r*-Value	Average expression
hsa-miR-423-5p	0.40	192.63	hsa-miR-126-5p	0.30	1021.75
hsa-miR-145-5p	0.37	80.97	hsa-miR-134-5p	0.30	19.46
hsa-miR-425-5p	0.37	240.80	hsa-miR-19a-3p	0.30	179.28
hsa-miR-22-5p	0.36	10.33	hsa-miR-339-3p	0.30	13.74
hsa-miR-140-5p	0.35	11.19	hsa-miR-29a-3p	0.30	67.12
hsa-miR-376a-3p	0.35	25.80	hsa-miR-199a-5p	0.30	57.71
hsa-miR-185-5p	0.34	436.12	hsa-miR-425-3p	0.30	14.47
hsa-miR-23b-5p	0.34	66.37	hsa-miR-424-5p	0.30	16.52
hsa-miR-23a-3p	0.34	804.32	hsa-miR-660-5p	0.30	10.43
hsa-miR-652-3p	0.34	22.15	hsa-miR-15a-5p	0.30	116.76
hsa-miR-25-3p	0.33	35.00	hsa-miR-339-5p	0.29	37.97
hsa-miR-128-3p	0.33	25.74	hsa-miR-99b-5p	0.29	47.06
hsa-miR-30d-5p	0.33	119.15	hsa-miR-136-5p	0.29	11.01
hsa-miR-485-3p	0.33	27.98	hsa-miR-27a-3p	0.29	105.93
hsa-miR-22-3p	0.33	325.32	hsa-miR-19b-3p	0.29	697.24
hsa-miR-221-3p	0.33	129.56	hsa-miR-625-3p	0.29	26.04
hsa-miR-382-5p	0.33	19.56	hsa-miR-106b-5p	0.29	29.31
hsa-miR-484	0.33	654.53	hsa-miR-103a-3p	0.29	824.95
hsa-miR-29c-3p	0.32	26.14	hsa-miR-199a-3p	0.29	78.57
hsa-miR-21-5p	0.32	190.64	hsa-miR-18a-5p	0.29	258.39
hsa-miR-92a-3p	0.32	203.81	hsa-miR-17-3p	0.29	20.08
hsa-miR-33a-5p	0.32	25.59	hsa-miR-186-5p	0.29	11.36
hsa-miR-421	0.32	11.50	hsa-miR-148a-3p	0.29	16.18
hsa-miR-146a-5p	0.32	152.48	hsa-miR-29b-3p	0.29	30.96
hsa-miR-376c-3p	0.32	227.40	hsa-miR-197-3p	0.29	123.44
hsa-let-7d-3p	0.32	32.72	hsa-let-7e-5p	0.29	34.63
hsa-miR-24-3p	0.31	246.04	hsa-miR-20a-5p	0.29	125.10
hsa-miR-664a-3p	0.31	10.75	hsa-miR-423-3p	0.28	255.35
hsa-miR-28-3p	0.31	20.59	hsa-miR-27b-3p	0.28	29.59
hsa-miR-766-3p	0.31	44.77	hsa-miR-199b-3p	0.28	39.08
hsa-miR-28-5p	0.31	20.26	hsa-miR-223-3p	0.28	8760.77
hsa-miR-590-5p	0.31	78.01	hsa-miR-378a-3p	0.28	22.60
hsa-miR-324-5p	0.31	18.93	hsa-let-7i-5p	0.28	94.64
hsa-miR-584-5p	0.31	69.43	hsa-miR-15b-3p	0.27	11.55
hsa-miR-1307-3p	0.30	10.92	hsa-miR-186-5p	0.27	11.36
hsa-miR-93-5p	0.30	141.86	hsa-miR-574-3p	0.27	39.23
hsa-miR-361-5p	0.30	27.69	hsa-let-7g-5p	0.26	302.03

examine the relationship of miRNA expression to MoCA scores, accounting for the influence of age. The analysis indicated that 13 miRNA exhibited a significant correlation with MoCA scores (**Table 3**) and 16 exhibited a trend ($p > 0.05 < 0.1$). In all cases, the correlations were negative such that increased miRNA expression was associated with decreased MoCA scores. Interestingly, three of the cognition related miRNA from **Table 3** exhibit relatively selective expression in the brain (hsa-miR-342-3p, hsa-miR-125b-5p, hsa-miR-125a-5p) (Hinske et al., 2014). Moreover, hsa-miR-342-3p and hsa-miR-125b-5p exhibited the strongest correlation with MoCA scores (**Table 3**). These three miRNAs exhibited relatively poor correlation with age (**Figure 3**). **Figure 4** illustrates the age and MoCA score correlations for has-miR-451a-3p, which exhibited the highest expression (**Table 3**), was correlated with cognition, and did not exhibit a correlation with age.

To study functionally related genes and their relationship, a biological interpretation was performed by GO enrichment analysis using DIANA tool web-based software to identify miRNA–gene interactions. To understand possible mechanisms through which miRNA could influence the brain, miRNA that correlated with MoCA scores were submitted to DIANA for miRNA pathway analysis. Combining the three brain selective miRNA (hsa-miR-342-3p, hsa-miR-125b-5p, hsa-miR-125a-5p) cluster enrichment indicated the top three pathways were associated with fatty acid biosynthesis (3 genes, $p = 1.9^{-16}$), hippo signaling (38 genes, $p = 1.8^{-9}$), and protein processing in the endoplasmic reticulum (43 genes, $p = 7.5^{-6}$). Brain specific

TABLE 3 | MoCA score multiple regression analysis.

	Coefficients			
miRNA	**miRNA**	**Age**	R^2	**Expression**
hsa-miR-342-3p	−1.26**	−0.069*	0.15	149.03
hsa-miR-125b-5p	−1.42*	−0.063*	0.14	21.73
hsa-miR-10a-5p	−1.39*	−0.065*	0.14	79.04
hsa-miR-140-3p	−1.74*	−0.065*	0.14	14.23
hsa-miR-451a	−1.14*	−0.074**	0.13	2372.06
hsa-miR-99a-5p	−1.03*	−0.067*	0.13	52.26
hsa-miR-23b-3p	−1.37*	−0.066*	0.13	64.87
hsa-miR-10b-5p	−1*	−0.069*	0.13	84.84
hsa-miR-125a-5p	−1.41*	−0.064*	0.13	114.18
hsa-miR-186-5p	−1.28*	−0.063*	0.13	11.59
hsa-miR-378a-3p	−1.74*	−0.063*	0.13	22.60
hsa-miR-26b-5p	−1.14*	−0.065*	0.13	49.22
hsa-miR-30c-5p	−1.01*	−0.065*	0.12	15.67

*Asterisks indicate a significant contribution *$p < 0.05$, **$p < 0.01$.*

pathways included neurotrophin signaling (27 genes, $p = 0.016$). For the highest expressing miRNA, hsa-miR-451a (**Table 3**), DIANA analysis indicated brain related cluster enrichment for Parkinson's disease (2 genes, $p = 1.0^{-5}$) and glioma (3 genes, $p = 0.02$), and clusters for signaling pathways related to aging, including mTOR signaling (6 genes, $p = 0.002$) and AMPK signaling (6 genes, $p = 0.027$). When all 13 miRNAs that correlated with MoCA scores were loaded into DIANA, the results indicate several pathways associated with brain function including prion disease (20 genes, 11 miRNA, $p = 1.0^{-6}$), glioma (44 genes, 13 miRNA, $p = 2.9^{-6}$), Huntington's disease (102 genes, 11 miRNA, $p = 0.015$), and axon guidance (71 genes, 12 miRNA, $p = 0.019$).

DISCUSSION

The results provide evidence that miRNA, from extracellular microvesicle enriched plasma samples, correlates with cognitive function in healthy elderly individuals. In discussing these results, there are several caveats that need to be considered. Exosomes have the potential to cross the blood–brain barrier and could provide a marker of brain health (Alvarez-Erviti et al., 2011). Alternatively, exosomes in the plasma could cross into the brain to deliver their cargo and influence brain function. Thus, it is important to consider the enrichment of exosomes. Elisa assays indicated that the samples were positive for the exosome marker CD63 indicating that the samples are enriched in exosomes. The enrichment of exosomes was supported by examination of microvesicle size, with ∼65% of particles in the range of exosomes. Exosomes are classically defined as 50–150 nm in diameter, although larger extracellular vesicles (>200 nm) have been described (Kowal et al., 2016). The 150 nm limit may represent a bias due to isolation techniques, and ignores the possible functional impact of increased volume of larger vesicles that have been described (van der Pol et al., 2012; Kowal et al., 2016). Regardless, it appears that the samples were enriched in exosomes.

A second consideration concerns the stringent criteria for the population of participants. Participants were screened in an attempt to exclude those with dementia or Alzheimer's disease. Interestingly, hsa-let-7g-5p, which is commonly found to decrease in plasma, serum, and blood from Alzheimer's patients (Kumar et al., 2013; Tan et al., 2014; Satoh et al., 2015), was observed to increase with age in our plasma samples and in previous studies using a wider age range (Freedman et al., 2016). Other miRNAs that were increased with age in our study and the Freedman study, and yet have been reported to decrease in blood or plasma from Alzheimer's patients, include hsa-let-7e-5p and hsa-miR-103a-3p (Kumar et al., 2013; Leidinger et al., 2013; Satoh et al., 2015; Nagaraj et al., 2017). In all cases, multiple regression indicated no correlation of these miRNA with the MoCA score when age was taken into consideration. The stringent criteria and the absence of suspected miRNA markers of Alzheimer's disease increases the confidence that these individuals did not have a neurodegenerative disease; although it is possible that they were pre-symptomatic. On the other hand, our results indicating that these miRNAs increase with age, emphasizing the importance of considering age when investigating biomarkers of disease. It has been suggested that the inability to reproduce expression differences may result from age differences across cohorts (Satoh et al., 2015; Cosin-Tomas et al., 2017; Nagaraj et al., 2017), and for studies that found decreased miRNA expression associated with Alzheimer's disease, the disease and control groups were age-matched.

Mild cognitive impairment is considered a transitional state between normal aging and Alzheimer's disease and previous research suggests a threshold cutoff MoCA score of 19–23 for designating MCI (Luis et al., 2009; Dong et al., 2012; Larner, 2012; Freitas et al., 2013). Previous studies have reported that specific miRNAs increase in plasma or serum in MCI patients (Sheinerman et al., 2013; Dong et al., 2015). In many cases, the previously reported miRNA exhibited expression levels below our cutoff and were not considered. The stringency for expression reduces the likelihood of type I error and increases the confidence in those miRNA that were correlated with age or MoCA scores. However, the stringency makes it likely that we missed low expressing miRNA that correlate with cognitive function. Indeed, considering that all cognition-related miRNAs exhibited increased expression associated with a decline in MoCA score, it is likely that we missed miRNA that exhibited low expression, particularly in cognitively intact individuals. In the case of miRNA that did satisfy our stringent cutoff, and have been reported to increase in MCI patients, expression of hsa-miR-128-3p, hsa-miR-134-5p, hsa-miR-382-5p, hsa-miR-146a-5p, and hsa-miR-93-5p was observed to increase with age and was not correlated with the MoCA score. We cannot rule out that individuals were pre-symptomatic for MCI. Thus, it will be important for future studies to track cognitive changes as well as miRNA markers over time to determine if miRNA are predictive of decline associated with normal aging and disease.

In comparing the pattern of miRNA expression to previous work, it is important to recognize that much of the previous

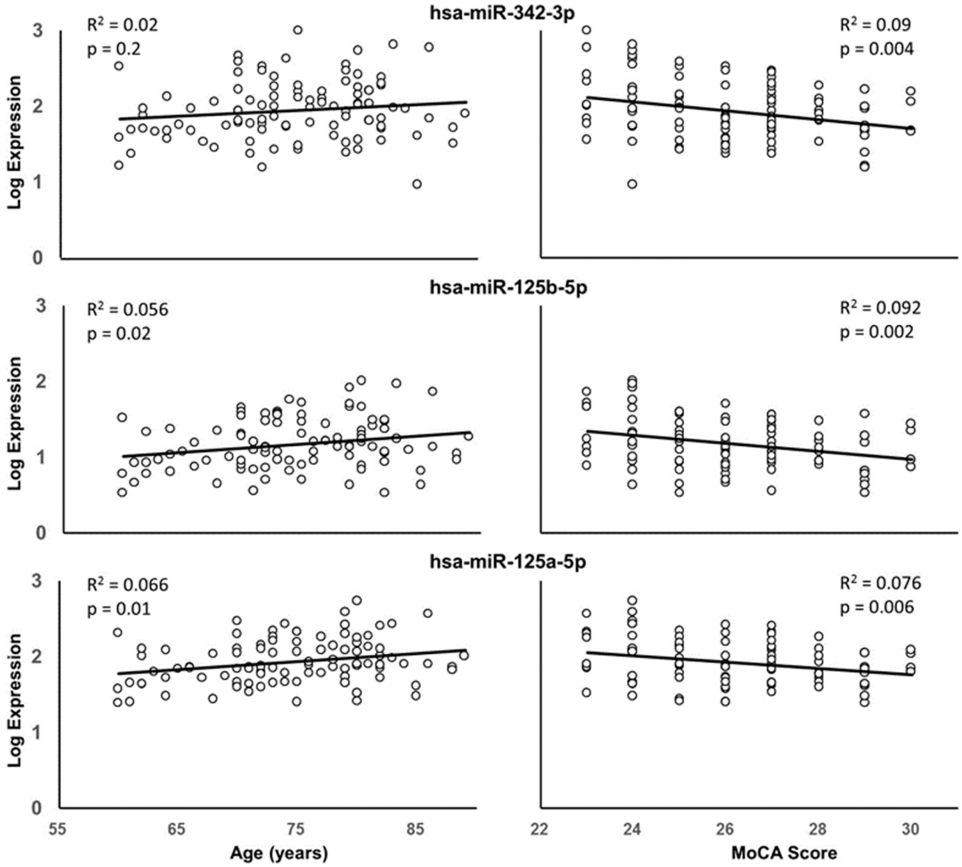

FIGURE 3 | Correlation of hsa-miR-342-3p **(top)**, hsa-miR-125b-5p **(middle)**, and hsa-miR-125a-5p **(bottom)** expression with age **(left)** or MoCA scores **(right)**. The R^2 and *p*-values for the simple regressions are provided.

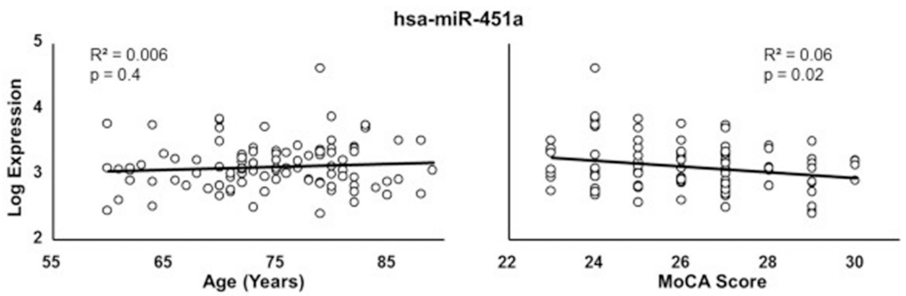

FIGURE 4 | Correlation of hsa-miR-451a with age **(left)** or MoCA scores **(right)**.

work has examined miRNA directly from plasma or serum, which includes exosomal and protein-bound miRNAs. It is expected that miRNA expression of plasma and exosomal enriched samples will be similar for many miRNAs; however, expression of some miRNAs may differ (Freedman et al., 2016). Our results confirm a high level of expression for mir-223-3p, mir-451a, mir-191-5p, mir-126-3p, mir-126-5p, mir-484, and mir-26a-5p, which are enriched in plasma exosomes (Hunter et al., 2008; Pritchard et al., 2012; Cheng et al., 2014; Mooney et al., 2015). Second, previous work indicates that chronological age provides a strong influence on expression of plasma miRNA. Indeed, we found over half the exosomal miRNAs examined at $p < 0.01$, exhibited increased expression with age (false discovery rate $p < 0.016$). The robustness of these 74 age-related miRNAs is emphasized by the fact that a well powered study reported 51 of these miRNAs increased in plasma across a broader age range (Freedman et al., 2016). Together, the results indicate that miRNA provide a good marker for chronological age. Together, the

results emphasize that age is a major risk factor for Alzheimer's disease and MCI. Thus, it should not be surprising that biological markers of chronological age provide good predictors of diseases. As such, age should be taken into account when attempting to link biological markers to age-related diseases.

Due to the correlation of age with measures of cognitive function and miRNA expression, multiple regressions were employed to examine the relationship between MoCA scores and miRNA expression, in order to account for age effects. Our analysis point to several miRNAs that may be good predictors of cognitive function in elderly individuals. Exosomes have the potential to cross the blood–brain barrier (Alvarez-Erviti et al., 2011). Thus, highly expressed miRNAs coming from white (mir-223-3p, mir-191-5p, mir-150-5p, mir-26a-5p, mir-19b-3p) or red (mir-451a) red blood cells (RBCs) (Hunter et al., 2008; Pritchard et al., 2012) could influence brain function. In the current study, we observed an increase in hsa-mir-19b-3p with age; however, this miRNA was not correlated with cognition. In contrast, MoCA scores were correlated with hsa-mir-451a. One possible confound is that hemolysis can increase the level of RBC enriched miRNA, hsa-mir-451a and hsa-mir-16-5p, in plasma and serum (Blondal et al., 2013; Kirschner et al., 2013), which could have contaminated our microvesicle enriched samples. A number of factors can influence the fragility of RBCs. However, it is important to note that the fragility of RBCs declines over the course of aging (Penha-Silva et al., 2007; de Freitas et al., 2014). Furthermore, when variability in cognition associated with age was taken into account, expression of hsa-mir-451a, but not hsa-mir-16-5p, was correlated with the MoCA scores. On the other hand, RBCs are not the only source of hsa-mir-451a and an increase in release of hsa-mir-451a containing microvesicles is associated with disease in other cell types as well as senescence of platelets (Ji et al., 2014; Dickman et al., 2017; Pienimaeki-Roemer et al., 2017; Takikawa et al., 2017). The manner in which hsa-mir-451a could influence cognition is unknown; however, an increase in plasma hsa-mir-451a has been reported to be associated with vascular dementia (Prabhakar et al., 2017) and increased expression in the brain may alter synaptic function (Mor et al., 2015).

The MoCA scores were also correlated with several miRNAs that are enriched in the brain (Hinske et al., 2014). An increase in brain specific miRNA in the plasma could result from increased leakiness of the blood–brain barrier, increased expression of specific miRNA, increased release of brain derived microvesicless or a combination. If an increase in plasma levels was due to increased leakiness of the blood–brain barrier, we might expect to have seen a whole host of brain specific miRNAs increase in the plasma of impaired individuals. This does not seem to be the case since other brain selective miRNAs (e.g., hsa-miR-320b, hsa-miR-328-3p, hsa-miR-744-5p) passed our expression criterion and did not correlate with MoCA score. On the other hand, an increase in brain selective miRNAs in the plasma may represent increased release of specific miRNA due to aberrant neural activity, damage, or disease (Lachenal et al., 2011; van der Vos et al., 2011; Wang et al., 2011; Serafini et al., 2014; Harrison et al., 2016).

CONCLUSION

In the current study, we describe miRNAs associated with extracellular microvesicles from plasma as possible biomarkers of cognitive decline during aging. A decrease in MoCA score was associated with increased expression of several miRNAs. The rise in expression of brain selective miRNA could signify conditions in the brain, such as aberrant neural activity, damage, or disease, that result in increased synthesis or release from the brain and a decline in function. In addition, it is possible that highly expressed miRNA are delivered to the brain from the circulation, to influence brain function. The miRNA biomarkers from plasma microvesicle exhibited an expression profile, which was different from that previously described for Alzheimer's disease, suggesting that these biomarkers may be specific to cognitive decline in normal aging. Alternatively, these miRNAs may be related to a pre-symptomatic stage of disease.

AUTHOR CONTRIBUTIONS

AR performed experiments. AO, AW, and RC collected behavior data. LI helped in analysis. TF designed experiments, analyzed data, constructed figures, and wrote manuscript.

ACKNOWLEDGMENTS

This work was supported by National Institutes of Aging Grants R01AG037984, R37AG036800, R01AG49711, RO1AG052258, K01AG050707, R01AG054077, the UF Center for Cognitive Aging and Memory, and the Evelyn F. McKnight Brain Research Foundation.

REFERENCES

Alexander, G. E., Ryan, L., Bowers, D., Foster, T. C., Bizon, J. L., Geldmacher, D. S., et al. (2012). Characterizing cognitive aging in humans with links to animal models. *Front. Aging Neurosci.* 4:21. doi: 10.3389/fnagi.2012.00021

Alvarez-Erviti, L., Seow, Y., Yin, H., Betts, C., Lakhal, S., and Wood, M. J. (2011). Delivery of siRNA to the mouse brain by systemic injection of targeted exosomes. *Nat. Biotechnol.* 29, 341–345. doi: 10.1038/nbt.1807

Barrientos, R. M., Frank, M. G., Watkins, L. R., and Maier, S. F. (2010). Memory impairments in healthy aging: Role of aging-induced microglial sensitization. *Aging Dis.* 1, 212–231.

Blondal, T., Jensby Nielsen, S., Baker, A., Andreasen, D., Mouritzen, P., Wrang Teilum, M., et al. (2013). Assessing sample and miRNA profile quality in serum and plasma or other biofluids. *Methods* 59, S1–S6. doi: 10.1016/j.ymeth.2012.09.015

Cai, L., Chan, J. S., Yan, J. H., and Peng, K. (2014). Brain plasticity and motor practice in cognitive aging. *Front. Aging Neurosci.* 6:31. doi: 10.3389/fnagi.2014.00031

Cheng, L., Doecke, J. D., Sharples, R. A., Villemagne, V. L., Fowler, C. J., Rembach, A., et al. (2015). Prognostic serum miRNA biomarkers associated with Alzheimer's disease shows concordance with neuropsychological and neuroimaging assessment. *Mol. Psychiatry* 20, 1188–1196. doi: 10.1038/mp.2014.127

Cheng, L., Sharples, R. A., Scicluna, B. J., and Hill, A. F. (2014). Exosomes provide a protective and enriched source of miRNA for biomarker profiling compared to intracellular and cell-free blood. *J. Extracell. Vesicles* 3, 1–14. doi: 10.3402/jev.v3.23743

Cosin-Tomas, M., Antonell, A., Llado, A., Alcolea, D., Fortea, J., Ezquerra, M., et al. (2017). Plasma miR-34a-5p and miR-545-3p as early biomarkers of Alzheimer's disease: potential and limitations. *Mol. Neurobiol.* 54, 5550–5562. doi: 10.1007/s12035-016-0088-8

Craft, S., Foster, T. C., Landfield, P. W., Maier, S. F., Resnick, S. M., and Yaffe, K. (2012). Session III: mechanisms of age-related cognitive change and targets for intervention: inflammatory, oxidative, and metabolic processes. *J. Gerontol. A Biol. Sci. Med. Sci.* 67, 754–759. doi: 10.1093/gerona/gls112

de Freitas, M. V., Marquez-Bernardes, L. F., de Arvelos, L. R., Paraiso, L. F., Gonçalves E Oliveira, A. F., Rde, C., et al. (2014). Influence of age on the correlations of hematological and biochemical variables with the stability of erythrocyte membrane in relation to sodium dodecyl sulfate. *Hematology* 19, 424–430. doi: 10.1179/1607845413Y.0000000145

Dickman, C. T., Lawson, J., Jabalee, J., MacLellan, S. A., LePard, N. E., Bennewith, K. L., et al. (2017). Selective extracellular vesicle exclusion of miR-142-3p by oral cancer cells promotes both internal and extracellular malignant phenotypes. *Oncotarget* 8, 15252–15266. doi: 10.18632/oncotarget.14862

Dong, H., Li, J., Huang, L., Chen, X., Li, D., Wang, T., et al. (2015). Serum MicroRNA profiles serve as novel biomarkers for the diagnosis of Alzheimer's disease. *Dis. Markers* 2015:625659. doi: 10.1155/2015/625659

Dong, Y., Lee, W. Y., Basri, N. A., Collinson, S. L., Merchant, R. A., Venketasubramanian, N., et al. (2012). The montreal cognitive assessment is superior to the mini-mental state examination in detecting patients at higher risk of dementia. *Int. Psychogeriatr.* 24, 1749–1755. doi: 10.1017/S1041610212001068

Fan, X., Wheatley, E. G., and Villeda, S. A. (2017). Mechanisms of hippocampal aging and the potential for rejuvenation. *Annu. Rev. Neurosci.* 40, 251–272. doi: 10.1146/annurev-neuro-072116-031357

Febo, M., and Foster, T. C. (2016). Preclinical magnetic resonance imaging and spectroscopy studies of memory, aging, and cognitive decline. *Front. Aging Neurosci.* 8:158. doi: 10.3389/fnagi.2016.00158

Fehlmann, T., Ludwig, N., Backes, C., Meese, E., and Keller, A. (2016). Distribution of microRNA biomarker candidates in solid tissues and body fluids. *RNA Biol.* 13, 1084–1088. doi: 10.1080/15476286.2016.1234658

Foster, T. C. (2006). Biological markers of age-related memory deficits: treatment of senescent physiology. *CNS Drugs* 20, 153–166. doi: 10.2165/00023210-200620020-00006

Foster, T. C., Kyritsopoulos, C., and Kumar, A. (2016). Central role for NMDA receptors in redox mediated impairment of synaptic function during aging and Alzheimer's disease. *Behav. Brain Res.* 322(Pt B), 223–232. doi: 10.1016/j.bbr.2016.05.012

Freedman, J. E., Gerstein, M., Mick, E., Rozowsky, J., Levy, D., Kitchen, R., et al. (2016). Diverse human extracellular RNAs are widely detected in human plasma. *Nat. Commun.* 7:11106. doi: 10.1038/ncomms11106

Freitas, S., Simoes, M. R., Alves, L., and Santana, I. (2013). Montreal cognitive assessment: validation study for mild cognitive impairment and Alzheimer disease. *Alzheimer Dis. Assoc. Disord.* 27, 37–43. doi: 10.1097/WAD.0b013e3182420bfe

Harrison, E. B., Hochfelder, C. G., Lamberty, B. G., Meays, B. M., Morsey, B. M., Kelso, M. L., et al. (2016). Traumatic brain injury increases levels of miR-21 in extracellular vesicles: implications for neuroinflammation. *FEBS Open Bio* 6, 835–846. doi: 10.1002/2211-5463.12092

Hinske, L. C., Franca, G. S., Torres, H. A., Ohara, D. T., Lopes-Ramos, C. M., Heyn, J., et al. (2014). miRIAD-integrating microRNA inter- and intragenic data. *Database* 2014:bau099. doi: 10.1093/database/bau099

Hunter, M. P., Ismail, N., Zhang, X., Aguda, B. D., Lee, E. J., Yu, L., et al. (2008). Detection of microRNA expression in human peripheral blood microvesicles. *PLOS ONE* 3:e3694. doi: 10.1371/journal.pone.0003694

Impey, S., Davare, M., Lesiak, A., Fortin, D., Ando, H., Varlamova, O., et al. (2010). An activity-induced microRNA controls dendritic spine formation by regulating Rac1-PAK signaling. *Mol. Cell. Neurosci.* 43, 146–156. doi: 10.1016/j.mcn.2009.10.005

Ji, H., Chen, M., Greening, D. W., He, W., Rai, A., Zhang, W., et al. (2014). Deep sequencing of RNA from three different extracellular vesicle (EV) subtypes released from the human LIM1863 colon cancer cell line uncovers distinct miRNA-enrichment signatures. *PLOS ONE* 9:e110314. doi: 10.1371/journal.pone.0110314

Jovasevic, V., Corcoran, K. A., Leaderbrand, K., Yamawaki, N., Guedea, A. L., Chen, H. J., et al. (2015). GABAergic mechanisms regulated by miR-33 encode state-dependent fear. *Nat. Neurosci.* 18, 1265–1271. doi: 10.1038/nn.4084

Kirschner, M. B., Edelman, J. J., Kao, S. C., Vallely, M. P., van Zandwijk, N., and Reid, G. (2013). The impact of hemolysis on cell-free microRNA biomarkers. *Front. Genet.* 4:94. doi: 10.3389/fgene.2013.00094

Kowal, J., Arras, G., Colombo, M., Jouve, M., Morath, J. P., Primdal-Bengtson, B., et al. (2016). Proteomic comparison defines novel markers to characterize heterogeneous populations of extracellular vesicle subtypes. *Proc. Natl. Acad. Sci. U.S.A.* 113, E968–E977. doi: 10.1073/pnas.1521230113

Kumar, A., Rani, A., Tchigranova, O., Lee, W. H., and Foster, T. C. (2012). Influence of late-life exposure to environmental enrichment or exercise on hippocampal function and CA1 senescent physiology. *Neurobiol. Aging* 33, e1–e17. doi: 10.1016/j.neurobiolaging.2011.06.023

Kumar, P., Dezso, Z., MacKenzie, C., Oestreicher, J., Agoulnik, S., Byrne, M., et al. (2013). Circulating miRNA biomarkers for Alzheimer's disease. *PLOS ONE* 8:e69807. doi: 10.1371/journal.pone.0069807

Lachenal, G., Pernet-Gallay, K., Chivet, M., Hemming, F. J., Belly, A., Bodon, G., et al. (2011). Release of exosomes from differentiated neurons and its regulation by synaptic glutamatergic activity. *Mol. Cell. Neurosci.* 46, 409–418. doi: 10.1016/j.mcn.2010.11.004

Landgraf, P., Rusu, M., Sheridan, R., Sewer, A., Iovino, N., Aravin, A., et al. (2007). A mammalian microRNA expression atlas based on small RNA library sequencing. *Cell* 129, 1401–1414. doi: 10.1016/j.cell.2007.04.040

Larner, A. J. (2012). Screening utility of the montreal cognitive assessment (MoCA): in place of–or as well as–the MMSE? *Int. Psychogeriatr.* 24, 391–396. doi: 10.1017/S1041610211001839

Leidinger, P., Backes, C., Deutscher, S., Schmitt, K., Mueller, S. C., Frese, K., et al. (2013). A blood based 12-miRNA signature of Alzheimer disease patients. *Genome Biol.* 14:R78. doi: 10.1186/gb-2013-14-7-r78

Lugli, G., Cohen, A. M., Bennett, D. A., Shah, R. C., Fields, C. J., Hernandez, A. G., et al. (2015). Plasma exosomal miRNAs in persons with and without Alzheimer disease: altered expression and prospects for biomarkers. *PLOS ONE* 10:e0139233. doi: 10.1371/journal.pone.0139233

Luis, C. A., Keegan, A. P., and Mullan, M. (2009). Cross validation of the montreal cognitive assessment in community dwelling older adults residing in the Southeastern US. *Int. J. Geriatr. Psychiatry* 24, 197–201. doi: 10.1002/gps.2101

Mooney, C., Raoof, R., El-Naggar, H., Sanz-Rodriguez, A., Jimenez-Mateos, E. M., and Henshall, D. C. (2015). High throughput qPCR expression profiling of circulating MicroRNAs reveals minimal sex- and sample timing-related variation in plasma of healthy volunteers. *PLOS ONE* 10:e0145316. doi: 10.1371/journal.pone.0145316

Mor, M., Nardone, S., Sams, D. S., and Elliott, E. (2015). Hypomethylation of miR-142 promoter and upregulation of microRNAs that target the oxytocin receptor gene in the autism prefrontal cortex. *Mol. Autism* 6:46. doi: 10.1186/s13229-015-0040-1

Mushtaq, G., Greig, N. H., Anwar, F., Zamzami, M. A., Choudhry, H., Shaik, M. M., et al. (2016). miRNAs as circulating biomarkers for Alzheimer's disease and Parkinson's disease. *Med. Chem.* 12, 217–225. doi: 10.2174/1573406411666151030112140

Nagaraj, S., Laskowska-Kaszub, K., Debski, K. J., Wojsiat, J., Dabrowski, M., Gabryelewicz, T., et al. (2017). Profile of 6 microRNA in blood plasma distinguish early stage Alzheimer's disease patients from non-demented subjects. *Oncotarget* 8, 16122–16143. doi: 10.18632/oncotarget.15109

Nasreddine, Z. S., Phillips, N. A., Bedirian, V., Charbonneau, S., Whitehead, V., Collin, I., et al. (2005). The montreal cognitive assessment, MoCA: a brief screening tool for mild cognitive impairment. *J. Am. Geriatr. Soc.* 53, 695–699. doi: 10.1111/j.1532-5415.2005.53221.x

Nissim, N. R., O'Shea, A. M., Bryant, V., Porges, E. C., Cohen, R., and Woods, A. J. (2017). Frontal structural neural correlates of working memory performance in older adults. *Front. Aging Neurosci.* 8:328. doi: 10.3389/fnagi.2016.00328

O'Shea, A., Cohen, R. A., Porges, E. C., Nissim, N. R., and Woods, A. J. (2016). Cognitive aging and the hippocampus in older adults. *Front. Aging Neurosci.* 8:298. doi: 10.3389/fnagi.2016.00298

Penha-Silva, N., Firmino, C. B., de Freitas Reis, F. G., da Costa Huss, J. C., de Souza, T. M., de Freitas, M. V., et al. (2007). Influence of age on the stability of human erythrocyte membranes. *Mech. Ageing Dev.* 128, 444–449. doi: 10.1016/j.mad.2007.06.007

Peterson, M. F., Otoc, N., Sethi, J. K., Gupta, A., and Antes, T. J. (2015). Integrated systems for exosome investigation. *Methods* 87, 31–45. doi: 10.1016/j.ymeth.2015.04.015

Pienimaeki-Roemer, A., Konovalova, T., Musri, M. M., Sigruener, A., Boettcher, A., Meister, G., et al. (2017). Transcriptomic profiling of platelet senescence and platelet extracellular vesicles. *Transfusion* 57, 144–156. doi: 10.1111/trf.13896

Porges, E. C., Woods, A. J., Edden, R. A., Puts, N. A., Harris, A. D., Chen, H., et al. (2017). Frontal gamma-aminobutyric acid concentrations are associated with cognitive performance in older adults. *Biol. Psychiatry Cogn. Neurosci, Neuroimaging* 2, 38–44. doi: 10.1016/j.bpsc.2016.06.004

Prabhakar, P., Chandra, S. R., and Christopher, R. (2017). Circulating microRNAs as potential biomarkers for the identification of vascular dementia due to cerebral small vessel disease. *Age. Ageing* 46, 861–864. doi: 10.1093/ageing/afx090

Pritchard, C. C., Kroh, E., Wood, B., Arroyo, J. D., Dougherty, K. J., Miyaji, M. M., et al. (2012). Blood cell origin of circulating microRNAs: a cautionary note for cancer biomarker studies. *Cancer Prev. Res.* 5, 492–497. doi: 10.1158/1940-6207.CAPR-11-0370

Rajman, M., Metge, F., Fiore, R., Khudayberdiev, S., Aksoy-Aksel, A., Bicker, S., et al. (2017). A microRNA-129-5p/Rbfox crosstalk coordinates homeostatic downscaling of excitatory synapses. *EMBO J.* 36, 1770–1787. doi: 10.15252/embj.201695748

Satoh, J., Kino, Y., and Niida, S. (2015). MicroRNA-Seq data analysis pipeline to identify blood biomarkers for Alzheimer's disease from public data. *Biomark Insights* 10, 21–31. doi: 10.4137/BMI.S25132

Schulte, C., Karakas, M., and Zeller, T. (2016). microRNAs in cardiovascular disease - clinical application. *Clin. Chem. Lab. Med.* 55, 687–704. doi: 10.1515/cclm-2016-0576

Schwarzenbach, H., Nishida, N., Calin, G. A., and Pantel, K. (2014). Clinical relevance of circulating cell-free microRNAs in cancer. *Nat. Rev. Clin. Oncol.* 11, 145–156. doi: 10.1038/nrclinonc.2014.5

Serafini, G., Pompili, M., Hansen, K. F., Obrietan, K., Dwivedi, Y., Shomron, N., et al. (2014). The involvement of microRNAs in major depression, suicidal behavior, and related disorders: a focus on miR-185 and miR-491-3p. *Cell Mol. Neurobiol.* 34, 17–30. doi: 10.1007/s10571-013-9997-5

Shao, N. Y., Hu, H. Y., Yan, Z., Xu, Y., Hu, H., Menzel, C., et al. (2010). Comprehensive survey of human brain microRNA by deep sequencing. *BMC Genomics* 11:409. doi: 10.1186/1471-2164-11-409

Sheinerman, K. S., Tsivinsky, V. G., Abdullah, L., Crawford, F., and Umansky, S. R. (2013). Plasma microRNA biomarkers for detection of mild cognitive impairment: biomarker validation study. *Aging* 5, 925–938. doi: 10.18632/aging.100624

Sheinerman, K. S., and Umansky, S. R. (2013). Circulating cell-free microRNA as biomarkers for screening, diagnosis and monitoring of neurodegenerative diseases and other neurologic pathologies. *Front. Cell Neurosci.* 7:150. doi: 10.3389/fncel.2013.00150

Speisman, R. B., Kumar, A., Rani, A., Foster, T. C., and Ormerod, B. K. (2013). Daily exercise improves memory, stimulates hippocampal neurogenesis and modulates immune and neuroimmune cytokines in aging rats. *Brain Behav. Immun.* 28, 25–43. doi: 10.1016/j.bbi.2012.09.013

Takikawa, T., Masamune, A., Yoshida, N., Hamada, S., Kogure, T., and Shimosegawa, T. (2017). Exosomes derived from pancreatic stellate cells: MicroRNA signature and effects on pancreatic cancer cells. *Pancreas* 46, 19–27. doi: 10.1097/MPA.0000000000000722

Tan, L., Yu, J. T., Tan, M. S., Liu, Q. Y., Wang, H. F., Zhang, W., et al. (2014). Genome-wide serum microRNA expression profiling identifies serum biomarkers for Alzheimer's disease. *J. Alzheimers Dis.* 40, 1017–1027. doi: 10.3233/JAD-132144

van der Pol, E., Boing, A. N., Harrison, P., Sturk, A., and Nieuwland, R. (2012). Classification, functions, and clinical relevance of extracellular vesicles. *Pharmacol. Rev.* 64, 676–705. doi: 10.1124/pr.112.005983

van der Vos, K. E., Balaj, L., Skog, J., and Breakefield, X. O. (2011). Brain tumor microvesicles: insights into intercellular communication in the nervous system. *Cell Mol. Neurobiol.* 31, 949–959. doi: 10.1007/s10571-011-9697-y

Vlachos, I. S., Zagganas, K., Paraskevopoulou, M. D., Georgakilas, G., Karagkouni, D., Vergoulis, T., et al. (2015). DIANA-miRPath v3.0: deciphering microRNA function with experimental support. *Nucleic Acids Res.* 43, W460–W466. doi: 10.1093/nar/gkv403

Wang, S., Cesca, F., Loers, G., Schweizer, M., Buck, F., Benfenati, F., et al. (2011). Synapsin I is an oligomannose-carrying glycoprotein, acts as an oligomannose-binding lectin, and promotes neurite outgrowth and neuronal survival when released via glia-derived exosomes. *J. Neurosci.* 31, 7275–7290. doi: 10.1523/JNEUROSCI.6476-10.2011

Woods, A. J., Cohen, R. A., and Pahor, M. (2013). Cognitive frailty: frontiers and challenges. *J. Nutr. Health Aging* 17, 741–743. doi: 10.1007/s12603-013-0398-8

Conflict of Interest Statement: The authors declare that the research was conducted in the absence of any commercial or financial relationships that could be construed as a potential conflict of interest.

frontiers in Aging Neuroscience

ORIGINAL RESEARCH
published: 19 December 2017
doi: 10.3389/fnagi.2017.00421

Mucuna pruriens Protects against MPTP Intoxicated Neuroinflammation in Parkinson's Disease through NF-κB/pAKT Signaling Pathways

*Sachchida N. Rai[1], Hareram Birla[1], Saumitra S. Singh[1], Walia Zahra[1], Ravishankar R. Patil[2], Jyoti P. Jadhav[2], Mallikarjuna R. Gedda[1] and Surya P. Singh[1]**

[1] Department of Biochemistry, Institute of Science, Banaras Hindu University, Varanasi, India, [2] Department of Biotechnology, Shivaji University, Kolhapur, India

Till date, drugs that have been used to manage Parkinson's disease (PD) have only shown symptomatic relief with several adverse effects besides their inability to prevent neurodegeneration. Neuroinflammation plays an important role in the advancement of PD and can be targeted for its effective treatment. Researchers have suggested that herbal plants exhibiting the anti-inflammatory and anti-oxidant properties are therefore beneficial to human health. Conventionally, *Mucuna pruriens* (Mp) seeds are used for maintaining male virility in India. Reportedly, Mp is used as a rejuvenator drug having neuroprotective property. Our study aimed to investigate effects of aqueous extract of Mp (100 mg/kgbwt) on neuroinflammation, orally administered to mice intoxicated with 1-methyl-4-phenyl-1,2,3,6-tetrahydropyridine (MPTP) as well as the molecular mechanism involved in the progression of PD. In this study, we have observed significant behavioral abnormalities beside decreased antioxidant defense in MPTP intoxicated mice. We have also observed significant increase in inflammatory parameters like Glial Fibrillary Acidic Protein, Inducible Nitric Oxide Synthase, Intercellular Cell Adhesion Molecule, and Tumor Necrosis Factor alpha in substantia nigra pars compacta (SNpc) of parkinsonian mice, while Mp treatment has notably reduced these inflammatory parameters. Mp also inhibited the MPTP induced activation of NF-κB and promoted pAkt1 activity which further prevented the apoptosis of the dopaminergic neurons. Moreover, Mp exhibited significant antioxidant defense by inhibiting the lipid peroxidation and nitrite level, and by improving catalase activity and enhancing GSH level in nigrostriatal region of mouse brain. Mp also recovered the behavioral abnormalities in MPTP treated mice. Additionally, Mp treatment considerably increased the immunoreactivity of Tyrosine Hydroxylase and Dopamine Transporter in SNpc of parkinsonian mice. Our high performance liquid chromatography analysis of the Mp seed extract have shown L-DOPA, gallic acid, phytic acid, quercetin, and catechin equivalents as the major components which might cause neuroprotection in PD mice. Our result suggested that Mp extract treatment containing L-DOPA and a mixture of

OPEN ACCESS

Edited by:
Ashok Kumar,
University of Florida, United States

Reviewed by:
Kempuraj Duraisamy,
University of Missouri, United States
Margarida Castro-Caldas,
Universidade Nova de Lisboa, Portugal

***Correspondence:**
Surya P. Singh
suryasinghbhu16@gmail.com

Received: *27 September 2017*
Accepted: *07 December 2017*
Published: *19 December 2017*

Citation:
Rai SN, Birla H, Singh SS, Zahra W, Patil RR, Jadhav JP, Gedda MR and Singh SP (2017) Mucuna pruriens Protects against MPTP Intoxicated Neuroinflammation in Parkinson's Disease through NF-κB/pAKT Signaling Pathways. Front. Aging Neurosci. 9:421. doi: 10.3389/fnagi.2017.00421

rich novel phytochemicals significantly alleviates the MPTP induced neurotoxicity by NF-κB and pAkt pathway. The findings observed thereby indicate that Mp extract have suggestively ameliorated MPTP induced neuroinflammation, restored the biochemical and behavioral abnormalities in PD mouse and thus provided a scientific basis for its traditional claim.

Keywords: Parkinson's disease, neuroinflammation, *Mucuna pruriens,* tyrosine hydroxylase, MPTP (1-methyl-4-phenyl-1,2,3,6-tetrahydropyridine), substantia nigra

INTRODUCTION

After Alzheimer's disease (AD), Parkinson's disease (PD) is considered to be the most common progressive neurodegenerative disease. PD is basically characterized by the loss of dopaminergic neurons in substantia nigra pars compacta (SNpc) and reduced level of dopamine (DA) within the striatum (ST) (Siderowf and Stern, 2003; Yadav et al., 2013, 2014; Rai et al., 2016). Among non-motor symptoms, cognitive decline appears the major one in the case of PD (Aarsland et al., 2017). Dopaminergic neuronal degradation, formation of inclusions called Lewy bodies and activation of glial cells are the hallmark of PD pathogenesis in brain. While the etiopathogenesis of PD still not fully known, it is identified to go worse on exposure to environmental neurotoxins such as MPTP, Paraquat (PQ), and several others (Bové et al., 2005; Khan et al., 2013; Yadav et al., 2013). In humans and primates, MPTP which is a potent inhibitor of mitochondrial complex-1 of electron transport chain creates parkinsonian characteristic, and in mice, it recapitulates dopaminergic degenerations via nigrostriatal pathway. For that reason, in animal models of PD, MPTP is extensively used to study and explore the molecular events responsible for dopaminergic neuronal degeneration and to check the efficacy of several neuroprotective agents (Jackson-Lewis et al., 2012). Biomolecules such as lipids, proteins, and DNA are damaged by reactive oxygen species (ROS) and reactive nitrogen species (RNS), by-products of which were observed in the SN and striatum of human PD post-mortem brains (Dexter et al., 1994; Khan et al., 2013). The oxidation of lipid and proteins can thus lead to loss of membrane integrity, enzyme inactivation leading to cell death in neurodegenerative disorders (Hald and Lotharius, 2005).

Previous literature suggests that in PD, prolonged neuroinflammation plays an important role during degeneration of neurons (Hirsch and Hunot, 2009; Joglar et al., 2009; Khan et al., 2013). Inflammatory response during neurodegeneration has not yet been thoroughly investigated. Proinflammatory mediators such as cytokines/chemokines, enzymes like cyclooxygenase-2 (COX-2) and inducible nitric oxide synthase (iNOS) are produced by glial (astroglial and microglial) cells in response to extracellular insult to dopaminergic neurons (Khan et al., 2013). In addition, nuclear transcription factor-κB (NF-κB) plays a central role in the PD pathogenesis by inducing the expression of tumor necrosis factor-alpha (TNF-α) and interleukin-1 beta (IL-1β) via oxidative stress mediated neurodegeneration (Hald and Lotharius, 2005). These cytokines and enzymes could cause neuronal death by the cytotoxic mechanism. Previous literature has also suggested that anti-inflammatory drugs significantly inhibit the neuroinflammatory processes and ultimately protect dopaminergic neuronal loss in different parkinsonian models (Choi et al., 2005; Jin et al., 2005).

In spite of important evidences in learning the pathobiology of neurodegeneration, various efforts to expand and advance successful treatment strategies are being done (Brotchie and Jenner, 2011) with minimal translational results. With this background, there has been a lot of focus on the herbal mediated neuroprotection of PD with special emphasis on the anti-oxidative and anti-inflammatory activities of these herbal plants and their derivatives. Recently, Kim et al. (2015) suggested that *Ligusticum officinale* exhibits potent anti-inflammatory activity via NF-κB/IκB-α and MAPK pathway. Pycnogenol, extracted from *Pinus maritima* bark also protects dopaminergic neuron in MPTP induced neuroinflammation (Khan et al., 2013).

In Indian system of medicine, *Mucuna pruriens* (Mp) is the most accepted drug. A number of reports have recommended that it exhibits various pharmacological properties like analgesic, anti-inflammatory, anti-neoplastic, anti-epileptic, and anti-microbial activities (Sathiyanarayanan and Arulmozhi, 2007; Adepoju and Odubena, 2009; Yadav et al., 2013). Mp has been found to be rich in bioactive compounds such as tannins, alkaloids, phenolics compounds, and flavonoids (Duke, 1995). Diabetes, atherosclerosis, rheumatoid arthritis, nervous disorders, and Parkinsonism are certain diseases that have been found to be effectively managed by free-radical mediated disease management property of Mp seeds (Bhaskar et al., 2011). Moreover, our high performance liquid chromatography (HPLC) data has shown the presence of different phytochemicals such as proanthocyanidin, tannin, gallic acid, quercetin, and phytic acid in the aqueous seed extract of Mp. The anti-neuroinflammatory activity of Mp might be due to the presence of these active constituents. Also, other phytochemicals can act in combination for exploring its synergistic effect. Recently, Uchegbu et al. (2016), have suggested the anti-inflammatory activity of Mp by administering the doses of 10 and 50 mg/kgbwt in carrageenan and formalin induced acute and chronic paw edema respectively. They compared the anti-inflammatory activity of Mp with diclofenac potassium as a standard anti-inflammatory drug. At the doses of 10 and 50 mg/kg, Mp showed an inhibition % of 9.8 and 47.8 and 6.6 and 38.8 respectively against their corresponding carrageenan and formalin induced acute paw edema (Uchegbu et al., 2016). Additionally, Yadav et al. (2017) showed that Mp seed extract (100 mg/kg bwt) has improved the neurobehavioral activity by reducing the oxidative stress in nigrostriatal tissue

effectively by mitigating the iNOS expression levels in Paraquat (PQ) induced parkinsonian mouse model. Mp contains L-DOPA and ursolic acid which has potent anti-parkinsonian property (Rai et al., 2016; Yadav et al., 2016). There is very little literature which shows the anti-inflammatory activity of Mp in PD. With all the background information, in the present study, we have chosen Mp seed extract in MPTP induced Parkinsonian mouse model to explore its potent anti-neuroinflammatory activity.

MATERIALS AND METHODS

Reagents and Antibodies

Acetic acid, disodium hydrogen phosphate, reduced glutathione (GSH), reduced nicotinamide adenine dinucleotide phosphate (NADPH), Potassium chloride, Ammonum chloride, Sodium dihydrogen phosphate, and Bovine Serum Albumin (BSA) were procured from Sisco Research Laboratories (SRL; Mumbai, India). 1-Methyl-4-phenyl-1,2,3,6-tetra hydropyridine (MPTP), Normal Goat Serum (NGS) from Sigma–Aldrich (St. Louis, MO, United States). Protein estimation kit by Bradford GeNeiTM, hydrogen peroxide (H_2O_2), and potassium dichromate were purchased from Merck (Darmstadt, Germany), Sodim dodecyl sulfate (SDS), Thiobarbituric acid (TBA), Griess reagent and DABCO were procured from HiMedia (Mumbai, India). Sodium nitrite and Paraformaldehyde were purchased from Lobachemie, India. Primary antibodies for TH (SC-25269), iNOS (SC-651), Glial Fibrillary Acidic Protein (GFAP) (SC-33673) and Intercellular Cell Adhesion Molecule (ICAM) (SC-8439) were procured from Santa Cruz, Biotechnology (Santa Cruz, CA, United States) and the primary antibodies for TNF-α (ab1793), NF-κB (ab16502), DAT (ab111468), and pAkt1 (ab81283) were purchased from Abcam Life Science, Biogenuix Medsystems, Pvt. Ltd. (New Delhi, India), secondary fluorescent tagged antibodies for IHCCy2-conjugated and cy3-conjugated were procured from Merck Millipore and Chemicon respectively.

Experimental Animals

Eight to ten weeks old male mice (Swiss Albino mice, 25–30 g) were purchased from animal research facility of Banaras Hindu University, Varanasi, India. Before starting the experiment, animals were made to adapt the laboratory conditions for about a week under standard laboratory conditions by keeping light and dark cycles of 12 h. Mice were fed with standard rodent food purchased from market and water *ad libitum*. Experiments were done in between 12:00 noon to 03:00 pm. The investigational protocol for animals on which the test was carried out, was approved by the Animal Ethics Committee of Banaras Hindu University, Varanasi, India.

Plant Extracts Preparation

Mp seed powder was purchased from the Ayurveda Pharmacy, Institute of Medical Sciences, Banaras Hindu University, Varanasi, India. Mp seed extract was prepared by the method of Uhegbu et al. (2005) in which distilled water was used as the solvent. 20 g of Mp seed powder was taken and soaked in 200 ml of autoclaved distilled water. The solution was stirred for about 6 min and left overnight for proper mixing. Next day, the solution was filtered by using filter paper (Whatman No. A-1) and the extract were allowed to dry in rotary vacuum evaporator under reduced pressure and temperature (below 40°C).

RP-HPLC Quantitative Analysis of L-DOPA and Phytochemicals

L-DOPA was quantified in Mp seeds using reverse phase high performance liquid chromatography (RP-HPLC) involved with diode array detection. Samples were prepared as described by Rathod and Patel (2014) with minor modifications. One gram powder of Mp seed was extracted using autoclaved doubled distilled water: 0.1 M HCl (70:30) for 30 min on rotary shaker (120 rpm) and sonicated for 5 min. Then sample was evaporated, dissolved in distilled water and filtered through 0.45 μm nylon filter (Axiva filters). RP-HPLC analysis was performed by Shimadzu prominence equipped with degasser DGU-20A 5R, photo diode array detector SPD- M20 A and low pressure quaternary pump LC 20 AD. Chromatographic separation was achieved using a Waters, Nova-Pak C18 column (4 μm, 4.6 mm × 250 mm). The commercially available synthetic L-DOPA (Himedia) was taken as a standard.

Total phenolics content of Mp seeds has been determined spectrophotometrically (Singleton and Rossi, 1965). The sample was mixed with 1.8 ml of Folin–Ciocalteu reagent and incubated for 5 min at 25°C with 1.2 ml of 15% sodium carbonate solution for neutralization of reaction and further kept for 90 min at room temperature. The absorbance was taken at 765 nm. Result was noted in terms of mg of gallic acid equivalent per gram (mg GAE g^{-1}) of dry mass.

Total flavonoids were quantified according to the method by Chang et al. (2002). In brief, 1 ml aqueous extract of Mp seed was added to 1.5 ml distilled water, 0.1 ml of aluminum chloride (10%) and 0.1 ml of potassium acetate (1 M). The total volume was made up to 4.5 ml by adding distilled water. Incubation was carried out for 30 min at room temperature and absorbance was recorded at 415 nm. Expression of flavonoids level was done as milligram of quercetin equivalents per gram (mg QUE g^{-1}) of dry weight.

Evaluation of proanthocyanidin was done as described by Sun et al. (1998). The 0.5 ml sample was mixed with 3 ml of 4% vanillin and 1.5 ml of concentration HCl. Reaction mixture was incubated for 15 min and absorbance was taken at 490 nm. Content of Proanthocyanidin was expressed as catechin equivalents per gram (mg CAE g-1) of dry weight.

As described by Kirk and Sawyer (1998), Tannin level was measured with the help of Folin–Denis colorimetric method. 5 ml Mp seed extract was mixed with 1 ml Folin–Ciocalteu reagent and 2.5 ml saturated sodium carbonate. The solution was further incubated for 90 min at 28°C after the final volume was made up to 50 ml. The color intensity was measured at 760 nm.

The content of phytic acid was estimated according to the method of Gao et al. (2007). In short, 1 ml of Mp seed extract was added with 1 ml volume of Wade reagent (0.03% $FeCl_3.6\ H_2O$ and 0.3% sulfosalicylic acid in D/W). Vortexing of the solution was done for 5 s and then it was put to centrifugation for about

10 min. Absorbance of supernatant was taken at 500 nm using UV-spectrophotometer.

Experimental Design

The first group, i.e., control ($n = 6$) was treated with normal saline (i.p.). MPTP (30 mg/kg body weight) was prepared by dissolving it in 0.9% saline. The mice were injected (i.p.) twice with MPTP (30 mg/kg body weight) within 16 h of interval to induce PD to the second group ($n = 6$) (Yadav et al., 2014). The third group ($n = 6$) was first given two injections (i.p.) of MPTP (30 mg/kg body weight) within 16 h of interval and then daily orally treated with Mp seed aqueous extract (100 mg/kg body weight) from next day till 21 days after second MPTP injection.

Group I: Mice ($n = 6$) were given intraperitoneal (i.p.) injections of saline (0.9%), this served as control.

Group II: Mice ($n = 6$) were administered i.p. injections of MPTP (30 mg/kg body wt.), twice within 16 h interval.

Group III: Mice ($n = 6$) were first intoxicated (i.p.) with MPTP (30 mg/kg body wt.), twice within 16 h interval and from the next day they were orally treated with aqueous seed extract of Mp (100 mg/kg body wt.) daily for 21 days.

Neurobehavioral Studies

Rotarod Test

In Rotarod test, prior to experiment, group animals were trained for 3 successive days at a fixed speed (5 rpm) and the time was noted after the mice fall up to a maximum of 5 min. The experiment was repeated four times for each animal; finally average time was calculated as described previously (Manna et al., 2006). The same procedure was repeated once the treatment was completed and the time taken by the mice to fall was noted down.

Hanging Test

In this test, mice were placed on a horizontal grid and allowed to have grip on it. This grid was then made upside down so that mouse hangs downward, gripping on it, until they lose their control and fall down. The experiment was repeated three times, and the hanging time was noted for each group (Mohanasundari et al., 2006).

Narrow Beam Walking Test

Motor coordination in mice was assessed using this test. Animals from each group were trained to move on stationary wooden narrow flat beam (1 cm) which was positioned at a height of 100 cm above the floor (L 100 cm × W 1 cm). Then according to Pisa, time spent in walking from one end of the beam to another was noted and the procedure was repeated thrice for each group's animals (Pisa, 1998).

Sample Preparation for Biochemical Studies

After completion of experiment, the animals were sacrificed by cervical decapitation from each groups ($n = 3$), the collection of nigrostriatal tissue was done individually and they were further homogenized in KCl buffer (Tris-HCl 10 mM, NaCl 140 mM, KCl 300 mM, ethylenediaminetetraacetic acid 1 mM, Triton-X 100 0.5%) at pH 8.0 complemented with phosphatase and protease inhibitor. Centrifugation of the tissue homogenates was done at 12,000 *g* at a temperature of 4°C for about 20 min for the estimation of antioxidant enzymes and different biochemical parameters.

Biochemical Test

Catalase and Nitrite Test

In accordance with the decomposition of hydrogen peroxide, the Catalase activity was estimated (Kumar et al., 2010). Briefly 10% w/v tissue homogenate was added in phosphate buffer pH-7, distilled water, hydrogen peroxide (0.02 M) and incubated at room temperature for 1 min then potassium dichromate and acetic acid (1:3) solution was added and solution was allowed to boil for 15 min in boiling water bath and absorbance was taken at 570 nm. The activity of enzyme was measured in nmoles/min/mg protein.

By using standard procedure, Nitrite level was estimated in the supernatant (Granger et al., 1996). Supernatant of 10% w/v tissue homogenate was taken and ammonum chloride (0.7 mM) mixed with Griess reagent (0.1% *N*-naphthyl ethylenediamine and 1% sulfanilamide in 2.5% phosphoric acid) was added. The solution was allowed to stand at 37°C for 30 min, and the supernatant was then taken out to record the absorbance at 540 nm. By using the standard curve for sodium nitrite (10–100 μM), the total content of nitrite was calculated in terms of μmoles/mL.

Lipid Peroxidation and GSH Test

Estimation of Lipid peroxidation was done in the same way as described previously (Ohkawa et al., 1979) with fewer modifications in the nigrostriatal tissue of the mouse brain. Briefly, for measuring the concentration of malondialdehyde (MDA), a reaction mixture containing 10% tissue homogenate (0.1 mL) was added in 10% SDS solution (0.1 mL) and was kept at room temperature for 5 min. After that, 20% acetic acid (0.6 mL) was added and the solution was incubated 2–5 min. At last 0.8% Thio-barbituric acid TBA (0.6 mL) was added and the solution was kept in a boiling water bath for 1 h. The reaction mixture was then allowed to cool, centrifugation was done and absorbance of the supernatant was taken at 532 nm against control. Expression of LPO levels was done as nano moles MDA/mg protein. Glutathione reductase (GSH) level in the brain homogenate was measured by the method described previously (Moron et al., 1979) and reported as μM GSH/mg tissue.

Immunofluorescence Staining of TH, NF-κB, TNF-α, DAT, iNOS, GFAP, ICAM, and pAkt1 in SNpc

In the SNpc of brain, Immunofluorescence staining of TH, NF-κB, TNF-α, DAT, iNOS, GFAP, ICAM, and pAkt1 in SNpc was performed (Gorbatyuk et al., 2008). Mice were anesthetized with pentobarbital and the perfusion was done with 4% paraformaldehyde and the brains were post-fixed and collected. Using a cryomicrotome, the brain was cut in 25 μ thick coronal sections at the SN level (Leica, Wetzlar, Germany). Washing of the sections were done twice with 0.01 M PBS at pH 7.4 and then they were allowed to incubate with blocking reagent (10% normal

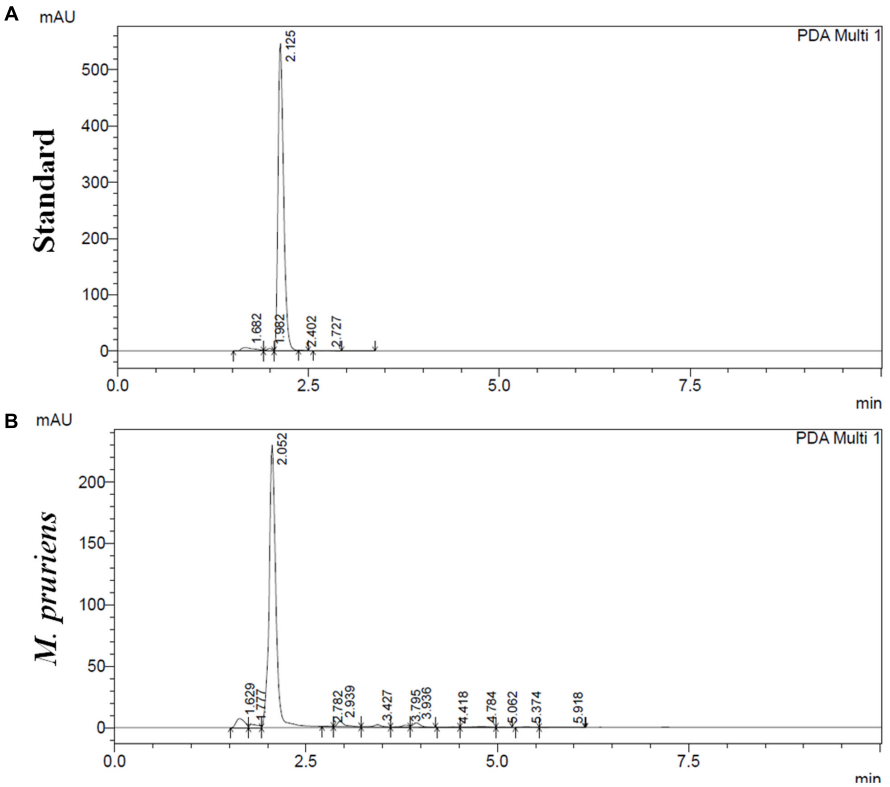

FIGURE 1 | High performance liquid chromatography (HPLC) analysis of *M. pruriens* seeds for L-DOPA. HPLC profile of standard L-DOPA **(A)**. HPLC profile of *M. pruriens* seed extract **(B)**.

goat serum in PBS, 0.3% Triton-X 100) for 1 h. Incubation of the sections with primary antibodies at 1:1000 dilutions was done with the polyclonal anti-mouse against TH, polyclonal anti-rabbit against NF-κB p65, monoclonal anti-mouse against TNF-α, polyclonal anti-rabbit against DAT, polyclonal anti-rabbit against iNOS, monoclonal anti-mouse against GFAP, monoclonal anti-mouse against ICAM, and monoclonal anti-rabbit against pAkt1 for 16 h at 4°C. The washing of the sections was again done five times in PBST and they were further incubated with Cy2-conjugated (Ex max 492 nm and Em max 510 nm) donkey anti-mouse and cy3-conjugated secondary antibodies (Ex max 550 nm and Em max 570 nm) donkey anti-rabbit in 1% BSA blocking solution for 1 h at Room Temperature. Washing of the sections was again done for three times and then mounted using mounting media, fluoro shield (Sigma–Aldrich). The images of the sections were taken with the help of fluorescent microscope Nikon (Thermo Fisher Scientific). Immunofluorescence was analyzed by Image J software (NIH, United States) and reported in mean integrated fluorescent value (IFV).

Statistical Analysis

Statistical analysis of differences between means of groups was determined by one way ANOVA followed by Student-Newman–Keuls *post hoc* test using GraphPad Prism 7.0 software. A $p < 0.05$ was considered statistically significant.

RESULTS

L-DOPA and Phytochemicals Content

Reverse phase high performance liquid chromatography analysis showed as compared to standard L-DOPA (**Figure 1A**), 65 mg g^{-1} of L-DOPA present in the aqueous extract of Mp seed (**Figure 1B**). Mp showed 38.9 ± 1.6 mg per gram of gallic acid equivalent (mg GAE g^{-1}) of phenolics and 54.14 ± 3.05 mg per gm of quercetin equivalent (mg QAE g^{-1}). The Mp seed showed 25.71 ± 4.13 mg per gram of catechin equivalents (mg CAE g^{-1}) proanthocyanidin level. Mp also showed 8.2 ± 0.15 mg g^{-1} of tannin level. Mp seed contain 6.72 ± 0.11 mg g^{-1} phytic acid.

Behavioral Studies

Effect of Mp on Behavioral Recovery

The result shows that the time taken by the MPTP treated mice for which it remained on the rotarod was significantly reduced ($p < 0.001$) compared to control. Whereas, when MPTP treated mice were treated with Mp, mice stayed on the rotarod significantly longer than MPTP mice ($p < 0.05$) (**Figure 2A**).

Our findings suggested that, in MPTP-treated mice, the time of gripping and hanging was significantly poorer ($p < 0.001$) as compared to control mice. When MPTP

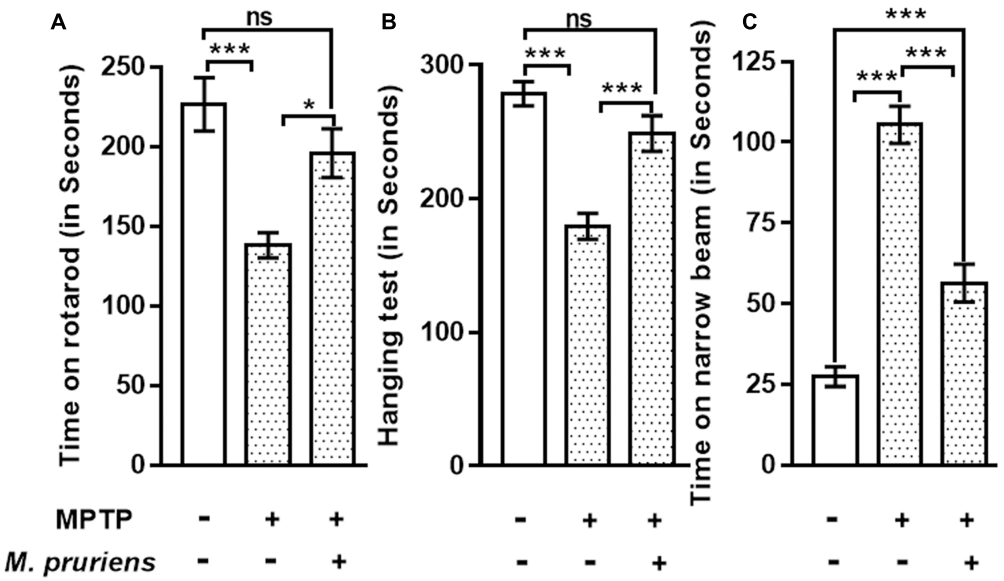

FIGURE 2 | Effect of Mp extract on behavioral parameters. **(A)** MPTP PD mice showed significantly reduced time of walking and staying on rotarod as compared to CONT group, which has been significantly improved on Mp supplementation to PD mice in comparison with untreated PD mice. **(B)** Hanging test showed significant improvement in Mp treated group compared to MPTP treated group. MPTP group mice fall early as compared to CONT group. **(C)** Narrow beam walking time was significantly increased in the MPTP treated mice in comparison with control group while Mp treatment declines the narrow beam walking time as compared to MPTP induced PD mouse (*$p < 0.05$, **$p < 0.01$, ***$p < 0.001$, $n = 6$). ns, non-significant.

mice were treated with Mp, the hanging time was increased ($p < 0.001$) when compared with MPTP treated mice (**Figure 2B**).

Result shows that in MPTP treated mice narrow beam walking time was increased ($p < 0.001$) as compared to CONT mice. When MPTP mice were treated with Mp the narrow beam walk time was decreased ($p < 0.001$) as compared to MPTP mice (**Figure 2C**).

Biochemical Studies

Effect of Mp on Catalase and Nitrite

We observed that MPTP injection significantly decrease the activity of CAT ($p < 0.001$) and increase the nitrite ($p < 0.001$) content in MPTP-injected mice when compared to CONT group. However, Mp treatment (MPTP+Mp) increased the activity of catalase ($p < 0.01$) (**Figure 3A**) and decreased nitrite level ($p < 0.01$) (**Figure 3B**) as compared to MPTP-treated group.

Effect of Mp on MDA and GSH Content

When compared to CONT group, the mice intoxicated with MPTP showed a significant increment ($p < 0.001$) in lipid peroxidation product, known as MDA. Conversely, MPTP administration caused a significant decline in GSH ($p < 0.001$) levels when compared with CONT group. Mp treatment (MPTP+Mp) significantly attenuated ($p < 0.001$) the rise in MDA level (**Figure 3C**) and improved ($p < 0.05$) the GSH levels (**Figure 3D**) compared to the MPTP group.

Effect of Mp on the Expression of TH, NF-κB, TNF-α, DAT, iNOS, GFAP, ICAM, and pAkt1 in SNpc

We have observed an increased in NF-κB ($p < 0.05$), TNF-α ($p < 0.01$), iNOS ($p < 0.01$), ICAM ($p < 0.01$), and GFAP ($p < 0.01$) positive cells expression in the MPTP treated mice as compared to CONT group. After Mp treatment (MPTP+Mp), a decrease in NF-κB ($p < 0.05$) (**Figure 4A**), TNF-α ($p < 0.01$) (**Figure 4B**), iNOS ($p < 0.01$) (**Figure 4C**), ICAM ($p < 0.01$) (**Figure 4D**), and GFAP ($p < 0.05$) (**Figure 5A**) expression was observed as compared to MPTP-treated mice. We also found decreased expression of pAkt1 positive cells ($p < 0.01$, **Supplementary Figure S1**) and DAT positive dopaminergic neurons ($p < 0.05$) as compared to control while Mp treatment (MPTP+Mp) significantly increased the expression of pAkt1 ($p < 0.05$) (**Figure 5B**) and DAT ($p < 0.05$) (**Figure 5C**) as compared to MPTP treated groups. A reduced ($p < 0.05$) level of TH positive dopaminergic neurons was seen in response to MPTP injection while comparing to the CONT group. However, following treatment with Mp in MPTP-administered mice, an increase in TH level ($p < 0.05$) (**Figure 5D**) was observed when compared to MPTP-treated mice.

Effect of Mp on the Nuclear Translocation of NF-κB in SNpc

We have observed that in MPTP injected mice, the nuclear translocation of NF-κB has occurred (**Figure 6B**) when compared with the control group (**Figure 6A**). Whereas, Mp treatment

(**Figure 6C**) has significantly inhibited this nuclear translocation of NF-κB as compared to MPTP treated mice.

DISCUSSION

In this study we demonstrate that Mp, an aqueous extract containing L-DOPA and a mixture of rich novel phytochemicals protect nigrostriatal degeneration of dopaminergic neurons by alleviating oxidative stress and neuroinflammation in PD mouse model. Dopaminergic neurons can be protected by neuroinflammation linked inhibition of iNOS, GFAP, ICAM as well as NF-κB activation and its responsive genes TNF-α. Protective effect of Mp on dopaminergic neurons suggest that it is an efficient herbal agent in PD research, corroborating previous studies (Yadav et al., 2013, 2014, 2017; Olson and Gendelman, 2016). From several decades there is a lot of focus on Mp's anti-parkinsonian activity specifically related to its anti-oxidative and metal chelating activity (Tharakan et al., 2007; Dhanasekaran et al., 2008; Yadav et al., 2013). Other than showing the anti-parkinsonian activity, Mp extract has also shown therapeutic potential in protecting against stroke and ischemia (Nayak et al., 2017). Mp extracts thus due to the presence of dopamine and 5-HT (5-hydroxytryptamine) has the potential to be an anti-cataleptic and antiepileptic drug (Champatisingh et al., 2011). *Ginkgo Biloba* extract 761 (EGb 761) is a well-defined mixture containing flavonoids (24%) and terpenoids (6%) and is patented (Rojas et al., 2009). This extract having the antioxidant and anti-apoptotic properties has the potential to show neuroprotection as it can help in the regulation of MAO. Phytomix-40 (PM-40) is a certified parapharmaceutical comprises extract from 40 plants including ginseng, eleutherococcus, *Rhodiola rosea* etc., which helps in improving hormonal, antioxidant and immune system of body. Administration of PM-40 along with standard anti- Parkinson's drugs improves Parkinson's symptoms and helps in decreasing negative activation of immune system which occurs during standard anti-Parkinson's therapy alone (Bocharov et al., 2010). Anti-Parkinson's activities of flavonoids have been also reported on 6-OHDA-induced experimental Parkinsonism *in vivo* and *in vitro* (Mu et al., 2009). Phenolics and flavonoids are important class of natural antioxidant substances having potential of scavenging free radicals, ultimately reducing the risk of oxidative stress related disorders including cancer and PD (Saxena et al., 2012; Patil et al., 2015). Recently, Cilia et al. (2017) have reported that 12.5–17.5 mg/kg Mp seed powder shows neuroprotective activity in PD patient with a more favorable tolerability profile.

The neuroprotective role of Mp in other neurodegenerative diseases such as AD and Multiple Sclerosis has not yet been investigated.

In this paper, we have reported the potential anti-neuroinflammatory activity of Mp in MPTP induced parkinsonian mouse model via NF-κB and Akt pathway.

Natural compounds containing flavonoids, phytochemicals having antioxidative and anti-inflammatory activities are neuroprotective in neurodegenerative diseases (Parkinson's disease, 2012). Past studies potentially exhibiting that orally

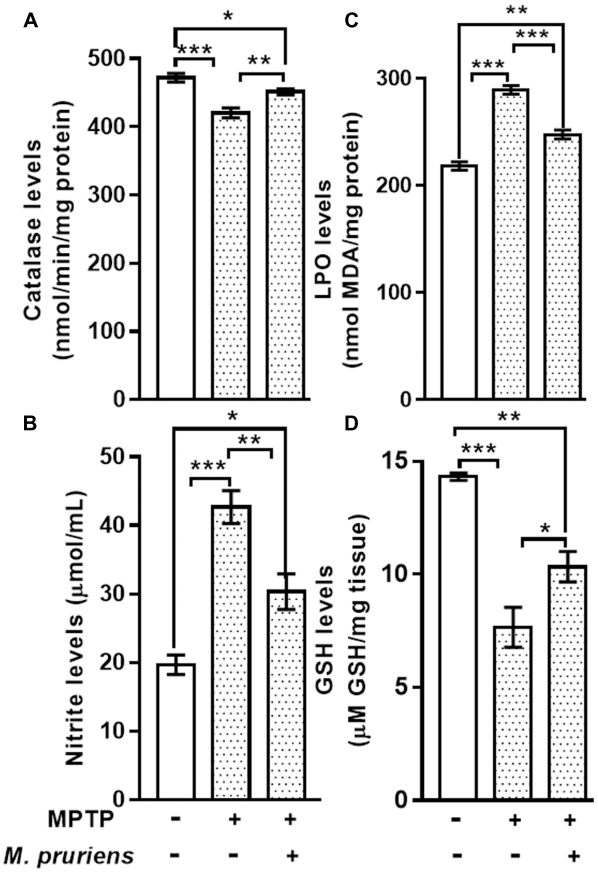

FIGURE 3 | Estimation of CAT, Nitrite, MDA, and GSH in nigrostriatal region of mice. MPTP injected mice showed significant decrease in CAT activity and GSH level and increase in Nitrite and MDA level as compared to control (CONT) group. While Mp treatment in MPTP group significantly increase the level of CAT **(A)**, decrease in the level of nitrite **(B)** and MDA **(C)**, increase in the level of GSH **(D)**. Values are expressed as mean ± SEM (*$p < 0.05$, **$p < 0.01$, ***$p < 0.001$, $n = 3$). ns, non-significant; MDA, malondialdehyde; GSH, glutathione; CAT, catalase; SEM, standard error of mean.

administered Mp reaches to the brain in adequate quantity to protect the dopaminergic neurons in PD (Katzenschlager et al., 2004; Yadav et al., 2013, 2014, 2017). To investigate the supplementary outcome of the drugs, oral route has been utilized as an efficient way of administration as it is the feasible and efficient way for drug delivery.

This study has demonstrated that in mice, MPTP intoxication creates behavioral impairment which is tested by rotarod, grip strength, and narrow beam walking test. Mp was found to significantly improve the motor deficits in parkinsonian mice. Our behavioral findings are in agreement with the earlier reports (Yadav et al., 2013, 2014).

Researchers have suggested that MPTP intoxication generates ROS and RNS which induces oxidative stress and neuroinflammation associated nigrostriatal degeneration of dopaminergic neurons (Yokoyama et al., 2008; Chung et al., 2011; More et al., 2013). Despite of the fact that, PQ poorly crosses the BBB, the patients died of PQ intoxication has been

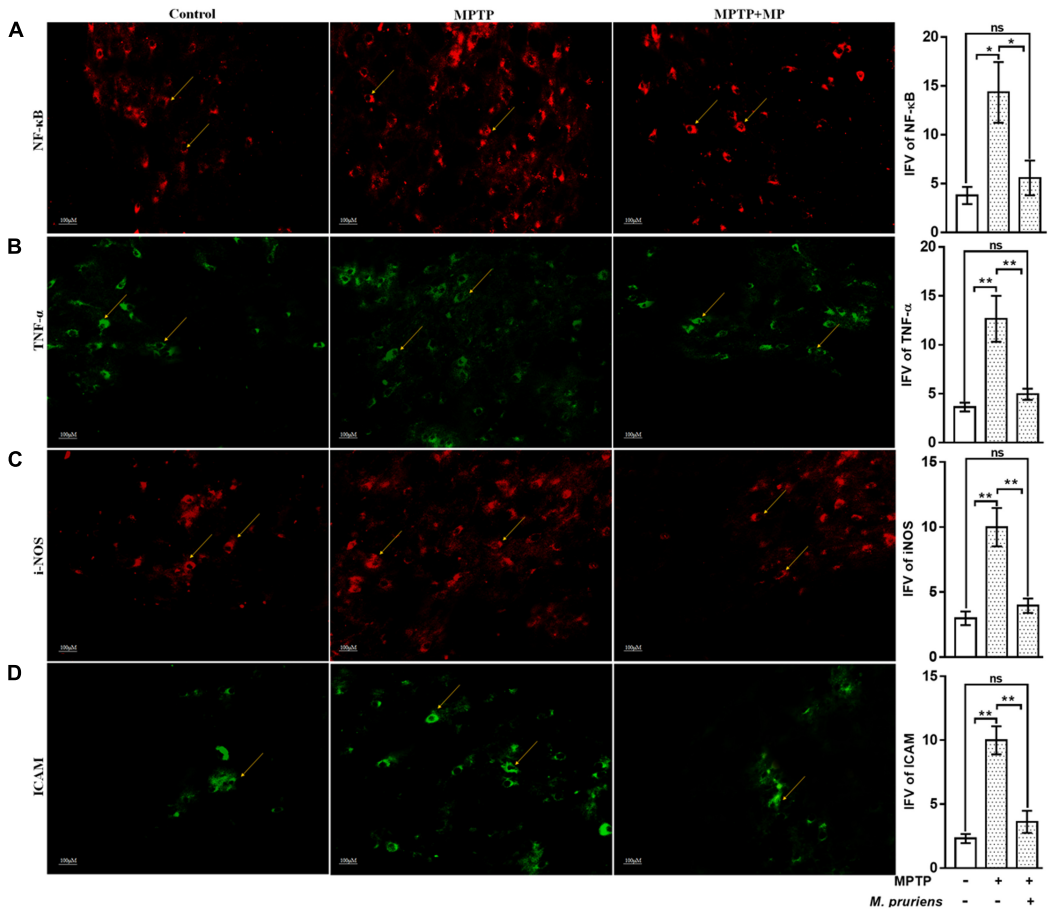

FIGURE 4 | Immunofluorescence expression of NF-κB, TNF-α, iNOS, and ICAM in SNpc. of CONT, MPTP, and MPTP+Mp mice by using Image J Software at 20x magnification. The MPTP intoxicated PD mice showed significantly enhanced expression level of NF-κB **(A)**, TNF-α **(B)**, iNOS **(C)**, and ICAM **(D)** positive cells as compared to control. On Mp supplementation in PD mice showed significantly alleviated expression level of NF-κB, TNF-α, iNOS, and ICAM positive cells as compared to MPTP mice. Values are expressed as mean ± SEM of integrated fluorescent value (IFV) (*$p < 0.05$, **$p < 0.01$, $n = 3$). ns, non-significant; TNF-α, tumor necrosis factor alpha; iNOS, inducible nitric oxide synthase; ICAM, intercellular adhesion molecule 1; SNpc, substantia nigra pars compacta.

detected with significant damage to the brain (Bové et al., 2005). MPTP intoxication has helped in mimicking most of the parkinsonian symptoms which can help us in understanding PD (Meredith and Rademacher, 2011). MPTP induced Parkinsonian Mouse models have been most widely used. MPTP, being lipophilic in nature crosses the BBB easily and binds mainly in astrocyte lysosomes, where it is converted to its toxic metabolite, the 1-methyl-4-phenylpyridinium (MPP^+) ion (Meredith and Rademacher, 2011). However, central dopaminergic neurons were not damaged upon systemic administration of MPP^+ as it is unable to cross the BBB due to its charge. But, much of the DAergic nigrostriatal pathway was destroyed by direct infusion into the brain. MPP^+ is selectively taken by the dopaminergic neurons because it is an excellent substrate for the dopamine transporter (DAT) (Meredith and Rademacher, 2011). So we have used MPTP induced mouse model instead of PQ.

Similarly, this study clearly shows that MPTP intoxication produces neuroinflammation induced ROS and RNS overproduction, whereas Mp reduces this ROS and RNS accumulation and downstream proceedings of this cascade. It is well-established that inflammation is the downstream event of oxidative stress. This might be suggested that Mp uses its antioxidative and anti-inflammatory activities to inhibit these oxidative and inflammatory loads. In PD, dopaminergic neurons possess reduced antioxidant ability which makes dopaminergic neurons more susceptible to oxidative stress, as exhibited by the low level of intracellular reduced glutathione. Reduced GSH is one of the main factors responsible for the antioxidant defense, which scavenges free radicals generated in brain tissue (Dringen, 2000). In this study, MPTP injection produces free radicals which creates oxidative damage and is eventually responsible for reduced GSH level along with decreased activity of antioxidant enzyme catalase, while it has also increased the level of lipid peroxidation. This finding in MPTP treated mice is consistent with earlier reports (Cheng et al., 2008; Khan et al., 2010; Lee et al., 2011; Yadav et al., 2013, 2014). Following MPTP injections, treatment with Mp reduced the oxidative injury by decreasing the MDA level along with restoration of GSH level and catalase

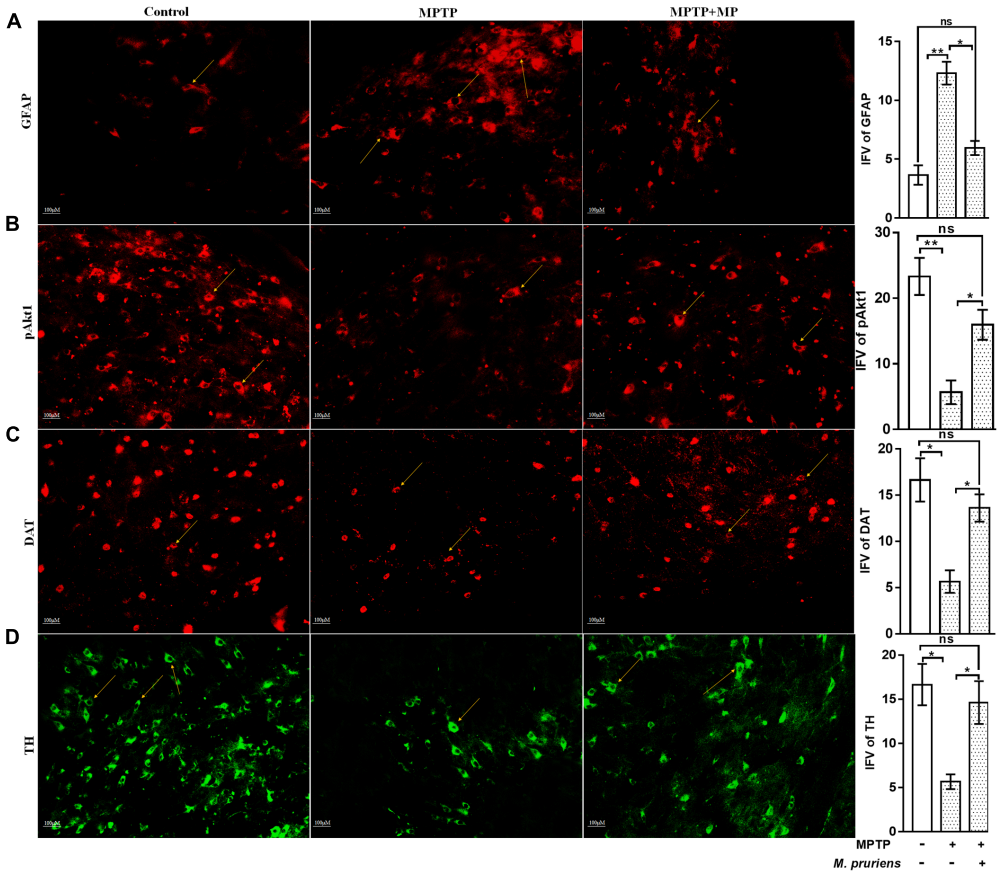

FIGURE 5 | Immunofluorescence expression of GFAP, pAkt1, DAT, and TH in SNpc. of CONT, MPTP, and MPTP+Mp mice by using Image J Software at 20x magnification. The MPTP intoxicated PD mice showed significantly enhanced expression level of GFAP positive cells **(A)** as compared to control, while on Mp supplementation in PD mice showed significantly alleviated expression level of GFAP positive cells as compared to MPTP mice. On the contrary immunofluorescence staining of pAkt1 positive cells were reduced in MPTP treated mice **(B)** while Mp treatment substantially enhanced the expression of pAkt1. Similarly, DAT **(C)** and TH **(D)** positive dopaminergic neurons expression were reduced in MPTP treated mice while Mp treatment in MPTP treated mice significantly enhanced the expression of DAT and TH. Values are expressed as mean ± SEM of IFV (*$p < 0.05$, **$p < 0.01$, $n = 3$). ns, non-significant; GFAP, glial fibrillary acidic protein; DAT, dopamine transporter; TH, tyrosine hydroxylase.

activity in the nigrostriatum. Recent findings have suggested that oxygen free radical and nitric oxide (NO) play a major role in stress mediated neurodegeneration. In addition, peroxynitrite is formed when NO react with superoxide, which then induces nitration of tyrosine to produce hydroxyl radicals. Therefore, NO along with peroxynitrite may adversely affect neuronal cell death in SN (Yokoyama et al., 2008). Our result exhibits that nitrite level was significantly reduced after Mp treatment which further protected the dopaminergic neurons from NO mediated neurodegeneration, corroborating previous studies (Yokoyama et al., 2008; Yadav et al., 2014).

During the pathogenesis of PD, activation of the glial cells is considered to be a rapid cellular response leading to neuroinflammation (Ghosh et al., 2007; Gordon et al., 2012; Hirsch et al., 2012). Upregulation in the expression of iNOS, ICAM GFAP, TNF-α, and NF-κB after MPTP administration signifies the process of glial activation. Different studies have suggested the presence of activated glial cells in SN and striatum of PD brains (Hirsch et al., 2003; Ouchi et al., 2009). Activation of Glial cells results in NF-κB activation which further triggers the upregulation and release of proinflammatory enzymes iNOS, and proinflammatory cytokine TNF-α in PD (Kim and Joh, 2006; Mosley et al., 2006). Studies done previously suggested that inhibition of glial activation by using some inhibitors prevents MPTP-induced neurotoxicity (Wu et al., 2003; Chung et al., 2011). In our study, inflammatory response due to glial cell activation and dopaminergic neuronal loss is suppressed on treatment with Mp. During neuroinflammation, redox sensitive transcription factor, e.g., NF-κB can be initiated by nitric oxide, ROS and RNS. NF-κB shows activity during neurodegeneration by regulating the expression of different proinflammatory mediators. NF-κB is kept in inhibited form, bounded to inhibitory protein IκB, in the cytoplasm to prevent its nuclear translocation necessary for transcriptional activity. NF-κB regulated transcription of certain proinflammatory genes such as TNF-α, IL-1β, COX-2, enzyme like iNOS, and adhesion molecules (ICAM) occurs only when IκB undergoes phosphorylation and proteolytic degradation resulting

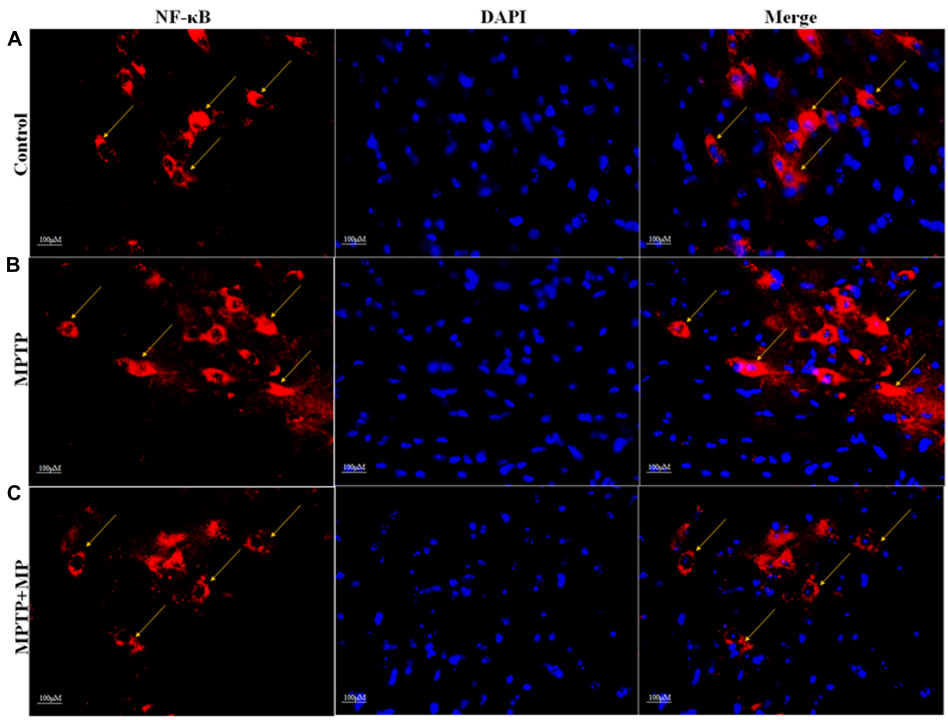

FIGURE 6 | Effect of Mp on the nuclear translocation of NF-κB in SNpc with 40x magnifications after staining. In substantia nigra (SN) as compared to control group **(A)**, nuclear translocation of NF-κB positive cells were increased in MPTP treated group **(B)** while Mp treatment inhibits this nuclear translocation of NF-κB **(C)**.

in translocation of free NF-κB to the nucleus, where it binds to target DNA elements (gene promoters containing κB binding sites) (Shen et al., 2010). Also, MPTP leads to impairment of the mitochondrial function in PD (Acuna-Castroviejo et al., 2011). As the activity of mitochondrial enzyme complex get inhibited, generation of superoxide anions occurs, which further helps in the process of neuroinflammation by up-regulating NF-κB activation. Thus, it can be suggested that drugs, which can be used in inhibiting the generation of ROS, can be used as neuroprotective agents to protect from the neurotoxin such as MPTP. In this study, Mp has significantly inhibited the production of ROS as well as the activation and translocation of NF-κB. Aqueous extract of Mp treatment improved the normal expression levels of iNOS and GFAP in MPTP treated animals (Yadav et al., 2014). Our aqueous extract of Mp also shows the similar activity as it improved the normal expression levels of iNOS, GFAP, ICAM, and TNF-α in SNpc of MPTP treated animals. Thus, antioxidative and anti-inflammatory drugs can be used effectively as therapeutic agents in the case of neurodegenerative diseases (Jin et al., 2005).

Akt activation helps in the survival of different types of cells including various neuronal types, as reported through various *in vitro* studies. Furthermore, Akt promotes the survival of different neurons by mediating the functions of different neurotrophic factors (Dudek et al., 1997; Crowder and Freeman, 1998; Brunet et al., 2001; Orike et al., 2001; Downward, 2004; Duronio, 2008). Death of cultured neurons occurs when interference with activation of Akt occurs, while, transfection with a constitutively active form of the kinase promotes the survival of neurons in the absence of any other support. Although studies about the Akt signaling is less in the case of survival of non-stressed neurons *in vivo*, it has been more studied in post-natal substantia nigra (SN), the brain area of high relevance in the case of PD (Ries et al., 2009). Dopaminergic neurons numbers get reduced in SN and incidence of apoptotic neurons was doubled due to a dominant negative form of Akt delivered by adeno-associated virus. On the other hand, developmental neuron death in the SN was reduced by transduction of a constitutively active form of Akt. The maintenance of the survival of dopaminergic neurons in SN under basal conditions has been highlighted by these significant findings. Phosphorylation of Akt at Ser473 (Malagelada et al., 2008; Timmons et al., 2009) and Thr308 (Malagelada et al., 2008) is considerably decreased in dopaminergic SN neurons of PD patients when compared with non-PD patients as indicated by the Immunostaining of post-mortem brains. A drop in total Akt staining in such neurons from PD patients was also seen (Timmons et al., 2009). Significantly, in the Ries et al. (2009) study cited above, reduction in number of individual TH^+ fibers correlated with decreased density of TH^+ fiber staining in the striatum was seen in the dominant-negative Akt mice model. Our result shows that MPTP inhibits the activation of pAkt1 in the SNpc while Mp treatment overcomes this inhibition, in accordance with the above citation. So, Mp treatment also suggests a possible neuroprotective pathway mediated by pAkt1.

Thus anti-inflammatory pathway especially NF-κB and Akt pathway plays a major role in PD treatment. As MPTP is converted to its active form MPP^+ inside the astroglial cells, then it is taken by dopaminergic neuron through transporter of dopamine, i.e., DAT (Kostic et al., 1996). These transporters get damaged during MPP^+ uptake process as number of DAT get reduced in the SN, after MPTP administration (Jakowec et al., 2004). Accordingly, our data also shows that DAT immunoreactivity was reduced in MPTP group while it is considerably improved in Mp treated group. The rate-limiting enzyme in the production of DA, i.e., TH is the marker for the dopaminergic neuron survival. Previous studies explore that TH immunoreactivity was decreased gradually in SN of mice after MPTP treatment. Their findings give important evidence about MPTP-induced neurodegeneration (Kurosaki et al., 2003; Ghosh et al., 2007). The immunohistochemical expression of TH in SNpc region indicates the protective action of Mp in MPTP injected parkinsonian mice, seen in the previous studies too (Kurosaki et al., 2003; Yadav et al., 2014).

The pathophysiology of different diseases such as gout, muscular pain, cancer, arthritis, and other vascular diseases have been seen to be associated with inflammation. Inflammatory symptoms are being treated by using different drugs and natural products (Ahmad et al., 2005). It has been discussed earlier too, that Mp is rich in different constituents such as saponins, tannins, alkaloids, flavonoids in addition to L-DOPA and has been used in the treatment of diseases like fever, muscular pains, spasms and dysmenorrhea in past (Javed et al., 2010) and is thus being tested for its anti-inflammatory activity and the reason behind its traditional use for pain and fever. The results of our present investigation indicates that seed powder of Mp possess significant anti-inflammatory activity by inhibiting the NF-κB and Akt dependent pathways as highlighted by the results of our study.

It is well-established that Mp contain L-DOPA as the primary component (Tripathi and Updhyay, 2001; Tomita-Yokotani et al., 2004; Kasture et al., 2009). The seed of Mp also contains Serotonin and its precursor 5-Hydroxytryptophan (5-HTP), *N,N*-dimethyltryptamine and 5-MeO-dimethyltryptamine (bufotenin) (Ghosal et al., 1971). Different saponins, anthraquinones, flavonoids, terpenoids, cardiac glycosides, and tannins are present in Mp (Agbafor and Nwachukwu, 2011). Data from RP-HPLC analysis of aqueous extract of Mp used in this study revealed a significant peak of L-DOPA correspond to standard L-DOPA peak, Mp also contain various phytochemicals like gallic acid, proanthocyanidin, tannin, quercetin, and phytic acid. Quercetin being one of the major component in our RP-HPLC result, might be showing anti-inflammatory activity. Querctin has shown both antioxidant and antiinflammatory activity as reported earlier by several studies (Haleagrahara et al., 2011; Weng et al., 2012; Costa et al., 2016; Lee et al., 2016). Moreover, other phytochemicals present in Mp might also act in combination to explore its synergistic effect.

CONCLUSION

Our study suggests that Mp extract appreciably ameliorate the neuroinflammatory processes and also restore biochemical and behavioral parameters along with TH and DAT immunoreactivity. NF-κB and Akt pathway might be responsible for the underlying mechanism of Mp. The anti-inflammatory activity along with potent anti-oxidant properties shown by Mp extract can be used in treating inflammatory condition in the case of PD.

AUTHOR CONTRIBUTIONS

SR, HB, SSS, and WZ: designed and performed the experiments, co-wrote the MS. RP and JJ: performed the HPLC experiments, co-wrote the MS. MG: assisted in the design of the study, statistical analysis, and MS writing. SPS: conceived, designed, directed, and supervised the complete study.

ACKNOWLEDGMENTS

The authors SR, HB, SSS, and WZ were sincerely thankful to ICMR, DBT, ICMR, BHU India for their respective fellowship. They are also thankful to the Head, Department of Biochemistry, I.O.S, B.H.U for providing the basic Departmental Facility and I.S.L.S, B.H.U for their central facility. They would also like to acknowledge Anand Prakash, Cytogenetics Lab, Department of Zoology, B.H.U for helping in fluorescence studies and Ashok Kumar Yadav, Lab attendant for his help in the animal care and other necessary assistance.

SUPPLEMENTARY MATERIAL

The Supplementary Material for this article can be found online at: https://www.frontiersin.org/articles/10.3389/fnagi.2017.00421/full#supplementary-material

FIGURE S1 | Immunofluorescence expression of pAkt1 in SNpc. of CONT, MPTP, and MPTP+Mp mice by using Image J Software at 20x magnification. The MPTP intoxicated PD mice showed significantly decreased expression level of pAkt1 positive cells as compared to control, while on Mp supplementation in PD mice showed significantly elevated expression level of pAkt1 positive cells as compared to MPTP mice. Values are expressed as mean ± SEM of integrated fluorescent value (IFV) (*$p < 0.05$, **$p < 0.01$, $n = 3$).

REFERENCES

Aarsland, D., Creese, B., Politis, M., Chaudhuri, K. R., Ffytche, D. H., Weintraub, D., et al. (2017). Cognitive decline in Parkinson disease. *Nat. Rev. Neurol.* 13, 217–231. doi: 10.1038/nrneurol.2017.27

Acuna-Castroviejo, D., Tapias, V., Lopez, L. C., Doerrier, C., Camacho, E., Carrion, M. D., et al. (2011). Protective effects of synthetic kynurenines on 1-methyl-4-phenyl-1,2,3,6- tetrahydropyridine-induced parkinsonism in mice. *Brain Res. Bull.* 85, 133–140. doi: 10.1016/j.brainresbull.2011.03.008

Adepoju, G. K. A., and Odubena, O. O. (2009). Effect of *Mucuna pruriens* on some haematological and biochemical parameters. *J. Med. Plants Res.* 3, 73–76.

Agbafor, K. N., and Nwachukwu, N. (2011). Phytochemical analysis and antioxidant property of leaf extracts of *Vitex doniana* and *Mucuna pruriens*. *Biochem. Res. Int.* 2011:459839. doi: 10.1155/2011/459839

Ahmad, N., Kumar, V., Raja, S., Mukherjee, K., and Mukherjee, P. K. (2005). Anti-nociceptive and anti-inflammatory activity of *Araucaria bidwillii* hook. *Iranian J. Pharmacol. Therap.* 4, 105–109.

Bhaskar, A., Nithya, V., and Vidhya, V. G. (2011). Phytochemical evaluation by GC-MS and antihyperglycemic activity of *Mucuna pruriens* on streptozotocin induced diabetes in rats. *J. Chem. Pharm. Res.* 3, 689–696.

Bocharov, E. V., Karpova, R. V., Bocharova, O. A., Kucheryanu, V. G., and Shprakh, Z. S. (2010). Effect of phytoadaptogen administration during early ontogeny on lifespan and somatic status of CBA mice with high incidence of tumors. *Bull. Exp. Biol. Med.* 149, 682–684. doi: 10.1007/s10517-017-3904-x

Bové, J., Prou, D., Perier, C., and Przedborski, S. (2005). Toxin-Induced Models of Parkinson's disease. *NeuroRX* 2, 484–494. doi: 10.1602/neurorx.2.3.484

Brotchie, J., and Jenner, P. (2011). New approaches to therapy. *Int. Rev. Neurobiol.* 98, 123–150. doi: 10.1016/B978-0-12-381328-2.00005-5

Brunet, A., Datta, S. R., and Greenberg, M. E. (2001). Transcription-dependent and -independent control of neuronal survival by the PI3K-Akt signaling pathway. *Curr. Opin. Neurobiol.* 11, 297–305. doi: 10.1016/S0959-4388(00)00211-7

Champatisingh, D., Sahu, P. K., Pal, A., and Nanda, G. S. (2011). Anticataleptic and antiepileptic activity of ethanolic extract of leaves of *Mucuna pruriens*: a study on role of dopaminergic system in epilepsy in albino rats. *Indian J. Pharmacol.* 43, 197–199. doi: 10.4103/0253-7613.77368

Chang, C., Yang, M., Wen, H., and Chern, J. (2002). Estimation of total flavonoid content in propolis by two complementary colorimetric methods. *J. Food Drug Anal.* 10, 178–182.

Cheng, Y., He, G., Mu, X., Zhang, T., Li, X., Hu, J., et al. (2008). Neuroprotective effect of baicalein against MPTP neurotoxicity: behavioral, biochemical and immunohistochemical profile. *Neurosci. Lett.* 441, 16–20. doi: 10.1016/j.neulet.2008.05.116

Choi, D. K., Pennathur, S., Perier, C., Tieu, K., Teismann, P., Wu, D. C., et al. (2005). Ablation of the inflammatory enzyme myeloperoxidase mitigates features of Parkinson's disease in mice. *J. Neurosci.* 25, 6594–6600. doi: 10.1523/JNEUROSCI.0970-05.2005

Chung, Y. C., Kim, S. R., Park, J. Y., Chung, E. S., Park, K. W., Won, S. Y., et al. (2011). Fluoxetine prevents MPTP-induced loss of dopaminergic neurons by inhibiting microglial activation. *Neuropharmacology* 60, 963–974. doi: 10.1016/j.neuropharm.2011.01.043

Cilia, R., Laguna, J., Cassani, E., Cereda, E., Pozzi, N. G., Isaias, I. U., et al. (2017). *Mucuna pruriens* in Parkinson disease: a double-blind, randomized, controlled, crossover study. *Neurology* 89, 432–438. doi: 10.1212/WNL.0000000000004175

Costa, L. G., Garrick, J. M., Roquè, P. J., and Pellacani, C. (2016). Mechanisms of neuroprotection by quercetin: counteracting oxidative stress and more. *Oxid. Med. Cell. Longev.* 2016:2986796. doi: 10.1155/2016/2986796

Crowder, R. J., and Freeman, R. S. (1998). Phosphatidylinositol 3-kinase and Akt protein kinase are necessary and sufficient for the survival of nerve growth factor-dependent sympathetic neurons. *J. Neurosci.* 18, 2933–2943.

Dexter, D. T., Holley, A. E., Flitter, W. D., Slater, T. F., Wells, F. R., Daniel, S. E., et al. (1994). Increased levels of lipid hydroperoxides in the parkinsonian substantia nigra: an HPLC and ESR study. *Mov. Disord.* 9, 92–97. doi: 10.1002/mds.870090115

Dhanasekaran, M., Tharakan, B., and Manyam, B. V. (2008). Antiparkinson drug – *Mucuna pruriens* shows antioxidant and metal chelating activity. *Phytother. Res.* 22, 6–11. doi: 10.1002/ptr.2109

Downward, J. (2004). PI 3-kinase, Akt and cell survival. *Semin. Cell Dev. Biol.* 15, 177–182. doi: 10.1016/j.semcdb.2004.01.002

Dringen, R. (2000). Metabolism and functions of glutathione in brain. *Prog. Neurobiol.* 62, 649–671. doi: 10.1016/S0301-0082(99)00060-X

Dudek, H., Datta, S. R., Franke, T. F., Birnbaum, M. J., Yao, R., Cooper, G. M., et al. (1997). Regulation of neuronal survival by the serine-threonine protein kinase Akt. *Science* 275, 661–665. doi: 10.1126/science.275.5300.661

Duke, A. T. (1995). *Handbook of Medicinal Herbs*, 3rd Edn. London: CRS Press, 220.

Duronio, V. (2008). The life of a cell: apoptosis regulation by the PI3K/PKB pathway. *Biochem. J.* 415, 333–344. doi: 10.1042/BJ20081056

Gao, Y., Shang, C., Maroof, S., and Buss, G. R. (2007). A modified colorimetric method for phytic acid analysis in soybean. *Crop. Sci.* 47, 1797–1803. doi: 10.2135/cropsci2007.03.0122

Ghosal, S., Singh, S., and Bhattacharya, S. K. (1971). Alkaloids of *Mucuna pruriens* chemistry and pharmacology. *Planta Med.* 19, 280–284. doi: 10.1055/s-0028-1099642

Ghosh, A., Roy, A., Liu, X., Kordower, J. H., Mufson, E. J., Hartley, D. M., et al. (2007). Selective inhibition of NF-B activation prevents dopaminergic neuronal loss in a mouse model of Parkinson's disease. *Proc. Natl. Acad. Sci. U.S.A.* 104, 18754–18759. doi: 10.1073/pnas.0704908104

Gorbatyuk, O. S., Li, S., Sullivan, L. F., Chen, W., Kondrikova, G., Manfredsson, F. P., et al. (2008). The phosphorylation state of Ser-129 in human alpha-synuclein determines neurodegeneration in a rat model of Parkinson disease. *Proc. Natl. Acad. Sci. U.S.A.* 105, 763–768. doi: 10.1073/pnas.0711053105

Gordon, R., Anantharam, V., Kanthasamy, A. G., and Kanthasamy, A. (2012). Proteolytic activation of proapoptotic kinase protein kinase Cdelta by tumor necrosis factor alpha death receptor signaling in dopaminergic neurons during neuroinflammation. *J. Neuroinflammation* 9:82. doi: 10.1186/1742-2094-9-82

Granger, D. L., Taintor, R. R., Boockvar, K. S., and Hibbs, J. B. (1996). Measurement of nitrate and nitrite in biological samples using nitrate reductase and Greiss reaction. *Methods Enzymol.* 268, 142–151. doi: 10.1016/S0076-6879(96)68016-1

Hald, A., and Lotharius, J. (2005). Oxidative stress and inflammation in Parkinson's disease: is there a causal link? *Exp. Neurol.* 193, 279–290. doi: 10.1016/j.expneurol.2005.01.013

Haleagrahara, N., Siew, C. J., Mitra, N. K., and Kumari, M. (2011). Neuroprotective effect of bioflavonoid quercetin in 6-hydroxydopamine-induced oxidative stress biomarkers in the rat striatum. *Neurosci. Lett.* 500, 139–143. doi: 10.1016/j.neulet.2011.06.021

Hirsch, E. C., Breidert, T., Rousselet, E., Hunot, S., Hartmann, A., and Michel, P. P. (2003). The role of glial reaction and inflammation in Parkinson's disease. *Ann. N. Y. Acad. Sci.* 991, 214–228. doi: 10.1111/j.1749-6632.2003.tb07478.x

Hirsch, E. C., and Hunot, S. (2009). Neuroinflammation in Parkinson's disease: a target for neuroprotection? *Lancet Neurol.* 8, 382–397. doi: 10.1016/S1474-4422(09)70062-6

Hirsch, E. C., Vyas, S., and Hunot, S. (2012). Neuroinflammation in Parkinson's disease. *Parkinsonism Relat. Disord* 18(Suppl. 1), S210–S212. doi: 10.1016/S1353-8020(11)70065-7

Jackson-Lewis, V., Blesa, J., and Przedborski, S. (2012). Animal models of Parkinson's disease. *Parkinsonism Relat. Disord.* 18, S183–S185. doi: 10.1016/S1353-8020(11)70057-8

Jakowec, M. W., Nixon, K., Hogg, E., McNeill, T., and Petzinger, G. M. (2004). Tyrosine hydroxylase and dopamine transporter expression following 1-methyl-4-phenyl-1,2,3,6-tetrahydropyridineinduced neurodegeneration of the mouse nigrostriatal pathway. *J. Neurosci. Res.* 76, 539–550. doi: 10.1002/jnr.20114

Javed, N., Alam, S. S., Subhani, H., Akhtar, M. S., and Khan, A. H. (2010). Evaluation of anti-inflammatory activity of *Mucuna pruriens* Linn. seeds. *Proc. S.Z.P.G.M.I.* 24, 97–102.

Jin, D. Q., Lim, C. S., Hwang, J. K., Ha, I., and Han, J. S. (2005). Anti-oxidant and anti-inflammatory activities of macelignan in murine hippocampal cell line and primary culture of rat microglial cells. *Biochem. Biophys. Res. Commun.* 331, 1264–1269. doi: 10.1016/j.bbrc.2005.04.036

Joglar, B., Rodriguez-Pallares, J., Rodriguez-Perez, A. I., Rey, P., Guerra, M. J., and Labandeira-Garcia, J. L. (2009). The inflammatory response in the MPTP model of Parkinson's disease is mediated by brain angiotensin: relevance to progression of the disease. *J. Neurochem.* 109, 656–669. doi: 10.1111/j.1471-4159.2009.05999.x

Kasture, S., Pontis, S., Pinna, A., Schintu, N., Spina, L., Longoni, R., et al. (2009). Assessment of symptomatic and neuroprotective efficacy of *Mucuna Pruriens* seed extract in rodent model of Parkinson's disease. *Neurotox. Res.* 15, 111–122. doi: 10.1007/s12640-009-9011-7

Katzenschlager, R., Evans, A., Manson, A., Patsalos, P. N., Ratnaraj, N., Watt, H., et al. (2004). *Mucuna pruriens* in Parkinson's disease: a double blind clinical and pharmacological study. *J. Neurol. Neurosurg. Psychiatry* 75, 1672–1677. doi: 10.1136/jnnp.2003.028761

Khan, M. M., Hoda, M. N., Ishrat, T., Ahmad, A., Khan, M. B., Khuwaja, G., et al. (2010). Amelioration of 1-methyl-4-phenyl-1,2,3,6-tetrahydropyridine-induced behavioural dysfunction and oxidative stress by Pycnogenol in mouse model of Parkinson's disease. *Behav. Pharmacol.* 21, 563–571. doi: 10.1097/FBP.0b013e32833d4186

Khan, M. M., Kempuraj, D., Thangavel, R., and Zaheer, A. (2013). Protection of MPTP-induced neuroinflammation and neurodegeneration by pycnogenol. *Neurochem. Int.* 62, 379–388. doi: 10.1016/j.neuint.2013.01.029

Kim, B.-W., Koppula, S., Park, S.-Y., Kim, Y.-S., Park, P.-J., Lim, J. H., et al. (2015). Attenuation of neuroinflammatory responses and behavioral deficits by *Ligusticum officinale* (Makino) Kitag in stimulated microglia and MPTP-induced mouse model of Parkinson's disease. *J. Ethnopharmacol.* 164, 388–397. doi: 10.1016/j.jep.2014.11.004

Kim, Y. S., and Joh, T. H. (2006). Microglia, major player in the brain inflammation: their roles in the pathogenesis of Parkinson's disease. *Exp. Mol. Med.* 38, 333–347. doi: 10.1038/emm.2006.40

Kirk, H., and Sawyer, R. (1998). Frait pearson chemical analysis of food. *Longman Sci. Techn.* 8, 211–212.

Kostic, V., Donovan, D. M., and Yokoyama, R. (1996). Transgenic mice with increased number of dopamine transporters (DAT) show greater sensitivity to MPTP. *Soc. Neurosci. Abstr.* 22:722.

Kumar, A., Ahmad, I., Shukla, S., Singh, B. K., Patel, D. K., Pandey, H. P., et al. (2010). Effect of zinc and PQ co-exposure on neurodegeneration: modulation of oxidative stress and expression of metallothioneins, toxicant responsive and transporter genes in rats. *Free Radical. Res.* 44, 950–965. doi: 10.3109/10715762.2010.492832

Kurosaki, R., Muramatsu, Y., Watanabe, H., Michimata, M., Matsubara, M., Imai, Y., et al. (2003). Role of dopamine transporter against MPTP (1-methyl-4-phenyl-1,2,3,6-tetrahydropyridine) neurotoxicity in mice. *Metab. Brain Dis.* 18, 139–146. doi: 10.1023/A:1023863003093

Lee, D. H., Kim, C. S., and Lee, Y. J. (2011). Astaxanthin protects against MPTP/MPP+-induced mitochondrial dysfunction and ROS production in vivo and in vitro. *Food Chem. Toxicol.* 49, 271–280. doi: 10.1016/j.fct.2010.10.029

Lee, M., McGeer, E. G., and McGeer, P. L. (2016). Quercetin, not caffeine, is a major neuroprotective component in coffee. *Neurobiol. Aging* 46, 113–123. doi: 10.1016/j.neurobiolaging.2016.06.015

Malagelada, C., Jin, Z. H., and Greene, L. A. (2008). RTP801 is induced in Parkinson's disease and mediates neuron death by inhibiting Akt phosphorylation/activation. *J. Neurosci.* 28, 14363–14371. doi: 10.1523/JNEUROSCI.3928-08.2008

Manna, S., Bhattacharyya, D., Mandal, T. K., and Dey, S. (2006). Neuropharmacological effects of deltamethrin in rats. *J. Vet. Sci.* 7, 133–136. doi: 10.4142/jvs.2006.7.2.133

Meredith, G. E., and Rademacher, D. J. (2011). MPTP mouse models of Parkinson's disease: an update. *J. Parkinsons Dis.* 1, 19–33.

Mohanasundari, M., Srinivasan, M. S., Sethupathy, S., and Sabesan, M. (2006). Enhanced neuroprotective effect by combination of bromocriptine and hypericum perforatum extract against MPTP-induced neurotoxicity in mice. *J. Neurol. Sci.* 249, 140–144. doi: 10.1016/j.jns.2006.06.018

More, S. V., Kumar, H., Kim, I. S., Song, S. Y., and Choi, D.-K. (2013). Cellular and molecular mediators of neuroinflammation in the pathogenesis of Parkinson's disease. *Med. Inflamm.* 2013:952375. doi: 10.1155/2013/952375

Moron, M. S., Depierre, J. W., and Mannervik, B. (1979). Levels of glutathione, glutathione reductase and glutathione S-transferaseactivities inrat lungand liver. *Biochim.Biophys. Acta* 582, 67–78. doi: 10.1016/0304-4165(79)90289-7

Mosley, R. L., Benner, E. J., Kadiu, I., Thomas, M., Boska, M. D., Hasan, K., et al. (2006). Neuroinflammation, oxidative stress and the pathogenesis of Parkinson's disease. *Clin. Neurosci. Res.* 6, 261–281. doi: 10.1016/j.cnr.2006.09.006

Mu, X., He, G., Cheng, Y., Li, X., Xu, B., and Du, G. (2009). Baicalein exerts neuroprotective effects in 6-hydroxydopamine-induced experimental Parkinsonism in vivo and in vitro. *Pharmacol. Biochem. Behav.* 92, 642–648. doi: 10.1016/j.pbb.2009.03.008

Nayak, V. S., Kumar, N., D'Souza, A. S., Nayak, S. S., Cheruku, S. P., and Pai, K. S. R. (2017). The effects of *Mucuna pruriens* extract on histopathological and biochemical features in the rat model of ischemia. *Neuroreport* 28, 1195–1201. doi: 10.1097/WNR.0000000000000888

Ohkawa, H., Ohishi, N., and Yagi, K. (1979). Assay for lipid peroxides in animal tissues by thiobarbituric acid reaction. *Anal. Biochem.* 95, 351–358. doi: 10.1016/0003-2697(79)90738-3

Olson, K. E., and Gendelman, H. E. (2016). Immunomodulation as a neuroprotective and therapeutic strategy for Parkinson's disease. *Curr. Opin. Pharmacol.* 26, 87–95. doi: 10.1016/j.coph.2015.10.006

Orike, N., Middleton, G., Borthwick, E., Buchman, V., Cowen, T., and Davies, A. M. (2001). Role of PI 3-kinase, Akt and Bcl-2-related proteins in sustaining the survival of neurotrophic factor-independent adult sympathetic neurons. *J. Cell. Biol.* 154, 995–1005. doi: 10.1083/jcb.200101068

Ouchi, Y., Yagi, S., Yokokura, M., and Sakamoto, M. (2009). Neuroinflammation in the living brain of Parkinson's disease. *Parkinsonism Relat. Disord.* 15, S200–S204. doi: 10.1016/S1353-8020(09)70814-4

Parkinson's disease (2012). Could dietary flavonoids be protective against Parkinson disease? *Nat. Rev. Neurol.* 8:298. doi: 10.1038/nrneurol.2012.88

Patil, R. R., Gholave, A. R., Jadhav, J. P., Yadav, S. R., and Bapat, V. A. (2015). *Mucuna sanjappae* Aitawade et Yadav: a new species of *Mucuna* with promising yield of anti-Parkinson's drug L-DOPA. *Genet. Resour. Crop Evol.* 62, 155–162. doi: 10.1007/s10722-014-0164-8

Pisa, M. (1998). Regional specialization of motor functions in the rat striatum: implications for the treatment of Parkinsonism. *Prog. Neuropsychopharmacol. Biol. Psychiatry* 12, 217–224.

Rai, S. N., Yadav, S. K., Singh, D., and Singh, S. P. (2016). Ursolic acid attenuates oxidative stress in nigrostriatal tissue and improves neurobehavioral activity in MPTP- induced Parkinsonian mouse model. *J. Chem. Neuroanat.* 71, 41–49. doi: 10.1016/j.jchemneu.2015.12.002

Rathod, B. G., and Patel, N. M. (2014). Development of validated RP-HPLC method for the estimation of L-Dopa from *Mucuna pruriens*, its extracts and in Aphrodisiac formulation. *Int. J. Pharma Sci. Res.* 5, 508–513.

Ries, V., Cheng, H. C., Baohan, A., Kareva, T., Oo, T. F., Rzhetskaya, M., et al. (2009). Regulation of the postnatal development of dopamine neurons of the substantia nigra in vivo by Akt/protein kinase B. *J. Neurochem.* 110, 23–33. doi: 10.1111/j.1471-4159.2009.06101.x

Rojas, P., Montes, S., Serrano-García, N., and Rojas-Castañeda, J. (2009). Effect of EGb761 supplementation on the content of copper in mouse brain in an animal model of Parkinson's disease. *Nutrition* 25, 482–485. doi: 10.1016/j.nut.2008.10.013

Sathiyanarayanan, L., and Arulmozhi, S. (2007). *Mucuna pruriens* Linn—a comprehensive review. *Pharmacogn. Rev.* 1, 157–162.

Saxena, M., Saxena, J., and Pradhan, A. (2012). Flavonoids and phenolic acids as antioxidants in plants and human health. *Int. J. Pharm. Sci. Rev. Res.* 16, 130–134.

Shen, H., Hu, X., Liu, C., Wang, S., Zhang, W., Gao, H., et al. (2010). Ethyl pyruvate protects against hypoxic-ischemic brain injury via anti-cell death and anti-inflammatory mechanisms. *Neurobiol. Dis.* 37, 711–722. doi: 10.1016/j.nbd.2009.12.010

Siderowf, A., and Stern, M. (2003). Update on Parkinson disease. *Ann. Intern. Med.* 138, 651–658. doi: 10.7326/0003-4819-138-8-200304150-00013

Singleton, V. L., and Rossi, J. A. (1965). Colorimetry of total phenolics with phosphomolybdic-phosphotungstic acid reagents. *Am. J. Enol. Vitic.* 16, 144–158.

Sun, B., Ricardo-da-Silva, J. M., and Spranger, I. (1998). Critical factors of vanillin assay for catechins and proanthocyanidins. *J. Agric. Food Chem.* 46, 4267–4274. doi: 10.1021/jf980366j

Tharakan, B., Dhanasekaran, M., Mize-Berge, J., and Manyam, B. V. (2007). Anti-Parkinson botanical *Mucuna pruriens* prevents levodopa induced plasmid and genomic DNA damage. *Phytother. Res.* 21, 1124–1126. doi: 10.1002/ptr.2219

Timmons, S., Coakley, M. F., Moloney, A. M., and O' Neill, C. (2009). Akt signal transduction dysfunction in Parkinson's disease. *Neurosci. Lett.* 467, 30–35. doi: 10.1016/j.neulet.2009.09.055

Tomita-Yokotani, K., Hashimoto, H., Fujii, Y., Nakamura, T., and Yamashita, M. (2004). Distribution of L-DOPA in the root of velvet bean plant (*Mucuna pruriens* L.) and gravity. *Biol. Sci. Space* 18, 165–166.

Tripathi, Y. B., and Updhyay, A. K. (2001). Antioxidant property of *Mucuna pruriens*. *Linn. Curr. Sci.* 80, 1377–1378.

Uchegbu, R. I., Ahuchaogu, A. A., Mbadiugha, C. N., Amanze, K. O., Igara, C. E., Iwu, I. C., et al. (2016). Antioxidant, anti-inflammatory and antibacterial

activities of the seeds of *Mucuna pruriens* (UTILIS). *Am. Chem. Sci. J.* 13, 1–8. doi: 10.9734/ACSJ/2016/24043

Uhegbu, A. F. O., Elekwa, I., and Ukoha, C. (2005). Comparative efficacy of crude aqueous extract of *Mangifera indica*, *Carica papaya* and sulfadoxine pyrimethamine on the mice infested with malaria parasite in vivo. *Global J. Pure Appl. Sci.* 11, 399–401.

Weng, Z., Zhang, B., Asadi, S., Sismanopoulos, N., Butcher, A., Fu, X., et al. (2012). Quercetin is more effective than cromolyn in blocking human mast cell cytokine release and inhibits contact dermatitis and photosensitivity in humans. *PLOS ONE* 7:e33805. doi: 10.1371/journal.pone.0033805

Wu, D. C., Teismann, P., Tieu, K., Vila, M., Jackson-Lewis, V., Ischiropoulos, H., et al. (2003). NADPH oxidase mediates oxidative stress in the 1-methyl-4-phenyl-1,2,3,6-tetrahydropyridine model of Parkinson's disease. *Proc. Natl. Acad. Sci. U.S.A.* 100, 6145–6150. doi: 10.1073/pnas.0937239100

Yadav, S. K., Prakash, J., Chouhan, S., and Singh, S. P. (2013). *Mucuna pruriens* seed extract reduces oxidative stress in nigrostriatal tissue and improves neurobehavioral activity in paraquat-induced Parkinsonian mouse model. *Neurochem. Int.* 62, 1039–1047. doi: 10.1016/j.neuint.2013.03.015

Yadav, S. K., Prakash, J., Chouhan, S., Westfall, S., Verma, M., Singh, T. D., et al. (2014). Comparison of the neuroprotective potential of *Mucuna pruriens* seed extract with estrogen in 1 methyl-4-phenyl-1,2,3,6-tetrahydropyridine (MPTP)-induced PD mice model. *Neurochem. Int.* 65, 1–13. doi: 10.1016/j.neuint.2013.12.001

Yadav, S. K., Rai, S. N., and Singh, S. P. (2016). *Mucuna pruriens* shows neuroprotective effect by inhibiting apoptotic pathways of dopaminergic neurons in the paraquat mouse model of parkinsonism. *Eur. J. Pharmaceut. Med. Res.* 3, 441–451.

Yadav, S. K., Rai, S. N., and Singh, S. P. (2017). Mp reduces inducible nitric oxide synthase expression in Parkinsonian mice model. *J. Chem. Neuroanat.* 80, 1–10. doi: 10.1016/j.jchemneu.2016.11.009

Yokoyama, H., Kuroiwa, H., Yano, R., and Araki, T. (2008). Targeting reactive oxygen species, reactive nitrogen species and inflammation in MPTP neurotoxicity and Parkinson's disease. *Neurol. Sci.* 29, 293–301. doi: 10.1007/s10072-008-0986-2

Conflict of Interest Statement: The authors declare that the research was conducted in the absence of any commercial or financial relationships that could be construed as a potential conflict of interest.

frontiers in Aging Neuroscience

ORIGINAL RESEARCH
published: 05 June 2018
doi: 10.3389/fnagi.2018.00169

Naringin Dihydrochalcone Ameliorates Cognitive Deficits and Neuropathology in APP/PS1 Transgenic Mice

Wenjuan Yang[1†], Keyan Zhou[1,2†], Yue Zhou[1†], Yuqian An[1], Tingting Hu[1], Jing Lu[1], Shichao Huang[3] and Gang Pei[1,4*]*

[1]State Key Laboratory of Cell Biology, CAS Center for Excellence in Molecular Cell Science, Shanghai Institute of Biochemistry and Cell Biology, Chinese Academy of Sciences, University of Chinese Academy of Sciences, Shanghai, China, [2]School of Life Science and Technology, ShanghaiTech University, Shanghai, China, [3]Shanghai Key Laboratory of Signaling and Disease Research, Laboratory of Receptor-based Bio-medicine, School of Life Sciences and Technology, Tongji University, Shanghai, China, [4]School of Life Science and Technology, The Collaborative Innovation Center for Brain Science, Tongji University, Shanghai, China

Alzheimer's disease (AD) is a multi-factorial neurodegenerative disorder with abnormal accumulation of amyloid-β (Aβ) plaques, neuroinflammation and impaired neurogenesis. Mounting evidences suggest that single-target drugs have limited effects on clinical treatment and alternative or multiple targets are required. In recent decades, natural compounds and their derivatives have gained increasing attention in AD drug discovery due to their inherently enormous chemical and structural diversity. In this study, we demonstrated that naringin dihydrochalcone (NDC), a widely used dietary sweetener with strong antioxidant activity, improved the cognitive function of transgenic AD mice. Pathologically, NDC attenuated Aβ deposition in AD mouse brain. Furthermore, NDC reduced periplaque activated microglia and astrocytes, indicating the inhibition of neuroinflammation. It also enhanced neurogenesis as investigated by BrdU/NeuN double labeling. Additionally, the inhibition of Aβ level and neuroinflammation by NDC treatment was also observed in an AD cell model or a microglia cell line. Taken together, our study indicated that NDC might be a potential therapeutic agent for the treatment of AD against multiple targets that include Aβ pathology, neuroinflammation and neurogenesis.

Keywords: naringin dihydrochalcone, Alzheimer's disease, amyloid-β, neuroinflammation, neurogenesis

OPEN ACCESS

Edited by:
Ashok Kumar,
University of Florida, United States

Reviewed by:
Fan Liao,
AbbVie Foundational Neuroscience Center, United States
Zhifang Dong,
Chongqing Medical University, China

***Correspondence:**
Shichao Huang
huangshichao@sibcb.ac.cn
Gang Pei
gpei@sibs.ac.cn

†Co-first authors.

Received: *23 March 2018*
Accepted: *18 May 2018*
Published: *05 June 2018*

Citation:
Yang W, Zhou K, Zhou Y, An Y, Hu T, Lu J, Huang S and Pei G (2018) Naringin Dihydrochalcone Ameliorates Cognitive Deficits and Neuropathology in APP/PS1 Transgenic Mice. Front. Aging Neurosci. 10:169. doi: 10.3389/fnagi.2018.00169

INTRODUCTION

Alzheimer's disease (AD) is the most common type of dementia and has no effective cure so far. Multiple factors are involved in the pathogenesis of AD: (1) the accumulation of amyloid-β (Aβ) and excessive Aβ (especially $A\beta_{42}$) aggregation into plaques are considered the trigger of pathological events for AD (Holtzman et al., 2011); (2) neurofibrillary tangles composed of hyperphosphorylated tau protein contribute to neuronal dysfunction and involve in the progression of AD (Holtzman et al., 2011); (3) neuroinflammation is mediated by microglia and astrocytes and in response to brain damage (e.g., Aβ accumulation, neurofibrillary tangles), proinflammatory cytokines and mediators are produced, leading to chronic inflammation and neurodegeneration.

(Bronzuoli et al., 2016); and (4) neurogenesis is reduced dramatically in AD, which can contribute to cognition impairment (Donovan et al., 2006; Drapeau and Nora Abrous, 2008). Multi-target compounds are proposed to tackle these factors and have attracted wide attention in recent years. For instance, curcumin and its derivatives which are suggested to have therapeutic potential for AD by inhibiting Aβ production and tau phosphorylation (Yang et al., 2005; Necula et al., 2007; Ma et al., 2009), stimulating embryonic neural stem cell proliferation via the MAP kinase pathways, and enhancing adult hippocampal neurogenesis (Kim et al., 2008). They are also reported to suppress inflammation process by reducing nuclear factor kappa-light-chain-enhancer of activated B cells (NF-κB)-mediated expression of proinflammatory cytokines (Jobin et al., 1999). These studies suggested that multi-target compounds might be promising drug candidates for AD.

Natural compounds and their derivatives have gained increasing attention due to their inherently enormous chemical diversity and many of them have turned into drug candidates (Lahlou, 2013; Guzior et al., 2015). Naringin is a major flavanone glycoside from Pomelo peel, and it has been experimentally demonstrated to improve long-term memory in the transgenic AD mouse model (Wang et al., 2013), it is interesting that whether its derivatives or other similar compounds may also have comparable or even better therapeutic effects on AD. Naringin dihydrochalcone (NDC) is a widely used natural compound derivative in food, medicine, and cosmetic industry as an artificial sweetener with antioxidant activity (Nakamura et al., 2003; Surana et al., 2006; Gaudette and Pickering, 2013). Large amount of evidence suggests that oxidative stress (OS) is involved in the development of AD (Feng and Wang, 2012), indicating NDC may have beneficial effects on the treatment of aging and neurodegenerative diseases. In our study, we investigated the effects of NDC on cognitive impairment and neuropathology in an AD mouse model. And the results suggest that oral administration of NDC ameliorated cognitive deficits, alleviated amyloid plaque burden and Aβ levels, suppressed neuroinflammation, and enhanced neurogenesis. Thus, NDC may be a promising multi-target drug candidate for the treatment of AD.

MATERIALS AND METHODS

Ethics Statement

All animal experiments in this study were performed properly according to the Guide for the Care and Use of Laboratory Animals from National Institutes of Health. The protocols for animals were approved by the Research Ethics Committee, Shanghai Institutes for biological Sciences, Chinese Academy of Sciences. Animal pain and discomfort were minimized with enough food and water and other efforts.

Animals and Drug Treatment

The APPswe/PS1ΔE9 (APP/PS1) transgenic mice (JAX Stock No. 004462) expressing mouse/human amyloid precursor protein (Mo/HuAPP695swe) and human Presenilin1 (PS1ΔE9) were used in our investigation and mice were maintained and genotyped according to the guidelines of Jackson Laboratory. The wild type (WT) littermates were used as age- and gender-matched controls. NDC (with a purity 95%–99%; Biopurify Phytochemicals Ltd., Chengdu, China[1]) was dissolved in vehicle (H_2O). WT and APP/PS1 mice chronically administered 200 μl of NDC (100 mg/kg) or vehicle per 20 g mouse body weight body weight by oral administration once a day from 3–4 to 6–7 months of age (n = 10–12 mice per group).

TABLE 1 | Primers used for qPCR.

Gene	Direction	Sequence
Il-1β	F	GTTGACGGACCCCAAAAGAT
	R	AAGGTCCACGGGAAAGACAC
Il-6	F	TAGTCCTTCCTACCCCAATTTCC
	R	TTGGTCCTTAGCCACTCCTTC
TGF-β	F	CACTGATACGCCTGAGTG
	R	GTGAGCGCTGAATCGAAA
TNF-α	F	ACCCTCACACTCAGATCATCTTC
	R	TGGTGGTTTGCTACGACGT

For assessment the effect of NDC on neurogenesis, these mice were intraperitoneally injected with 5-bromo-2-deoxyuridine (BrdU, Sigma, 50 mg/kg/d) once a day, from days 73 to 79 during drug administration, as described by Encinas et al. (2011).

Morris Water Maze

The Morris Water Maze (MWM) were carried out as previously described (Morris, 1984; Teng et al., 2010). The apparatus was a 120-cm-diameter circular water pool containing small white plastic particles, with four different cues located on the four directions of pool wall. At a fixed position in the target quadrant, 11-cm- diameter transparent platform was placed 1 cm below the water surface. During the whole experiment, the water temperature was maintained at 21.0 ± 0.5° and the room temperature was 23.0 ± 0.5°. The training consisted of four trials 1 day for six consecutive days. To assess spatial memory, on day 7, we performed a probe trial. During the probe trial, the platform was removed away from the target quadrant of water pool and mice were allowed to explore for 1 min freely. All tracks from all trials were monitored using an automated tracking system (Ethovision XT software) for the animal performance analysis.

Novel Object Recognition

The Novel Object Recognition test (NOR) is also widely used to evaluate recognition memory in mice. The detailed protocol with modifications is as previously described (Bevins and Besheer, 2006; Liu et al., 2013; Hou et al., 2014). The procedure included two phases: training phase and testing phase. On the first day, mice were placed in an evenly illuminated sound proof box with a Plexiglas box (25 cm × 25 cm × 25 cm). In the presence of two equal objects, each mouse was allowed to explore for 10 min freely. On the second day, one of the equal objects was replaced by a novel, unfamiliar object. Animals were placed back in the arena to freely explore for

[1]http://www.biopurify.com

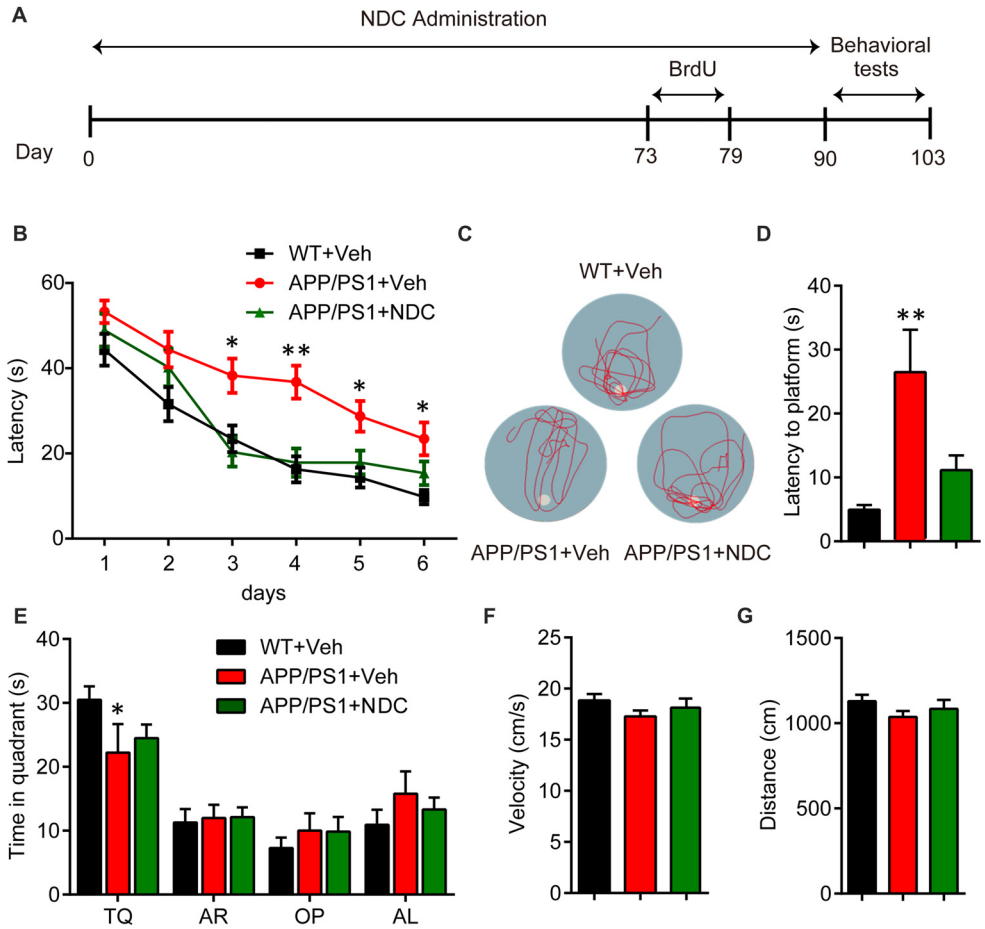

FIGURE 1 | Naringin dihydrochalcone (NDC) ameliorates learning and memory deficits in APP/PS1 mice. **(A)** Experimental procedure for Morris water maze (MWM) analysis. **(B)** MWM test of wild type (WT) mice and vehicle- or NDC-treated APP/PS1 mice. **(C)** Representative track images of each group mice in day 7 probe trial test. **(D)** Latency to platform of each group mice in day 7 probe trial test. **(E)** Time spent of each group mice in the target quadrant in day 7 probe trial test. TQ, target quadrant; AR, adjacent right; OP, opposite; AL, adjacent left. **(F)** Swimming velocity of each group mice in probe trial. **(G)** Swimming distance of each group mice in probe trial. Data are presented as mean ± SEM, WT group $n = 8$, Veh group $n = 7$, NDC group $n = 7$, $^{*}p < 0.05$, $^{**}p < 0.01$, analyzed by two-way ANOVA **(B,E)** or one-way ANOVA **(D,F,G)** followed by Bonferroni test.

10 min. During the whole trial, to eliminate olfactory cues, the arena and objects were cleaned thoroughly with 10% ethanol. Object exploration time was the time of a mouse was sniffing, directing and pawing the object. The time was recorded in a double-blinded manner. In the training phase, location preference means the time of a mouse exploring one object relative to the time of exploring two objects, and in the testing phase, recognition index means the time of a mouse exploring the novel object relative to the time of exploring two objects.

ELISA for Human Aβ and Western Blot Analysis

$A\beta_{40}$ and $A\beta_{42}$ in APP/PS1 mouse hippocampus and cortex were extracted as previously reported (Lazarov et al., 2005), for ELISA measurement of human $A\beta_{40}$ and $A\beta_{42}$, the frozen hippocampal and cortical tissue (400 mg) stored in −80°C were homogenized in 1 ml 2% SDS (dissolved in PBS), then centrifuged at 1,20,000 *g* for 60 min at room temperature. The supernatant was collected as the soluble fraction and quantified with human Aβ ELISA kits according to the users' guidelines (ExCell Bio). Total Aβ levels in HEK293/APPswe cell culture medium were also quantified with ELISA.

Supernatant is also used for Western blot analyses. Proteins in supernatant were separated by SDS-PAGE, and transferred onto membrane. Proteins were labeled with β-actin (AB0035, Abways) and IL-1β rabbit polyclonal antibody (16806-1-AP, Proteintech) and the immunoreactive bands were detected by chemiluminescent detection (Bio-Rad) of peroxidase-conjugated antibody (M21002, Abmart). The intensity of each band was quantified by ImageJ and normalized to β-actin.

Immunohistochemistry and Image Analysis

After behavioral tests, the mice were anesthetized with chloral hydrate and transcardially perfused with phosphate-buffered

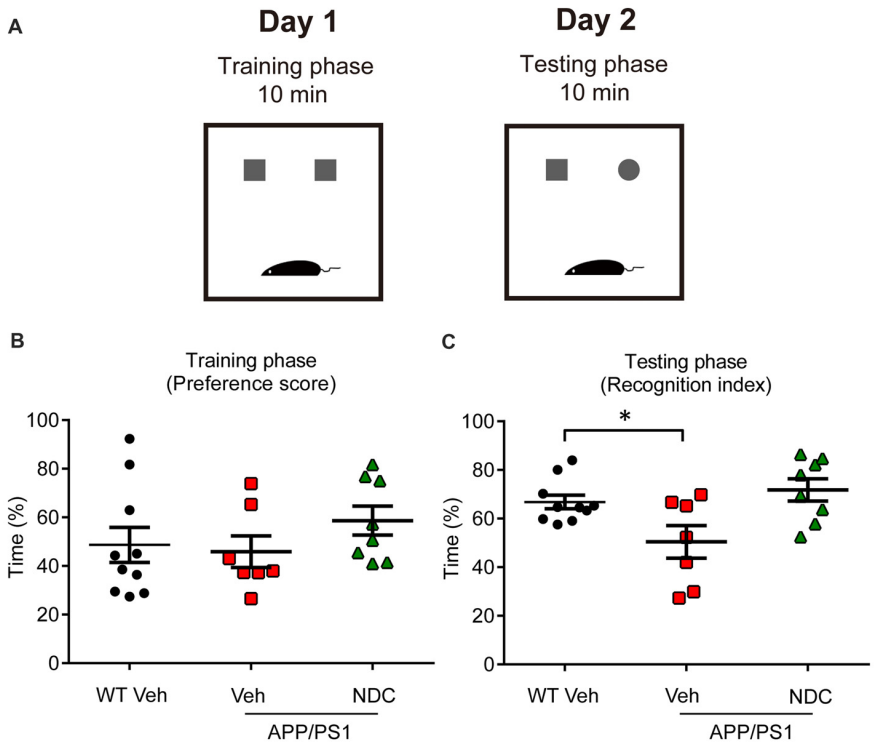

FIGURE 2 | NDC improves memory retention in APP/PS1 mice. **(A)** Diagram of Novel object recognition (NOR) analysis. **(B,C)** Preference scores of training phase **(B)** and Recognition Index of testing phase **(C)** during a 10-min testing phase are shown, respectively. Data are presented as mean ± SEM, WT group $n = 10$, Veh group $n = 7$, NDC group $n = 8$. $^*p < 0.05$, analyzed by one-way ANOVA followed by Bonferroni test.

saline (PBS) buffer and then with 4% paraformaldehyde (PFA) in PBS. The half brain tissue were serially sectioned at 30 μm thickness and stained using Thioflavin S (ThioS; Sigma) and anti-Aβ antibody 6E10 (Covance, SIG-39300) for amyloid plaques, a polyclonal rabbit antibody against GFAP (DAKO) for astrocytes, a mouse antibody against Iba1(WAKO) for microglia and anti-NeuN antibody for neurons.

According to previous studies (Galea et al., 2015; Krauthausen et al., 2015), GFAP-positive astrocytes within an 80 μm radius surrounding Aβ plaques were quantified in hippocampus and cortex. The proportion of GFAP-positive areas in cortex means the GFAP-positive areas in cortex relative to total areas of cortex, and the same in hippocampus.

All images of brain slices were captured using a confocal laser scanning microscope (Leica TCS SP8). Each section was captured by confocal microscopy in z stack, covered all layers of cells and all positive-staining cells were counted. For counting the $NeuN^+BrdU^+$ double-stained cells, the co-localization of different channels in each cell was carefully confirmed. Quantification was performed using ImageJ software and the percentage of antibody-positive area was calculated. Five to six sections were analyzed per mouse and all assessments were analyzed in a blinded manner.

Cell Culture and Treatment

HEK293 cells were purchased from ATCC. HEK293/APPswe cells were transfected, selected and maintained in our lab. BV2 cell lines were cultured and maintained in Dulbecco's Minimal Essential Medium (DMEM), with 10% fetal bovine serum and 100 U/ml penicillin and 0.1 mg/ml streptomycin. HEK293/APPswe cells were cultured in MEM under the same condition. BV2 cells were treated with 0.3 μg/ml lipopolysaccharides (LPS; 055:B5, Sigma) and various concentrations of NDC for 6 h. HEK293/APPswe cells were treated with various concentrations of NDC for 24 h.

Quantitative Real-Time PCR

The analysis of mRNA expression was performed as previously reported (Cai et al., 2017), 3e4 BV2 cells per well were seeded into 96-well plates. After NDC treatment, total RNA was extract according to the instructions of TRI Reagent® (Sigma) and used NanoDrop 1000 Spectrophotometer (Thermo Scientific) to assess the RNA purity and integrity. TIANScript M-MLV kit (TIANGEN) was used to synthesis cDNA according to protocols, and rRNasin® (Recombinant rRNasin® Ribonuclease Inhibitor, Promega) was used in the synthesis. The expression level of mRNA was measured by quantitative Real-time PCR (qPCR) using the 2× HotStart SYBR Green qRT-PCR Master Mix kit from ExCell. The reaction parameters were: 95°C for 10 min; 95°C for 30 s, 40 cycles; 60°C for 30 s; 72°C for 30 s. An additional cycle was performed for evaluation of primer's dissociation curve: 95°C for 1 min, 60°C for 30 s and 95°C for 30 s. Each cDNA sample was amplified in duplicates. Primer sequences are listed in **Table 1**.

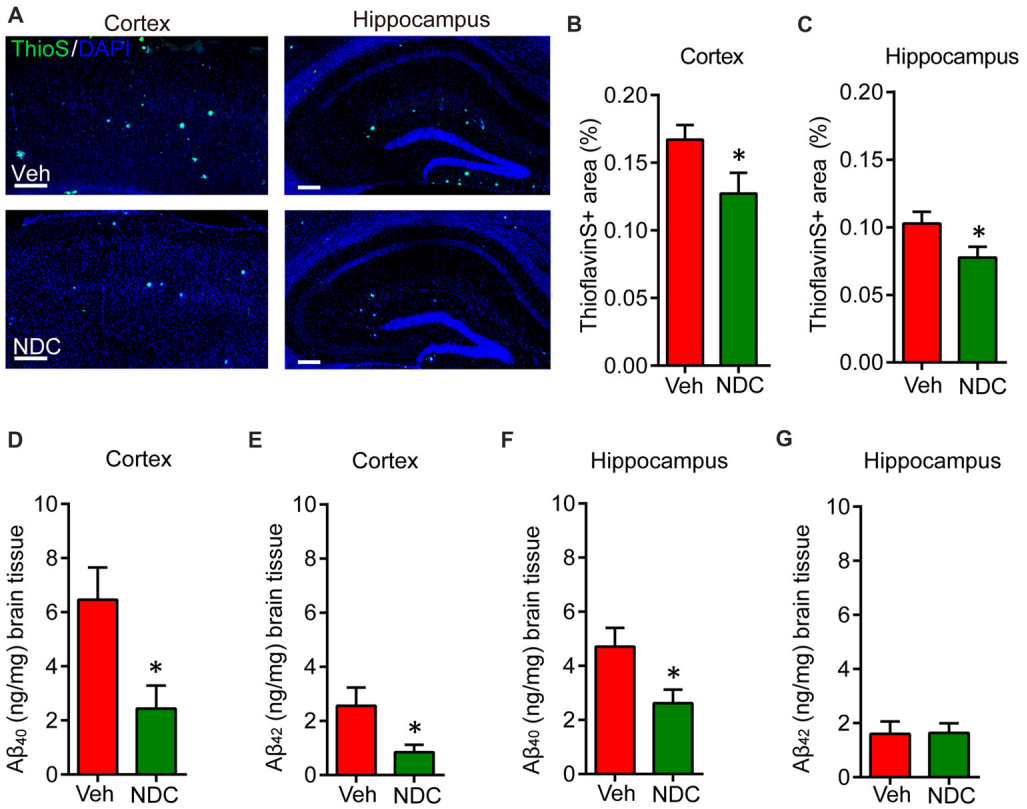

FIGURE 3 | NDC alleviates amyloid plaque burden and Aβ levels in APP/PS1 mice. **(A)** Representative half brain sections of vehicle- or NDC-treated APP/PS1 mice brain stained with ThioS and DAPI in cortex and hippocampus are shown. Scale bar = 200 μm. **(B,C)** Quantitative analysis of the of ThioS-positive amyloid plaques covered area in cortex **(B)** and hippocampus **(C)**. **(D,E)** ELISA of soluble $A\beta_{40}$ and $A\beta_{42}$ levels in cortical tissues of APP/PS1 mice. **(F,G)** ELISA of soluble $A\beta_{40}$ and $A\beta_{42}$ levels in hippocampal tissues of APP/PS1 mice. Data are presented as mean ± SEM. ThioS: Veh group $n = 5$, NDC group $n = 5$; ELISA: Veh group $n = 6$, NDC group $n = 6$. $^*p < 0.05$, analyzed by two-tailed t test compared with APP/PS1 vehicle group.

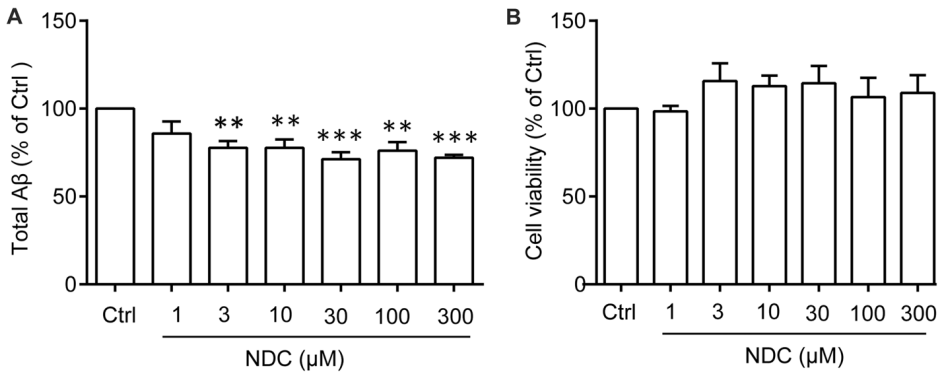

FIGURE 4 | NDC reduces Aβ level in HEK293/APPswe cells. **(A)** The total Aβ level in HEK293/APPswe culture medium. **(B)** Cell viability of HEK293/APPswe cells after treatment with NDC for 24 h. Data are presented as mean ± SEM, $n = 3$ independent experiments, $^{**}p < 0.01$, $^{***}p < 0.005$, analyzed by one-way ANOVA **(A,B)** followed by Bonferroni test.

CellTiter-Glo Assay

Cell viability of NDC-treated HEK293/APPswe or BV2 cells was investigated with CellTiter-Glo luminescent Cell Viability Assay (Promega) according to the manufacturer's instructions.

Statistical Analysis

All data are presented as mean ± SEM. Statistical analysis was performed with GraphPad Prism 6 Software (San Diego, CA, USA). Results were analyzed by two-tailed t-test to

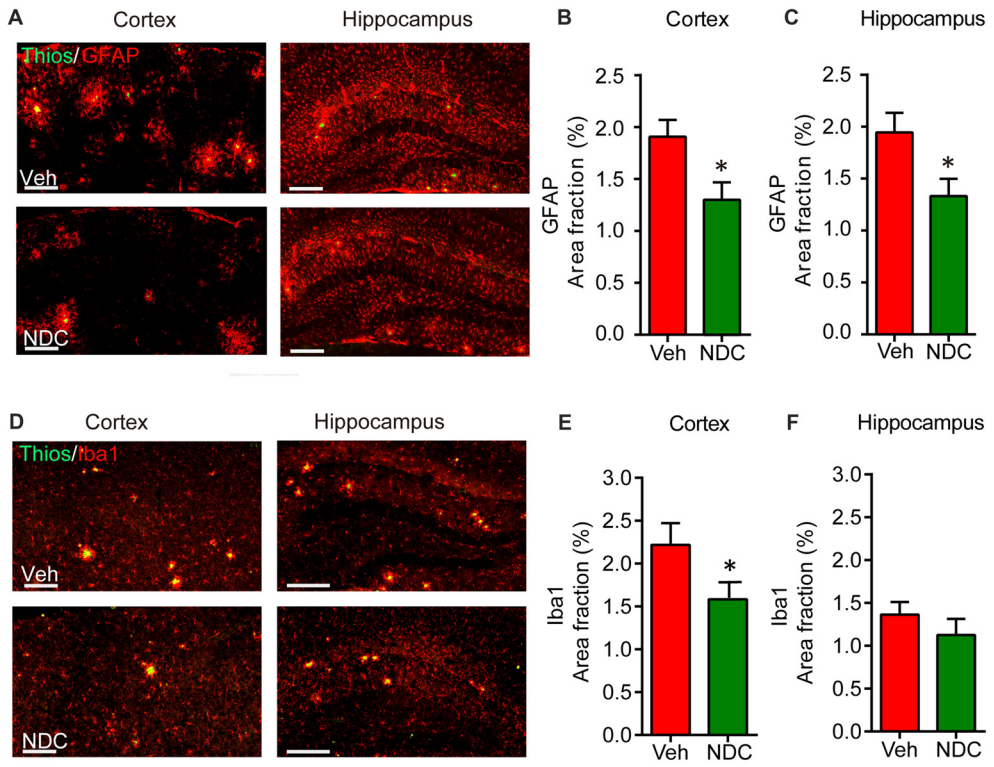

FIGURE 5 | NDC reduces periplaque activated microglia and astrocytes in APP/PS1 mice. **(A)** Representative sections of vehicle- and NDC-treated APP/PS1 mice brain immunostained with ThioS and GFAP in cortex and hippocampus are shown. Scale bar = 200 μm. **(B,C)** Quantitative analysis of ThioS and GFAP double staining in cortex **(B)** and hippocampus **(C)**. **(D)** Representative sections of vehicle- and NDC-treated APP/PS1 mice brain immunostained with ThioS and microglial makers Iba1 in cortex and hippocampus are shown. Scale bar = 200 μm. **(E,F)** Quantitative analysis of ThioS and Iba1 double staining in cortex **(E)** and hippocampus. **(F)** Data are presented as mean ± SEM, $n = 5$ per group, $^*p < 0.05$, analyzed by two-tailed t-test compared with APP/PS1 vehicle group.

determine the statistical significance of treatment sets. For multiple comparisons, one-way ANOVA or two-way ANOVA were performed, followed by Bonferroni test. Differences were considered significant when $p < 0.05$.

RESULTS

NDC Ameliorates Learning and Memory Deficits in APP/PS1 Mice

To investigate the potential therapeutic of NDC for AD, we began the oral administration of NDC from 3- to 4-month-old APP/PS1 mice for 3 months. During drug administration, all treated animals' body weight was recorded and there was no body weight loss or obvious adverse effects among groups (data not shown). After drug administration, the behavioral tests were performed to investigate the cognitive function of these mice. MWM was carried out to assess spatial learning and memory ability (**Figure 1A**). The latency to platform was analyzed using two-way ANOVA ($F_{(2,114)} = 18.65$, $p < 0.001$). We found that compared with WT mice, APP/PS1 mice spent more time in locating the platform ($p < 0.001$), indicating it exhibited significant cognitive decline in learning, and there was no significant difference between NDC-treated mice and WT mice ($p > 0.05$), indicating that the cognitive function of spatial memory was significantly improved by treatment of NDC (**Figure 1B**). On day 7, probe trials were performed to assess the maintenance of spatial memory. Compared with WT mice, APP/PS1 vehicle mice crossed the platform position was less frequently (**Figure 1C**) and spent more time to reach position of missing platform. However, no significant difference in latency was observed between NDC-treated mice and WT mice ($F_{(2,19)} = 8.650$, $p < 0.005$; **Figure 1D**).The time in quadrant was Two-way ANOVA revealed no significant effect for group ($F_{(2,76)} = 0.000097$, $p > 0.05$), compared with WT mice, APP/PS1 mice spent less time in target quadrant ($p = 0.0415$; **Figure 1E**). Among three groups, there was no significant difference in velocity ($F_{(2,19)} = 1.340$, $p > 0.05$) or distance ($F_{(2,19)} = 1.334$, $p > 0.05$) of swimming, suggesting that NDC treatment did not influence locomotor activity of mice (**Figures 1F,G**). These results suggest that administration of NDC ameliorates the spatial learning and memory of APP/PS1 mice.

To further evaluate the learning and recognition memory of AD mice, we performed the NOR test (**Figure 2A**). In the training phase, there was no significant difference among groups, the preference scores were all about 50% in all groups (**Figure 2B**). In the testing phase, APP/PS1 vehicle mice

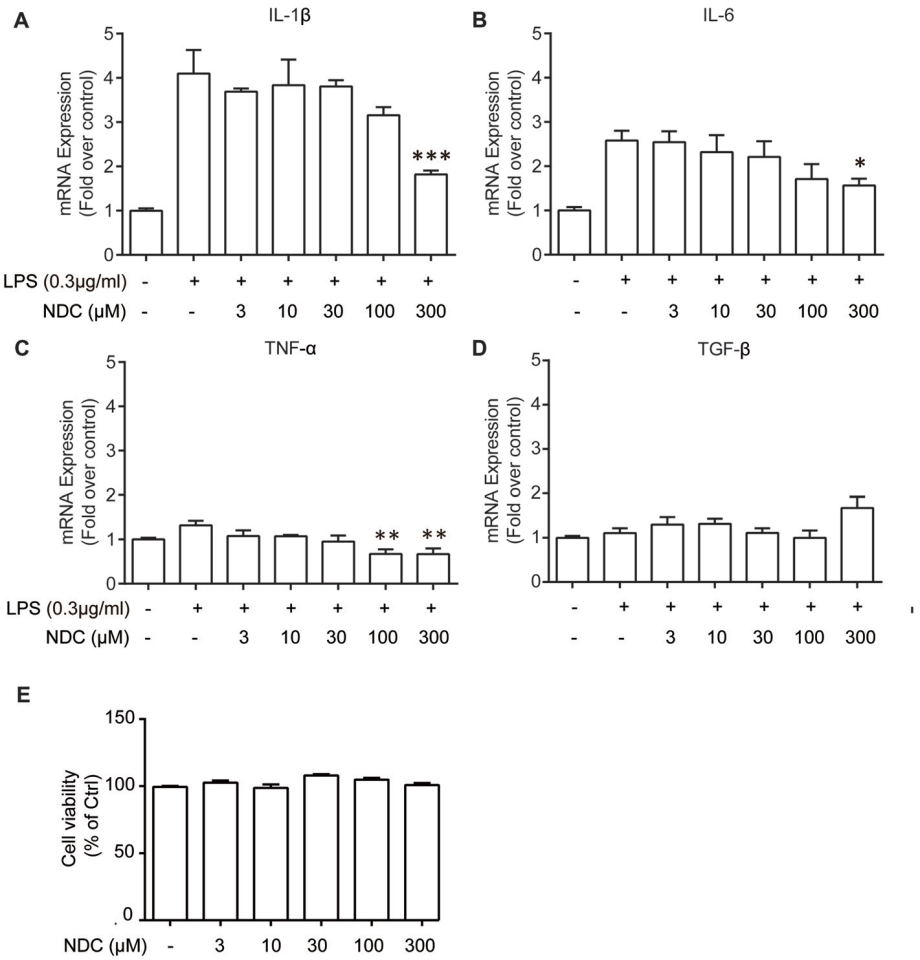

FIGURE 6 | NDC reduces levels of inflammation cytokines in BV2 cells. **(A–D)** Quantitative PCR (qPCR) quantification of proinflammatory cytokines IL-1β **(A)**, TNF-α **(B)**, IL-6 **(C)** and one anti-inflammatory cytokine, TGF-β **(D)**. **(E)** Cell viability of BV2 cells after 6 h NDC treatment. Data are presented as mean ± SEM, $n = 3$ independent experiments, $^{*}p < 0.05$, $^{**}p < 0.01$, $^{***}p < 0.005$, analyzed by one-way ANOVA followed by Bonferroni test revealed difference between NDC- and lipopolysaccharides (LPS)-treated condition **(A–D)**, as well as difference between control and NDC-treated condition **(E)**.

spent less time to explore the novel object than WT mice, NDC-treated APP/PS1 mice spent much longer time to explore the novel object than APP/PS1 vehicle mice ($F_{(2,22)} = 5.412$, $p < 0.05$), the recognition index of NDC-treated mice was similar with that of WT mice (**Figure 2C**), indicating that NDC-treatment efficiently improved memory retention of APP/PS1 mice.

NDC Alleviates Amyloid Plaque Burden and Aβ Levels in APP/PS1 Mice

The Aβ levels or deposits in the brain of APP/PS1 mice can be detected on 6 month. To explore the effects of NDC on Aβ levels and Aβ deposits, ThioS staining for amyloid plaques was performed on these fixed brain tissues (**Figure 3A**). Detailed statistical analysis showed that, ThioS-positive amyloid plaque areas were markedly reduced in the brains of NDC-treated APP/PS1 mice compared with that in the brains of vehicle-treated APP/PS1 mice (**Figures 3B,C**), and 6E10-positive amyloid plaque areas were also significantly reduced (Supplementary Figure S1), indicating that NDC treatment alleviates the deposition of amyloid plaques.

Simultaneously, we performed ELISA assay to quantify Aβ levels in the cortex and hippocampus of these mice. Results showed that the Aβ levels were high in cortex and hippocampus of APP/PS1 transgenic mice. NDC treatment significantly reduced SDS-soluble $A\beta_{40}$ and $A\beta_{42}$ levels in cortex (**Figures 3D,E**). In hippocampus, the level of SDS-soluble $A\beta_{40}$ was also reduced significantly (**Figure 3F**), but there is no significant differences between the hippocampus $A\beta_{42}$ level in NDC-treated and vehicle-treated mice (**Figure 3G**). These results suggest that NDC reduced Aβ levels in APP/PS1 mice brain.

To identify whether NDC could reduce Aβ level *in vitro*, we treated HEK293/APPswe cells with various concentrations of NDC. The culture medium was collected to evaluate total Aβ level using ELISA assay and the cell were used

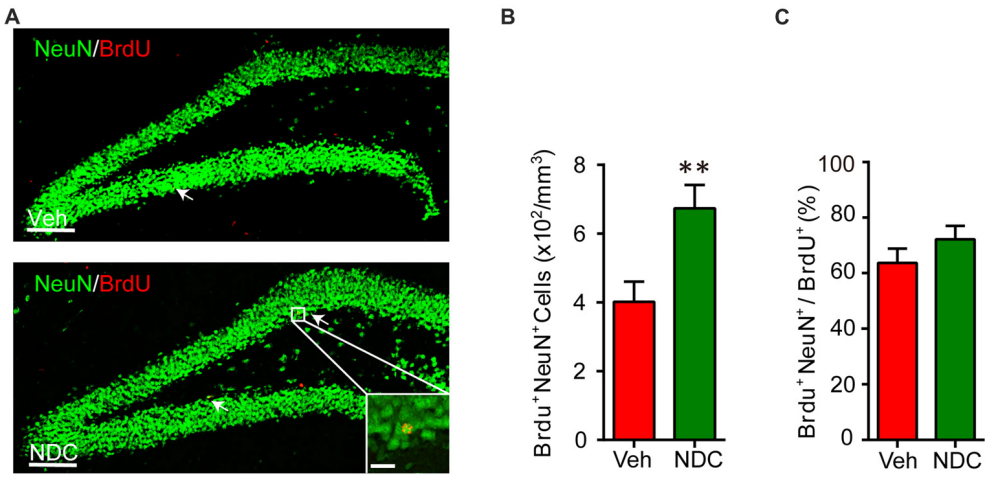

FIGURE 7 | NDC enhances neurogenesis in APP/PS1 mice. **(A)** NeuN (green) and BrdU (red) staining in dentate gyrus (DG) of brain sections from mice treated with vehicle **(A)** and NDC **(B)**. **(B)** Quantification of BrdU$^+$ NeuN$^+$ cells in the brain sections of vehicle- and NDC-treated mice. **(C)** Proportion of BrdU$^+$ NeuN$^+$ cells in all BrdU$^+$ cells. Data are presented as mean ± SEM, Veh group $n = 7$, NDC group: $n = 8$, $^{**}p < 0.01$, analyzed by two-tailed t-test **(B,C)** compared with APP/PS1 vehicle group. Scale bars in **(A)**, 100 μm; insets, 20 μm.

to evaluate cell viability. Compared to the vehicle treatment, NDC significantly reduced the total extracellular Aβ level ($F_{(6,28)} = 5.459$, $p < 0.001$; **Figure 4A**). The viability of cells was not declined after 24 h treatment as revealed by the CellTiter-Glo assay ($F_{(6,14)} = 0.3613$, $p > 0.05$; **Figure 4B**). These results suggest that NDC can reduce Aβ generation in an AD cell model.

NDC Attenuates Neuroinflammation in APP/PS1 Mice

Abnormal neuroinflammation, including activated astrocytes and microglia, is a typical hallmark of neurodegenerative disease, and amyloid plaques are surrounded by activated microglia and astrocytes in the brains of AD patients (McGeer and McGeer, 2003). To investigate its possible anti-inflammatory effects of NDC in APP/PS1 mice, we stained brain sections with polyclonal antibodies against Iba1 and GFAP, which are indications of active microglia and astrocytes, respectively. As previously reported (Hou et al., 2014), we observed that amyloid plaques were surrounded by GFAP-positive astrocytes and Iba1-positive microglia. Compared with vehicle-treated APP/PS1 mice, we found that NDC-treated APP/PS1 mice showed lower GFAP-positive area and Iba1-positive area in cortex and hippocampus (**Figures 5A,D**). Further statistical analysis demonstrated that compared with the vehicle-treated APP/PS1 mice, the proportion of GFAP-positive areas surrounding Aβ in the cortex and hippocampus of NDC-treated APP/PS1 mice were reduced (**Figures 5B,C**). Similarly, we found the proportion of Iba1-positive microglia areas surrounding Aβ also decreased in the cortex and hippocampus (**Figures 5E,F**). These results demonstrate that NDC treatment could significantly reduce the area fraction of activated microglia and astrocytes in APP/PS1 Mice.

We then investigated the effect of NDC on the LPS-induced microglia activation. The BV2 cells were incubated with various concentrations of NDC in the presence of LPS (0.3 ug/mL) for 6 h. qPCR results demonstrated that NDC inhibited LPS-induced proinflammatory cytokines, interleukin 1 beta (IL-1β; $F_{(6,24)} = 13.04$, $p < 0.001$), Interleukin 6 (IL-6; $F_{(6,32)} = 6.350$, $p < 0.001$), and tumor necrosis factor alpha (TNF-α) expression ($F_{(6,23)} = 4.825$, $p < 0.01$; **Figures 6A–C**). These cytokines were effectively reduced mainly by NDC at 300 μM. In addition, NDC slightly up-regulated the expression of anti-inflammatory cytokine transforming growth factor beta (TGF-β) in the presence of LPS (**Figure 6D**), and NDC had no obvious cytotoxicity to BV2 cells as assessed by the CellTiter-Glo assay (**Figure 6E**). Furthermore, Western blot results suggested that NDC also reduced IL-1β level in AD mouse brain (Supplementary Figure S2). Thus, our results indicate that NDC inhibited the expression of proinflammatory cytokines and promoted the expression of anti-inflammatory cytokines.

NDC Enhances Neurogenesis in APP/PS1 Mice

In AD patients and animal models, abnormal neurogenesis is related to cognitive decline. We investigated whether NDC could affect neurogenesis in APP/PS1 mice with the improvement in cognition. APP/PS1 mice were intraperitoneally injected with bromodeoxyuridine (BrdU) for 7 days and then euthanized after behavioral tests. Brain sections were stained with BrdU/NeuN (**Figure 7A**). Compared with vehicle-treated APP/PS1 mice, the number of BrdU/NeuN double-positive cells in the hippocampus of NDC-treatment APP/PS1 mice was increased significantly (**Figure 7B**). However, the proportion of BrdU/NeuN double-positive cells in the BrdU-positive cells was not altered among two groups after NDC treatment (**Figure 7C**). These

results indicated that NDC treatment promotes neurogenesis in APP/PS1 transgenic mice.

DISCUSSION

In this study, NDC significantly ameliorated cognitive impairment and neuropathology in transgenic AD mice through reducing amyloid plaque burden and Aβ levels, suppressing neuroinflammation and promoting neurogenesis, which is in line with previous findings on other natural compounds, such as curcumin and Naoling decoction (Ono et al., 2002; Hamaguchi et al., 2006, 2010; Hatcher et al., 2008; Xia et al., 2017). Taken together, these studies suggest that natural compounds such as NDC could achieve multi-target directed therapy in the treatment of AD.

In current AD drug research, many targets or strategies are considered, such as preventing Aβ accumulation or tau phosphorylation, inhibition of secretase activity that directly modulates Aβ generation, OS, neuroinflammation, as well as mitochondrial damage (Tundis et al., 2018). On the basis of these targets and processes, most therapeutic strategies for AD focus on Aβ and phosphorylated tau levels and OS (Selkoe, 2001; Dysken et al., 2014a). However, it has been observed that drugs directed to a single target with high specificity often lacked clinical efficacy on AD, highlighting the complexity of this disorder (León et al., 2013). Notably, antioxidants such as rutin, resveratrol and vitamin E have been reported to exert beneficial effects on the treatment of AD (Zuo et al., 2015). Interestingly, in addition to its antioxidant effect, vitamin E can also reduce Aβ levels and amyloid deposition in the brain of transgenic AD mice (Sung et al., 2004). It also suppresses inflammatory responses (reduction of GFAP, IL-1β) and decreases tau pathology (Nakashima et al., 2004; Yao et al., 2004). Clinical trials further showed that vitamin E has protective effects in patients with mild to moderate AD and the cognitive performance of patients was changed significantly (Dysken et al., 2014b). In our study, NDC exhibited beneficial effects on Aβ, NDC reduced Aβ levels and alleviated the deposition of amyloid plaques in AD mice similar with vitamin E. Neurogenesis is an essential process to maintain hippocampus-dependent cognitive abilities (Deng et al., 2010), and the impaired neurogenesis is involved in the progression of AD (Martinez-Canabal, 2014). Here, NDC also enhanced neurogenesis in transgenic mice model. All these suggest that the beneficial effects of NDC may not only due to its antioxidant activity but also possess other activities.

In previous studies, the relationship between neuroinflammation and Aβ is complicated. On the one hand cerebral inflammation could increase Aβ production (Iadecola, 2003; Walker and Lue, 2007), and on the other hand aggregated Aβ peptide could activate microglia to a proinflammatory state (Walker and Lue, 2005, 2007). In our study, NDC not only reduced the activated microglia and astrocytes but also reduced Aβ plaques in AD mice brain. It has been reported that NDC possesses anti-inflammatory properties as an antioxidant (Nakamura et al., 2003). Therefore we guess that in our study NDC may suppress the neuroinflammation, which further leads to the decrease of Aβ production. What's more, we also found that NDC treatment reduced production of inflammatory cytokines in BV2 cells, which further suggests NDC may affect microglia directly. To prove this hypothesis, more *in vitro* assays including treatment of NDC and Aβ in primary microglia culture should be carried out.

In summary, the current study first demonstrates the protective effects of NDC on AD pathology by targeting multiple processes in an AD mouse model, which suggests that NDC may serve as a promising therapeutic agent for AD.

AUTHOR CONTRIBUTIONS

GP substantially designed and controlled the study. WY and YZ performed the behavioral tests. KZ, WY and YZ performed histopathological and data analysis. YA and TH performed the *in vitro* experiments. KZ and WY contributed to the manuscript preparation. SH and JL contributed to critical revision of the manuscript. All the authors reviewed and commented on the manuscript.

FUNDING

This study was supported by the "Strategic Priority Research Program" of the Chinese Academy of Sciences (XDA16020502), the National Key Research and Development Program of China Stem Cell and Translational Research (2016YFA0101200, 2016YFA0101202), the Ministry of Science and Technology (2015CB964502), Shanghai Municipal Commission for Science and Technology (15JC1400202).

ACKNOWLEDGMENTS

The work using a confocal laser scanning microscope Leica TCS SP8 was performed at the National Center for Protein Science Shanghai, and we grateful to Yan Wang for technical supports. We thank Shunmei Xin for technical assistance. We thank all members of our laboratory for sharing reagents and advice.

SUPPLEMENTARY MATERIAL

The Supplementary Material for this article can be found online at: https://www.frontiersin.org/articles/10.3389/fnagi.2018.00169/full#supplementary-material

REFERENCES

Bevins, R. A., and Besheer, J. (2006). Object recognition in rats and mice: a one-trial non-matching-to-sample learning task to study 'recognition memory'. *Nat. Protoc.* 1, 1306–1311. doi: 10.1038/nprot.2006.205

Bronzuoli, M. R., Iacomino, A., Steardo, L., and Scuderi, C. (2016). Targeting neuroinflammation in Alzheimer's disease. *J. Inflamm. Res.* 9, 199–208. doi: 10.2147/JIR.S86958

Cai, Q., Li, Y., and Pei, G. (2017). Polysaccharides from Ganoderma lucidum attenuate microglia-mediated neuroinflammation and modulate

microglial phagocytosis and behavioural response. *J. Neuroinflammation* 14:63. doi: 10.1186/s12974-017-0839-0

Deng, W., Aimone, J. B., and Gage, F. H. (2010). New neurons and new memories: how does adult hippocampal neurogenesis affect learning and memory? *Nat. Rev. Neurosci.* 11, 339–350. doi: 10.1038/nrn2822

Donovan, M. H., Yazdani, U., Norris, R. D., Games, D., German, D. C., and Eisch, A. J. (2006). Decreased adult hippocampal neurogenesis in the PDAPP mouse model of Alzheimer's disease. *J. Comp. Neurol.* 495, 70–83. doi: 10.1002/cne.20840

Drapeau, E., and Nora Abrous, D. (2008). Stem cell review series: role of neurogenesis in age-related memory disorders. *Aging Cell* 7, 569–589. doi: 10.1111/j.1474-9726.2008.00369.x

Dysken, M. W., Guarino, P. D., Vertrees, J. E., Asthana, S., Sano, M., Llorente, M., et al. (2014a). Vitamin E and memantine in Alzheimer's disease: clinical trial methods and baseline data. *Alzheimers Dement.* 10, 36–44. doi: 10.1016/j.jalz.2013.01.014

Dysken, M. W., Sano, M., Asthana, S., Vertrees, J. E., Pallaki, M., Llorente, M., et al. (2014b). Effect of vitamin E and memantine on functional decline in Alzheimer disease: the TEAM-AD VA cooperative randomized trial. *JAMA* 311, 33–44. doi: 10.1001/jama.2013.282834

Encinas, J. M., Michurina, T. V., Peunova, N., Park, J. H., Tordo, J., Peterson, D. A., et al. (2011). Division-coupled astrocytic differentiation and age-related depletion of neural stem cells in the adult hippocampus. *Cell Stem Cell* 8, 566–579. doi: 10.1016/j.stem.2011.03.010

Feng, Y., and Wang, X. (2012). Antioxidant therapies for Alzheimer's disease. *Oxid. Med. Cell. Longev.* 2012:472932. doi: 10.1155/2012/472932

Galea, E., Morrison, W., Hudry, E., Arbel-Ornath, M., Bacskai, B. J., Gómez-Isla, T., et al. (2015). Topological analyses in APP/PS1 mice reveal that astrocytes do not migrate to amyloid-β plaques. *Proc. Natl. Acad. Sci. U S A* 112, 15556–15561. doi: 10.1073/pnas.1516779112

Gaudette, N. J., and Pickering, G. J. (2013). Modifying bitterness in functional food systems. *Crit. Rev. Food Sci. Nutr.* 53, 464–481. doi: 10.1080/10408398.2010.542511

Guzior, N., Wieckowska, A., Panek, D., and Malawska, B. (2015). Recent development of multifunctional agents as potential drug candidates for the treatment of Alzheimer's disease. *Curr. Med. Chem.* 22, 373–404. doi: 10.2174/0929867321666141106122628

Hamaguchi, T., Ono, K., and Yamada, M. (2006). Anti-amyloidogenic therapies: strategies for prevention and treatment of Alzheimer's disease. *Cell. Mol. Life Sci.* 63, 1538–1552. doi: 10.1007/s00018-005-5599-9

Hamaguchi, T., Ono, K., and Yamada, M. (2010). REVIEW: curcumin and Alzheimer's disease. *CNS Neurosci. Ther.* 16, 285–297. doi: 10.1111/j.1755-5949.2010.00147.x

Hatcher, H., Planalp, R., Cho, J., Torti, F. M., and Torti, S. V. (2008). Curcumin: from ancient medicine to current clinical trials. *Cell. Mol. Life Sci.* 65, 1631–1652. doi: 10.1007/s00018-008-7452-4

Holtzman, D. M., John, C. M., and Goate, A. (2011). Alzheimer's disease: the challenge of the second century. *Sci. Transl. Med.* 3:77sr1. doi: 10.1126/scitranslmed.3002369

Hou, Y., Wang, Y., Zhao, J., Li, X., Cui, J., Ding, J., et al. (2014). Smart soup, a traditional Chinese medicine formula, ameliorates amyloid pathology and related cognitive deficits. *PLoS One* 9:e111215. doi: 10.1371/journal.pone.0111215

Iadecola, C. (2003). Cerebrovascular effects of amyloid-beta peptides: mechanisms and implications for Alzheimer's dementia. *Cell. Mol. Neurobiol.* 23, 681–689. doi: 10.1023/A:1025092617651

Jobin, C., Bradham, C. A., Russo, M. P., Juma, B., Narula, A. S., Brenner, D. A., et al. (1999). Curcumin blocks cytokine-mediated NF-κB activation and proinflammatory gene expression by inhibiting inhibitory factor I-κB kinase activity. *J. Immunol.* 163, 3474–3483.

Kim, S. J., Son, T. G., Park, H. R., Park, M., Kim, M. S., Kim, H. S., et al. (2008). Curcumin stimulates proliferation of embryonic neural progenitor cells and neurogenesis in the adult hippocampus. *J. Biol. Chem.* 283, 14497–14505. doi: 10.1074/jbc.m708373200

Krauthausen, M., Kummer, M. P., Zimmermann, J., Reyes-Irisarri, E., Terwel, D., Bulic, B., et al. (2015). CXCR3 promotes plaque formation and behavioral deficits in an Alzheimer's disease model. *J. Clin. Invest.* 125, 365–378. doi: 10.1172/jci66771

Lahlou, M. (2013). The success of natural products in drug discovery. *Pharmacol. Pharm.* 04, 17–31. doi: 10.4236/pp.2013.43a003

Lazarov, O., Robinson, J., Tang, Y.-P., Hairston, I. S., Korade-Mirnics, Z., Lee, V. M. Y., et al. (2005). Environmental enrichment reduces Aβ levels and amyloid deposition in transgenic mice. *Cell* 120, 701–713. doi: 10.1016/j.cell.2005.01.015

León, R., Garcia, A. G., and Marco-Contelles, J. (2013). Recent advances in the multitarget-directed ligands approach for the treatment of Alzheimer's disease. *Med. Res. Rev.* 33, 139–189. doi: 10.1002/med.20248

Liu, X., Zhao, X., Zeng, X., Bossers, K., Swaab, D. F., Zhao, J., et al. (2013). β-arrestin1 regulates γ-secretase complex assembly and modulates amyloid-β pathology. *Cell Res.* 23, 351–365. doi: 10.1038/cr.2012.167

Ma, Q. L., Yang, F., Rosario, E. R., Ubeda, O. J., Beech, W., Gant, D. J., et al. (2009). β-amyloid oligomers induce phosphorylation of tau and inactivation of insulin receptor substrate via c-Jun N-terminal kinase signaling: suppression by omega-3 fatty acids and curcumin. *J. Neurosci.* 29, 9078–9089. doi: 10.1523/JNEUROSCI.1071-09.2009

Martinez-Canabal, A. (2014). Reconsidering hippocampal neurogenesis in Alzheimer's disease. *Front. Neurosci.* 8:147. doi: 10.3389/fnins.2014.00147

McGeer, E. G., and McGeer, P. L. (2003). Inflammatory processes in Alzheimer's disease. *Prog. Neuropsychopharmacol. Biol. Psychiatry* 27, 741–749. doi: 10.1016/S0278-5846(03)00124-6

Morris, R. (1984). Developments of a water-maze procedure for studying spatial learning in the rat. *J. Neurosci. Methods* 11, 47–60. doi: 10.1016/0165-0270(84)90007-4

Nakamura, Y., Watanabe, S., Miyake, N., Kohno, H., and Osawa, T. (2003). Dihydrochalcones: evaluation as novel radical scavenging antioxidants. *J. Agric. Food Chem.* 51, 3309–3312. doi: 10.1021/jf0341060

Nakashima, H., Ishihara, T., Yokota, O., Terada, S., Trojanowski, J. Q., Lee, V. M., et al. (2004). Effects of α-tocopherol on an animal model of tauopathies. *Free Radic. Biol. Med.* 37, 176–186. doi: 10.1016/j.freeradbiomed.2004.04.037

Necula, M., Kayed, R., Milton, S., and Glabe, C. G. (2007). Small molecule inhibitors of aggregation indicate that amyloid β oligomerization and fibrillization pathways are independent and distinct. *J. Biol. Chem.* 282, 10311–10324. doi: 10.1074/jbc.m608207200

Ono, K., Hasegawa, K., Yoshiike, Y., Takashima, A., Yamada, M., and Naiki, H. (2002). Nordihydroguaiaretic acid potently breaks down pre-formed Alzheimer's β-amyloid fibrils *in vitro*. *J. Neurochem.* 81, 434–440. doi: 10.1046/j.1471-4159.2002.00904.x

Selkoe, D. J. (2001). Alzheimer's disease: genes, proteins and therapy. *Physiol. Rev.* 81, 741–766. doi: 10.1152/physrev.2001.81.2.741

Sung, S., Yao, Y., Uryu, K., Yang, H., Lee, V. M., Trojanowski, J. Q., et al. (2004). Early vitamin E supplementation in young but not aged mice reduces Abeta levels and amyloid deposition in a transgenic model of Alzheimer–s disease. *FASEB J.* 18, 323–325. doi: 10.1096/fj.03-0961fje

Surana, S. J., Gokhale, S. B., Rajmane, R. A., and Jadhav, R. B. (2006). Non-saccharide natural intense sweeteners—an overview of current status. *Nat. Prod. Radiance* 5, 270–278. Available online at: http://www.niscair.res.in/sciencecommunication/researchjournals/rejour/npr/npr0_march07.asp

Teng, L., Zhao, J., Wang, F., Ma, L., and Pei, G. (2010). A GPCR/secretase complex regulates β- and γ-secretase specificity for Aβ production and contributes to AD pathogenesis. *Cell Res.* 20, 138–153. doi: 10.1038/cr.2010.3

Tundis, R., Loizzo, M. R., Nabavi, S. M., Orhan, I. E., Skalicka-Woźniak, K., D'Onofrio, G., et al. (2018). "Natural compounds and their derivatives as multifunctional agents for the treatment of alzheimer disease," in *Discovery and Development of Neuroprotective Agents from Natural Products: Natural Product Drug Discovery* (Elsevier), 63–102. doi: 10.1016/B978-0-12-809593-5.00003-3

Walker, D. G., and Lue, L. F. (2005). Investigations with cultured human microglia on pathogenic mechanisms of Alzheimer's disease and other neurodegenerative diseases. *J. Neurosci. Res.* 81, 412–425. doi: 10.1002/jnr.20484

Walker, D., and Lue, L. F. (2007). Anti-inflammatory and immune therapy for Alzheimer's disease: current status and future directions. *Curr. Neuropharmacol.* 5, 232–243. doi: 10.2174/157015907782793667

Wang, D. M., Yang, Y. J., Zhang, L., Zhang, X., Guan, F. F., and Zhang, L. F. (2013). Naringin enhances CaMKII activity and improves long-term memory in a mouse model of Alzheimer's disease. *Int. J. Mol. Sci.* 14, 5576–5586. doi: 10.3390/ijms14035576

Xia, Z., Peng, W., Cheng, S., Zhong, B., Sheng, C., Zhang, C., et al. (2017). Naoling decoction restores cognitive function by inhibiting the neuroinflammatory network in a rat model of Alzheimer's disease. *Oncotarget* 8, 42648–42663. doi: 10.18632/oncotarget.17337

Yang, F., Lim, G. P., Begum, A. N., Ubeda, O. J., Simmons, M. R., Ambegaokar, S. S., et al. (2005). Curcumin inhibits formation of amyloid beta oligomers and fibrils, binds plaques, and reduces amyloid *in vivo*. *J. Biol. Chem.* 280, 5892–5901. doi: 10.1074/jbc.m404751200

Yao, Y., Chinnici, C., Tang, H., Trojanowski, J. Q., Lee, V. M., and Pratico, D. (2004). Brain inflammation and oxidative stress in a transgenic mouse model of Alzheimer-like brain amyloidosis. *J. Neuroinflammation* 1:21. doi: 10.1186/1742-2094-1-21

Zuo, L., Hemmelgarn, B. T., Chuang, C. C., and Best, T. M. (2015). The role of oxidative stress-induced epigenetic alterations in amyloid-beta production in Alzheimer's disease. *Oxid. Med. Cell. Longev.* 2015:604658. doi: 10.1155/2015/604658

Conflict of Interest Statement: The authors declare that the research was conducted in the absence of any commercial or financial relationships that could be construed as a potential conflict of interest.

frontiers in Aging Neuroscience

ORIGINAL RESEARCH
published: 23 May 2018
doi: 10.3389/fnagi.2018.00149

The Expression of Hippocampal NRG1/ErbB4 Correlates With Neuronal Apoptosis, but Not With Glial Activation During Chronic Cerebral Hypoperfusion

Yue Hei[1†], Rong Chen[2†], Xicai Yi[1], Lizhou Wei[1], Qianfa Long[3] and Weiping Liu[1]*

[1]*Department of Neurosurgery, Xijing Hospital, Fourth Military Medical University, Xi'an, China,* [2]*Department of Neurology, Xijing Hospital, Fourth Military Medical University, Xi'an, China,* [3]*Department of Neurosurgery, Institute of Mini-invasive Neurosurgery and Translational Medicine, Xi'an Central Hospital, Xi'an, China*

Permanent bilateral common carotid occlusion (2VO) is well-established to investigate the chronic cerebral hypoperfusion (CCH)-induced cognitive deficits. Besides, previous studies suggested that disturbance of Neuregulin1 (NRG1)/ErbB4 signaling is associated with cognitive impairments, as well as neuronal apoptosis and neuroinflammation in CNS. However, the expression pattern of hippocampal NRG1/ErbB4 has not been systematically investigated during CCH. Here, we aim to investigate the temporal changes of hippocampal NRG1/ErbB4 during CCH and their possible relationship with neuronal apoptosis and glial activation. Morris water maze (MWM) and Radial arm water maze (RAWM) tests were used to analyze cognitive impairment in 2VO rats at 28 days post-surgery, and Enzyme-Linked Immunosorbent Assay (ELISA), western blotting and immunostaining were performed at different time points (24 h, 7 days, 14 days, 28 days) to detect the expression pattern of NRG1/ErbB4 and the distribution of ErbB4. Neuronal nuclei (NeuN), NeuN/TUNEL, Iba1 and GFAP immunostaining and caspase activity in hippocampal CA1 subarea were assessed during CCH as well. We found that the expression of NRG1 and phosphorylated ErbB4 (pErbB4)/ErbB4 changed in a time-dependent manner (up-regulated in the acute phase and then decreased in the chronic phase of CCH). Besides, ErbB4-expressed neurons and selective types of GABAergic cells decreased after CCH, but the distribution pattern of ErbB4 remained unchanged. In addition, the expression of hippocampal NRG1/ErbB4 positively correlated with the level of neuronal apoptosis (both NeuN/TUNEL immunostaining and caspase-3 activity), but not with glial activation according to Pearson's correlation. These findings indicated that hippocampal NRG1/ErbB4 may be involved in the pathogenesis of CCH, especially neuronal apoptosis during CCH.

Keywords: chronic cerebral hypoperfusion, neuronal apoptosis, glial activation, NRG1, ErbB4

OPEN ACCESS

Edited by:
Yogesh Dwivedi,
University of Alabama at Birmingham, United States

Reviewed by:
Wei-jiang Zhao,
Shantou University Medical College, China
Yuriko Iwakura,
Niigata University, Japan

***Correspondence:**
Weiping Liu
liuwp@fmmu.edu.cn

†These authors have contributed equally to this work.

Received: *18 March 2018*
Accepted: *02 May 2018*
Published: *23 May 2018*

Citation:
Hei Y, Chen R, Yi X, Wei L Long Q and Liu W (2018) The Expression of Hippocampal NRG1/ErbB4 Correlates With Neuronal Apoptosis, But Not With Glial Activation During Chronic Cerebral Hypoperfusion. Front. Aging Neurosci. 10:149. doi: 10.3389/fnagi.2018.00149

INTRODUCTION

Chronic cerebral hypoperfusion (CCH) may cause dramatic cognitive decline and neurodegenerative changes that are closely associated with Alzheimer's disease and vascular dementia (Farkas et al., 2007; Zhao and Gong, 2015), but the underlying mechanisms are poorly understood so far. It is known that hippocampal neuronal death and glial activation contribute to cognitive decline (Farkas et al., 2007; Du et al., 2017) in the permanent bilateral common carotid artery occlusion (2VO) rats (a well-established animal model for CCH). More specifically, neuronal apoptosis and glial activation were found to be directly correlated with CCH-induced cognitive deficits (Xi et al., 2014). Bennett et al. (1998) previously reported selectively increased level of neuronal apoptosis in CA1 subarea during CCH, and a number of studies have further demonstrated that neuroprotection in CA1 region could improve cognitive ability in 2VO rats (Anastacio et al., 2014; Kwon et al., 2015; Liu et al., 2015). Besides, activated microglia and astrocytes take an essential role in neuroinflammation by producing inflammatory chemokines and cytokines (such as IL-1β, IL-6 and TNF-α) (Cechetti et al., 2012; Yang et al., 2014; Du et al., 2017), which may further accelerate the disease progression. These findings suggest the key role of both hippocampal neuronal apoptosis and glial activation in CCH.

Neuregulin1 (NRG1) is a growth factor that contains the epidermal growth factor (EGF)-like domain (Wu et al., 2015). Mature NRG1 is largely diffusible and exerts its effects via tyrosine kinase receptors like ErbB4, which can bind NRG1 and activate downstream signaling (Mei and Xiong, 2008; Guan et al., 2015). NRG1/ErbB4 signaling has been heavily implicated in neuronal migration, synaptic plasticity (Mei and Xiong, 2008), etc. Besides, recent studies have suggested NRG1/ErbB4 signaling may be also involved in cognitive processes, neuronal protection and anti-inflammatory actions (Li et al., 2014; Lu et al., 2016; Tian et al., 2016). With regard to cognitive processes, endogenous hippocampal ErbB4 receptors in Parvalbumin (PV) interneurons were found to mediate NRG1's action in long-term potentiation (LTP), which is essential for cognitive process (Chen et al., 2010). Furthermore, a number of studies have suggested that NRG1 administration can ameliorate cognitive impairments in cerebral ischemia and neurodegenerative diseases (Rong et al., 2015; Ryu et al., 2016). On the other hand, emerging evidence has demonstrated that NRG1 can effectively protect neurons directly (attenuate neuronal apoptosis) and indirectly (preserve blood-brain barrier integrity and reduce glial activation) (Simmons et al., 2016; Gao et al., 2017). However, all these beneficial effects of NRG1 could be abolished by ErbB4 inhibition (Tan et al., 2011; Guan et al., 2015; Zhang et al., 2017), indicating the role of ErbB4 in NRG1's actions. Taken together, the expression of hippocampal NRG1/ErbB4 signaling may be associated with cognitive ability, neuroprotection and glial activation in CCH. But the expression of hippocampal NRG1/ErbB4 in CCH has not been systematically investigated so far, as well as their possible relationship with neuropathological changes during CCH.

Therefore, the present study aimed to investigate the temporal changes of NRG1/ErbB4 expression in hippocampus (especially CA1 region) and their possible relationship with neuronal apoptosis and glial activation in a rat model of CCH.

MATERIALS AND METHODS

Animals and 2VO Model

All male Sprague-Dawley rats (230–250 g) were purchased from the Experimental Animal Center of the Fourth Military Medical University. Rats were housed in groups under controlled conditions (12-h light/dark cycle; 22–24°C) with free access to food and water. All experiments were approved by the Ethics Committee of the Fourth Military Medical University and followed the guidelines for the Care and Use of Laboratory Animals of the National Institute of Health (Publication No. 85–23, revised 1996). 2VO was used here. Food and water were withheld for 1 day prior to surgery. Rats were anesthetized with 10% chloral hydrate (300 mg/kg, i.p.). The bilateral common carotid arteries and vagal nerves were gently exposed and separated. Each artery was permanently ligated with silk suture. Then the wound caused by midline ventral incision was carefully sutured and closed. A total of 140 rats underwent the 2VO surgery and 44 of them died within the first 3 days. Rats that underwent a sham operation were treated similarly, but the common carotid arteries were not ligated.

Behavioral Assessment

Rats (sham group: $n = 6$; 2VO group: $n = 6$) underwent Morris water maze (MWM) tests at 28 days post-operation. The procedure has been described previously (Long et al., 2015). Briefly, the black circular tank was divided into four quadrants (I, II, III and IV) and the platform (1 cm below the water surface) was located in the center of quadrant IV for the hidden platform tasks, during which the rats were released from a randomized quadrant to search for the platform within 60 s. Rats would be gently guided to the platform and took a rest for 10 s if they failed to find it. The escape latency and swimming speed were collected during the five training days for hidden platform tasks. Then we removed the platform and performed the 1-day probe trial. The animals were allowed to swim freely for 60 s in the pool, during which the percentage of time spent in the target and the number of platform crossings were recorded. Apart from this, we also conducted radial arm water maze (RAWM) as described previously (Murray et al., 2011; Penley et al., 2013). This RAWM test is specialized to evaluate the hippocampal-dependent spatial memory ability, and it is a modified version of the traditional land-based tests. There are eight equally sized arms (numbered I to VIII) radiated from a central area (50 cm in diameter) and extra-maze cues are set around the room. As previously described (Murray et al., 2011), the escape platforms were placed at the ends of four arms (I, III, V, VII), and animals were released from the starting arm (II) to find the hidden platform within 120 s. The cumulative data of working and reference memory errors over the 5 days were collected (four trials per day).

Enzyme-Linked Immunosorbent Assay (ELISA)

Since mature NRG1 is largely diffusible (Mei and Xiong, 2008), the concentration of NRG1 in the hippocampus was evaluated by ELISA at different time points (24 days, 7 days, 14 days, 28 days) during CCH as described in previous studies (Li et al., 2014; Gao et al., 2017). Briefly, the tissue of bilateral hippocampal CA1 from rats (sham group: $n = 6$; 2VO group: $n = 6$ per time point) was carefully isolated under microscope. Afterwards, the tissue was homogenized (using ice-cold water) and centrifuged (12,000 rpm for 5 min) to get the supernatant. The concentration of NRG1 was analyzed using ELISA kit following the manufacturer's instructions (R&D Systems, Minneapolis, MN, USA). We also tested the concentration of EGF using the specific Human EGF ELISA kit (Abcam, Burlingame, CA, USA) at the same time during CCH, which was described previously (David et al., 2014).

Western Blotting

In order to detect the dynamic changes of ErbB4 expression in the hippocampal subareas during CCH, rats (sham group: $n = 6$; 2VO group: $n = 6$ per time point) were sacrificed for western blotting analysis at different time points (24 days, 7 days, 14 days, 28 days). The proteins were extracted from the tissue using the BioRad protein assay kit (Hercules, Wilmington, DE, USA). The normalized protein samples were subjected to sodium dodecyl sulfate-polyacrylamide gel, and then transferred to nitrocellulose membranes (Whatman, Germany). The membranes were blocked using 5% skim milk in TBST at room temperature for 1.5 h and incubated with anti-β-actin (Cell Signaling Technology, Danvers, MA, USA), anti-phosphorylated ErbB4 (pErbB4) (Abcam, Burlingame, CA, USA) and anti-ErbB4, anti- phosphorylated ErbB1 (pErbB1) and anti-ErbB1 (Cell Signaling Technology, Danvers, MA, USA) antibodies overnight at 4°C. After incubation at room temperature for 1 h, the membranes were thoroughly washed and incubated with peroxidase-conjugated secondary antibody (Santa Cruz Biotechnology, Santa Cruz, CA, USA) for 1 h. Finally, the labeled proteins were visualized with chemiluminescence (SuperSignal West Pico, Pierce), and the quantification of pErbB4, ErbB4 expression on X-ray films was analyzed using Quantity One 4.5.2 software. The value for the sham group was defined as 100%.

Immunostaining and Cell Counting

Rats (sham group: $n = 6$; 2VO group: $n = 6$ per time point) were anesthetized with 300 mg/kg chloral hydrate intraperitoneally and perfused using 4% paraformaldehyde. The rat brains were then removed, and routinely dehydrated, embedded in paraffin and cut into 2 μm sections. The sections were incubated overnight with rabbit-anti ErbB4 (1:100, Santa Cruz Biotechnology, Santa Cruz, CA, USA) or mouse anti-ErbB4 (1:50, Abcam, CA, USA), and mouse antibodies of neuronal nuclei (NeuN; 1:200), GFAP (1:200), GABA (1:50), GAD67 (1:100), PV(1:50), Somatostatin (SOM) (1:50; Abcam, CA, USA), or rabbit anti-Iba1 (1:100, Abcam, CA, USA), and then detected with secondary antibodies (goat anti-rabbit Alexa Fluor 488-conjugated and goat anti-mouse Alexa Fluor 594-conjugated) (Invitrogen, Carlsbad, CA, USA) (room temperature for 3 h followed by 0.0001% DAPI (Beyotime, China) staining) to see the distribution and location of ErbB4 receptors. The co-expression of ErbB4 and other markers in the hippocampus (including stratum oriens (SO), pyramidale (SP) and radiatum (SR) according to Paxinos and Watson (2005) was determined by counting the cells that clearly represented with DAPI staining. The images were captured using a confocal microscope (Olympus, Japan; magnification, 200×). Data obtained from at least 10 sections for each rat by three investigators were averaged to get a single estimate for each animal.

TUNEL Assay

To further determine the co-localization of apoptotic cells and neurons in the hippocampus, immunofluorescent double staining of TUNEL/NeuN was performed. Briefly, the brain sections were prepared as above. Sections were incubated in permeabilization solution (0.1% Triton X-100, 0.1% sodium citrate) for 2 min on ice, and then incubated with TUNEL reaction mixture (*In Situ* Cell Death Detection Kit (Roche, Germany)) in a humid chamber at 37°C for 60 min. Afterwards, the sections were incubated with mouse anti-NeuN (Abcam, CA, USA) overnight at 4°C and then mounted with DAPI (Beyotime, China) for 5 min in the dark. All the double-labeled cells (NeuN/TUNEL) were carefully counted by three investigators to analyze the neuronal apoptosis in the hippocampal CA1 subarea during CCH.

Caspase Activity

Caspase-3, -8 and -9 activity was measured by colorimetric assay kits (EMD Millipore, Billerica, MA, USA) according to the manufactures' protocol. In brief, the hippocampal CA1 tissue was carefully isolated from the rat brain (sham group: $n = 6$; 2VO group: $n = 6$ per time point) under microscope and homogenized with 1 ml ice-cold lysis buffer supplied with the kit. After centrifugation (10,000 rpm for 15 min) and assessment of protein concentration, the samples were assayed for caspase activity based on the detection of the chromophore p-nitroaniline (pNA) after cleavage from the labeled substrates (Ercan et al., 2015). The cleavage of synthetic caspase-3, -8 and -9 were spectrophotometrically detected at 405 nm in a microplate reader. The value for the sham group was defined as 1 and the ratio of optical density (OD) was finally used in the present study to show the caspase activity at different time points during CCH.

Statistical Analysis

SPSS 19.0.0 was used for statistical analysis of the data. Data were presented as the mean ± SEM. Repeated measures were used to analyze time latency and swimming speed in MWM tests, and comparisons in the individual day were analyzed by Student's *t*-test, which was also used to analyze results from time spent in the target quadrant and the number of target crossings. Other multiple comparisons were analyzed using one-way ANOVA followed by *post hoc* Bonferroni's test. Values of $P < 0.05$ were considered to be statistically significant.

RESULTS

Cognitive Deficits and Neuronal Loss in 2VO Rats

Behavioral assessments were performed on day 28 after surgery. For MWM tests (**Figures 1A–D**), the 2VO group showed obvious longer time latencies in comparison to the sham group (training day 2: $P = 0.0001 < 0.001$; training day 3: $P < 0.0001$; training day 4: $P < 0.0001$; training day 5: $P < 0.0001$). Besides, the percentage of time (PT (%)) and the number of platform crossings in the 2VO group increased significantly compared to the sham group (PT (%): $P = 0.0035 < 0.01$; platform crossings: $P = 0.0001 < 0.001$). No significant difference was found in the swimming speed between the two groups. For RAWM tests (**Figures 1E,F**), 2VO group showed remarkably increased numbers of working memory errors ($P < 0.0001$) and reference memory errors ($P = 0.0082 < 0.01$) compared to the sham group. In addition, we further performed NeuN immunostaining to see the neuronal loss in the hippocampal CA1 subarea at different time points during CCH (**Figures 2A,B**). Although no significant difference was found between the sham group and 2VO group at 7 days ($P > 0.05$), reduced NeuN-positive cells were clearly observed at 14 days ($P = 0.0338 < 0.05$) and 28 days ($P = 0.0026 < 0.01$).

The Expression of Hippocampal CA1 NRG1/ErbB4 During CCH

In order to determine the spatial and temporal changes of hippocampal NRG1/ErbB4 during CCH, ELISA, western blotting and immunofluorescence were conducted at different time points (**Figure 3**). ELISA results showed that the concentration of NRG1 in the 2VO group significantly improved at 24 h in 2VO rats in comparison to the sham group

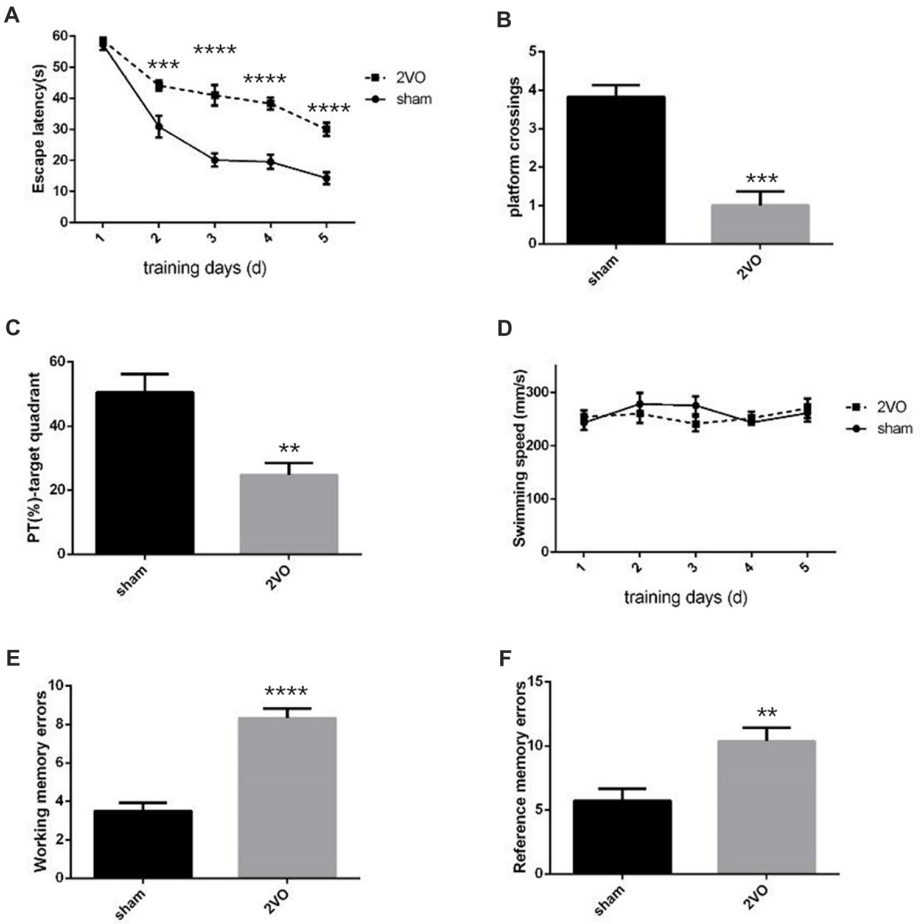

FIGURE 1 | Decreased spatial learning and memory abilities in permanent bilateral common carotid occlusion (2VO) rats. **(A)** The escape latency in the hidden platform task. **(B)** The number of platform crossings in the single probe task. **(C)** Percentage of time spent in the target quadrant during the single probe task. **(D)** The swimming speed. **(E)** The cumulative data of working memory errors in Radial arm water maze (RAWM). **(F)** The cumulative data of reference memory errors in RAWM. Working memory errors defined as re-entries into arms which had previously been explored. Reference memory errors scored as first entries into arms not containing the platform. Data are expressed as mean ± SEM. $n = 6$ for each group. The changes in escape latency and swimming speed were first evaluated using repeated measures, then comparisons between the two groups were analyzed using Student's *t*-test, which is also used for others. $^{**}p < 0.01$, $^{***}p < 0.001$, $^{****}p < 0.0001$ vs. sham group.

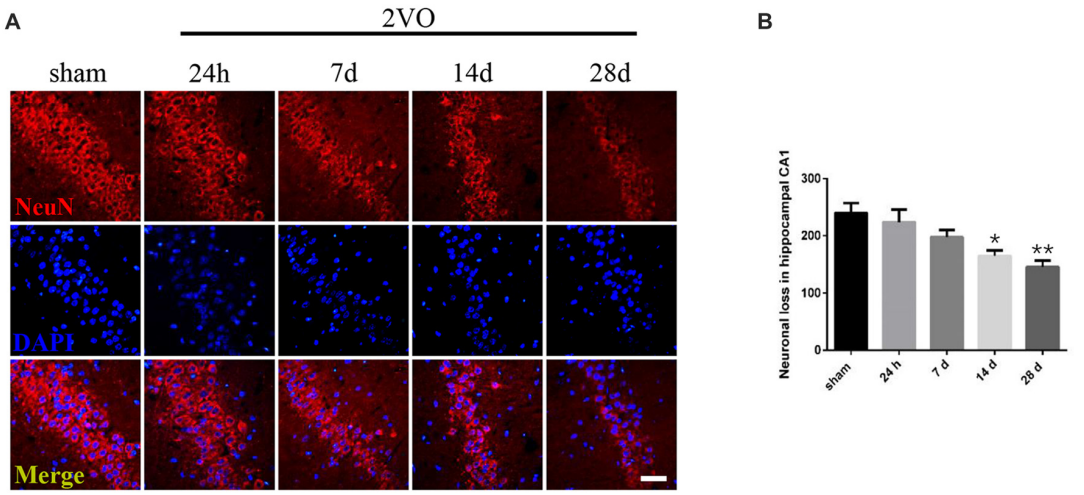

FIGURE 2 | Neuronal loss in the hippocampal CA1 subarea at different time points during Chronic Cerebral Hypoperfusion (CCH). **(A)** Neuronal nuclei (NeuN) immunostaining in the sham group and in the 2VO group (24 h, 7 days, 14 days, 28 days). Horizontal bar = 50 μm. **(B)** The quantification of NeuN-positive cells. Data are expressed as mean ± SEM. $n = 6$ for each group. Multiple comparisons were evaluated using one-way ANOVA. Individual comparisons were analyzed by *post hoc* Bonferroni's test. $^{*}p < 0.05$, $^{**}p < 0.01$ vs. sham group.

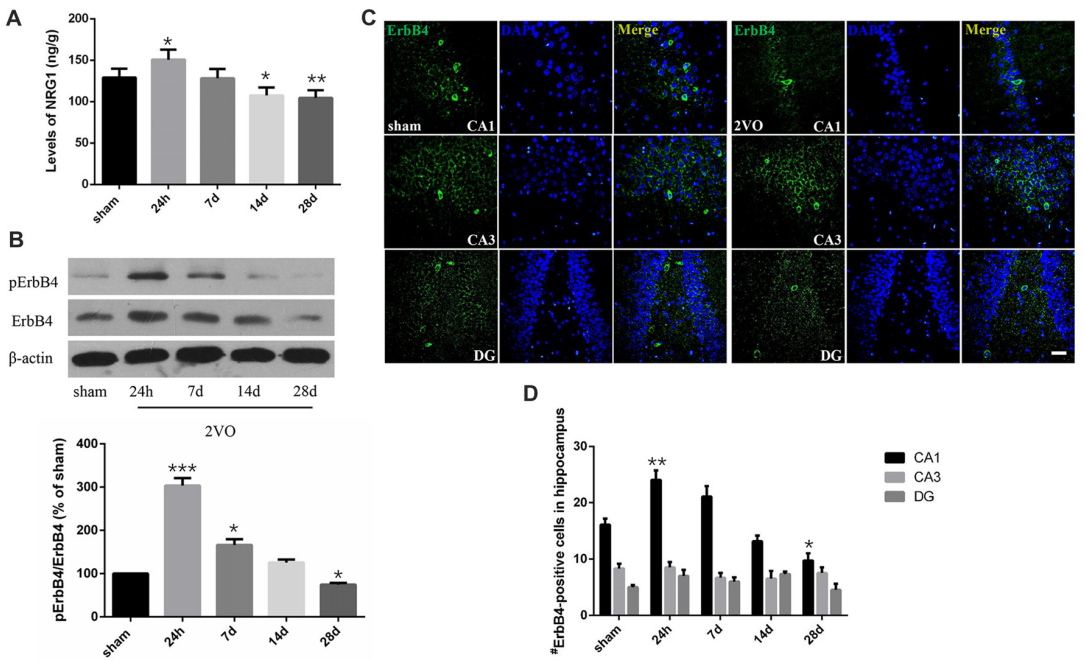

FIGURE 3 | Dynamic changes of NRG1 and pErbB4/ErbB4 in hippocampal CA1 subarea at different time points during CCH. **(A)** The concentration of NRG1 detected by Enzyme-Linked Immunosorbent Assay (ELISA). **(B)** Relative protein expression and the quantification of pErbB4/ErbB4. Densities were normalized to β-actin and the value for the sham group was defined as 100%. **(C)** Representative images of ErbB4-immunostaining in the hippocampal subareas. Horizontal bar = 50 μm. **(D)** Quantification of ErbB4-positive cells. The data are expressed as mean ± SEM. For ELISA, western blotting and immunostaining, $n = 6$ for each group. Multiple comparisons were evaluated using one-way ANOVA. Individual comparisons were analyzed by *post hoc* Bonferroni's test. $^{*}p < 0.05$, $^{**}p < 0.01$, $^{***}p < 0.001$ vs. sham group.

($P = 0.0173 < 0.05$), and then gradually decreased from day 7 to day 28 ($P = 0.0141 < 0.05$ for 14 days; $P = 0.0043 < 0.01$ for 28 days). For western blotting, similarly, the relative protein levels of pErbB4/ErbB4 in the 2VO group increased at 24 h ($P = 0.0002 < 0.001$) and 7 days ($P = 0.0381 < 0.05$) compared to that of the sham group, and gradually reduced later

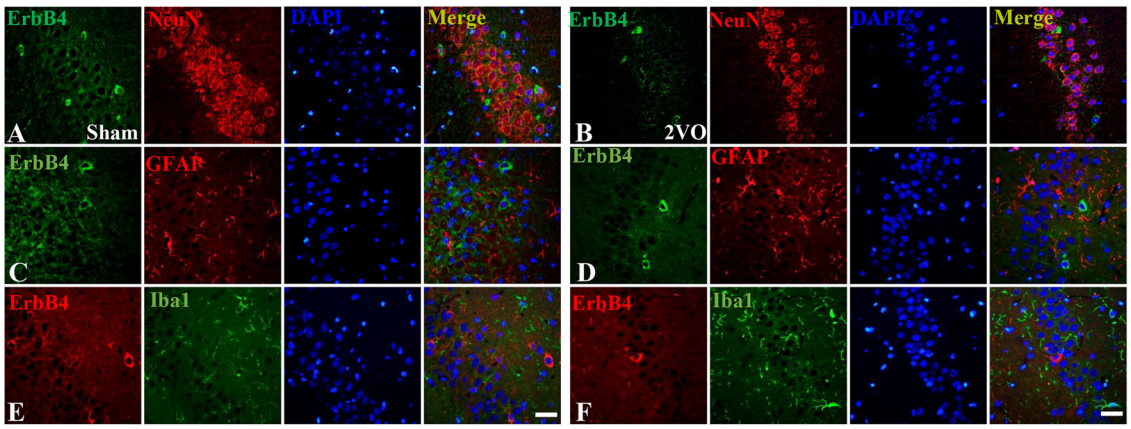

FIGURE 4 | The co-localization of ErbB4 with neurons, microglia and astrocytes at 28 days. The representative images in the sham group are listed in the left four columns **(A,C,E)** and the images in the 2VO group are listed in the right **(B,D,F)**. Horizontal bar = 50 μm. Note that ErbB4 is mainly expressed in NeuN-positive cells.

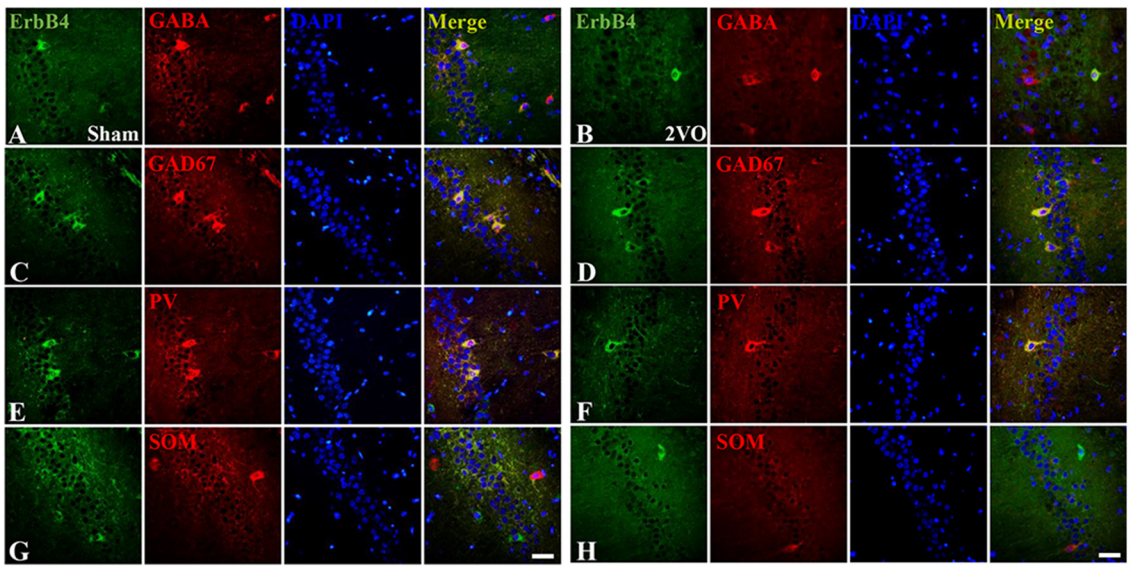

FIGURE 5 | The co-localization of ErbB4 with GABAergic cells (GABA, GAD67, Parvalbumin (PV) and Somatostatin (SOM)) at 28 days. The representative images in the sham group are listed in the left four columns **(A,C,E,G)** and the images in the 2VO group are listed in the right **(B,D,F,H)**. Horizontal bar = 50 μm. Note that ErbB4 is expressed in GABA, GAD67 and PV-positive cells, but not in SOM-positive cells.

($P = 0.0130 < 0.05$ at 28 days). Meanwhile, the population of ErbB4-positive cells in the hippocampal CA1 subarea in the 2VO group remarkably increased at 24 h compared to the sham group ($P = 0.0056 < 0.01$), and then significantly reduced on day 28 ($P = 0.0393 < 0.05$) in comparison to the sham group. However, no significant difference was found in regard to CA3 and DG.

The Distribution of ErbB4 in Hippocampal CA1 Subarea in 2VO Rats

First, we investigated the co-expression of ErbB4 and the main cell-types in the brain including neurons, microglia and astrocytes on day 28 (**Figure 4**). Double-immunofluorescence revealed that ErbB4 was largely expressed in the NeuN-positive cells, but rarely in Iba1 and GFAP-positive cells, indicating that the ErbB4 expression was mainly located in neurons. To further determine the distribution of ErbB4 in GABAergic cell types, GABA, GAD67, PV and SOM antibodies were used here (**Figure 5**). As expected, ErbB4 is largely expressed in the GAD67 and PV-positive cells, but rarely expressed in SOM-positive cells in the hippocampal CA1 subarea. In addition, the difference of expression patterns between the sham group and the 2VO group was analyzed using Student's *t*-test (**Figure 6A**) and no significant difference was found between the two groups, indicating that the co-expression pattern of ErbB4 remained unchanged during CCH. Furthermore, ErbB4 expressed neurons ($P = 0.0411 < 0.05$) and GABAergic cells ($P = 0.0091 < 0.01$ for

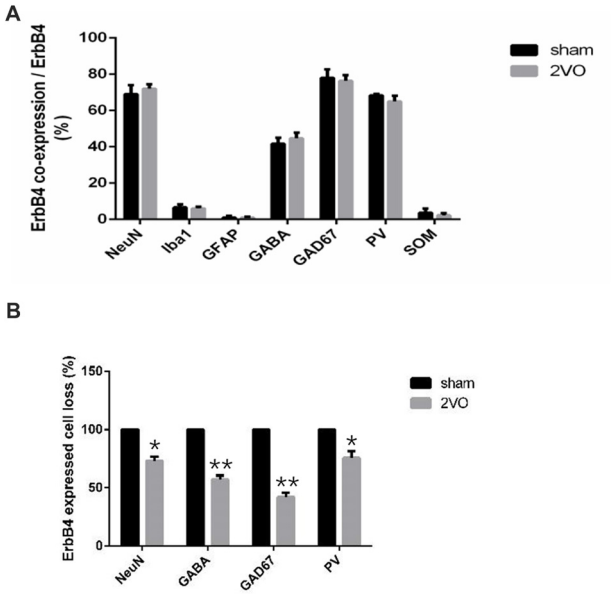

FIGURE 6 | The distribution pattern of ErbB4 in the hippocampal CA1 subarea after CCH. **(A)** Comparison of the co-expression pattern of ErbB4 between the sham group and the 2VO group at 28 days. No significant difference was found between the two groups. **(B)** The quantification of ErbB4-expressed cell loss (NeuN, GABA, GAD67, PV) at 28 days. The value for the sham group was defined as 100%. Data are expressed as mean ± SEM. Comparisons in the two groups ($n = 6$ for each group) were analyzed by Student's *t*-test. $^{*}p < 0.05$, $^{**}p < 0.01$ vs. sham group.

GABA; $P = 0.0071 < 0.01$ for GAD67; $P = 0.0233 < 0.05$ for PV) in the 2VO group significantly reduced at 28 days compared to the sham group (**Figure 6B**), which may contribute to the decreased expression of hippocampal ErbB4 in 2VO rats.

The Expression of NRG1/ErbB4 Directly Correlated With Neuronal Apoptosis, But Not With Glial Activation During CCH

We analyzed the dynamic changes of NeuN/TUNEL, Iba1 and GFAP-positive cells at different time points (**Figure 7**). The level of NeuN/TUNEL positive cells significantly increased and peaked at 24 h ($P < 0.0001$ vs. sham group), and then remained high after that ($P < 0.0001$ for 7 days; $P = 0.0002 < 0.001$ for 14 days; $P = 0.0006 < 0.001$ for 28 days). For glial activation, similarly, the positive cells dramatically increased and peaked at 24 h in the 2VO group (Iba1: $P < 0.0001$ vs. sham group; GFAP: $P < 0.0001$ vs. sham group), and then remained at a relatively high level (Iba1: $P < 0.0001$ for 7 days and 28 days, $P = 0.0014 < 0.01$ for 14 days; GFAP: $P < 0.0001$ for 7 days, $P = 0.0068 < 0.01$ for 14 days).

Pearson's correlation was used here to detect the possible relationship between the expression of hippocampal CA1 NRG1/ErbB4 and neuronal apoptosis and glial activation. The concentration of NRG1 and the numbers of immunostained cells in the hippocampal CA1 subarea counted at different time points (24 h, 7 days, 14 days, 28 days) were analyzed (**Table 1**). Interestingly, both the concentration of NRG1 and the number of ErbB4 immunostained cells were positively correlated with TUNEL-positive cells (NRG1: $r = 0.869$, $P < 0.05$; ErbB4: $r = 0.859$, $P < 0.05$), but no significant results were found in regard to Iba1 or GFAP ($P > 0.05$).

Since positive correlation exists between the NRG1/ErbB4 expression and TUNEL/NeuN positive cell counts, we further performed caspase activity assay to validate the role of NRG1/ErbB4 in hippocampal apoptosis (**Figure 8**). And we found the caspase-3, -8 and -9 activities peaked at 24 h post-operation ($P < 0.001$) compared to the sham group and gradually decreased after that. The temporal profile of caspase activation seemed to coincide with the expression of NRG1/ErbB4 and Pearson's correlation further revealed that caspase-3 activity positively correlated with the levels of NRG1 ($r = 0.671$, $P < 0.05$).

DISCUSSION

Numerous studies have demonstrated the neuroprotective and anti-inflammatory effects of NRG1, and even reported improved cognitive function after NRG1 administration (Guan et al., 2015; Lu et al., 2016). And in the present study, we explored the expression pattern of hippocampal NRG1/ErbB4 during CCH and its possible relationship with neuronal apoptosis and glial activation. We found that: (1) the expression of NRG1 and pErbB4/ErbB4 peaked in the acute phase and then decreased in the chronic phase of CCH; (2) ErbB4 expressed neurons and selective types of GABAergic cells decreased after CCH, but the distribution pattern of ErbB4 remained unchanged; and (3) the expression of hippocampal NRG1/ErbB4 positively correlated with the degree of neuronal apoptosis (both NeuN/TUNEL immunostaining and caspase-3 activity), but not with glial activation according to Pearson's correlation.

To begin with, thorough analysis of the expression pattern of NRG1/ErbB4 in the hippocampal CA1 subarea is crucial for us to explore their possible involvement in the pathogenesis of CCH. According to the previous studies, the expression of NRG1 and ErbB4 receptors significantly increased in the acute phase in cerebral ischemia (24 h after surgery) and in traumatic brain injury (Erlich et al., 2000; Tokita et al., 2001). Meanwhile, a number of studies have also reported down-regulated expression of NRG1/ErbB4 signaling in sepsis-associated encephalopathy (SAE) 20 days after model establishment (Gao et al., 2017). In agreement of these studies, here we found that hippocampal CA1 NRG1 and pErbB4/ErbB4 expression changed in a time-dependent manner during CCH. Lu et al. (2016) recently reported the decreased expression of membrane ErbB4 receptors in neurons in cerebral ischemia, suggesting that recruitment or translocation of ErbB4 stimulated by NRG1 treatment is disrupted (Ma et al., 2003). Therefore, the specific location of ErbB4 should be noted too.

It is known that EGF and NRG1's actions on GABAergic neurons are inconsistent among the ErbB ligands (Namba et al., 2006; Nagano et al., 2007). More specifically, exogenous EGF administration can reduce the expression of GAD67 and PV in neocortical cultures (Nawa et al., 2014), while NRG1/ErbB4 signaling seems to improve the development

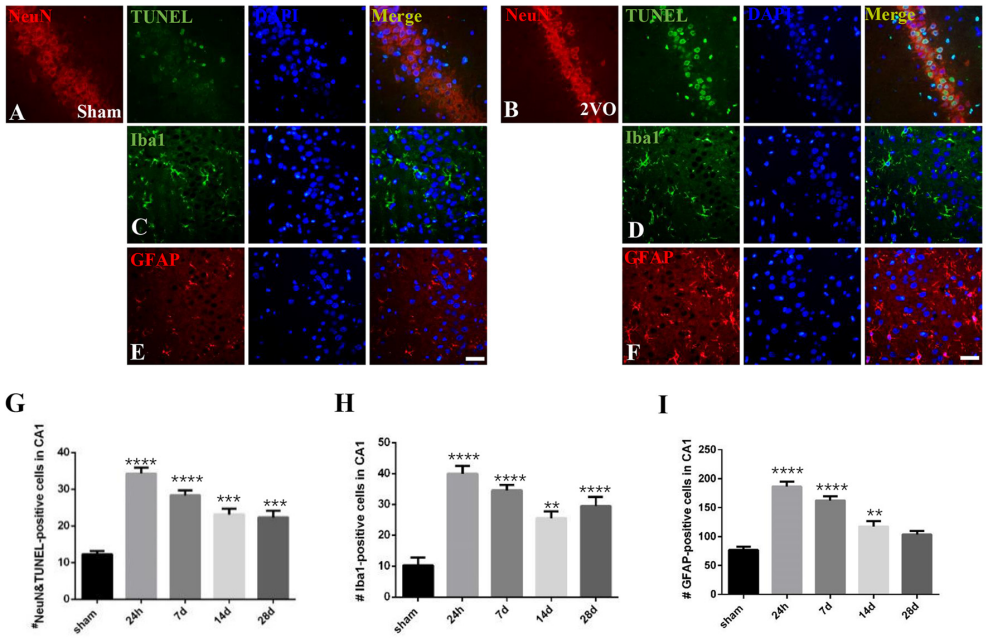

FIGURE 7 | The dynamic changes of neuronal apoptosis and glial activation during CCH. **(A–F)** Representative images of ErbB4/TUNEL, NeuN/TUNEL, Iba1 and GFAP-positive cells in the sham group (left) and 2VO group (right) at 28 days. Horizontal bar = 50 μm. **(G–I)** The quantification of NeuN/TUNEL, Iba1 and GFAP-positive cells at different time points. The data are expressed as mean ± SEM. $n = 6$ for each group. Multiple comparisons were evaluated using one-way ANOVA. Individual comparisons were analyzed by *post hoc* Bonferroni's test. $^{**}p < 0.01$, $^{***}p < 0.001$, $^{****}p < 0.0001$ vs. sham group.

TABLE 1 | The concentration of Neuregulin1 (NRG1) (detected by Enzyme-Linked Immunosorbent Assay (ELISA)) and the number of immunostained cells (hippocampal CA1 subarea) during chronic cerebral hypoperfusion (CCH).

Time point	NRG1 (ng/g)[a]	ErbB4[b]	NeuN & TUNEL[c]	Iba1[d]	GFAP[e]
Sham	129.33 ± 4.10	16.12 ± 0.79	12.33 ± 0.81	10.23 ± 1.157	77.00 ± 5.20
24 h	150.72 ± 4.98	24.06 ± 1.70	34.33 ± 1.54	39.95 ± 2.47	186.30 ± 8.86
7 days	128.31 ± 4.49	21.10 ± 1.85	28.33 ± 1.33	34.57 ± 1.79	162.31 ± 6.98
14 days	107.53 ± 3.97	13.12 ± 1.01	23.17 ± 1.54	25.50 ± 2.19	117.49 ± 9.52
28 days	104.71 ± 3.72	9.74 ± 1.29	22.33 ± 1.86	29.47 ± 2.90	103.69 ± 6.15

Data are expressed as mean ± SEM. n = 6 for each group. Pearson's correlational analysis showed significant results between [a] and [c] ($r = 0.869$, $P < 0.05$), [b] and [c] ($r = 0.859$, $P < 0.05$). But no significant correlation was found between [a] and [d] ($r = 0.020$, $P > 0.05$), [b] and [d] ($r = 0.078$, $P > 0.05$), [a] and [e] ($P > 0.05$), [b] and [e] ($P > 0.05$).

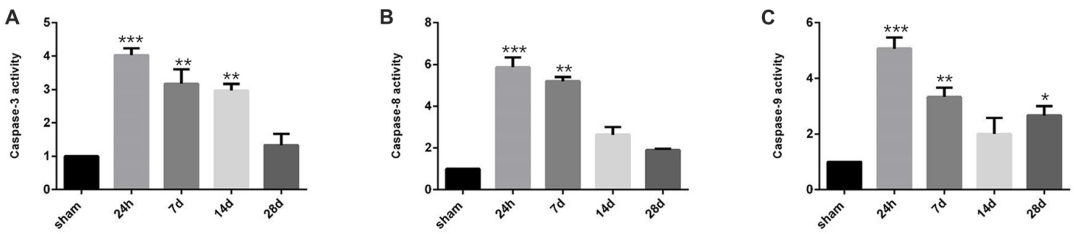

FIGURE 8 | Caspase activity in the hippocampal CA1 subarea at different time points during CCH. **(A)** The quantification of caspase-3 activity. **(B)** The quantification of caspase-8 activity. **(C)** The quantification of caspase-9 activity. Data are expressed as mean ± SEM. $n = 6$ for each group. The values in the sham group was defined as 100%. Multiple comparisons were evaluated using one-way ANOVA. Individual comparisons were analyzed by *post hoc* Bonferroni's test. $^{*}p < 0.05$, $^{**}p < 0.01$, $^{***}p < 0.001$ vs. sham group.

of GABAergic cells. We further analyzed the hippocampal expression of EGF and ErbB1 using ELISA and western blotting respectively (see details in the **Supplementary Figure S1**) and observed the up-regulation of EGF and ErbB1 expression during CCH, which is consistent with the previous research (Ashok et al., 2016). In view of the opposite changes of NRG1/ErbB4 and EGF/ErbB1, the expression of hippocampal NRG1/ErbB4 seems to be more directly linked with cognitive deficits in CCH.

By the way, since the protein levels of NRG1 and ErbB4 in the hippocampus changed after 2VO surgery in our study, the transcription/translation level of them could probably present corresponding changes as well. As far as we know, the mRNA levels of NRG1 and ErbB4 have not been investigated during CCH, but similar changes have been reported in other animal models of neurodegenerative diseases (Croll et al., 1998; Dickerson et al., 2009). Interestingly, Dickerson et al. (2009) reported that the ErbB4 mRNA transcripts in rat brain selectively decreased prior to other biochemical changes in aged rats, indicating that the change of ErbB4 in translation level, rather than the protein level, can predict functional changes in neurodegenerative disorders. Therefore, time-dependent changes of NRG1/ErbB4 mRNA levels should be systematically investigated in the future.

Emerging evidence has showed the protective role of NRG1/ErbB4 in neuronal and non-neuronal cells in the hippocampal subareas (Shyu et al., 2004; Simmons et al., 2016). To further determine the role of NRG1/ErbB4 signaling on different cell types, we performed double-immunofluorescence to investigate the distribution of ErbB4 receptors and found that ErbB4 largely co-expressed in neurons (NeuN-positive cells), especially selective subtypes of GABAergic interneurons (GAD67 and PV-positive cells, but not in SOM-positive cells) in the hippocampal CA1 region. These findings were consistent with others (Neddens and Buonanno, 2010; Vullhorst et al., 2009; Li et al., 2014). Besides, we found the distribution of ErbB4 remained unchanged during CCH, while the ErbB4 expressed neurons and selective types of GABAergic cells significantly decreased in the chronic phase of CCH. In fact, we have counted the GABAergic cells in hippocampal CA1 subarea in CCH before and found decreased expression of GABA, GAD67 and $GABA_BRs$ in hippocampal CA1 region (Long et al., 2015). It is likely that the remarkable decrease of ErbB4 expression in the chronic phase is caused by the reduction of these neurons and GABAergic cells (especially GAD67 and PV).

The long-lasting cognitive impairments, as well as improved degrees of hippocampal CA1 neuronal apoptosis and neuroinflammation, in CCH have been well-established over the years (Cechetti et al., 2012; Du et al., 2017), but there are still some details that should be addressed in this study. First, Ji et al. (2010) reported that the expression of hippocampal NRG1/ErbB4 significantly reduced during spatial learning tests (Tian et al., 2016). Therefore, rats that underwent cognitive tests (WMW and RAWM) in this study were not used for biochemical analysis. Second, increased neuronal death and glial activation in CCH have been reported to present early at 7 days post-operation and continue for long (Cechetti et al., 2012). However, some of the molecular changes in the hippocampus seem to change in a different way. For example, the expression of anti-apoptotic factors (such as Bcl-2) was reported to increase only in the acute phase, followed by a remarkable reduction in the chronic phase of CCH (Bang et al., 2013; Yang et al., 2013). We also found transiently increased expression of NRG1/ErbB4 signaling in the current study. The mismatch of these factors in the chronic phase of CCH may further contribute to cognitive impairment and neuropathologic changes during CCH.

Although the mismatch occurs between the NRG1/ErbB4 expression and neuropathologic changes in the chronic phase of CCH, all these factors seemed to increase in the acute phase, and then gradually decreased later during CCH. Pearson's correlation in our study further revealed that both the expression of NRG1 and ErbB4 positively correlated with NeuN/TUNEL cell counts during CCH. Besides, delayed hippocampal neuronal death after CCH is mediated, at least in part, through the activation of terminal caspases, particularly caspase-3 (Ji et al., 2010). Caspase-8 and caspase-9 probably mediate the activation of caspase-3 under an ischemic condition via extrinsic and intrinsic pathways respectively (Cao et al., 2002). Consistently, we found up-regulated expression of caspase activities and positive correlation between caspase-3 activity and NRG1 expression. Taken together, our results suggest the protective role of NRG1/ErbB4 signaling in CCH is closely related to direct inhibition of neuronal apoptosis, thus providing a friendly environment for cognitive improvement.

By the way, some studies have demonstrated that NRG1/ErbB signaling could improve proliferation in microglia and astrocytes (Calvo et al., 2011; Simmons et al., 2016), while both we and others found that only a few ErbB4 receptors co-expressed in glial cells, especially GFAP-positive astrocytes (Xu and Ford, 2005). Furthermore, Ghashghaei et al. (2006) further reported that these cells do not respond to exogenous NRG1 infusion in the brain. These findings may explain the reason the NRG1/ErbB4 signaling failed to correlate with glial activation. Finally, in order to further determine the neuroprotective effects of NRG1/ErbB4 signaling during CCH, the bilateral regulation of NRG1/ErbB4 signaling using an agonist/antagonist and ErbB4 knockout rats can be more useful.

AUTHOR CONTRIBUTIONS

YH and RC, performed the experiments, analyzed the data and drafted the manuscript. QL and WL, designed the experiments and approved the final manuscript. LW and XY, contributed reagents/materials/analysis tools. All authors read and approved the final manuscript.

FUNDING

This research was supported by Natural Science Foundation of China (No. 81627806).

SUPPLEMENTARY MATERIAL

The Supplementary Material for this article can be found online at: https://www.frontiersin.org/articles/10.3389/fnagi.2018.00149/full#supplementary-material

FIGURE S1 | Analysis of the hippocampal expression of epidermal growth factor (EGF) and ErbB1 using Enzyme-Linked Immunosorbent Assay (ELISA) and western blotting.

REFERENCES

Anastacio, J. R., Netto, C. A., Castro, C. C., Sanches, E. F., Ferreira, D. C., Noschang, C., et al. (2014). Resveratrol treatment has neuroprotective effects and prevents cognitive impairment after chronic cerebral hypoperfusion. *Neurol. Res.* 36, 627–633. doi: 10.1179/1743132813y.0000000293

Ashok, A., Rai, N. K., Raza, W., Pandey, R., and Bandyopadhyay, S. (2016). Chronic cerebral hypoperfusion-induced impairment of Aβ clearance requires HB-EGF-dependent sequential activation of HIF1α and MMP9. *Neurobiol. Dis.* 95, 179–193. doi: 10.1016/j.nbd.2016.07.013

Bang, J., Jeon, W. K., Lee, I. S., Han, J. S., and Kim, B. Y. (2013). Biphasic functional regulation in hippocampus of rat with chronic cerebral hypoperfusion induced by permanent occlusion of bilateral common carotid artery. *PLoS One* 8:e70093. doi: 10.1371/journal.pone.0070093

Bennett, S. A., Tenniswood, M., Chen, J. H., Davidson, C. M., Keyes, M. T., Fortin, T., et al. (1998). Chronic cerebral hypoperfusion elicits neuronal apoptosis and behavioral impairment. *Neuroreport* 9, 161–166. doi: 10.1097/00001756-199801050-00033

Calvo, M., Zhu, N., Grist, J., Ma, Z., Loeb, J. A., and Bennett, D. L. (2011). Following nerve injury neuregulin-1 drives microglial proliferation and neuropathic pain via the MEK/ERK pathway. *Glia* 59, 554–568. doi: 10.1002/glia.21124

Cao, G., Luo, Y., Nagayama, T., Pei, W., Stetler, R. A., Graham, S. H., et al. (2002). Cloning and characterization of rat caspase-9: implications for a role in mediating caspase-3 activation and hippocampal cell death after transient cerebral ischemia. *J. Cereb. Blood Flow. Metab.* 22, 534–546. doi: 10.1097/00004647-200205000-00005

Cechetti, F., Pagnussat, A. S., Worm, P. V., Elsner, V. R., Ben, J., Da, C. M., et al. (2012). Chronic brain hypoperfusion causes early glial activation and neuronal death and subsequent long-term memory impairment. *Brain Res. Bull.* 87, 109–116. doi: 10.1016/j.brainresbull.2011.10.006

Chen, Y. J., Zhang, M., Yin, D. M., Wen, L., Ting, A., Wang, P., et al. (2010). ErbB4 in parvalbumin-positive interneurons is critical for neuregulin 1 regulation of long-term potentiation. *Proc. Natl. Acad. Sci. U S A* 107, 21818–21823. doi: 10.1073/pnas.1010669107

Croll, S. D., Ip, N. Y., Lindsay, R. M., and Wiegand, S. J. (1998). Expression of BDNF and trkB as a function of age and cognitive performance. *Brain Res.* 812, 200–208. doi: 10.1016/s0006-8993(98)00993-7

David, M., Sahay, D., Mege, F., Descotes, F., Leblanc, R., Ribeiro, J., et al. (2014). Identification of heparin-binding EGF-like growth factor (HB-EGF) as a biomarker for lysophosphatidic acid receptor type 1 (LPA1) activation in human breast and prostate cancers. *PLoS One* 9:e97771. doi: 10.1371/journal.pone.0097771

Dickerson, J. W., Hemmerle, A. M., Numan, S., Lundgren, K. H., and Seroogy, K. B. (2009). Decreased expression of ErbB4 and tyrosine hydroxylase mRNA and protein in the ventral midbrain of aged rats. *Neuroscience* 163, 482–489. doi: 10.1016/j.neuroscience.2009.06.008

Du, S., Wang, X., Xiao, L., Tu, J., Zhu, W., He, T., et al. (2017). Molecular mechanisms of vascular dementia: what can be learned from animal models of chronic cerebral hypoperfusion? *Mol. Neurobiol.* 54, 3670–3682. doi: 10.1007/s12035-016-9915-1

Ercan, S., Kencebay, C., Basaranlar, G., Derin, N., and Aslan, M. (2015). Induction of xanthine oxidase activity, endoplasmic reticulum stress and caspase activation by sodium metabisulfite in rat liver and their attenuation by Ghrelin. *Food Chem. Toxicol.* 76, 27–32. doi: 10.1016/j.fct.2014.11.021

Erlich, S., Shohami, E., and Pinkas-Kramarski, R. (2000). Closed head injury induces up-regulation of ErbB-4 receptor at the site of injury. *Mol. Cell. Neurosci.* 16, 597–608. doi: 10.1006/mcne.2000.0894

Farkas, E., Luiten, P. G. M., and Bari, F. (2007). Permanent, bilateral common carotid artery occlusion in the rat: A model for chronic cerebral hypoperfusion-related neurodegenerative diseases. *Brain Res. Rev.* 54, 162–180. doi: 10.1016/j.brainresrev.2007.01.003

Gao, R., Ji, M., Gao, D., Yang, R., Zhang, S., Yang, J., et al. (2017). Neuroinflammation-induced downregulation of hippocampacal neuregulin 1-ErbB4 signaling in the parvalbumin interneurons might contribute to cognitive impairment in a mouse model of sepsis-associated encephalopathy. *Inflammation* 40, 387–400. doi: 10.1007/s10753-016-0484-2

Ghashghaei, H. T., Weber, J., Pevny, L., Schmid, R., Schwab, M. H., Lloyd, K. C., et al. (2006). The role of neuregulin-ErbB4 interactions on the proliferation and organization of cells in the subventricular zone. *Proc Natl Acad Sci U S A* 103, 1930–1935. doi: 10.1073/pnas.0510410103

Guan, Y. F., Wu, C. Y., Fang, Y. Y., Zeng, Y. N., Luo, Z. Y., Li, S. J., et al. (2015). Neuregulin 1 protects against ischemic brain injury via ErbB4 receptors by increasing GABAergic transmission. *Neuroscience* 307, 151–159. doi: 10.1016/j.neuroscience.2015.08.047

Ji, H. J., Hu, J. F., Wang, Y. H., Chen, X. Y., Zhou, R., and Chen, N. H. (2010). Osthole improves chronic cerebral hypoperfusion induced cognitive deficits and neuronal damage in hippocampus. *Eur. J. Pharmacol.* 636, 96–101. doi: 10.1016/j.ejphar.2010.03.038

Kwon, K. J., Lee, E. J., Kim, M. K., Kim, S. Y., Kim, J. N., Kim, J. O., et al. (2015). Diabetes augments cognitive dysfunction in chronic cerebral hypoperfusion by increasing neuronal cell death: implication of cilostazol for diabetes mellitus-induced dementia. *Neurobiol. Dis.* 73, 12–23. doi: 10.1016/j.nbd.2014.08.034

Li, X., Su, F., Ji, M., Zhang, G., Qiu, L., Jia, M., et al. (2014). Disruption of hippocampal neuregulin 1-ErbB4 signaling contributes to the hippocampus-dependent cognitive impairment induced by isoflurane in aged mice. *Anesthesiology* 121, 79–88. doi: 10.1097/aln.0000000000000191

Liu, L., Li, C. J., Lu, Y., Zong, X. G., Luo, C., Sun, J., et al. (2015). Baclofen mediates neuroprotection on hippocampal CA1 pyramidal cells through the regulation of autophagy under chronic cerebral hypoperfusion. *Sci. Rep.* 5:14474. doi: 10.1038/srep14474

Long, Q., Hei, Y., Luo, Q., Tian, Y., Yang, J., Li, J., et al. (2015). BMSCs transplantation improves cognitive impairment via up-regulation of hippocampal GABAergic system in a rat model of chronic cerebral hypoperfusion. *Neuroscience* 311, 464–473. doi: 10.1016/j.neuroscience.2015.10.055

Lu, Y., Gao, Y., Tao, R., Liao, M., Huang, J., Wu, G., et al. (2016). Calpain-dependent ErbB4 cleavage is involved in brain ischemia-induced neuronal death. *Mol. Neurobiol.* 53, 2600–2609. doi: 10.1007/s12035-015-9275-2

Ma, L., Huang, Y. Z., Pitcher, G. M., Valtschanoff, J. G., Ma, Y. H., Feng, L. Y., et al. (2003). Ligand-dependent recruitment of the ErbB4 signaling complex into neuronal lipid rafts. *J. Neurosci.* 23, 3164–3175. doi: 10.1523/jneurosci.23-08-03164.2003

Mei, L., and Xiong, W. C. (2008). Neuregulin 1 in neural development, synaptic plasticity and schizophrenia. *Nat. Rev. Neurosci.* 9, 437–452. doi: 10.1038/nrn2392

Murray, A. J., Sauer, J., Riedel, G., McClure, C., Ansel, L., Cheyne, L., et al. (2011). Parvalbumin-positive CA1 interneurons are required for spatial working but not for reference memory. *Nat. Neurosci.* 14, 297–299. doi: 10.1038/nn.2751

Nagano, T., Namba, H., Abe, Y., Aoki, H., Takei, N., and Nawa, H. (2007). *In vivo* administration of epidermal growth factor and its homologue attenuates developmental maturation of functional excitatory synapses in cortical GABAergic neurons. *Eur. J. Neurosci.* 25, 380–390. doi: 10.1111/j.1460-9568.2007.05297.x

Namba, H., Nagano, T., Iwakura, Y., Xiong, H., Jourdi, H., Takei, N., et al. (2006). Transforming growth factor alpha attenuates the functional expression of AMPA receptors in cortical GABAergic neurons. *Mol. Cell. Neurosci.* 31, 628–641. doi: 10.1016/j.mcn.2005.12.002

Nawa, H., Sotoyama, H., Iwakura, Y., Takei, N., and Namba, H. (2014). Neuropathologic implication of peripheral neuregulin-1 and EGF signals in dopaminergic dysfunction and behavioral deficits relevant to schizophrenia: their target cells and time window. *Biomed Res. Int.* 2014:697935. doi: 10.1155/2014/697935

Neddens, J., and Buonanno, A. (2010). Selective populations of hippocampal interneurons express ErbB4 and their number and distribution is altered in ErbB4 knockout mice. *Hippocampus* 20, 724–744. doi: 10.1002/hipo.20675

Paxinos, G., and Watson, C. (2005). *The Rat Brain in Sterotaxic Coordinates*, 5th Edn. Cambridge, MA: Academic Press

Penley, S. C., Gaudet, C. M., and Threlkeld, S. W. (2013). Use of an eight-arm Radial water maze to assess working and reference memory following neonatal brain injury. *J. Vis. Exp.* 82:50940. doi: 10.3791/50940

Rong, L., Ding, K., Zhang, M., and Guo, Y. (2015). Neuregulin1beta improves cognitive dysfunction and up-regulates expression of p-ERK1/2 in rats with chronic omethoate poisoning. *Behav. Brain Funct.* 11:5. doi: 10.1186/s12993-014-0050-8

Ryu, J., Hong, B., Kim, Y., Yang, E., Choi, M., Kim, H., et al. (2016). Neuregulin-1 attenuates cognitive function impairments in a transgenic mouse model of Alzheimer's disease. *Cell Death Dis.* 7:e2117. doi: 10.1038/cddis.2016.30

Shyu, W., Lin, S., Chiang, M., Yang, H., Thajeb, P., and Li, H. (2004). Neuregulin-1 reduces ischemia-induced brain damage in rats. *Neurobiol. Aging* 25, 935–944. doi: 10.1016/j.neurobiolaging.2003.10.012

Simmons, L. J., Surles-Zeigler, M. C., Li, Y., Ford, G. D., Newman, G. D., and Ford, B. D. (2016). Regulation of inflammatory responses by neuregulin-1 in brain ischemia and microglial cells *in vitro* involves the NF-κB pathway. *J. Neuroinflammation* 13:237. doi: 10.1186/s12974-016-0703-7

Tan, G. H., Liu, Y. Y., Hu, X. L., Yin, D. M., Mei, L., and Xiong, Z. Q. (2011). Neuregulin 1 represses limbic epileptogenesis through ErbB4 in parvalbumin-expressing interneurons. *Nat. Neurosci.* 15, 258–266. doi: 10.1038/nn.3005

Tian, J., Geng, F., Gao, F., Chen, Y., Liu, J., Wu, J., et al. (2016). Down-regulation of neuregulin1/ErbB4 signaling in the hippocampus is critical for learning and memory. *Mol. Neurobiol.* 54, 3976–3987. doi: 10.1007/s12035-016-9956-5

Tokita, Y., Keino, H., Matsui, F., Aono, S., Ishiguro, H., Higashiyama, S., et al. (2001). Regulation of neuregulin expression in the injured rat brain and cultured astrocytes. *J. Neurosci.* 21, 1257–1264.

Vullhorst, D., Neddens, J., Karavanova, I., Tricoire, L., Petralia, R. S., McBain, C. J., et al. (2009). Selective expression of ErbB4 in interneurons, but not pyramidal cells, of the rodent hippocampus. *J. Neurosci.* 29, 12255–12264. doi: 10.1523/jneurosci.2454-09.2009

Wu, L., Walas, S. J., Leung, W., Lo, E. H., and Lok, J. (2015). Neuregulin-1 and neurovascular protection.

Xi, Y., Wang, M., Zhang, W., Bai, M., Du, Y., Zhang, Z., et al. (2014). Neuronal damage, central cholinergic dysfunction and oxidative damage correlate with cognitive deficits in rats with chronic cerebral hypoperfusion. *Neurobiol. Learn. Mem.* 109, 7–19. doi: 10.1016/j.nlm.2013.11.016

Xu, Z., and Ford, B. D. (2005). Upregulation of ErbB receptors in rat brain after middle cerebral arterial occlusion. *Neurosci. Lett.* 375, 181–186. doi: 10.1016/j.neulet.2004.11.039

Yang, Y., Zhang, J., Liu, H., Wang, J., Xin, J., and Deng, M. (2013). Changes in levels of hypoxia-induced mediators in rat hippocampus during chronic cerebral hypoperfusion. *Neurochem. Res.* 38, 2433–2439. doi: 10.1007/s11064-013-1158-1

Yang, Z., Zhang, N., Shen, H., Lin, C., Lin, L., and Yuan, B. (2014). Microglial activation with reduction in autophagy limits white matter lesions and improves cognitive defects during cerebral hypoperfusion. *Curr. Neurovasc. Res.* 11, 223–229. doi: 10.2174/1567202611666140520124407

Zhang, H., Zhang, L., Zhou, D., He, X., Wang, D., Pan, H., et al. (2017). Ablating ErbB4 in PV neurons attenuates synaptic and cognitive deficits in an animal model of Alzheimer's disease. *Neurobiol. Dis.* 106, 171–180. doi: 10.1016/j.nbd.2017.07.001

Zhao, Y., and Gong, C. X. (2015). From chronic cerebral hypoperfusion to alzheimer-like brain pathology and neurodegeneration. *Cell. Mol. Neurobiol.* 35, 101–110. doi: 10.1007/s10571-014-0127-9

Conflict of Interest Statement: The authors declare that the research was conducted in the absence of any commercial or financial relationships that could be construed as a potential conflict of interest.

frontiers in Aging Neuroscience

GENERAL COMMENTARY
published: 25 June 2018
doi: 10.3389/fnagi.2018.00192

Commentary: Mild endoplasmic reticulum stress ameliorates lpopolysaccharide-induced neuroinflammation and cognitive impairment via regulation of microglial polarization

*Sachchida N. Rai, Walia Zahra, Hareram Birla, Saumitra S. Singh and Surya P. Singh**

Department of Biochemistry, Institute of Science, Banaras Hindu University, Varanasi, India

Keywords: endoplasmic reticulum, lipopolysaccharide, neuroinflammation, cognitive impairment, microglia

A commentary on

Mild endoplasmic reticulum stress ameliorates lipopolysaccharide-induced neuroinflammation and cognitive impairment via regulation of microglial polarization
by Wang, Y. W., Zhou, Q., Zhang, X., Qian, Q. Q., Xu, J. W., Ni, P. F., et al. (2017). J. Neuroinflammation 14:233. doi: 10.1186/s12974-017-1002-7

OPEN ACCESS

Edited by:
Ashok Kumar,
University of Florida, United States

Reviewed by:
Udai Pandey,
University of Pittsburgh Medical Center, United States
Lakshmi Rajagopal,
Northwestern University, United States
Deep R. Sharma,
SUNY Downstate Medical Center, United States

****Correspondence:***
Surya P. Singh
suryasinghbhu16@gmail.com

Received: *29 December 2017*
Accepted: *07 June 2018*
Published: *25 June 2018*

Citation:
Rai SN, Zahra W, Birla H, Singh SS and Singh SP (2018) Commentary: Mild endoplasmic reticulum stress ameliorates lpopolysaccharide-induced neuroinflammation and cognitive impairment via regulation of microglial polarization. Front. Aging Neurosci. 10:192. doi: 10.3389/fnagi.2018.00192

In this article, Wang and colleagues have discussed the non-harmful levels of Endoplasmic reticulum (ER) stress in rats focusing mainly on primary microglia. Specifically, they sought to investigate the regulation of lipopolysaccharide (LPS) driven neuroinflammation in male Sprague-Dawley rats through mild ER-stress (MERS). In experiment 1, to determine the extent of unfolded protein response (UPR), they measured expression of phosphorylated total protein kinase RNA-like ER kinase (p-PERK), phosphorylated eukaryotic translation initiation factor 2α (p-EIF2α), phosphorylated inositol-requiring protein 1α (p-IRE1α), spliced X-box-binding protein-1 (XBP1s), XBP1u, activating transcription factor-4 (ATF4) and CCAAT/enhancer-binding protein homologous protein (CHOP) through western blot and Immunofluorescence (Wang et al., 2017). During ER stress, IRE1α gets phosphorylated & activated and cuts unspliced XBP1u mRNA into spliced XBP1s mRNA which further encodes XBP1 protein (Gardner et al., 2013). They found that expressions of p-IRE1α and XBP1s were considerably increased on administration of different doses of tunicamycin (TM), while the expression of XBP1u was significantly reduced. Expression of hippocampal p-PERK, p-EIF2α, ATF4, and CHOP were also assessed. p-PERK causes phosphorylation of EIF2α (Walter and Ron, 2011; Hetz et al., 2015) which on prolonged phosphorylation induces paradoxical translation of ATF4 mRNA into its corresponding protein, in turn inducing upregulation of pro-apoptotic components such as CHOP (Gardner et al., 2013).

Furthermore, Caspase-3 and cleaved caspase-3 expressions were assessed in the CA1 region of the hippocampus. Increased expression of p-PERK and p-EIF2-α were seen at a range of different doses of TM administration, but ATF4, CHOP and cleaved caspase-3 were only elevated at the highest dose of TM. Thus, the authors concluded that low doses of TM, i.e.; 0.3 and 3 μg/2 μl *in vivo* & 0.5 and 5 ng/ml *in vitro* led to modest UPR without cell or organism lethality as assessed by TUNEL labeling, while the higher concentrations of 30 μg/2 μl *in vivo* and 50 ng/ml *in vitro* have shown serious ER perturbations and a robust UPR. In experiment 2, the authors studied the role of MERS in LPS-induced neuroinflammation and cognitive impairment

in rats. MERS was induced by using 3 μg/2 μl TM and treated with or without sodium 4-phenylbutyrate (a stabilizing agent), an hour before the LPS administration both *in vivo* and *in vitro*. This low dose of TM (3 μg) significantly improved freezing behavior and learning trials, indicating its role in protection against memory dysfunction caused by LPS.

They have also shown that TM prevented neurons from undergoing LPS-induced apoptosis. To clarify whether MERS was responsible for neuroprotective activity of TM, they administered rats with 100 mg/kg 4-Phenylbutyric acid (4-PBA) known to reduce ER stress, which at this dose does not affect normal functioning of nervous system. Treatment with 4-PBA significantly reduced expression levels of p-IRE1α and XBP1s as compared to non-PBA treated groups. Also, neuroprotection conferred by TM was partially blocked by concomitant administration of 4-PBA as revealed by increased numbers of TUNEL-positive cells. Therefore, significant reductions in cognitive function in the TM+LPS+4-PBA group confirmed that low dose of TM protects against LPS-induced cognitive dysfunction by inducing MERS which inhibits caspase-3 activation (Wang et al., 2017). As in neurodegenerative disorders, microglia activation indicates an early sign of neuronal death, thus the authors tried to explore the effect of MERS on microglia *in vitro* by measuring expression of microglial genes associated with classic (M1), alternative repair and regeneration (M2a) and, immunomodulation (M2b) (Tang and Le, 2016). The relative expression of classical M1 genes CD86, CD32 and inducible nitric oxide synthase (iNOS), M2a genes YM1/2 and CD206 and, M2b gene suppressor of cytokine signaling 3 were assessed. LPS was shown to significantly increase mRNA levels of M1 and M2b markers in hippocampus compared with levels in the naïve group, while M2a genes were significantly reduced as compared to the naïve group. Alternatively, TM pretreatment led to alteration in balance of M1 and M2 microglia expression patterns in hippocampus significantly increasing expression of M2a genes and decreasing expression of M1 and M2b genes. Thus, the authors concluded that LPS-induced neuroinflammation was significantly attenuated by MERS, leading to a shift of the microglia population from M1/2b to M2a in hippocampus. Further, the authors also used double immunofluorescent staining of iNOS and CD206 with microglial marker Iba1 in the hippocampal CA1 region, to show that TM inhibited LPS-induced microglia activation and shifted the phenotype of microglia toward M2a.

The authors also detected levels of TNF-α, IL-1β, and IL-6 proinflammatory factors thought to play major role in neuroinflammation. They have seen increased expression of these proinflammatory factors induced by LPS, while TM has significantly reduced this inflammatory response. But, the expression levels of these factors were significantly enhanced after 4-PBA co-treatment through reversal of anti-neuroinflammatory effects of TM. Results were further validated *in vitro* by demonstrating that dose of 5 ng/ml of TM was able to induce MERS in microglial culture. They have confirmed that TM has inhibited cytokine production and induced microglial polarization from M1/2b to M2a. Moreover, 4-PBA led to impairment of anti-inflammatory effects and M2a differentiation conferred by TM.

Since authors talk about neuroinflammation, they must have studied role of MERS on Astrogliosis. NF-kB plays important role in neuroinflammation, hence must have been investigated. The biochemical parameters such as Catalase and Lipid Peroxidation must have been checked in the hippocampal region. Moreover, on Page: 8, in line "LPS significantly increased the mRNA levels of M1 and M2a markers in the hippocampus compared with the levels observed in the naïve group"; there should be M2b instead of M2a.

Thus, MERS has an important role in neuroinflammation and cognitive impairment. Since, ER stress has also been seen in astrocytes, an important cell type that plays a vital role in neurodegenerative disorders through neuroinflammation, the question arises whether MERS in astrocyte in LPS-induced neuroinflammation could also have contributed to the beneficial properties of MERS.

Finally, they reported that MERS preconditioning can alleviate neuroinflammation and cognitive impairment induced by LPS, thereby suggesting that moderate level of ER stress can act as a new therapeutic possibility to suspend or delay progression of neurodegenerative diseases (Wang et al., 2017).

AUTHOR CONTRIBUTIONS

All authors listed have made a substantial, direct and intellectual contribution to the work, and approved it for publication.

REFERENCES

Gardner, B. M., Pincus, D., Gotthardt, K., Gallagher, C. M., and Walter, P. (2013). Endoplasmicreticulum stress sensing in the unfolded protein response. *Csh Perspect. Biol.* 5:a13169. doi: 10.1101/cshperspect.a013169

Hetz, C., Chevet, E., and Oakes, S. A. (2015). Proteostasis control by the unfolded proteinresponse. *Nat. Cell Biol.* 17, 829–838. doi: 10.1038/ncb3184

Tang, Y., and Le, W. (2016). Differential roles of M1 and M2 microglia inneurodegenerative diseases. *Mol. Neurobiol.* 53, 1181–1194. doi: 10.1007/s12035-014-9070-5

Walter, P., and Ron, D. (2011). The unfolded protein response: from stress pathway tohomeostatic regulation. *Science* 334, 1081–1086. doi: 10.1126/science.1209038

Wang, Y. W., Zhou, Q., Zhang, X., Qian, Q. Q., Xu, J. W., Ni, P. F., et al.. (2017). Mild endoplasmic reticulum stress ameliorates lipopolysaccharide-induced neuroinflammation and cognitive impairment via regulation of microglial polarization. *J. Neuroinflammation* 14:233. doi: 10.1186/s12974-017-1002-7

Conflict of Interest Statement: The authors declare that the research was conducted in the absence of any commercial or financial relationships that could be construed as a potential conflict of interest.

frontiers in Aging Neuroscience

ORIGINAL RESEARCH
published: 27 September 2018
doi: 10.3389/fnagi.2018.00291

Withaferin A Suppresses Beta Amyloid in APP Expressing Cells: Studies for Tat and Cocaine Associated Neurological Dysfunctions

*Sneham Tiwari[1], Venkata Subba Rao Atluri[1], Adriana Yndart Arias[1], Rahul Dev Jayant[1], Ajeet Kaushik[1], Jonathan Geiger[2] and Madhavan N. Nair[1]**

[1]*Institute of NeuroImmune Pharmacology, Center for Personalized Nanomedicine, Department of Immunology, Herbert Wertheim College of Medicine, Florida International University, Miami, FL, United States,* [2]*Biomedical Sciences, School of Medicine and Health Sciences, University of North Dakota, Grand Forks, ND, United States*

Neurological disorders are the biggest concern globally. Out of ∼36 million human immunodeficiency virus (HIV) positive people, about 30%–60% exhibit neurological disorders, including dementia and Alzheimer's disease (AD) like pathology. In AD or AD like neurological disorders, the pathogenesis is mainly due to the abnormal accumulation of extracellular amyloid beta (Aβ). In this era of antiretroviral therapy, the life span of the HIV-infected individuals has increased leading towards increased neurocognitive dysfunction in nearly 30% of HIV-infected individuals, specifically older people. Deposition of the Aβ plaques in the CNS is one the major phenomenon happening in aging HIV patients. ART suppresses the viral replication, but the neurotoxic protein (Tat) is still produced and results in increased levels of Aβ. Furthermore, drugs of abuse like cocaine (coc) is known to induce the HIV associated neurocognitive disorders as well as the Aβ secretion. To target the Tat and coc induced Aβ secretion, we propose a potent bifunctional molecule Withaferin A (WA) which may act as a neuro-protectant against Aβ neurotoxicity. In this study, we show that WA reduces secreted Aβ and induced neurotoxicity in amyloid precursor protein (APP)-plasmid transfected SH-SY5Y cells (SH-APP). In this study, we show that in SH-APP cells, Aβ secretion is induced in the presence of HIV-1 Tat (neurotoxic) and drug of abuse coc. Our fluorescent microscopy studies show the increased concentration of Aβ40 in Tat (50 ng/ml) and coc (0.1 μM) treated SH-APP cells as compared to control. Our dose optimization study show, lower concentrations (0.5–2 μM) of WA significantly reduce the Aβ40 levels, without inducing cytotoxicity in the SH-APP cells. Additionally, WA reduces the Tat and cocaine induced Aβ levels. Therefore, we propose that Aβ aggregation is induced by the presence of Tat and coc and WA is potent in reducing the secreted Aβ and induced neurotoxicity. Our study provides new opportunities for exploring the pathophysiology and targeting the neurological disorders.

Keywords: beta amyloid (Aβ), Withaferin A, HIV-1 Tat, cocaine, neurological disorders

OPEN ACCESS

Edited by:
Ashok Kumar,
University of Florida, United States

Reviewed by:
Bo Zhou,
Stanford University, United States
Santosh Kumar,
University of Tennessee Health Science Center, United States

****Correspondence:***
Madhavan N. Nair
nairm@fiu.edu

Received: *03 July 2018*
Accepted: *04 September 2018*
Published: *27 September 2018*

Citation:
Tiwari S, Atluri VSR, Yndart Arias A, Jayant RD, Kaushik A, Geiger J and Nair MN (2018) Withaferin A Suppresses Beta Amyloid in APP Expressing Cells: Studies for Tat and Cocaine Associated Neurological Dysfunctions. Front. Aging Neurosci. 10:291. doi: 10.3389/fnagi.2018.00291

INTRODUCTION

The overall life expectancy of people living with human immunodeficiency virus (HIV; People living with HIV, PLWH) has increased moderately due to introduction of effective anti-HIV therapies (Oguntibeju, 2012; Sabin, 2013). As per WHO Number of AIDS related death decreased from 1.5 million (2010) to 1.1 million (2015) globally (World Health Organization, 2016). Longer drug (anti-retroviral) consumption and virus living cycle leads to increased prevalence of HIV-1 associated neurocognitive disorder (HAND; Saylor et al., 2016). Additionally, PLWH (∼2 million as per World Health Organization, 2018) are more prone to the risk of developing neurological diseases like Alzheimer's disease and (AD)-like neurocognitive problems. HIV-infection and associated neurological disease synergism has become a pressing health issue to be managed, globally' because HIV-infection progression facilitates AD like pathology (Koppel et al., 1985; Levy et al., 1985). Though, neurological disorders are irreversible but investigating novel therapies of better efficacy to manage these serious disorders without side-effects are urgently required.

AD is one of the prominent neurodegenerative disease, and is characterized as a progressive impairment of memory and neurocognitive functions due to abnormal accumulation of extracellular amyloid beta (Aβ) and intracellular neurofibrillary tangles (NFTs; Dorszewska et al., 2016). Aβ aggregation is prominent in the cortical and limbic regions of the brain (Snider et al., 1983; Kurapati et al., 2013, 2014). Alternative or abnormal cleavage of integral membrane amyloid precursor protein (APP) by β and γ secretases (Ghosh et al., 2008; Guardia-Laguarta et al., 2010) lead to abnormal Aβ processing, resulting into insoluble Aβ aggregation (Zheng et al., 2002; Kretner et al., 2016). Aβ peptides then aggregate into extracellular insoluble senile plaques (Echeverria et al., 2004; Guardia-Laguarta et al., 2010; Ahyayauch et al., 2012). This Aβ accumulation leads to decreased neuronal health and stability, increased deterioration, synaptic depression (Venkitaramani et al., 2007; Palop and Mucke, 2010; Li et al., 2017), oxidative stress (Butterfield et al., 2013; Arimon et al., 2015; Cheignon et al., 2018), augmented neuronal dysfunctions and inflammation (Barage and Sonawane, 2015; Marottoli et al., 2017). These dysfunctions caused by Aβ aggregation, become worst upon the presence of HIV-1 (András and Toborek, 2013; Martínez-Bonet et al., 2018) and drugs of abuse. HIV patients are reported to have augmented Aβ plaques deposition in the brain compared to HIV negative individuals (Esiri et al., 1998; Becker et al., 2004; Valcour et al., 2004). HIV associated Aβ dysfunction can be due to either the entire HIV virus, or mainly by neurotoxic Tat (transactivator of transcription) protein (Bagashev and Sawaya, 2013). HIV-1 Tat is neurotoxic and even though ART targets all the active virus, Tat could still be produced by the provirus in the viral reservoirs, such as brain (Daily et al., 2006). Tat protein as a neurotoxin, plays a prominent role in HIV neuropathogenesis as it gets secreted extracellularly and has the ability to cause neurotoxicity in the healthy cells (Chandra et al., 2005; Tahirov et al., 2010). Tat may have specific reaction with the Aβ in the CNS and facilitate Aβ aggregation, in the CNS (Hategan et al., 2017). Moreover, Aβ aggregations are studied to be increased in cortex of HIV brains when compared to age matched non-HIV controls (Achim et al., 2009; Soontornniyomkij et al., 2012).

Another factor, which augments the Aβ aggregation induced pathogenesis, are the drugs of abuse (Ramage et al., 2005; Dublin et al., 2017). These powerfully addictive stimulant drug molecules have been studied to have an exaggerating effect during HIV infection (Jayant et al., 2017). Cocaine (coc), a very common abused drug within PLWH, exerts malicious effects on the CNS (Javadi-Paydar et al., 2017; Meade et al., 2017; Wakim et al., 2017). In the presence of coc, the additive effect of HIV-1 Tat and coc may increase Aβ aggregation, which is a common factor in aging and HIV associated neurological disorders. Therefore, investigating desired therapies for coc abusing aging PLWH, are required for devising new therapeutic agent with multifunctional abilities to manage neurological disorders.

In this article, we have studied therapeutic properties of Withaferin A (WA) against multiple disease associated factors including Aβ, HIV-1 Tat and drug of abuse, coc. WA is an active purified drug moiety extracted from Ashwagandha (ASH), isolated from the root extract of a medicinal plant *Withania Somnifera* and expected to reverse $A\beta_{1-42}$ induced toxicity in human neuronal cells (Kurapati et al., 2013, 2014). WA is a steroidal lactone, derived from *Withania somnifera* (Indian Winter cherry or Ashwagandha). ASH has been traditionally used in ayurvedic medicine. WA is the first member of the withanolide class of ergostane type product to be discovered (Mirjalili et al., 2009). The beneficial effects of WA has been studied in the field of tumor inhibition (Bargagna-Mohan et al., 2007), antiangiogenic activity (Mohan et al., 2004; Challa et al., 2012; Mohan and Bargagna-Mohan, 2016), and against angioproliferative and malignant diseases like pancreatic cancer (Yu et al., 2010), leukemia, breast cancer and colon cancer (Choi and Kim, 2015), as well as anti-metastasis (Lee and Choi, 2016) and anti-carcinogenic properties (Rah et al., 2012). However, the therapeutic ability of WA against neurological disorders, as a protective agent is not well studied yet. WA is also explored in the field of apoptosis and adipogenesis inhibitor in 3T3-L1 adipocytes (Park et al., 2008). In this systematic study, we have explored for the first time the neuroprotective role of WA against Aβ secretion and aggregation *in vitro*. During our study we observed the deleterious effect of Aβ on the neuronal health, function and morphology. In our step by step dose dependent studies, we explored the role of WA in reducing Aβ induced neurotoxicity in the HIV-1 Tat and coc treated APP-plasmid transfected SH-SY5Y cells (SH-APP) cells, towards neurological dysfunctions. The outcomes of this research claim that WA has a great potential to be promoted as a natural neuro therapeutic agent in order to manage age or viral infection associated neurological disorders. Our studies open new areas of drug efficacy against neurological conditions.

MATERIALS AND METHODS

Chemicals and Reagents

Withaferin A (WA) was commercially purchased from Sigma Aldrich (Cat# W4394 SIGMA). Methylthiazolyldiphenyl-

tetrazolium bromide (MTT; Cat# M2003) and paraformaldehyde was purchased from Sigma Aldrich. HIV-1 clade B recombinant Tat protein (86-amino acid) was obtained from NIH AIDS research and reference reagent program (Cat# 2222).

Cell Culture

The cell type used in this study are SH-APP cells which is a human neuroblastoma cell line stably over-expressing human APP751 which was a kind gift from Dr. Jonathan Geiger (University of North Dakota, Grand Forks, ND, USA). SH-APP Cells were cultured in Dulbecco Eagle's minimum essential medium (DMEM; Gibco®; Life Technologies, Grand Island, NY, USA) supplemented with 10% fetal bovine serum, 100 U/ml penicillin/streptomycin, nonessential amino acids, and sodium pyruvate (1 mM) at 37°C in 5% CO_2.

Cell Viability Assay

Cells were plated at a density of 1×10^4 cells per well into 96-well plates and maintained at 37°C for 24 h. Cells were treated with various concentrations of WA for 48 h. Fresh medium containing 50μL of MTT solution (0.5 mg/mL) was added to each well. After 3 h incubation, the MTT formazan crystals were dissolved in dimethyl sulfoxide (DMSO) and viable cells were detected by measuring the absorbance at 570 nm using a microplate reader (Molecular Devices, Sunnyvale, CA, USA).

For Tat and coc toxicity study on cell viability, we performed Cell viability test using 0.4% Trypan Blue Solution (T8154) Live dead screening. Ten microliter of cells were taken from the pellet resuspended in fresh media, after centrifugation at 1,500 rpm for 5 min, and was mixed with 10 μl of Trypan blue dye (1:1 ratio). The cells were then loaded on a cell counting slide and counted for live count on a cell counter (BioRad TC20™ Automated cell counter).

Tat and Coc Treatment of SH-APP Cells

SH-APP cells (1×10^6 cells) were cultured overnight in T-25 flasks in complete DMEM media with 10% FBS and 1% Penicillin streptomycin solution. After 48 h, cells were treated with different concentrations of HIV-1 Tat (5–100 ng/ml) and coc (0.1–10 μM) and the cells and supernatant were collected after 48 h after the treatment. The optimized dose of Tat and coc were selected based on their effect on increasing Aβ levels significantly compared to untreated controls. In further experiments, 1×10^5 SH-APP cells were seeded in six wells plates and were cultured for 48 h. Cells were treated with optimized concentrations of HIV-1 Tat1–72 and/or coc.

Quantification of Aβ40 Levels

Secreted Aβ levels were measured using human Aβ40 ELISA kit as per the manufacturer's protocol (Thermo Fisher Scientific, Catalog# KHB3481). For secreted Aβ measurements, SH-APP cells were cultured in six well plates and after 48 h, cells were treated with HIV-1 Tat/coc in combination with WA. The media from cultured cells was collected and protease inhibitor was added to it. The supernatant was utilized as samples for the AB_{40} ELISA as per the specific reagents and protocol provided with the kit. Each sample was analyzed in duplicate. Cells were saved for flow cytometry studies to estimate intracellular Aβ40 level.

Flow Cytometry

Cells from Tat, $coc^{+/-}$ WA treated samples were utilized for flow cytometry studies. Flow Cytometry was used to identify the expression of Aβ40 protein in SH-APP cells after treatment with various concentrations of Withaferin A, Tat and coc. 1×10^6 SH-APP cells were stained with primary anti-human Aβ40 (#PA3–16760) and secondary anti-rabbit Fluorescein isothiocyanate (FITC)-labeled antibody (catalog #AP187F, Millipore). Auto fluorescence of the cells was based on the unstained cells. Cells were gated based on the secondary antibody. Accuri BD flow and Amnis® Imaging Flow Cytometers were used for acquisition. Analysis was conducted in Flow Jo software and Amnis® FlowSight® Imaging Flow Cytometer and analysis by IDEAS® image software.

Single-Cell Flow Cytometry

The SH-APP were treated with different concentrations of WA. The cells were then harvested at 24 h after treatment, washed and counted; equal amounts of cells (1× 106) were aliquoted in 1.5 ml Eppendorf centrifuge tubes in 250 μl 1× PBS. Cells were analyzed by ImageStreamX Imaging Flow Cytometer (Amnis Corporation, Seattle, WA, USA) having with INSPIRE software. A magnification of 60× was employed for all readings. Ten-thousand cells (events) were analyzed for each sample. FITC and DAPI were excited with a 100 mW of 488 nm argon laser. FITC and DAPI fluorescence was collected on channel two (505–560 nm) and channel seven (560–595 nm), respectively. Intensity adjusted bright field images were collected on channel one. Bright field area and total fluorescence intensity were calculated using IDEAS software. Data analysis was performed using the IDEAS software (Amnis Corporation), with proper data compensation with respect to singly stained samples. The compensated data was then gated to eliminate cells that were out of field of focus and doublets or debris was eliminated too.

Immunofluorescence Staining and Analysis for Studying Beta Amyloid Aggregation

To study the effect of WA on the morphology aggregation, we conducted immunofluorescence imaging experiment. The cells were cultured to 80% confluency on the 4-well microscopy slides and were then exposed to HIV-1 Tat+/− WA. After 48 h, the supernatant was discarded and the cells were fixed in 4% PFA. PFA embedded slides were then immunostained by using Aβ40 primary antibody (1:100) and GFP secondary antibody (1:100). Immunohistochemically stained sections were captured using the Keyence microscope. The images were captured at a magnification of 10×.

Immunofluorescence Staining for Studying Effect of WA on Neuronal Morphology

To study the effect of WA on the neuronal morphology, we conducted immunofluorescence imaging experiment. The cells were cultured to 80% confluency on the 4-well microscopy slides and were then treated with HIV-1

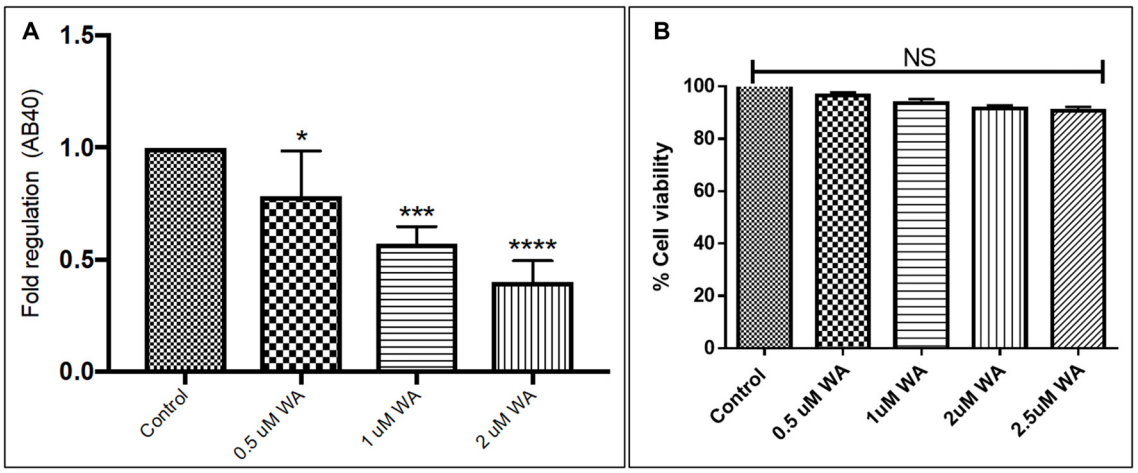

FIGURE 1 | Effect of Withaferin A (WA) on amyloid beta (Aβ) secretion. **(A)** Cells were treated with different dose of WA and the supernatants were collected 48 h after treatment. The supernatant collected were analyzed by $A\beta_{1-40}$ ELISA which demonstrated that at an optimum dose of 2 μM WA, the levels of secreted Aβ40 showed significant decrease compared to control untreated samples. **(B)** The dosage of WA used for this experiment were also analyzed for the associated cellular toxicity. The cell toxicity assay showed that the lower doses of WA were not toxic to cells. Optimum dose of 2 μM, WA did not cause any loss in cell viability or toxicity in amyloid precursor protein (APP)-plasmid transfected SH-SY5Y (SH-APP) cells (*$p \leq 0.05$; ***$p \leq 0.001$; ****$p \leq 0.0001$).

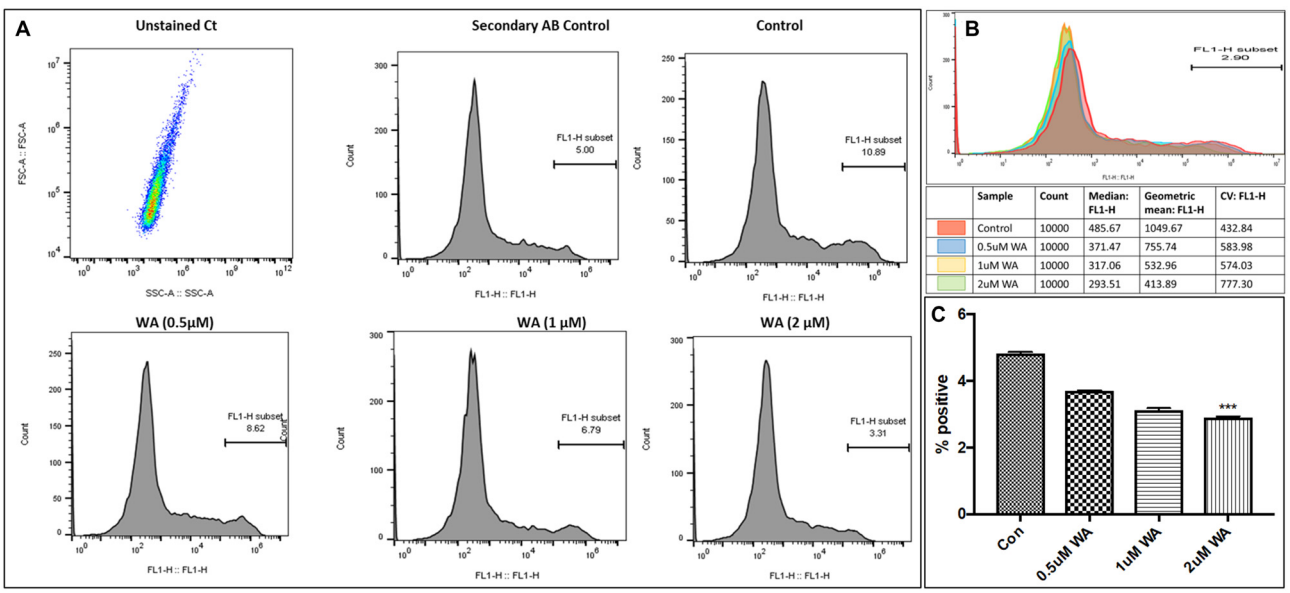

FIGURE 2 | WA inhibits $A\beta_{1-40}$ in concentration dependent manner. Panel **(A)** shows histograms of Aβ secretion by the SH-APP cells upon treatment with varying dose of WA. Panel **(B)** shows the layover of the peaks in one histogram, and **(C)** shows the quantification of the same. The cells were treated with WA concentrations, and after 48 h of treatment were analyzed by Flow cytometry for determining $A\beta_{1-40}$ levels. Flow cytometry was used to identify the expression of $A\beta_{1-40}$ in SH-APP cells after treatment with three different concentration of WA. 1× 106 SH-APP cells were stained with primary anti-human Aβ40 (#PA3–16760) and secondary anti-rabbit Fluorescein isothiocyanate (FITC)-labeled antibody (catalog #AP187F, Millipore). Auto fluorescence of the cells was based on the unstained cells. Cells were gated based on the secondary antibody. Accuri BD flow and Amnis® Imaging Flow Cytometers were used for acquisition. Analysis was conducted in Flow Jo software and Amnis® FlowSight® Imaging Flow Cytometer and analysis by IDEAS® Image software. For each experiment, from all events collected, FITC positive cells were gated from single cells (***$p \leq 0.001$).

Tat protein/coc +/− WA. After 48 h, the supernatant was discarded and the cells were fixed in 4% PFA. PFA embedded slides were then washed and immunostained using MAP2 primary antibody (1:100) and anti-FITC secondary antibody (1:100). Immunohistochemically stained sections were captured using the ImageScope AT2 image scanner (Aperio Technologies) and analyzed using the ImageScope software; Scale 50 μm.

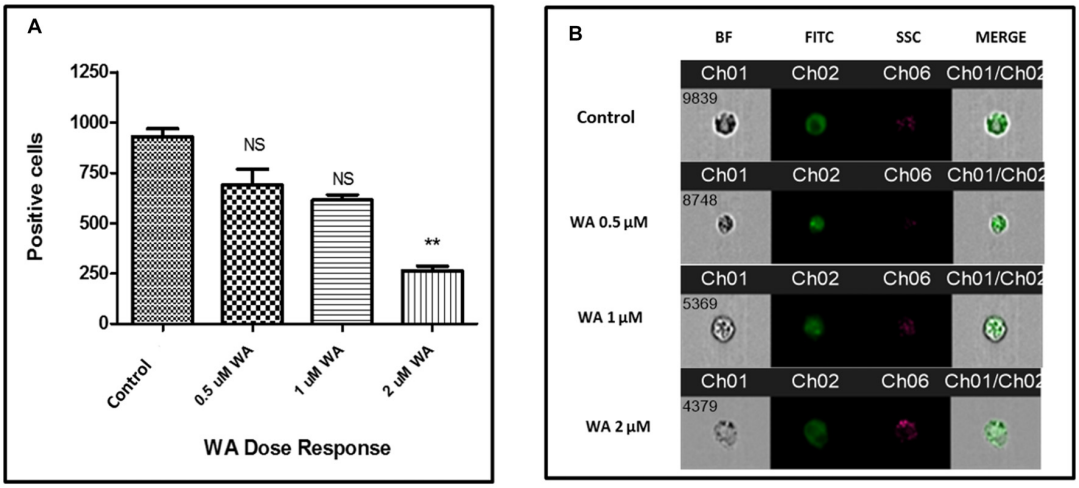

FIGURE 3 | WA inhibits Aβ production: single cell flow Cytometry was used to identify the expression of $A\beta_{1-40}$ protein in SH-APP cells after treatment with different concentration of WA. **(A)** Bar graph representing the mean ± standard error of percent of mean fluorescence intensity. **(B)** Representative single cell images. We have observed significantly reduced Aβ with WA exposure dose dependently ($n = 3$; $^{**}p \leq 0.01$; NS: Non Significant).

Data Analysis

Results in this study are representative of three or more independent experiments. Statistical significance was analyzed using Graph Pad Prism5 software, La Jolla, CA, USA by performing ANOVA or the Student's *t*-test for unpaired observations. The values are presented as means ± SEM.

RESULTS

WA Dose Optimization and Aβ Neutralizing Efficacy Studies in SH-APP Cells

To optimize the non-toxic dose of WA, different concentrations of WA (0.5–10 µM) were treated to SH-APP (neuroblastoma cell lines stably expressing human APP751) cells and results showed that 2 µM of WA reduces the secreted Aβ40 in SH-APP cells significantly when compared to non-treated control, (**Figure 1A**) without inducing cytotoxicity to the cells (**Figure 1B**). Further, results were confirmed with the flow cytometry and showed (**Figures 2A–C**) dose dependent reduction in the $A\beta_{1-40}$ levels and the maximum reduction was reported at 2 µM WA concentration without causing cellular toxicity. Additional single cell flow cytometry and imaging also showed the same trend highlighting the effective role of 2 µM WA against $A\beta_{1-40}$ (**Figures 3A,B**).

Effect of HIV-Tat Protein and coc on Aβ Production in SH-APP Cells

Human Aβ40 ELISA was performed with the supernatant collected from control and WA treated SH-APP cell samples

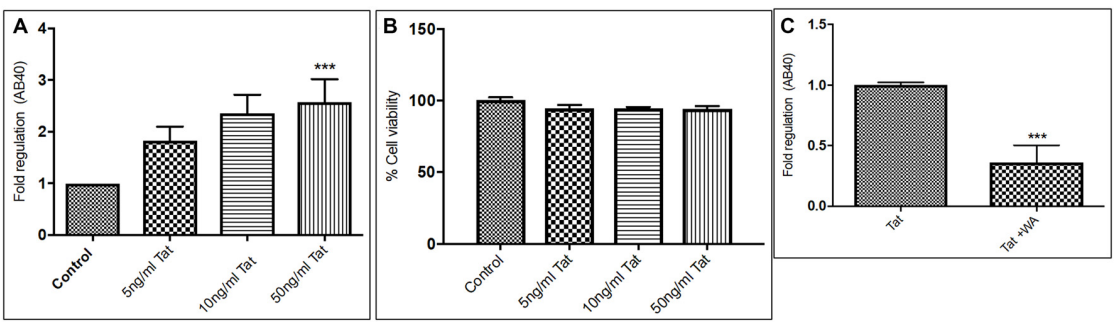

FIGURE 4 | Tat induce increase in secreted Aβ40 levels **(A)**. Human Amyloid Beta ELISA analysis showing that Tat (5–50 ng/mL) increased the secreted $A\beta_{1-40}$ significantly in SH-APP cells. **(B)** Cellular toxicity assay showing viability of the cells in the Tat treated samples. **(C)** 2µM WA reduced the Tat levels significantly when compared to Tat (50 ng/mL) only treated samples. 1× 106 SH-APP cells were seeded in 6-well plates and were grown for 48 h and then treated with human immunodeficiency virus (HIV)-1 Tat in different doses and the cells were then incubated for 48 h at 37°C. The supernatant from the culture was collected and treated with protease inhibitor (1µl/ml) and analyzed by $A\beta_{1-40}$ ELISA (Sigma). The results are from three independent experiments and the statistical significance was calculated by Student's *t*-test. Cell viability study was performed by Trypan blue live dead screening, to study the toxicity levels of various Tat dose. Dose selected for Tat treatment for further experiment was elected on the basis of increase in Aβ40 secretion levels and correlated with cell viability ($^{***}p \leq 0.001$).

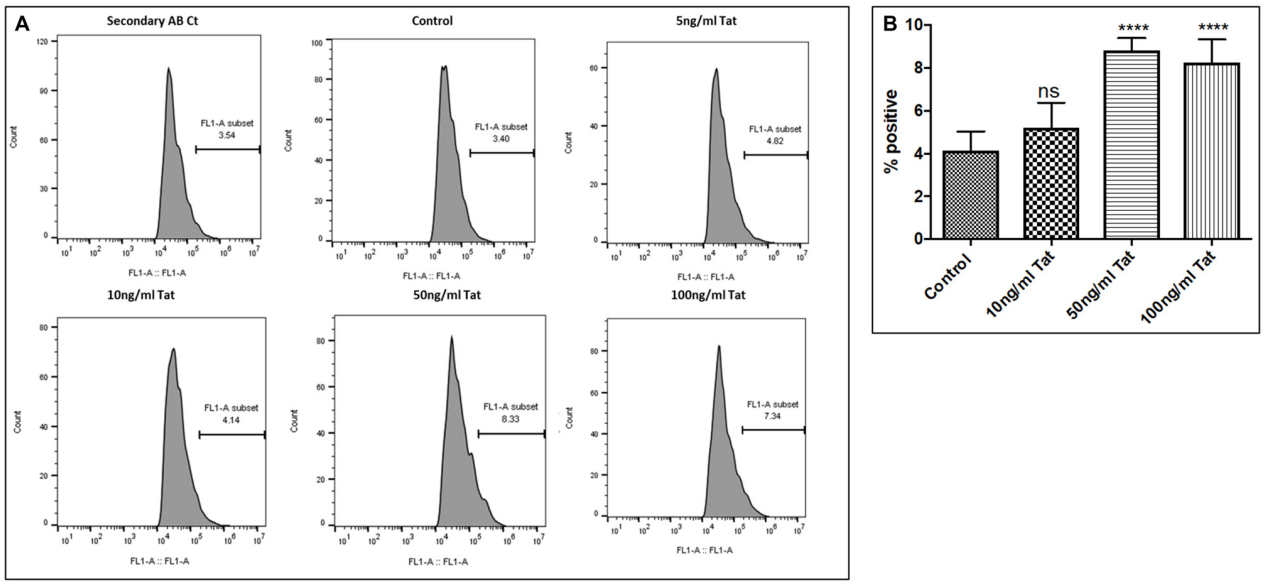

FIGURE 5 | Dose response. **(A)** Histograms showing Tat (5–100 ng/mL) increases the $A\beta_{1-40}$ levels. SHAPP cells were treated with different concentrations of Tat and after 48 h of treatment were analyzed by Flow cytometry for determining the $A\beta_{1-40}$ levels. **(B)** Quantification representation of the percent positive cells (****$p \leq 0.0001$; ns: Non Significant).

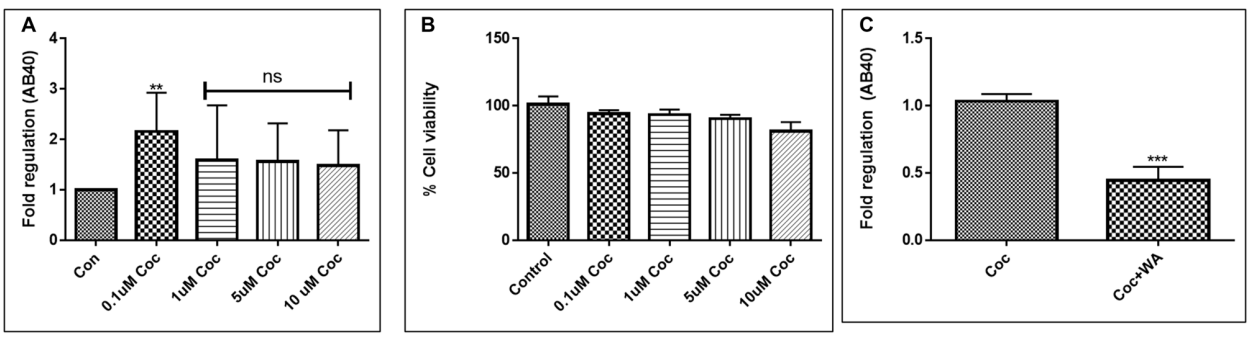

FIGURE 6 | Coc induces increase in secreted Aβ40 levels. Similar study pattern of ELISA and flow cytometry, like in the case of HIV-1 Tat, was performed with various concentrations of coc to choose an optimized dose of coc for further studies. **(A)** Coc increases $A\beta_{1-40}$ secretion. Coc (0.1–10 μM) increased the secreted $A\beta_{1-40}$ but the significant increase was found in the samples treated with 0.1 μM coc. **(B)** Cellular toxicity assay showing viability of the cells in the coc treated samples. **(C)** 2μM WA reduced the coc (0.1 μM) induced $A\beta_{1-40}$ levels significantly when compared to coc only treated samples (**$p \leq 0.01$; ***$p \leq 0.001$; ns, not significant).

in order to evaluate the efficacy of WA in reducing the HIV-Tat and coc induced Aβ secretion. SH-APP cells were treated with different concentrations of Tat (5–50 ng/ml) and coc (0.1–10 μM). **Figure 4** shows that the SH-APP cells treated with Tat exhibited upregulation of $A\beta_{1-40}$ secretion compared to untreated control (**Figures 4A,B**). Effective dose of Tat (50 ng/ml) when treated with 2 μM WA, showed significant decrease in $A\beta_{1-40}$ (**Figure 4C**). Further, the results were also confirmed by the flow cytometry using $A\beta_{1-40}$ specific primary antibody. The dose of 50 ng/ml Tat most significantly increased the Aβ levels when compared to control (**Figures 5A,B**). Additionally, we studied the effect of coc in the similar study pattern, and observed the increase in $A\beta_{1-40}$ secretion (**Figures 6A,B**). We report that 0.1 μM showed most significant upregulation in $A\beta_{1-40}$ secretion compared to untreated controls. Effective dose of coc (0.1 μM) when treated with 2 μM WA, showed significant decrease in $A\beta_{1-40}$ (**Figure 6C**). This trend was also confirmed by the flow cytometry experiment which showed a coc induced increase in Aβ levels (**Figures 7A,B**).

Tat and coc Induced Increase in Aβ40 Levels, in Combination

An optimized dose of Tat (50 ng/mL) and coc (0.1 μM) alone or in combination were used to study the neutralizing efficacy of WA (2 μm) in SH-APP cells. Results showed the combined effect of Tat and coc together in increasing the $A\beta_{1-40}$ levels. (**Figures 8A,B**). Individual optimized dose of Tat (50 ng/mL)

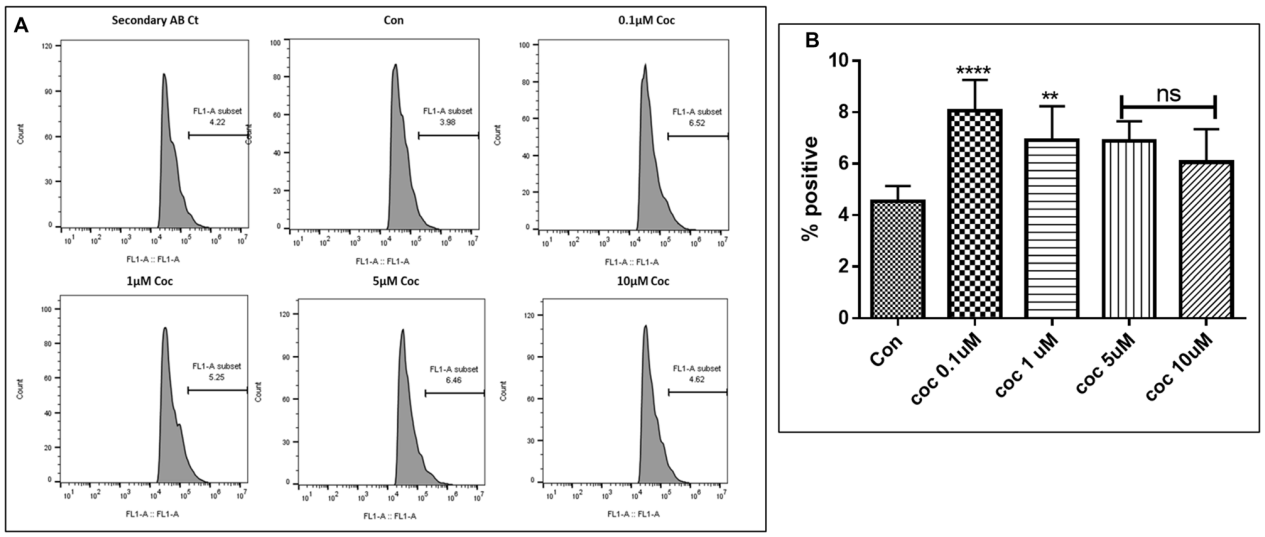

FIGURE 7 | Dose response. **(A)** Histograms showing coc (0.1–10 μM) increases the $A\beta_{1-40}$ levels. The cells were treated with different concentrations of coc and after 48 h of treatment were analyzed by flow cytometry for determining the $A\beta_{1-40}$ levels. **(B)** Quantification representation of the percent positive cells (**$p \leq 0.01$; ****$p \leq 0.0001$; ns, not significant).

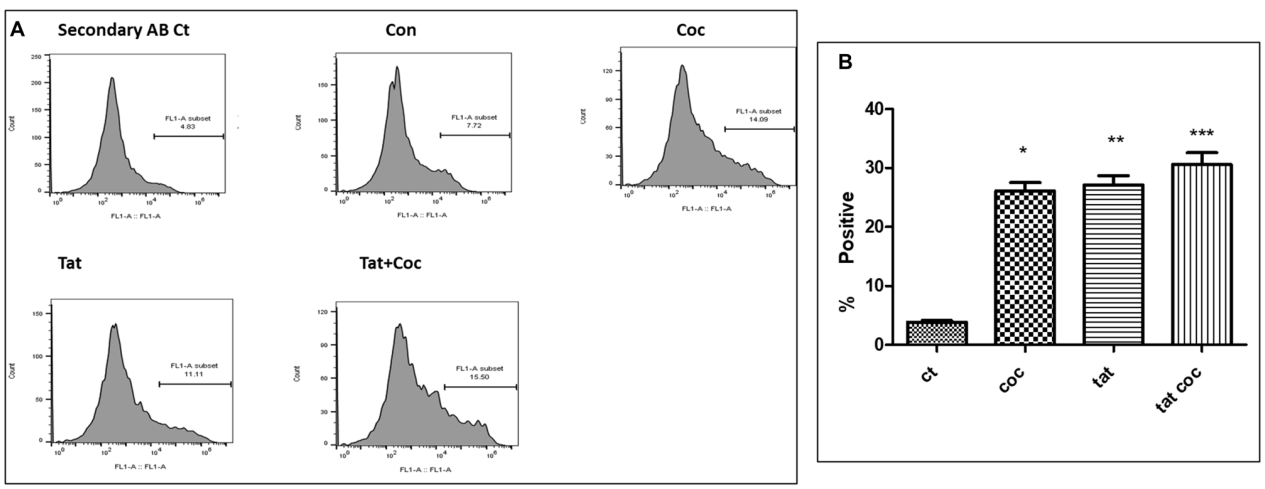

FIGURE 8 | Tat and coc combination. **(A)** Tat (50 ng/mL) and coc (0.1 μM) individually and in combination increase the $A\beta_{1-40}$ levels. The cells were treated with selected Tat and coc concentrations and combination of both, and after 48 h of treatment were analyzed by flow cytometry for determining the $A\beta_{1-40}$ levels. **(B)** Quantification representation of the percent positive cells (*$p \leq 0.05$; **$p \leq 0.01$; ***$p \leq 0.001$).

and coc (0.1 μM) were used for further WA neutralizing efficacy studies from here on.

WA Reverses Tat and coc Induced Amyloid Aggregates *in vitro*

Immunocytochemistry studies showed that WA was able to reduce the amyloid aggregation when compared to the untreated control SH-APP cells. The cells were grown in the microscopic slides (eight wells) and after 24 h of growth, the wells were treated individually with Tat+/− WA and coc+/− WA for 48 h and control wells had fresh media added. The cells were then collected, fixed and stained with primary Beta amyloid 1–40 antibody (1:100) and GFP secondary antibody (1:100). We observed that the cells exposed to Tat and coc had strong signals for amyloid beta aggregations, which was mitigated by WA treatment as seen in the Tat + WA and coc + WA microscopic chambers, when compared to control well (**Figures 9A–G**).

WA Reverses/Decreases coc Induced Neurotoxicity

Additionally, to study derogatory effects of coc on the SH-APP cells and the effect of WA on the neuronal morphology, we

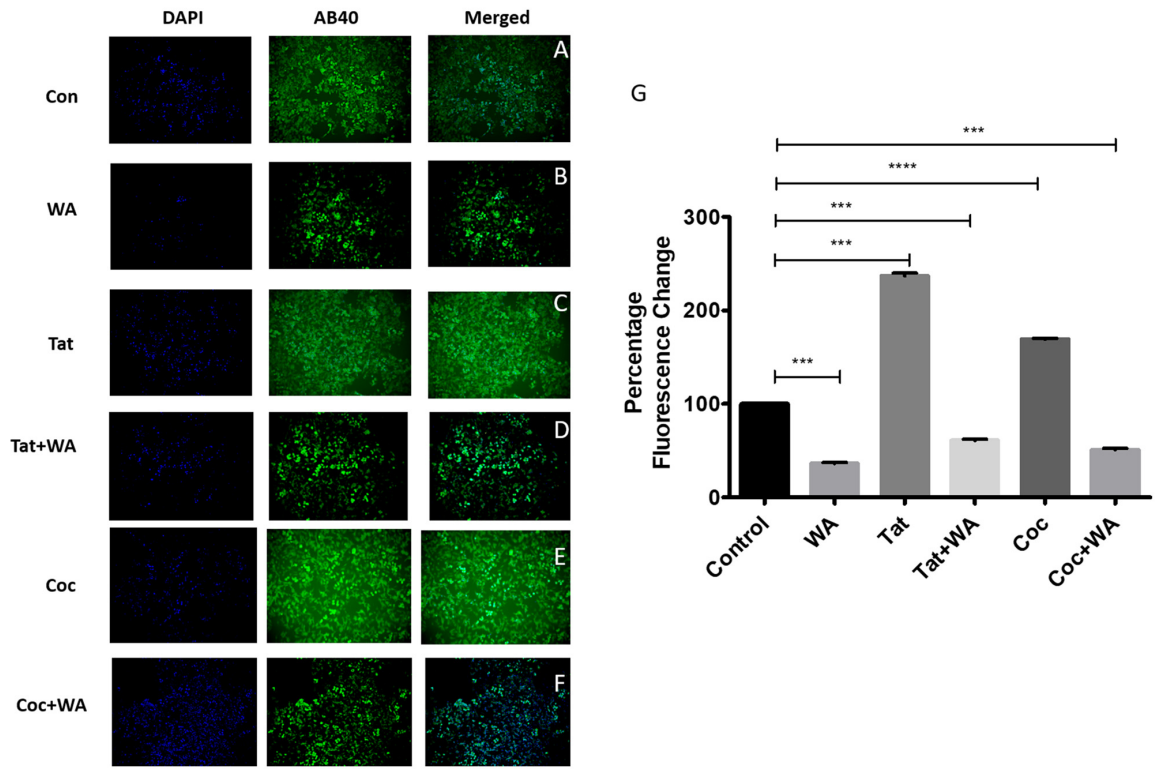

FIGURE 9 | WA inhibits HIV-1 Tat induced Aβ-production, respectively. SH-APP cells were treated with HIV-1 Tat (50 ng/mL; **C**) coc (0.1 μM; **E**) +/− WA (2 μM; **(D,F)** respectively) were compared to Control **(A)** and only WA treated cells **(B)**. After 24 h, cells were fixed and stained with Anti-Human Aβ40 overnight. Cells were washed and stained with secondary anti-rabbit FITC-labeled antibody (catalog #AP187F, Millipore). Images were acquired using Keyence ALL in one microscope (10×). WA significantly suppressed Tat and coc induced Aβ-secretion, respectively ($n = 3$). Florescent intensity of these stained cells was quantified using the ImageJ software (**G**; $^{***}p \leq 0.001$; $^{****}p \leq 0.0001$).

conducted immunofluorescence imaging experiment. Cultures of SH-APP cells grown on the eight well imaging slides for 48 h, and then the cells were stained by MAP2 primary antibody. We observed that the cells exposed to coc for 48 h exhibited heavy dendritic beading (indicated by yellow arrows) and cytoplasmic vacuoles (**Figure 10C**). The control SH-APP cells (**Figure 10A**) and WA only treated cells (**Figure 10B**) showed no abnormal beading or thickening of the dendrites, when compared. Upon treatment with WA, in coc exposed cells (**Figure 10D**), we observed reduced dendritic beading and more pronounced and elongated dendrites, communicating with other neuronal cells. We also observed reduced cytoplasmic vacuoles in the WA treated cells. This indicates that coc induces the stressed environment in the cell culture system which leads to neuronal damage (**Figure 10**).

DISCUSSION

Currently, the studies focusing towards neurodegeneration caused by either aging or due to viral infections, are extremely important. The accumulation of Aβ in the CNS is major factor contributing towards neurodegeneration (Green et al., 2005). The introduction of HAART gives a longer life span, giving a major opportunity to age related disorders in these recovering patients (Ellis et al., 2010; Heaton et al., 2010, 2011). The currently available drugs against Aβ aggregation, for example, Memantine (*N*-methyl-D-aspartic acid (NMDA) receptor antagonist), helps in repair of damaged neurons (van Marum, 2008), but does not aid in overall cure for neurological issues. Another drug which is very well studied for its anti-inflammatory, antioxidant and neuroprotective properties is Cucurmin/Curcuminoid, obtained from the roots of a plant Curcuma longa (Sharma et al., 2007). It has been reported that Curcuma may have potential role in AD treatment by targeting Aβ aggregates and associated toxicity in the neuronal cells (Ringman et al., 2005; Ishrat et al., 2009). Unfortunately, Curcuma is weakly stable and easily hydrolyzed, and gets photodegraded or even oxidized. This makes it very challenging and leads to its minimal bioavailability in the CNS (Anand et al., 2007).

Currently, there is no direct cure available for AD or AD-like neurodegenerative symptoms. Therefore in this paper we have focused on a drug compound WA, as a neuroprotective agent against Aβ induced neuronal toxicity. Our studies show that WA reduces the levels of secreted Aβ significantly without causing cytotoxicity in the cell cultures. Our microscopic studies demonstrate the protective role of WA as the human neuroblastoma cells showed healthy growth in the presence of

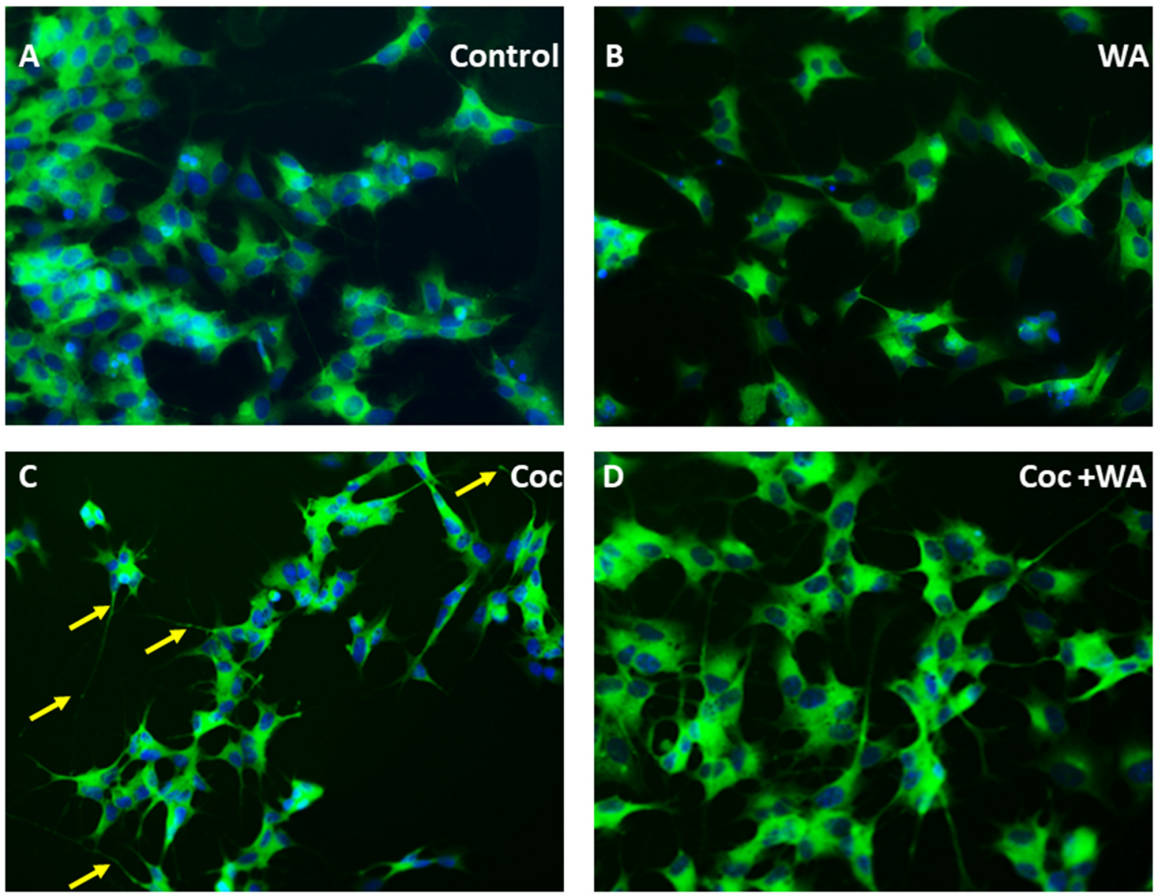

FIGURE 10 | WA reverses coc induced dendritic beading and cytoplasmic vacuoles. SH-APP cells were treated with coc (0.1 μM) +/− WA (2 μM). After 24 h, cells were fixed and stained with MAP2 primary antibody overnight. Cells were washed and stained with secondary anti-rabbit FITC-labeled antibody (catalog #AP187F, Millipore). **(A)** Control SH-APP cells and **(B)** WA only treated cells showed no abnormal beading or thickening of the dendrites when compared to **(C)** coc exposed SH-APP cells which exhibited heavy dendritic beading (yellow arrows) and cytoplasmic vacuoles, measure of the cells being in drug-induced stress, **(D)** WA treated coc exposed cells on the other HIV-1 associated neurocognitive disorder (HAND) displayed reduced dendritic beading and elongated dendrites, with minimal cytoplasmic vacuoles.

WA. We observed that WA treatment reduced dendritic beading and cytoplasmic vacuoles in the SH-APP cells, conferring towards protective role of WA. Our observation coincides with other studies as well, which show that *W. somnifera* whole root extract treatment promotes neuronal health by inducing dendrite formation *in vitro* (Tohda et al., 2000; Zhao et al., 2002). Moreover, our study shows for the first time that a small sized active moiety of Withania root extract, termed as WA neutralizes secreted Aβ, in the SH-APP cells *in vitro*. Our previous lab has studied the role of Ashwagandha (ASH) which is a big molecule extracted from roots of *W. Somnifera*. We reported the properties of ASH towards neutralizing Aβ in the neuronal cells *in vitro*. ASH showed the reduction of Aβ in treated cells significantly when compared to untreated controls, suggesting anti-amyloid role of ASH (Kurapati et al., 2013, 2014). Even though ASH is capable of reducing the secreted Aβ, the understanding of ASH's efficacy in the CNS across the BBB is minimum, as it is a big moiety. Therefore, the systematic delivery of the drug into the CNS and increased bioavailability becomes a pressing issue. This urged a need to find potent smaller molecular weight molecules with similar properties. Systematic chromatographic studies show the various components, upon breakdown of ASH molecule. This gave us an opportunity to study small molecule WA and assess its ability as a neuroprotectant to target the Aβ levels.

We further wanted to explore the effect of WA on induced Aβ production by the exposure of HIV-1 Tat. Therefore, in this study, we have analyzed the effect of HIV-1 Tat protein (Nuovo et al., 1994; Nath et al., 1996; Merino et al., 2011) on the Aβ secretion in SH-APP neuronal cells and found significantly increased Aβ production. Our results are in agreement with other studies which have reported the role of Tat protein in increased neuronal Aβ secretion (Rempel and Pulliam, 2005; Giunta et al., 2009; Aksenov et al., 2010). Tat is a neurotoxin and we show that it aggravates the Aβ aggregation *in vitro*. The mechanism through which this happens is still not understood well (Chen et al., 2013; Hategan et al., 2017), Tat may have a direct interaction with the Aβ fibrils, resulting in induced

aggregation of monomers, towards plaques. This hypothesis is supported by our Immunocytochemistry studies which show dense accumulation of Aβ, in the cell medium exposed to HIV-1Tat (50 ng/ml). Our human Aβ40 ELISA experiment detected increased concentration of Aβ in Tat treated samples as well. This leads us to a conclusion that Tat is extremely neurotoxic and has an ability to interact with Aβ, increasing the overall toxicity of the cell system, and urging more and more release and aggravation of Aβ. HIV-1 Tat tends to have a direct physical interaction with Aβ peptide, leading to excessive aggregation of Aβ leading to neurotoxicity (Hategan et al., 2017).

Further, among the most abused drugs by People living with HIV (PLWH), coc abuse has been one of the major contributors towards the increased severity of neurocognitive disorders in the patients (Fiala et al., 1998; Gannon et al., 2011; Buch et al., 2012). Additionally, the percentage of drug abusers in the HIV positive population and aging population is very high. Drug abuse/addiction and HIV/AIDS are linked since the beginning of the HIV/AIDS epidemic. People who inject drugs accounted for about six percent of HIV diagnoses in 2015 (CDC, 2018). Even though the association of coc is shown with the exaggeration in HIV neuropathogenesis, the underlying mechanisms remain unclear. We elucidate the mechanism, in this study, for the first time, we observed the increased levels of Aβ production by coc. We also observed in our Immunocytochemistry experiments that coc affects neuronal morphology and communications, and aggregation of Aβ in the SH-APP cells, *in vitro*. This verifies the toxic effect of coc on the neuronal cells, which contribute in the increased accumulation of the amyloids. Coc alone and in combination with HIV-1 Tat is highly neurotoxic. These results coincide with various *in vivo* studies done by other research groups which show that the peritoneal injection of coc in rats stimulates hyperphosphorylation of tau and neurofilament in cortex, hippocampus and caudato-putamen regions of brain, indirectly contributing to the Aβ toxicity (Liu et al., 2003). These observations indicate that coc addiction may be associated with neurofibrillary degeneration. Therefore, here we report that coc in addition to HIV-1 Tat increases Aβ secretion *in vitro*. Our findings suggest that HIV-1 Tat and coc introduce cellular toxicity and cause neuronal dysfunctions by increasing amyloid secretion and modulating neuronal morphology and communications. Moreover, accumulation and deposition of Aβ in the brain of HIV patients (active infection or latent infection) drive the pathogenic cascades of neurological disorders, contributing towards aging or associated dementias (Pulliam, 2009). Targeting Aβ secretion, will have a translational significance in the treatment of HIV coc abusers and other neurological disorders like AD.

Additionally, the main rationale behind introducing WA is the unavailability of the direct medicine/drugs which target neurological disorders. Moreover the drugs, get rejected due to pharmacotherapy failures like inadequate physical chemistry, minimal absorption, unfavorable pharmacokinetic parameters, instability and toxicity. This urges the need of the alternate medicine/nanomedicine. Therefore, our next step is to address the limitation or incapability of drugs to cross BBB into the CNS, by employing nanotechnology assisted approaches, where our developed drug magneto-liposomes (which are a biopolymeric vesicle with capacity to deliver drugs across BBB) would be able to transmigrate across BBB (Ding et al., 2014; Kaushik et al., 2016).

In summary, it is critical to design and identify compounds that specifically target and inhibit Aβ secretion and aggregation, and also the interaction between Aβ and HIV-Tat 1 and drug of abuse, against their synergistic role towards neurodegenerative disorders. When combined with other strategies targeting Aβ, including immunotherapy, these approaches might allow for a reduction, if not elimination, of Aβ-related toxicity. Further *in vivo* efficacy and drug delivery mechanistic studies are necessary to explore WA's therapeutic role in neurological disorders like HIV associated neurocognitive disorders and Alzheimer's disease.

AUTHOR CONTRIBUTIONS

ST designed and coordinated the research, performed experiments, data analysis and manuscript writing. AYA helped in flow cytometry experiments and analysis. VA and RJ helped in data analysis and manuscript review. AK helped in manuscript review. JG reviewed the manuscript. MN guided in experimental research plan and provided continuous supervision and reviewed the manuscript.

FUNDING

The National Institute of Health (Grant# R01DA034547), Florida Department of Health's Ed, and Ethel Moore Alzheimer's Disease Research Program (Grant# 800009191) supported this work.

ACKNOWLEDGMENTS

We would like to acknowledge the Dissertation Year Fellowship 2018 awarded to ST (graduate student) by University Graduate School, Florida International University.

REFERENCES

Achim, C. L., Adame, A., Dumaop, W., Everall, I. P., Masliah, E., and Neurobehavioral Research Center. (2009). Increased accumulation of intraneuronal amyloid β in HIV-infected patients. *J. Neuroimmune Pharmacol.* 4, 190–199. doi: 10.1007/s11481-009-9152-8

Ahyayauch, H., Raab, M., Busto, J. V., Andraka, N., Arrondo, J.-L. R., Masserini, M., et al. (2012). Binding of β-amyloid (1–42) peptide to negatively charged phospholipid membranes in the liquid-ordered state: modeling and experimental studies. *Biophys. J.* 103, 453–463. doi: 10.1016/j.bpj.2012.06.043

Aksenov, M., Aksenova, M., Mactutus, C., and Booze, R. (2010). HIV-1 protein-mediated amyloidogenesis in rat hippocampal cell cultures. *Neurosci. Lett.* 475, 174–178. doi: 10.1016/j.neulet.2010.03.073

Anand, P., Kunnumakkara, A. B., Newman, R. A., and Aggarwal, B. B. (2007). Bioavailability of curcumin: problems and promises. *Mol. Pharm.* 4, 807–818. doi: 10.1021/mp700113r

András, I. E., and Toborek, M. (2013). Amyloid beta accumulation in HIV-1-infected brain: the role of the blood brain barrier. *IUBMB Life* 65, 43–49. doi: 10.1002/iub.1106

Arimon, M., Takeda, S., Post, K. L., Svirsky, S., Hyman, B. T., and Berezovska, O. (2015). Oxidative stress and lipid peroxidation are upstream of amyloid pathology. *Neurobiol. Dis.* 84, 109–119. doi: 10.1016/j.nbd.2015.06.013

Bagashev, A., and Sawaya, B. E. (2013). Roles and functions of HIV-1 Tat protein in the CNS: an overview. *Virol. J.* 10:358. doi: 10.1186/1743-422X-10-358

Barage, S. H., and Sonawane, K. D. (2015). Amyloid cascade hypothesis: pathogenesis and therapeutic strategies in Alzheimer's disease. *Neuropeptides* 52, 1–18. doi: 10.1016/j.npep.2015.06.008

Bargagna-Mohan, P., Hamza, A., Kim, Y.-E., Ho, Y. K. A., Mor-Vaknin, N., Wendschlag, N., et al. (2007). The tumor inhibitor and antiangiogenic agent withaferin A targets the intermediate filament protein vimentin. *Chem. Biol.* 14, 623–634. doi: 10.1016/j.chembiol.2007.04.010

Becker, J. T., Lopez, O. L., Dew, M. A., and Aizenstein, H. J. (2004). Prevalence of cognitive disorders differs as a function of age in HIV virus infection. *AIDS* 18, 11–18. doi: 10.1097/00002030-200401001-00003

Buch, S., Yao, H., Guo, M., Mori, T., Mathias-Costa, B., Singh, V., et al. (2012). Cocaine and HIV-1 interplay in CNS: cellular and molecular mechanisms. *Curr. HIV Res.* 10, 425–428. doi: 10.2174/157016212802138823

Butterfield, D. A., Swomley, A. M., and Sultana, R. (2013). Amyloid β-peptide (1–42)-induced oxidative stress in alzheimer disease: importance in disease pathogenesis and progression. *Antioxid. Redox Signal.* 19, 823–835. doi: 10.1089/ars.2012.5027

CDC. (2018). *Injection Drug Use and HIV Risk*. Available online at: https://www.cdc.gov/hiv/risk/idu.html

Challa, A. A., Vukmirovic, M., Blackmon, J., and Stefanovic, B. (2012). Withaferin-A reduces type I collagen expression *in vitro* and inhibits development of myocardial fibrosis *in vivo*. *PLoS One* 7:e42989. doi: 10.1371/journal.pone.0042989

Chandra, T., Maier, W., König, H.-G., Hirzel, K., Kögel, D., Schüler, T., et al. (2005). Molecular interactions of the type 1 human immunodeficiency virus transregulatory protein Tat with *N*-methyl-d-aspartate receptor subunits. *Neuroscience* 134, 145–153. doi: 10.1016/j.neuroscience.2005.02.049

Cheignon, C., Tomas, M., Bonnefont-Rousselot, D., Faller, P., Hureau, C., and Collin, F. (2018). Oxidative stress and the amyloid beta peptide in Alzheimer's disease. *Redox Biol.* 14, 450–464. doi: 10.1016/j.redox.2017.10.014

Chen, X., Hui, L., Geiger, N. H., Haughey, N. J., and Geiger, J. D. (2013). Endolysosome involvement in HIV-1 transactivator protein-induced neuronal amyloid beta production. *Neurobiol. Aging* 34, 2370–2378. doi: 10.1016/j.neurobiolaging.2013.04.015

Choi, B. Y., and Kim, B.-W. (2015). Withaferin-A inhibits colon cancer cell growth by blocking STAT3 transcriptional activity. *J. Cancer Prev.* 20, 185–192. doi: 10.15430/JCP.2015.20.3.185

Daily, A., Nath, A., and Hersh, L. B. (2006). Tat peptides inhibit neprilysin. *J. Neurovirol.* 12, 153–160. doi: 10.1080/13550280600760677

Ding, H., Sagar, V., Agudelo, M., Pilakka-Kanthikeel, S., Atluri, V. S. R., Raymond, A., et al. (2014). Enhanced blood-brain barrier transmigration using a novel transferrin embedded fluorescent magneto-liposome nanoformulation. *Nanotechnology* 25:055101. doi: 10.1088/0957-4484/25/5/055101

Dorszewska, J., Prendecki, M., Oczkowska, A., Dezor, M., and Kozubski, W. (2016). Molecular basis of familial and sporadic Alzheimer's disease. *Curr. Alzheimer Res.* 13, 952–963. doi: 10.2174/1567205013666160314150501

Dublin, S., Walker, R. L., Gray, S. L., Hubbard, R. A., Anderson, M. L., Yu, O., et al. (2017). Use of analgesics (opioids and nonsteroidal anti-inflammatory drugs) and dementia-related neuropathology in a community-based autopsy cohort. *J. Alzheimers Dis.* 58, 435–448. doi: 10.3233/JAD-160374

Echeverria, V., Ducatenzeiler, A., Dowd, E., Jänne, J., Grant, S. M., Szyf, M., et al. (2004). Altered mitogen-activated protein kinase signaling, tau hyperphosphorylation and mild spatial learning dysfunction in transgenic rats expressing the β-amyloid peptide intracellularly in hippocampal and cortical neurons. *Neuroscience* 129, 583–592. doi: 10.1016/j.neuroscience.2004.07.036

Ellis, R. J., Rosario, D., Clifford, D. B., Mcarthur, J. C., Simpson, D., Alexander, T., et al. (2010). Continued high prevalence and adverse clinical impact of human immunodeficiency virus-associated sensory neuropathy in the era of combination antiretroviral therapy: the CHARTER study. *Arch. Neurol.* 67, 552–558. doi: 10.1001/archneurol.2010.76

Esiri, M. M., Biddolph, S. C., and Morris, C. S. (1998). Prevalence of Alzheimer plaques in AIDS. *J. Neurol. Neurosurg. Psychiatry* 65, 29–33. doi: 10.1136/jnnp.65.1.29

Fiala, M., Gan, X. H., Zhang, L., House, S. D., Newton, T., Graves, M. C., et al. (1998). Cocaine enhances monocyte migration across the blood-brain barrier. Cocaine's connection to AIDS dementia and vasculitis? *Adv. Exp. Med. Biol.* 437, 199–205. doi: 10.1007/978-1-4615-5347-2_22

Gannon, P., Khan, M. Z., and Kolson, D. L. (2011). Current understanding of HIV-associated neurocognitive disorders pathogenesis. *Curr. Opin. Neurol.* 24, 275–283. doi: 10.1097/WCO.0b013e32834695fb

Ghosh, A. K., Gemma, S., and Tang, J. (2008). β-secretase as a therapeutic target for Alzheimer's disease. *Neurotherapeutics* 5, 399–408. doi: 10.1016/j.nurt.2008.05.007

Giunta, B., Hou, H., Zhu, Y., Rrapo, E., Tian, J., Takashi, M., et al. (2009). HIV-1 Tat contributes to Alzheimer's disease-like pathology in PSAPP mice. *Int. J. Clin. Exp. Pathol.* 2, 433–443.

Green, D. A., Masliah, E., Vinters, H. V., Beizai, P., Moore, D. J., and Achim, C. L. (2005). Brain deposition of beta-amyloid is a common pathologic feature in HIV positive patients. *AIDS* 19, 407–411. doi: 10.1097/01.aids.0000161770.06158.5c

Guardia-Laguarta, C., Pera, M., and Lleo, A. (2010). γ-Secretase as a therapeutic target in Alzheimers disease. *Curr. Drug Targets* 11, 506–517. doi: 10.2174/138945010790980349

Hategan, A., Bianchet, M. A., Steiner, J., Karnaukhova, E., Masliah, E., Fields, A., et al. (2017). HIV Tat protein and amyloid-β peptide form multifibrillar structures that cause neurotoxicity. *Nat. Struct. Mol. Biol.* 24, 379–386. doi: 10.1038/nsmb.3379

Heaton, R., Clifford, D., Franklin, D., Woods, S., Ake, C., Vaida, F., et al. (2010). HIV-associated neurocognitive disorders persist in the era of potent antiretroviral therapy CHARTER study. *Neurology* 75, 2087–2096. doi: 10.1212/WNL.0b013e318200d727

Heaton, R. K., Franklin, D. R., Ellis, R. J., McCutchan, J. A., Letendre, S. L., Leblanc, S., et al. (2011). HIV-associated neurocognitive disorders before and during the era of combination antiretroviral therapy: differences in rates, nature and predictors. *J. Neurovirol.* 17, 3–16. doi: 10.1007/s13365-010-0006-1

Ishrat, T., Hoda, M. N., Khan, M. B., Yousuf, S., Ahmad, M., Khan, M. M., et al. (2009). Amelioration of cognitive deficits and neurodegeneration by curcumin in rat model of sporadic dementia of Alzheimer's type (SDAT). *Eur. Neuropsychopharmacol.* 19, 636–647. doi: 10.1016/j.euroneuro.2009.02.002

Javadi-Paydar, M., Roscoe, R. F. Jr., Denton, A. R., Mactutus, C. F., and Booze, R. M. (2017). HIV-1 and cocaine disrupt dopamine reuptake and medium spiny neurons in female rat striatum. *PLoS One* 12:e0188404. doi: 10.1371/journal.pone.0188404

Jayant, R. D., Atluri, V. S., Tiwari, S., Pilakka-Kanthikeel, S., Kaushik, A., Yndart, A., et al. (2017). Novel nanoformulation to mitigate co-effects of drugs of abuse and HIV-1 infection: towards the treatment of NeuroAIDS. *J. Neurovirol.* 23, 603–614. doi: 10.1007/s13365-017-0538-8

Kaushik, A., Jayant, R. D., Tiwari, S., Vashist, A., and Nair, M. (2016). Nano-biosensors to detect beta-amyloid for Alzheimer's disease management. *Biosens Bioelectron.* 80, 273–287. doi: 10.1016/j.bios.2016.01.065

Koppel, B. S., Wormser, G. P., Tuchman, A. J., Maayan, S., Hewlett, D. Jr., et al. (1985). Central nervous system involvement in patients with acquired immune deficiency syndrome (AIDS). *Acta Neurol. Scand.* 71, 337–353. doi: 10.1111/j.1600-0404.1985.tb03211.x

Kretner, B., Trambauer, J., Fukumori, A., Mielke, J., Kuhn, P. H., Kremmer, E., et al. (2016). Generation and deposition of Aβ43 by the virtually inactive presenilin-1 L435F mutant contradicts the presenilin loss-of-function hypothesis of Alzheimer's disease. *EMBO Mol. Med.* 8, 458–465. doi: 10.15252/emmm.201505952

Kurapati, K. R., Atluri, V. S., Samikkannu, T., and Nair, M. P. (2013). Ashwagandha (Withania somnifera) reverses beta-amyloid1–42 induced toxicity in human neuronal cells: implications in HIV-associated neurocognitive disorders (HAND). *PLoS One* 8:e77624. doi: 10.1371/journal.pone.0077624

Kurapati, K. R., Samikkannu, T., Atluri, V. S., Kaftanovskaya, E., Yndart, A., and Nair, M. P. (2014). β-Amyloid1–42, HIV-1Ba-L (clade B) infection and drugs of abuse induced degeneration in human neuronal cells and protective effects

of ashwagandha (Withania somnifera) and its constituent Withanolide A. *PLoS One* 9:e112818. doi: 10.1371/journal.pone.0112818

Lee, I.-C., and Choi, B. Y. (2016). Withaferin-A—a natural anticancer agent with pleitropic mechanisms of action. *Int. J. Mol. Sci.* 17:290. doi: 10.3390/ijms17030290

Li, Y., Sun, Z., Cao, Q., Chen, M., Luo, H., Lin, X., et al. (2017). Role of amyloid β protein receptors in mediating synaptic plasticity. *Biomed. Rep.* 6, 379–386. doi: 10.3892/br.2017.863

Liu, S.-J., Fang, Z.-Y., Yang, Y., Deng, H.-M., and Wang, J.-Z. (2003). Alzheimer-like phosphorylation of tau and neurofilament induced by cocaine *in vivo*. *Acta Pharmacol. Sin.* 24, 512–518.

Marottoli, F. M., Katsumata, Y., Koster, K. P., Thomas, R., Fardo, D. W., and Tai, L. M. (2017). Peripheral inflammation, apolipoprotein E4 and amyloid-β interact to induce cognitive and cerebrovascular dysfunction. *ASN Neuro* 9:1759091417719201. doi: 10.1177/1759091417719201

Martínez-Bonet, M., Muñoz-Fernández, M. A., and Álvarez, S. (2018). HIV-1 increases extracellular amyloid-beta levels through neprilysin regulation in primary cultures of human astrocytes. *J. Cell. Physiol.* doi: 10.1002/jcp.26462 [Epub ahead of print].

Meade, C. S., Hobkirk, A. L., Towe, S. L., Chen, N.-K., Bell, R. P., and Huettel, S. A. (2017). Cocaine dependence modulates the effect of HIV infection on brain activation during intertemporal decision making. *Drug Alcohol Depend.* 178, 443–451. doi: 10.1016/j.drugalcdep.2017.05.043

Merino, J. J., Montes, M., Blanco, A., Bustos, M. J., Oreja-Guevara, C., Bayon, C., et al. (2011). HIV-1 neuropathogenesis: therapeutic strategies against neuronal loss induced by gp120/Tat glycoprotein in the central nervous system. *Rev. Neurol.* 52, 101–111.

Mirjalili, M. H., Moyano, E., Bonfill, M., Cusido, R. M., and Palazón, J. (2009). Steroidal lactones from Withania somnifera, an ancient plant for novel medicine. *Molecules* 14, 2373–2393. doi: 10.3390/molecules14072373

Mohan, R., and Bargagna-Mohan, P. (2016). The use of withaferin A to study intermediate filaments. *Methods Enzymol.* 568, 187–218. doi: 10.1016/bs.mie.2015.09.025

Mohan, R., Hammers, H., Bargagna-Mohan, P., Zhan, X., Herbstritt, C., Ruiz, A., et al. (2004). Withaferin A is a potent inhibitor of angiogenesis. *Angiogenesis* 7, 115–122. doi: 10.1007/s10456-004-1026-3

Nath, A., Psooy, K., Martin, C., Knudsen, B., Magnuson, D., Haughey, N., et al. (1996). Identification of a human immunodeficiency virus type 1 Tat epitope that is neuroexcitatory and neurotoxic. *J. Virol.* 70, 1475–1480.

Nuovo, G. J., Becker, J., Burk, M. W., Margiotta, M., Fuhrer, J., and Steigbigel, R. T. (1994). in situ detection of PCR-amplified HIV-1 nucleic acids in lymph nodes and peripheral blood in patients with asymptomatic HIV-1 infection and advanced-stage AIDS. *J. Acquir. Immune Defic. Syndr.* 7, 916–923.

Oguntibeju, O. O. (2012). Quality of life of people living with HIV and AIDS and antiretroviral therapy. *HIV/AIDS* 4, 117–124. doi: 10.2147/HIV.s32321

Palop, J. J., and Mucke, L. (2010). Amyloid-β induced neuronal dysfunction in Alzheimer's disease: from synapses toward neural networks. *Nat. Neurosci.* 13, 812–818. doi: 10.1038/nn.2583

Park, H. J., Rayalam, S., Della-Fera, M. A., Ambati, S., Yang, J.-Y., and Baile, C. A. (2008). Withaferin A induces apoptosis and inhibits adipogenesis in 3T3–L1 adipocytes. *Biofactors* 33, 137–148. doi: 10.1002/biof.5520330206

Pulliam, L. (2009). HIV regulation of amyloid beta production. *J. Neuroimmune Pharmacol.* 4, 213–217. doi: 10.1007/s11481-009-9151-9

Rah, B., Amin, H., Yousuf, K., Khan, S., Jamwal, G., Mukherjee, D., et al. (2012). A novel MMP-2 inhibitor 3-azidowithaferin A (3-azidoWA) abrogates cancer cell invasion and angiogenesis by modulating extracellular Par-4. *PLoS One* 7:e44039. doi: 10.1371/journal.pone.0044039

Ramage, S., Anthony, I., Carnie, F., Busuttil, A., Robertson, R., and Bell, J. (2005). Hyperphosphorylated tau and amyloid precursor protein deposition is increased in the brains of young drug abusers. *Neuropathol. Appl. Neurobiol.* 31, 439–448. doi: 10.1111/j.1365-2990.2005.00670.x

Rempel, H. C., and Pulliam, L. (2005). HIV-1 Tat inhibits neprilysin and elevates amyloid β. *AIDS* 19, 127–135. doi: 10.1097/00002030-200501280-00004

Ringman, J. M., Frautschy, S. A., Cole, G. M., Masterman, D. L., and Cummings, J. L. (2005). A potential role of the curry spice curcumin in Alzheimer's disease. *Curr. Alzheimer Res.* 2, 131–136. doi: 10.2174/1567205053585882

Levy, R. M., Bredesen, D. E., and Rosenblum, M. L. (1985). Neurological manifestations of the acquired immunodeficiency syndrome (AIDS): experience at UCSF and review of the literature. *J. Neurosurg.* 62, 475–495. doi: 10.3171/jns.1985.62.4.0475

Sabin, C. A. (2013). Do people with HIV infection have a normal life expectancy in the era of combination antiretroviral therapy? *BMC Med.* 11:251. doi: 10.1186/1741-7015-11-251

Saylor, D., Dickens, A. M., Sacktor, N., Haughey, N., Slusher, B., Pletnikov, M., et al. (2016). HIV-associated neurocognitive disorder—pathogenesis and prospects for treatment. *Nat. Rev. Neurol.* 12, 234–248. doi: 10.1038/nrneurol.2016.27

Sharma, R. A., Steward, W. P., and Gescher, A. J. (2007). Pharmacokinetics and pharmacodynamics of curcumin. *Adv. Exp. Med. Biol.* 595, 453–470. doi: 10.1007/978-0-387-46401-5_20

Snider, W. D., Simpson, D. M., Nielsen, S., Gold, J. W., Metroka, C. E., and Posner, J. B. (1983). Neurological complications of acquired immune deficiency syndrome: analysis of 50 patients. *Ann. Neurol.* 14, 403–418. doi: 10.1002/ana.410140404

Soontornniyomkij, V., Moore, D. J., Gouaux, B., Soontornniyomkij, B., Tatro, E. T., Umlauf, A., et al. (2012). Cerebral β-amyloid deposition predicts HIV-associated neurocognitive disorders in APOE ε4 carriers. *AIDS* 26, 2327–2335. doi: 10.1097/QAD.0b013e32835a117c

Tahirov, T. H., Babayeva, N. D., Varzavand, K., Cooper, J. J., Sedore, S. C., and Price, D. H. (2010). Crystal structure of HIV-1 Tat complexed with human P-TEFb. *Nature* 465, 747–751. doi: 10.1038/nature09131

Tohda, C., Kuboyama, T., and Komatsu, K. (2000). Dendrite extension by methanol extract of Ashwagandha (roots of Withania somnifera) in SK-N-SH cells. *Neuroreport* 11, 1981–1985. doi: 10.1097/00001756-200006260-00035

Valcour, V. G., Shikuma, C. M., Watters, M. R., and Sacktor, N. C. (2004). Cognitive impairment in older HIV-1-seropositive individuals: prevalence and potential mechanisms. *AIDS* 18, 79–86. doi: 10.1097/00002030-200418001-00012

van Marum, R. J. (2008). Current and future therapy in Alzheimer's disease. *Fundam. Clin. Pharmacol.* 22, 265–274. doi: 10.1111/j.1472-8206.2008.00578.x

Venkitaramani, D. V., Chin, J., Netzer, W. J., Gouras, G. K., Lesne, S., Malinow, R., et al. (2007). β-amyloid modulation of synaptic transmission and plasticity. *J. Neurosci.* 27, 11832–11837. doi: 10.1523/JNEUROSCI.3478-07.2007

Wakim, K.-M., Molloy, C. J., Bell, R. P., Ross, L. A., and Foxe, J. J. (2017). White matter changes in HIV+ women with a history of cocaine dependence. *Front. Neurol.* 8:562. doi: 10.3389/fneur.2017.00562

World Health Organization (2016). *Global Aids Update.* Available online at: http://www.who.int/hiv/pub/arv/global-AIDS-update-2016_en.pdf

World Health Organization (2018). *HIV/AIDS.* Available online at: http://www.who.int/mediacentre/factsheets/fs360/en/

Yu, Y., Hamza, A., Zhang, T., Gu, M., Zou, P., Newman, B., et al. (2010). Withaferin A targets heat shock protein 90 in pancreatic cancer cells. *Biochem. Pharmacol.* 79, 542–551. doi: 10.1016/j.bcp.2009.09.017

Zhao, J., Nakamura, N., Hattori, M., Kuboyama, T., Tohda, C., and Komatsu, K. (2002). Withanolide derivatives from the roots of Withania somnifera and their neurite outgrowth activities. *Chem. Pharm. Bull.* 50, 760–765. doi: 10.1248/cpb.50.760

Zheng, W. H., Bastianetto, S., Mennicken, F., Ma, W., and Kar, S. (2002). Amyloid β peptide induces tau phosphorylation and loss of cholinergic neurons in rat primary septal cultures. *Neuroscience* 115, 201–211. doi: 10.1016/s0306-4522(02)00404-9

Conflict of Interest Statement: The authors declare that the research was conducted in the absence of any commercial or financial relationships that could be construed as a potential conflict of interest.

Advantages of publishing in Frontiers

OPEN ACCESS
Articles are free to read for greatest visibility and readership

FAST PUBLICATION
Around 90 days from submission to decision

HIGH QUALITY PEER-REVIEW
Rigorous, collaborative, and constructive peer-review

TRANSPARENT PEER-REVIEW
Editors and reviewers acknowledged by name on published articles

Frontiers
Avenue du Tribunal-Fédéral 34
1005 Lausanne | Switzerland

Visit us: www.frontiersin.org
Contact us: info@frontiersin.org | +41 21 510 17 00

REPRODUCIBILITY OF RESEARCH
Support open data and methods to enhance research reproducibility

DIGITAL PUBLISHING
Articles designed for optimal readership across devices

FOLLOW US
@frontiersin

IMPACT METRICS
Advanced article metrics track visibility across digital media

EXTENSIVE PROMOTION
Marketing and promotion of impactful research

LOOP RESEARCH NETWORK
Our network increases your article's readership